NGU
Norges geologiske undersøkelse
Geological Survey of Norway

GEOLOGI FOR SAMFUNNET
GEOLOGY FOR SOCIETY

NGU Report 2013.014

Investigations on unstable rock slopes in Møre og Romsdal - status and plans after field surveys in 2012

NGU
Norges geologiske undersøkelse
Geological Survey of Norway

Geological Survey of Norway
Postboks 6315 Sluppen
NO-7491 Trondheim, Norway
Tel.: +4773904000
Telefax +4773921620

REPORT

Report no.: 2013.014	ISSN: 0800–3416	Grading: Open

Title:
Investigations on unstable rock slopes in Møre og Romsdal – status and plans after field surveys in 2012

Authors:	Client:
T. Oppikofer, A. Saintot, S. Otterå, R.L. Hermanns, E. Anda, H. Dahle, T. Eiken	Norwegian Water Resources and Energy Directorate (NVE)
County: Møre og Romsdal	Commune:
Map-sheet name (M=1:250.000): Ålesund, Kristiansund, Røros, Ulsteinvik	Map-sheet no. and -name (M=1:50.000)
Deposit name and grid-reference:	Number of pages: 323 Price (NOK): 1285,- Map enclosures: 0

Fieldwork carried out:	Date of report:	Project no.:	Quality control:
2006–2012	13.11.2013	309900	Halvor Bunkholt

Summary:

This report presents investigations, analyses and displacement measurements made between 2006 and 2012 on 131 unstable or potential unstable rock slopes in Møre og Romsdal County (Western Norway). An extract of this report is available in Norwegian (NGU rapport 2013.053).

These investigations are part of the national plan for mapping of unstable rock slopes in Norway from the Norwegian Water Resources and Energy Directorate (NVE) and NGU. A total of 245 sites are known in Møre og Romsdal, but only 77 sites are classified as unstable rock slopes that are relevant for this project by being large enough to create either a rock avalanche or a displacement wave if impacting a water body. The remaining sites are classified either as potential unstable rock slopes (29 sites), not unstable rock slopes (91 sites) or have not yet been visited (48 sites) and have thus unknown status.

Helicopter reconnaissance flights were made in Eikesdalen and Romsdalen Valleys, Romsdalsfjord, Søre Sunnmøre region and the coastal region between Ålesund and Molde to get an overview over unstable rock slopes in these previously uninvestigated areas. Field mapping was done on several unstable rock slopes in these areas, along with other sites in Storfjord region and Sunndal municipality.

At 28 unstable rock slopes periodical displacement measurements are made by NGU using differential Global Navigation Satellite Systems, terrestrial laser scanning and tape extensometers. Three unstable rock slopes (Åknes, Hegguraksla and Mannen) are continuously monitored by the Åknes/Tafjord Early-Warning Centre. In addition to Åknes and Mannen do NGU's periodic measurements shows significant displacements on four unstable rock slopes (Børa, Gikling, Middagstinden, Oppstadhornet) with displacement rates ranging from 0.1 to 2.4 cm/year. Other periodically measured sites have either no significant displacements measured over several years (16 sites) or displacements are unknown as no repetitive measurements are made up to now (8 sites). According to the recommendations given in this report, periodic measurements should not be continued at 8 sites because they are no longer classified as unstable rock slopes.

Recommendations for further investigations in this report are preliminary. Final recommendations will be made in the next years based on the systematic hazard and risk classification system for large unstable rock slopes in Norway.

Keywords: Rock avalanche	Unstable rock slope	Structural mapping
Periodic displacement measurements	Global Navigation Satellite Systems	Terrestrial laser scanning
Cosmogenic nuclide dating	Hazard and risk classification	

CONTENTS

APPENDIXES

1. INTRODUCTION

1.1 Goals

The Geological Survey of Norway (NGU) is systematically mapping unstable or potential unstable rock slopes in Norway. The recommendations that arised from results of field surveys and additional investigations carried out between 2006 and 2012 in Møre og Romsdal County are presented in this report. A Norwegian extract of this report is published as NGU report 2013.053 (Oppikofer et al. 2013).

This project deals with unstable or potential unstable rock slopes that have the potential to cause either rock avalanches and/or secondary effects, such as displacement waves or damming of a valley. The rock slopes investigated in this project have thus large volumes ranging from hundred thousands to several million m^3. The catastrophic, sudden failure of such rock slopes may form rock avalanches ("fjellskred" in Norwegian) that have much longer run-out distances than rockfalls ("steinsprang" in Norwegian) and small rock slope failures ("steinskred" in Norwegian). The terms "unstable rock slope" and "instability" are used as synonyms and as generic term for the landslide features studied in this project.

This project was a common project between NGU, the Møre og Romsdal County and Oslo University and became a common project between NGU, the Norwegian Water Resources and Energy directorate (NVE), the Møre og Romsdal County and Oslo University on 1 January 2009 when NVE took over the responsibility for landslide mapping in Norway. It participates to the national plan for mapping of unstable rock slopes in Norway and has been financed since 2009 by NVE (Devoli et al. 2011, Øydvin et al. 2011). Similar systematic studies have been carried out for the same goal during these years in Troms (e.g. Bunkholt et al. 2011, 2013) and Sogn og Fjordane (e.g. Hermanns et al. 2011).

1.2 Background and earlier works

The Møre og Romsdal County in Western Norway is characterized by numerous fjords and valleys surrounded by high mountain sides and its relief belong to the extreme alpine class. These steep mountain sides let to several large rockslides and rock avalanches since the last glaciation. NGU has for example completed a systematic inventory of 108 rockslide and rock avalanche deposits in the Storfjord (Longva et al. 2009). Many of them occurred between 11 000 and 9000 years ago, i.e. shortly after the deglaciation, even though several rock avalanches were also recorded in Møre og Romsdal in the following millennia and in historic times (Blikra et al. 2006, Furseth 2006). These historic events caused casualties, mainly because of displacement waves (tsunamis) created by the rock avalanche when impacting a water body. The last major event in Møre og Romsdal was the rock avalanche from Langhammaren into Tafjord in 1934, which caused an up to 63 m high displacement wave and killed 40 people in nearby villages (Furseth 2009). A number of fjords and valleys in Møre og Romsdal were also affected by rock avalanches in the past, such as Romsdalen Valley where tens of rock avalanche deposits are mapped (Blikra et al. 2002a, Farsund 2010). Because of this large number of catastrophic historic events the Møre og Romsdal County is in the highest priority group of regions for the systematic mapping of unstable rock slopes (Devoli et al. 2011, Øydvin et al. 2011).

Several rock slopes in Møre og Romsdal evidenced past and present movements and might produce catastrophic rock avalanches in the future. More than 240 potential unstable rock slopes were detected by NGU in collaboration with Einar Anda, county geologist of Møre og Romsdal (Dahle et al. 2011a). The systematic mapping and investigation of these unstable rock slopes started in 2005 in the Storfjord area (Henderson et al. 2006), rapidly followed by the Romsdalen and Sunndalen Valleys (Henderson and Saintot 2007, Saintot et al. 2008). These investigations are still going on and will conclude with the hazard and risk classification of all unstable rock slopes (Hermanns et al. 2012) in the coming years.

Three unstable rock slopes in Møre og Romsdal were classified as high-risk sites in the 2000s and are now continuously monitored and equipped with an early-warning system operated by the Åknes/Tafjord Early-Warning Centre (www.aknes.no). The Åknes rockslide in the Sunnylvsfjord was studied within the Åknes/Tafjord Project with a very high level of detail using a multitude of surface and subsurface surveys and continuous monitoring instruments (e.g. Blikra 2008, Ganerød et al. 2008). The rock slope instabilities at Hegguraksla in Tafjord (e.g. Oppikofer 2009) and a large rockslide at Mannen in the Romsdal Valley (e.g. Dahle et al. 2008, Dahle et al. 2011c, Saintot et al. 2011a, Oppikofer et al. 2012b) are also analysed in great detail and continuously monitored.

2. METHODS

This report is written for the general public and mainly intended for NVE, the Møre og Romsdal County and the different municipalities. Most of the background data (field mapping, field data and analyses) are therefore only shortly described in this report but obviously found the basis for the considerations given in this report. The collected data and conducted analyses are available upon request and include structural data, kinematic analyses, and measurements from differential Global Navigation Satellite Systems, terrestrial laser scanning and tape extensometer, as well as dating with terrestrial cosmogenic nuclides.

2.1 Approach for systematic mapping of unstable rock slopes in Norway

The systematic mapping of unstable rock slopes that could cause rock avalanches started in Norway in 2005 (Henderson et al. 2006). The goals of these ongoing mapping activities are (1) to find all rock slopes that could fail catastrophically and (2) to indicate areas that would be potentially affected by their failure so that any consequences can be systematically communicated to the Norwegian society. Since the beginning of 2013, mapping activities are focused on collecting the necessary information for the hazard and risk classification system (Hermanns et al. 2012) recently developed by a team of Norwegian and international experts. This classification system does not take into account earthquakes as triggering mechanism of a rock avalanche, due to the fact that earthquakes cannot be predicted. However, this is not regarded as a major problem in Norway since the risk of an earthquake that is strong enough to trigger a rockslide is low (Bungum et al. 2000). Keefer (1984) based upon 40 case studies worldwide in seismically active areas set an earthquake with a magnitude M6 as a minimum threshold for triggering rock avalanches. However in areas with low seismic activity this threshold might be lower, but no empirical data exist. In any case, there is no knowledge about a historical earthquake-triggered rock avalanche in Norway. The classification system is now the standard tool for defining the risk level, which in turn will be used to decide on further actions on the investigated unstable rock slopes (a list of follow-up actions and the conditions of how and where they will be applied will be specified in an upcoming NVE document). The application of this classification system has allowed developing a systematic mapping approach as presented in Figure 1: low-risk sites are ruled out at an early stage and more detailed investigations focus on the possible medium- and high-risk sites only. Therefore, this mapping approach guarantees a similar level of geological information for all unstable rock slopes with the same risk level over the entire country.

The information about each investigated unstable rock slope will become publicly accessible through www.skrednett.no in 2014. This database will include a general description of the site (location, observations, structures…), conducted site investigations, recommendations for further work and the hazard and risk classification. More detailed geological information will be available upon request. Information on www.skrednett.no will also be downloadable in 2014, and then NGU reports will only be published to summarize geological information for risk-classified sites. Meanwhile, county status reports will continue being used 1) to inform the public on the progress of the site investigations and 2) document the geological information gained at each site.

The 2013 county status reports are published with information collected prior to the establishment of the hazard and risk classification system, and thus do not strictly follow the same mapping approach. Therefore, the status reports fulfil both above-mentioned tasks, i.e. information and documentation. To make the status reports easy to read all content has been standardized. For every site the general description and geological information is written in normal style font, while recommendations for further investigations are given in bold style font. All reports summarize future work plans in a separate chapter (see chapter 10).

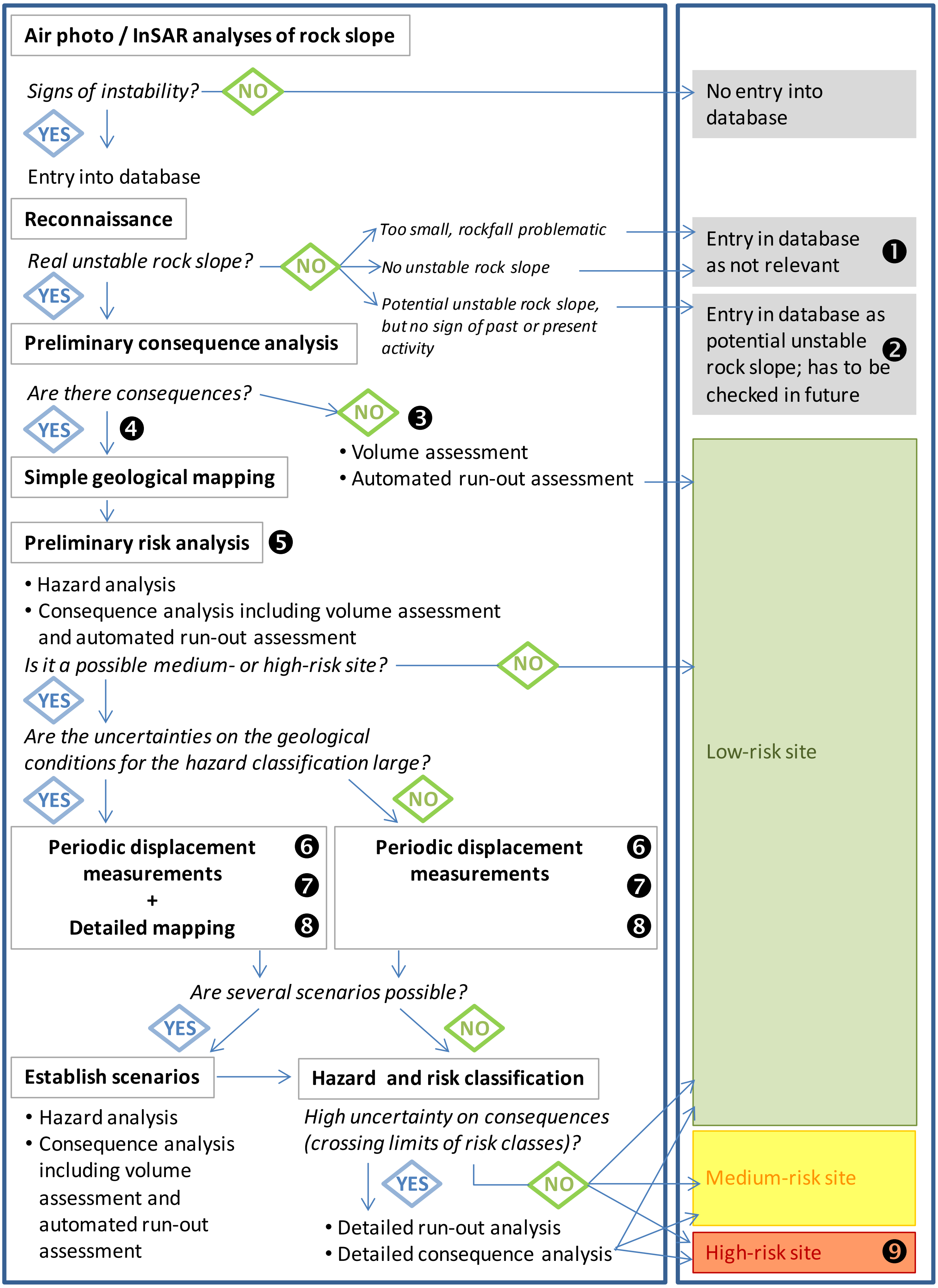

Figure 1: **Work-flow diagram for site investigations on unstable rock slopes. Goal of this approach is to filter low-risk sites out at an early stage in order to reduce the amount of work and costs in the mapping program, while creating essential knowledge for society. More detailed investigations and displacement measurements will focus on the possible medium- and high-risk sites. Numbers refer to the standard recommendations described in section 2.1.2.**

2.1.1 Site investigation statuses

The investigation status of every site is systematically shown on overview maps and is defined as:

Continuous monitoring: Permanent real-time monitoring systems are installed on the site and continuously transmit data to an early-warning centre. Works on those sites are not under NGU's responsibility as the risk has already been defined and the responsibility was transferred to the relevant communities.

Periodic measurements: Displacement measurements are conducted with one to several years interval using geodetic/geotechnical methods such as global navigation satellite systems (GNSS), extensometers, terrestrial laser scanning (TLS) or radar interferometry (InSAR). Sites under periodic displacement measurements have also been mapped in the field. It is expected that for most of these sites the amount and quality of geological data allow their final hazard and risk classification with sufficiently low uncertainties. However, some sites require longer time-series of displacement measurements in order to decrease the uncertainty in the hazard classification.

Detailed mapping: Sites have been mapped in detail in the field. Data collected during mapping is sufficient to perform kinematic analyses and to elaborate geological models of the unstable rock slope. It is expected that for most of these sites the amount and quality of geological data allow their hazard and risk classification.

Simple mapping: Sites have been mapped in the field and limited geological data have been collected. Possibly, more geological data will be needed to reduce uncertainties in the hazard and risk assessment. However, if there are minor or no consequences, the hazard and risk classification obtained based on the available geological data will be sufficient.

Reconnaissance: Sites have not been visited or mapped on the ground, but an evaluation has been performed based on observations from helicopter or from the valley bottom. These sites need to be mapped in the field prior to making the final hazard and risk classification, except if there are no consequences due to a potential failure so that large geological uncertainties are acceptable.

Not investigated: Sites have only been recognized by aerial photo analysis and/or InSAR analysis. Hence, they might either represent an unstable rock slope, a slope with a morphology that only suggests an unstable rock slope (e.g. eroded inherited structure(s) on the slope) or superficial deformation of Quaternary deposits. Reconnaissance is required to identify real unstable rock slopes, possibly followed by simple mapping prior to the hazard and risk classification.

Not relevant: Reconnaissance or simple mapping indicated that these sites are not unstable rock slopes, even though aerial photographs showed suspicious morphological signs suggesting an unstable rock slope. These sites are divided into three sub-categories: A) potential unstable rock slopes that have no signs of displacements (past or present) or deformation (see note below), B) unstable rock slopes with a too small volume to form rock avalanches and whose run-out areas therefore lie within the run-out area of rockfalls (covered by the nationwide rockfall susceptibility map and local rockfall hazard maps), and C) rock slopes that due to the geological conditions cannot develop an unstable rock slope. Not relevant rock slopes are discarded (no further investigations), but will be kept in the database with restricted access to avoid duplication of work in later years or decades. Potential unstable rock slopes (category A) should however be revisited after years to decades and followed-up on InSAR data.

Note: There is no relation between the different investigation statuses and any preliminary or final hazard and risk classification, except for the status "Continuous monitoring". It is only the level of investigations carried out at each site that determines the investigation status.

Note: "Potential unstable rock slopes" were previously not separated from "unstable rock slopes", but this distinction is now necessary in the frame of the hazard and risk classification. An "unstable rock slope" has clear signs of past or present displacements (i.e. head scarps, open back-cracks, obvious boundaries of the unstable area and deformation in the rock mass). In contrast, a "potential unstable rock slope" has no signs of past or present displacement or deformation, but the necessary geological conditions are present so that the site may develop into an unstable rock slope in the future. However, such a development takes decades to millennia, and can thus be detected with new aerial photo analyses and InSAR data.

2.1.2 Standard recommendations

Field work in years before 2013 did not follow the hazard and risk classification system and the classification can thus not be given yet. Standard recommendations are therefore used in the 2013 county status reports. These standard recommendations are described in the following. Numbers refer to the work-flow diagram (Figure 1) and texts in italics provide a more detailed explanation of the standard recommendation in relation to the work-flow diagram.

1. **No unstable rock slope**

   Recommendation: There are no signs that this rock slope might fail in a massive rock slope failure. No further investigations or displacement measurements are necessary and the hazard and risk classification will not be made. However, rockfalls are possible and their run-out area is given by the rockfall susceptibility map or more detailed hazard maps, where available.

   This recommendation signifies in the work-flow diagram (Figure 1) that reconnaissance or simple field mapping is finished. These investigations demonstrated that this site is not an unstable rock slope.

2. **Potential unstable rock slope**

   Recommendation: This site is classified as a potential unstable rock slope. At present the remaining rock slope does not show any signs of past or present displacements or deformation of a large volume. No further investigations or displacement measurements are necessary and the hazard and risk classification will not be made. However, this site may lead to rockfalls and develop over time into an unstable rock slope, due to structural and geological conditions. The site should be revisited after years to decades to detect any changes and be followed-up on InSAR data.

This recommendation signifies in the work-flow diagram (Figure 1) that reconnaissance or simple field mapping is finished. These investigations demonstrated that this site does not represent an unstable rock slope up to now. Yet, this site is classified as a potential unstable rock slope due to its structural and geological conditions that may favour over time the development of an unstable rock slope. A new reconnaissance is recommended after some years or decades in order to detect possible changes and InSAR data should be used to detect any displacements.

3. **Reconnoitred unstable rock slope without consequences**

   Recommendation: A possible rock avalanche from this unstable rock slope will have no consequences. No further investigations or displacement measurements are necessary. The hazard and risk classification will be made after a simple run-out assessment. Further follow-up activities will be based on this classification.

   This recommendation signifies in the work-flow diagram (Figure 1) that reconnaissance is finished. The unstable rock slope is located in a remote, uninhabited location without consequences for people. Geological field mapping is thus not necessary.

4. **Reconnoitred unstable rock slope with consequences**

   Recommendation: A possible rock avalanche from this unstable rock slope will have consequences. Geological field mapping is necessary to evaluate the structural and geological conditions and to quantify past displacements. The hazard and risk classification will be made after this field mapping. Further follow-up activities will be decided based on this classification.

   This recommendation signifies in the work-flow diagram (Figure 1) that reconnaissance is finished and field mapping has to be carried out. A volume estimation and automated run-out assessment are needed to evaluate the potential consequences. The preliminary hazard and risk classification of the site is performed thereafter. If the site is classified as a possible medium- or high-risk site, periodic displacement measurements and maybe detailed mapping need to be undertaken. In turn, if it is classified as low-risk site, periodic displacement measurements or further mapping are not necessary.

5. **Mapped unstable rock slope**

   Recommendation: A possible rock avalanche from this unstable rock slope will have consequences, which will be assessed in the hazard and risk classification. Further follow-up activities will be decided based on this classification.

   This recommendation signifies in the work-flow diagram (Figure 1) that field mapping is finished. A volume estimation and automated run-out assessment are needed to evaluate the potential consequences. The preliminary hazard and risk classification of the site is performed thereafter. If the site is classified as a possible medium- or high-risk site, periodic displacement measurements and maybe detailed mapping need to be undertaken. In turn, if it is classified as low-risk site, periodic displacement measurements or further mapping are not necessary.

6. **Periodically measured unstable rock slope with unknown movements**

   Recommendation: Periodic displacement measurements are started at this unstable rock slope, but the time-series is not sufficiently long to determine displacement rates. Periodic displacement measurements using the currently employed technique(s) should be continued with 1–3 years interval. The hazard and risk classification needs to be made and further follow-up activities will be decided based on this classification.

This recommendation signifies in the work-flow diagram (Figure 1) that mapping is finished, but periodic displacement measurements should continue in order to obtain a sufficiently long time-series (at least 3 measurements) and until the hazard and risk classification is completed.

7. **Periodically measured unstable rock slope without active movements**

   Recommendation: No significant displacements are measured up to now at this unstable rock slope. Periodic displacement measurements using the currently employed technique(s) should be continued with 3–5 years interval. The hazard and risk classification needs to be made and further follow-up activities will be decided based on this classification.

   This recommendation signifies in the work-flow diagram (Figure 1) that mapping is finished and no significant displacements were measured up to now. Periodic displacement measurements should continue until the hazard and risk classification is completed.

8. **Periodically measured unstable rock slope with active movements**

   Recommendation: Significant displacements are measured at this unstable rock slope. Periodic displacement measurements using the currently employed technique(s) should be continued with 1–3 years interval. The hazard and risk classification needs to be made and further follow-up activities will be decided based on this classification.

   This recommendation signifies in the work-flow diagram (Figure 1) that mapping is finished and significant displacements were measured. Periodic displacement measurements should continue until the hazard and risk classification is completed.

9. **Continuously monitored unstable rock slope**

   Recommendation: This unstable rock slope is under continuous monitoring and data are being sent to an early-warning centre, which is also responsible for further follow-up activities.

   This recommendation signifies in the work-flow diagram (Figure 1) that this unstable slope is already classified as high-risk site and is under continuous monitoring by an early-warning centre.

2.2 Mapping of unstable rock slopes

Unstable and potential unstable rock slopes are detected on aerial photos, field photos, digital elevation models and on maps. The purpose of mapping is to document slope deformation that can be associated with gravitational movements. Typical geomorphologic features indicating past deformation of a rock slope are head scarps or back-cracks, major open cracks, scarps and counterscarps, flanks (lateral release surfaces), sliding surfaces, morphological depressions and faults (modified from Hermanns et al. 2011). These features are presented in this report using a consistent symbology for edited photographs (Figure 2a) and maps (Figure 2b).

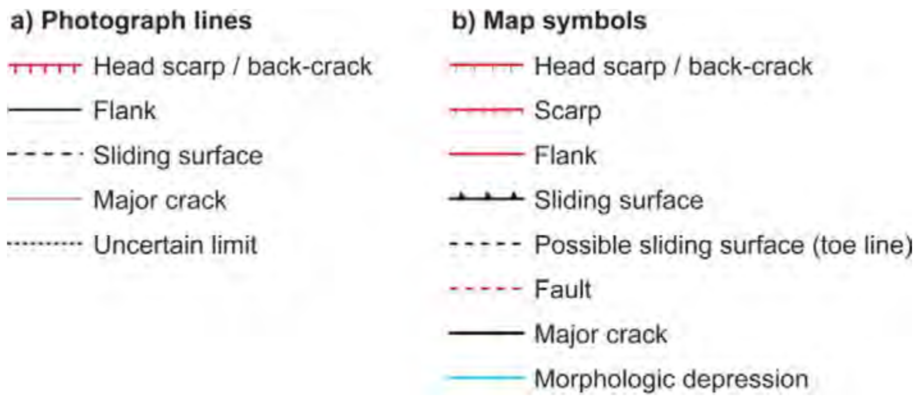

Figure 2: Legend used in this report for: a) edited photographs; b) maps.

2.3 Structural and kinematic analyses

Discontinuities are natural pre-existing planar structures in the rock mass such as metamorphic foliation and other schistosity, joints, fractures and faults. Their orientation is measured in the field using structural compasses or remotely using high-resolution digital elevation models (DEM) and appropriate software tools (e.g. Coltop3D, Terranum 2013). The structural pattern formed by these pre-existing discontinuities influences the rock slope stability, which in a first estimation can be assessed using simple kinematic analyses. The standard criteria from rock mechanics (Hoek and Bray 1981, Wyllie and Mah 2004) are used in this report, however with some adaptations to large rock slope failures as proposed by Hermanns et al. (2012).

2.4 Displacement measurements

2.4.1 Global Navigation Satellite Systems

Global Navigation Satellite Systems (GNSS) is a general term for satellite-based radionavigation, timing and positioning systems, such as the American Global Positioning System (GPS) or the Russian GLONASS system. By tracking the electromagnetic waves that the GNSS satellites are sending continuously to the world, the system can obtain the exact location of a receiving antenna (longitude, latitude and height or X, Y and Z Cartesian coordinates) (modified from SafeLand 2010).

The measurement technique is a static phase-difference measurement between the different GNSS antennas, leading to a network of vectors between all the antennas. The measurement time is generally 60 minutes (minimally 30 minutes) with one measurement every 5 seconds (Eiken 2012). The coordinates of each GNSS-point are calculated using a least squares adjustment of the measured vectors and expressed relative to one or several fixed point, installed on presumably stable areas. This common measurement technique is often called differential GNSS or dGNSS, as also used in this report.

The accuracy of the coordinates are estimated for each GNSS-point and are generally ca. 1 mm in planimetry and ca. 2 mm in elevation. These values are found to be too optimistic, so that the real accuracy is approximately 2–3 times higher than the estimated values (Eiken 2012). In this report, a factor of 3 is used to obtain the realistic accuracy from the standard deviations estimated by the processing software. Thus, the error on the total horizontal, total vertical and total 3D displacement, $\sigma_{tot.H}$, $\sigma_{tot.V}$ and $\sigma_{tot.3D}$, respectively, is given by:

$$\sigma_{tot.H} = 3 \cdot \sqrt{\bar{\sigma}_X{}^2 + \bar{\sigma}_Y{}^2}$$

$$\sigma_{tot.V} = 3 \cdot \bar{\sigma}_Z$$

$$\sigma_{tot.3D} = 3 \cdot \sqrt{\bar{\sigma}_X^{\,2} + \bar{\sigma}_Y^{\,2} + \bar{\sigma}_Z^{\,2}}$$

where $\bar{\sigma}_X$, $\bar{\sigma}_Y$ and $\bar{\sigma}_Z$ are the averages of the accuracies estimated by the processing software for the entire time-series at each point.

The differences on the X, Y and Z coordinates of the measurements with one or several years interval enable the calculation of displacement rates (velocities) and displacement directions. These may significantly vary from year to year as most points have displacement rates that are close to the level of accuracy of the measurement method. Robust linear regressions over the entire time series were thus applied to determine average yearly displacement rates as described in Böhme et al. (2013).

If the computed yearly displacement rates, v, exceeds the errors on the displacement, σ_{tot}, divided by the time interval between the first and last measurement, Δt (in years), then the displacements are considered as statistically significant from a methodological point of view:

$$v > \frac{\sqrt{2} \cdot \sigma_{tot}}{\Delta t}$$

This equation is used for horizontal, vertical or 3D displacement rates using the appropriate σ_{tot}. However, as described in Hermanns et al. (2011) and Böhme et al. (2013) the measured displacements do not always follow a coherent trend over time, but can be relatively chaotic. Coherent trends are a good indication of "certain gravitational movement", while chaotic trends do not allow to ascertain gravitational movement. Reasons for chaotic trends are for example meteorological conditions, thermal expansion of the rock mass and opening and closing of cracks due to the change of pore water pressure (Hermanns et al. 2011). Finally, each GNSS-point has been checked if the displacement trend is coherent over time or not.

Only GNSS-points with statistically significant displacements and coherent trends are considered as significant in this report. The displacement trend (horizontal direction) and plunge (vertical angle) were computed for every GNSS-point with significant horizontal and/or vertical displacement(s) based on the regression results.

Detailed results of dGNSS measurements in Møre og Romsdal are presented in Appendix 1.

2.4.2 Terrestrial laser scanning

Terrestrial laser scanning (TLS) is based on the reflectorless and contactless acquisition of a point cloud of the topography using the time-of-flight distance measurement of an infrared laser pulse. The Optech ILRIS-3D ER used for this study has a wavelength of 1500 nm and a range in practice of about 800 to 1200 m on rock slopes, depending on the reflectivity of the object. See Oppikofer et al. (2009) for a detailed description of the instrument. Since 2012, NGU possess also the Optech ILRIS-3D LR with a range in practice of up to 3500 m and the capability to scan even in wet conditions.

The high-resolution point clouds of the topography provided by TLS can be used for the structural analysis of rock slopes and for displacement measurements using multi-temporal TLS data. The detailed methodology is described by Oppikofer et al. (2009, 2012a) and includes several steps:

- Co-registration (alignment) of individual scans of the same epoch
- Co-registration of multi-temporal TLS scans using only the (supposed) stable area , i.e. the surroundings of the rock slope instability
- Georeferencing of the entire dataset using ground-control points or a DEM
- Structural analysis using Coltop3D software (Terranum 2013)

- Shortest distance comparison between sequential scans for the visualisation and a preliminary quantification of displacements

Detailed results on TLS data acquired in Møre og Romsdal between 2006 and 2009 are presented in Appendix 2.

2.4.3 Tape extensometer

The tape extensometer is a compact, portable and easy-to-use instrument for measuring the distance between pairs of eyebolts that are permanently fixed into the rock surface. Repetitive measurements over time allow measuring the displacements between the pairs of eyebolts. Typical use of the tape extensometer is to measure the opening of the back-crack or internal cracks of an unstable rock slope, by having one eyebolt on each side of the crack.

NGU uses a Digital Tape Extensometer from Soil Instruments (serial no. TXO-807) that comprises a 20 m long stainless steel measuring tape with equally spaced precision punched holes. The tape winds onto a reel, which incorporates a tape tensioning device (with an optical tension indicator) and a digital LCD readout (itmsoil 2012). The tape extensometer has an accuracy of readings of 0.01 mm and a repeatability of 0.1 mm. Own repeatability tests in 2012 by several NGU geologists shows a standard deviation between 0.04 and 0.19 mm.

2.5 Terrestrial cosmogenic nuclide dating

Surface exposure dating using terrestrial cosmogenic nuclides has been established as a reliable method to date rock avalanche deposits (Hermanns et al. 2001, 2004) and for slope deformation (Bigot-Cormier et al. 2005, Hermanns et al. 2012). Although dating with this method is expensive and the entire process takes a long time, it has the advantage that the dateable material is produced by the rockslide event itself by exposing fresh material surfaces to the cosmic radiation. In general every deposit older than about 1000 years can be dated (modified from Hermanns et al. 2011).

The sampling procedure is described by Hermanns et al. (2012) and focussed on taking at least two samples for each rock avalanche deposit to have a control on pre-exposure, uncontrolled shielding or block rotation of deposits. Sliding surfaces were sampled along direction of movement and at least two samples were dated from each sliding surface to have a control on post-sliding erosion (modified from Hermanns et al. 2011).

All ages reported here were calibrated according to the geographical latitude, altitude, angle of the sampled exposed surface, shielding, and snow cover as outlined in Gosse and Philips (2001). Ages were obtained with the CRONUS calculator (Balco et al. 2008), which takes into account the various discussed production rates for cosmogenic nuclides and are given as mean values of all possible ages . No calibration for uplift related to isostatic rebound was made, since it varies significantly over the region, it is relatively poorly mapped and its effect on the final age is small in comparison to other errors (Fenton et al. 2011) (modified from Hermanns et al. 2011).

The reported ages are average ages based on individual sample ages. The standard deviation on the mean age, σ_{mean}, is calculated based on the standard deviation, σ_i, of n individual sample ages:

$$\sigma_{mean} = \frac{\sqrt{\sum \sigma_i{}^2}}{n}$$

3. OVERVIEW OVER UNSTABLE ROCK SLOPES IN MØRE OG ROMSDAL

In this report, the unstable rock slopes are classified in chapters according to their location (economic region and municipality) (Figure 3). The Møre og Romsdal County is divided into five economic regions comprising each between 5 and 11 municipalities as defined by the Confederation of Norwegian Enterprise (www.nho.no):

- Nordmøre: Aure, Averøy, Eide, Gjemnes, Halsa, Kristiansund, Rindal, Smøla, Sunndal, Surnadal and Tingvoll (chapter 4);
- Romsdal: Aukra, Fræna, Midsund, Molde, Nesset, Rauma and Vestnes (chapter 5);
- Storfjord: Norddal, Stordal, Stranda, Sykkylven and Ørskog (chapter 6);
- Søre Sunnmøre: Hareid, Herøy, Sande, Ulstein, Vanylven, Volda and Ørsta (chapter 7);
- Ålesund: Giske, Haram, Sandøy, Skodje, Sula and Ålesund (chapter 8).

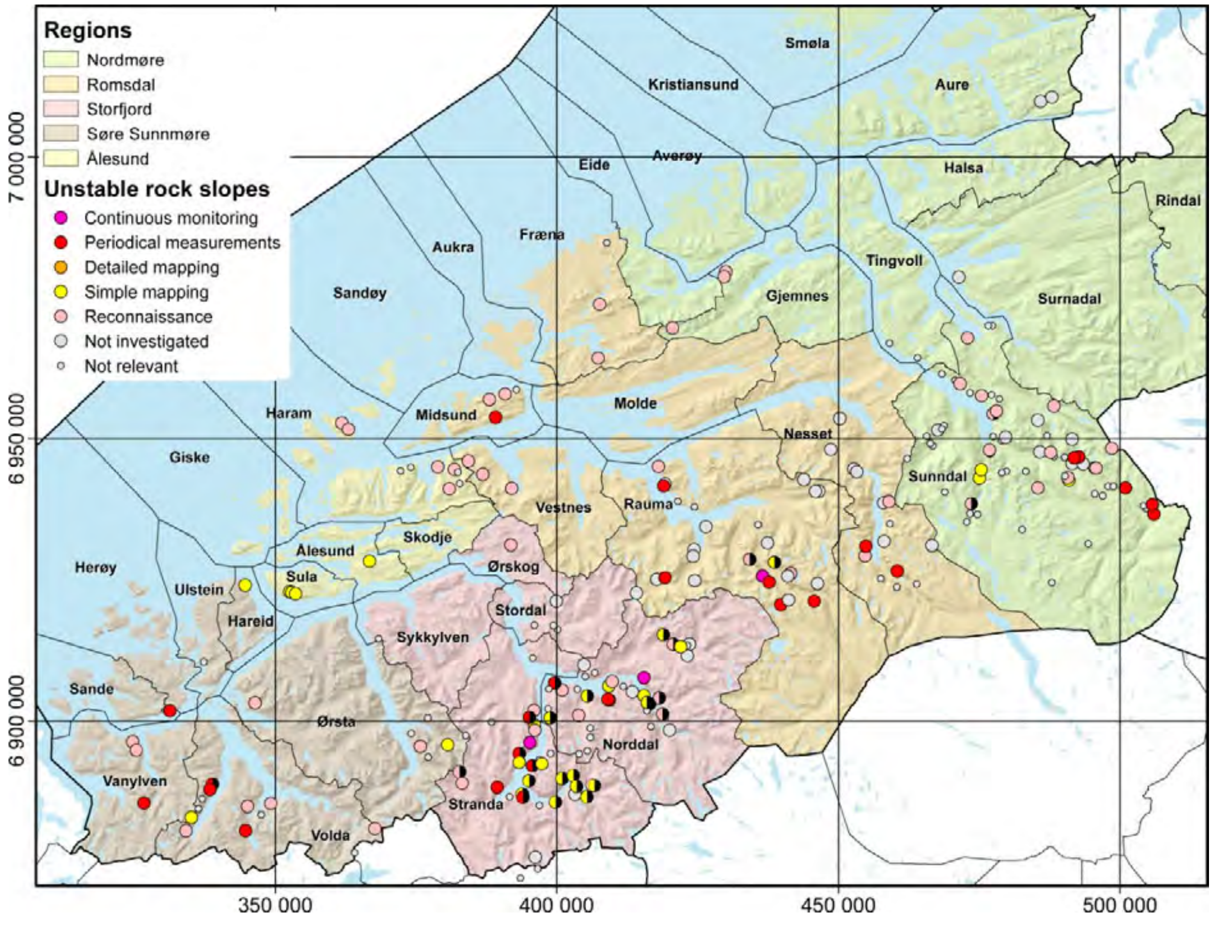

Figure 3: **Overview map of the unstable or potential unstable rock slopes in Møre og Romsdal. The investigation status of each unstable rock slope is shown. Potential unstable rock slopes are also shown with a half-masked symbol (◑). The county is divided into five economic regions (Nordmøre, Romsdal, Storfjord, Søre Sunnmøre and Ålesund).**

3.1 Investigated areas

Nearly the entire Møre og Romsdal County has been investigated by aerial photograph analysis, except the southeastern parts of Rauma, Norddal and Stranda municipalities (Figure 4), where snow cover on the mountain tops avoids to get high quality aerial photographs. Many fjords and valleys with unstable rock slopes have been visited by helicopter reconnaissance flights or from the road in the past years (Figure 4).

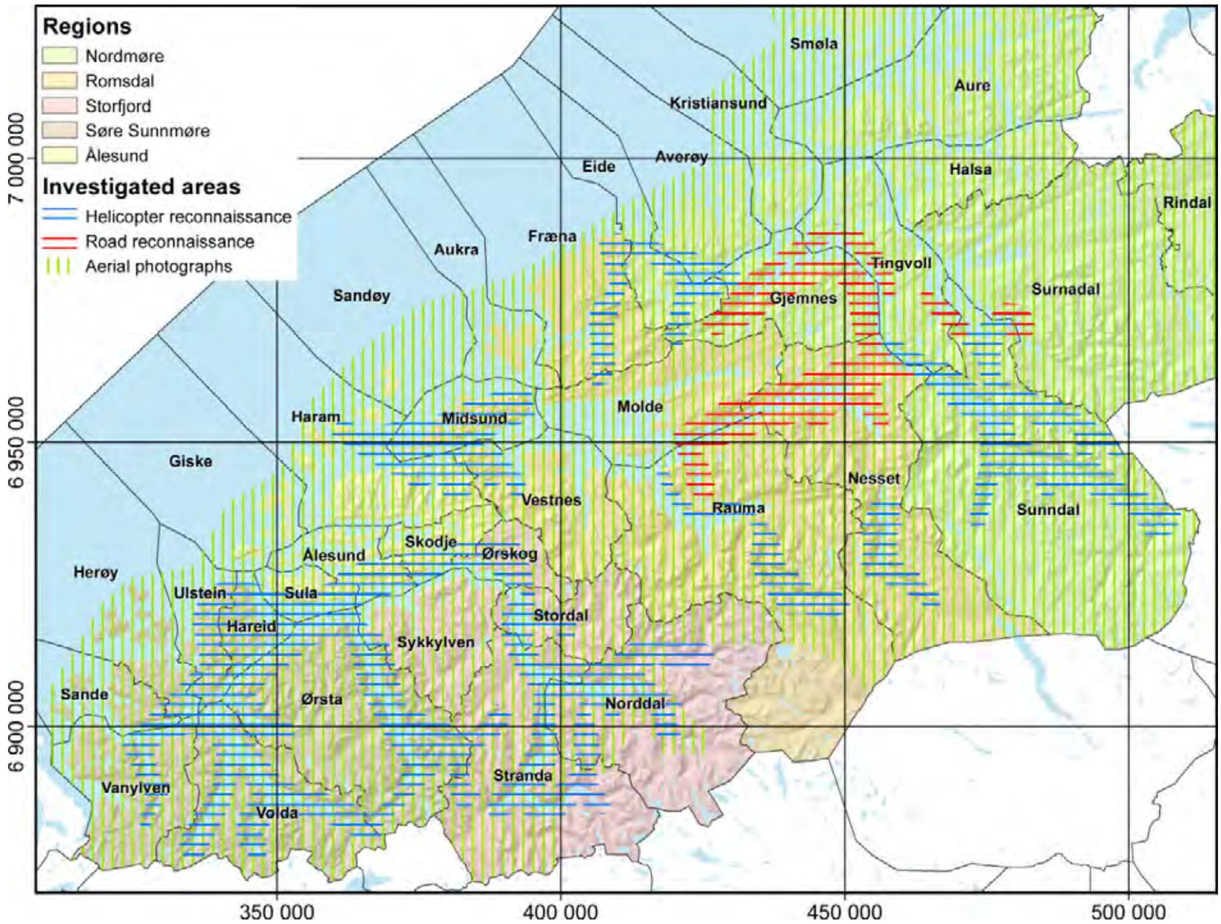

Figure 4: **Map of the investigated areas in Møre og Romsdal by aerial photograph analysis, reconnaissance from the road or reconnaissance from helicopter.**

3.2 Registered unstable rock slopes in Møre og Romsdal

The database on unstable rock slopes contains 245 sites in Møre og Romsdal (Figure 3). Appendix 3 shows an overview of unstable rock slopes in Møre og Romsdal extracted from this database with the current investigation status, recommendations for further work and references to previous reports. A list of different names for the sites is given where applicable. **Amongst those 245 registered sites, 77 are classified as unstable rock slopes, 29 as potential unstable rock slopes and 91 as not relevant sites** (see chapter 2.1.1 for definitions). Furthermore, 48 sites are not yet inspected and have therefore an unknown status.

Recommendations for further investigations given in this report are preliminary. Final recommendations will be made in the next years based on the systematic hazard and risk classification system for unstable rock slopes in Norway (Hermanns et al. 2012).

Rockfalls and small rockslides may occur from "not relevant" sites, but the volume of these rock slope failures is too small to create a rock avalanche or a displacement wave. Other mapping products from NGU and NVE, such as the rockfall susceptibility map and more detailed rockfall hazard maps, provide the area affected by the run-out of these small rock slope failures.

3.3 Unstable rock slopes described in this report

NGU has investigated and worked on 131 unstable rock slopes in Møre og Romsdal, since the last county status reports (Henderson et al. 2006, Henderson and Saintot 2007, Saintot et al. 2008). These sites are reported herein (Figure 5, Table 1).

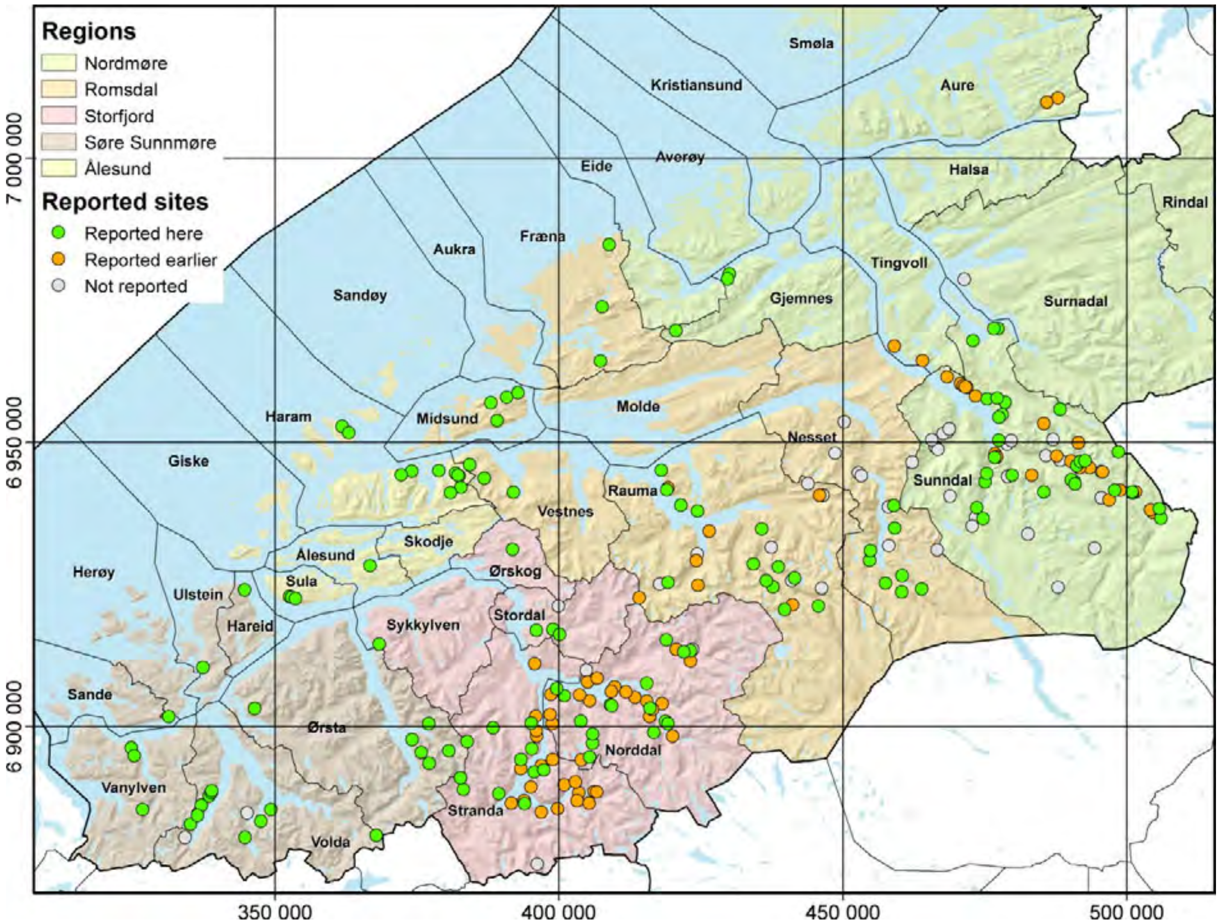

Figure 5: Overview map of the unstable rock slopes in Møre og Romsdal with the reporting status.

Table 1: List of investigated sites described in this report.

Site name	Investigation status	Investigations reported here (year)					
		Recon-naissance	Field mapping	dGNSS[1]	TLS[1]	Extenso-meter[1]	Dating[2]
Nordmøre region							
Gjemnes municipality							
Geitaskaret	Reconnaissance	2012					
Trolldalsfjellet	Reconnaissance	2012					
Ørnstolen	Reconnaissance	2012					
Sunndal municipality							
Bårsveinhamran	Reconnaissance	2011					
Fulånebba	Reconnaissance	2011					
Gammelseterhaugen	Reconnaissance	2011					
Gammelurkollen	Reconnaissance	2011					
Gikling 1	Periodic measurements			2011			
Gikling 2	Periodic measurements			2011			
Gjersvollsetra	Reconnaissance	2011					
Grøvelnebba	Reconnaissance	2011					
Gråhøa 1	Simple mapping	2011	2010				
Gråhøa 2	Reconnaissance	2011					
Gråhøa 3	Reconnaissance	2011					
Hovennebba	Reconnaissance	2011					
Hovsnebba 1	Reconnaissance	2011					
Høghamran	Reconnaissance	2011					
Ivasnasen	Periodic measurements				2012	2011	2012
Kammen	Reconnaissance	2011					
Klingfjellet 2	Reconnaissance	2011					
Litlkalkinn 3	Reconnaissance	2011					
Merrakammen	Reconnaissance	2011					
Mohaugen 1	Reconnaissance	2011					
Mohaugen 2	Reconnaissance	2011					
Ottdalskammen	Reconnaissance	2011					
Ottem 2	Periodic measurements	2007			2010		
Ottem 3	Periodic measurements			2009	2011		
Serkjenebba	Reconnaissance	2011					
Steinbruhøa	Reconnaissance	2011					
Storbotnen	Simple mapping	2011					
Storurhamran	Simple mapping				2010		
Vollan	Periodic measurements			2011			
Romsdal region							
Fræna municipality							
Røssholfjellet	Reconnaissance	2012					
Stemshesten	Reconnaissance	2012					
Talstadhesten	Reconnaissance	2012					
Midsund municipality							
Bendsethornet	Reconnaissance	2012					
Oppstadhornet	Periodic measurements			2011			2003
Ræstadhornet	Reconnaissance	2012					
Sundsbørøra	Reconnaissance	2012					
Nesset municipality							
Børa i Eikesdalen	Simple mapping	2010	2010				
Ellingbenken	Reconnaissance	2010					
Evelsfonnhøa	Periodic measurements	2010			2012		
Kjøtåfjellet	Periodic measurements	2010			2012	2011	2010
Litleaksla	Reconnaissance	2010					
Martinskora	Reconnaissance	2011					
Vikesoksa	Reconnaissance	2010					
Vikesætra	Reconnaissance	2010					
Rauma municipality							
Børa	Periodic measurements			2012	2012		

Table 1: List of investigated sites described in this report.

Site name	Investigation status	Investigations reported here (year)					
		Recon-naissance	Field mapping	dGNSS[1]	TLS[1]	Extenso-meter[1]	Dating[2]
Flatmark	Periodic measurements			2011	2012	2011	2003
Frisvollfjellet	Reconnaissance	2011					
Kvarvesnippen	Reconnaissance	2011					
Kvitfjellgjølet	Periodic measurements	2011			2012		
Mannen	Continuous monitoring			2010			2009
Marsteinskora 1	Reconnaissance	2010					
Middagstinden	Periodic measurements		2010	2011	2010		
Mjølvafjellet	Reconnaissance	2011					
Olaskarstinden	Reconnaissance	2010					
Svarttinden	Periodic measurements			2010			2003
Trolltindan	Reconnaissance	2006					
Veten	Reconnaissance	2011					2003
Vestnes municipality							
Seteraksla	Reconnaissance	2012					
Snaufjellet	Reconnaissance	2012					
Strandastolen	Reconnaissance	2012					
Storfjord region							
Norddal municipality							
Alstadfjellet	Simple mapping		2007				2003
Alvikhornet 3	Simple mapping	2006	2006				
Hegrehamrane	Reconnaissance	2007					
Hegguraksla	Continuous monitoring			2007	2008		
Jimdalen	Reconnaissance	2007					
Kallen	Reconnaissance	2007					2003
Kilstiheia	Reconnaissance	2011					
Kleivahammaren	Reconnaissance	2007					
Kloven	Reconnaissance	2007					
Krikeberget	Simple mapping		2007				
Kvitfjellet 1	Periodic measurements			2011	2012		
Kvitfjellet 2	Periodic measurements			2011	2012		
Remsfjellet	Simple mapping	2007	2007				
Skorene 1	Reconnaissance	2007					
Skorene 2	Reconnaissance	2007					
Skrednakken 1	Periodic measurements			2012			
Stordal municipality							
Storhornet 1	Reconnaissance	2007					
Storhornet 2	Reconnaissance	2007					
Tuva	Reconnaissance	2007					
Stranda municipality							
Aksla	Simple mapping		2006				
Fivelstadnibba	Reconnaissance	2011					
Fremste Blåhornet	Periodic measurements			2009			2009
Furneset	Periodic measurements			2007			
Herdalsnibba	Periodic measurements			2012			
Kvitegga	Reconnaissance	2011					
Nokkenibba 2	Periodic measurements			2010			2009
Rindalseggene	Periodic measurements			2012	2011		
Ytstevatnet	Reconnaissance	2011					
Åknes	Continuous monitoring			2007	2008		
Sykkylven municipality							
Hundatindan	Reconnaissance	2011					
Ørskog municipality							
Giskemonibba	Reconnaissance	2011					
Søre Sunnmøre region							
Hareid municipality							
Grøthornet	Simple mapping	2011	2012				

Table 1: List of investigated sites described in this report.

Site name	Investigation status	Investigations reported here (year)					
		Recon-naissance	Field mapping	dGNSS[1]	TLS[1]	Extenso-meter[1]	Dating[2]
Sande municipality							
Laupsnipa	Periodic measurements	2011	2012		2012	2012	
Ulstein municipality							
Haddalura	Periodic measurements	2011		2009			
Vanylven municipality							
Sandfjellet	Reconnaissance	2011					
Sandnestua	Reconnaissance	2011					
Storehornet	Periodic measurements	2011	2012	2012	2012	2012	2012
Volda municipality							
Bjørnasethornet	Reconnaissance	2011					
Heida	Reconnaissance	2011					
Hestefjellet	Periodic measurements	2011	2012		2012		
Keipedalen	Simple mapping	2011	2012				
Kvanndalsskåla	Simple mapping	2011	2012				
Kvivsdalshornet	Reconnaissance	2011					
Midnakken	Reconnaissance	2011					
Skylefjellet	Periodic measurements	2011			2012		
Solahylla	Periodic measurements	2011			2012		
Trongedalen	Reconnaissance	2011					
Ørsta municipality							
Blåhornet	Reconnaissance	2011					
Jakta	Reconnaissance	2011					
Keipen	Simple mapping	2011			2012		
Litlehornet	Reconnaissance	2011					
Maudekollen	Reconnaissance	2011					
Skorgeurda	Reconnaissance	2011					2012
Stålberghornet	Reconnaissance	2011					
Ålesund region							
Haram municipality							
Branddalsryggen	Reconnaissance	2012					
Byrkjevollhornet	Reconnaissance	2012					
Hellenakken	Reconnaissance	2012					
Otrefjellet	Reconnaissance	2012					
Skjerveheian	Reconnaissance	2012					
Skulen	Reconnaissance	2012					
Skoraegga	Reconnaissance	2012					
Tindfjellet	Reconnaissance	2012					
Vassbotnen 1	Reconnaissance	2012					
Vassbotnen 2	Reconnaissance	2012					
Sula municipality							
Tverrfjellet 1	Simple mapping	2011	2012				
Tverrfjellet 2	Simple mapping	2011	2012				
Tverrfjellet 3	Simple mapping	2011	2012				
Ålesund municipality							
Rambjøra	Simple mapping	2011	2012				

[1] For sites with periodic displacement measurements using dGNSS, TLS or tape extensometer only the last year of measurement is indicated.
[2] For terrestrial cosmogenic nuclide dating the sampling year is given. Dating results are generally available 1–3 years after sampling.

4. NORDMØRE REGION

4.1 Gjemnes municipality

There are three known sites located in Gjemnes municipality, which are all described in this report (Figure 6).

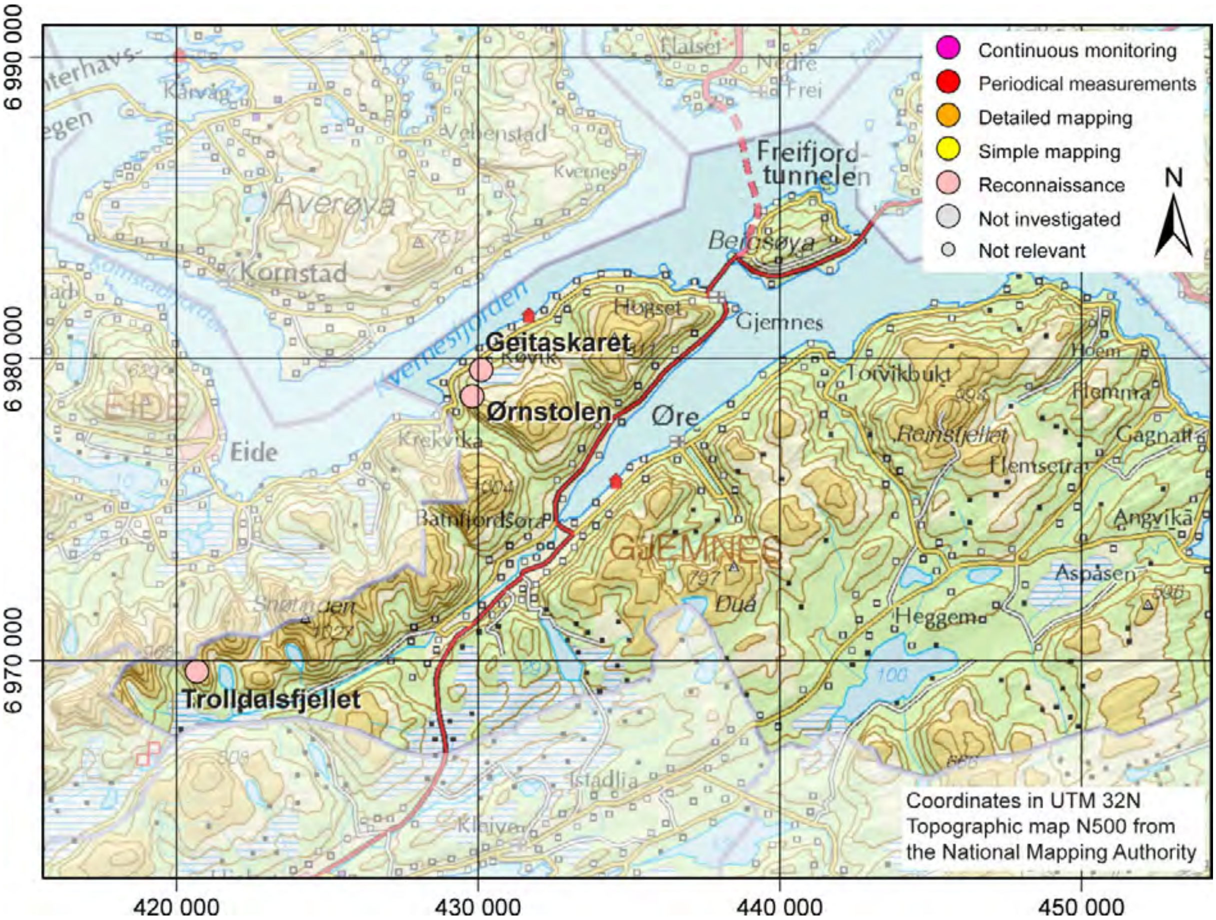

Figure 6: Map of the three known sites in the Gjemnes municipality with their investigation status. The name of the sites described in this report is shown.

4.1.1 Geitaskaret

Geitaskaret (Figure 6) is situated on a north-facing slope 220 m above Skjerset. The site was surveyed during a helicopter reconnaissance flight in 2012. A 90 m wide and 30 m long instability is clearly detached from the back-scarp (Figure 7). Several cracks with a few meters opening divide the instability into distinct, small blocks with volumes smaller than 20 000 m³. A small waterfall runs into the back-crack and through the detached rock body. The water runs partly through the blocky deposits from previous failures. Previous failures from Geitaskaret have been of limited volumes (few thousand m³) and did likely not reach inhabited areas. Potential future failures are also expected not to reach inhabited areas (Dahle et al. 2011a).

Recommendation: A possible rock avalanche from the Geitaskaret instability will have no consequences. No further investigations or displacement measurements are necessary. The hazard and risk classification will be made after a simple run-out assessment. Further follow-up activities will be based on this classification.

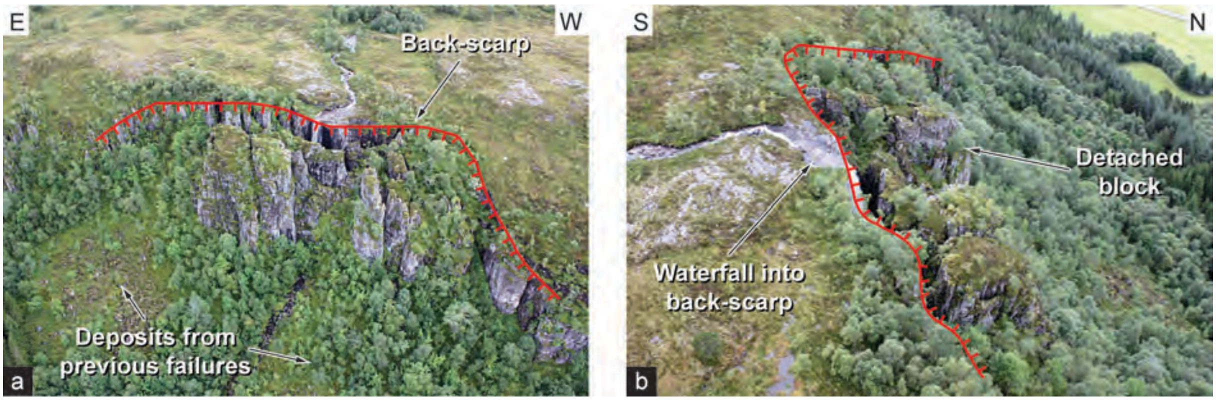

Figure 7: **Photographs of the Geitaskaret instability. The instability is divided by cracks into several blocks with of small volumes (<20 000 m³).**

4.1.2 Trolldalsfjellet

Trolldalsfjellet (Figure 6) is located on a west-facing slope 400 m above Litlvassdalen Valley. During a helicopter reconnaissance flight in 2012 the main back-scarp controlling the highest extent of the disturbed mass was observed together with several parallel cracks downslope that can be followed over a few tens of meters (Figure 8a). At 650 m a.s.l. the slope is continuously covered with blocks over a length of 600 m (Figure 8a). Depressions are present above and inside the blocky area. Especially in the northern part of the disintegrated area structures in the rock mass show a dense fracturing that enables toppling of small blocks downslope to the west or to the south (Figure 8b). This style of deformation let suppose that this unstable rock slope is formed locally by the in-situ disintegration of the rock mass into small blocks. Given this deformation style, a massive rock slope failure from Trolldalsfjellet seems unlikely, but cannot be ruled out. A rock slope failure from Trolldalsfjellet would only affect the uninhabited Litlvassdalen Valley (Dahle et al. 2011a).

Recommendation: A possible rock avalanche from the Trolldalsfjellet instability will have no consequences. No further investigations or displacement measurements are necessary. The hazard and risk classification will be made after a simple run-out assessment. Further follow-up activities will be based on this classification.

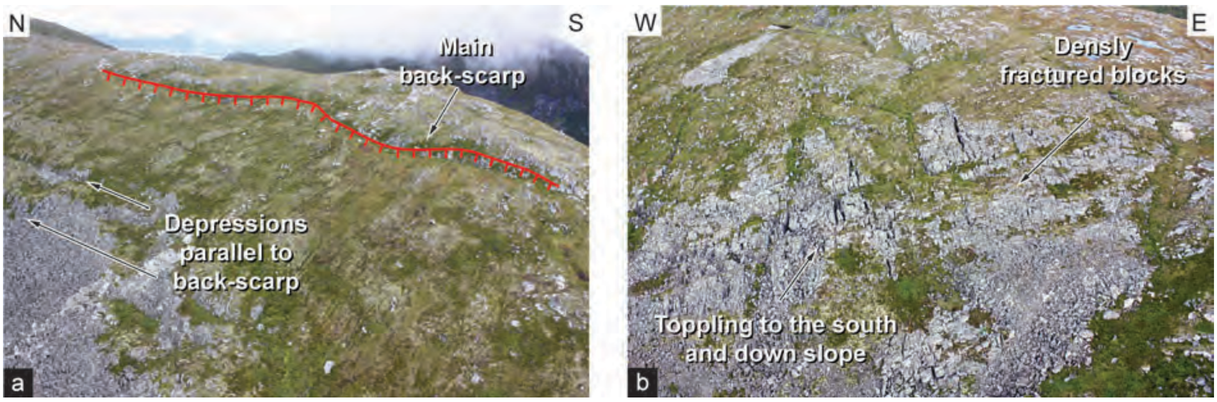

Figure 8: **Photographs of the Trolldalsfjellet unstable rock slope with large block fields originating likely from in-situ disintegration of the rock mass due to a dense fracture network which enables toppling of small blocks.**

4.1.3 Ørnstolen

Ørnstolen (Figure 6) is situated on a west-facing slope 430 m above Sevika. A helicopter reconnaissance flight made in 2012 revealed a steeply NW-dipping foliation in the upper part that flattens out in the lower part (Figure 9a). The exposed foliation surfaces are likely the scar of a former rockslide, but no large rock avalanche deposits can be seen at the foot of the slope (Figure 9b). The same foliation surfaces could also be the basal sliding surface of the remaining unstable rock slope at Ørnstolen. However, there are no signs of deformation, except a small escarpment, where the foliation surface crosses the present topography on the top of the instability (inset in Figure 9b). Furthermore, there are rockfall deposits accumulating at the foot of the cliff of the Ørnstolen instability. A catastrophic failure of the Ørnstolen instability would likely reach some of the buildings in Sevika.

Recommendation: A possible rock avalanche from the Ørnstolen instability will have consequences. Geological field mapping is necessary to evaluate the structural and geological conditions, to quantify past displacements and assess the structures involved in the previous rockslide. The hazard and risk classification will be made after this field mapping. Further follow-up activities will be decided based on this classification.

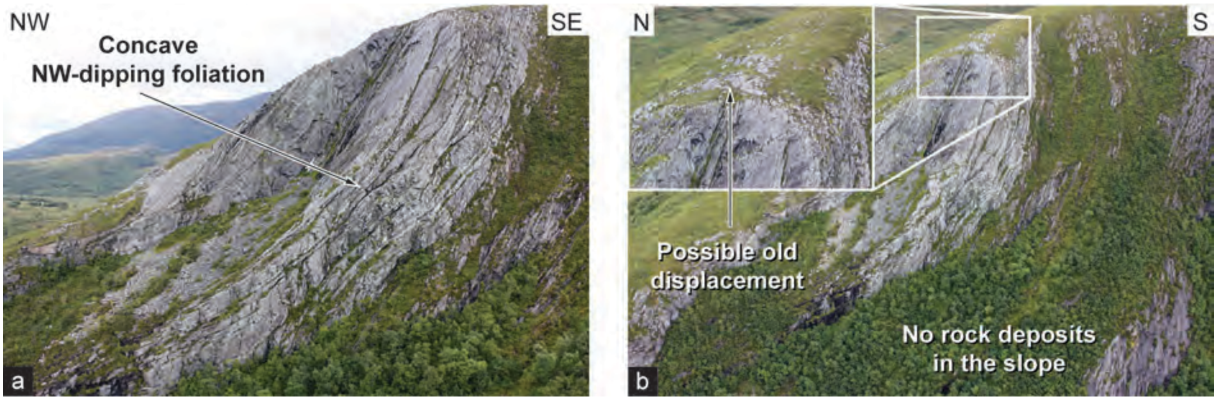

Figure 9: **Photographs of the Ørnstolen instability with the foliation as basal sliding surface of a former rockslide and of the present instability. A small escarpment is observed on top of the instability in the continuation of the foliation surface (inset in b).**

4.2 Sunndal municipality

There are 74 known sites located in Sunndal municipality. Twenty-nine of them are described in this report (Figure 10). The high number of known sites in comparison with other municipalities in Møre og Romsdal County is due to a very detailed analysis of high-resolution orthophotos made by a summer job student at NGU in 2011. Seventeen of the known sites are however only lineaments that were interpreted as open cracks, and do not show any signs of past deformations of an unstable rock slope. These 17 sites were therefore directly classified as not relevant without any reconnaissance or field investigations and not described in the present report (red-crossed, not relevant sites in Figure 10).

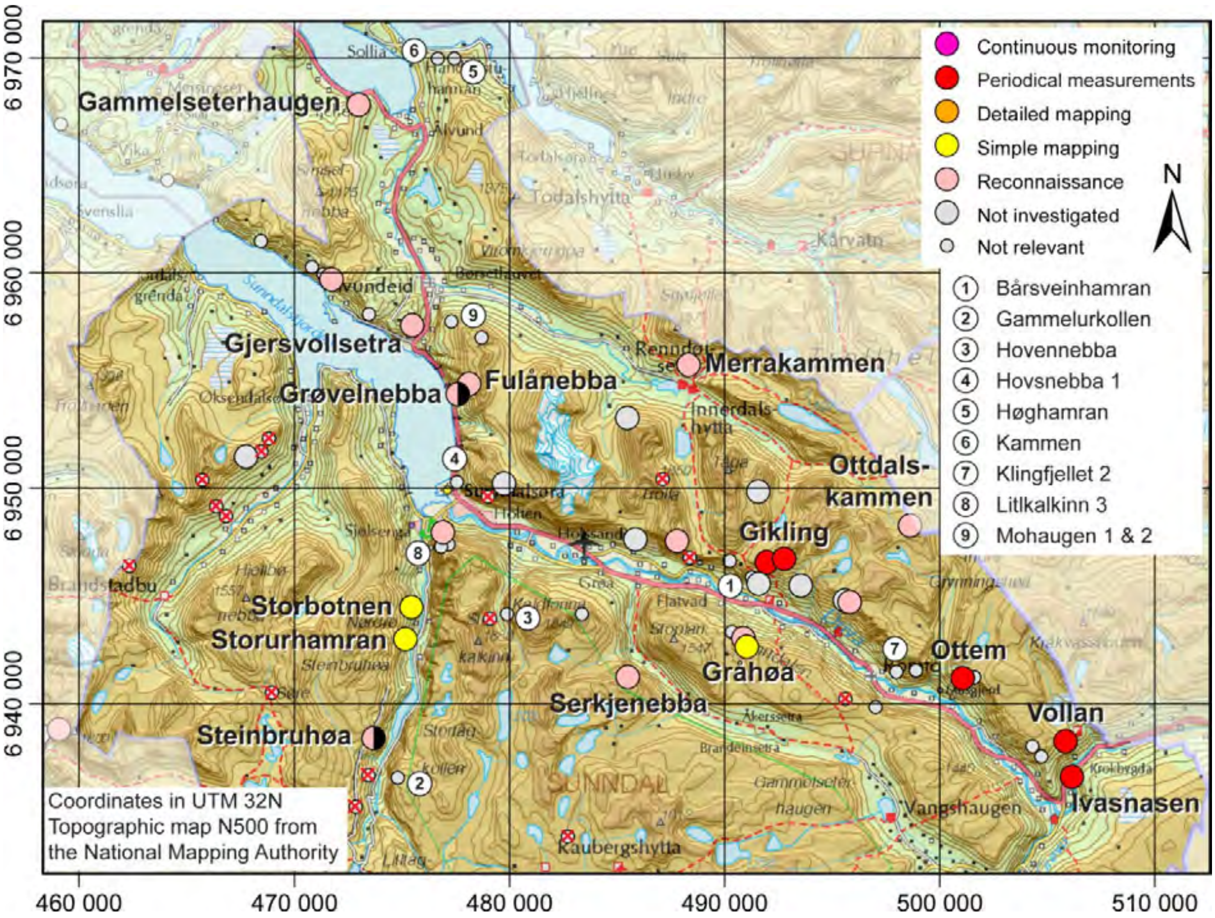

Figure 10: **Map of the known sites in the Sunndal municipality with their investigation status. Potential unstable rock slopes are also shown with a half-masked symbol (◑). The name of the sites described in this report is shown (numbers are used for not relevant sites for clarity of the map). Red-crossed sites are classified as not relevant based on orthophoto analysis.**

4.2.1 Bårsveinhamran

Bårsveinhamran is located on a southwest-facing slope at 590 m above the farm Gikling in Sunndalen Valley (Figure 10). A helicopter reconnaissance flight was made in 2011. An old fault forms a deep depression back of the rock spur, but there are no signs of deformation along this fault in the recent past (Figure 11). The fault would serve as back-bounding structure for this potential unstable rock slope, but no basal sliding surface and no the lateral release surface are developed although pre-existing planar structures favourable for sliding exist at Bårsveinhamran (Figure 11).

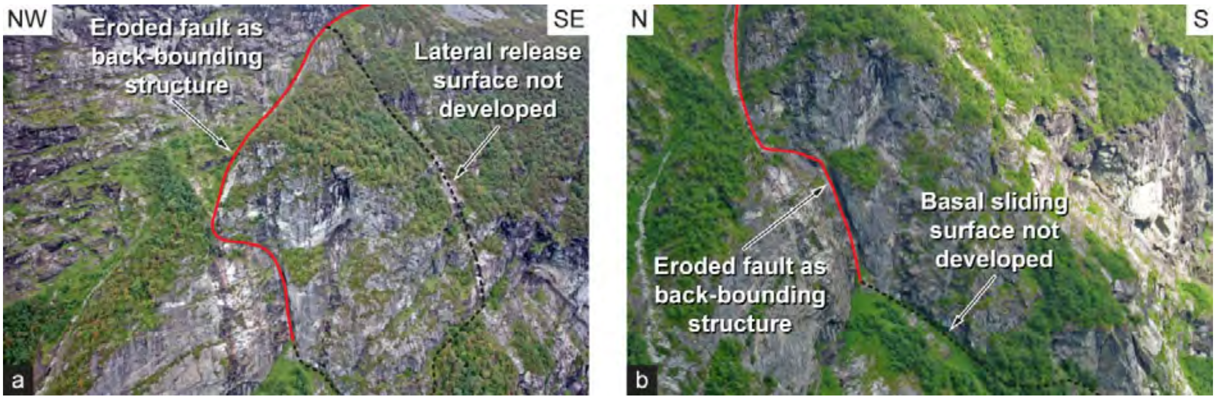

Figure 11: **Photographs of the potential unstable rock slope at Bårsveinhamran. No signs of past deformation can be seen.**

Recommendation: Bårsveinhamran is classified as a potential unstable rock slope. At present the remaining rock slope does not show any signs of past or present displacements or deformation of a large volume. No further investigations or displacement measurements are necessary and the hazard and risk classification will not be made. However, this site may lead to rockfalls and develop over time into an unstable rock slope, due to structural and geological conditions. The site should be revisited after years to decades to detect any changes and be followed-up on InSAR data.

4.2.2 Fulånebba

Fulånebba is located on a southwest-facing slope at 1220 m above Oppdølstranda in Sunndalsfjord (Figure 10). The site was investigated by helicopter reconnaissance in 2011. Fulånebba shows significant signs of past displacements with several meters of downward movement of a vegetated plateau relatively to the surrounding crest (Figure 12). To the east a obvious lateral release surface is visible. Other lateral and basal structures are not observable, partly due to an extensive cover with rockfall deposits. A massive failure of this unstable rock slope would likely reach Sunndalsfjord and subsequently create a displacement wave.

Recommendation: A possible rock avalanche from the Fulånebba instability will have consequences. Geological field mapping is necessary to evaluate the structural and geological conditions and to quantify past displacements. The hazard and risk classification will be made after this field mapping. Further follow-up activities will be decided based on this classification.

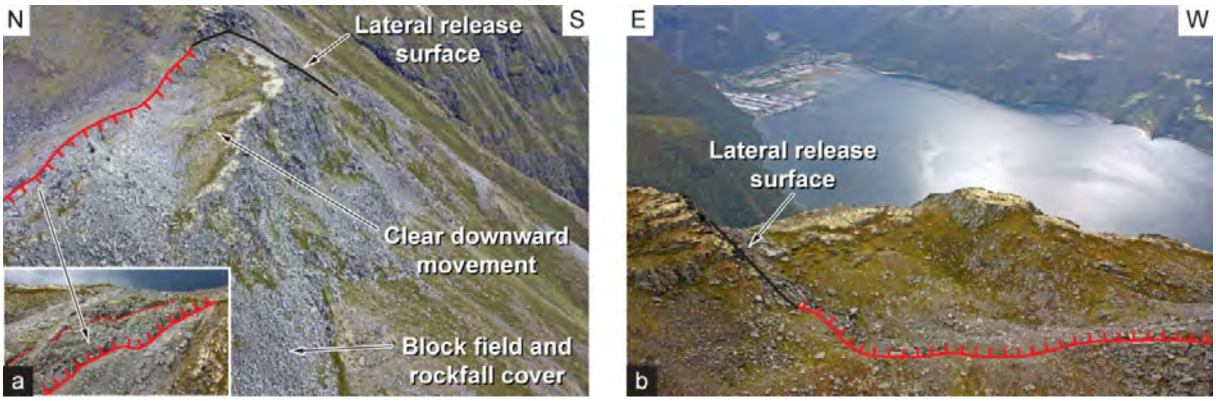

Figure 12: **Photographs of the Fulånebba unstable rock slope: a) lateral view showing the clear downward movement of the vegetated plateau and cracks parallel to the back-scarp along the crest (inset); b) downward view with the east-bounding lateral release surface. Sunndalsøra is in the back-ground.**

4.2.3 Gammelseterhaugen

Gammelseterhaugen is located on a north-facing slope at 490 m above Ålvundfjord, close to Ålvund (Figure 10). A helicopter reconnaissance flight was made in 2011. There are several valley-dipping failure surfaces of previous shallow rockslides (Figure 13a). One of them may form the basal sliding surface of a small unstable rock slope (Figure 13b). Surface depressions in the back of the instability are possible morphologic expressions of a developing back-scarp. In turn, the western lateral release surface is clearly well developed. The volume of the Gammelseterhaugen instability is approximately of 25 000 m³ and thus too small to generate a significant displacement wave in Ålvundfjord and a total failure of the instability will therefore probably only affect the road Rv70.

Recommendation: A possible rock avalanche from the Gammelseterhaugen instability will have no consequences. No further investigations or displacement measurements are necessary. The hazard and risk classification will be made after a simple run-out assessment. Further follow-up activities will be based on this classification.

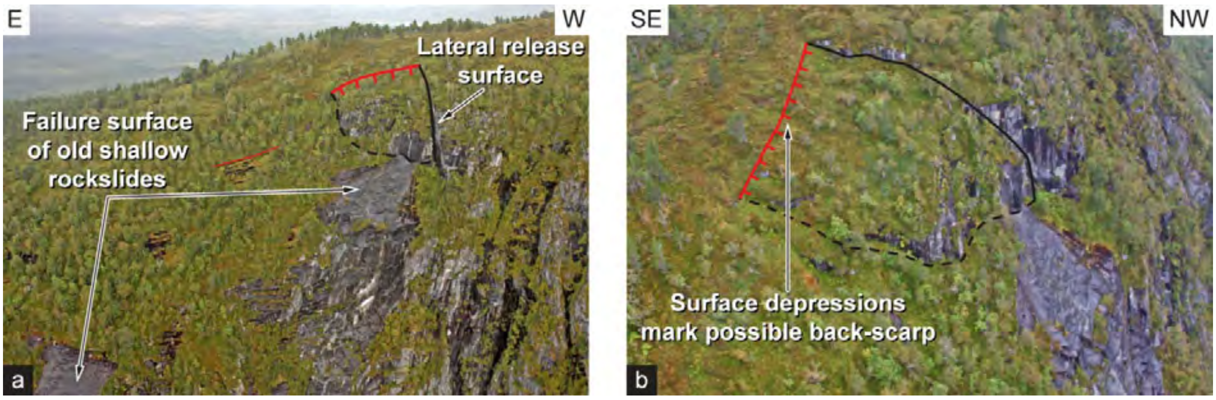

Figure 13: Photographs of the Gammelseterhaugen unstable rock slope showing the scars of past small rockslides and the present unstable rock slope. Small cracks are also observed in other parts of the slope.

4.2.4 Gammelurkollen

Gammelurkollen (Figure 10) is located on a west-facing slope approximately 870 m above Sandvatnet in Litldalen Valley. A helicopter reconnaissance flight was made in 2011. The site is situated in a linear depression and is delimited northward by an old fault that is partly eroded (Figure 14). It is likely that this entire depression is a wide ductile shear zone that is a typical tectonic structure in Western Norway. Other necessary structures to delimit an unstable rock slope, i.e. back-scarp, basal sliding surface or lateral release surface to the south, are missing or not visible. There is a large talus slope at the foot of the Gammelurkollen slope, which is formed by rockfalls originating from the rock wall, but also partly by transport along the gully from further uphill.

Recommendation: There are no signs that the Gammelurkollen rock slope might fail in a massive rock slope failure. No further investigations or displacement measurements are necessary and the hazard and risk classification will not be made. However, rockfalls are possible and their run-out area is given by the rockfall susceptibility map or more detailed hazard maps, where available.

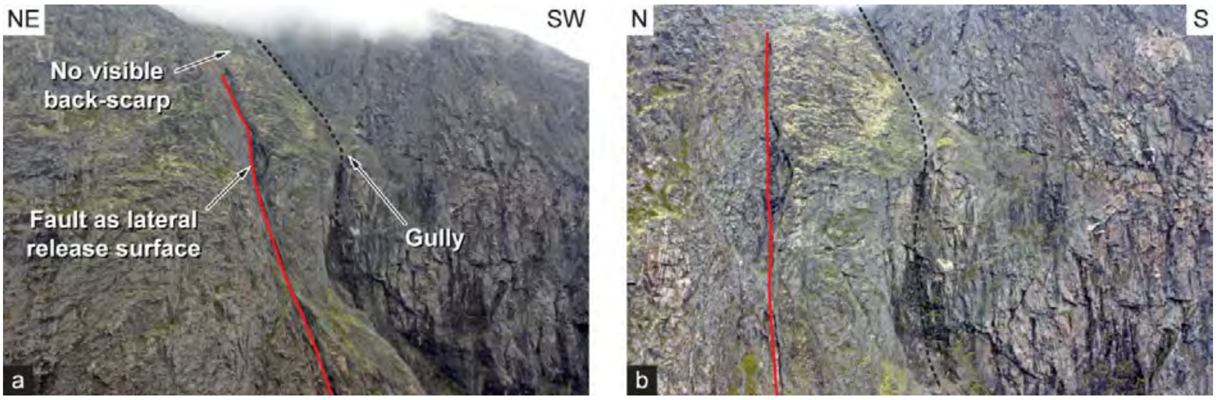

Figure 14: **Photographs of the Gammelurkollen slope with the fault as north-bounding lateral release surface. Other necessary structures to delimit an unstable rock slope are however missing.**

4.2.5 Gikling 1 & 2

The unstable rock slope Gikling is located on a south-facing slope at 1240 m above the farm Gikling in Sunndalen Valley (Figure 10). Following a helicopter reconnaissance in 2007, the site has been extensively studied and geophysical and geological investigations led to the production of a detailed map and to a reliable estimation of the unstable volumes (Henderson and Saintot 2007, Saintot et al. 2008, Dalsegg et al. 2010). Since 2007 the site is also periodically measured using dGNSS. The area is divided into two distinct unstable rock slopes: to the east, a large complex unstable rock slope named Gikling 1 with estimated volumes of 30 million m³ for the frontal subblock and 100 million m³ for the total deformed rock slope, and to the west a small well delimited rockslide named Gikling 2 with an estimated volume of 0.7 million m³ (Figure 15).

Herein, we present the results from dGNSS measurements in the years 2007, 2008, 2009 and 2011 (4 years interval). The fixed point is located above the back-scarp of Gikling 1, two measurement points (GI-2 and GI-3) are on Gikling 1 and one measurement point (GI-4) is on Gikling 2 (Figure 15). In the measurement period between 2007 and 2011, both points on Gikling 1 show significant horizontal and vertical displacements, however with an incoherent vertical trend for GI-3. The yearly three-dimensional displacement rates are 4.0 mm/year towards the South for GI-2 and 2.6 mm/year towards the SSW for GI-3. The measurement point GI-4 on Gikling 2 does not show significant horizontal or vertical displacements.

The measured displacement rates for Gikling 1 are relatively low compared to other large unstable rock slopes in Norway. The unstable rock slope Gikling 1 is likely in a creep state sliding downwards to the valley. Fresh debris slides in the scree deposits at the front of Gikling 1 are possibly caused by the advancing rock mass and thus a further sign of activity. A massive failure from Gikling 1 would form a rock avalanche that would cross Sunndalen Valley, destroy several buildings and likely dam the Driva River with the probability of a subsequent dam breach and outburst flood (Dahle et al. 2011a).

Recommendation: Significant displacements are measured at Gikling 1, while no significant displacements are measured up to now at Gikling 2. Periodic displacement measurements using dGNSS should be continued with 1–3 years interval. The hazard and risk classification needs to be made and further follow-up activities will be decided based on this classification.

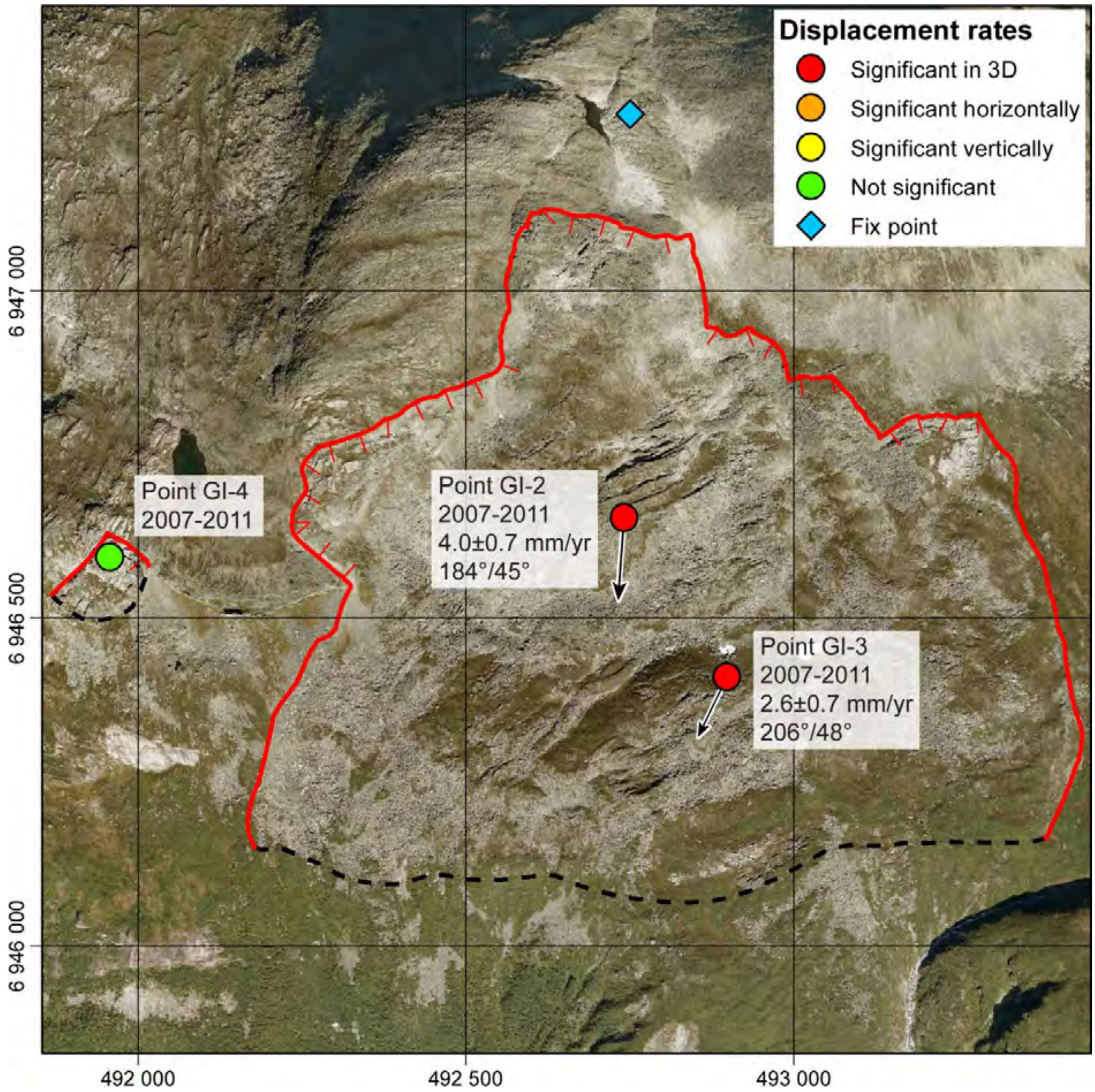

Figure 15: **Map of the unstable rock slopes Gikling 1 and Gikling 2 with the location of dGNSS points for periodic displacement measurements and average displacement vectors for the 2007–2011 measurement period.**

4.2.6 Gjersvollsetra

Gjersvollsetra is situated on a southeast-facing slope 300 m above Gjersvollen on the northern side of Sunndalsfjord (Figure 10). A helicopter reconnaissance flight in 2011 permitted the identification of two eroded ancient faults, acting as possible lateral release surface to the east and as limit between compartments of the instability, respectively (Figure 16). A partly open back-crack is observable at the western limit of the instability but its continuation is masked by the vegetation on the slope (Figure 16). The past displacements of the Gjersvollsetra instability were likely only small and there are no obvious signs of present activity. The Gjersvollsetra instability is of a relatively small volume (~150 000 m³) and a failure will likely not reach inhabited areas.

Recommendation: A possible rock avalanche from the Gjersvollsetra instability will have no consequences. No further investigations or displacement measurements are necessary. The hazard and risk classification will be made after a simple run-out assessment. Further follow-up activities will be based on this classification.

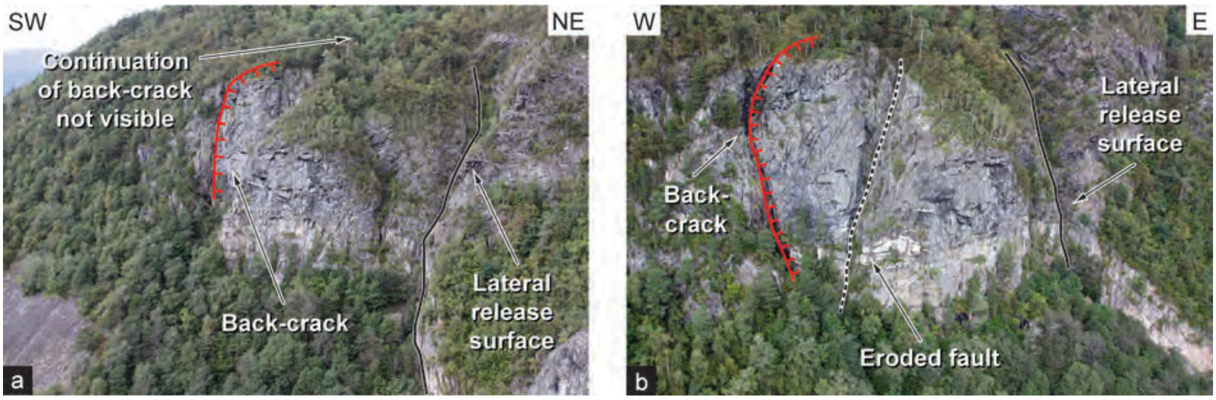

Figure 16: **Photographs of the Gjersvollsetra instability showing the partly open back-crack in the western part and eroded faults as lateral release surfaces to the East and as delimitation between two compartments of the unstable rock slope.**

4.2.7 Grøvelnebba

Grøvelnebba is located on a west-facing slope 620 m above Sunndalsfjord between Sunndalsøra and Oppdøl (Figure 10). A lineament, making out a small step in the morphology and favorably orientated to form the back-crack of a potential unstable rock slope, was closely observed during a helicopter reconnaissance flight in 2011 (Figure 17). No signs of openings or past displacements were observed along the lineament. Laterally the potential instability is delimited by deeply eroded gullies. Moderately valley-dipping surfaces are observed at the base of the Grøvelnebba rock slope (Figure 17), which might provide a potential sliding surface. Rockfalls are very frequent from the cliffs above the county road Fv70 at Oppdølstranda, including the Grøvelnebba rock slope.

Recommendation: Grøvelnebba is classified as a potential unstable rock slope. At present the remaining rock slope does not show any signs of past or present displacements or deformation of a large volume (except for rockfall activity). No further investigations or displacement measurements are necessary and the hazard and risk classification will not be made. However, this site may lead to rockfalls and develop over time into an unstable rock slope, due to structural and geological conditions. The site should be revisited after years to decades to detect any changes and be followed-up on InSAR data.

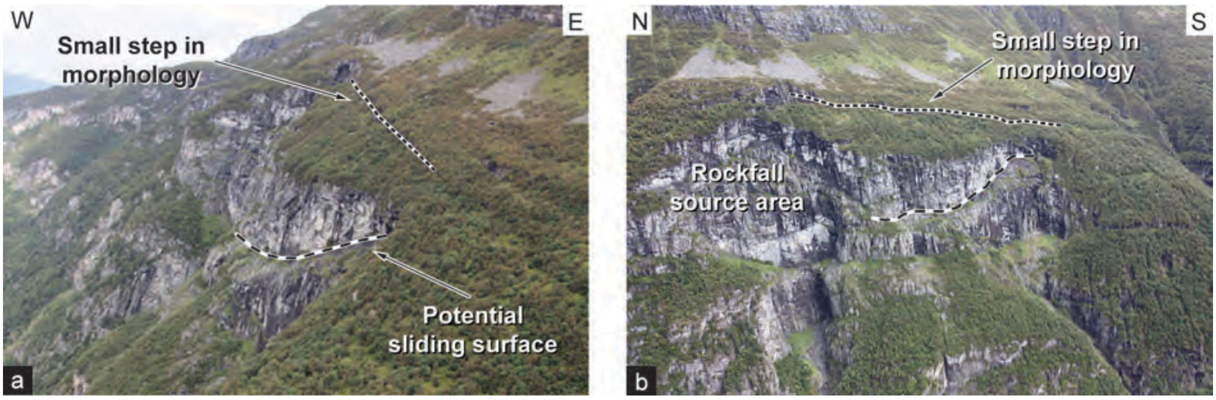

Figure 17: **Photographs of the Grøvelnebba potential unstable rock slope with the moderately valley-dipping potential sliding surface and the lineament forming a small step that might develop as the back-crack of a potential unstable rock slope.**

4.2.8 Gråhøa 1, 2 & 3

The unstable rock slopes at Gråhøa are located on the north-facing slope 1080 m to 1210 m above Molykkja in Sunndalen Valley (Figure 10). Three sites were investigated by helicopter survey in 2011 (Figure 18). Gråhøa 1 was also mapped in the field in 2010 (Figure 19). Gråhøa 2 was already observed from helicopter in 2007 (Henderson and Saintot 2007). Several ENE-WSW-trending lineaments, which are parallel to the steep gneiss foliation, and NW-SE-trending depressions are visible on the plateau (Figure 19).

Gråhøa 1 is a complex unstable rock slope with several possible extents (Figure 19). The foliation-parallel lineaments form the lateral limits of the Gråhøå 1 instability and display a clear offset (Figure 18c). Their dip directions change from SSE-dipping in the north to NNW-dipping in the south leading to a wedge sliding mechanism (Figure 18b). The rock mass at the base of the instability is highly fractured that may indicate internal deformation of the instability. A 2–3 m wide and 10–15 m deep back-crack was opened by past displacements in ENE direction (Figure 18c). The total volume of the Gråhøa 1 instability is large enough to develop a rock avalanche that may reach the bottom of Sunndalen Valley, impact several buildings and maybe dam the river Driva with the probability of a subsequent dam breach and outburst flood (Dahle et al. 2011a).

An ESE-WNW-trending depression forms the potential back-crack of the Gråhøa 2 instability. This structure appears to be an ancient fault that is eroded out and there are no signs of past displacements of the instability (Figure 18d). Gråhøa 2 is a relatively small column and its volume is probably not large enough to create a large rock avalanche.

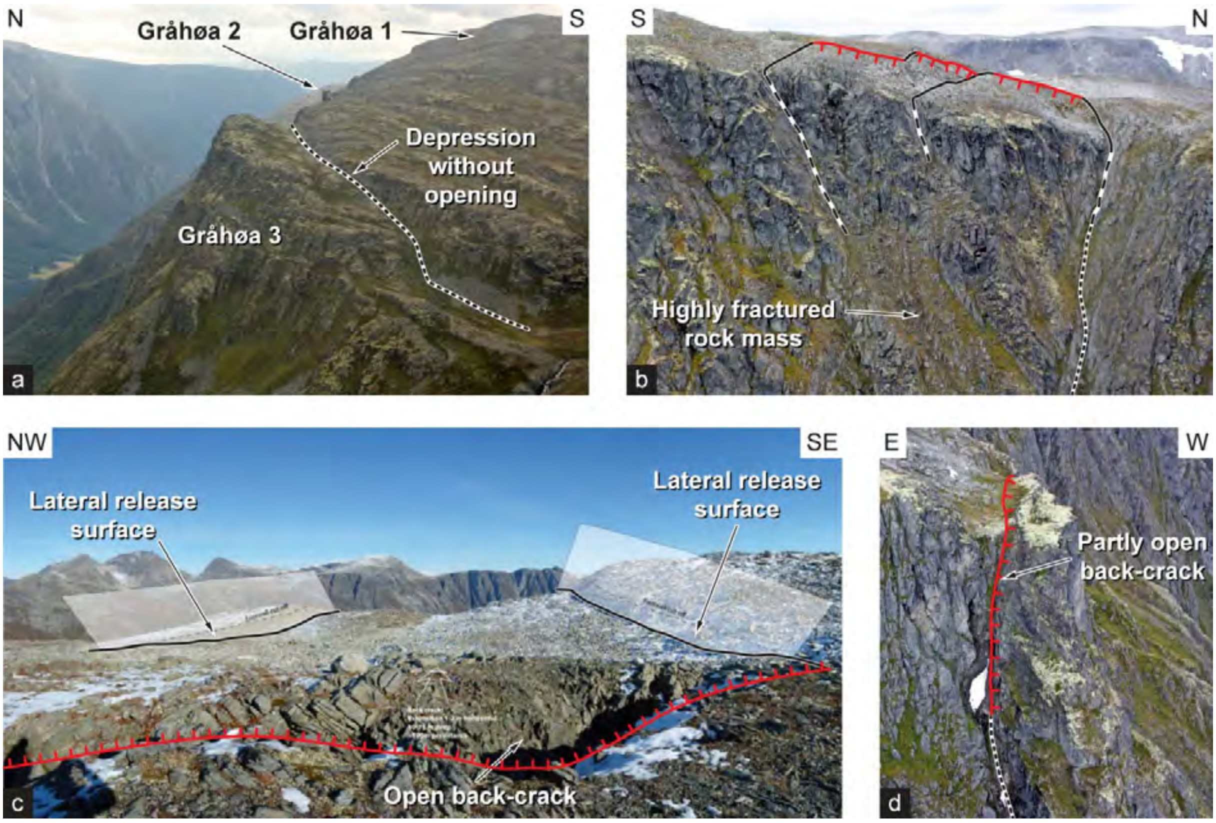

Figure 18: Photographs of the Gråhøa instabilities: a) the depression without visible opening in the back of Gråhøa 3 is probably created by an old fault; b) Gråhøå 1 is delimited by two lateral release surfaces resp. sliding surfaces forming a wedge. The rock mass at the base of the instability is highly fractured; c) view of the 2–3 m wide back-crack at Gråhøa 1 and the lateral release surfaces showing a clear offset (photo: H. Bunkholt, NGU); d) Gråhøa 2 is a small column detached by a partly open back-crack.

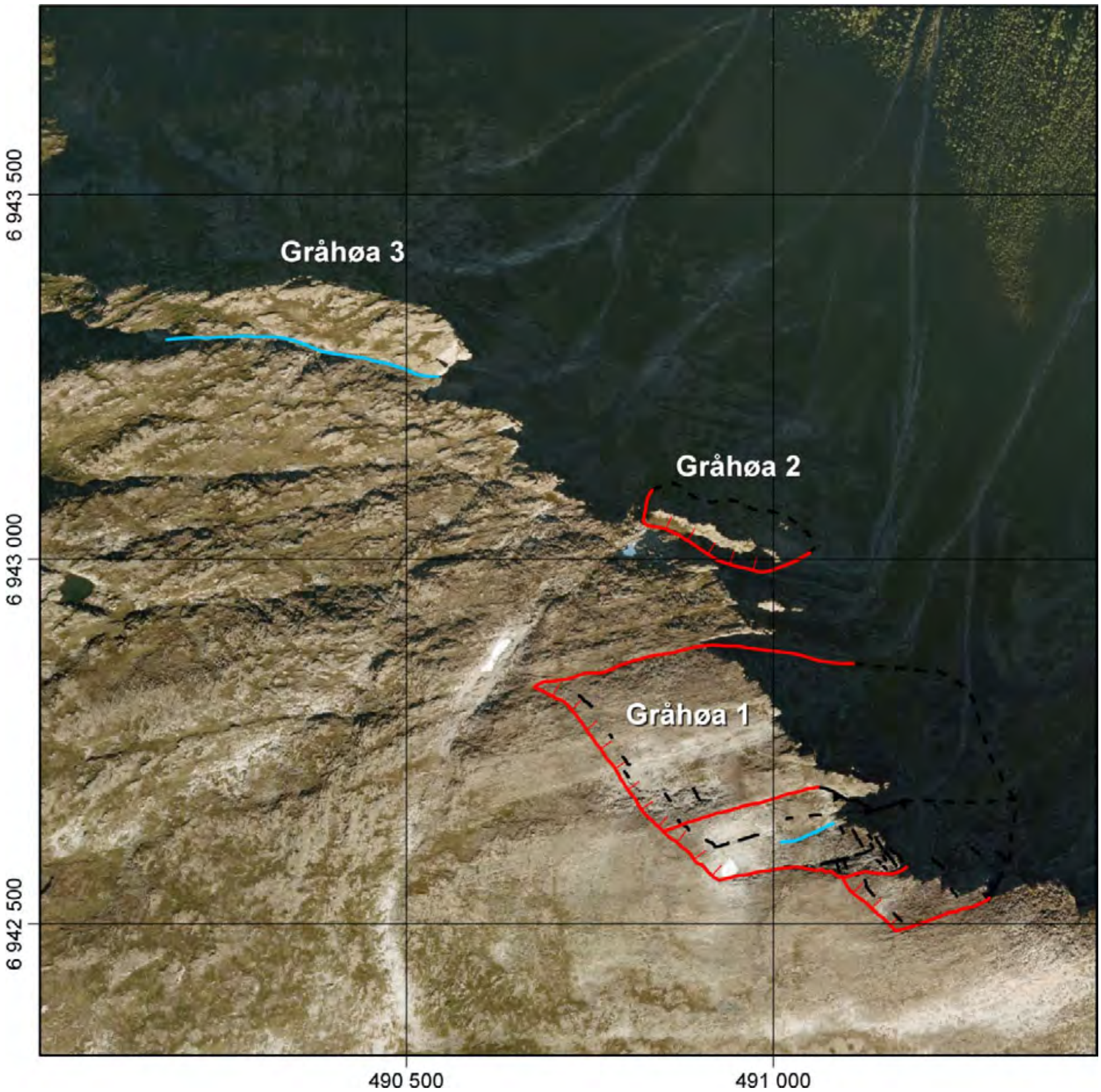

Figure 19: **Map of the Gråhøa instabilities.**

The back limit of the rock slope at Gråhøa 3 is also formed by one of these depressions, but there is no visible sign of opening and is thus also possibly an old eroded fault (Figure 18a). Other structures necessary for sliding are missing and Gråhøå 3 is thus not an unstable rock slope.

Recommendation: Possible rock avalanches from the Gråhøa 1 and Gråhøa 2 instabilities will have consequences. Geological field mapping is necessary to evaluate the structural and geological conditions, define the extents of different compartments, estimate volumes and to quantify past displacements. The hazard and risk classification will be made after this field mapping. Further follow-up activities will be decided based on this classification.

There are no signs that the Gråhøa 3 rock slope might fail in a massive rock slope failure. No further investigations or displacement measurements are necessary. However, rockfalls are possible and their run-out area is given by the rockfall susceptibility map or more detailed hazard maps, where available.

4.2.9 Hovennebba

Hovennebba is situated on the west-facing slope 420 m above a small lake in Hareimdalen Valley, a small side-valley to Sunndalen Valley (Figure 10). A 500 m long lineament was observed in aerial photographs and interpreted as a potential back-crack (Figure 20a). A helicopter reconnaissance flight in 2011 allowed however to show that this lineament lacks openings or other signs of past displacements (Figure 20b). A deeply eroded gully delimits the Hovenebba rock slope to the north. Small rockslides have occurred along moderately valley-dipping sliding surfaces and similar small rockslides are likely to develop again. A large catastrophic collapse of the entire rock slope can however be ruled out according to the present structural development of the site. Moreover, a rock slope failure from Hovennebba would only affect the uninhabited Hareimdalen valley and have thus no major consequences.

Recommendation: There are no signs that the Hovenebba rock slope might fail in a massive rock slope failure. No further investigations or displacement measurements are necessary and the hazard and risk classification will not be made. However, rockfalls are possible and their run-out area is given by the rockfall susceptibility map or more detailed hazard maps, where available.

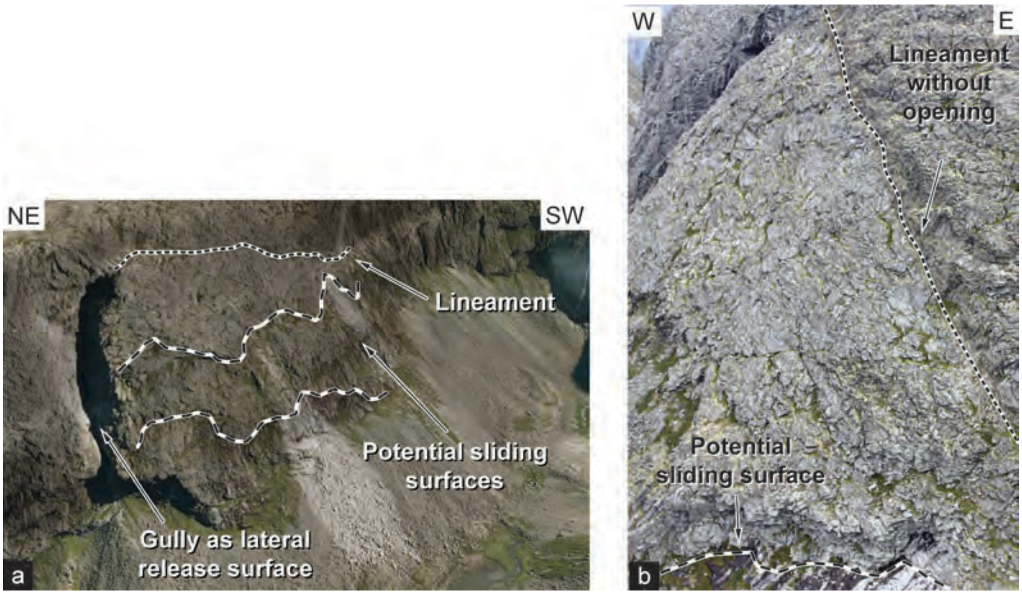

Figure 20: Photographs of the Hovennebba rock slope: a) 3D view from Norge i 3D showing past small rockslides; b) the back-bounding lineament is not open.

4.2.10 Hovsnebba 1

Hovsnebba 1 is located on a SW-facing slope 570 m above Sunndalsøra (Figure 10). The mountain side has been surveyed from helicopter in 2011. An old cataclasite-filled fault makes an approximately 900 m long and 80 m high escarpment at 570 m a.s.l. (Figure 21a). This fault crops out in the SE and forms a gully due to preferential erosion (Figure 21b). This fault would form a back-scarp of a large rock slope, but is too steep to daylight the topography and thus to allow sliding. There are no signs of recent movement along this fault.

The foliation is inward-dipping or flat-lying and thus unfavourably orientated for sliding. Two perpendicular sets of steep joints are the principal structures in the rock mass. Together with the foliation they delimit small blocks that might fail as rockfalls. Rockfalls occur frequently from the steep mountainsides and pose a major hazard for the county road Rv70 (Figure 21b). Ground-based InSAR measurements (by Åknes/Tafjord Early-Warning Centre) and terrestrial laser scanning (by University of Lausanne/NGU) are used to monitor the rockfall activity.

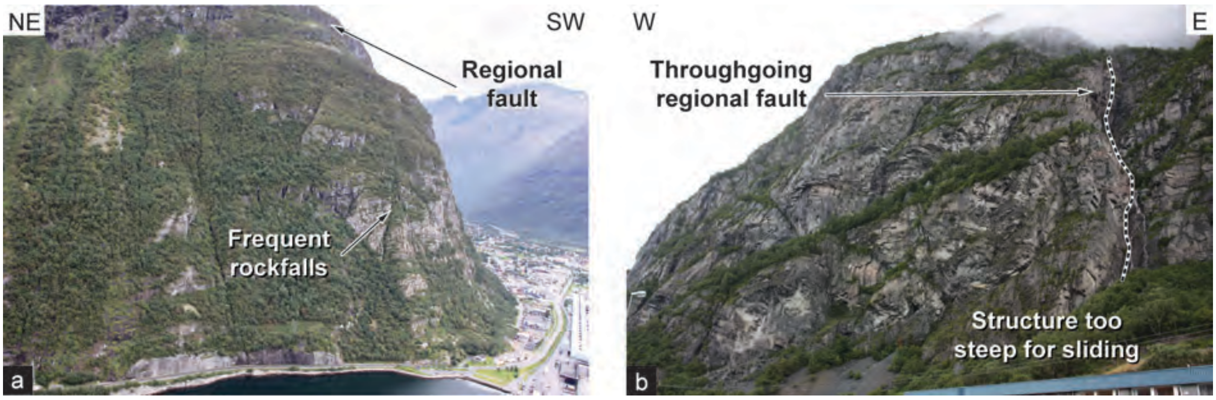

Figure 21: **Photographs of the Hovsnebba 1 rock slope: a regional fault is a potential back-scarp for a large volume, but necessary structures to delimit an instability are missing.**

Striated glacial surfaces are still present in the central and south-eastern part of the Hovsnebba 1 rock slope and testify to the lack of recent gravitational failure along the slope. The slope Hovsnebba 1 above Sunndalsøra lacks necessary structures to delimit a massive unstable rock slope.

Recommendation: There are no signs that the Hovsnebba 1 rock slope might fail in a massive rock slope failure. No further investigations or displacement measurements are necessary and the hazard and risk classification will not be made. However, rockfalls are possible and their run-out area is given by the rockfall susceptibility map or more detailed hazard maps, where available.

4.2.11 Høghamran

Høghamran (Figure 10) is located on a NE-facing slope 510 m above Stangvikfjord. A 500 m long shallow depression was observed during a helicopter survey in 2011 (Figure 22). This depression follows a contact between different bedrock units (fine bands of augengneiss, micaschist and metaarkose within the granitic to dioritic gneiss) (Tveten et al. 1998) and is thus not caused by gravitational deformation. Small rockfall scars are visible to the east of the Høghamran slope (Figure 22a), but there are no evidences for a large rock slope deformation.

Recommendation: There are no signs that the Høghamran rock slope might fail in a massive rock slope failure. No further investigations or displacement measurements are necessary and the hazard and risk classification will not be made. However, rockfalls are possible and their run-out area is given by the rockfall susceptibility map or more detailed hazard maps, where available.

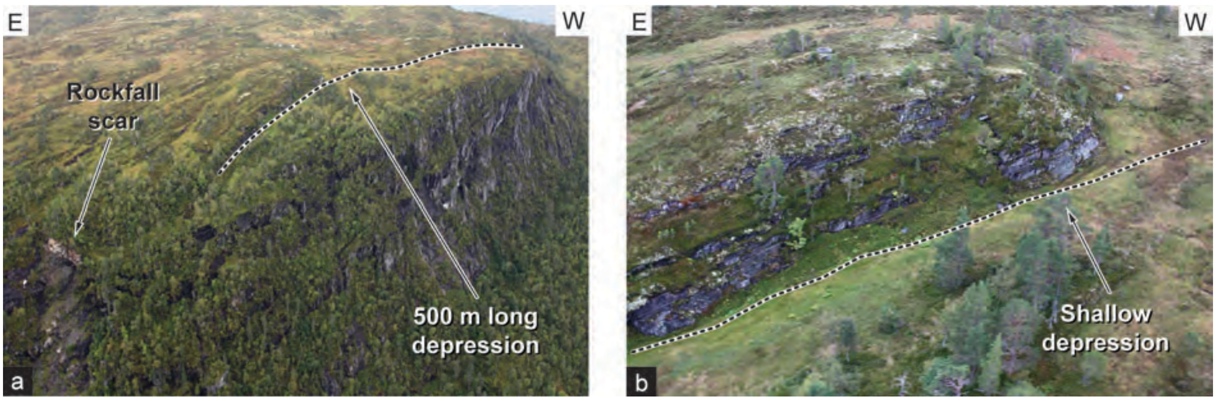

Figure 22: **Photographs of the Høghamran rock slope with a 500 m long depression caused by lithological differences and not by gravitation deformation.**

4.2.12 Ivasnasen

Ivasnasen (Figure 10) is an unstable rock slope located on a west-facing slope 295 m above Sunndalen Valley close to Gjøra. The site has been investigated since 2007 with helicopter reconnaissance and field work (Henderson and Saintot 2007, Saintot et al. 2008). A detailed mapping and analysis of the Ivasnasen instability and of the past rock slope failure at Ivasnasen was made in 2011-2012 in a MSc thesis at NTNU (Dreiås 2012). The orientation of the gneiss foliation at Ivasnasen is favourable for a planar sliding mechanism (Figure 23a). However, numerical slope stability modelling indicates that the present-day deformed volume might be stable (Dreiås 2012). The sliding surface of the present instability follows the same structure as the past rockslide. Samples for cosmogenic nuclide dating were taken in 2012 along this sliding surface in order to date the past rockslide and quantify past displacement rates at the Ivasnasen instability. The deposits of the past rockslide were also sampled.

The Ivasnasen instability is periodically measured since 2010 using TLS and tape extensometers (Figure 24). Both tape extensometer points were measured again in 2011, but no significant displacements are detected. Repetitive TLS data acquired in 2011 and 2012 did also not reveal any significant displacements or rockfall activity. However, there has been recent opening or widening of a crack on the instability, which is evidenced by disturbed and twisted roots of a tree (Figure 23b).

The volume of the Ivasnasen instability was assessed in detail and equals approximately 2.1 million m³ for the entire instability (Dreiås 2012). A rock avalanche from Ivasnasen will likely dam the river Driva with the consequence of upstream flooding and also downstream flooding in the event of a dam breach (Dahle et al. 2011a).

Recommendation: No significant displacements are measured up to now at Ivasnasen. Periodic displacement measurements using tape extensometer and TLS should be continued with 3–5 years interval and to compare to past displacement rates obtained from cosmogenic nuclide dating. The hazard and risk classification needs to be made and further follow-up activities will be decided based on this classification.

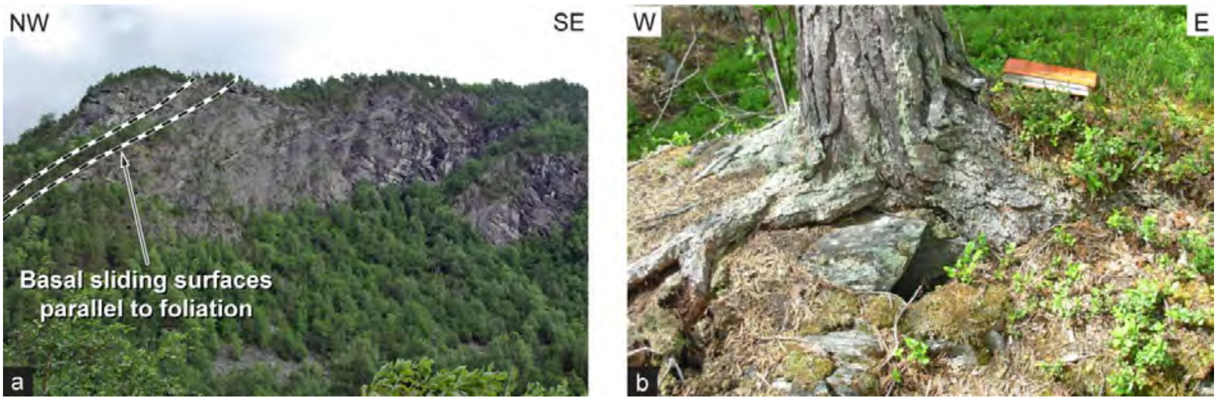

Figure 23: Photographs of the Ivasnasen instability: a) basal sliding surfaces of the present instability are parallel to foliation and are in the continuation of the sliding surface of the past rockslide; b) disturbed tree growth due to (recent) opening or widening of a local crack on the instability.

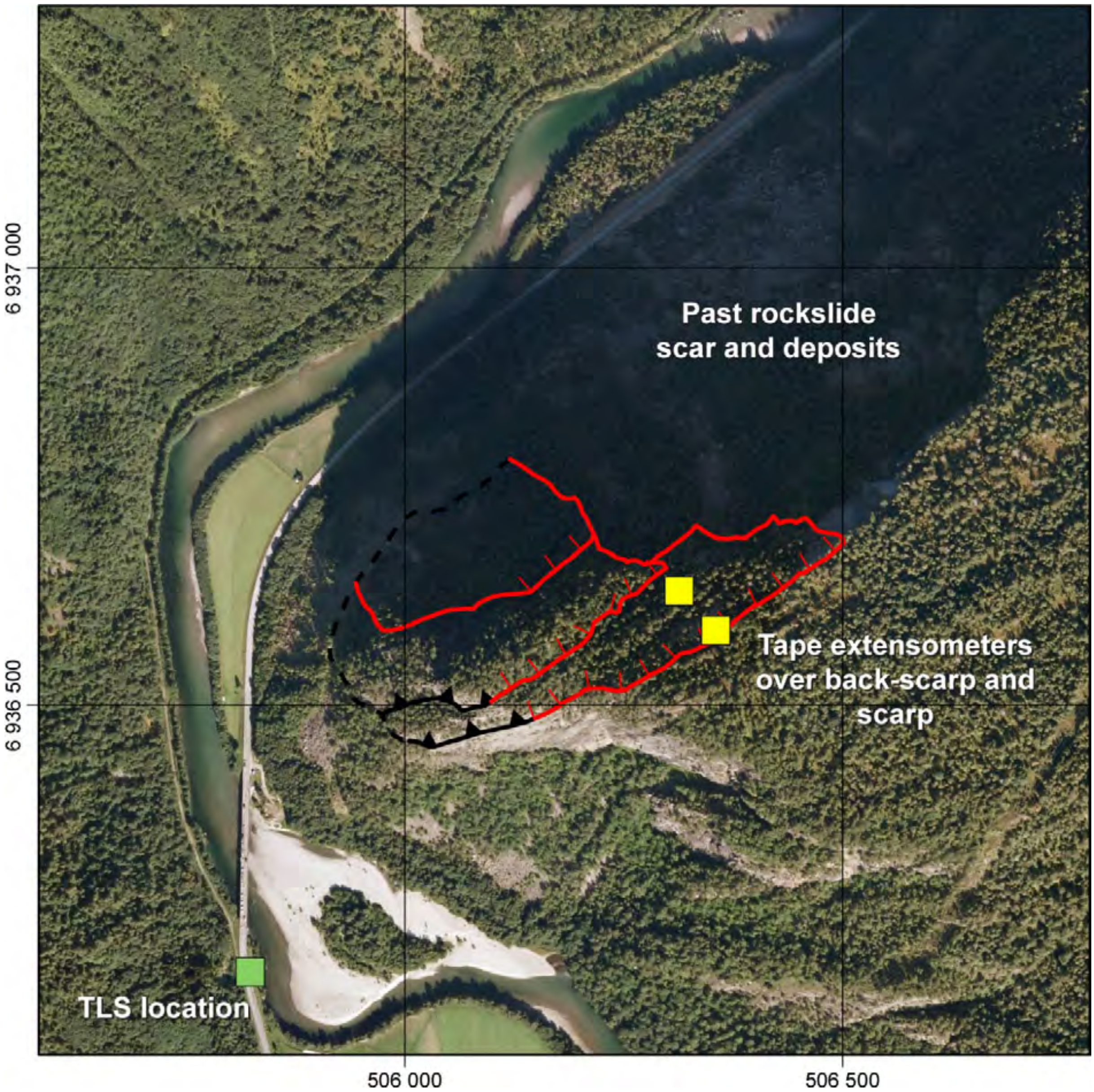

Figure 24: Map of the Ivasnasen instability showing three different compartments, as well as the location of measurement instrumentation (tape extensometer & TLS).

4.2.13 Kammen

Kammen is located on a north-facing slope 410 m above Stangvikfjord, on the same slope section as the site Høghamran (Figure 10). Kammen was observed in a helicopter survey in 2011 (Figure 25). Several sets of vertical cracks delimit small columns along the front of the cliff. These detached blocks have only small volumes (few tens to hundreds of cubicmeters) and their failure as rockfalls would not cause a displacement wave in Stangvikfjord.

Recommendation: There are no signs that the Kammen rock slope might fail in a massive rock slope failure. No further investigations or displacement measurements are necessary and the hazard and risk classification will not be made. However, rockfalls are possible and their run-out area is given by the rockfall susceptibility map or more detailed hazard maps, where available.

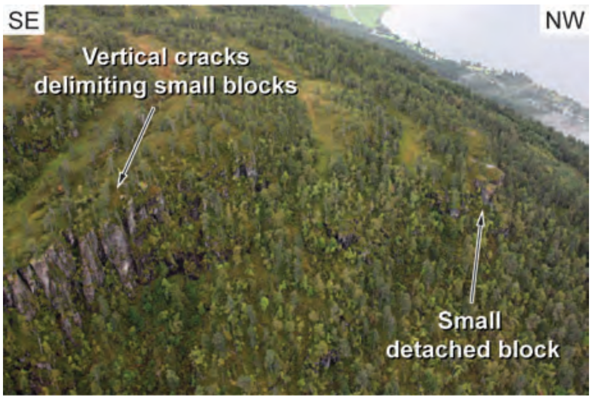

Figure 25: Photograph of the Kammen rock slope. Only small blocks are delimited by vertical cracks.

4.2.14 Klingfjellet 2

Klingfjellet 2 (Figure 10) is situated on the south-facing slope 500 m above Sunndalen Valley close to Romfo. The site was identified from aerial photos and surveyed from helicopter in 2011 (Figure 26). A large valley-parallel linear depression was interpreted as a potential back-crack from aerial photos. A helicopter survey in 2011 allowed however to ascertain that the depression is not caused by gravitational movements, but more likely by erosion of an old fault. Furthermore, lateral and basal structures are missing to delimit a potential instability (Figure 26).

Recommendation: There are no signs that the Klingfjellet 2 rock slope might fail in a massive rock slope failure. No further investigations or displacement measurements are necessary and the hazard and risk classification will not be made. However, rockfalls are possible and their run-out area is given by the rockfall susceptibility map or more detailed hazard maps, where available.

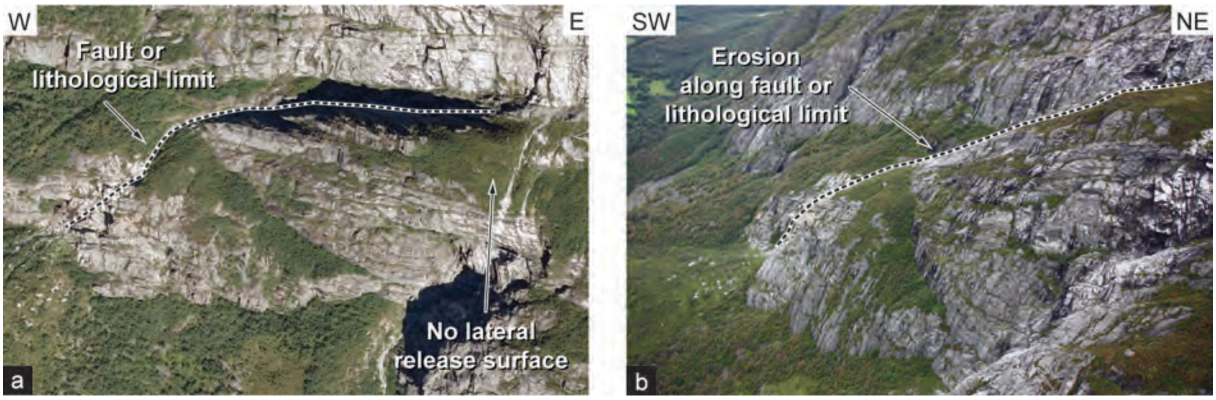

Figure 26: Photographs of the Klingfjellet 2 rock slope: the lineament is formed by erosion of an old fault and is not a back-crack of an instability.

4.2.15 Litlkalkinn 3

Litlkalkinn 3 is located on a west-facing slope above Litldalen Valley close to Sunndalsøra (Figure 10). The steep rock slope was surveyed during a helicopter reconnaissance flight in 2011 (Figure 27). A steep fault with high fracturing and preferential erosion was observed, but there are no signs of past displacements or present activity along it. Other structures necessary to delimit an instability are lacking and Litlkalkinn3 is therefore not an unstable rock slope.

Recommendation: There are no signs that the Litlkalkinn 3 rock slope might fail in a massive rock slope failure. No further investigations or displacement measurements are necessary and the hazard and risk classification will not be made. However, rockfalls are possible and their run-out area is given by the rockfall susceptibility map or more detailed hazard maps, where available.

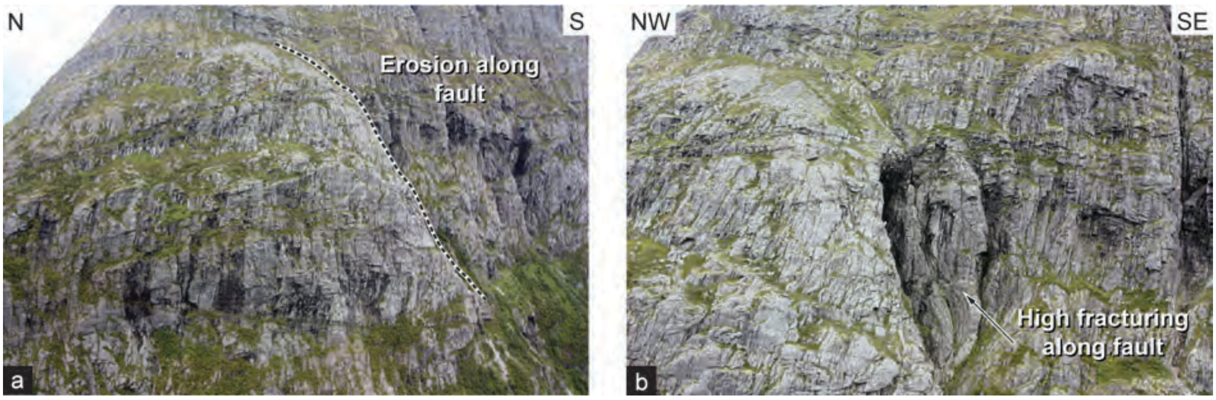

Figure 27: Photographs of the Litlkalkinn 3 rock slope: the lineament is an old eroded fault and not related to an unstable rock slope.

4.2.16 Merrakammen

Merrakammen is located on a south-facing slope 525 m above Innerdalsvatna Lake in Innerdalen Valley (Figure 10). A helicopter survey was made in 2011 at Merrakammen. Eroded lateral release surfaces delimit a small volume on two sides (Figure 28). No back-crack might have developed at the site since no visible opening is observed along the linear structure that joins the lateral release surfaces. Only based on helicopter survey it is not possible to ascertain whether past displacement occurred at Merrakammen or not. A catastrophic failure of this instability might reach the cabins at Oppdølsetra, but will likely not cause a major displacement wave in the lake.

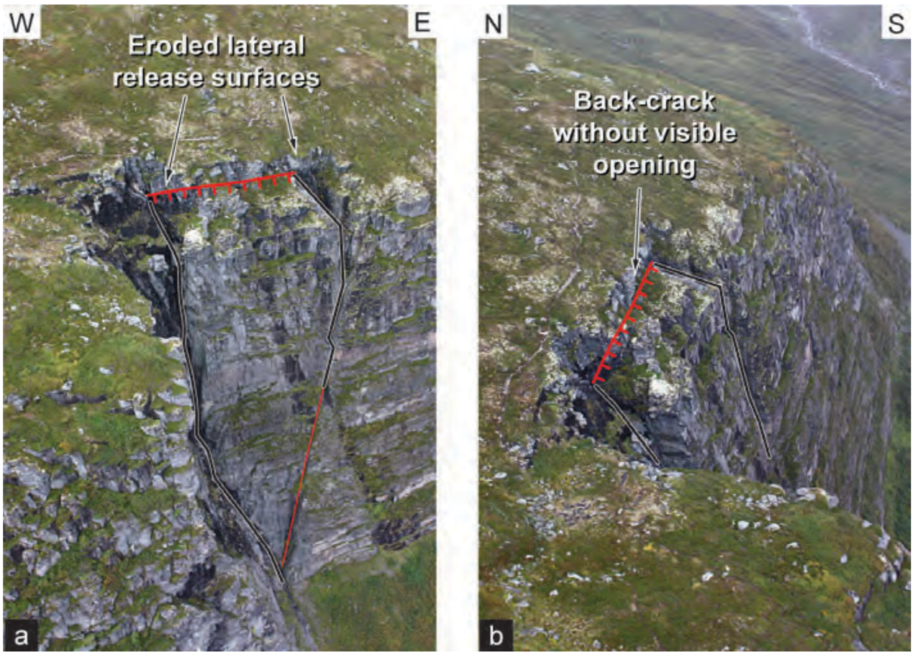

Figure 28: Photographs of the Merrakammen instability with its free lateral release surfaces and an apparent back-crack.

Recommendation: A possible rock avalanche from the Merrakammen instability will have consequences. Geological field mapping is necessary to evaluate the structural and geological conditions and to quantify past displacements. The hazard and risk classification will be made after this field mapping. Further follow-up activities will be decided based on this classification.

4.2.17 Mohaugen 1

Mohaugen 1 (Figure 10) is situated on a northeast-facing slope 1130 m above Viromdalen Valley. Two 200 and 100 meter long depressions were observed from helicopter in 2011 (Figure 29). These depressions display no openings or other signs of past gravitational deformation and other structures are lacking to delimit an unstable rock slope. The rock mass is heavily fractured and small blocks are detached along the front cliff and from the southern side of the Mohaugen 1 rock slope (Figure 29b). These small blocks lead to rockfalls.

Recommendation: There are no signs that the Mohaugen 1 rock slope might fail in a massive rock slope failure. No further investigations or displacement measurements are necessary and the hazard and risk classification will not be made. However, rockfalls are possible and their run-out area is given by the rockfall susceptibility map or more detailed hazard maps, where available.

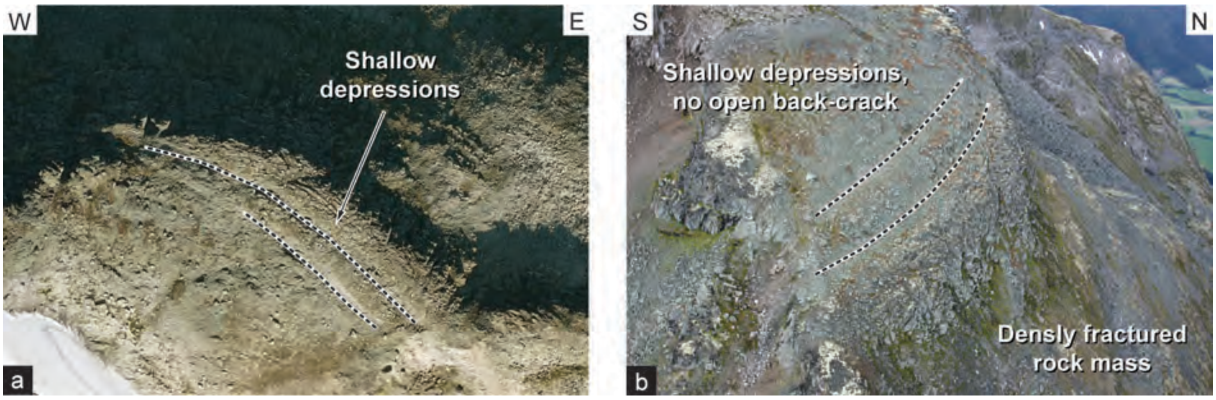

Figure 29: Photographs of the Mohaugen 1 rock slope: shallow depressions are likely not caused by gravitational movements of the rock slope; rockfalls from the densely fractured rock mass will occur.

4.2.18 Mohaugen 2

Mohaugen 2 (Figure 10) is located on a northwest-facing slope above the valley between Oppdøl and Ålvundseid. The site was observed from helicopter in 2011. A depression in a relatively flat terrain seems to delimit a small volume toward the cliff (Figure 30). This depression follows probably an old fault and water ponds inside the depression indicate that there are no recent openings indicating a back-crack formation (Figure 30b). Other structures to delimit an unstable rock slope are missing.

Recommendation: There are no signs that the Mohaugen 2 rock slope might fail in a massive rock slope failure. No further investigations or displacement measurements are necessary and the hazard and risk classification will not be made. However, rockfalls are possible and their run-out area is given by the rockfall susceptibility map or more detailed hazard maps, where available.

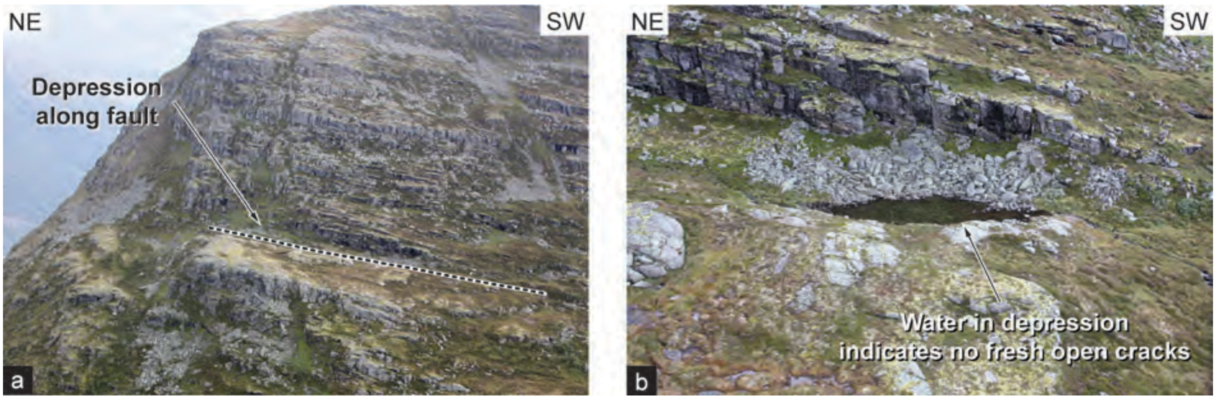

Figure 30: **Photographs of the Mohaugen 2 rock slope: an old fault forms a depression that is locally filled with water, indicating no recent openings.**

4.2.19 Ottdalskammen

Ottdalskammen (Figure 10) is located on a NW-facing slope 410 m above the valley bottom in the inner end of Innerdalen Valley. The slope was surveyed from helicopter in 2011. The unstable rock slope has a clear south-bounding lateral release surface along an eroded fault and is delimited to the east by two open back-cracks (Figure 31a). The detached rock body shows a displacement of several tens of meters and has several internal slope-parallel cracks (Figure 31b). The foliation is moderately valley-dipping and may form the basal sliding surface of Ottdalskammen rockslide. Small compartments delimited by internal cracks have failed in the past (Figure 31b). Eventual failures at Ottdalskammen will only affect uninhabited areas and have no major consequences (Dahle et al. 2011a).

Recommendation: A possible rock avalanche from the Ottdalskammen rockslide will have no consequences. No further investigations or displacement measurements are necessary. The hazard and risk classification will be made after a simple run-out assessment. Further follow-up activities will be based on this classification.

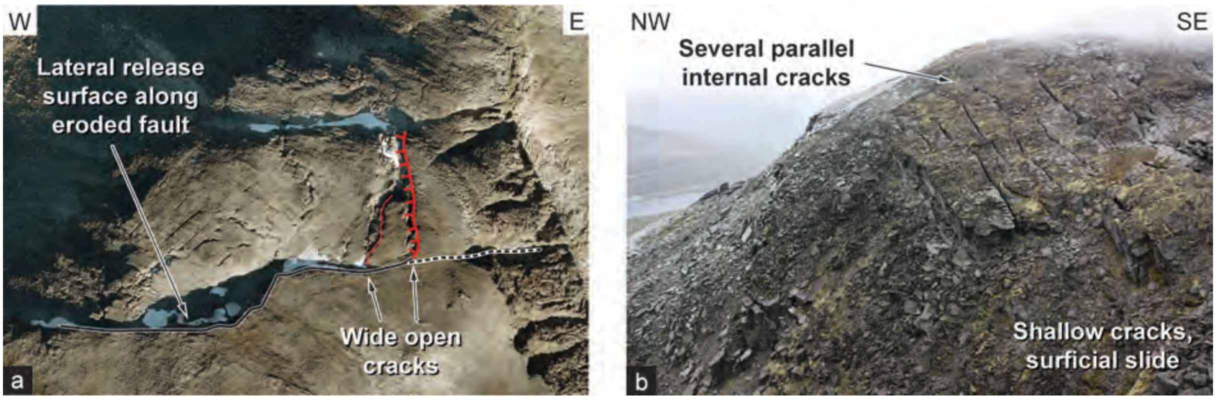

Figure 31: **Photographs of the Ottdalskammen unstable rock slope: a) aerial photograph of the rock slope showing major structures and internal cracks; b) internal cracks delimit compartments that may fail individually towards the NW.**

4.2.20 Ottem 1, 2 & 3

Ottem is located on a south-facing slope 830 m to 1100 m above Sunndalen Valley (Figure 10). The area is divided in three zones and has been investigated since 2007 with helicopter reconnaissance and field work (Henderson and Saintot 2007, Saintot et al. 2008).

Ottem 1 is described in Saintot et al. (2008) (Figure 32). No new investigations have been made on this site. Ottem 1 is probably not an unstable rock slope due to the lack of necessary lateral and back structures delimiting an unstable rock slope and the absence of signs of gravitational deformation.

Ottem 2 is a talus slope formed by rockfalls and small rock avalanches from the steep cliffs at Ottem (Figure 32). A detached, highly fractured block lies on this talus slope (Figure 33). This block has a relatively small volume and the high fracturing lets suppose that it will disintegrate in smaller blocks. Ottem 2 is too small to form a large rock avalanche that would affect the settlements in Sunndalen Valley. This talus slope stretches down to the cliffs above Ottemsøyan at 240 m a.s.l., but is grass- and forest-covered in the lower part. There are signs of movements of single blocks on this talus (Figure 33c) and the cliffs above Ottemsøyan are prone to rockfalls (Figure 33d). However, there are no indications for a large unstable rock slope affecting the entire mountain side as it has been previously supposed (Henderson and Saintot 2007, Dahle et al. 2011a). The cliffs above Ottemsøyan were scanned by TLS in 2010 for structural characterization of the cliffs and possible detection of rockfall activity. No repetitive scans are made yet. The foliation is subhorizontal, while other discontinuity sets are steep to subvertical with variable dip directions (N, NE, S, SW and NW). This structural setting enables rockfalls from the steep cliffs, but no planar or wedge sliding mechanism for a large unstable rock slope.

Ottem 3 is described in previous reports (Henderson and Saintot 2007, Saintot et al. 2008). Periodic displacement measurements using dGNSS started in 2008 with two points on the unstable rock slope (Figure 32). The points were measured again in 2009, but no significant displacements were recorded in this relatively short time period (1 year). TLS data were acquired in 2011 from the valley bottom, but no repetitive scans are made yet.

Recommendations: No significant displacements are measured up to now at Ottem 3. Periodic displacement measurements using dGNSS should be continued with 3–5 years interval. The hazard and risk classification needs to be made and further follow-up activities will be decided based on this classification.

There are no signs that the Ottem 1 and Ottem 2 rock slopes might fail in massive rock slope failures. No further investigations or displacement measurements are necessary and the hazard and risk classification will not be made. However, rockfalls are possible and their run-out area is given by the rockfall susceptibility map or more detailed hazard maps, where available.

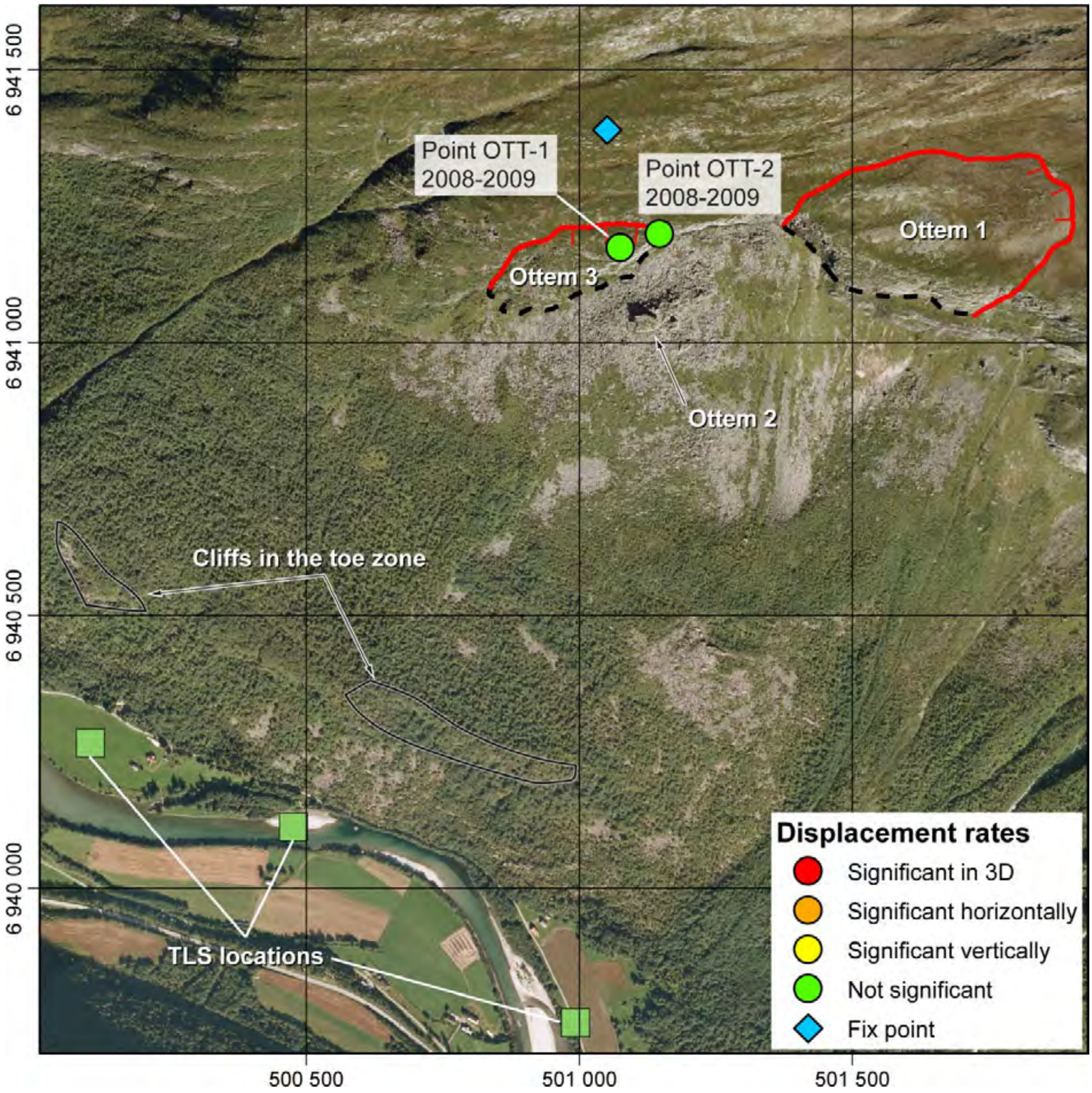

Figure 32: Map of the unstable rock slopes at Ottem with the location of dGNSS points for periodic displacement measurements. No significant displacements were detected over the 2008–2009 measurement period. The cliffs in the toe zone above Ottemsøyan were scanned by TLS in 2010 for structural analysis and possible detection of rockfall activity.

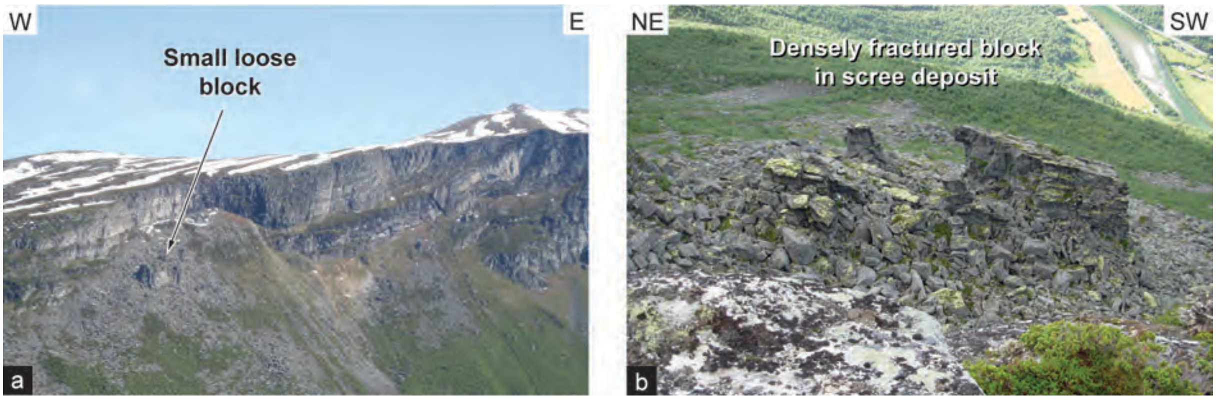

Figure 33: Photographs of the Ottem 2 instability: a) the fully detached block lies on a blocky talus slope; b) the block is highly fractured and will likely disintegrate into small blocks.

4.2.21 Serkjenebba

Serkjenebba (Figure 10) is located on a northeast-facing slope 1065 m above Dalavatnet Lake in Grødalen Valley. The unstable rock slope was observed by helicopter in 2011 and is delimited by an old fault to the SE and basal sliding surface to the north (Figure 34a). Foliation attitude changes along the mountainside and a basal sliding surface could have developed along the foliation where it is moderately SE-dipping in the northern part of the instability (Figure 34b). A lineament on the plateau marks the potential back-crack of the Serkjenebba instability, but there are no visible openings and only a small vertical apparent offset is seen. There are signs of high rockfall and debris flow activity at the unstable rock slope and its surroundings. A catastrophic failure of the Serkjenebba instability will reach Grødalen Valley and likely dam the river Grøa.

Recommendation: A possible rock avalanche from the Serkjenebba, characterise the basal sliding surface instability will have consequences. Geological field mapping is necessary to evaluate the structural and geological conditions and to quantify past displacements. The hazard and risk classification will be made after this field mapping. Further follow-up activities will be decided based on this classification.

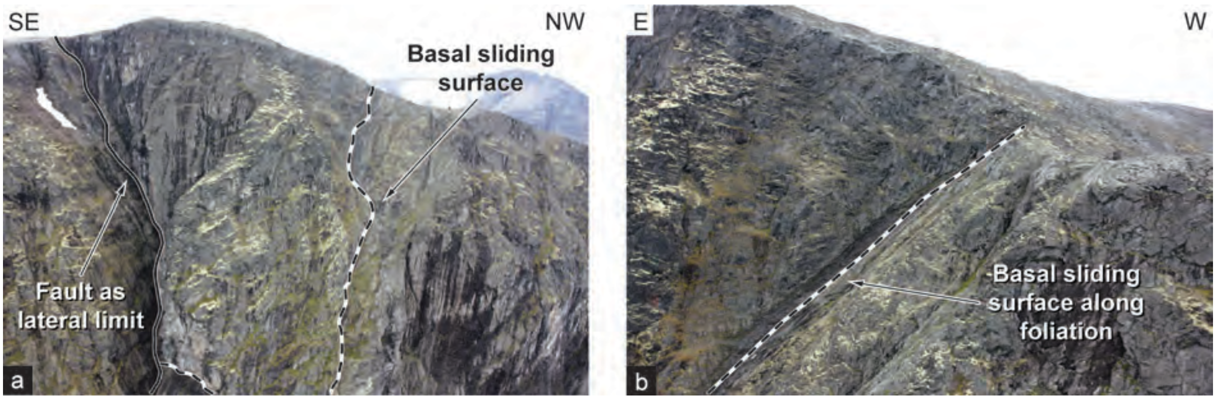

Figure 34: Photographs of the Serkjenebba instability: a) the instability is delimited by a NE-dipping fault to the SE and by a basal sliding surface to the NW; b) the moderately S-dipping basal sliding surface at the NW-limit of the instability is parallel to foliation.

4.2.22 Steinbruhøa

Steinbruhøa (Figure 10) is located on an east-facing slope 850 m above Litldalen Valley. A helicopter survey in 2011 has allowed the observation of an old fault zone forming the basal sliding surface of the potential unstable rock slope. This fault daylights on the plateau and forms small depressions probably due to preferential erosion (Figure 35a). A small gully marks a possible southern lateral limit of the instability, but this structure is very poorly developed (Figure 35b). Rockfall scars and possible small, shallow rockslides are observed along the frontal cliff (Figure 35b). There are no signs of recent activity (opening of back-cracks, offsettings etc.) of the potential unstable rock slope at Steinbruhøa.

Recommendation: Steinbruhøa is classified as a potential unstable rock slope. At present the remaining rock slope does not show any signs of past or present displacements or deformation of a large volume. No further investigations or displacement measurements are necessary and the hazard and risk classification will not be made. However, this site may lead to rockfalls and develop over time into an unstable rock slope, due to structural and geological conditions. The site should be revisited after years to decades to detect any changes and be followed-up on InSAR data.

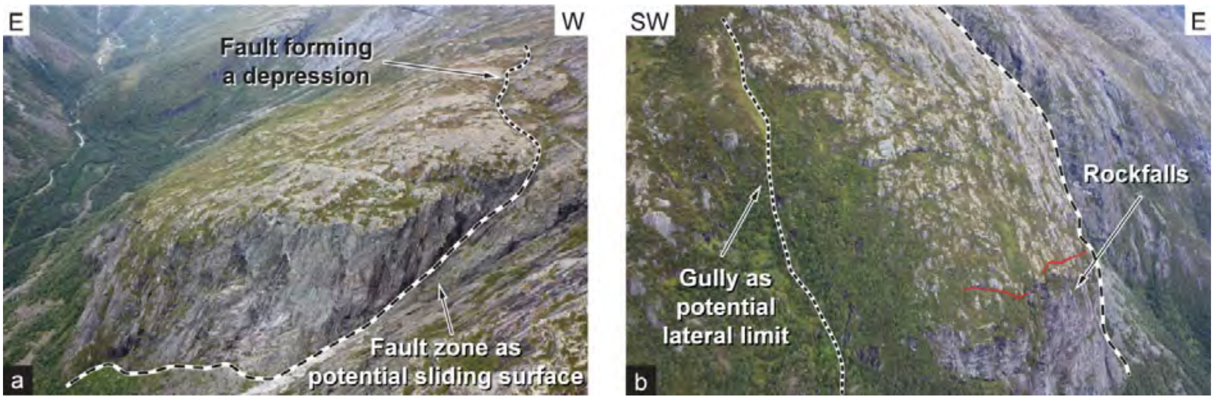

Figure 35: Photographs of the potential unstable rock slope at Steinbruhøa: a) a fault zone delimits the potential instability at its base and back; b) the lateral limit to the south is poorly marked by a small gully, cracks along the front cliff delimit small rockslides and rockfalls.

4.2.23 Storbotnen

Storbotnen is located on an east-facing slope at 520 m above Litldalen Valley (Figure 10). A first helicopter reconnaissance and field mapping was made in 2007 and 2008 (Henderson and Saintot 2007, Saintot et al. 2008). Based on new aerial photographs and a helicopter survey in 2011, the unstable rock slope at Storbotnen was redefined and divided into several compartments and subblocks. Several valley-parallel and moderately valley-dipping faults are the most remarkable structural features at Storbotnen. They are located approximately at 500 (fault A), 550 (B), 700 (C) and 800 m a.s.l. (D) and can be followed over several km.

Fault A is a steeply east-dipping cataclasite-filled tectonic fault zone of approximately 1 m width. This fault delimits the base and back of the main unstable rock slope at Storbotnen, which affects the frontal part of the mountainside (Figure 36a, b). There are indications of past displacements along this fault with the presence of fine-grained breccia, which has been sampled for grain size distribution and clay composition analysis. Laboratory results show a mature, matrix-supported breccia with possible clay content (illite) (NGU-Lab analysis report no. 2013.0057). However, no significant recent activity can be observed. Rockfalls are, however, frequent from the steep cliffs at the front of the unstable rock slope. A catastrophic failure of this unstable rock slope seems unlikely, but would affect several buildings and create a major rock avalanche dam in the narrow Litldalen Valley.

The subblock Hamran is located at the southern end of the main unstable rock slope (Figure 36a). There are morphologic indications for a back-crack and a lateral release surface, but no openings or signs of past displacements can be detected. Hamran is however a cliff with high rockfall activity.

The subblock Høglia is delimited laterally by two parallel faults (A & B) and a partly open back-crack (Figure 36b). The subblock Hårstad has also a partly open back-crack, but its western lateral limit is poorly developed. However, there are several small detached columns in front of the subblock Hårstad (Figure 36b). Another series of detached columns is located further downslope below the subblock Hårstad, as described by Saintot et al. (2008) (Figure 36c). All columns slid and may further slide along the favourably orientated foliation.

Three subblocks are located between the two uppermost faults (C & D). All subblocks use the shallow valley-dipping foliation as basal sliding surface and fault D as lateral release surface (subblock A) or as back-crack (subblocks B and C) (Figure 36d-f). Subblock A at the northern end of the Storbotnen area has a small depression at the back, but there is no open back-crack, which indicates that little to no past displacements occurred at subblock A. The available observations do not enable to assess the amount of past displacement at subblocks B and C.

Recommendation: A possible rock avalanche from the Storbotnen instability will have consequences. Geological field mapping is necessary to evaluate the structural and geological conditions, define the extents of different compartments and subblocks, estimate volumes and quantify past displacements. The hazard and risk classification will be made after this field mapping. Further follow-up activities will be decided based on this classification.

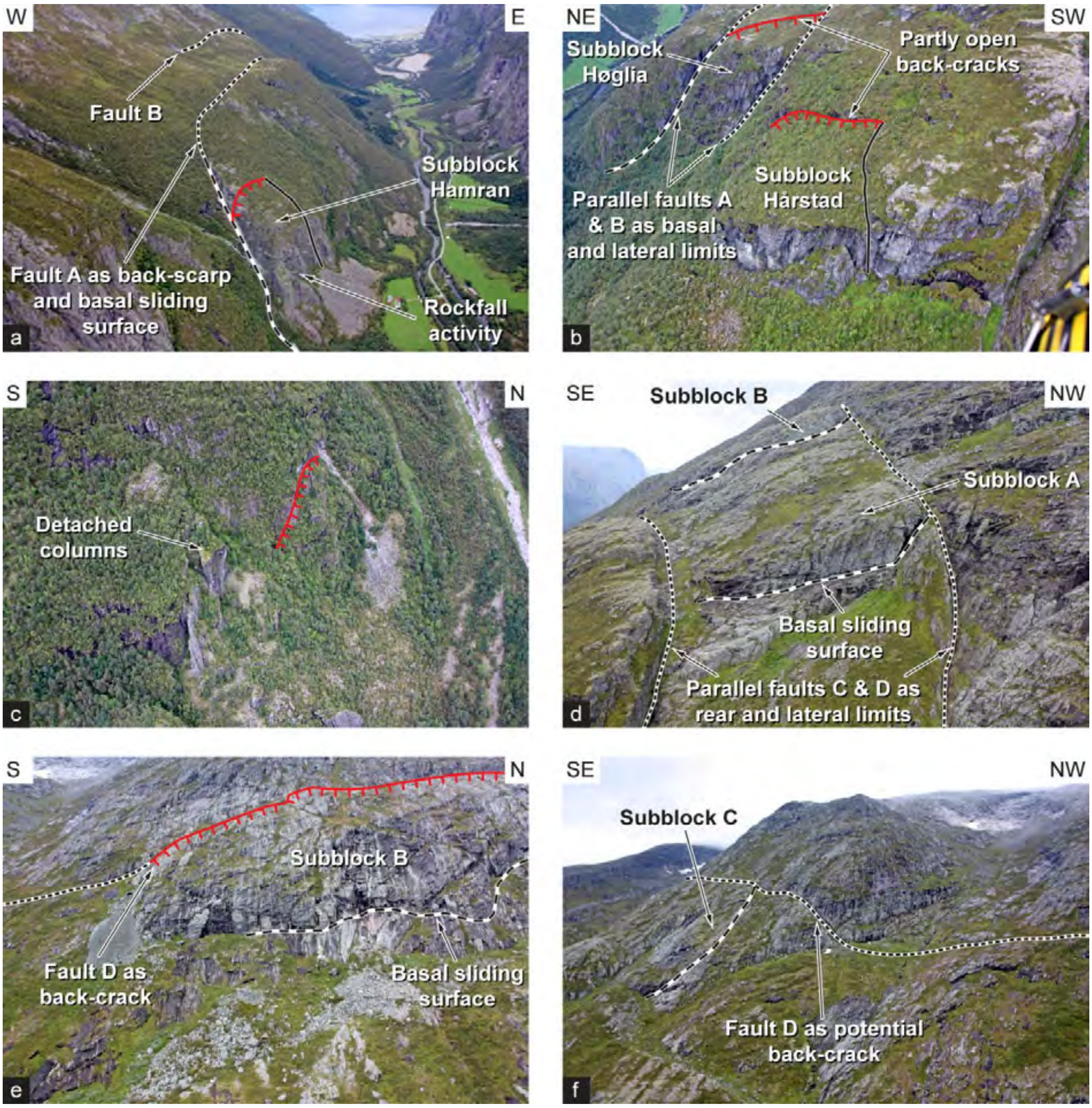

Figure 36: **Photographs of the Storbotnen unstable rock slope: a) viewing north, the main unstable rock slope with an old fault as back-scarp and basal sliding surface. The subblock Hamran is prone to rockfalls; b) viewing SE, parallel faults delimiting the main unstable rock slope and two subblocks namely, Høglia and Hårstad; c) detached columns and small local instabilities at the foot of the slope at Hårstad; d) subblocks A and B located above Hårstad subblock; e) frontal view of subblock B with a well-defined basal sliding surface and a fault as back-crack; f) the fault forming the potential back-crack of subblock C has no visible opening.**

4.2.24 Storurhamran

Storurhamran is located on the east-facing slope 400 m above Litldalen Valley (Figure 10). The site was investigated by helicopter in 2007 and described by Henderson & Saintot (2007) (Figure 37a). The steep cliffs at Storurhamran make this site nearly inaccessible to an eventual field work. The slope was therefore scanned by TLS in 2010 in order to assess the main structures of the cliff. The foliation is steeply dipping southwards, which is roughly perpendicular to the slope face. The cliff at Storurhamran is characterised by overhanging walls formed by SW- to W-dipping discontinuity sets and moderately E-dipping exfoliation surfaces. The latter appear to have formed the basal sliding surface of ancient rockslides and might also form the basal sliding surface of the present unstable rock slope (Figure 37b). These ancient rockslides explain the huge boulders found at the foot of the Storurhamran instability. A catastrophic failure would hit the road in Litldalen Valley and probably dam the Litldalselva River, but will not directly impact inhabited areas.

Recommendation: A possible rock avalanche from the Storurhamran instability will have no consequences. No further investigations or displacement measurements are necessary. The hazard and risk classification will be made after a simple run-out assessment. Further follow-up activities will be based on this classification.

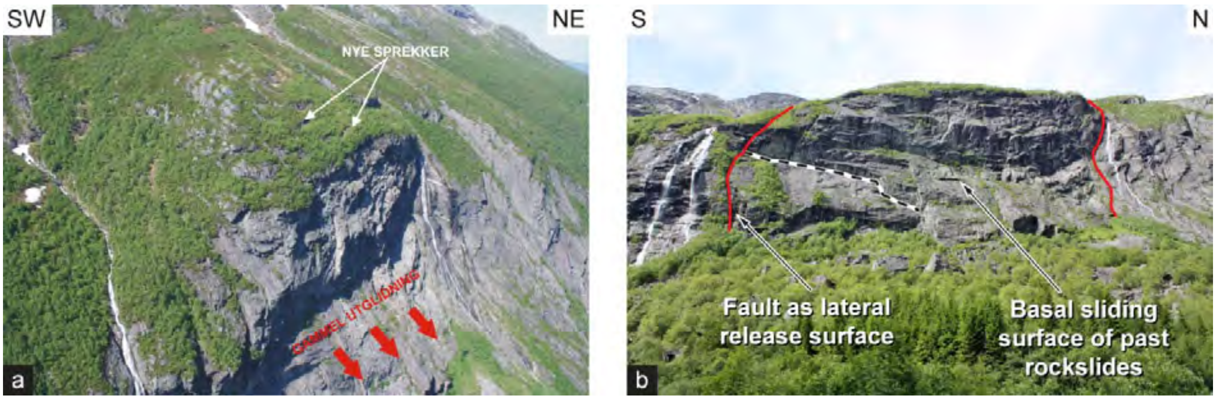

Figure 37: Photographs of the Storurhamran instability: a) aerial photograph (from Henderson & Saintot 2007); b) frontal view of the instability showing the past sliding surfaces and the huge boulders at the foot of the slope.

4.2.25 Vollan

Vollan (Figure 10) is an unstable rock slope located on a southeast-facing slope 840 m above Sunndalen Valley close to Gjøra (Saintot et al. 2008). Extensive field work was carried out on the site in 2008 (Saintot et al. 2011b) including the installation of three dGNSS-points for periodic displacement measurements (Figure 38). The points were measured again in 2009 and 2011, but no significant displacements were recorded over the 3 years measurement period. A detailed mapping and analysis of the Vollan unstable rock slope was completed in 2012 in a MSc thesis at NTNU (Dreiås 2012). A massive failure from Vollan will likely dam the river Driva with the consequence of upstream flooding and also downstream flooding in the event of a dam breach (Dahle et al. 2011a).

Recommendation: No significant displacements are measured up to now at Vollan. Periodic displacement measurements using dGNSS should be continued with 3–5 years interval. The hazard and risk classification needs to be made and further follow-up activities will be decided based on this classification.

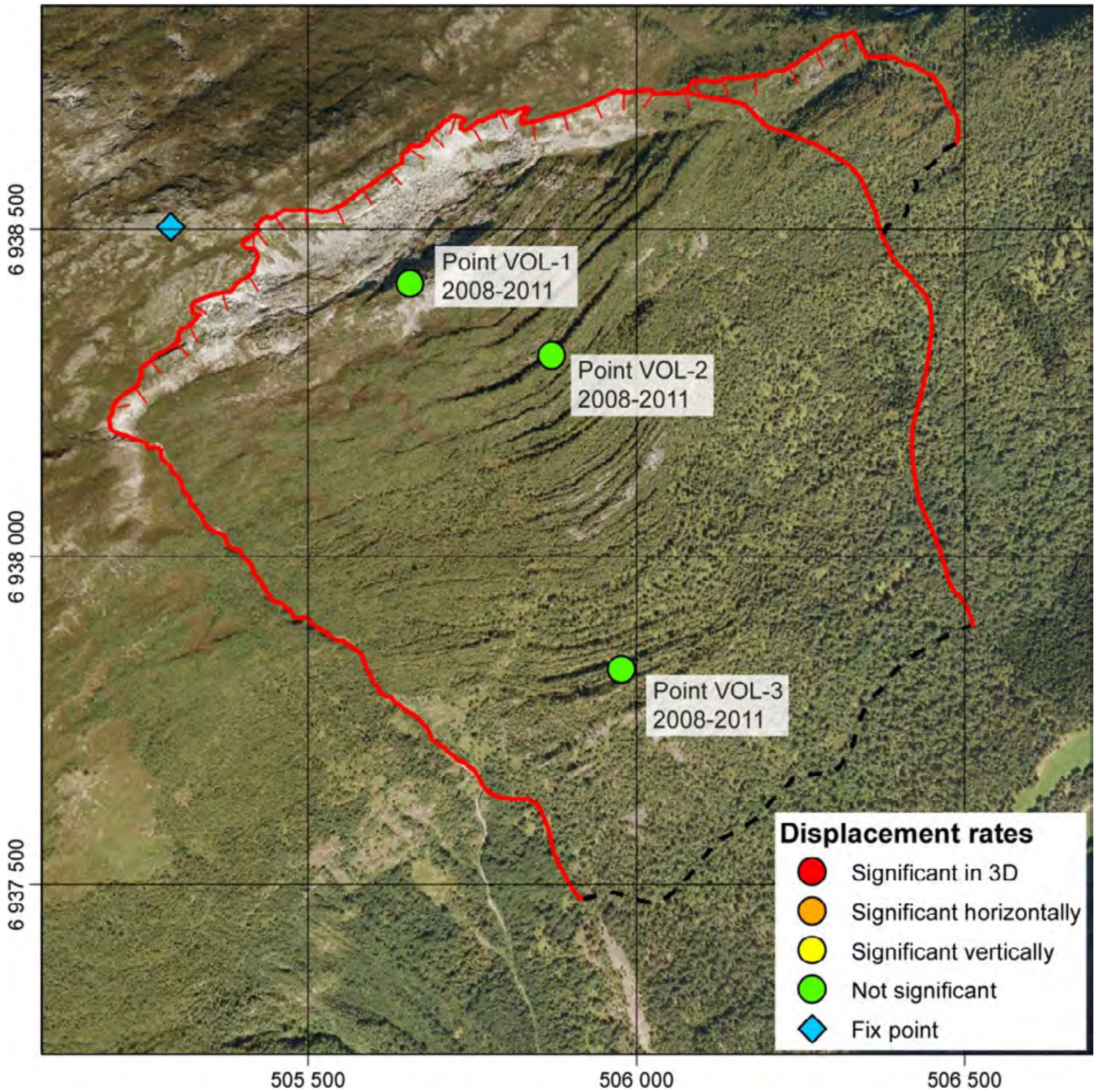

Figure 38: Map of the Vollan unstable rock slope with the location of dGNSS points for periodic displacement measurements. No significant displacements were detected over the 2006–2011 measurement period.

5. ROMSDAL REGION

5.1 Fræna municipality

There are three known sites located in Fræna municipality, which are all described in this report (Figure 39).

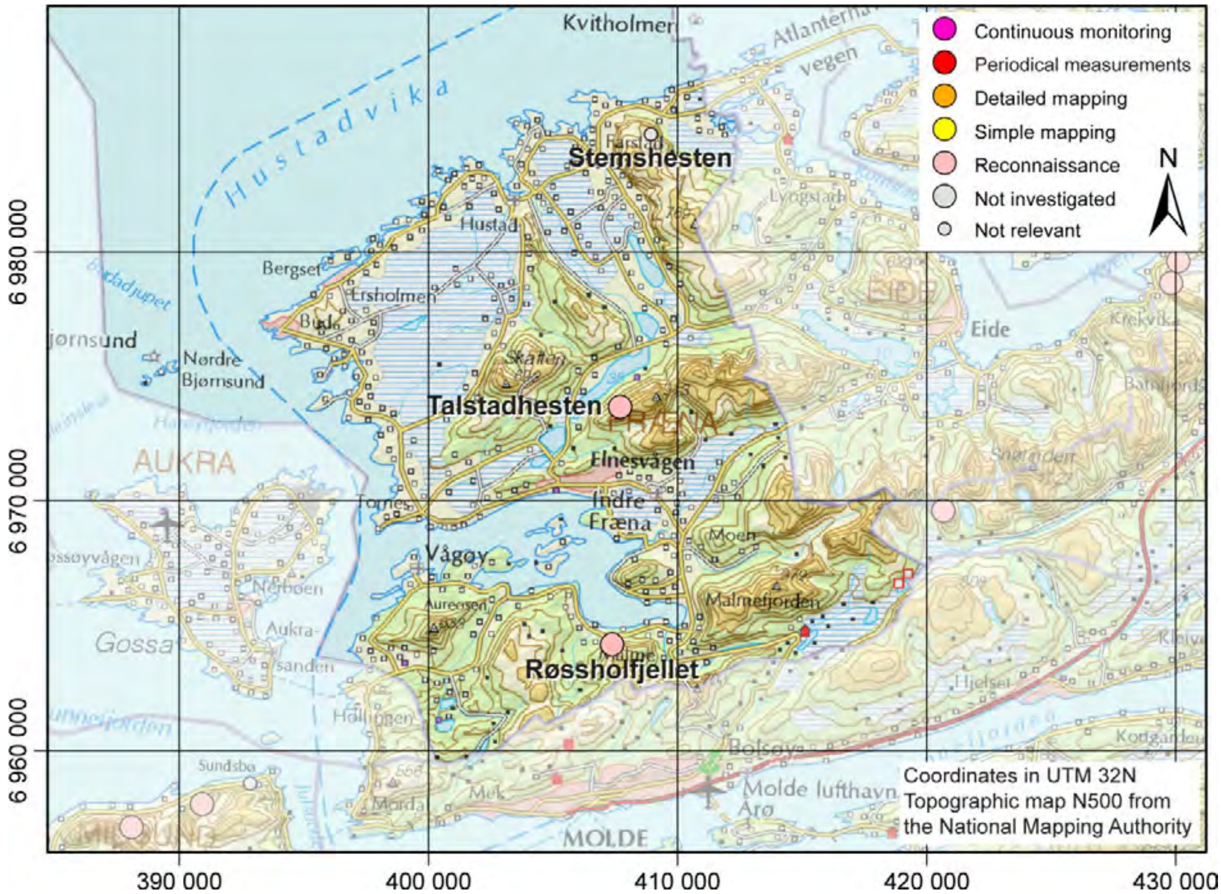

Figure 39: Map of the three known sites in the Fræna municipality with their investigation status. The name of the sites described in this report is shown.

5.1.1 <u>Røssholfjellet</u>

Røssholfjellet (Figure 39) is situated on a north-facing slope 380 m above Malmefjord. A helicopter reconnaissance flight was made in 2012. Røssholfjellet is a complex unstable rock slope with two instabilities located at the front of a possible deep-seated gravitational slope deformation (Figure 40). One of these instabilities, named Alteret, is a rockslide with free lateral surfaces and fully detached by a 10–30 m wide graben at the back. Alteret has been earlier described in Dahle et al. (2011). There are only few cracks visible within the Alteret instability indicating a relatively intact rock mass. A smaller instability is located above Alteret and has a partly developed back-crack. Scars of previous rockslides are visible east of both instabilities and blocky deposits, completely overgrown by vegetation, cover the slope below the instabilities down to the fjord. A persistent lineament in the form of a surface depression is observed at 500 m a.s.l. The helicopter reconnaissance flight did not allow ascertaining the nature and origin of this lineament. It could be either a crack caused by a deep-seated gravitational slope deformation or a fault carved by preferential erosion.

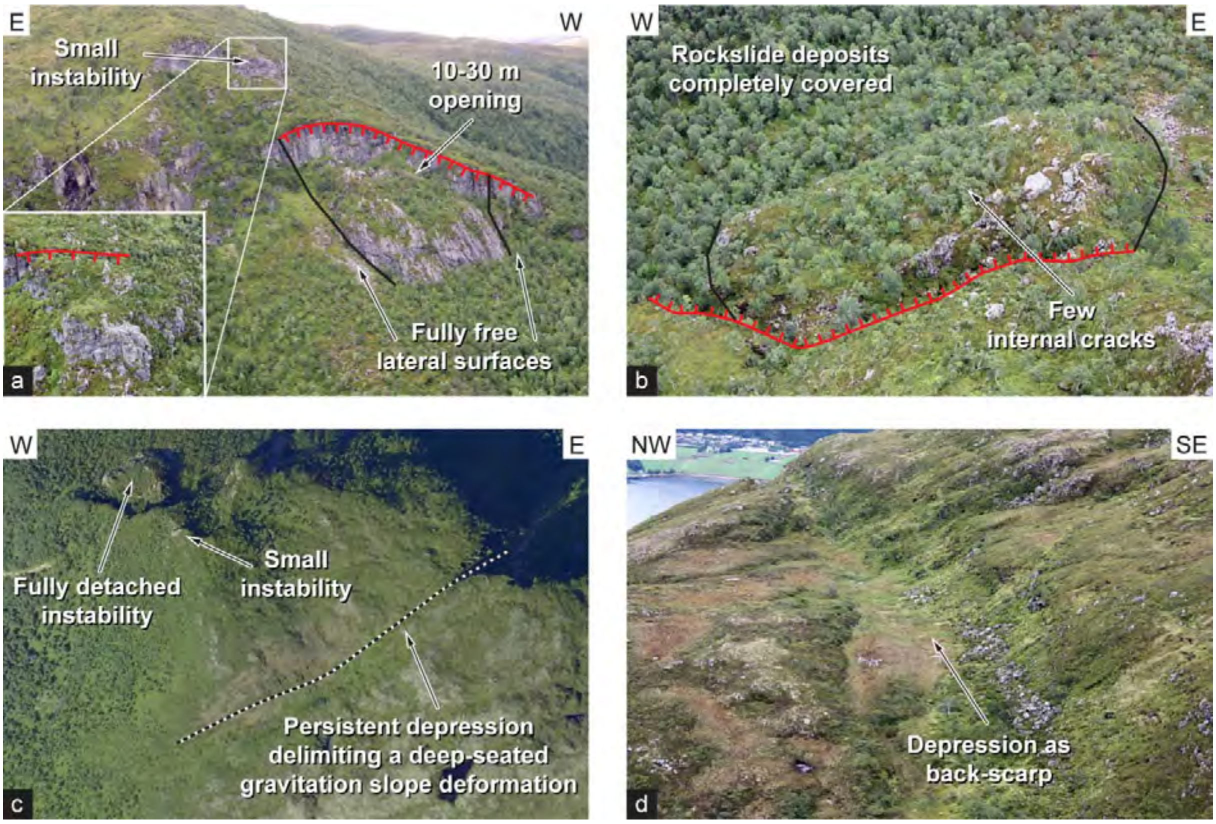

Figure 40: Photographs of the Røssholfjellet instability: a) and b) the instability Alteret is delimited by a wide open graben structure in the back and has free lateral surfaces; c) orthophoto showing a persistent depression delimiting a deep-seated gravitational slope deformation with the fully detached instability Alteret at its front; d) depression as back-scarp of the deep-seated gravitational slope deformation.

Recommendation: A possible rock avalanche from the Røssholfjellet instability will have consequences. Geological field mapping is necessary to evaluate the structural and geological conditions and to quantify past displacements. The hazard and risk classification will be made after this field mapping. Further follow-up activities will be decided based on this classification.

5.1.2 Stemshesten

Stemhesten (Figure 39) is situated on a northeast-facing slope 510 m above Austheim. The site has been earlier described by Dahle et al. (2011). A helicopter reconnaissance flight in 2012 revealed several 2–4 meters long open vertical cracks on the mountain top without visible connectivity of the crack system (Figure 41b). An intact block with a volume of 20 000 to 30 000 m³ is observed at the front of Stemhesten (Figure 41). A spur with little internal deformation is separated from the mountain side by a saddle (Figure 41a), but there are no structures delimiting a large unstable rock slope. The subvertical valley-dipping foliation enables toppling failures. Large boulders are deposited at the foot of the slope and a fresh rock slope failure of a smaller volume shows that there is some activity at Stemhesten. The possible rock slope failures at Stemshesten have relatively small volumes and they would not form a rock avalanche with an excessive run-out distance, i.e. longer than that of rockfalls.

Recommendation: There are no signs that the Stemshesten rock slope might fail in a massive rock slope failure. No further investigations or displacement measurements are necessary and the hazard and risk classification will not be made. Rockfalls and small rock avalanches are however possible and their run-out area is given by the rockfall susceptibility map or more detailed hazard maps, where available.

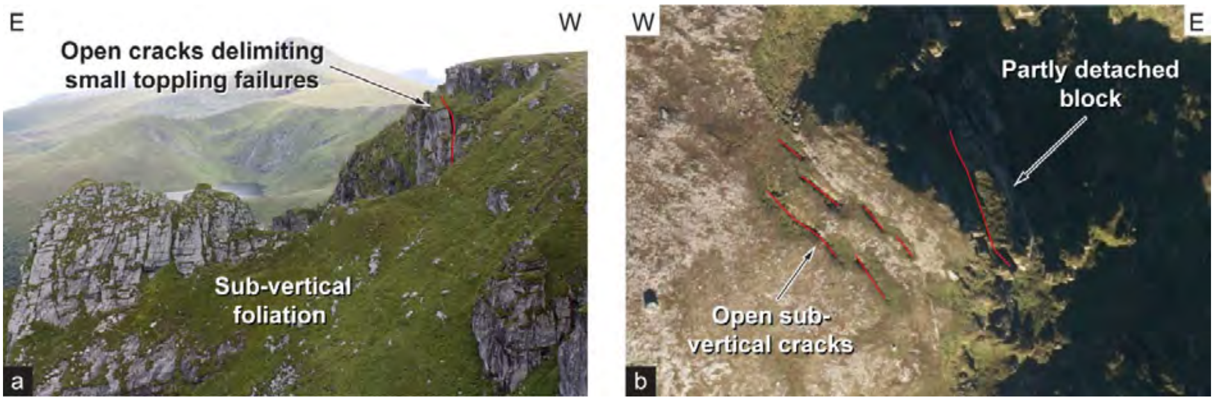

Figure 41: **Photographs of the Stemshesten: a) the intact spur in the East is separated from the mountainside by a saddle, but there are no indications of past displacements; b) toppling failures are possible along the subvertical foliation delimiting small blocks.**

5.1.3 Talstadhesten

Talstedhesten (Figure 39) is located on a northwest-facing slope 600 m above Langvatnet Lake. A helicopter reconnaissance flight made in 2012 showed an unstable rock slope that is delimited by a 350 m long discontinuous back-crack (Figure 42a). It is partly open and partly a shallow depression. The unstable rock slope is free on both lateral sides, but no basal sliding surface is visible. The apparent downthrow indicates small past displacements. Foliation is mainly steeply NE-dipping (dipping perpendicular to the mountain side), but is folded and the axial plane seems to be valley-dipping (Figure 42b). The absence of large scree deposits below the densely fractured mountainside indicates little activity. A massive rock slope failure from Talstadhesten would form a rock avalanche and create a displacement wave in Langvatnet Lake.

Recommendation: A possible rock avalanche from the Talstadhesten instability will have consequences. Geological field mapping is necessary to evaluate the structural and geological conditions and to quantify past displacements. The hazard and risk classification will be made after this field mapping. Further follow-up activities will be decided based on this classification.

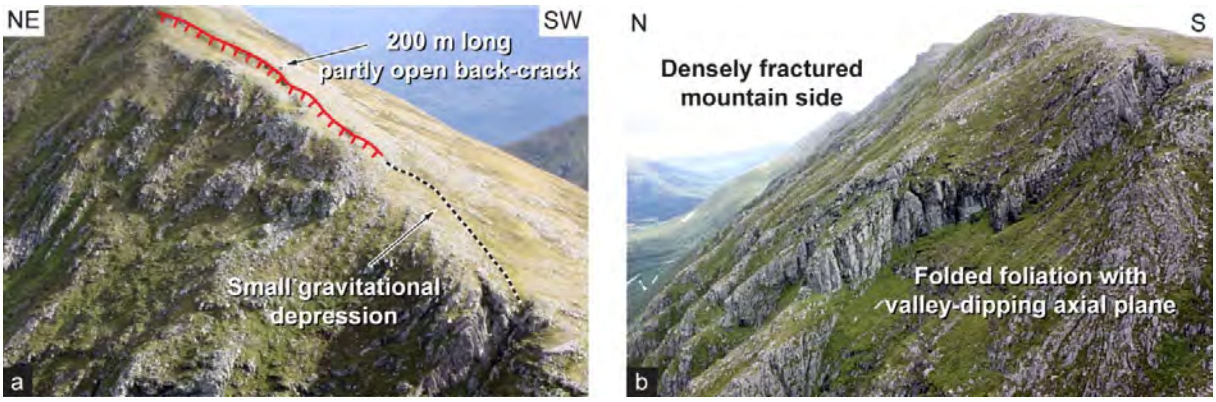

Figure 42: **Photographs of the Talstadhesten unstable rock slope: a) the back-scarp is partly open and partly a shallow depression; b) the rock mass is highly fractured and folded along a valley-dipping axial plane.**

5.2 Midsund municipality

There are four known sites located in Midsund municipality, which are all described in this report (Figure 43).

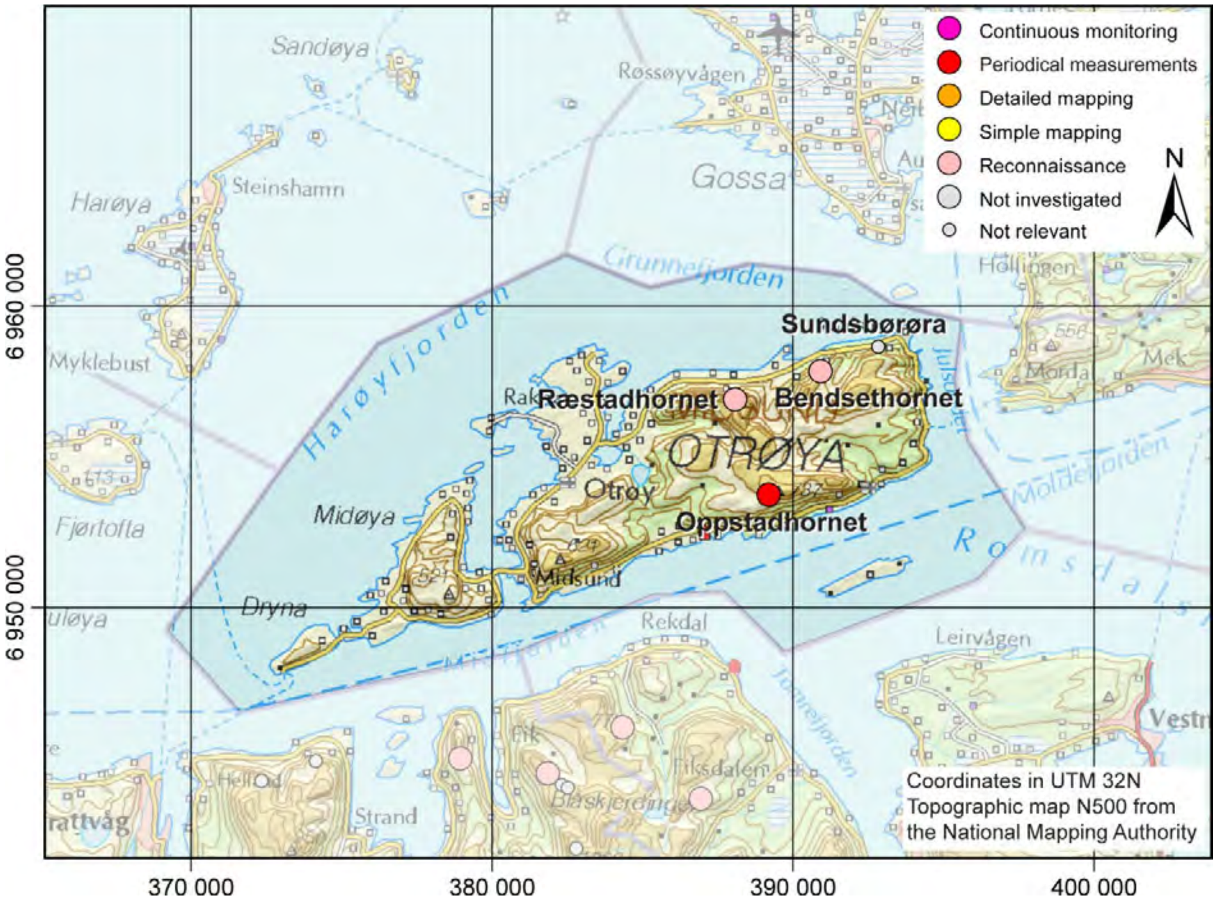

Figure 43: Map of the four known sites in the Midsund municipality with their investigation status. The name of the sites described in this report is shown.

5.2.1 Bendsethornet

Bendsethornet is located on a northwest-facing slope 540 m above Grunnefjord (Figure 43) between Ræstad and Bendset. The site has earlier been described under the name Kløvhaugen by Dahle et al. (2011) and overflown by helicopter in 2012. The back-crack is not fully developed (Figure 44b). A set of persistent steep N-dipping fractures forms possible sliding surfaces in the upper part of the slope (Figure 44a). Foliation is moderately S-dipping (Figure 44b). Observations from helicopter suggest that the instability is possibly separated into two compartments: a relatively intact upper block is resting on a lower block with a strongly fractured or even crushed base (Figure 44a). The total volume is estimated to approximately 2 million m³. A small part of the instability was blasted in the 1930s and iron bolts were installed across the back-crack in 1937. The bolt distances were measured in 2009 and no opening of the crack was recorded (Dahle et al. 2011a). A rock avalanche from Bendsethornet would impact some buildings and might create a displacement wave in Grunnefjord.

Recommendation: A possible rock avalanche from the Bendsethornet instability will have consequences. Geological field mapping is necessary to evaluate the structural and geological conditions and to quantify past displacements. The hazard and risk classification will be made after this field mapping. Further follow-up activities will be decided based on this classification.

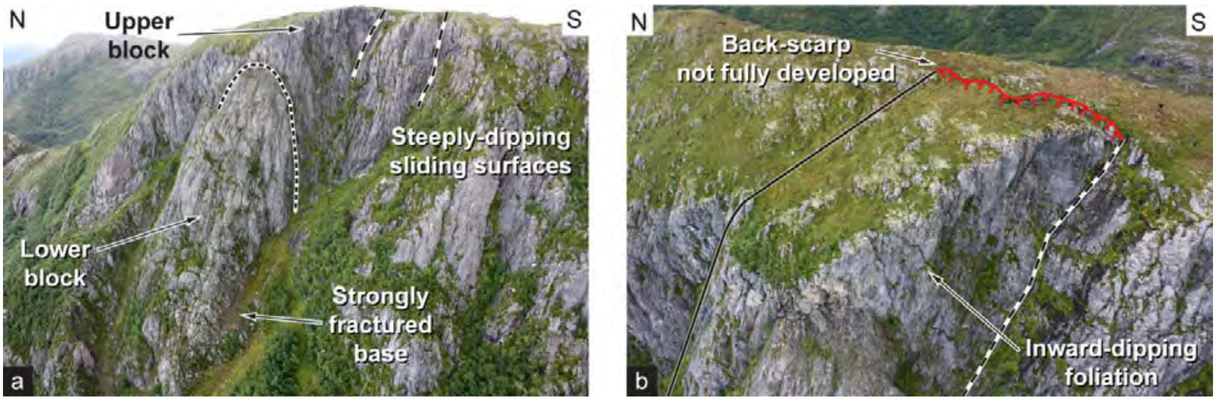

Figure 44: Photographs of the Bendsethornet instability: a) the instability is divided into an intact upper block and a strongly fractured lower block; b) detail of the upper block showing a partly open back-scarp and one of the possible sliding surfaces.

5.2.2 Oppstadhornet

Oppstadhornet is located on a southeast-facing slope 730 m above Midfjord (Figure 43). This large, complex unstable rock slope has been studied in the field since the 1990s (Robinson et al. 1997, Anda et al. 2000, Blikra et al. 2002a, Blikra et al. 2002b, Braathen et al. 2004, Dahle et al. 2011a). Further investigations included geophysical investigations (Dalsegg et al. 2007), numerical modelling (Bhasin and Kaynia 2004, Dahle 2004, Derron et al. 2005b) and cosmogenic nuclide dating (Hermanns et al. 2013). Since 2003 the unstable rock slope is measured periodically using dGNSS. Here, the latest results from dGNSS measurements and cosmogenic nuclide dating are presented.

A total of 12 measurement points were set out between 2003 and 2004 on the south-western part of the Oppstadhornet unstable rock slope, which has undergone large displacements in the past and is actively moving (Figure 45). The points were yearly measured between 2003 and 2008, and again in 2011. The points in the uppermost part of the slope (OT-2, OT-4 to OT-7 and OT-15) have significant displacements in 3D with displacement rates ranging from 2.1 to 2.8 mm/year. The displacement vectors are downslope SSE to SSW directed and moderately to steeply (46° to 70°) plunging. In the middle part of the unstable rock slope (at points OT-9 and OT-11) displacement vectors have a shallower plunge angle of 37°. The high displacement rates at OT-9 of 4.3 mm/year are incoherent with the other measurements and a field verification of the setting of this point needs to be undertaken. The points in the lower part of the slope do not have significant displacements over the 2003–2011 measurement period.

Seven additional measurement points were installed in 2005 on the north-eastern part of the slope based on results of geophysical investigations that indicate a possible sliding surface under this slope section. However, no significant displacements are recorded between 2005 and 2011 (Figure 45).

Terrestrial cosmogenic nuclide dating of the back-scarp indicates that the Oppstadhornet rockslide became active ca. 14 200–16 600 years ago when the Scandinavian ice sheet exposed the island from the continental ice sheet (Hermanns et al. 2013). This old age of the Oppstadhornet rockslides contradicts previously published models of the rockslide, which postulate that the slope would fail under an earthquake with a recurrence period of 475 years (Bhasin and Kaynia 2004). Also, such seismic accelerations or even stronger ones have repeatedly occurred in the past thousands of years and did not cause the total failure of the slope. Displacement rates inferred from cosmogenic nuclide dating indicated a deceleration from 3.2 mm/year until 10 300 years ago to 0.6 mm/year afterwards. The difference between these long-term slip rates and present displacement rates measured dGNSS is explained by the difference in displacement direction of the uppermost part of the Oppstadhornet rockslide (SSW) compared to the dip direction of the back-scarp (SSE), which is foliation-parallel. The change in long-term slip rates around 10 000 years ago might indicate a possible change in deformation style going from foliation-parallel sliding to oblique displacements (Hermanns et al. 2013).

These results from dGNSS measurements and cosmogenic nuclide dating need to be further analysed in order to propose an improved geological model and included in the hazard and risk classification of the Oppstadhornet unstable rock slope.

Recommendation: Significant displacements are measured at Oppstadhornet. Periodic displacement measurements using dGNSS should be continued with 1–3 years interval. The setting of dGNSS measurement point OT-9 needs to be verified in the field. The hazard and risk classification needs to be made and further follow-up activities will be decided based on this classification.

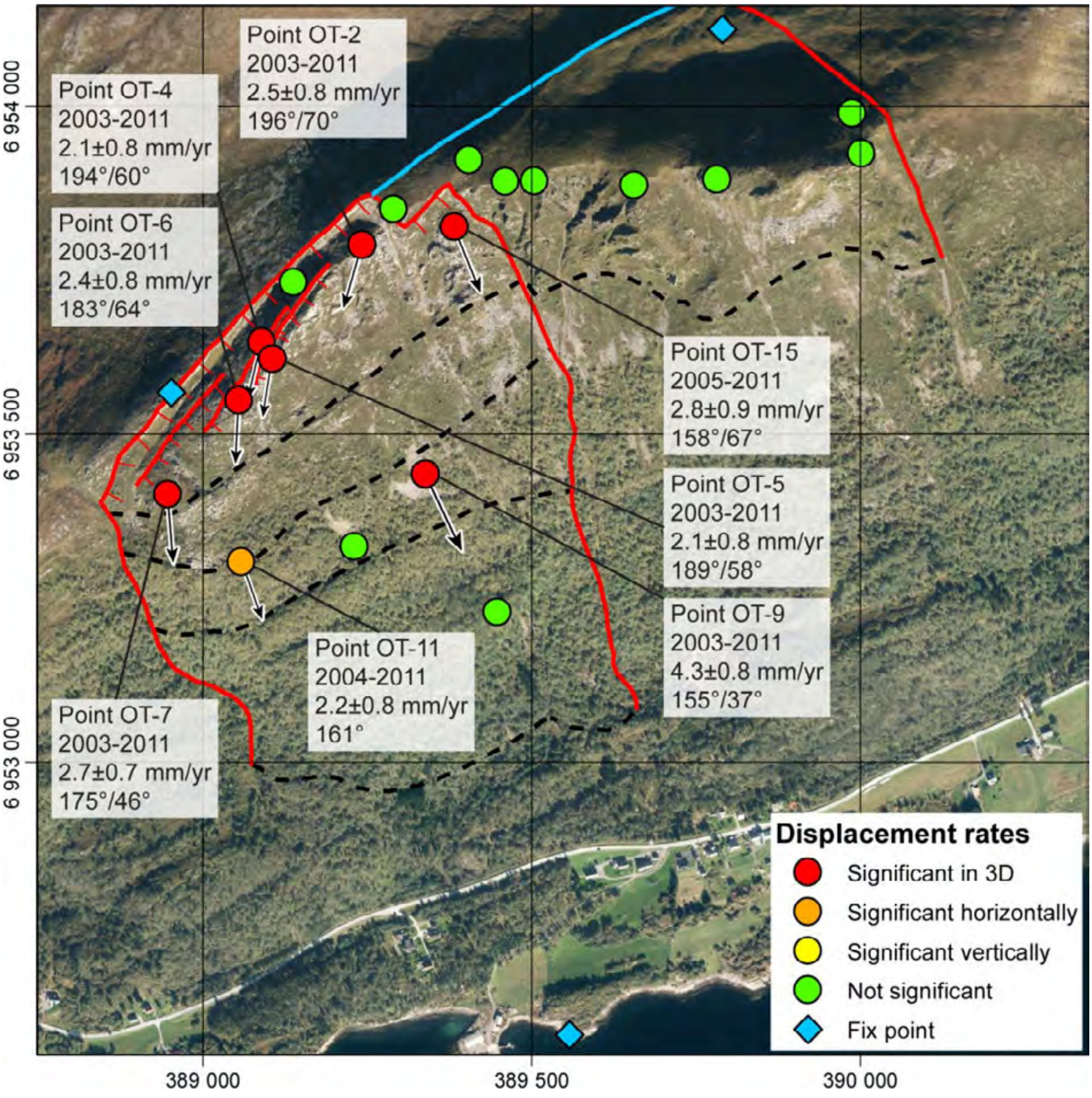

Figure 45: Map of the Oppstadhornet unstable rock slope with the location of dGNSS points for periodic displacement measurements and average displacement vectors for the 2003–2011 measurement period.

5.2.3 Ræstadhornet

Ræstadhornet is situated on a north-facing slope at 650 m above Ræstadvika Bay (Figure 43). The site has been earlier described by Dahle et al. (2011). A helicopter reconnaissance flight in 2012 revealed evident signs of past deformation with a 70 m long, partly open back-crack (Figure 46a). The unstable rock slope is delimited to the SE by a steeply N-dipping surface. This red-coloured surface is relatively planar and might form the basal sliding surface of the Ræstadhornet instability (Figure 46). Inward-dipping foliation surfaces at the western limit of the unstable rock slope might form with the basal sliding surface a wedge failure mechanism (Figure 46b). However, the exact extent of the instability could not be determined based on aerial photographs and helicopter reconnaissance, which impedes to estimate the volume. Large rock slope failures have occurred in the past from Ræstadhornet creating a large talus slope. The debris could be remobilised by a new failure from Ræstadhornet, but this would likely slow down the rock avalanche due to the low angle of the talus slope.

Recommendation: A possible rock avalanche from the Ræstadhornet instability will have consequences. Geological field mapping is necessary to evaluate the structural and geological conditions and to quantify past displacements. The hazard and risk classification will be made after this field mapping. Further follow-up activities will be decided based on this classification.

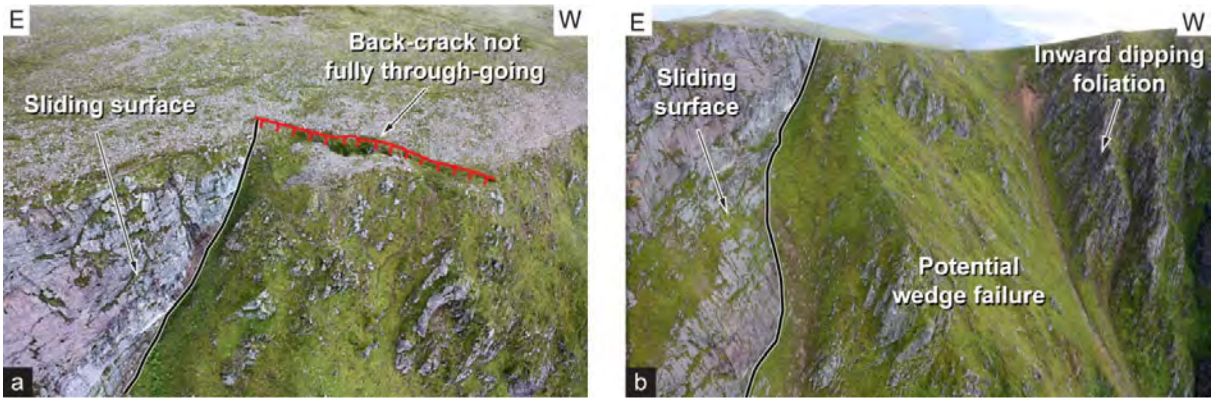

Figure 46: Photographs of the Ræstadhornet instability: a) the back-crack is partly open; b) a potential wedge failure is delimited by the planar, red-coloured sliding surface in the SE and inward-dipping foliation surfaces in the W.

5.2.4 Sundsbørøra

Sundsbørøra is located on a north-facing slope 330 m above Grunnefjord (Figure 43). An old heavily eroded subvertical fault was observed during a helicopter reconnaissance flight in 2012 (Figure 47a). This fault is mostly filled and vegetated and there are no signs of past gravitational displacements. Other major structures are inward-dipping foliation surfaces and do not favor sliding (Figure 47b). There are no structures delimiting a large unstable rock slope. However, rockfall activity is observed at the western end of the investigated rock slope.

Recommendation: There are no signs that the Sundsbørøra rock slope might fail in a massive rock slope failure. No further investigations or displacement measurements are necessary and the hazard and risk classification will not be made. However, rockfalls are possible and their run-out area is given by the rockfall susceptibility map or more detailed hazard maps, where available.

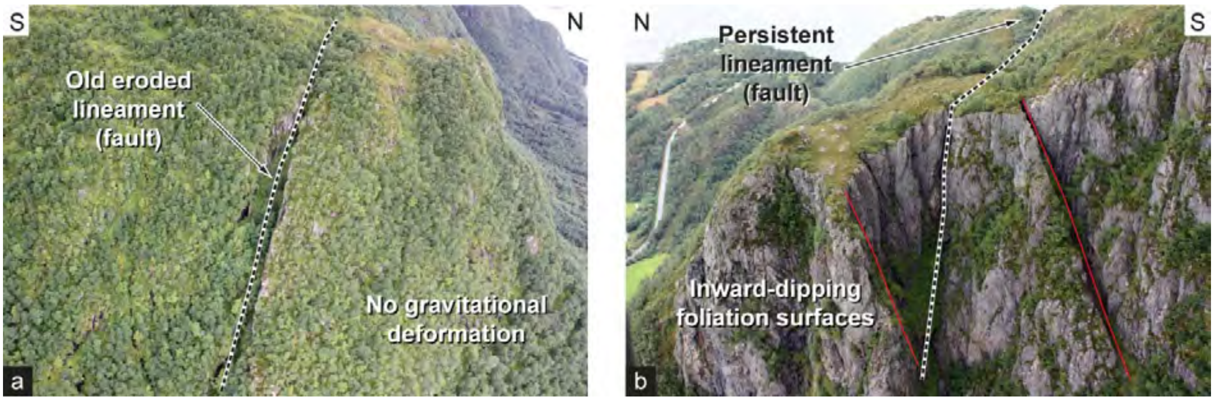

Figure 47: **Photographs of the Sundsbørøra rock slope: a) an old eroded fault delimits the spur to the South; b) main structures are inward-dipping foliation surfaces and impede sliding.**

5.3 Nesset municipality

There are fourteen known sites located in Nesset municipality. Eight of them are described in this report (Figure 48).

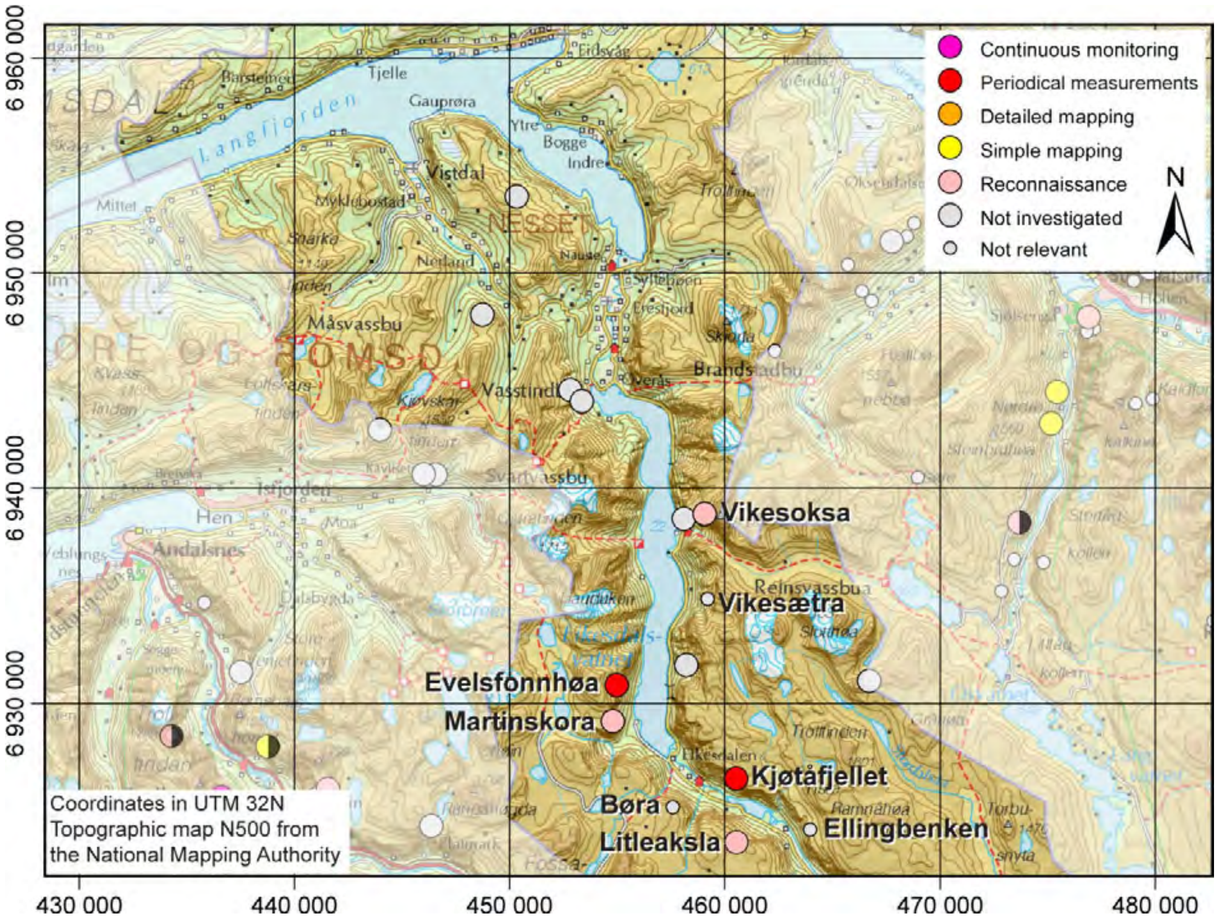

Figure 48: **Map of the 14 known sites in the Nesset municipality with their investigation status. The name of the sites described in this report is shown.**

5.3.1 Børa

Børa is situated on a north-facing slope 1160 m above Eikesdalen Valley (Figure 48). The site was visited in field in 2010. Glacial deposits with sub-rounded blocks mixed with soil cover the top surface at Børa (Figure 49). Soil-creep could lead to shallow landslides. Erosion along a NW-SE-trending fault seems to form the western limit of a potential instability (Figure 49), but there are no open cracks or other structures delimiting an unstable rock slope at Børa. W-E-trending depressions near the edge are likely not related to any gravitational deformation, but are possibly carved out during the last glaciation by drainage near the lateral margin of the glacier in Eikesdalen Valley.

Recommendation: There are no signs that Børa rock slope might fail in a massive rock slope failure. No further investigations or displacement measurements are necessary and the hazard and risk classification will not be made. Rockfalls and debris slides are however possible and their run-out area is given by the rockfall susceptibility map or more detailed hazard maps, where available.

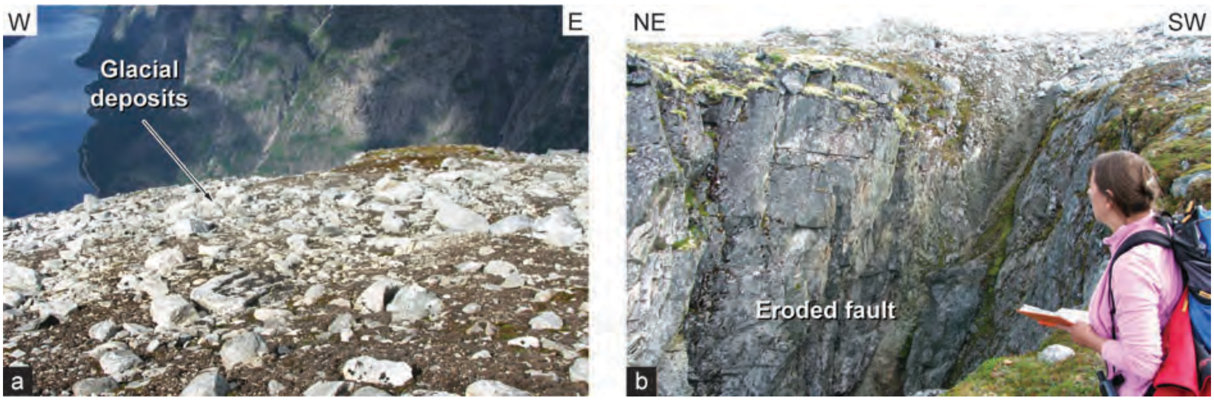

Figure 49: Photographs of the Børa rock slope in Eikesdalen Valley: a) glacial deposits cover the slope; b) an eroded fault could form a lateral release surface, but there are no visible openings and other structures are missing to delimit an unstable rock slope.

5.3.2 Ellingbenken

Ellingbenken is located on a southwest-facing slope 700 m above Setra in Eikesdalen Valley (Figure 48). A helicopter reconnaissance flight in 2010 revealed a conspicuous 2 km-long and 50–100 m wide depression (Figure 50). This depression marks the lithological contact between two gneiss units (Tveten et al. 1998) and is thus not related to gravitational movements of the Ellingbenken rock slope. No major visible cracks were detected. Water ponds inside the depression are also indicating absence of fractured and deformed bedrock. Rockfall deposits are however evident inside the depression and at the cliff side (Figure 50b).

Recommendation: There are no signs that Ellingbenken rock slope might fail in a massive rock slope failure. No further investigations or displacement measurements are necessary and the hazard and risk classification will not be made. However, rockfalls are possible and their run-out area is given by the rockfall susceptibility map or more detailed hazard maps, where available.

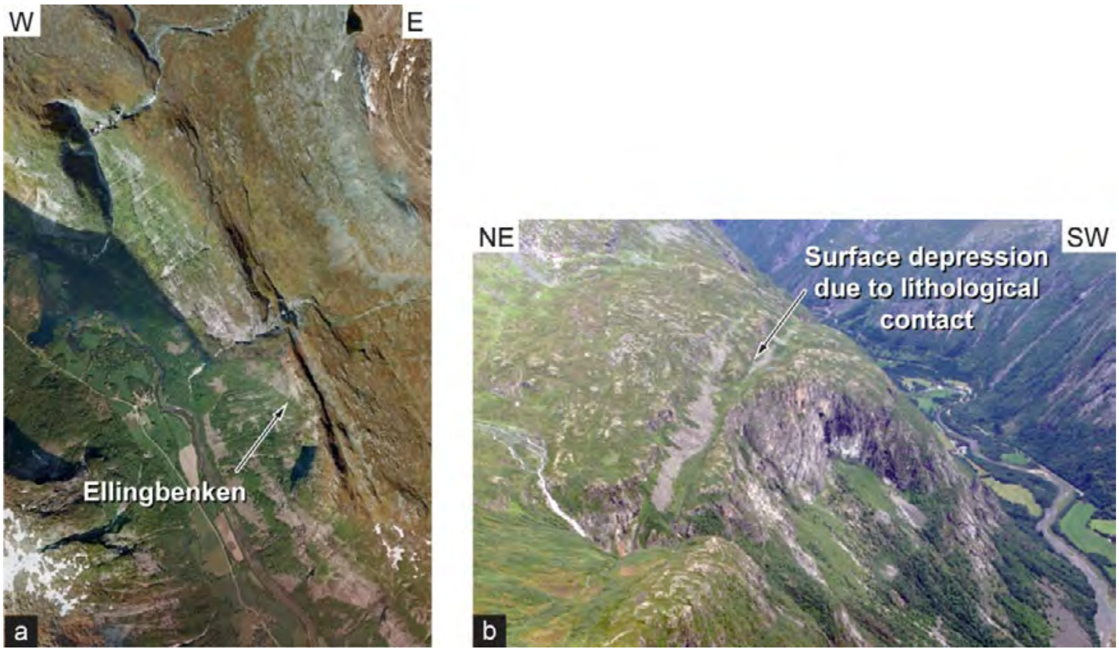

Figure 50: **Photographs of the Ellingbenken rock slope: a) aerial photograph showing a long lineament and depression marking the contact between two gneiss units; b) the lithological contact does not delimit a large unstable rock slope toward the valley.**

5.3.3 Evelsfonnhøa

Evelsfonnhøa is situated on an east-facing slope 980 m above Eikedalsvatnet Lake (Figure 48). A helicopter reconnaissance flight in 2010 showed a large column delimited by an open back-crack (Figure 51). The column has a free lateral limit to the southwest, but there is no visible open lateral release surface in the north. A possible sliding surface is visible at the base of the column (Figure 51b). The structures present at Evelsfonnhøa enable sliding and toppling of the instability.

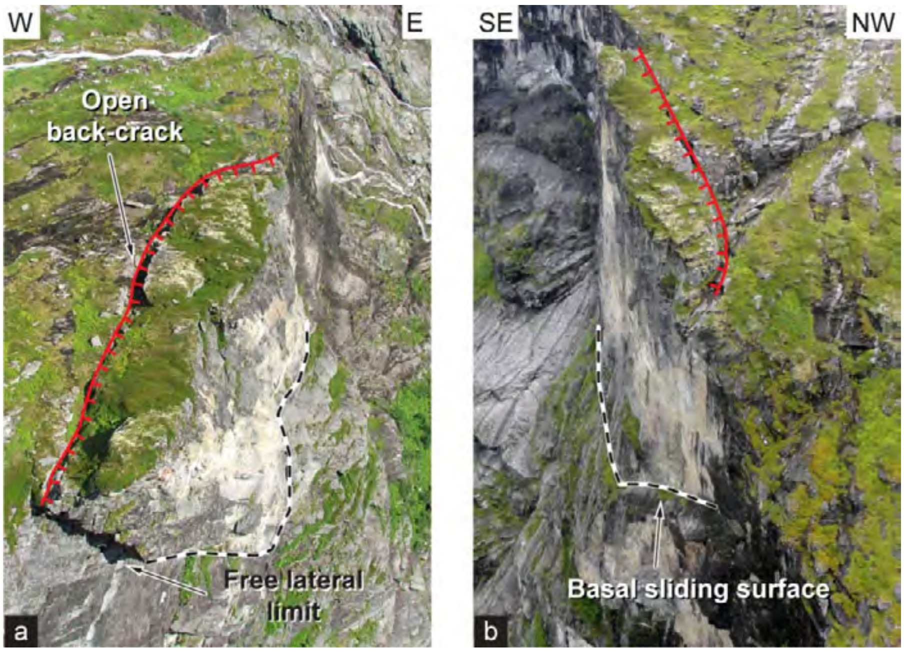

Figure 51: **Photographs of a columnar failure of ca. 110000 m³ developed on Evelsfonnhøa rock slope.**

The Evelsfonnhøa instability is inaccessible to field work. Therefore it was scanned by TLS from two locations around Eikedalsvatnet Lake providing a reference dataset for periodic displacement measurements (Figure 52). TLS data allowed estimating the orientation of the basal sliding surface to moderately NE-dipping (046°/48°) and the back-crack is subvertical dipping to the SE (132°/86°), i.e. straight to the valley side. The volume of the Evelsfonnhøa instability was assessed to 110000 m³ based on TLS data. A failure from Evelsfonnhøa is likely to reach Eikedalsvatnet Lake and cause a displacement wave (Dahle et al. 2011a).

Recommendation: Periodic displacement measurements are started at the Evelsfonnhøa instability, but the time-series is not sufficiently long to determine displacement rates. Periodic displacement measurements using TLS should be continued with 1–3 years interval. Additionally, geological field mapping is necessary to evaluate the structural and geological conditions and to quantify past displacements. The hazard and risk classification needs to be made and further follow-up activities will be decided based on this classification.

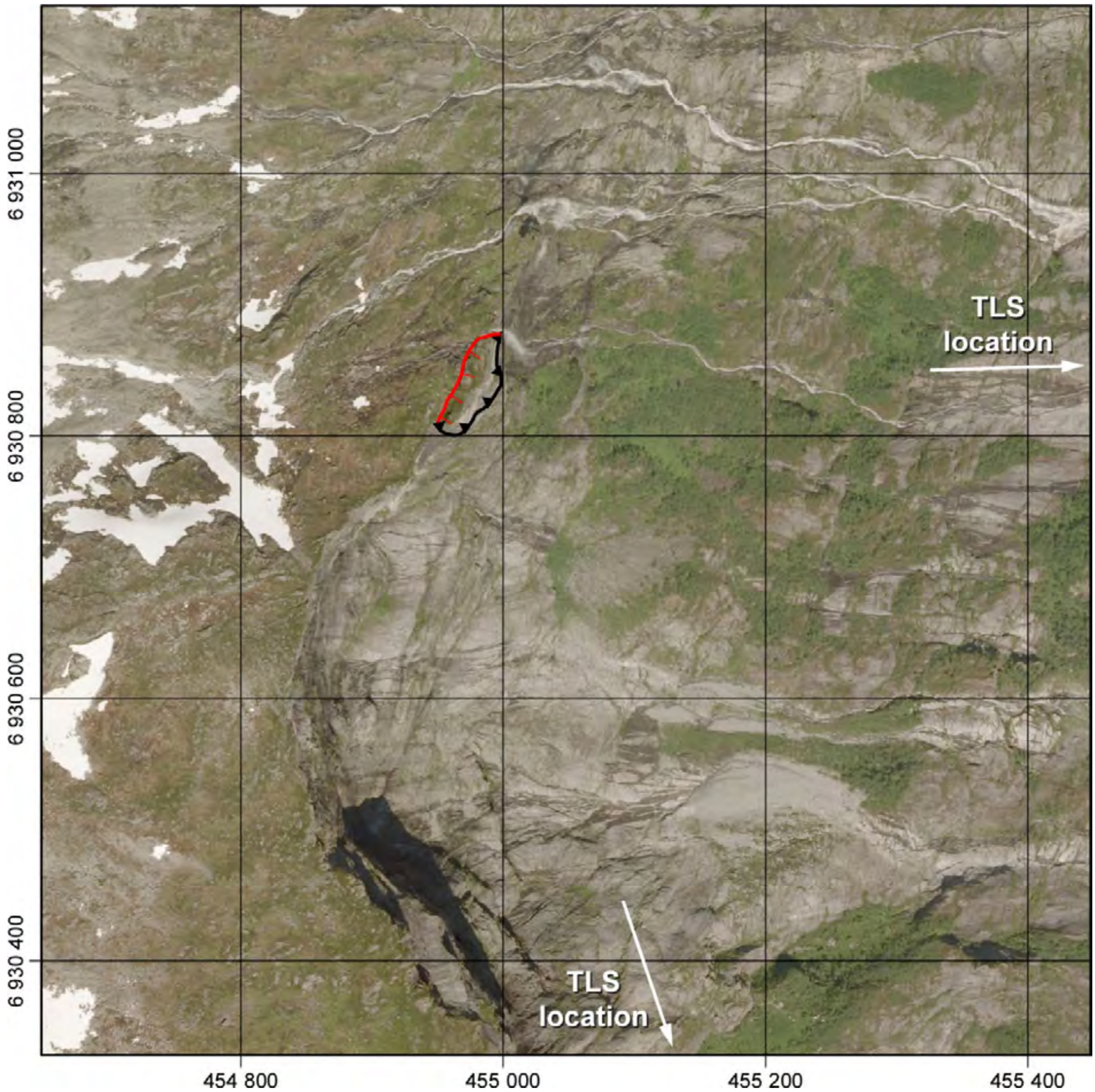

Figure 52: Map of the Evelsfonnhøa instability showing directions to the locations of measurement instrumentation (TLS).

5.3.4 Kjøtåfjellet

Kjøtåfjellet is located on a southwest-facing slope 900 m above Litlevatnet Lake in Eikesdalen Valley (Figure 48). A helicopter reconnaissance flight in 2010 showed an instability with an open back-crack and free lateral limits (Figure 53). A second, partly open back-crack further inward in the mountainside delimits two additional compartments that are separated by a brecciated ancient fault (Figure 53a). In 2011 bolts for tape extensometer measurements were installed at three locations over the back-crack and an internal crack (Figure 54), in order to detect possible widening of the cracks. The Kjøtåfjellet instability was scanned by TLS from two locations in the valley for structural characterization and providing a reference dataset for periodic displacement measurements (Figure 54).

Rock avalanche deposits are found in the Eikesdalen Valley below the Kjøtåfjellet instability (Figure 54). This rock avalanche dammed the valley to form Litlevatnet Lake. The source area of the rock avalanche is not exactly known, but could be located in the surroundings of the present instability at Kjøtåfjellet. Cosmogenic nuclide dating of three rock avalanche deposit samples taken gives an age of 2900 ± 400 years BP.

Recommendation: Periodic displacement measurements are started at the Kjøtåfjellet instability, but the time-series is not sufficiently long to determine displacement rates. Periodic displacement measurements using TLS should be continued with 1–3 years interval. Additionally, geological field mapping is necessary to evaluate the structural and geological conditions and to quantify past displacements. The hazard and risk classification needs to be made and further follow-up activities will be decided based on this classification.

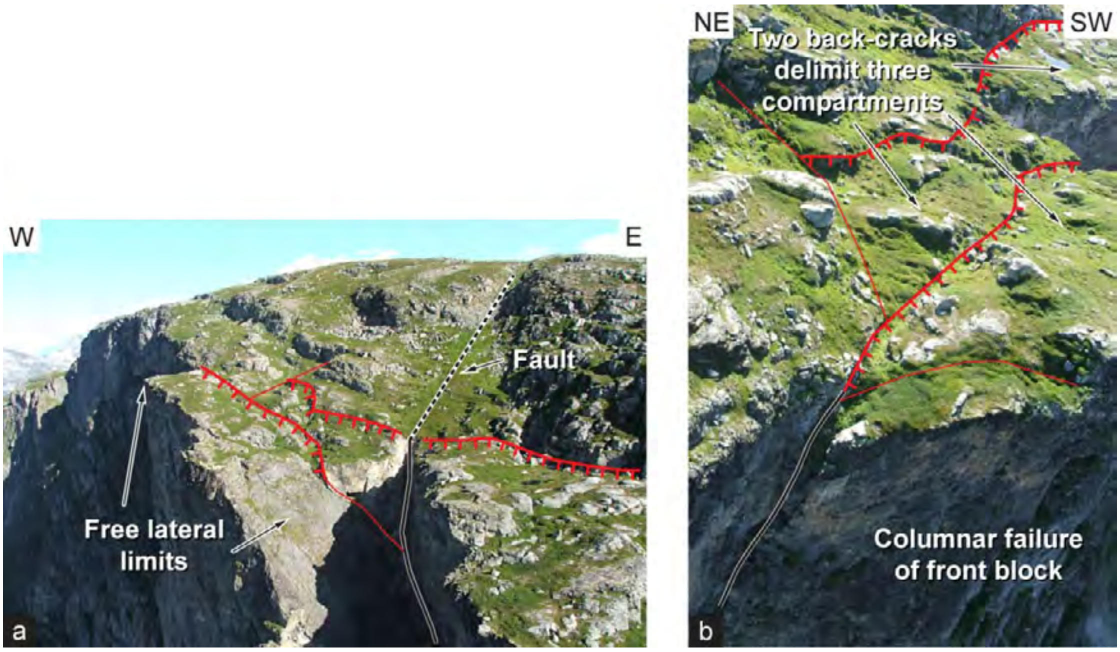

Figure 53: Photographs of the Kjøtåfjellet instability showing the free lateral side limits of the frontal block (left) and the three unstable blocks (right).

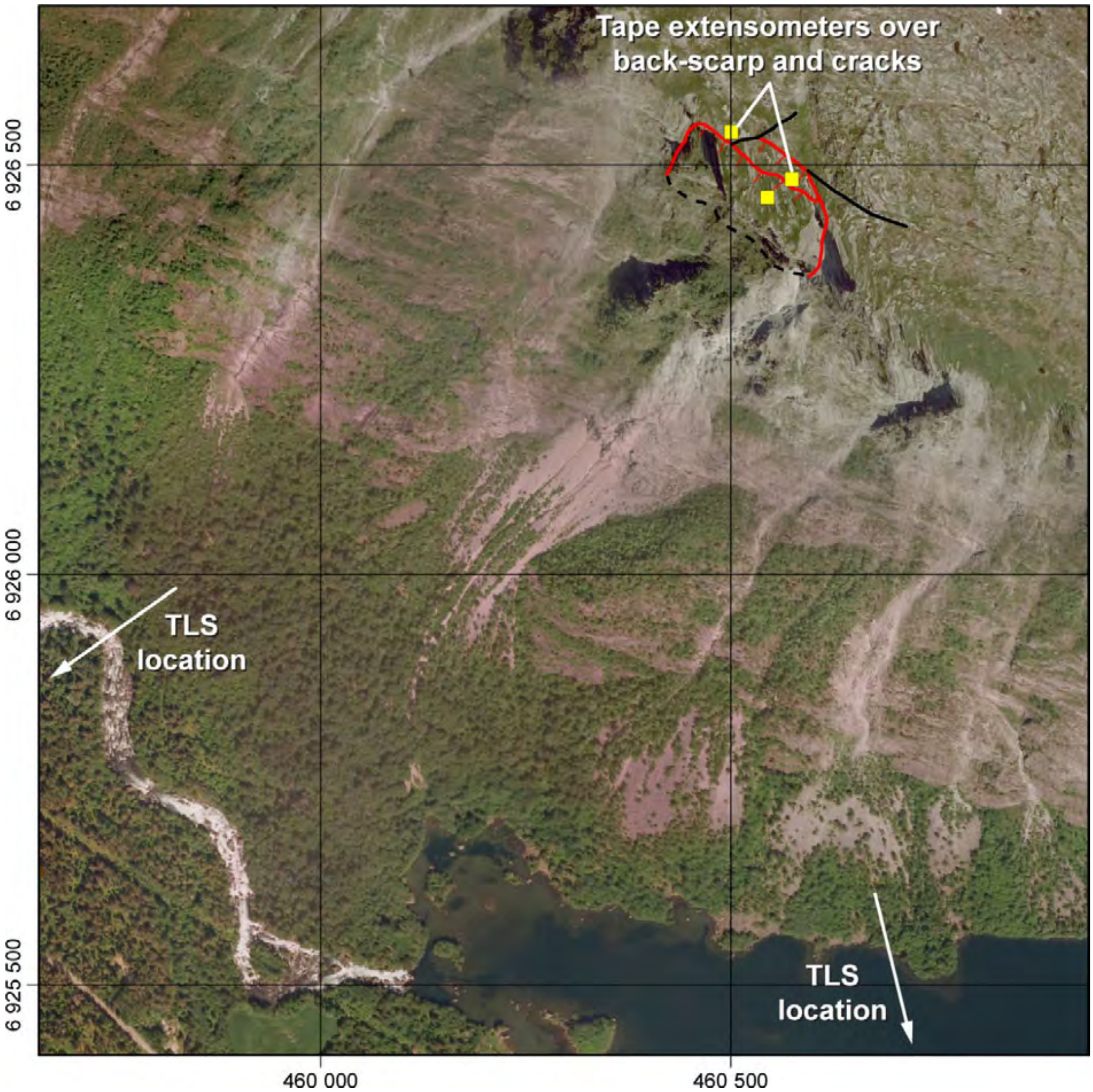

Figure 54: Map of the Kjøtåfjellet instability showing locations of measurement instrumentation (tape extensometer), respectively directions to the locations of measurement instrumentation (TLS).

5.3.5 <u>Litleaksla</u>

Litleaksla is located on a northeast-facing slope at ca. 1060 meters above Litlevatnet Lake in Eikesdalen Valley (Figure 48). The site was observed by helicopter in 2010 and no large instability is currently developed despite the presence of old sliding surfaces, which likely continue inside the remaining rock mass (Figure 55b). Surface depressions form the lateral and rear limit of a potential instability, but no signs of opening or past displacement were observed (Figure 55a). No major cracks are visible on the slope. The surface of the rock slope was probably dismantled by glacial erosion and rockfall activity is conspicuous from the site.

Recommendation: There are no signs that Litleaksla rock slope might fail in a massive rock slope failure. However, a more detailed helicopter reconnaissance flight is planned, focussing on the observed surface depressions.

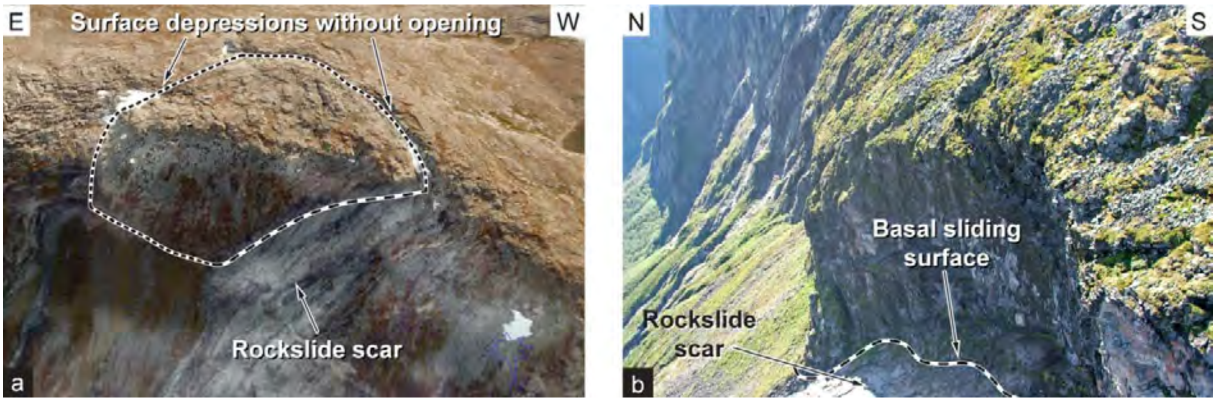

Figure 55: **Photograph of the Litleaksla rock slope: a) 3D view from Norgei3D showing depressions as lateral and rear limit of a potential instability, but no signs of opening or past displacement were observed; b) the basal sliding surface of a past rockslide continues likely into the remaining rock mass.**

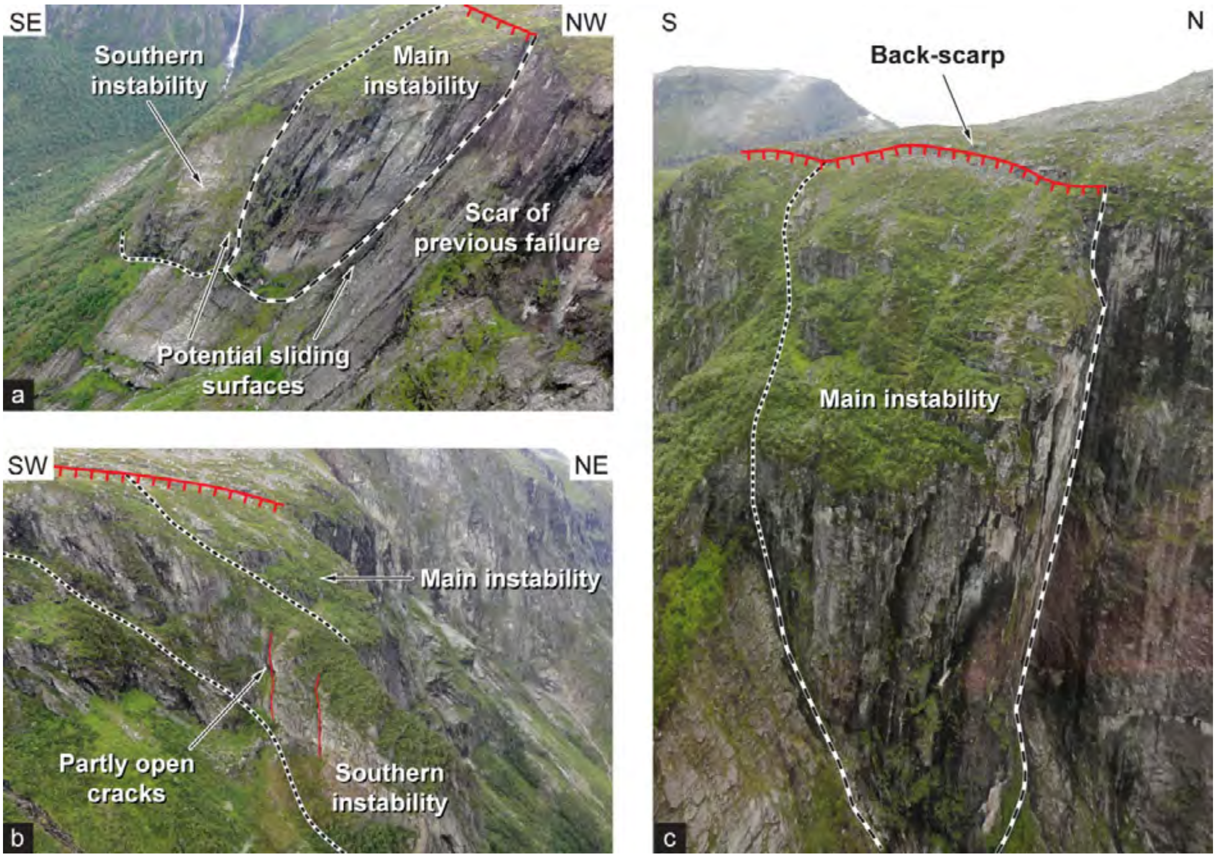

Figure 56: **Photographs of Martinskora unstable rock slope: a) large valley-dipping surfaces form sliding surfaces for past rock slides and the present instabilities; b) the southern instability with fractures inside the block parallel to the main back-crack and with a moderately valley-dipping basal sliding surface; c) wedge failure on steeply NE- and E-dipping sliding surfaces.**

5.3.6 Martinskora

Martinskora is located on an east-facing slope at 820 m above Mardalsbøen settlement on the shore of Eikedalsvatnet Lake (Figure 48). The site was observed by helicopter in 2011 and appears to be a complex unstable rock slope composed of several compartments with different deformation mechanisms (Figure 56).

A previous rockslide occurred along a unique steeply E-dipping surface and large boulders are deposited on the entire slope down to Eikedalsvatnet Lake. The continuation of the same back-bounding surface to the south and a steeply NE-dipping surface may delimit a large unstable rock slope (Figure 56a, c). The two failure surfaces may compose a wedge failure. Structures in the rock body are parallel to these surfaces, but few cracks are opened.

Further to the south, another instability is delimited at its back by the steep E-dipping surface and its base may follow moderately E-dipping sliding surfaces (Figure 56b). A planar rockslide is envisaged to develop at this location and fractures observed in the rock mass appear to be parallel to the main back-crack. The structure separating this southern instability from the main instability is poorly developed and might correspond to the steeply NE-dipping surface involved in the wedge sliding mechanism of the main instability.

The present knowledge about the Martinskora unstable rock slope is insufficient to assess the volume, to define scenarios and thus to assess possible consequences.

Recommendation: A possible rock avalanche from the Martinskora instability will have consequences. Geological field mapping is necessary to evaluate the structural and geological conditions, to quantify past displacements and assess the structures involved in the previous rockslide. The hazard and risk classification will be made after this field mapping. Further follow-up activities will be decided based on this classification.

5.3.7 Vikesoksa

Vikesoksa is situated on a southwest-facing slope 1390 m above Vikeelva River, an eastern tributary of Eikesdalsvatnet Lake (Figure 48). Vikesoksa was observed during a helicopter reconnaissance flight in 2010. At the western tip of the ridge, a steep structure partly detaches a column (Figure 57). The nature of this structure is however unknown, but it is more likely formed by preferential erosion along a pre-existing fault rather than opening of a crack by any displacements of the column. A penetrating set of inherited steeply SW-dipping structures can be seen in the column and provides possible basal sliding surfaces. However, there is no visible activity along the structures delimiting the instability. Rockfall activity from the steep faces of the column is evident.

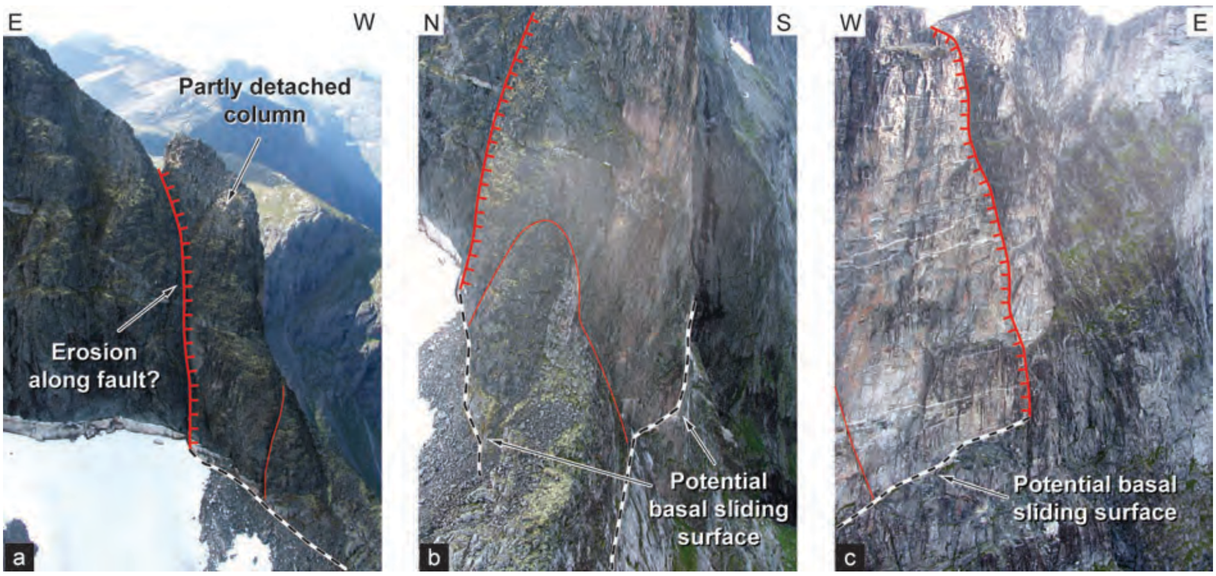

Figure 57: Photographs of Vikesoksa instability displaying the structures which delimit a column. However, no signs of past displacements are observable, apart from rockfall activity from the steep faces of the column.

Recommendation: A possible rock avalanche from the Vikesoksa instability will have consequences. Geological field mapping is necessary to evaluate the structural and geological conditions and to quantify past displacements. The hazard and risk classification will be made after this field mapping. Further follow-up activities will be decided based on this classification.

5.3.8 Vikesætra

Vikesætra is located on a west-facing slope 950 m above Eikesdalsvatnet Lake (Figure 48). The rock slope was observed during a helicopter reconnaissance flight in 2010, but no signs of gravitational movements or open cracks delimiting an unstable rock slope were observed (Figure 58). Some weathering and rockfall activity exists from the rock face.

Recommendation: There are no signs that the Vikesætra rock slope might fail in a massive rock slope failure. No further investigations or displacement measurements are necessary and the hazard and risk classification will not be made. However, rockfalls are possible and their run-out area is given by the rockfall susceptibility map or more detailed hazard maps, where available.

Figure 58: Photograph of Vikesætra rock slope showing rockfall activity from the steep cliff.

5.4 Rauma municipality

There are 27 known sites located in Rauma municipality. Thirteen of them are described in this report (Figure 59).

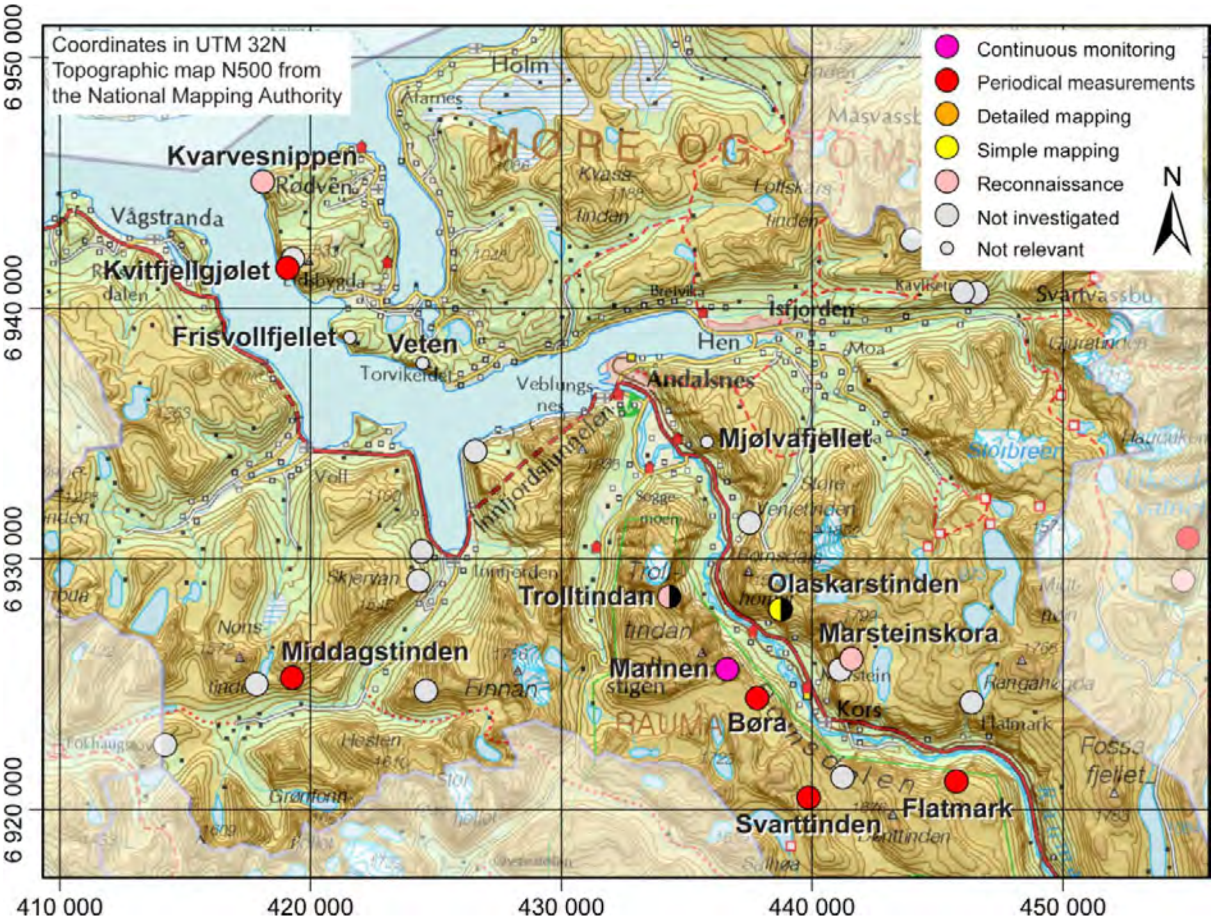

Figure 59: Map of the 27 known sites in the Rauma municipality with their investigation status. Potential unstable rock slopes are also shown with a half-masked symbol (◑). The name of the sites described in this report is shown.

5.4.1 <u>Børa</u>

Børa is located on a northeast-facing slope 990 m above Marstein in Romsdalen Valley (Figure 59). This large, complex unstable rock slope has been studied in the field since the 1990s (Anda et al. 2000, Blikra et al. 2002a, Braathen et al. 2004, Blikra et al. 2006, Henderson and Saintot 2007, Dahle et al. 2011a, Saintot et al. 2011b, Saintot et al. 2012) and investigated by geophysics (Dalsegg and Tønnesen 2004). The unstable rock slope is periodically measured using dGNSS since 2003 and TLS since 2008. New TLS acquisitions from the valley bottom were made in 2012, but they cannot be compared to previous scans acquired from the top of the unstable rock slope due to the large difference in view angles and coverage. Here, the latest results from dGNSS measurements are presented.

A total of 17 measurement points (15 in 2003, one in 2004 and one in 2009) were set out on the Børa unstable rock slope, as well as on localised, detached blocks along the front cliff of the unstable rock slope (Figure 60). All points were measured in 2004, 2006 and 2010, but only selected points were measured in 2008, 2009 and 2012. Points with significant displacements over the 9 years measurement period are mainly located along the frontal cliff on detached blocks (points B-4 and B-6) and compartments of the unstable rock slope, which might fail individually from the main instability (points B-1, B-TP and B-N1).

The displacement rates measured on the detached blocks are 13.8 and 6.3 mm/year for points B-4 and B-6, respectively (Figure 60). The displacement directions to the NE and to the N, respectively, are matching with the kinematics given by the orientation of major structures delimiting these blocks. The plunge of the displacement vectors are relatively gentle (10° and 30°, respectively). This indicates a toppling component of the movement, especially for the detached block at point B-4.

Point BN-1 at the SE-end of the unstable rock slope moves 5.0 mm/year in a downslope direction with a plunge angle of 45° (Figure 60). These high displacement rates compared to the surroundings suggest that the ridge surrounding point BN-1 is detached from the total unstable area. However, the lateral limit of this compartment is not visible in the field. The prominent graben structure observed behind this ridge might also be the expression of these increased displacement rates.

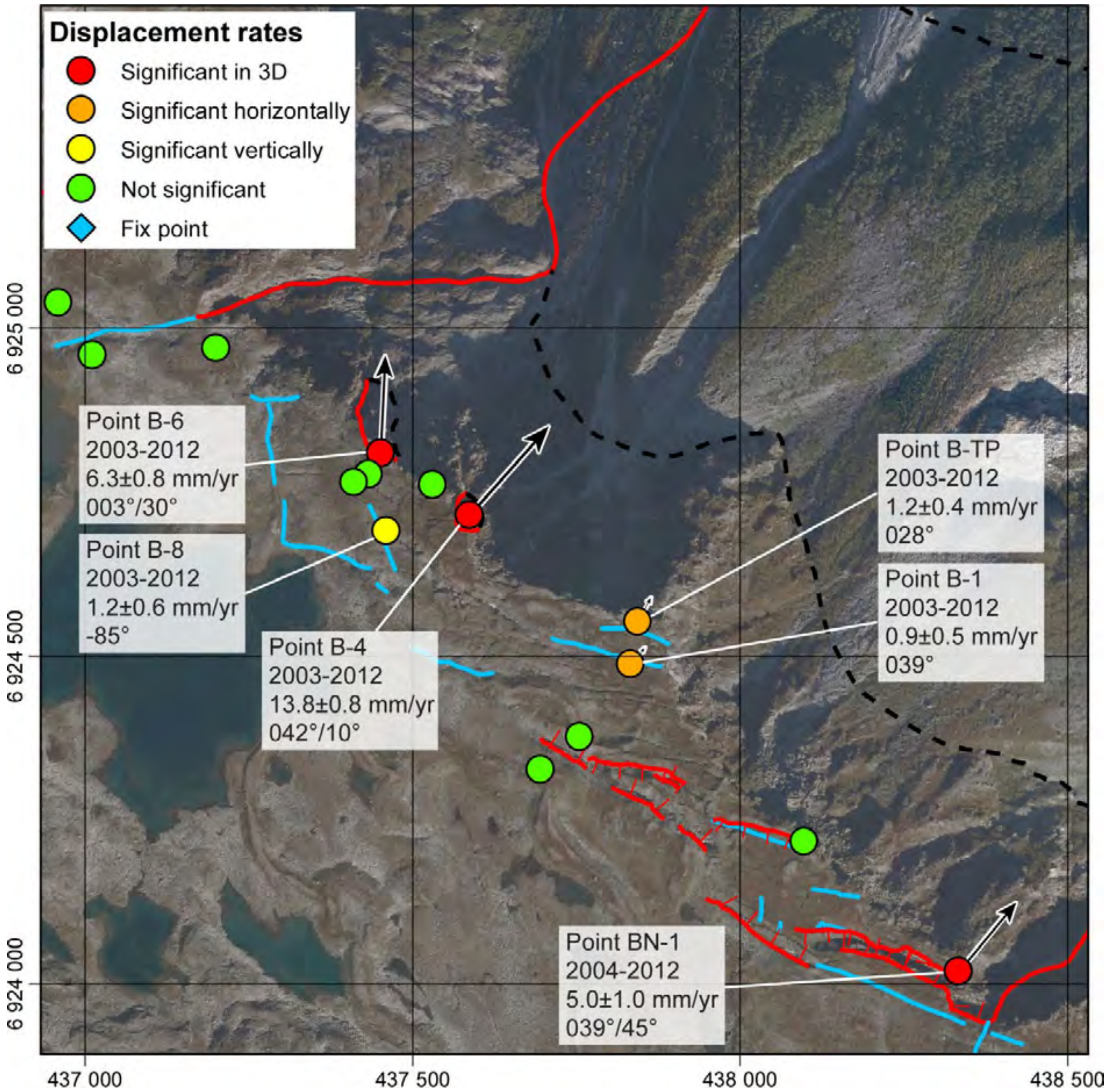

Figure 60: **Map of the Børa unstable rock slope with the location of dGNSS points for periodic displacement measurements and average displacement vectors for the 2003–2012 measurement period.**

Two points in the central part of the Børa unstable rock slope (B-1 and B-TP) have significant horizontal displacements with 0.9 to 1.2 mm/year in NNE-direction (Figure 60). However, no vertical trend was observed, which might also indicate toppling movements. The measurement point B-8 is located on the plateau more than 100 m inwards from the frontal cliff, where active movements are generally observed at Børa. It shows a significant vertical displacement in upward direction by 1.2 mm/year. Such a displacement is inconsistent with general gravitational deformation and has only limited significance since other surrounding points are not significantly moving (Figure 60). Point B-8 might thus be placed on a small, local block that is extruded due to differential movements between compartments of the unstable rock slope.

Recommendation: Significant displacements are measured at Børa. Periodic displacement measurements using dGNSS and TLS should be continued with 1–3 years interval. The hazard and risk classification needs to be made and further follow-up activities will be decided based on this classification.

5.4.2 Flatmark

Flatmark is located on a north-facing slope 920 m above Skiri and Flatmark in Romsdalen Valley (Figure 59). This complex unstable rock slope is divided into several compartments (Figure 61) that could individually fail although they are structurally similar. Field mapping was made in 2006 and several studies describe this unstable rock slope (Henderson and Saintot 2007, Dahle et al. 2011a, Saintot et al. 2011b, Saintot et al. 2012). The unstable rock slope is periodically measured using dGNSS since 2006, TLS since 2007 and tape extensometer since 2011. Here, the latest results from dGNSS and TLS measurements and cosmogenic nuclide dating of rock avalanche deposits are presented. No repetitive tape extensometer measurements are made up to now.

Six dGNSS measurement points were installed at Flatmark in 2006 (Figure 61). The points FM-3, FM-4 and FM-7 are located on detached compartments that have obviously moved in the past. All points were measured again in 2007, 2008 and 2011, but no significant displacements were recorded over the 5 years measurement period.

Periodic displacement measurements by TLS focused on the western compartment of the Flatmark unstable rock slope, which is back-bound by a more than 20 m wide graben (located at dGNSS measurement point FM-3) (Figure 61). Repetitive TLS acquisitions were made in 2011, but no significant changes are detected over the 3 years measurement period. New TLS acquisitions from the valley bottom were made in 2012, but they cannot be compared to previous scans acquired from the top of the unstable rock slope due to the difference in the view angles.

Old rock avalanche deposits that have probably dammed the Rauma River are located downward of the Flatmark unstable rock slope. Cosmogenic nuclide dating of three rock avalanche deposit samples give an age of 11 700 ± 1000 years.

Recommendation: No significant displacements are measured up to now at Flatmark. Periodic displacement measurements using dGNSS should be continued with 3–5 years interval. The hazard and risk classification needs to be made and further follow-up activities will be decided based on this classification.

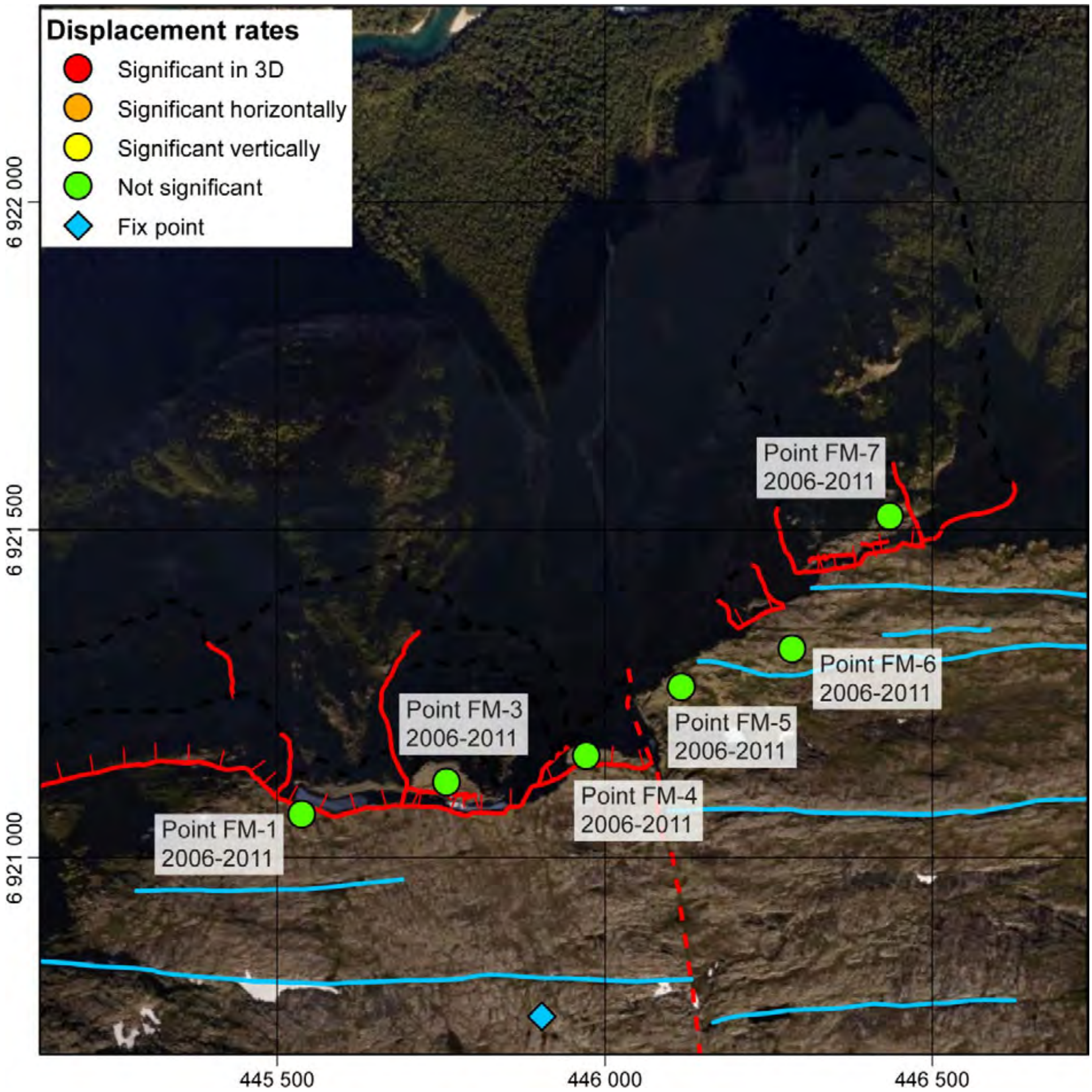

Figure 61: **Map of the Flatmark unstable rock slope with the location of dGNSS points for periodic displacement measurements. No significant displacements were detected over the 2006–2011 measurement period.**

5.4.3 Frisvollfjellet

Frisvollfjellet (Figure 59) is situated on a southwest-facing slope above Romsdalsfjord south of Norvika. The site was surveyed from helicopter in 2011. Several gullies are eroded along the subvertical foliation (Figure 62). At Frisvollfjellet there is neither an open back-crack nor other structures necessary to delimit an unstable rock slope. Small columns delimited by the foliation and subvertical discontinuities might fail by toppling, but the volume (tens to hundreds of m^3) is too small to cause a significant displacement wave in Romsdalsfjord.

Recommendation: There are no signs that the Frisvollfjellet rock slope might fail in a massive rock slope failure. No further investigations or displacement measurements are necessary and the hazard and risk classification will not be made. However, rockfalls are possible and their run-out area is given by the rockfall susceptibility map or more detailed hazard maps, where available.

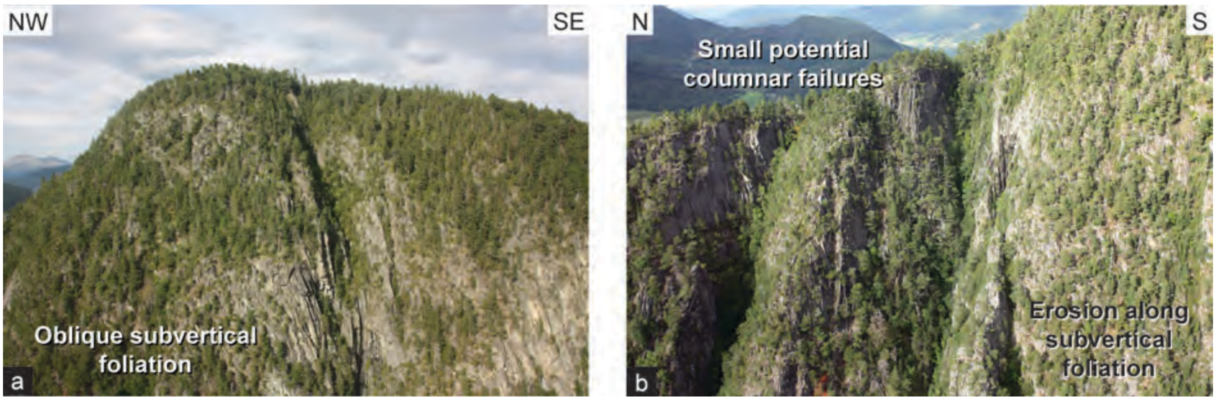

Figure 62: **Photographs of the Frisvollfjellet rock slope: a) the subvertical foliation is locally eroded forming deep gullies; b) small columns are delimited by the foliation and subvertical joints.**

5.4.4 Kvarvesnippen

Kvarvesnippen (Figure 59) is located on a southwest-facing slope 390 m above Romsdalsfjord. A helicopter reconnaissance flight in 2012 revealed an eroded, persistent lineament (Figure 63), which might form the lateral release surface for an instability located south of it. There are no visible openings along this potential lateral release surface. The instability is free on all other sides, including upward at the back due to erosion. However, there are no major discontinuities visible that might form a basal sliding surface. A massive failure of the Kvarvesnippen instability would create a displacement wave in Romsdalsfjord.

Recommendation: A possible rock avalanche from the Kvarvesnippen instability will have consequences. Geological field mapping is necessary to evaluate the structural and geological conditions and to quantify past displacements. The hazard and risk classification will be made after this field mapping. Further follow-up activities will be decided based on this classification.

Figure 63: **Photographs of the Kvarvesnippen instability: an eroded regional fault forms a potential lateral release surface and the instability is free on all other sides.**

5.4.5 Kvitfjellgjølet

Kvitfjellgjølet (Figure 59) is located on a southwest-facing slope 310 m above Romsdalsfjord. A helicopter reconnaissance flight in 2011 revealed an open continuous back-crack delimiting an unstable rock slope (Figure 64, Figure 65). The instability has also a clear basal sliding surface, which was likely already involved in rock slope failures of the surrounding slopes. Fresh rockfall scars above the basal sliding surface might indicate internal deformation of the rock slope and is thus a sign of activity of the rockslide (Figure 64a). The northern boundary of the instability is formed by a deeply eroded gully and is thus free. A possible subblock is found in the upper part of the instability with a clear sliding surface at its base (Figure 64a).

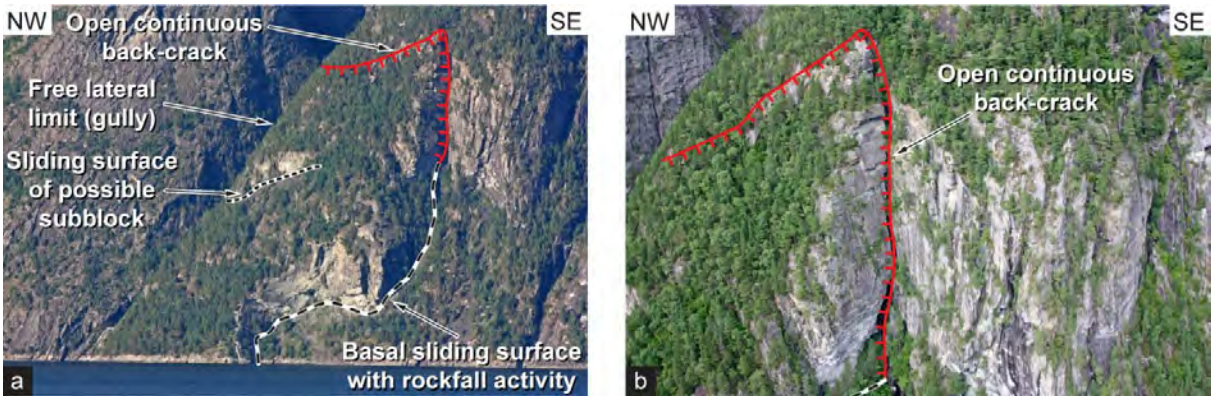

Figure 64: **Photographs of the Kvitfjellgjølet instability: a) the unstable rock slope is delimited by an open back-crack, a gully as free lateral limit and a well marked basal sliding surface; b) detail of the open continuous back-crack.**

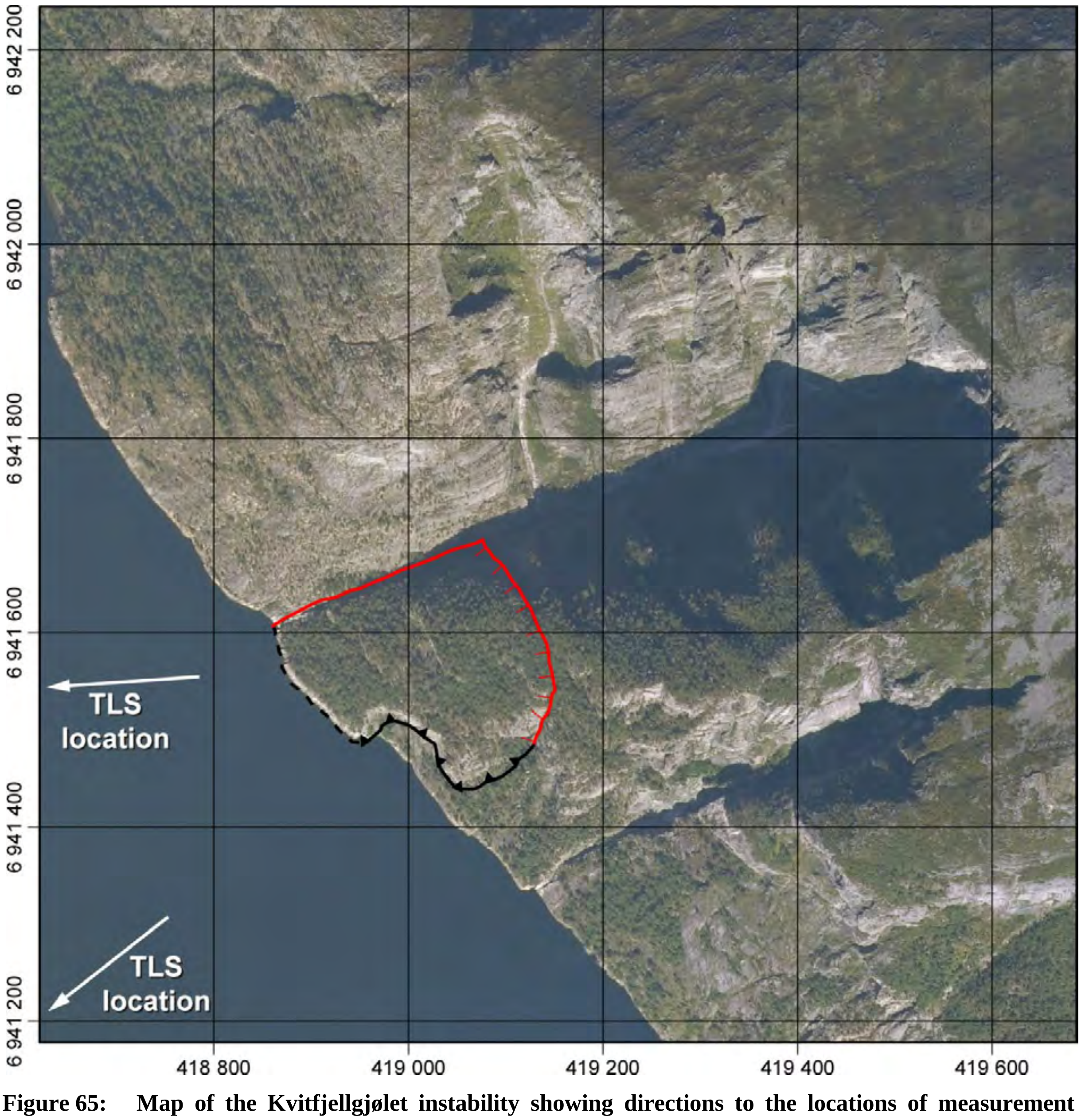

Figure 65: **Map of the Kvitfjellgjølet instability showing directions to the locations of measurement instrumentation (TLS).**

The Kvitfjellgjølet instability is inaccessible for field work. Therefore it was scanned by TLS in 2012 from two locations on the opposite side of Romsdalsfjord providing a reference dataset for periodic displacement measurements (Figure 65). Additionally, a test with ground-based InSAR measurements was performed in 2012 by Åknes/Tafjord Early-Warning Centre. This test showed that periodic displacement measurements with ground-based InSAR is feasible, but the results may not be optimal due to (1) poor signal strength inherent to the long distance and (2) atmospheric disturbances caused by the fjord (Kristensen 2012).

The TLS dataset and the observed structures allow estimating the volume of the Kvitfjellgjølet instability to 2.5 million m³. A massive failure from Kvitfjellgjølet will cause a displacement wave in Romsdalsfjord.

Recommendation: Periodic displacement measurements are started at the Kvitfjellgjølet instability, but the time-series is not sufficiently long to determine displacement rates. Periodic displacement measurements using TLS should be continued with 1–3 years interval. The hazard and risk classification needs to be made and further follow-up activities will be decided based on this classification.

5.4.6 Mannen

Mannen is located on a northeast-facing slope 1215 m above Rønningen in Romsdalen Valley (Figure 59). This large, complex unstable rock slope has been extensively studied since the 2000s with:

- field mapping and geomorphic interpretations (Henderson and Saintot 2007, Dahle et al. 2008, Dahle et al. 2011a, Dahle et al. 2011c, Saintot et al. 2011b, Saintot et al. 2012);
- geophysical investigations of the unstable rock slope (Dalsegg and Rønning 2012) and deposits in the valley (Tønnesen 2009);
- borehole investigations (Saintot et al. 2011a, Elvebakk 2012, Oppikofer et al. 2012b);
- numerical slope stability modelling (Farsund 2011);
- run-out modelling (Dahle et al. 2011b);
- continuous monitoring instrumentation (Kristensen and Blikra 2011).

The unstable rock slope was measured periodically using dGNSS between 2004 and 2010 and by TLS from 2008 to 2010. Since 2009 the Mannen unstable rock slope is continuously monitored by the Åknes/Tafjord Early-Warning Centre. Results from the periodic displacement measurements by TLS are reported in Saintot et al. (2011a). Here, the latest results from dGNSS measurements are presented.

Two measurement points were installed on the Mannen unstable rock slope in 2004 and two more in 2006 (Figure 66). The measurement point BM-5 located on the top of the instability is actively moving with an average displacement rate of 45.5 mm/year towards the ENE with a plunge angle of 50° (Figure 66). The instability in this case certainly refers to scenario A or in a lesser extent to scenario B as defined by Dahle et al. (2011b) (Figure 66). These scenarios A and B involve volumes of 2–3.5 Mm^3 and of 25–30 Mm^3, respectively (Saintot et al. 2011a, Saintot et al. 2012). The other measurement points are located on top of the plateau and have no significant displacements over the measurement period (6 years for BM-1 and BM-2, 4 years for BM-3). These results signify that scenario C as defined by Dahle et al. (2011b) is not actively moving, even though open cracks indicate some displacements in the past (see also discussion in Dahle et al. 2008, Dahle et al. 2011c, Saintot et al. 2012).

Recommendation: Mannen is under continuous monitoring and data are being sent to the Åknes/Tafjord Early-Warning Centre, which is also responsible for further follow-up activities. New scenarios should be defined for the Mannen unstable rock slope based on the latest monitoring results and investigations.

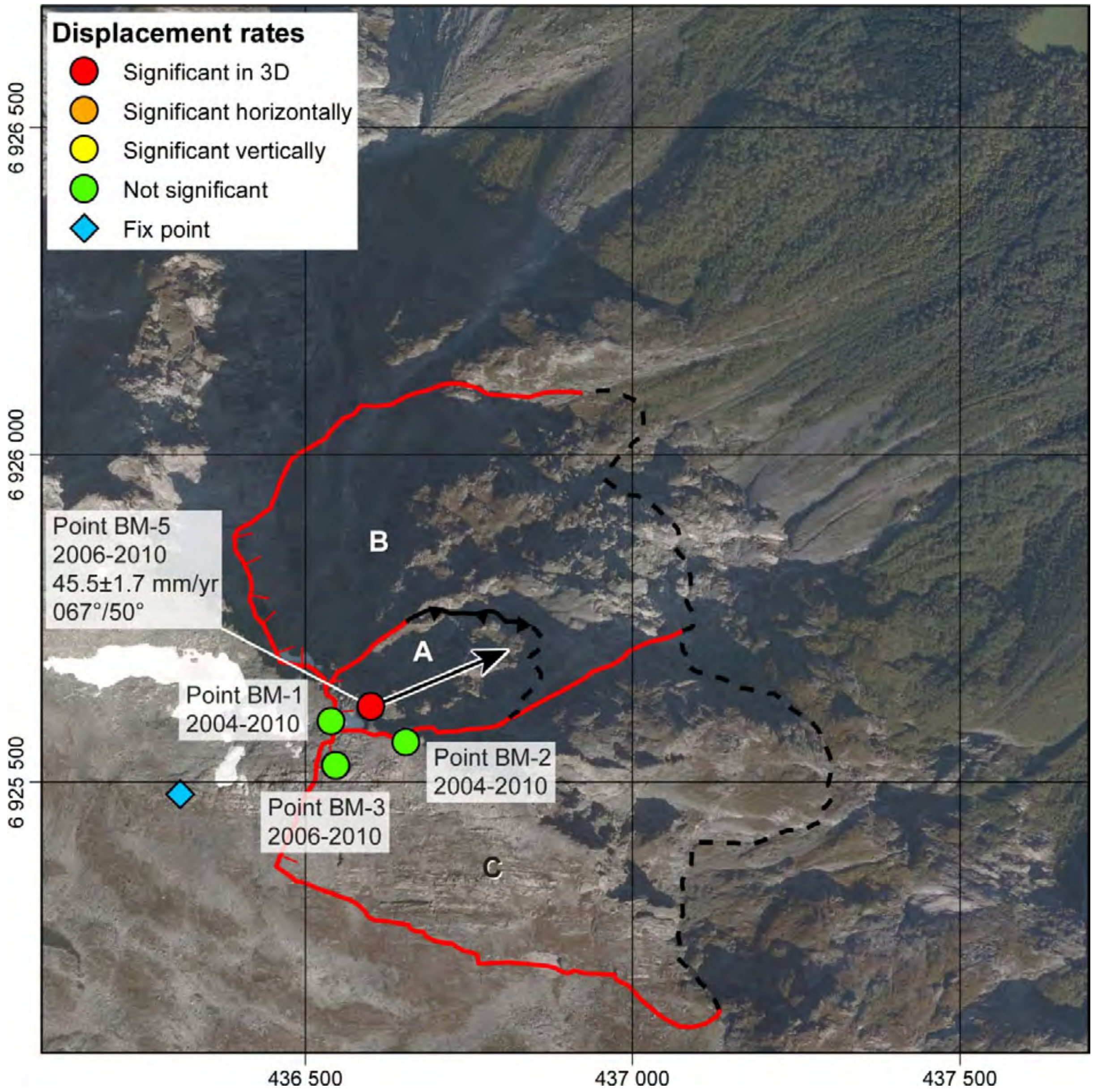

Figure 66: Map of the Mannen unstable rock slope with the location of dGNSS points for periodic displacement measurements and average displacement vectors for the 2004–2010 measurement period. Letters A, B and C refer to scenarios as defined by Dahle et al. (2011b).

5.4.7 Marsteinskora 1

Marsteinskora 1 is located on a west-facing slope 1020 m above Marstein in Romsdalen Valley (Figure 59). The site has been identified based on the analysis of a high-resolution digital elevation model and aerial photographs (Farsund 2010). A helicopter reconnaissance flight in 2010 revealed a deeply eroded contact between two gneiss units and a gully forming the lateral limits of an instability (Figure 67). Both structures show signs of active erosion with fresh debris lying at the foot of the instability. The lithological boundary as northern boundary is partly filled with rock debris (Figure 67b). The top of the site is covered by boulders. A surface depression marks the scarp of a shallow landslide developing in the boulder cover. However, it cannot be ruled out that it also corresponds to the surface expression of a fracture affecting the bedrock, and if so, the back-crack of an instability (Figure 67a). The present knowledge on this site does not allow to ascertain whether or not Marsteinskora 1 is an unstable rock slope or not.

Recommendation: A possible rock avalanche from the Marsteinskora 1 instability will have consequences. Geological field mapping is necessary to evaluate the structural and geological conditions and to quantify past displacements. The hazard and risk classification will be made after this field mapping. Further follow-up activities will be decided based on this classification.

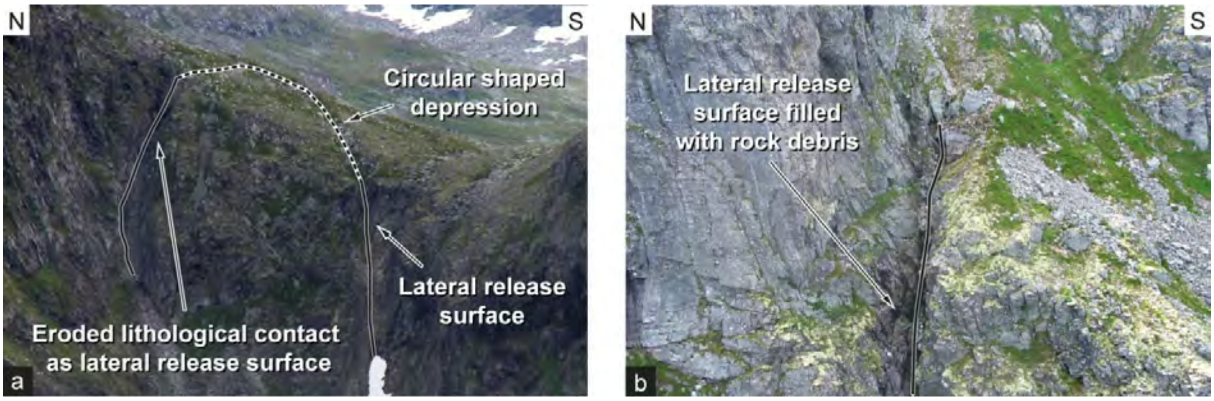

Figure 67: Photographs of the Marsteinskora 1 rock slope: a) well-defined lateral release surfaces and a surface depression may delimit an instability; b) the N-bounding lateral release surface is formed by deeply eroded contact between two gneiss units and is partly filled with debris.

5.4.8 Middagstinden

Middagstinden (Figure 59) is located on a south-facing slope 700 m above Berillvatnet Lake in Innfjorddalen Valley. A complex unstable rock slope has been identified in the early 2000s in relation with the Berill fault (Anda et al. 2002, Blikra et al. 2002a), which is SSW-NNE-trending and delimits the unstable rock slope to the SE. The back-scarp is formed by moderately S-dipping gneiss foliation surfaces and shows several tens of meters of displacement. These past movements have led to strong deformation of the instability with open cracks, depressions, counter-scarps and ridges (Figure 68). Past rock slope failures have likely occurred from the western part of the unstable rock slope, which is heavily disintegrated and covered by debris. Directly west of the large unstable rock slope is a smaller located instability with a relatively newly opened back-crack (Anda et al. 2002, Blikra et al. 2002a). A strong post-glacial earthquake along the Berill fault is discussed as possible trigger of the Middagstinden rockslide (Anda et al. 2002, Blikra et al. 2002a), but geophysical investigations and trenches dug out in the valley sediments did not reveal post-glacial seismic activity along the Berill fault (Krieger et al. 2013).

Field mapping, structural analyses and slope stability modelling is going on as part of Markus Schleier's PhD project at the University of Erlangen, Germany, in collaboration with NGU. The unstable rock slopes is periodically measured using dGNSS since 2008 and TLS since 2010. Here, the latest results from dGNSS and TLS measurements are presented.

Four dGNSS measurement points were set out in 2008 and 2009 on the Middagstinden unstable rock slope (Figure 68). Repetitive measurements were made in 2009, 2010 and 2011 and all four points show significant horizontal and vertical displacements: the points BER-1, BER-2 and BER-3 are located on the main part of the unstable rock slope and move with 6.5 to 9.1 mm/year towards the S to SSW with a plunge angle ranging from 37° to 47° (Figure 68). Point BER-4 is located on the located instability west of the main unstable rock slope and moves with 24.4 mm/year towards the S with a plunge angle of 56°.

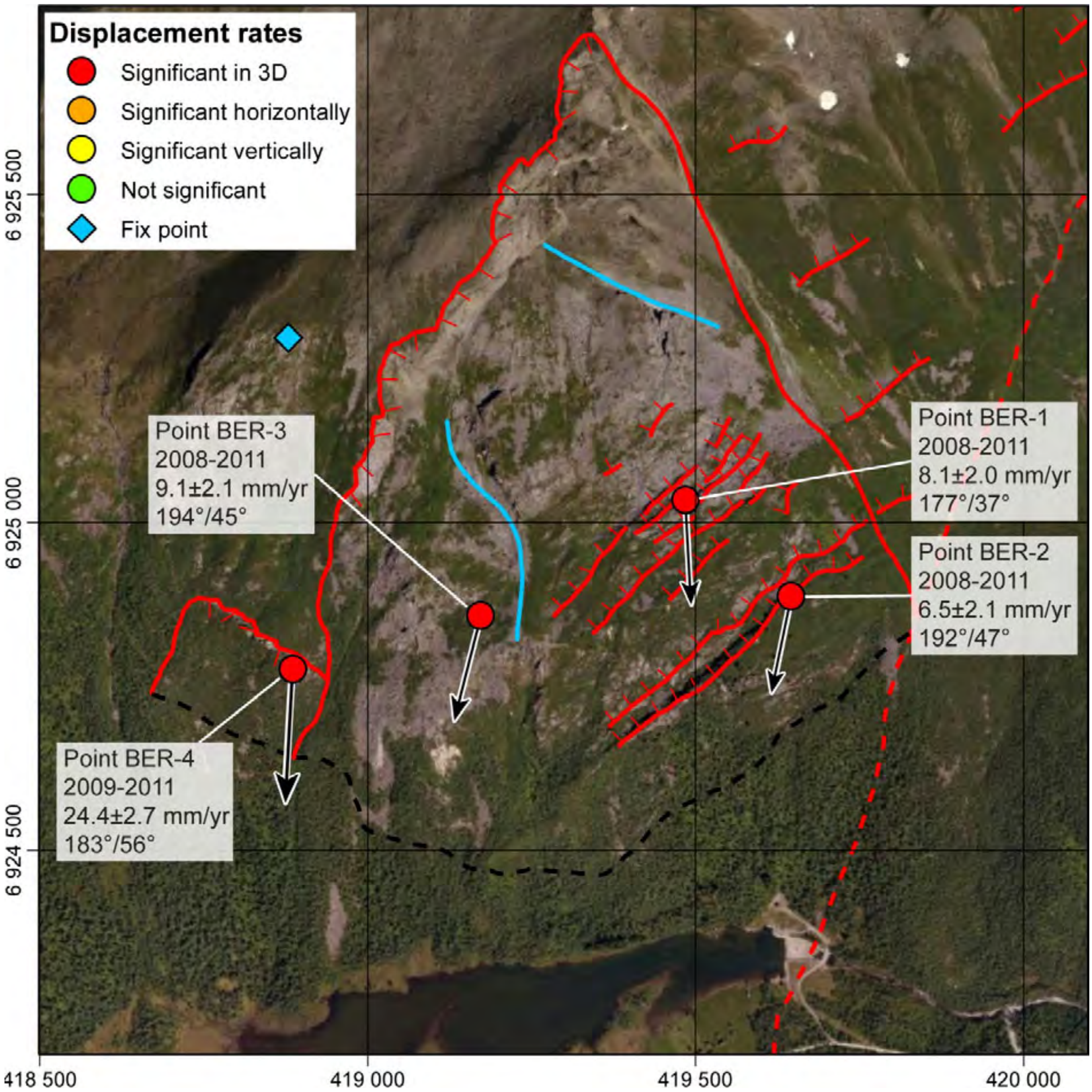

Figure 68: Map of the Middagstinden unstable rock slope with the location of dGNSS points for periodic displacement measurements and average displacement vectors for the 2008–2011 measurement period.

TLS acquisitions were made in 2010 and 2012 from the valley bottom along Berillvatnet Lake and from the eastern lateral release surface. Structural analyses based on the 2010 TLS dataset show a steeply SSE-dipping foliation that forms a basal sliding surface cropping out in the upper part of the slope due to downward motion of the rock mass. Other discontinuity sets are all very steep to subvertical and delimit the unstable rock slope into different compartments. One of these discontinuity set forms overhanging cliffs and the uphill facing counter-scarps. The structures observed in the field and on TLS data do not enable a simple planar or wedge sliding mechanism. Deformation at Middagstinden involves a more complex mechanism that is investigated in Markus Schleier's PhD project. The volume of the Middagstinden unstable rock slope is estimated to 21.5 million m³, but is somewhat speculative due to the uncertain orientation and location of the basal sliding surface in the instability toe zone.

A catastrophic of the Middagstinden rockslide would cross and possibly dam the narrow Innfjorddalen Valley, create a displacement wave in the shallow Berillvatnet Lake and affect several buildings (Dahle et al. 2011a).

Recommendation: Significant displacements are measured at Middagstinden. Periodic displacement measurements using dGNSS and TLS should be continued with 1–3 years interval. Terrestrial cosmogenic nuclide dating of the sliding surface exposed at the back-scarp is planned in order to date the onset of displacement and assess paleo-displacement rates. The hazard and risk classification needs to be made and further follow-up activities will be decided based on this classification.

5.4.9 Mjølvafjellet

Mjølvafjellet is situated on a southwest-facing slope 640 m above Halsa in the outer part of Romsdalen Valley (Figure 59). A helicopter reconnaissance flight was made in 2011 and showed vertical cracks that are partly open and delimit small columns that may lead to rock-falls (Figure 69). The slope is vegetated and there are no significant traces of recent rockfall activity. The observed structures do not delimit a large unstable rock slope.

Recommendation: There are no signs that the Mjølvafjellet rock slope might fail in a massive rock slope failure. No further investigations or displacement measurements are necessary and the hazard and risk classification will not be made. However, rockfalls are possible and their run-out area is given by the rockfall susceptibility map or more detailed hazard maps, where available.

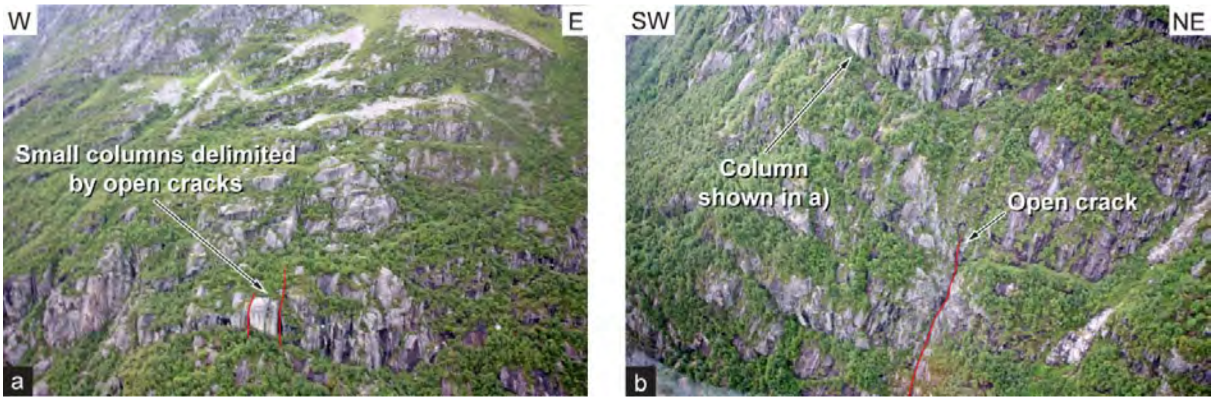

Figure 69: Photographs of the Mjølvafjellet rock slope: open vertical cracks affect the vegetated rock slope and locally delimit small columns that might lead to rockfalls.

5.4.10 Olaskarstinden

Olaskarstinden is located on a southeast-facing slope 1150 m above Horgheim in Romsdalen Valley (Figure 59). The site has been identified based on the analysis of a high-resolution digital elevation model and aerial photographs, then overflown by helicopter and studied in the field (Farsund 2010).

The bedrock displays steep NW- or SE-dipping foliation and associated meter-scale amplitude folds with axial planes gently dipping to the SE. An undulating SE-dipping basal sliding surface crops out on the southwestern edge of the site (Figure 70b). It follows a SE-dipping schistosity (likely a cleavage) that developed nearly parallel to the fold axial planes. Two SSW-NNE-trending surface depressions are observed to the northwest, on the top of the unstable rock slope (Figure 70). These discontinuous depressions are of unknown nature and no bedrock openings are actually visible (Figure 70b). No eastern lateral limit can be defined. In the lower SE-part of the rock slope the rock mass looks more heavily fractured than in the upper NW-part (Figure 70a), which could be related to internal deformation of the rock mass, but more likely to surface alteration processes. Finally, Olaskarstinden is classified as a potential unstable rock slope because no clear signs of past displacements are observable.

Downward the steep slope and at various locations in the surrounding of the site sliding surfaces of previous failures are well displayed. The SE-dipping schistosity acted as sliding surfaces, NW-SE steep fractures as lateral surfaces, and the steep NW-dipping or SE-dipping foliation detached the blocks at the back. The volumes involved in those previous events could have reached several 100 000 m³.

Recommendation: Olaskarstinden is classified as a potential unstable rock slope. At present the remaining rock slope does not show any signs of past or present displacements or deformation of a large volume (except for rockfall activity). No further investigations or displacement measurements are necessary and the hazard and risk classification will not be made. However, this site may lead to rockfalls and develop over time into an unstable rock slope, due to structural and geological conditions. The site should be revisited after years to decades to detect any changes and be followed-up on InSAR data.

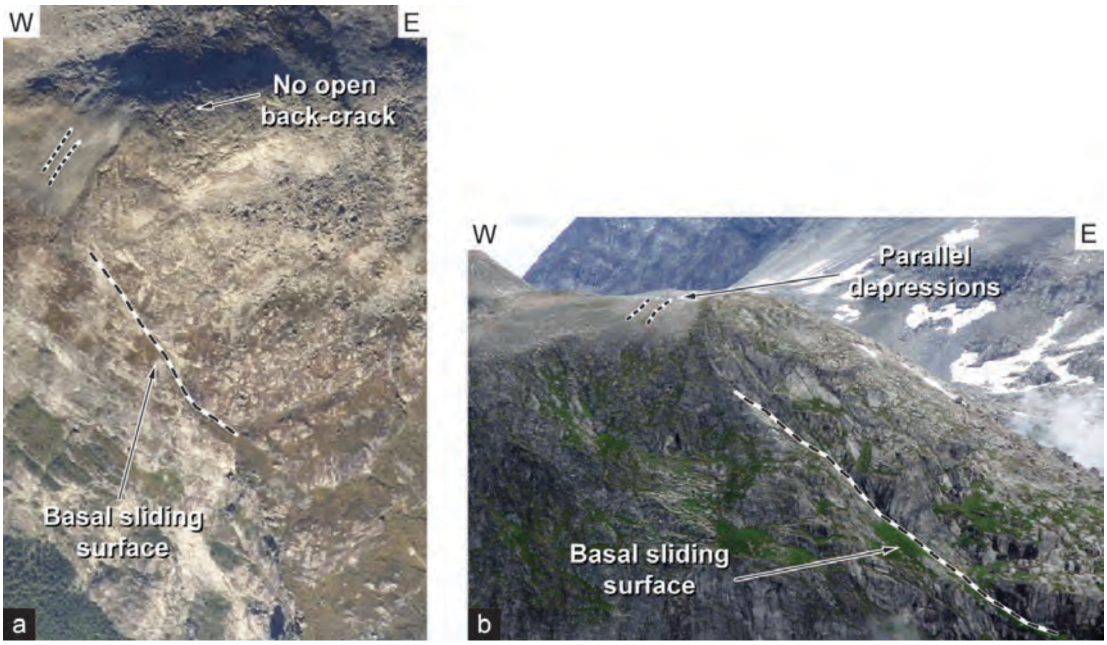

Figure 70: Photographs of the potential unstable rock slope at Olaskarstinden with a possible basal sliding surface and surface depressions: a) aerial photograph showing higher fracturing in the lower SE-part of the rock slope; b) the possible basal sliding surface formed along an undulating schistosity.

5.4.11 Svarttinden

Svarttinden is located on a northeast-facing slope 1520 m above Remmem in Romsdalen Valley (Figure 59). Field mapping was made in 2006 and several studies describe this unstable rock slope (Henderson and Saintot 2007, Dahle et al. 2011a, Saintot et al. 2011b, Saintot et al. 2012). Svarttinden is lying on a single, moderately NE-dipping basal sliding surface and has an estimated volume of 4.3 million m³. There are signs of past displacement along this basal sliding surface, notably in the form of fine-grained breccia, but there is no apparent offset at the back, where the sliding surface daylights (modified from Saintot et al. 2012). The unstable rock slope is measured periodically using dGNSS since 2005 and TLS since 2006. No repetitive TLS measurements are made up to now. Here, the latest results from dGNSS and cosmogenic nuclide dating of rock avalanche deposits are presented.

Three dGNSS measurement points were installed at Svarttinden in 2005 (Figure 71). All points were measured again in 2006, 2007 and 2010, but no significant displacements were recorded over the 5 years measurement period.

A previous rock slope failure occurred from the eastern part of the basal sliding surface. Its volume is estimated to 3–4 million m³ based on a reconstruction of the pre-failure topography. The rock avalanche reached the edge of the plateau, but not the valley floor (or only a small part of it). Rock avalanche deposits at Remmen likely originated from the steep cliffs of the southern flank of Romsdalen Valley (modified from Saintot et al. 2012). Cosmogenic nuclide dating of 3 rock avalanche deposit samples at Svarttinden provide an age between 7800 ± 700 and 10 500 ± 900 years.

Recommendation: No significant displacements are measured up to now at Svarttinden. Periodic displacement measurements using dGNSS should be continued with 3–5 years interval. The hazard and risk classification needs to be made and further follow-up activities will be decided based on this classification.

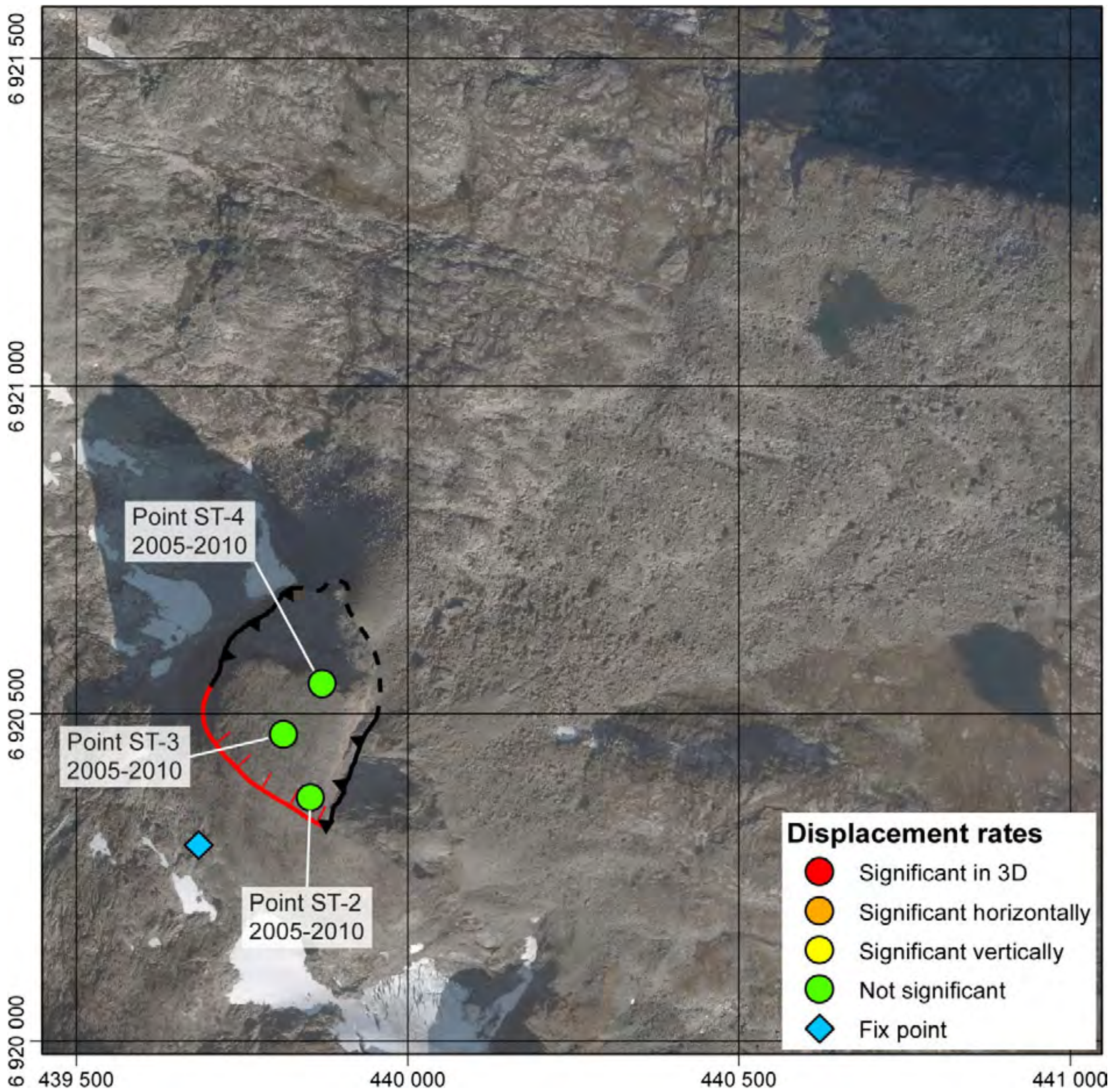

Figure 71: **Map of the Svarttinden instability with the location of dGNSS points for periodic displacement measurements. No significant displacements were detected over the 2005–2010 measurement period.**

5.4.12 Trolltindan

Trolltindan is located on a northeast- to east-facing slope 1510 m above Romsdalen Valley (Figure 59) and comprises the steep high cliffs of Trollveggen, which is a major tourist attraction in the valley. A helicopter reconnaissance flight was made in 2006 along the pinnacles forming the mountain crest of Trolltindan (Figure 72). Several rock slope failures occurred in the past, mainly in the form of rockfalls, but also as larger failures. In 1998 a volume of approximately 75 000 m³ collapsed and formed a small rock slope failure, which did not have an excessive run-out distance. The foliation is subhorizontal, while other discontinuity sets are very steeply dipping to subvertical (Figure 72). A persistent fault is inward-dipping and crosses the Trolltindan mountain (Figure 72a). This structural setting delimits relatively small volumes that may fail as rockfalls or small rock slope failures. On the other hand, there is a moderately valley-dipping structure at the foot of Trolltindan, which might form the basal sliding surface of an unstable rock slope. However, there are no morphologic evidences to define an unstable rock slope, but a closer look at the steep cliffs at Trolltindan is necessary.

Recommendation: Trolltindan is classified as a potential unstable rock slope. At present the remaining rock slope does not show any signs of past or present displacements or deformation of a large volume (except for rockfall activity). However, this site may lead to rockfalls and develop over time into an unstable rock slope, due to structural and geological conditions. Nonetheless, a more detailed helicopter reconnaissance flight is planned, focussing on the valley-dipping structure at the foot of Trolltindan and cracks within the cliff delimiting potential instabilities.

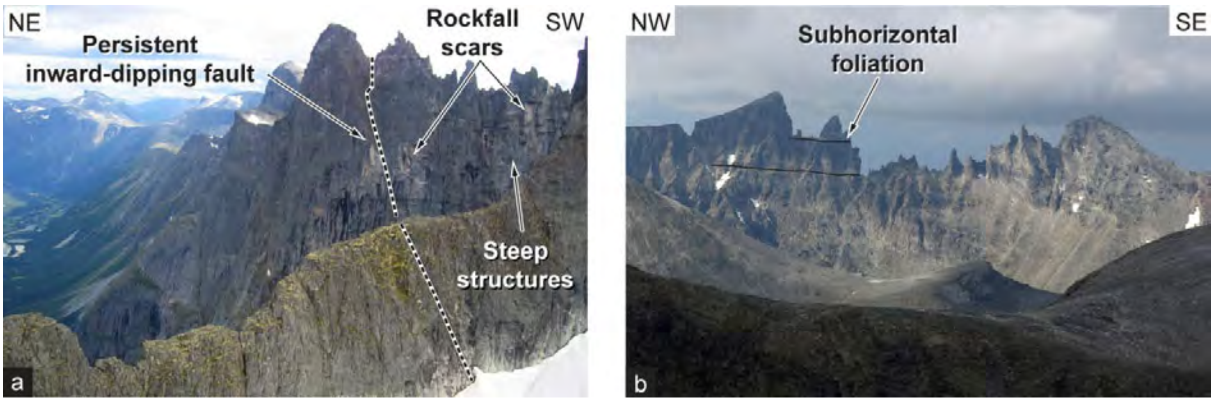

Figure 72: Photographs of the Trolltindan rock slope: a) lateral view showing the inward-dipping fault and other steep structures; b) view from the back-side of Trolltindan showing the subhorizontal foliation.

5.4.13 Veten

Veten (Figure 59) is located on a southwest-facing slope 410 meter above Romsdalsfjord, NW of Klungnes. A helicopter reconnaissance flight in 2011 revealed steeply S-dipping structures parallel to foliation (Figure 73a), which may favour sliding. On the other hand, no open cracks were observed and other necessary structures to delimit an unstable rock slope are missing. There are no signs of past displacements or current activity, except for rockfalls from the subvertical frontal cliff.

On the northwest-facing slope of Veten a past rock slope failure occurred. The rock avalanche (also called Gråura or Raudfonna) had its source area along small cliffs along the mountain crest. Also along these cliffs there are no large open cracks that would delimit a current unstable rock slope. Cosmogenic nuclide dating of 2 samples of the Gråura rock avalanche deposits give an age of 14 600 ± 1600 years.

Recommendation: There are no signs that the Veten rock slope might fail in a massive rock slope failure. No further investigations or displacement measurements are necessary and the hazard and risk classification will not be made. However, rockfalls are possible and their run-out area is given by the rockfall susceptibility map or more detailed hazard maps, where available.

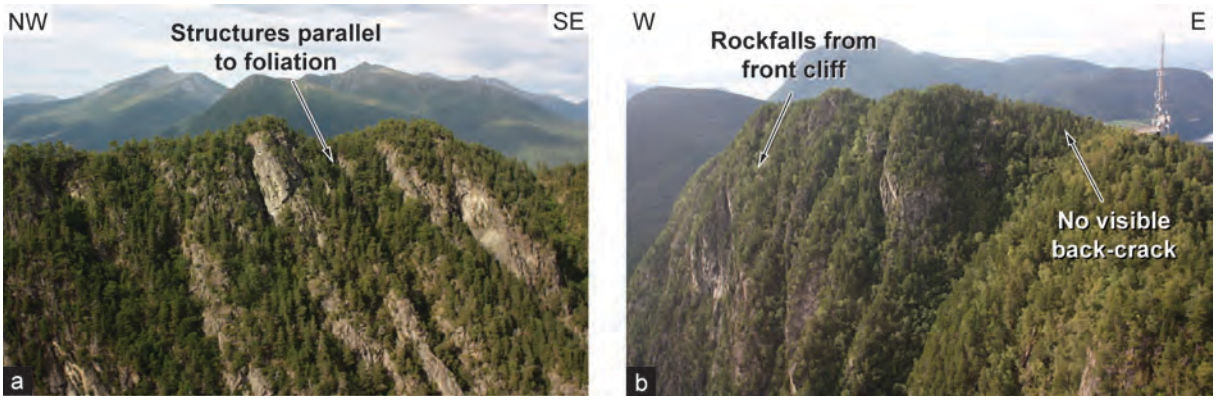

Figure 73: Photographs of the Veten rock slope: a) the foliation is steeply S-dipping, but the observed structures do not delimit an unstable rock slope; b) there are no visible open cracks and no signs of activity except rockfalls from the steep frontal cliff.

5.5 Vestnes municipality

There are three known sites located in Vestnes municipality, which are all described in this report (Figure 74).

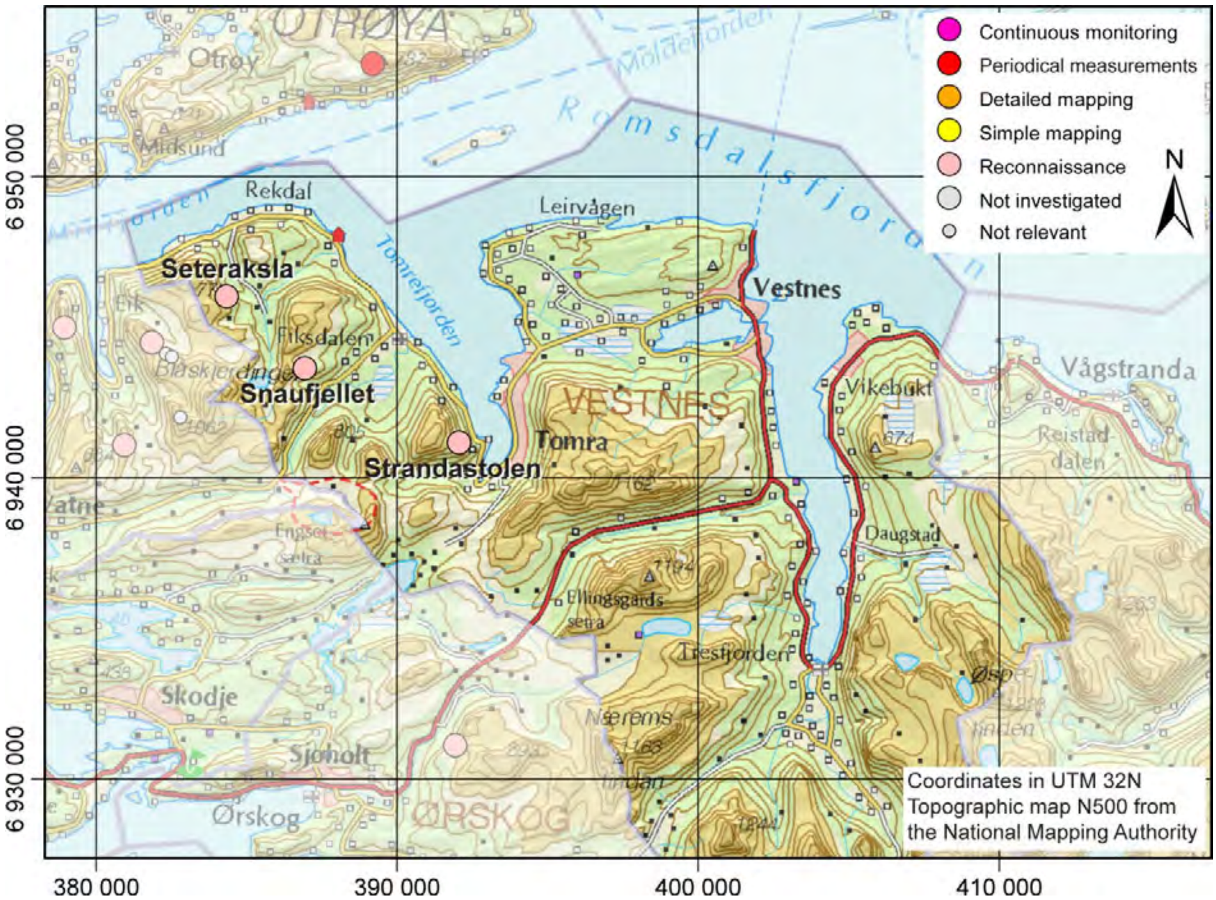

Figure 74: Map of the three known sites in the Vestnes municipality with their investigation status. The name of the sites described in this report is shown.

5.5.1 Seteraksla

Seteraksla (Figure 74) is located on a northeast-facing slope 330 m above Rekdalsdalen Valley. A helicopter reconnaissance flight in 2012 showed an obvious back-scarp that has developed over 800 m in length and fully delimits the unstable rock slope (Figure 75). The back-scarp is marked as a surface depression in the ESE-part of the slope and by an up to 10 m high escarpment in its NW-part (Figure 75a). The lateral and basal limits of the unstable rock slope are poorly developed and not conspicuous on the terrain. There are no major cracks on the instability and no signs of recent displacement of the unstable rock slope as a whole. However, there are open cracks at several locations at the front of the instability (Figure 75b). They delimit small blocks that might induce rockfalls with volumes of tens to hundreds of m^3. A massive failure from Seteraksla is unlikely and consequences would be small, since there are only very few buildings in Rekdalsdalen Valley (Dahle et al. 2011a).

Recommendation: A possible rock avalanche from the Seteraksla unstable rock slope will have no consequences. No further investigations or displacement measurements are necessary. The hazard and risk classification will be made after a simple run-out assessment. Further follow-up activities will be based on this classification.

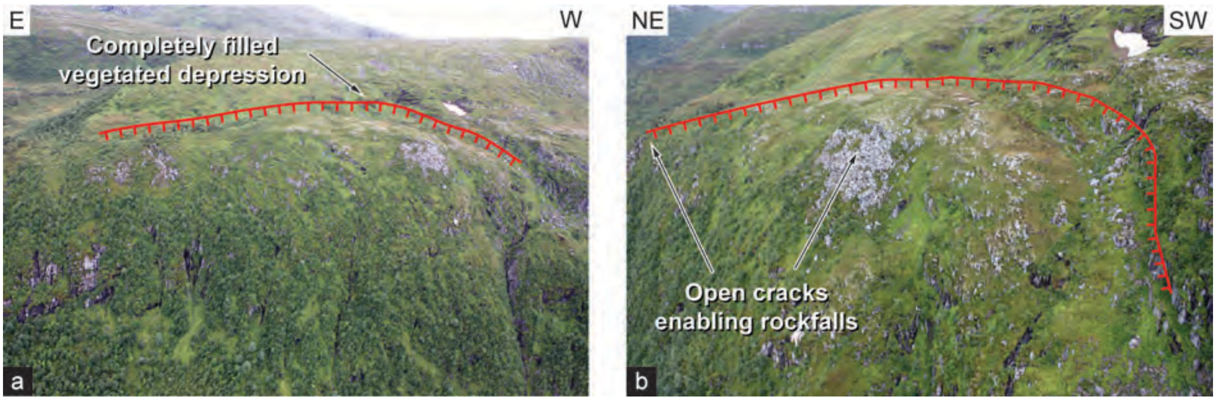

Figure 75: Photographs of the Seteraksla unstable rock slope: a) an escarpment and depression form the back-scarp; b) open cracks delimit small blocks that lead to rockfalls.

5.5.2 Snaufjellet

Snaufjellet (Figure 74) is located on a south-facing slope 345 m above Botnavatn Lake in Nakkedalen Valley. A helicopter reconnaissance flight was made in 2012 and revealed an 800 m long lineament north of, and parallel to, the ridge where the instability is located. It might be the result of past gravitational movements of the unstable rock slope (Figure 76). However, there are no signs of current activity, and necessary structures to delimit a large unstable rock slope are missing. Few, steep outcrops are visible along a two meter high back-scarp in the western part of the instability (Figure 76a). A large talus slope testifies of past rockfall activity. However, dense vegetation cover on the slope indicates only minor current rockfall activity. A massive failure from Snaufjellet could reach Botnavatn Lake and the road Fv147, but no buildings are located in the run-out area (Dahle et al. 2011a).

Recommendation: A possible rock avalanche from the Snaufjellet unstable rock slope will have no consequences. No further investigations or displacement measurements are necessary. The hazard and risk classification will be made after a simple run-out assessment. Further follow-up activities will be based on this classification.

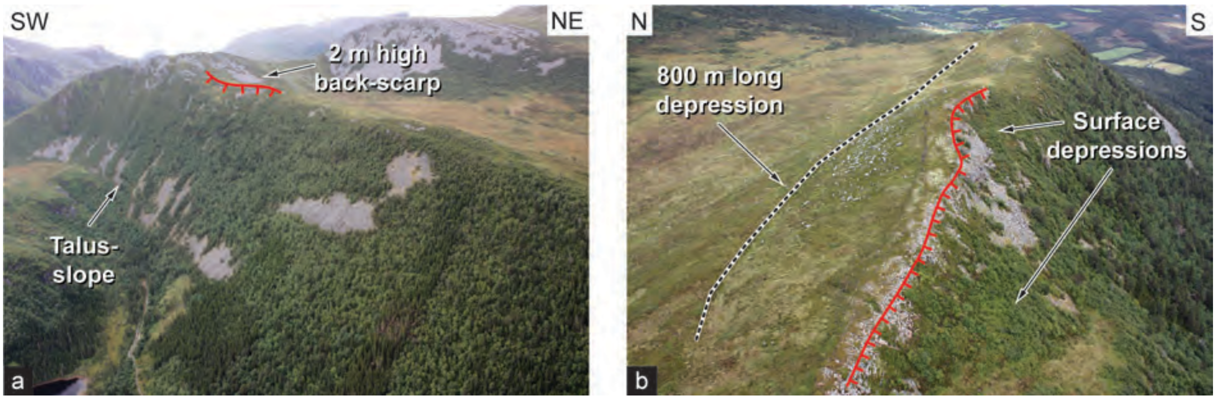

Figure 76: **Photographs of the Snaufjellet unstable rock slope: a) cliffs along the ridge lead to rockfalls forming a large talus slope; b) a surface depression behind the mountain ridge indicates possible past displacements of a large unstable rock slope.**

5.5.3 Strandastolen

Strandastolen is located on a northeast-facing slope 510 m above the inner part of Tomrefjord close to the town of Tomra (Figure 74). A helicopter reconnaissance flight in 2012 showed a small instability that is laterally delimited by eroded and partly filled, vertical cracks (Figure 77). No through-going open back-crack was observed and there were only small to no past displacements (Figure 77b). However, a field survey by H. Dahle showed locally open cracks with up to 30 cm in width. The dimensions of the instability are roughly 60 m wide, 30 m long and 50 m high. This gives a maximum volume of approximately 90 000 m³. The massive failure of this instability would reach Tomrefjord and would create a minor displacement wave.

Recommendation: A possible rock avalanche from the Strandastolen instability will have consequences, which will be assessed in the hazard and risk classification. Further follow-up activities will be decided based on this classification.

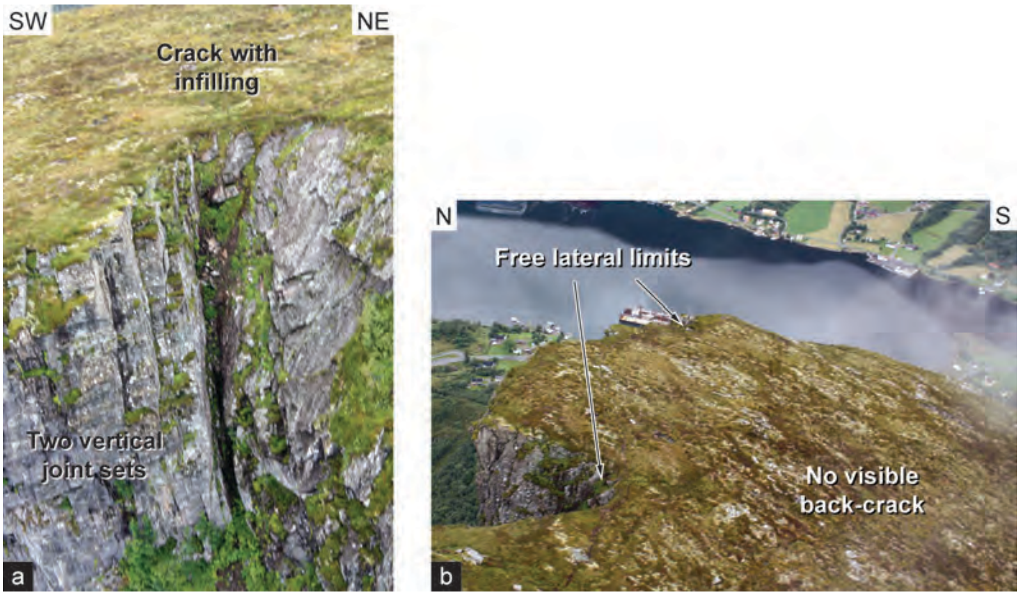

Figure 77: **Photographs of the Strandastolen instability: a) the south-western lateral release surface is partly open and filled with loose debris; b) no recent displacement is visible.**

6. STORFJORD REGION

6.1 Norddal municipality

There are 37 known sites located in Norddal municipality. Sixteen of them are described in this report (Figure 78).

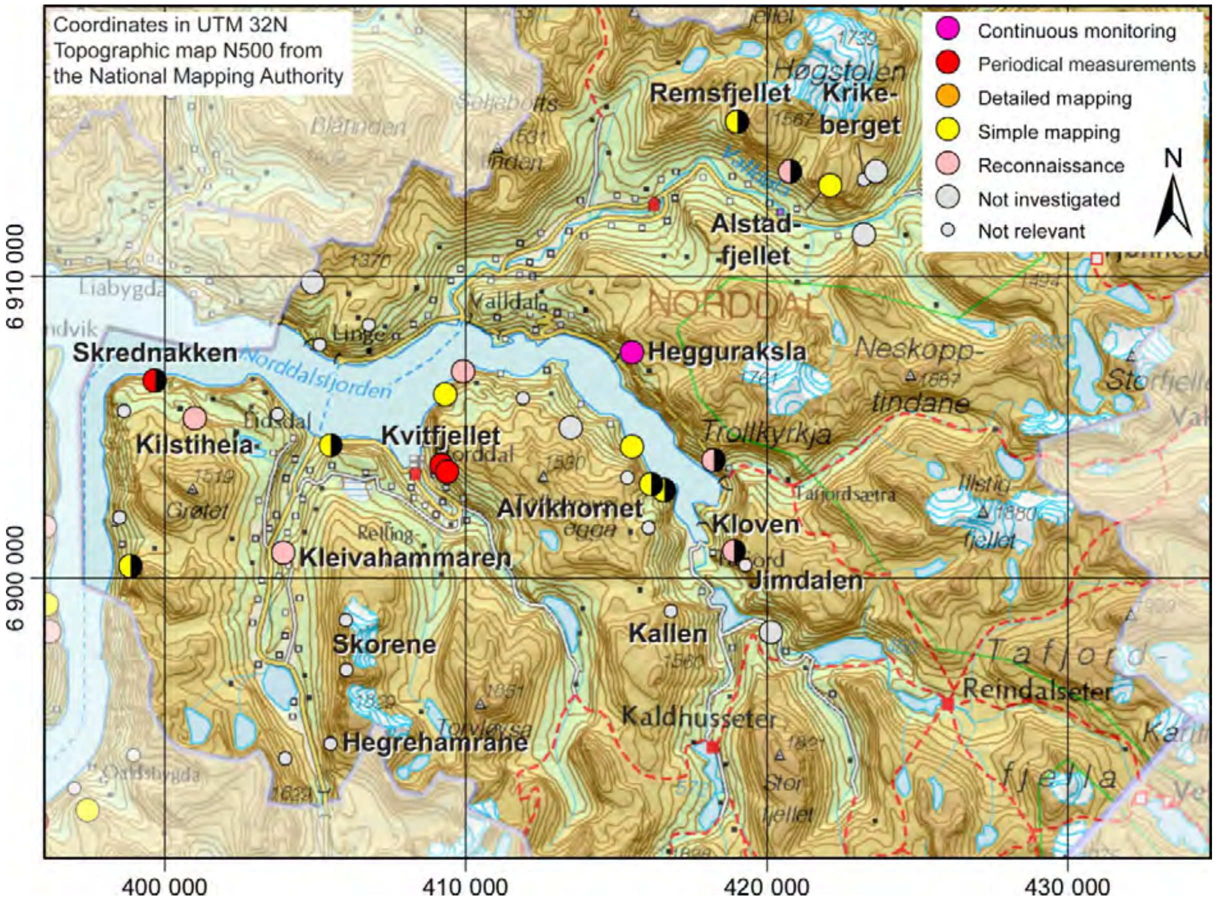

Figure 78: Map of the 37 known sites in the Norddal municipality with their investigation status. Potential unstable rock slopes are also shown with a half-masked symbol (◑). The name of the sites described in this report is shown.

6.1.1 <u>Alstadfjellet</u>

Alstadfjellet (Figure 78) is located on a south-facing slope 1040 m above Alstad in Valldalen Valley. Several past rockslides occurred in the western part of Alstadfjellet slope with moderately SE-dipping structures as basal sliding surfaces (Figure 79). The largest of the past rockslides formed a rock avalanche that crossed Valldalen Valley. Two samples of these rock avalanche deposits were dated to 9700 ± 900 years BP using cosmogenic nuclide dating.

Field mapping was carried out in 2007, but was limited to the top surface of the site because of the steepness of the slope. The foliation is moderately NE- to E-dipping at the top of the slope, thus acting against sliding. However, it cannot be ruled out that the foliation changes its orientation within the mountainside and forms the sliding surfaces of ancient rock slides observed downward the slope (Figure 79b). In any case, the bedrock at the top is densely fractured by a predominant orthogonal pattern of NE-SW and NW-SE steep fractures, which are also present downward the slope and participated to the previous failures. No back-crack and lateral release surfaces delimiting a large unstable rock slope were observed. However, there are rock masses remaining on the basal sliding surfaces of past rockslides (Figure 79b).

Recommendation: There are no signs that the Alstadfjellet rock slope might fail in a massive rock slope failure. However, a more detailed helicopter reconnaissance flight is planned, focussing on rock masses that remain on the sliding surfaces of past rockslides.

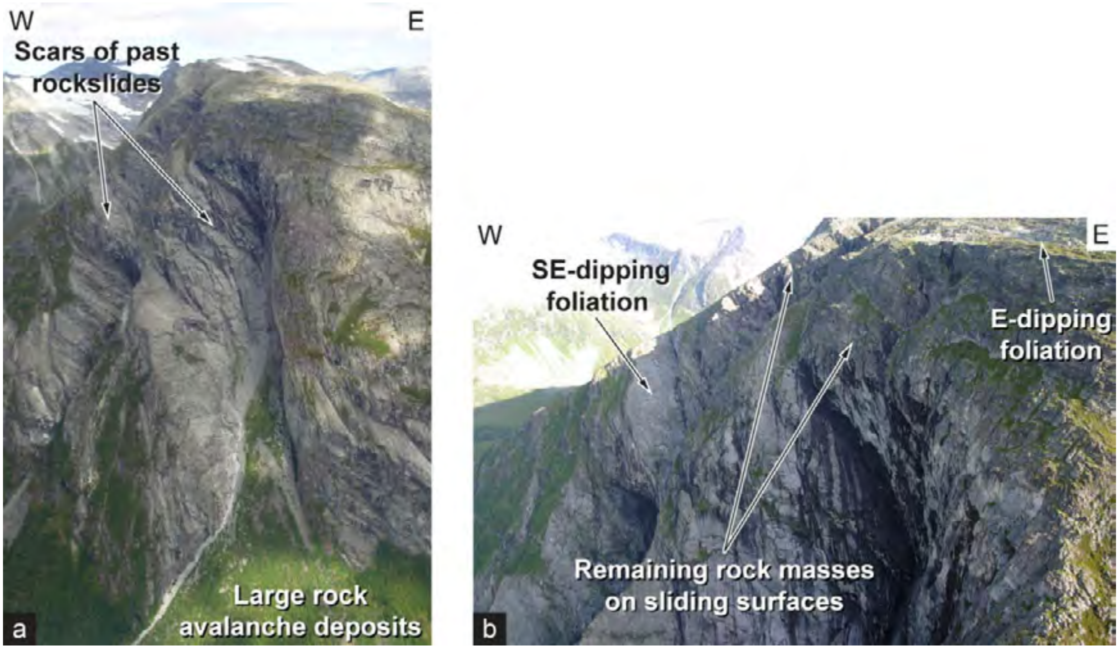

Figure 79: Photographs of the Alstadfjellet rock slope: numerous past failures occurred along SE-dipping foliation surfaces, but no large potential instability is delimited at present.

6.1.2 Alvikhornet 3

Alvikhornet 3 is located on a northeast-facing slope 600 m above Tafjord (Figure 78). Reconnaissance by boat and field mapping in 2006 showed a potential back-crack that follows the back-scarp of a past failure (Figure 80). Deposits of this past rock slope failure with a volume of 0.7 million m³ are found in the fjord (Longva et al. 2009). A potential instability with an estimated volume of 2 million m³ (Dahle et al. 2011a) is delimited by this potential back-crack, a poorly developed lateral release surface and a moderately ENE-dipping basal sliding surface probably formed by an exfoliation surface.

Figure 80: Photograph of the potential instability Alvikhornet 3 that is delimited by a possible back-crack, a poorly developed lateral release surface and a basal sliding surface probably formed by exfoliation.

Recommendation: Alvikhornet 3 is classified as a potential unstable rock slope. At present the remaining rock slope does not show any signs of past or present displacements or deformation of a large volume. No further investigations or displacement measurements are necessary and the hazard and risk classification will not be made. However, this site may lead to rockfalls and develop over time into an unstable rock slope, due to structural and geological conditions. The site should be revisited after years to decades to detect any changes and be followed-up on InSAR data.

6.1.3 Hegrehamrane

Hegrehamrane (Figure 78) is located on a west-facing cliff 690 m above Eidsdalen Valley. Reconnaissance by car and helicopter in 2007 showed steep cliffs that are prone to rockfalls (Figure 81). Past rockfalls have formed large talus slopes at the foot of the cliff, while large single blocks are observed on the valley floor (Figure 81a). There are no visible structures that would delimit a large unstable rock slope.

Recommendation: There are no signs that the Hegrehamrane rock slope might fail in a massive rock slope failure. No further investigations or displacement measurements are necessary and the hazard and risk classification will not be made. However, rockfalls are possible and their run-out area is given by the rockfall susceptibility map or more detailed hazard maps, where available.

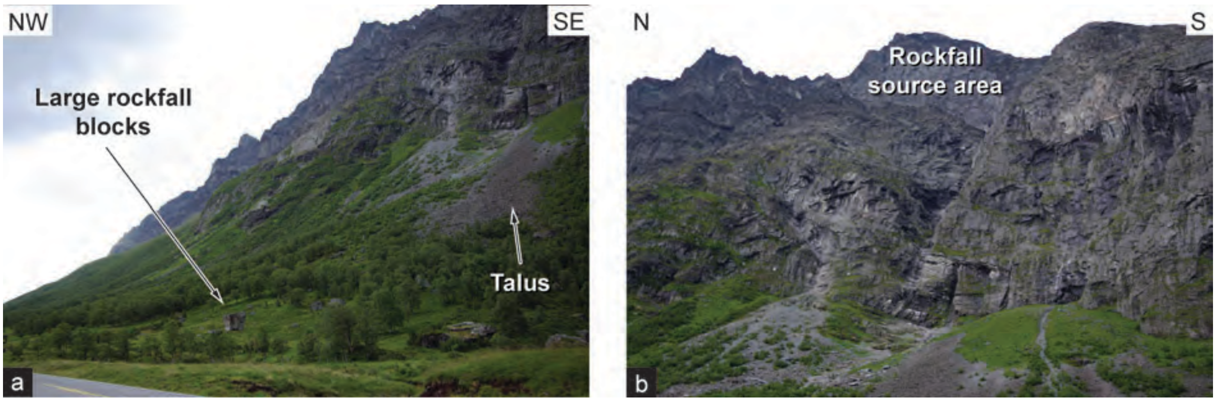

Figure 81: Photographs of the Hegrehamrane cliffs: a) talus slopes and large rockfall boulders on the valley floor indicate past rockfall activity; b) fresh rockfall scars are visible at several locations on the steep cliffs.

6.1.4 Hegguraksla

Hegguraksla (Figure 78) is located on a southwest-facing slope 930 m above Tafjord. Hegguraksla is continuously monitored by the Åknes/Tafjord Early-Warning Centre and has been investigated within the international Åknes/Tafjord project by:

- field mapping, structural mapping and analysis of high-resolution digital elevation models and aerial photographs (Braathen et al. 2004, Oppikofer and Jaboyedoff 2008, Oppikofer 2009);
- geophysical investigations (Rønning et al. 2006, Rønning et al. 2008);
- periodic displacement measurements using terrestrial laser scanning (Oppikofer and Jaboyedoff 2008);
- risk analyses (Blikra et al. 2006, Dahle et al. 2011a);
- continuous monitoring instrumentation (Kristensen and Blikra 2010).

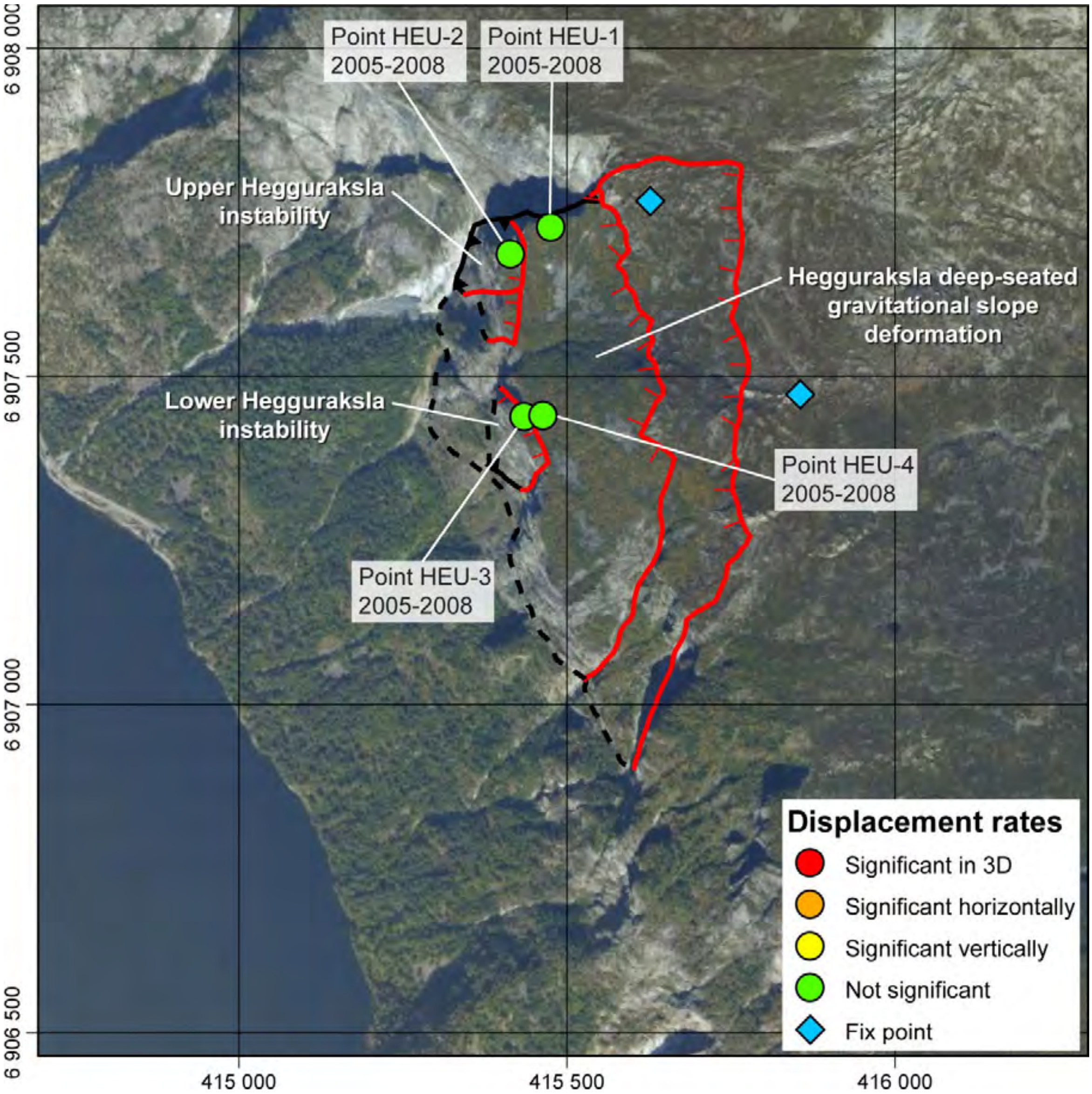

Figure 82: Map of the Hegguraksla unstable rock slope with the location of dGNSS points for periodic displacement measurements. No significant displacements were detected over the 2005–2008 measurement period.

The Hegguraksla rock slope is affected by a deep-seated gravitational slope deformation over a width of more than 600 m (Figure 82). A several meter high escarpments marks the back-scarp of this large unstable rock slope with an estimated volume of approximately 24 million m³ (Oppikofer 2009). Two instabilities are located along the frontal cliff of the Hegguraksla deep-seated gravitational slope deformation (Figure 82) with estimated volumes of 0.78–1.0 million m³ for the Upper Hegguraksla instability and 0.40 million m³ for the Lower Hegguraksla instability (Oppikofer 2009). Open back-cracks indicate past displacements of the instabilities and most continuous monitoring instrumentation focuses on these instabilities (Kristensen and Blikra 2010). Crackmeters installed in the back-crack of the Upper Hegguraksla instability indicate small displacements of less than 1 mm/year.

The Upper and Lower Hegguraksla instabilities were measured periodically using dGNSS between 2005 and 2008. Four dGNSS points were installed in August 2005 (Figure 82). One point is located on each of the localised instabilities (HEU-2 and HEU-3) and two other points are located on the deep-seated gravitational slope deformation (HEU-1 and HEU-4). All points were measured again in October 2005, August 2006, August 2007 and August 2008, but no significant displacements were recorded in the 3 years measurement period.

Recommendation: Hegguraksla is under continuous monitoring and data are being sent to the Åknes/Tafjord Early-Warning Centre, which is also responsible for further follow-up activities.

6.1.5 Jimdalen

Jimdalen is located on a southwest-facing slope 710 m above the Jimdalen Valley, 1.8 km SE of Tafjord (Figure 78). A helicopter reconnaissance flight in 2007 showed a large talus slope formed by past rockfalls and a small rock avalanche (Figure 83). The fresh scar in the upper part of the cliff is from a small rock avalanche that occurred in 1992. The foliation orientation is very variable due to strong folding. There are no open cracks or other visible structures that might delimit a large unstable rock slope.

Recommendation: There are no signs that the Jimdalen rock slope might fail in a massive rock slope failure. No further investigations or displacement measurements are necessary and the hazard and risk classification will not be made. However, rockfalls are possible and their run-out area is given by the rockfall susceptibility map or more detailed hazard maps, where available.

Figure 83: Photograph of the Jimdalen rock slope: the scar and deposits of past rockfalls and a small rock avalanche are visible, but no open cracks or structures delimiting a large unstable rock slope are visible.

6.1.6 Kallen

Kallen is located on a northeast-facing slope 1030 m above Onilsavatnet Lake, 1.8 km south of Tafjord (Figure 78). A large post-glacial rockslide with an estimated volume of 100 million m³ originated from Kallen and dammed Onilsavatnet Lake (Longva et al. 2009). The steeply N-dipping cliffs at Kallen were probably the southern lateral release surface of this past rockslide (Figure 84). Three samples of the rock avalanche deposits were dated to 11 200 ± 1500 years BP using cosmogenic nuclide dating. Colour differences in the bedrock at Kallen (Figure 84a) were interpreted as signs of an unstable rock slope, but a helicopter reconnaissance flight in 2007 did not reveal any open cracks or other signs of past displacements at the mountain top of Kallen and the ridge trending eastwards down to Onilsavatnet Lake (Figure 84b).

Recommendation: There are no signs that the Kallen rock slope might fail in a massive rock slope failure. No further investigations or displacement measurements are necessary and the hazard and risk classification will not be made. However, rockfalls are possible and their run-out area is given by the rockfall susceptibility map or more detailed hazard maps, where available.

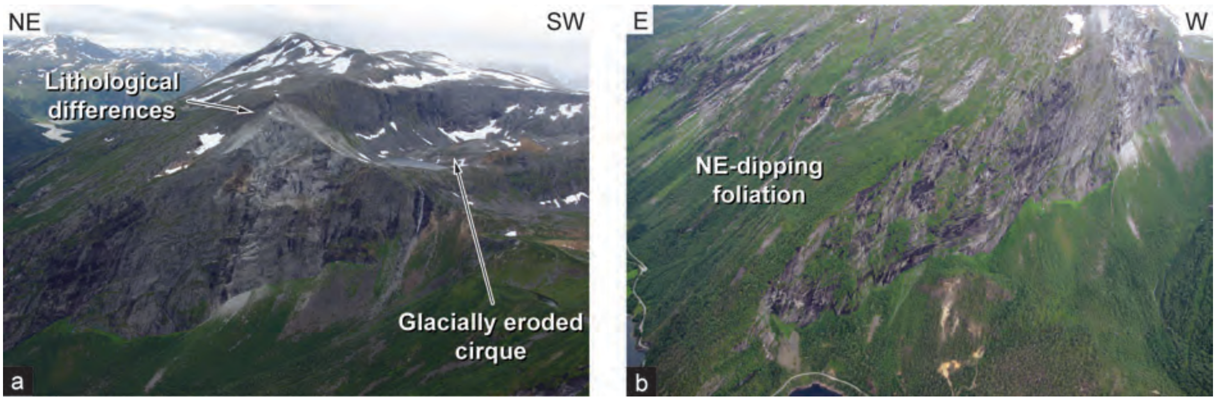

Figure 84: Photographs of the Kallen rock slope: a) the steeply N-dipping cliffs at Kallen were the lateral release surface of a large post-glacial rockslide, but no large unstable rock slope remains; b) there are no visible open cracks on the mountain ridge running eastward from Kallen down to Onilsavatnet Lake.

6.1.7 Kilstiheia

Kilstiheia (Figure 78) is located on a north-facing slope 600 m above Verpesdalen Valley. An unstable rock slope was identified during a helicopter reconnaissance flight in 2011. An instability is delimited by a well-developed back-crack that is filled and vegetated (Figure 85). The gneiss foliation is moderately dipping towards the valley and served as basal sliding surface in past rockslides, whose scars are well visible on the rock slope (Figure 85a). The foliation also likely forms the basal sliding surface of the present instability at Kilstiheia. Lateral release surfaces are however not well-developed although structures along which they can develop, i.e. parallel to the presumed sliding direction, exist (Figure 85a). A massive failure from Kilstiheia would affect a few houses in Verpesdalen Valley.

Recommendation: A possible rock avalanche from the Kilstiheia instability will have consequences. Geological field mapping is necessary to evaluate the structural and geological conditions, to quantify past displacements and assess the structures involved in previous rockslides. The hazard and risk classification will be made after this field mapping. Further follow-up activities will be decided based on this classification.

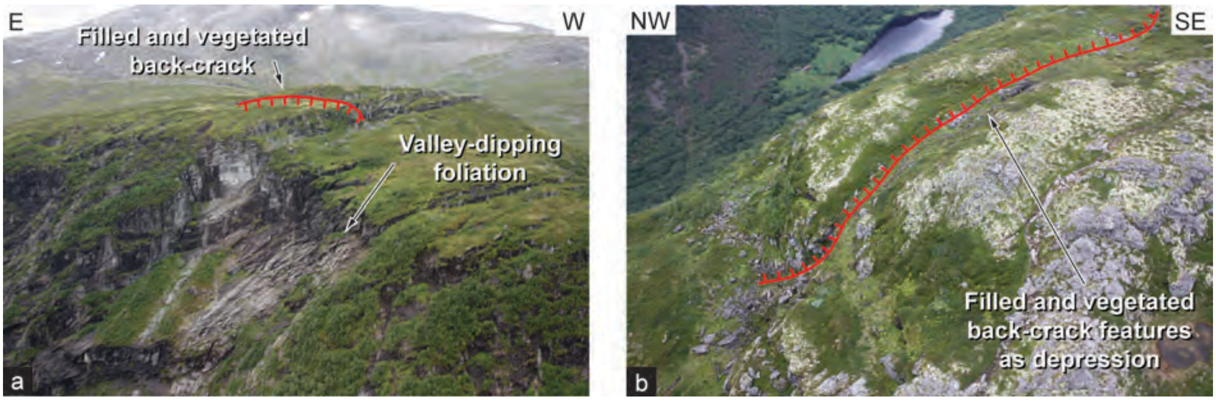

Figure 85: Photographs of the Kilstiheia instability: a) rockslides occurred along the valley-dipping foliation forming the basal sliding surface; b) the instability is delimited by a filled and vegetated back-crack.

6.1.8 Kleivahammaren

Kleivahammaren (Figure 78) is situated close to Kleiva on a west-facing slope 270 m above Eidsdalen Valley. Reconnaissance by car in 2007 revealed a sub-vertical fault that forms the back-crack of an unstable rock slope (Figure 86). No openings of the back-crack can be seen on the top of the hill as it is covered by forest, but the fault trace is nonetheless visible as a shallow surface depression. A small compartment along the front cliff is delimited by a sub-vertical crack (Figure 86a), but there are no signs of past displacements. A talus slope below cliff indicates high rockfall activity.

Recommendation: A possible rock avalanche from the Kleivahammaren instability will have consequences. Geological field mapping is necessary to evaluate the structural and geological conditions and to quantify past displacements. The hazard and risk classification will be made after this field mapping. Further follow-up activities will be decided based on this classification.

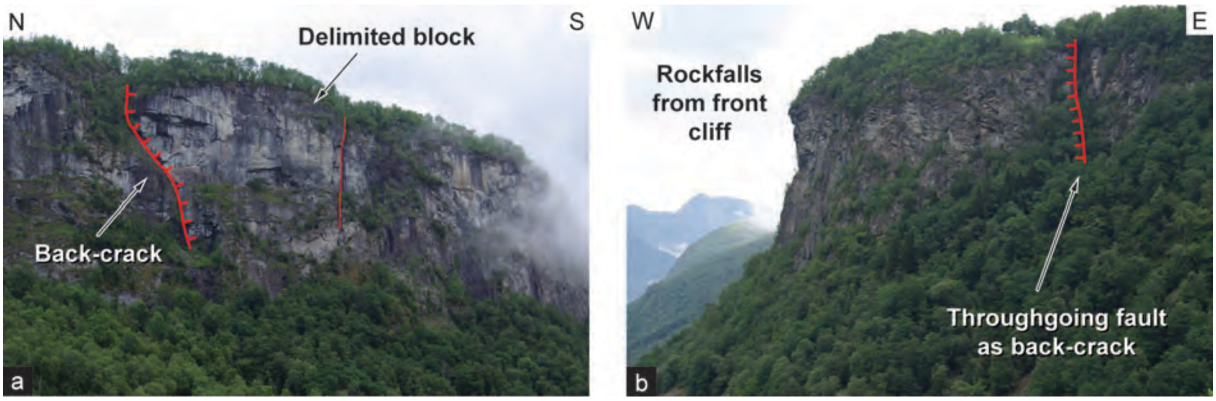

Figure 86: Photographs of the Kleivahammaren instability: a through-going structure that may act as the back-crack of a large instability is observed and should be further investigated.

6.1.9 Kloven

Kloven is located on a southwest-facing slope 770 m above Jimdalen Valley, 1 km SE of Tafjord (Figure 78). A helicopter reconnaissance flight in 2007 showed a past rockslide scar with a planar basal sliding surface and a subvertical lateral release surface (Figure 87). This basal sliding surface likely continues into the mountainside and might thus be activated in a future rockslide. However, there is currently no open back-crack or lateral release surface to delimit an unstable rock slope (Figure 87).

Recommendation: Kloven is classified as a potential unstable rock slope. At present the remaining rock slope does not show any signs of past or present displacements or deformation of a large volume. No further investigations or displacement measurements are necessary and the hazard and risk classification will not be made. However, this site may lead to rockfalls and develop over time into an unstable rock slope, due to structural and geological conditions. The site should be revisited after years to decades to detect any changes and be followed-up on InSAR data.

Figure 87: **Photograph of the potential unstable rock slope at Kloven: the basal sliding surface of a past rockslide likely continues into the mountainside. The lack of back-crack and lateral release surface indicates that no past displacement occurred at this potential instability.**

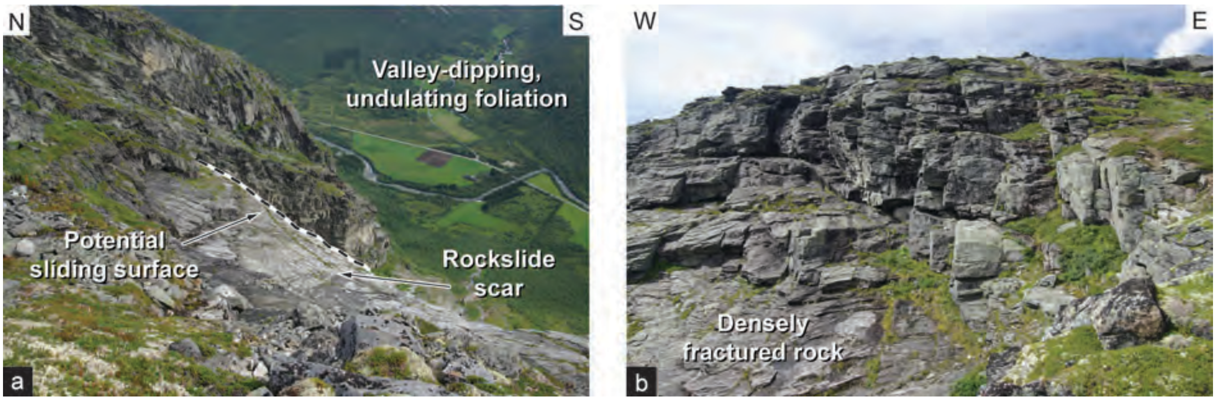

Figure 88: **Photographs of the Krikeberget rock slope: rockslides occurred in the past along a gently valley-dipping foliation.**

6.1.10 Krikeberget

Krikeberget (Figure 78) is situated on a southeast-facing slope 750 m above Valldalen Valley. Field mapping in 2007 showed a gently valley-dipping foliation that formed the basal sliding surface of past rockslides (Figure 88). These failure were however of small volume and did not form a rock avalanche with excessive run-out distance. Furthermore, there is no open back-crack or other structures linked to a large gravitational deformation within the slope. The bedrock is densely fractured and may currently lead to rockfalls.

Recommendation: There are no signs that the Krikeberget rock slope might fail in a massive rock slope failure. No further investigations or displacement measurements are necessary and the hazard and risk classification will not be made. However, rockfalls are possible and their run-out area is given by the rockfall susceptibility map or more detailed hazard maps, where available.

6.1.11 Kvitfjellet 1 & 2

Kvitfjellet 1 & 2 are located on a southwest-facing slope 620–720 m above Norddal village (Figure 78). Both instabilities were mapped in 2006 and field work results are described in previous reports (Henderson et al. 2006, Dahle et al. 2011a, Saintot et al. 2011b). The unstable rock slope is measured periodically using dGNSS since 2005 and TLS since 2006. Here, the latest results from dGNSS and TLS measurements are presented.

Two dGNSS points were installed in 2005 (Figure 89). Point 21-02 is located on Kvitfjellet 1 and point 21-03 on Kvitfjellet 2. Both points were measured again in 2006, 2007 and 2011, but no significant displacements were recorded over the 6 years measurement period.

Kvitfjellet 1 was scanned by TLS from several locations in the valley bottom and the talus slope formed by previous rockfalls (Figure 89). Repetitive scans made in 2009, 2010, 2011 and 2012 did not reveal significant displacements of the unstable rock slopes. However, more than ten rockfalls from the Kvitfjellet 1 instability are detected between 2006 and 2012.

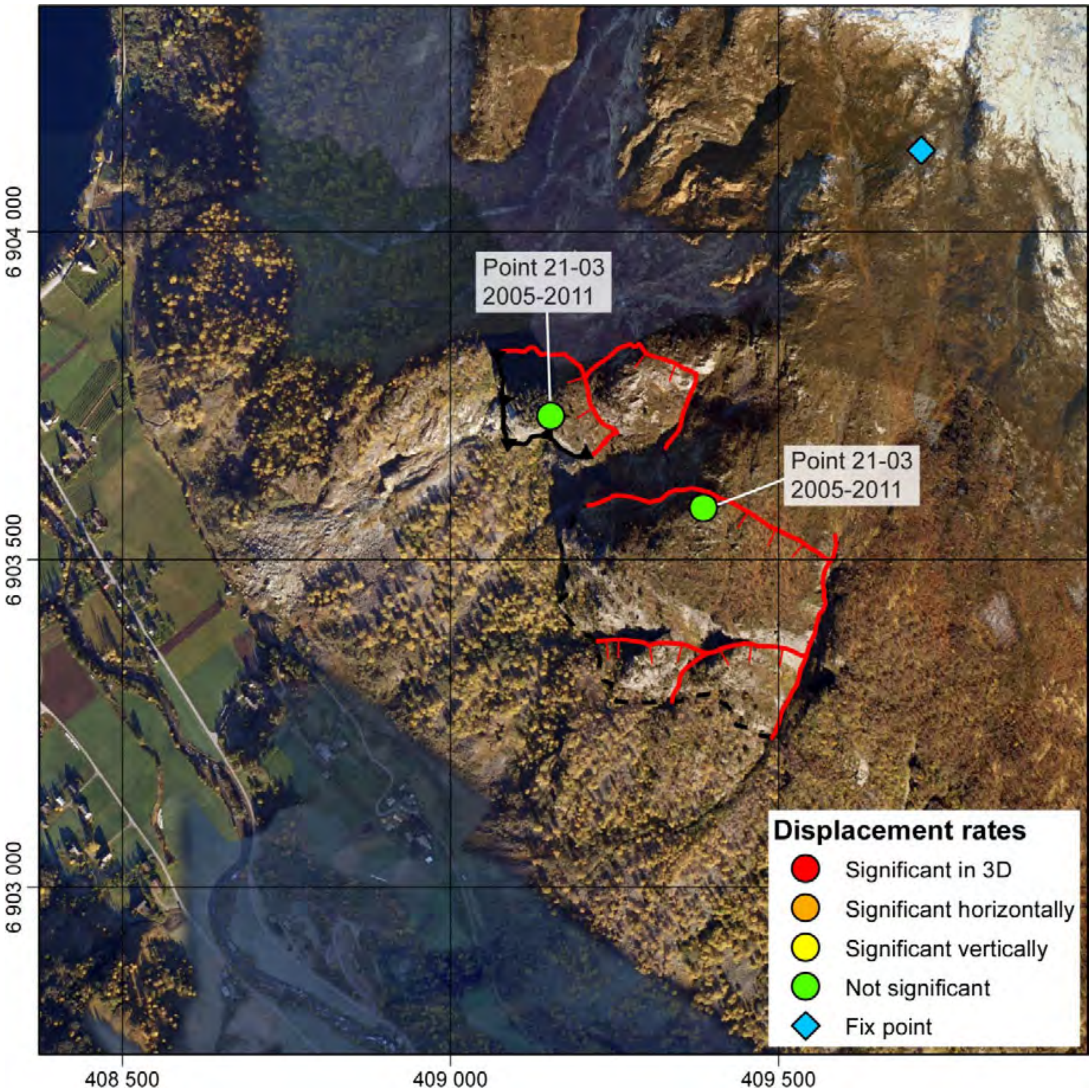

Figure 89: Map of the Kvitfjellet 1 & 2 instabilities with the location of dGNSS points for periodic displacement measurements. No significant displacements were detected over the 2005–2011 measurement period.

Several of these rockfalls occurred along the basal sliding surfaces and a major SW-NE open fracture. This may be an indication for deformation of the entire unstable rock slope, i.e. sliding along the basal surfaces and opening along the steep fracture (Oppikofer et al. 2012a).

A massive rock slope failure from Kvitfjellet 1 & 2 would cross the valley, impact several buildings in Norddal and dam the Storelva River with the possibility of subsequent dam breach and outburst flooding (Dahle et al. 2011a).

Recommendations: No significant displacements are measured up to now at Kvitfjellet 1 & 2. Periodic displacement measurements using dGNSS and TLS should be continued with 3–5 years interval. The hazard and risk classification needs to be made and further follow-up activities will be decided based on this classification.

6.1.12 Remsfjellet

Remsfjellet (Figure 78) is located on a south-facing slope 1120 m above Rem village in Valldalen Valley. Helicopter reconnaissance and field mapping was carried out in 2007. The instability is on the western termination of a mountain ridge with a deeply eroded vertical N-S-trending brecciated fault as eastern lateral free limit (Figure 90). The instability stands on a moderately valley-dipping basal sliding surface denuded downward by past rockslides (Figure 90). However, there are no signs of past displacements of the remaining block along the sliding surface as well as no visible offset at the back of the potential instability. The volume of the potential unstable rock slope is probably less than 0.5 million m³.

Recommendation: Remsfjellet is classified as a potential unstable rock slope. At present the remaining rock slope does not show any signs of past or present displacements or deformation of a large volume. No further investigations or displacement measurements are necessary and the hazard and risk classification will not be made. However, this site may lead to rockfalls and develop over time into an unstable rock slope, due to structural and geological conditions. The site should be revisited after years to decades to detect any changes and be followed-up on InSAR data.

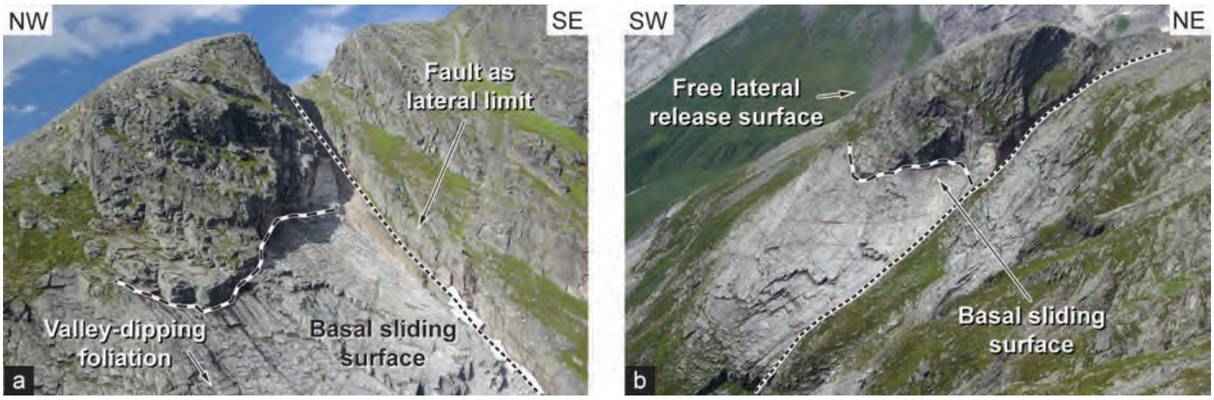

Figure 90: Photographs of the potential instability at Remsfjellet: a remaining block is located on a planar basal sliding surface and delimited to the east by an eroded fault. There are however no signs of past displacements.

6.1.13 Skorene 1 & 2

Skorene 1 & 2 (Figure 78) are located at 1185 m to 1360 m above Løvoll and Eide settlements and Eidsvatnet Lake in Eidsdalen Valley (Figure 91). Along the entire mountain side the foliation is flat-laying. Subvertical cross-cutting structures lead to rockfall activity and delimit front columns with a volume of tens of thousands of m³ that might topple. Further downslope gullies are eroded out. On the northern part of the mountain range, a N-S-trending brecciated hematite-rich fault cuts the ridge in two parts (Figure 91a) and highly fractured rocks are at the crest of the ridges. Scree deposits cover the slope at the foot of the cliffs. Some big blocks are present in the scree deposits.

Recommendations: There are no signs that the Skorene 1 & 2 rock slopes might fail in massive rock slope failures. No further investigations or displacement measurements are necessary and the hazard and risk classification will not be made. However, rockfalls are possible and their run-out area is given by the rockfall susceptibility map or more detailed hazard maps, where available.

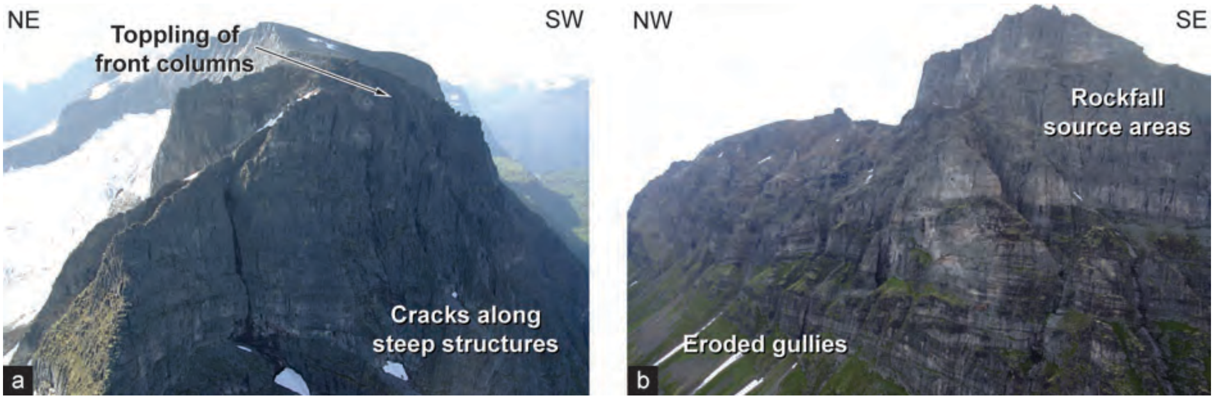

Figure 91: Photographs of the Skorene cliffs: the foliation is flat lying but a dense network of cross-cutting subvertical fractures leads to columnar failures and rockfall formation; the northern part of the site is a double ridge separated by a large fault zone.

6.1.14 Skrednakken 1

Skrednakken 1 is located on a north-facing slope 440 m above Norddalsfjord (Figure 78). The potential unstable rock slope was mapped in 2005 and described in previous reports (Henderson et al. 2006, Dahle et al. 2011a, Saintot et al. 2011b). The potential instability is measured periodically using dGNSS since 2006. Here, the latest results from dGNSS measurements are presented.

One dGNSS measurement points was installed on Skrednakken 1 in 2006 (Figure 92) and measured again in 2007 and 2012. No significant displacement was recorded over the 6 years measurement period. A potential collapse of this instability would impact Norddalsfjord and create a displacement wave (Dahle et al. 2011a).

Recommendation: Skrednakken 1 is classified as a potential unstable rock slope. At present the remaining rock slope does not show any signs of past or present displacements or deformation of a large volume. Periodic displacement measurements with dGNSS did not reveal significant displacements. No further investigations or displacement measurements are necessary and the hazard and risk classification will not be made. However, this site may lead to rockfalls and develop over time into an unstable rock slope, due to structural and geological conditions. The site should be revisited after years to decades to detect any changes and be followed-up on InSAR data.

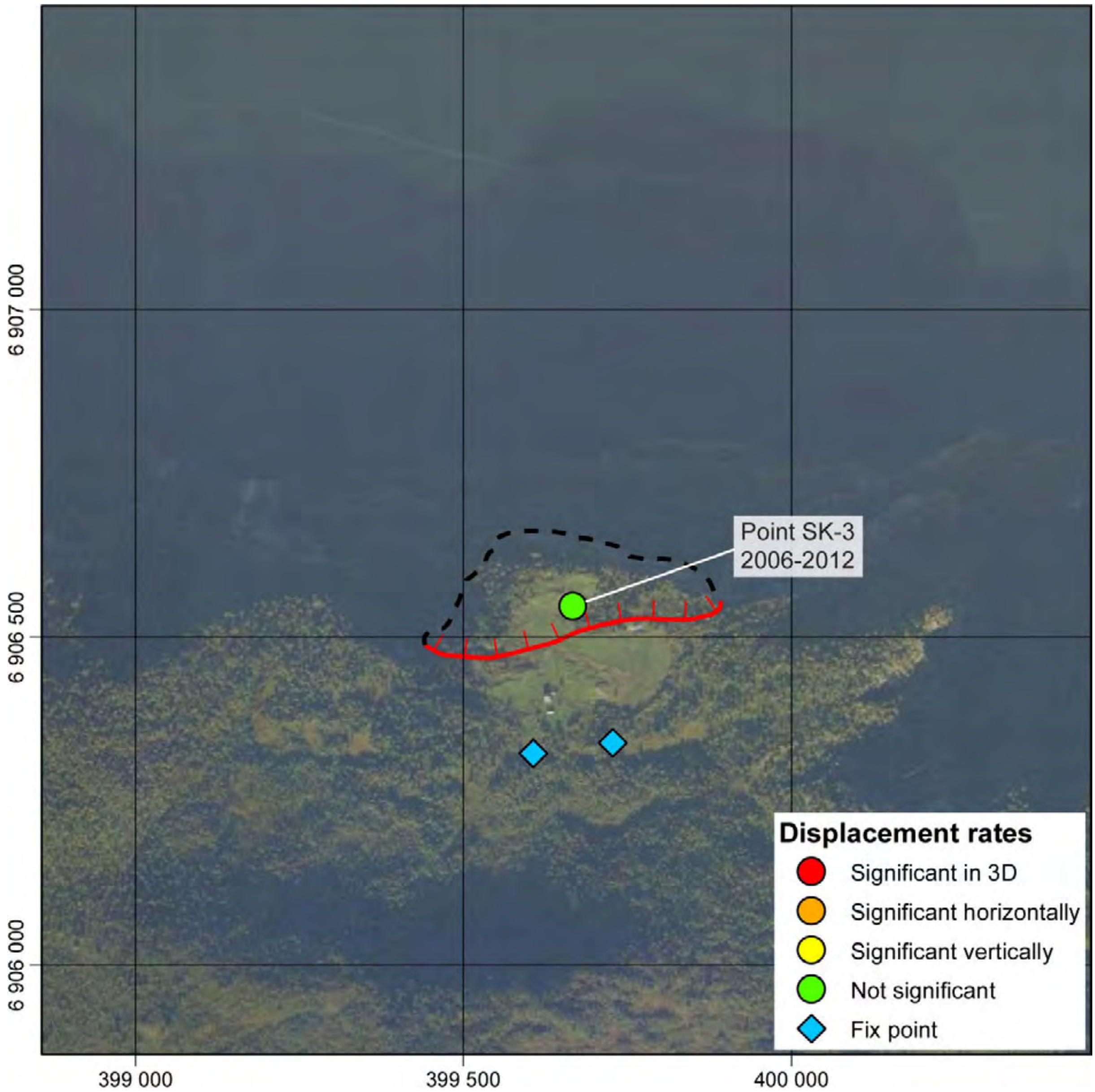

Figure 92: Map of the potential instability at Skrednakken 1 with the location of dGNSS points for periodic displacement measurements. No significant displacements were detected over the 2006–2012 measurement period.

6.2 Stordal municipality

There are four known sites located in Stordal municipality. Two of them are described in this report (Figure 93).

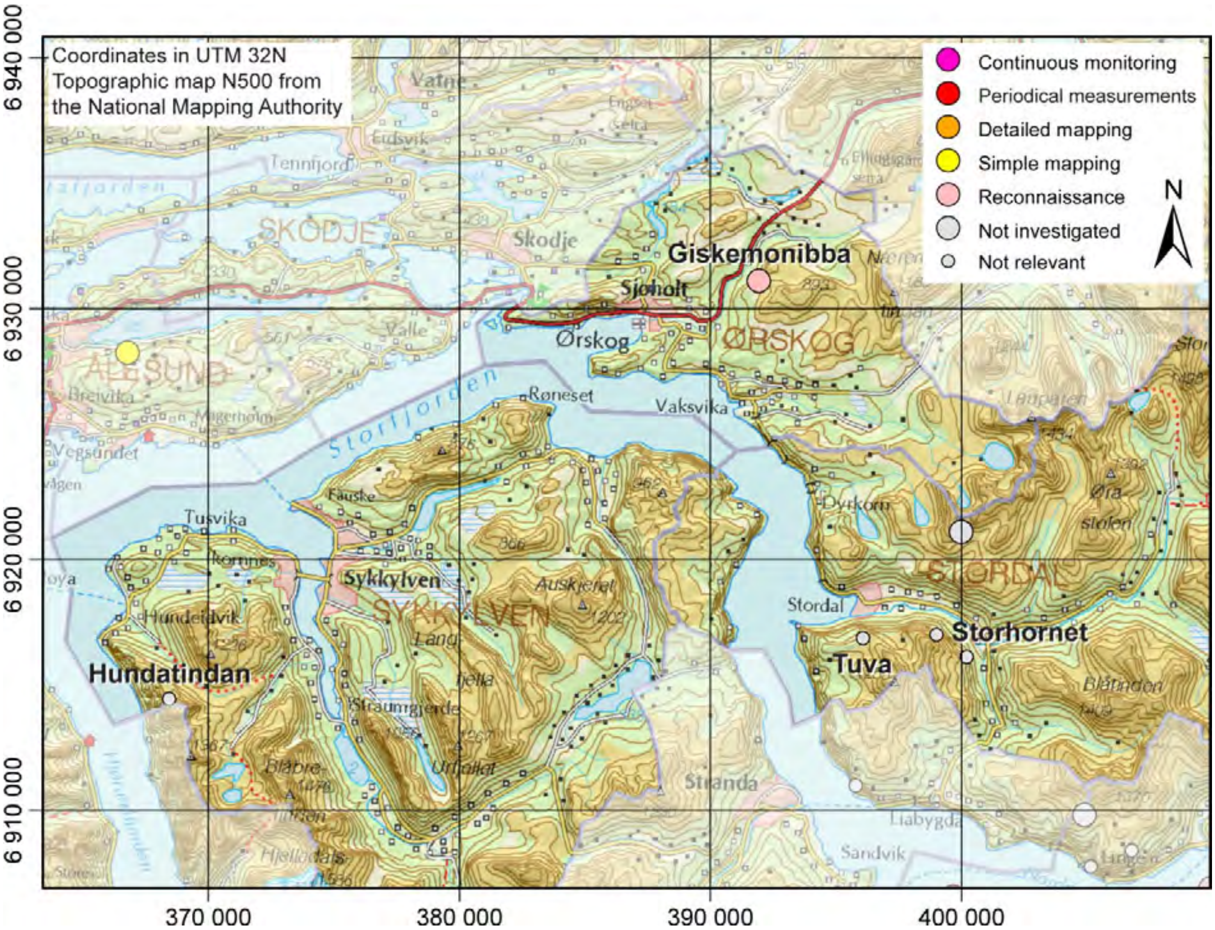

Figure 93: **Map of the known sites in the Stordal municipality (4 sites), Sykkylven municipality (1 site) and Ørskog municipality (1 site) with their investigation status. The name of the sites described in this report is shown.**

6.2.1 Storhornet 1 & 2

Storhornet 1 & 2 (Figure 93) are located on a northeast-facing cliff 1020 m respectively 500 m above Stordalen Valley. A helicopter reconnaissance flight made in 2007 did not show large unstable rock slopes at Storhornet 1 & 2. A past rockslide at Storhornet 1 used the moderately S-dipping foliation as basal sliding surface (Figure 94a). On the other hand, there are no open cracks above this scar and no large unstable rock slope is delimited at Storhornet 1. Two several meter high WNW-ESE and N-S-trending escarpments were identified on aerial photographs and supposed to delimit an instability at Storhornet 2 (Figure 94b). However, there are no visible openings or other signs of past displacements. No large unstable rock slope is delimited at Storhornet 2.

Recommendations: There are no signs that the Storhornet 1 & 2 rock slopes might develop toward massive rock slope failures. No further investigations or displacement measurements are necessary and the hazard and risk classification will not be made. However, rockfalls are possible and their run-out area is given by the rockfall susceptibility map or more detailed hazard maps, where available.

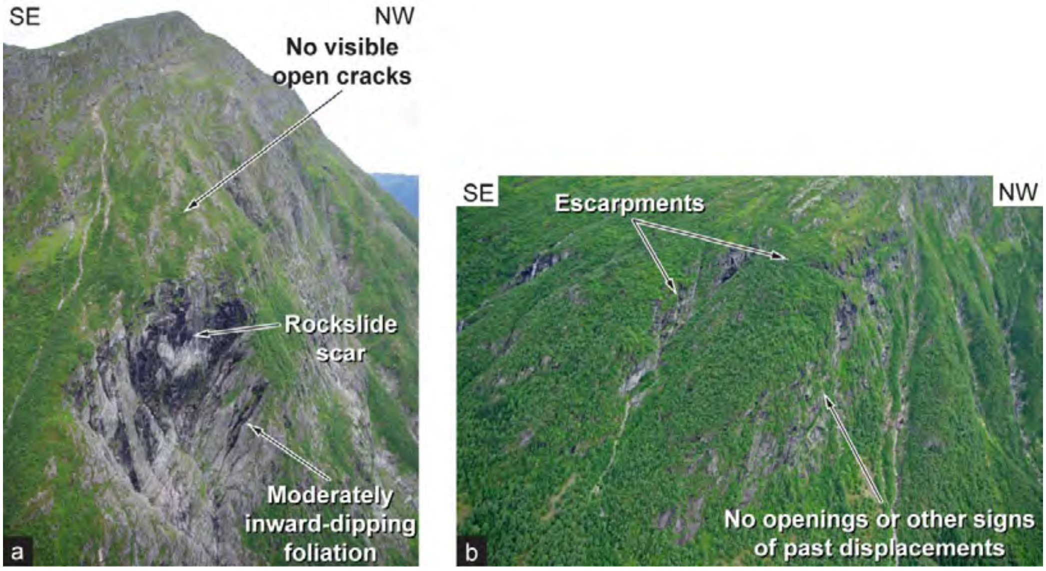

Figure 94: **Photographs of the Storhornet 1 & 2 rock slopes (in a and b respectively): a) no open cracks are visible above the scar of a past rockslide at Storhornet 1; b) several meters high escarpments were supposed to delimit an instability at Storhornet 2, but no openings or other signs of past displacements are visible.**

6.2.2 Tuva

Tuva is located on a north-facing slope 750 m above Stordal (Figure 93). The site was identified as potential deep-seated gravitational slope deformation based on aerial photograph analysis in Henderson et al. (2006). A helicopter reconnaissance flight and field survey in 2007 did not reveal any large gravitational structures delimiting an unstable rock slope (Figure 95). The foliation is gently S-dipping and thus not favourably oriented for sliding. A subvertical NNE-SSW-trending discontinuity set might delimit laterally small blocks that could fail as rockfalls.

Recommendation: There are no signs that the Tuva rock slope might fail in a massive rock slope failure. No further investigations or displacement measurements are necessary and the hazard and risk classification will not be made. However, rockfalls are possible and their run-out area is given by the rockfall susceptibility map or more detailed hazard maps, where available.

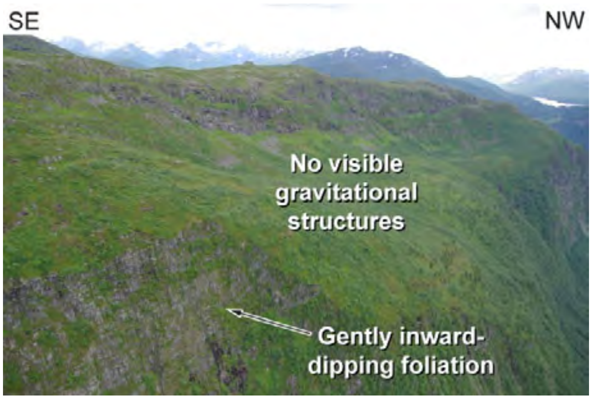

Figure 95: **Photographs of the Tuva rock slope: no signs of large gravitational deformation are visible.**

6.3 Stranda municipality

There are 30 known sites located in Stranda municipality. Ten of them are described in this report (Figure 96).

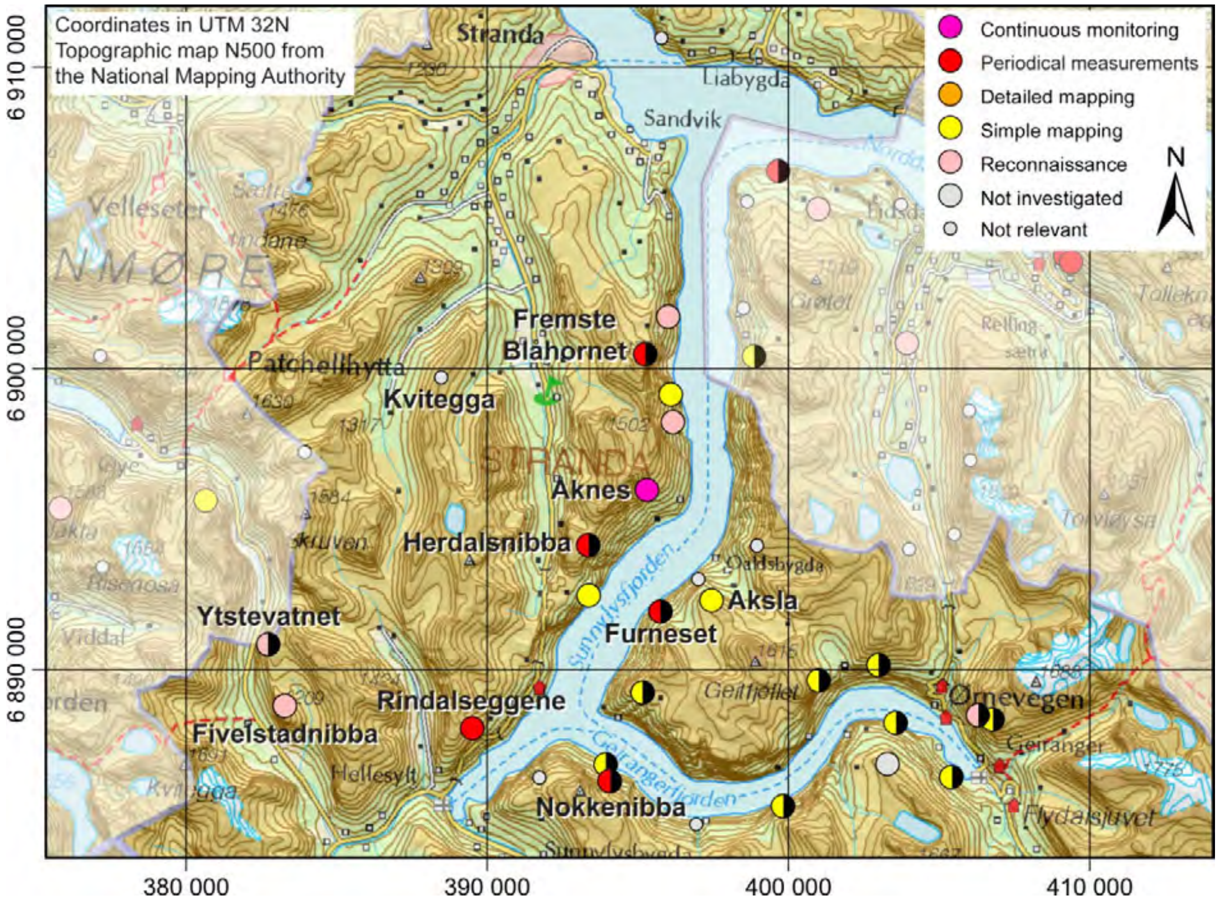

Figure 96: Map of the 30 known sites in the Stranda municipality with their investigation status. Potential unstable rock slopes are also shown with a half-masked symbol (◑). The name of the sites described in this report is shown.

6.3.1 <u>Aksla</u>

Aksla is situated on a northeast-facing slope 710 m above Sætredalen Valley and Oaldalsbygda (Figure 96). Helicopter reconnaissance in 2005 and field mapping in 2006 on top of the instability showed a linear depression that might be the morphologic expression of a back-crack (Figure 97b, Figure 98). Secondary open cracks within the instability are parallel to it. The foliation is steeply inward-dipping (Figure 97b), but a persistent moderately NW-dipping structure forms the basal sliding surface of the instability (Figure 97a). The eastern lateral release surface is not fully developed and marked by a gully due to preferential erosion of more fractured rock mass (Figure 97a). A small, highly fractured wedge is located at the western limit of the main instability and standing on the same basal surface. A massive failure or the Aksla instability would form a rock avalanche that would reach the buildings at Oaldalsbygda, but likely not form a significant displacement wave in Sunnylvsfjord.

Recommendation: A possible rock avalanche from the Aksla instability will have consequences, which will be assessed in the hazard and risk classification. Further follow-up activities will be decided based on this classification.

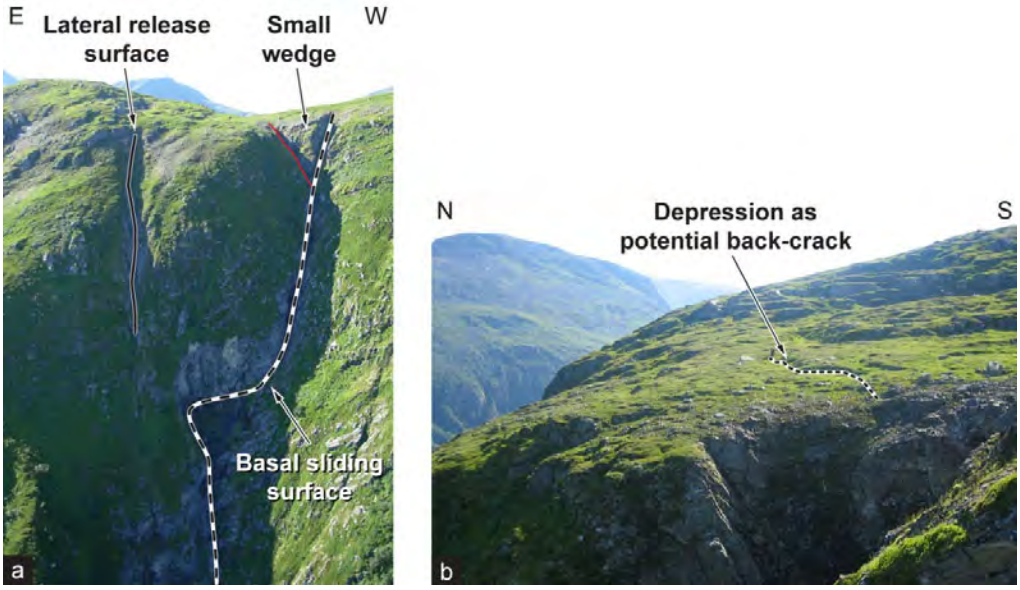

Figure 97: **Photographs of the Aksla instability: a) the basal sliding surface is formed by a moderately NW-dipping planar structure and the eastern limit is marked by a gully; b) a shallow surface depression marks the location of the potential back-crack.**

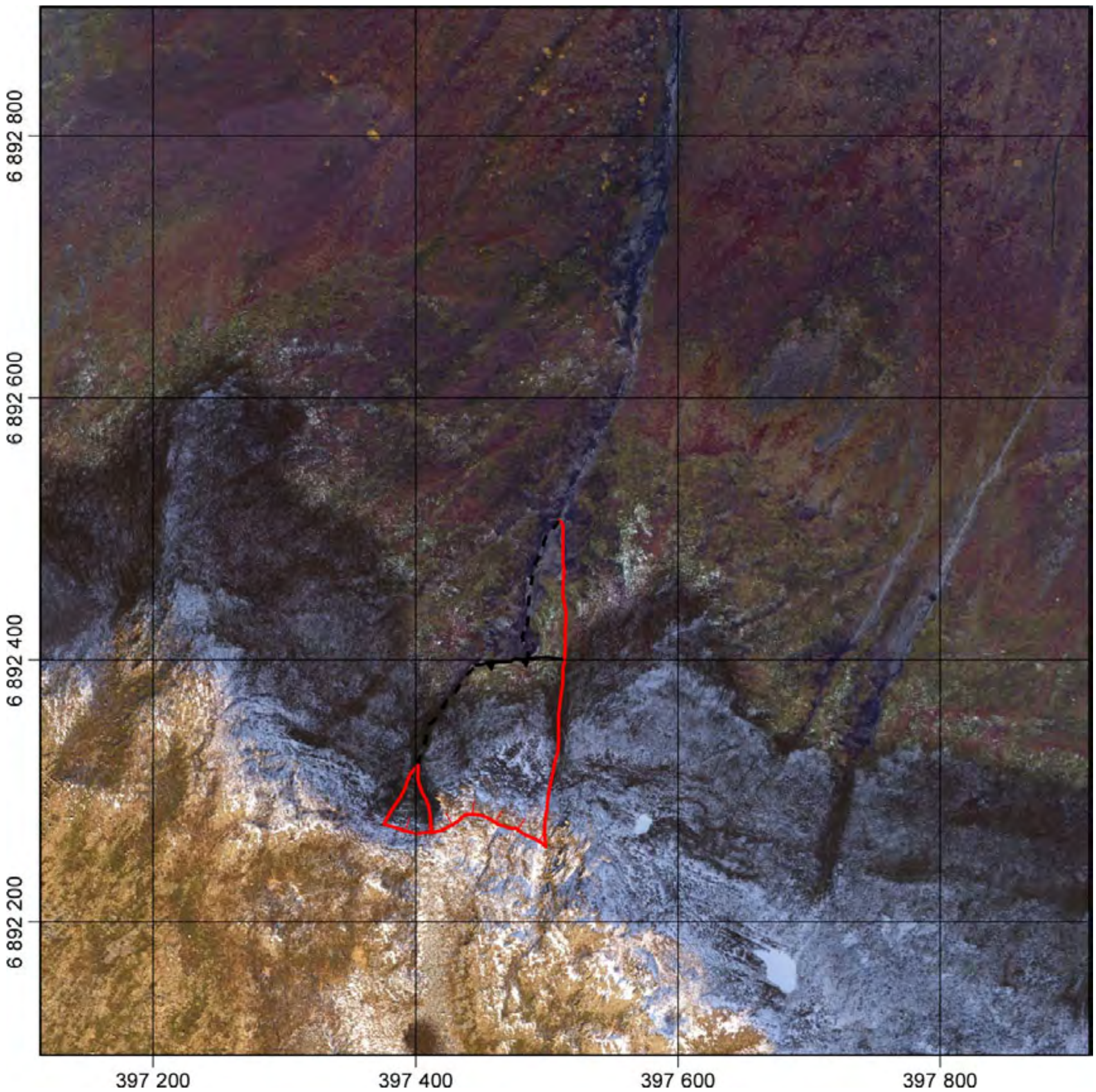

Figure 98: **Map of the Aksla instability.**

6.3.2 Fivelstadnibba

Fivelstadnibba is a mountain ridge 1209 m a.s.l. that separates the perched Sætredalen Valley from Norangsdalen Valley (Figure 96). A helicopter reconnaissance flight was made in 2011. On the northeast-facing slope 375 m above Sætredalen Valley several cracks enable sliding and toppling of relatively small (thousands to tens of thousands of m³) compartments (Figure 99a). Their failure would only affect the uninhabited Sætredalen Valley and have thus no major consequences (Dahle et al. 2011a). Rockfalls may occur on the subvertical west-facing cliffs of Fivelstadnibba and fall toward Norangsdalen Valley (Figure 99b). There are no visible structures that would delimit a large unstable rock slope that could fail towards Norangsdalen Valley.

Recommendation: A possible rock avalanche from the Fivelstadnibba instability will have no consequences. No further investigations or displacement measurements are necessary. The hazard and risk classification will be made after a simple run-out assessment. Further follow-up activities will be based on this classification.

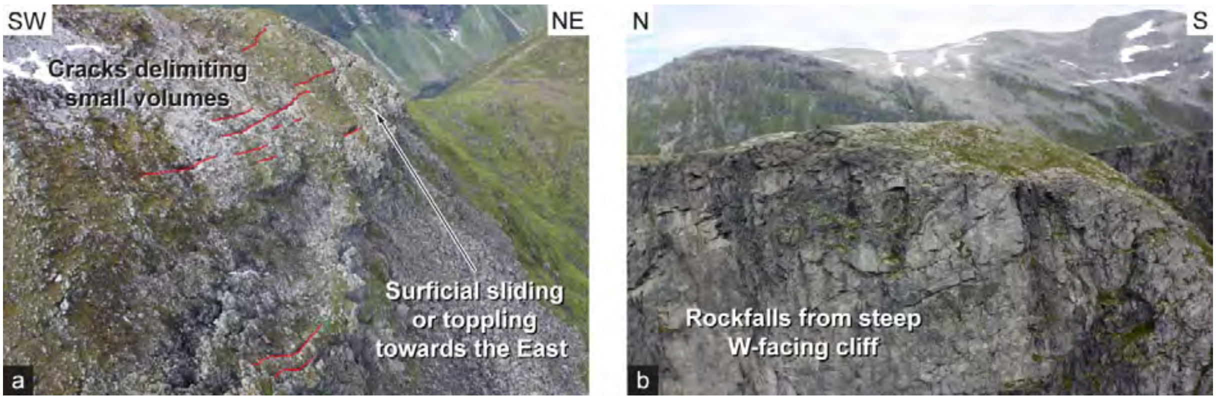

Figure 99: Photographs of the Fivelstadnibba rock slope: a) open cracks delimit slices that could slide or topple towards the East; b) rockfalls occur from the W-facing cliff above Norangsdalen Valley.

6.3.3 Fremste Blåhornet

Fremste Blåhornet is located on an east-facing slope 1100 m above Sunnylvsfjord (Figure 96). The potential unstable rock slope was mapped in 2005 and described in previous reports (Henderson et al. 2006, Dahle et al. 2011a, Saintot et al. 2011b). The potential instability is measured periodically using dGNSS since 2005. The scar of a large post-glacial rockslide from Fremste Blåhornet (Longva et al. 2009) was sampled for cosmogenic nuclide dating in 2009. Here, the latest results from dGNSS measurements and cosmogenic nuclide dating are presented.

Three dGNSS measurement points were installed on Fremste Blåhornet in 2005 (Figure 100) and measured again in 2006, 2007 and 2009. No significant displacements were recorded over the 4 years measurement period.

The deposits of the rock avalanche from Fremste Blåhornet were previously dated to 11 000–12 500 years BP (Longva et al. 2009). Cosmogenic nuclide dating of three samples of the rockslide scar at Fremste Blåhornet however gives an age of 2200 ± 300 years. It is thus likely that the deposits in Sunnylvsfjord do not correspond to the sampled sliding rockslide scar.

Recommendation: Fremste Blåhornet is classified as a potential unstable rock slope. At present the remaining rock slope does not show any signs of past or present displacements or deformation of a large volume. Periodic displacement measurements with

dGNSS did not reveal significant displacements. No further investigations or displacement measurements are necessary and the hazard and risk classification will not be made. However, this site may lead to rockfalls and develop over time into an unstable rock slope, due to structural and geological conditions. The site should be revisited after years to decades to detect any changes and be followed-up on InSAR data.

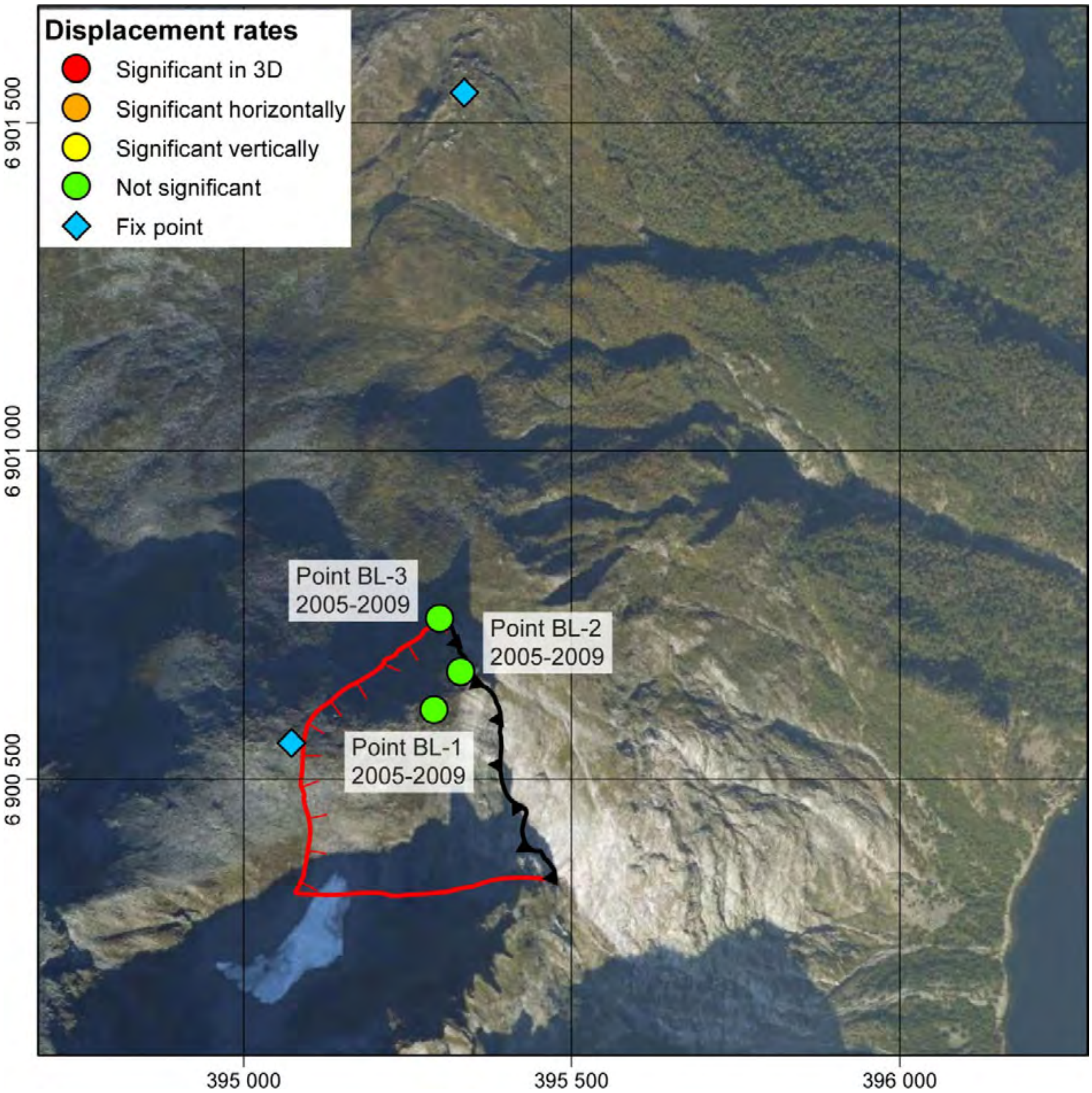

Figure 100: Map of the potential unstable rock slope at Fremste Blåhornet with the location of dGNSS points for periodic displacement measurements. No significant displacements were detected over the 2005–2009 measurement period.

6.3.4 Furneset

Furneset is located on a northwest-facing slope 450 m above Sunnylvsfjord (Figure 96). The potential unstable rock slope was mapped in 2005 and described in previous reports (Henderson et al. 2006, Dahle et al. 2011a, Saintot et al. 2011b). The potential instability is measured periodically using dGNSS since 2006. Here, the latest results from dGNSS measurements are presented.

One dGNSS measurement points was installed on Furneset in 2006 (Figure 101) and measured again in 2007. No significant displacement was recorded over the 1 year measurement period.

Recommendation: Furneset is classified as a potential unstable rock slope. At present the remaining rock slope does not show any signs of past or present displacements or deformation of a large volume (except for rockfall activity). Periodic displacement measurements with dGNSS did not reveal significant displacements. No further investigations or displacement measurements are necessary and the hazard and risk classification will not be made. However, this site may lead to rockfalls and develop over time into an unstable rock slope, due to structural and geological conditions. The site should be revisited after years to decades to detect any changes and be followed-up on InSAR data.

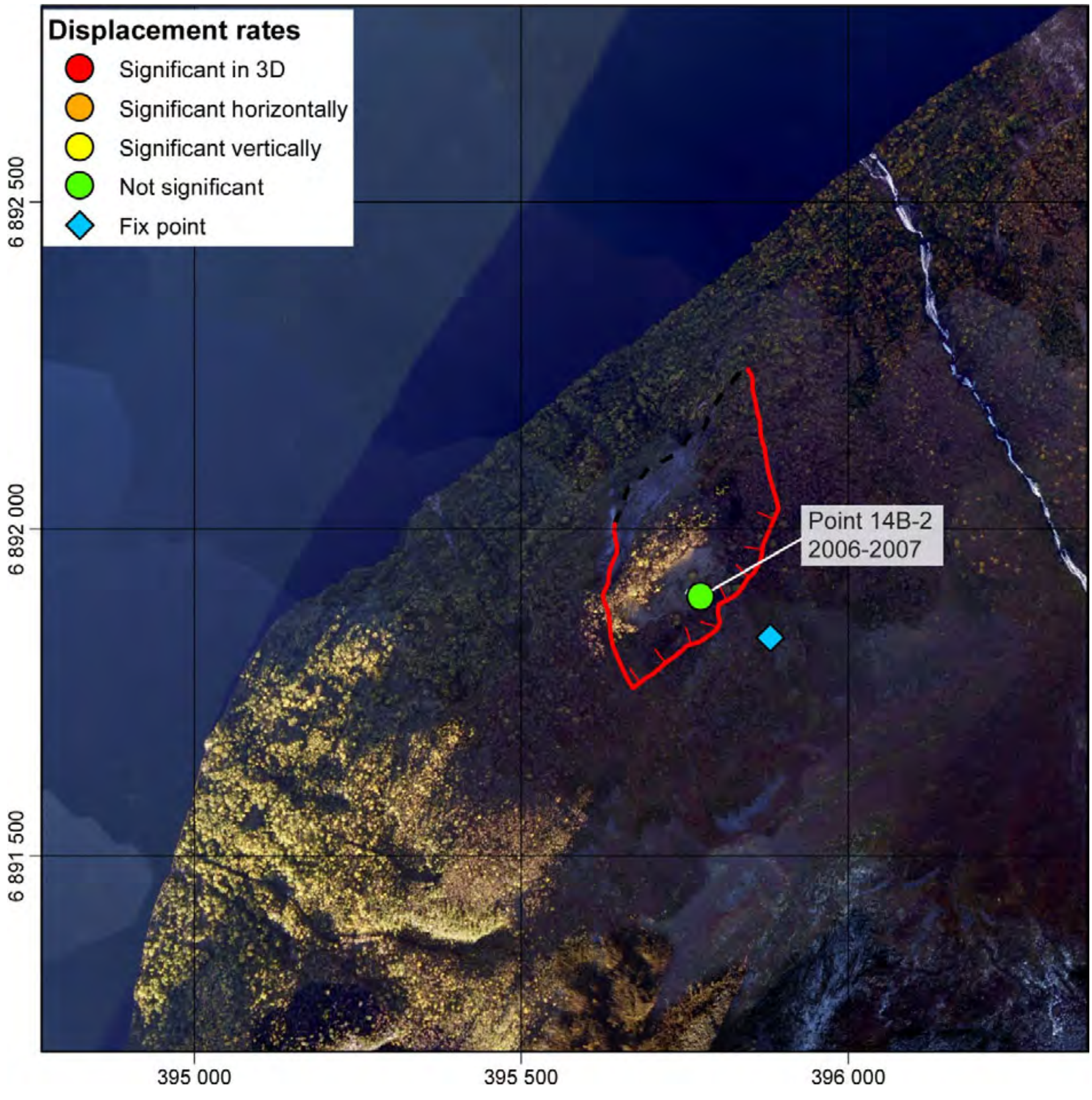

Figure 101: Map of the potential instability at Furneset with the location of dGNSS points for periodic displacement measurements. No significant displacements were detected over the 2006–2007 measurement period.

6.3.5 Herdalsnibba

Herdalsnibba is located on an east-facing slope 1120 m above Sunnylvsfjord (Figure 96). The potential unstable rock slope was mapped in 2005 and described in previous reports (Henderson et al. 2006, Dahle et al. 2011a, Saintot et al. 2011b). A past rockslide from the slope in front of Herdalsnibba was studied in detail by Oppikofer et al. (Oppikofer et al. 2011). The potential instability is measured periodically using dGNSS since 2006. Here, the latest results from dGNSS measurements are presented.

Four dGNSS measurement points were installed on Herdalsnibba (three points in 2006, one point in 2010) (Figure 102) and measured yearly until 2010 and again in 2012. No significant displacements were recorded over the 6 years measurement period.

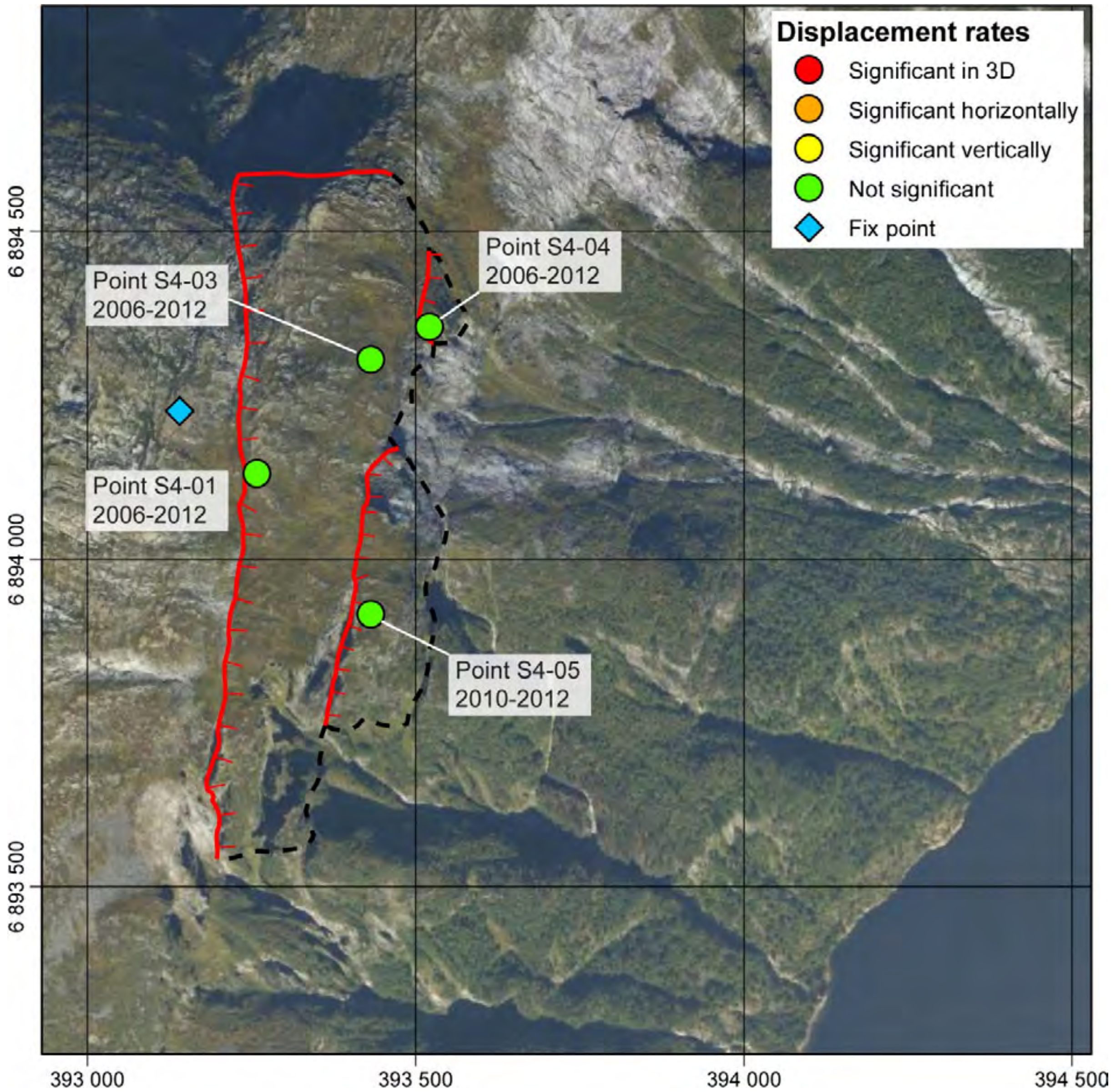

Figure 102: Map of the potential unstable rock slope at Herdalsnibba with the location of dGNSS points for periodic displacement measurements. No significant displacements were detected over the 2006–2012 measurement period.

Recommendation: Herdalsnibba is classified as a potential unstable rock slope. At present the remaining rock slope does not show any signs of past or present displacements or deformation of a large volume. Periodic displacement measurements with dGNSS did not reveal significant displacements. No further investigations or displacement measurements are necessary and the hazard and risk classification will not be made. However, this site may lead to rockfalls and develop over time into an unstable rock slope, due to structural and geological conditions. The site should be revisited after years to decades to detect any changes and be followed-up on InSAR data.

6.3.6 Kvitegga

Kvitegga (Figure 96) is a long mountain ridge separating the Strandamolskreddalen and Emdalsdalen Valleys. The locality was surveyed from helicopter in 2011 and there are no signs indicating that Kvitegga is an unstable rock slope. The 2 km long lineament on the SE flank is likely due to creep in glacial deposits (Figure 103) and not to gravitational deformation of the entire mountainside towards the WNW.

Recommendation: There are no signs that the Kvitegga rock slope might fail in a massive rock slope failure. No further investigations or displacement measurements are necessary and the hazard and risk classification will not be made. However, rockfalls are possible and their run-out area is given by the rockfall susceptibility map or more detailed hazard maps, where available.

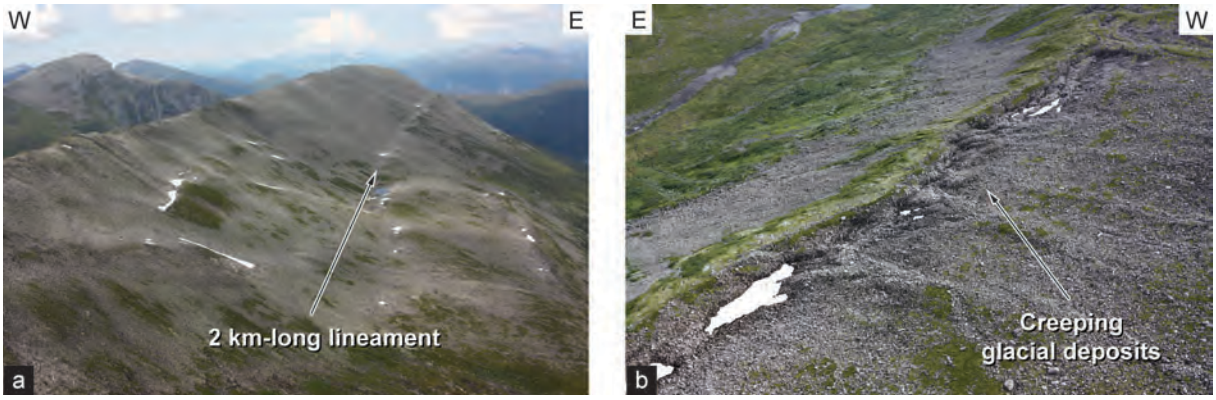

Figure 103: Photographs of the Kvitegga ridge: a) a 2 km long lineament on the SE-facing slope is likely caused by creep of loose glacial deposits; b) detail of the lineament.

6.3.7 Nokkenibba 2

Nokkenibba 2 is located on a northeast-facing slope 700 m above Geirangerfjord (Figure 96). The potential unstable rock slope was surveyed from helicopter in 2005 and described in previous reports (Henderson et al. 2006, Dahle et al. 2011a, Saintot et al. 2011b). The potential instability is measured periodically using dGNSS since 2006. The scar of a large post-glacial rockslide from Nokkenibba (Longva et al. 2009) was sampled for cosmogenic nuclide dating in 2009. Here, the latest results from dGNSS measurements and cosmogenic nuclide dating are presented.

One dGNSS measurement point was installed on Nokkenibba 2 in 2006 (Figure 104) and measured again in 2007 and 2010. No significant displacements were recorded over the 4 years measurement period.

The deposits of the rock avalanche from Nokkenibba were previously dated to 8000–9000 years BP (Longva et al. 2009). Cosmogenic nuclide dating of two samples of the rock-slide scar at Nokkenibba gives an age of 7100 ± 900 years and thereby match relatively well with previous results.

Recommendation: Nokkenibba 2 is classified as a potential unstable rock slope. At present the remaining rock slope does not show any signs of past or present displacements or deformation of a large volume (except for rockfall activity). Periodic displacement measurements with dGNSS did not reveal significant displacements. No further investigations or displacement measurements are necessary and the hazard and risk classification will not be made. However, this site may lead to rockfalls and develop over time into an unstable rock slope, due to structural and geological conditions. The site should be revisited after years to decades to detect any changes and be followed-up on InSAR data.

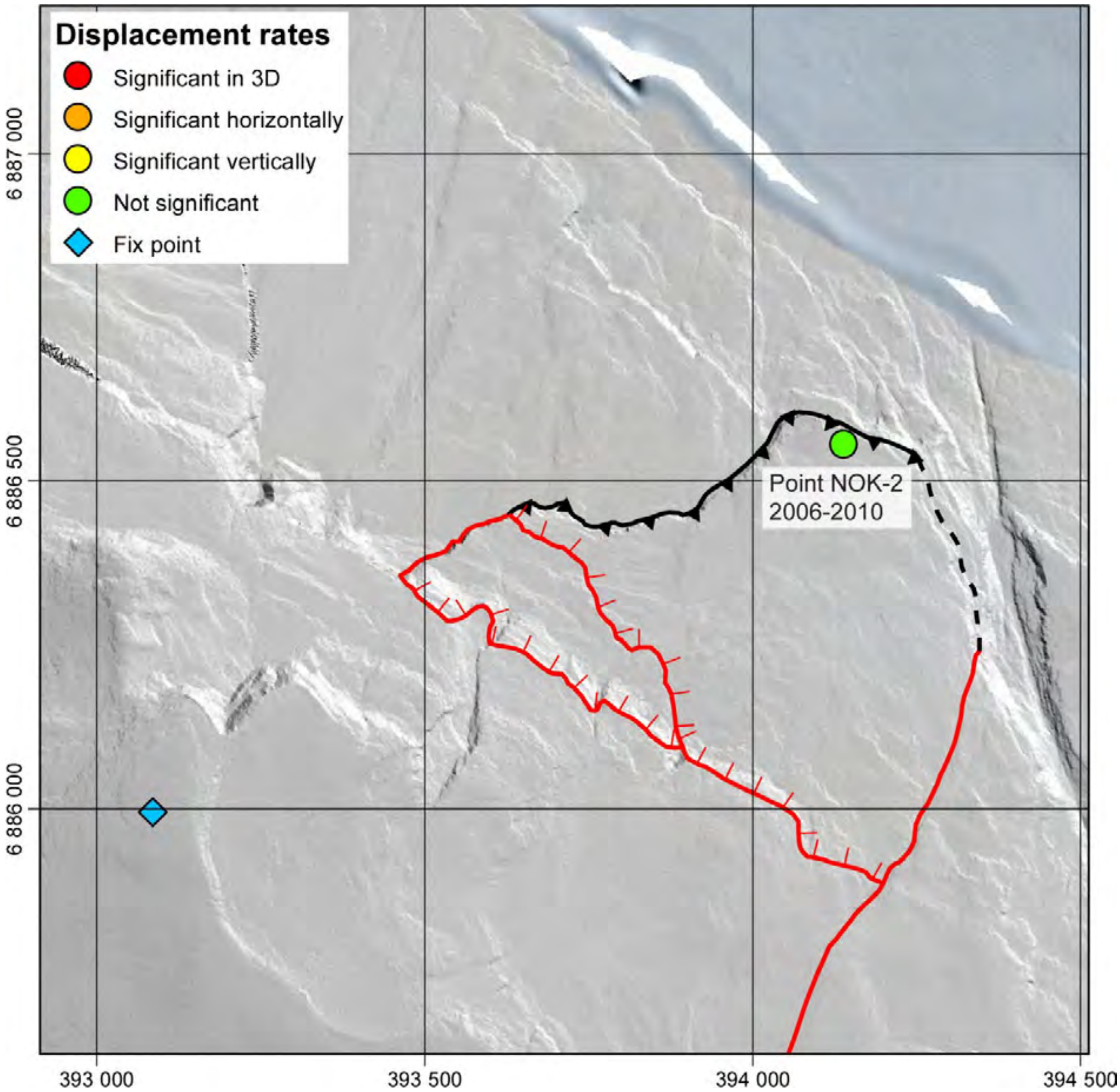

Figure 104: Map of the potential unstable rock slope at Nokkenibba 2 with the location of dGNSS points for periodic displacement measurements. No significant displacements were detected over the 2006–2010 measurement period.

6.3.8 Rindalseggene

Rindalseggene is located on a southeast-facing slope 950 m above Sunnylvsfjord (Figure 96). The unstable rock slope was mapped in 2005 and described in previous reports (Henderson et al. 2006, Dahle et al. 2011a, Saintot et al. 2011b). The Rindalseggene instability is measured periodically using dGNSS since 2005 and TLS since 2006. Here, the latest results from dGNSS and TLS measurements are presented.

Three dGNSS measurement points were installed on the Rindalseggene instability in 2005 (Figure 105) and measured yearly until 2012, except in 2009. No significant displacements were recorded over the 7 years measurement period, even though some of the yearly measurements indicate some deformation at point 6B-03. This was however not confirmed by further measurements.

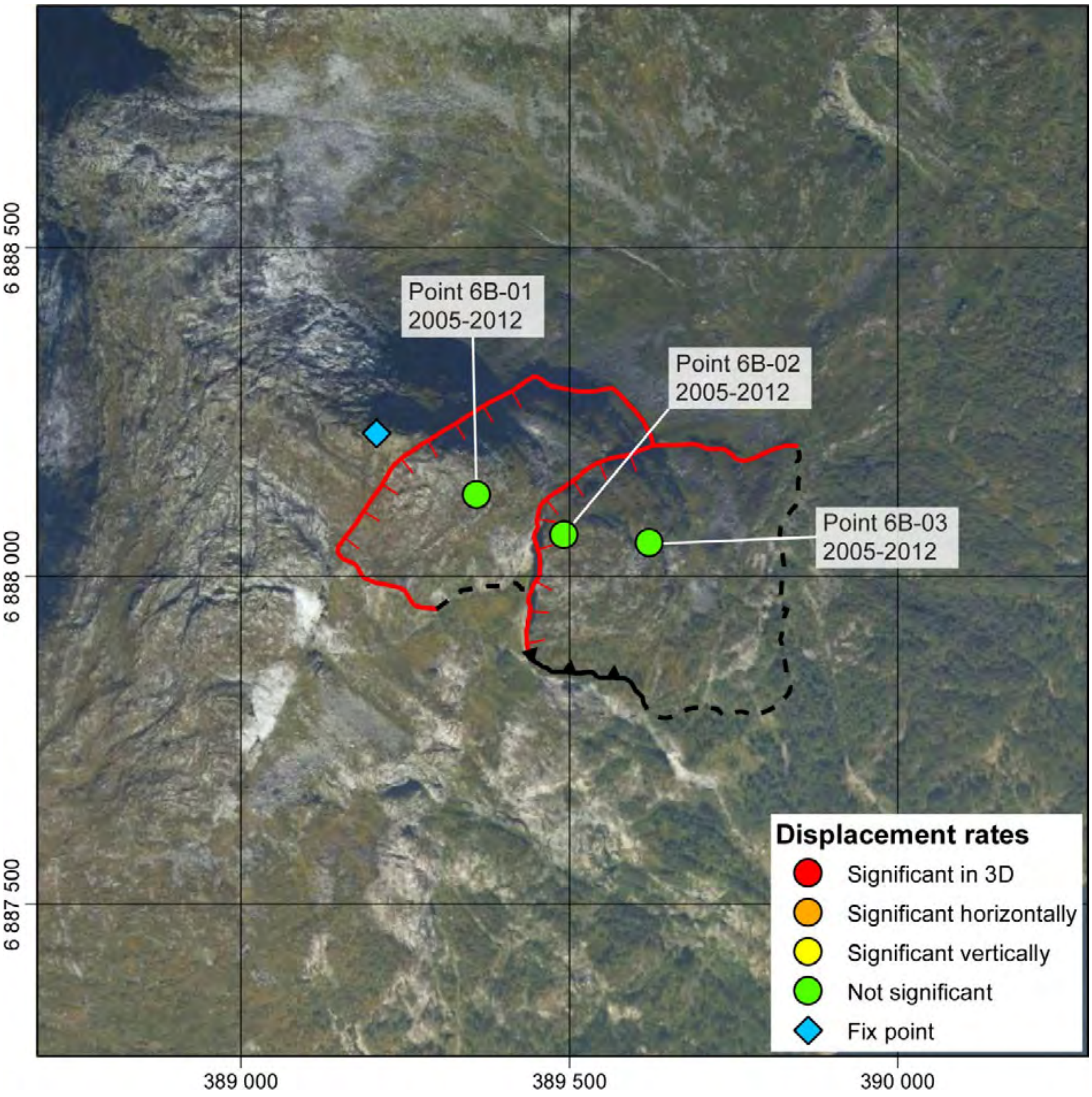

Figure 105: Map of the Rindalseggene unstable rock slope with the location of dGNSS points for periodic displacement measurements. No significant displacements were detected over the 2005–2012 measurement period.

The Rindalseggene instability was scanned by TLS in 2006 and 2011 from one viewpoint SW of the instability. The analysis of these repetitive TLS datasets does not reveal significant displacements of the instability over the 5 years measurement period.

Recommendation: No significant displacements are measured up to now at Rindalseggene. Periodic displacement measurements using dGNSS and TLS should be continued with 3–5 years interval. The hazard and risk classification needs to be made and further follow-up activities will be decided based on this classification.

6.3.9 Ytstevatnet

Ytstevatnet (Figure 96) is situated on a west-facing slope 780 m above Norangsdalen Valley. The site was surveyed from helicopter in 2011 and is characterized by a potential back-crack that follows subvertical valley-parallel discontinuities (Figure 106). The back-crack curves to become steeply valley-dipping at the foot of the slope and might act as a potential basal sliding surface (Figure 106a). However, there are no signs of past displacements or openings along this basal sliding surface. The foliation is gently dipping into the mountainside. The potential instability has a free lateral surface to the north, but there is no visible lateral release surface to the south (Figure 106a). There are no major signs of activity or recent displacements, but past rockslides have occurred from the surrounding rock slopes, which is underlined by several rock avalanche deposits in Norangsdalen Valley. A massive failure of the Ytstevatnet instability would likely also form a rock avalanche and cross Norangsdalen Valley, but not lead to major consequences since the valley is uninhabited.

Recommendation: Ytstevatnet is classified as a potential unstable rock slope. At present the remaining rock slope does not show any signs of past or present displacements or deformation. No further investigations or displacement measurements are necessary and the hazard and risk classification will not be made. However, this site may lead to rockfalls and develop over time into an unstable rock slope, due to structural and geological conditions. The site should be revisited after years to decades to detect any changes and be followed-up on InSAR data.

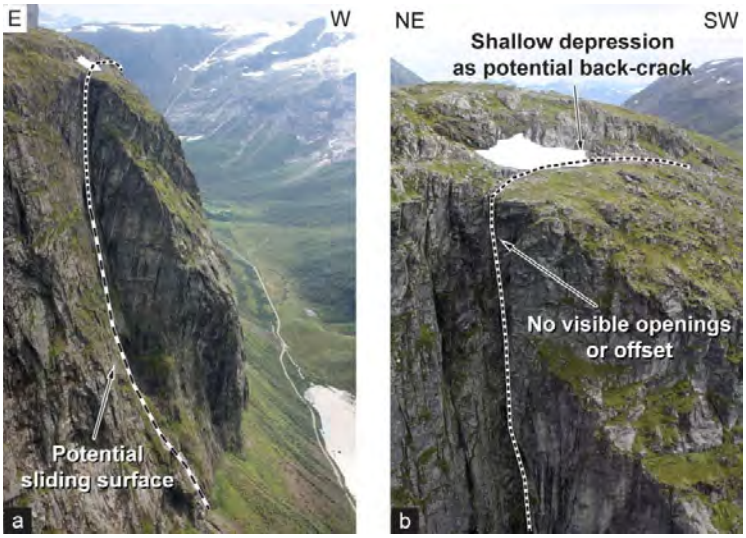

Figure 106: Photographs of the potential unstable rock slope at Ytstevatnet: a) the back-bounding surface is slightly changing in dip angle and forms a potential sliding surface in the lower part; b) no signs of past displacements are visible along the potential back-crack.

6.3.10 Åknes

Åknes is located on a southeast-facing slope 860 m above Sunnylvsfjord (Figure 96). Åknes is continuously monitored by the Åknes/Tafjord Early-Warning Centre and has been investigated within the international Åknes/Tafjord project by:

- field mapping, structural mapping and analysis of high-resolution digital elevation models and aerial photographs (Braathen et al. 2004, Derron et al. 2005a, Blikra et al. 2006, Ganerød et al. 2008, Nordvik et al. 2009, Ganerød 2010, Jaboyedoff et al. 2011, Oppikofer et al. 2011);
- geophysical investigations (Rønning et al. 2006, Rønning et al. 2008, Heincke et al. 2010);
- borehole logging and investigations (Ganerød et al. 2007, Elvebakk 2008);
- geomechanical analyses (Grøneng et al. 2009, Grøneng et al. 2010);
- groundwater analyses (Frei 2008, Storrø and Gaut 2009);
- numerical slope stability modelling (Kveldsvik et al. 2008, Kveldsvik et al. 2009a, Kveldsvik et al. 2009b);
- modelling of rockslide-triggered displacement waves (Eidsvig and Harbitz 2005);
- periodic displacement measurements using terrestrial laser scanning (Oppikofer et al. 2009);
- high-resolution satellite-based InSAR measurements (Dehls et al. 2012);
- continuous monitoring instrumentation (Kveldsvik et al. 2006, Blikra 2008, Nordvik and Nyrnes 2009, Kristensen et al. 2010)();
- risk analyses (Blikra et al. 2006, Lacasse 2008, Dahle et al. 2011a, Eidsvig et al. 2011).

The Åknes rockslide was measured periodically using dGNSS between 2004 and 2008. Nine dGNSS points were installed in October 2004 in the upper, middle and lower part of the unstable rock slope (Figure 107). The dGNSS network was extended in August 2005 in the lower part of the slope with 5 additional measurement points. Repetitive measurements were made in June 2005 for the first series of measurement points and in October 2005, August 2006, August 2007 and August 2008 for all points.

High displacement rates are measured in the uppermost part of the rockslide with up to 151 mm/year (Figure 107). Displacement directions are roughly southward with relatively steep plunge angles, which is consistent with results from periodic TLS measurements between 2006 and 2008 (Oppikofer et al. 2009). Three measurement points in the middle part of the slope show coherent displacement rates (19 to 27 mm/year) and displacement directions towards the SE. No significant displacements are detected in the lower section of the Åknes unstable rock slope (Figure 107).

The displacement directions measured by periodic dGNSS measurements are in agreement with the conceptual model of the Åknes rockslide from Jaboyedoff et al. (2011). The model relates the diverging displacement directions to the different orientations of the basal sliding surface that should follow the conspicuous undulation of the gneiss foliation. High-resolution InSAR data from TerraSAR-X and Radarsat-2 satellites show active displacements in the upper and middle part of the slope and thus confirm the periodic dGNSS measurements (Dehls et al. 2012).

Recommendation: Åknes is under continuous monitoring and data are being sent to the Åknes/Tafjord Early-Warning Centre, which is also responsible for further follow-up activities. New scenarios should be defined for the Åknes rockslide based on the latest monitoring results and investigations.

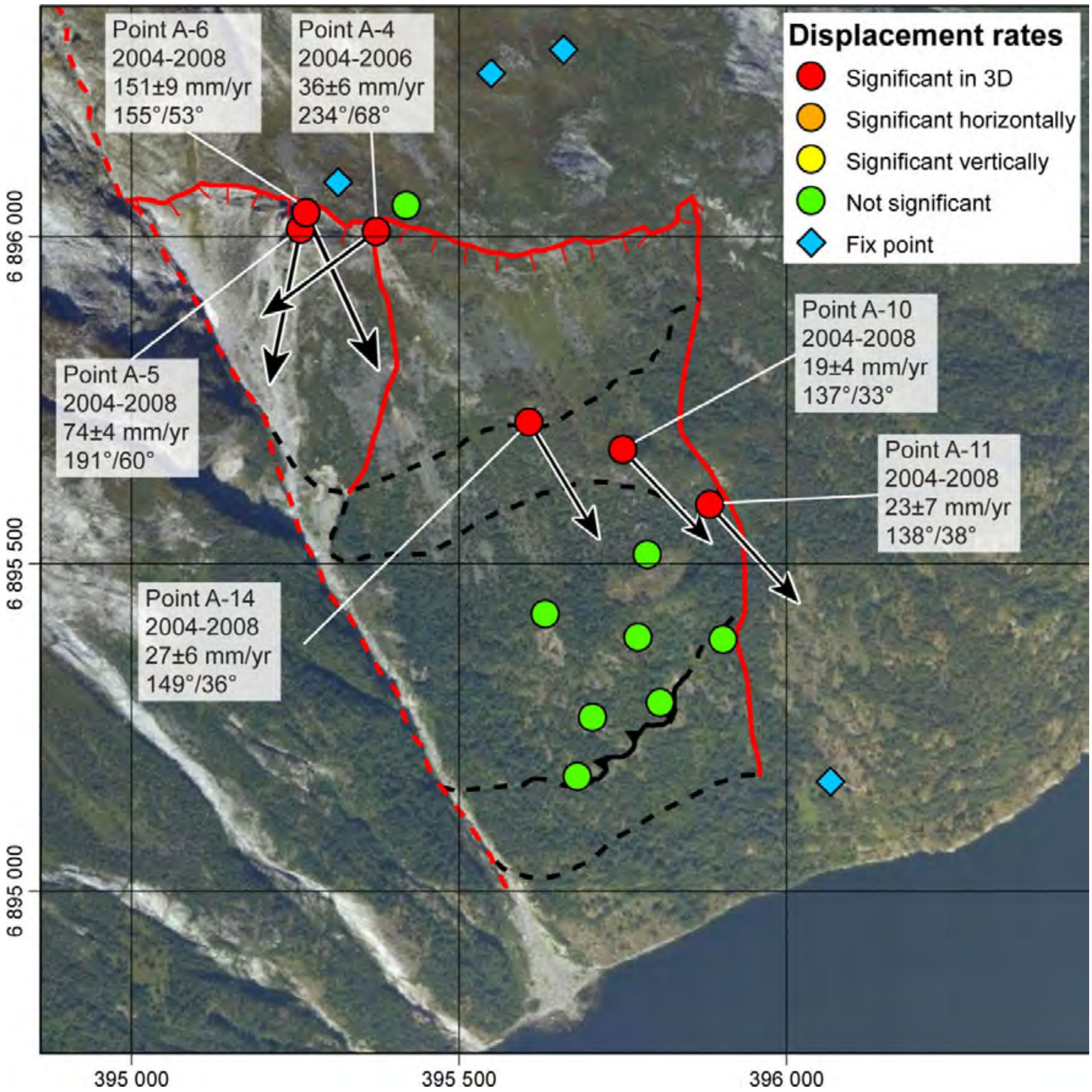

Figure 107: Map of the Åknes unstable rock slope with the location of dGNSS points for periodic displacement measurements and average displacement vectors for the 2004–2008 measurement period.

6.4 Sykkylven municipality

There is one known site located in Sykkylven municipality, which is described in this report (Figure 93).

6.4.1 Hundatindan

Hundatinden is located on a west-facing slope 910 m above of Hjørundfjord (Figure 93). A series of four valley-parallel depressions are visible on the plateau (Figure 108a). A helicopter reconnaissance flight in 2011 revealed that these depressions are not caused by gravitational movements, but are more likely paleodrainage systems and/or lateral moraines. There are no visible structures at Hundatinden to delimit a large unstable rock slope. Rockfalls may however originate from the highly fractured rock mass along the front cliff (Figure 108b).

Recommendation: There are no signs that the Hundatindan rock slope might fail in a massive rock slope failure. No further investigations or displacement measurements are necessary and the hazard and risk classification will not be made. However, rockfalls are possible and their run-out area is given by the rockfall susceptibility map or more detailed hazard maps, where available.

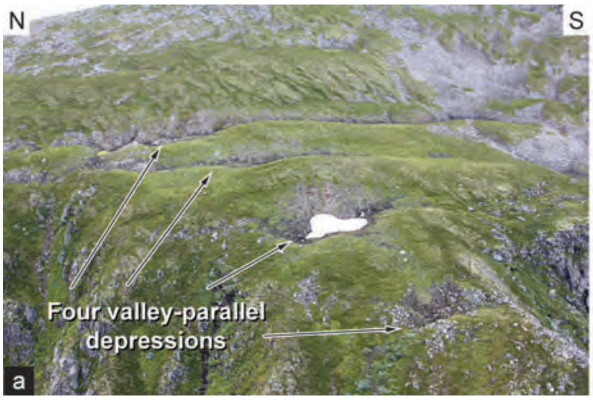

Figure 108: Photographs of the Hundatindan rock slope: a) valley-parallel depressions formed by a paleodrainage system or/and lateral moraines; b) rockfalls may occur from the highly fractured rock mass along the front cliff.

6.5 Ørskog municipality

There is one known site located in Ørskog municipality, which is described in this report (Figure 93).

6.5.1 Giskemonibba

Giskemonibba (Figure 93) is situated on a northwest-facing slope 330 m above Landedalen Valley. A helicopter reconnaissance flight in 2011 showed several open cracks that delimit an unstable rock slope (Figure 109). The foliation is gently-dipping into the mountainside and subvertical discontinuities delimit several small columns that may topple towards the valley. Toppling failures have occurred in the past, but the deposits remained at the foot of the gentle slope (Figure 109). An eventual a massive failure from Giskemonibba would not reach the valley bottom and would thus have no major consequences (Dahle et al. 2011a).

Recommendation: A possible rock avalanche from the Giskemonibba instability will have no consequences. No further investigations or displacement measurements are necessary. The hazard and risk classification will be made after a simple run-out assessment. Further follow-up activities will be based on this classification.

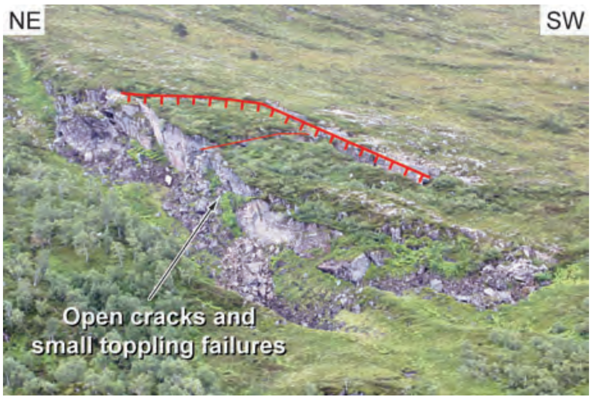

Figure 109: Photograph of the Giskemonibba instability: open cracks delimit the instability and divide it into small blocks that may topple.

7. SØRE SUNNMØRE REGION

7.1 Hareid municipality

There is one known site located in Hareid municipality, which is described in this report (Figure 110).

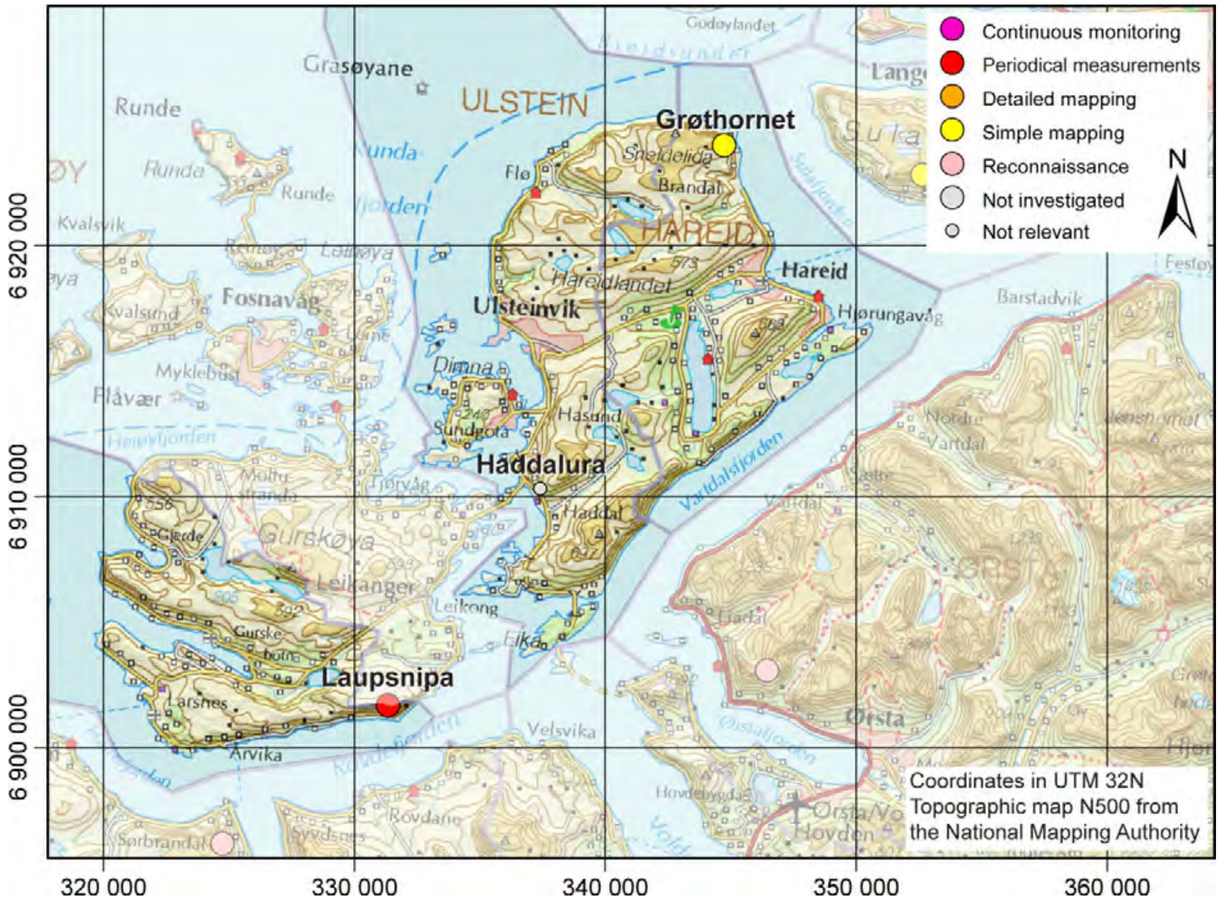

Figure 110: Map of the known sites in the Hareid municipality (1 site), Sande municipality (1 site) and Ulstein municipality (1 site) with their investigation status. The name of the sites described in this report is shown.

7.1.1 Grøthornet

Grøthornet is located on a northeast-facing slope 420 m above Sulafjord (Figure 110). A helicopter reconnaissance flight was made in 2011 and followed by field mapping in 2012 (Figure 111). The potential unstable rock slope is delimited to the west by a more than 130-m-long, open back-crack, and to the south by a lateral release surface that is marked by a surficial linear depression (Figure 112). The gneiss foliation is folded and changes from moderately SSE-dipping in the north to shallow NNE-dipping at the lateral release surface in the south and to moderately N-dipping at the back-crack. A foliation-parallel potential basal sliding surface is observed at the base of the instability in the north (Figure 112c).

The past deformations at Grøthornet exceed several dm to m (Figure 112b). However, the measured discontinuities do not allow for a planar or wedge sliding mechanism, except at the back-crack where the foliation is favourably oriented for planar sliding. This makes possible that the gneiss foliation also is favourably oriented in the inaccessible lower part of the instability to form a basal sliding surface.

The volume of the Grøthornet instability was computed using the available digital elevation model and is approximately 0.5 million m³. The collapse of this instability could create a rock avalanche that impacts Sulafjord and creates a displacement wave (Dahle et al. 2011a).

Recommendation: A possible rock avalanche from the Grøthornet instability will have consequences, which will be assessed in the hazard and risk classification. Further follow-up activities will be decided based on this classification.

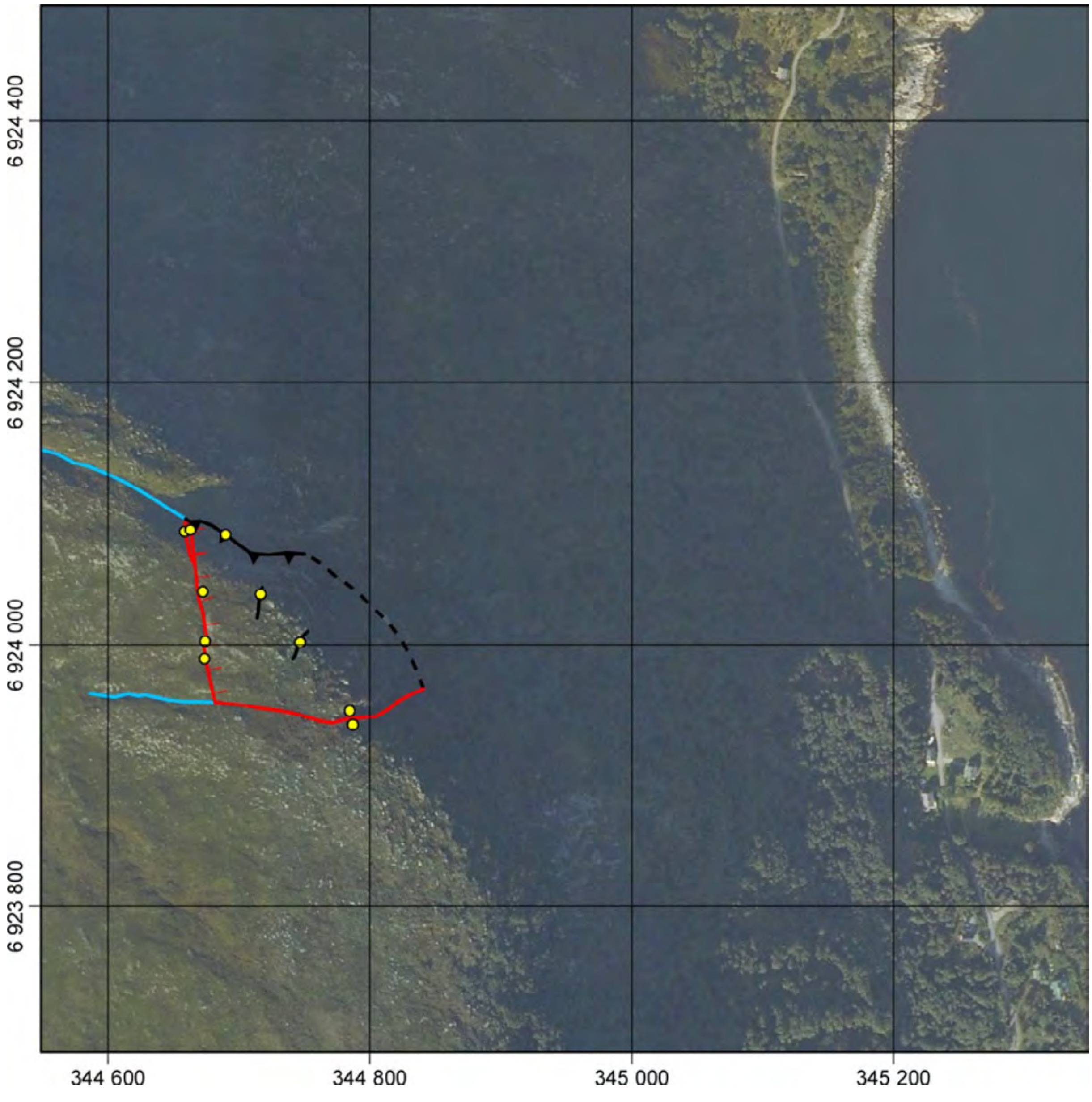

Figure 111: Map of the Grøthornet instability showing locations of field measurements (yellow dots).

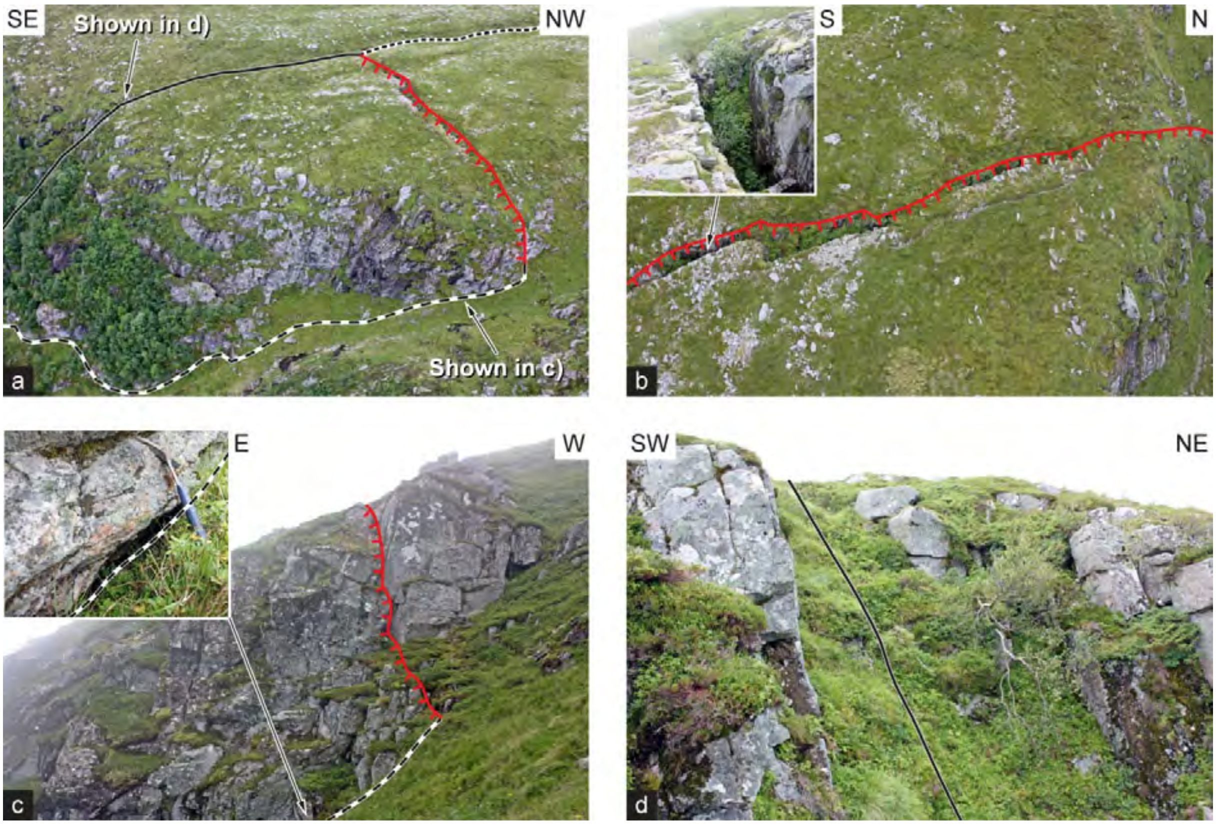

Figure 112: **Photographs of the Grøthornet instability: a) overview of the instability; b) the back-crack is mainly formed by subvertical N-S-trending discontinuities and shows several dm to m opening; c) northern face of the instability with the continuous back-crack and the possible basal sliding surface (inset: apparent opening along the foliation-parallel basal sliding surface); d) lateral release surfaces marked by a surface depression.**

7.2 Sande municipality

There is one known site located in Sande municipality, which is described in this report (Figure 110).

7.2.1 <u>Laupsnipa</u>

Laupsnipa is situated on a south-facing slope 540 m above Rovdefjord (Figure 110). A helicopter reconnaissance flight was made in 2011 followed by field mapping in 2012 (Figure 113). A series of steeply south-dipping faults form surface depressions and apparent counterscarps on the inward-facing slope (Figure 114a). It could not be clarified whether these morphologic features are related to past movements of an unstable rock slope or to preferential erosion along the faults. The gneiss foliation is folded and undulating. Orientations vary from steeply N-dipping to vertical to steeply S-dipping.

An unstable column is located at the front cliff (Figure 114a, b). The measured structures allow this instability to topple along steeply N-dipping foliation surfaces. The instability is laterally delimited by NE-SW-trending vertical discontinuities and a steeply NW-dipping regional fault in the east. Gently fjord-dipping surfaces form the basal limit of the instability. The latter are similar to the stepped basal failure surface of past rockslides or rock topples in the western part of Laupsnipa.

Large rockfall scars and a large talus slope at the foot of the cliff are observed (Figure 114a, d). A past debris slide happened on the talus slope close to the shoreline (Figure 114d), indicating that the talus slope is reaching its stability limit and might be destabilized by the impact of larger blocks falling from the Laupsnipa instability. The resulting rock and debris avalanche would create a displacement wave in Rovdefjord (Dahle et al. 2011a).

Recommendation: Periodic displacement measurements are started at the Laupsnipa instability, but the time-series is not sufficiently long to determine displacement rates. Periodic displacement measurements using tape extensometer and TLS should be continued with 1–3 years interval. The hazard and risk classification needs to be made and further follow-up activities will be decided based on this classification.

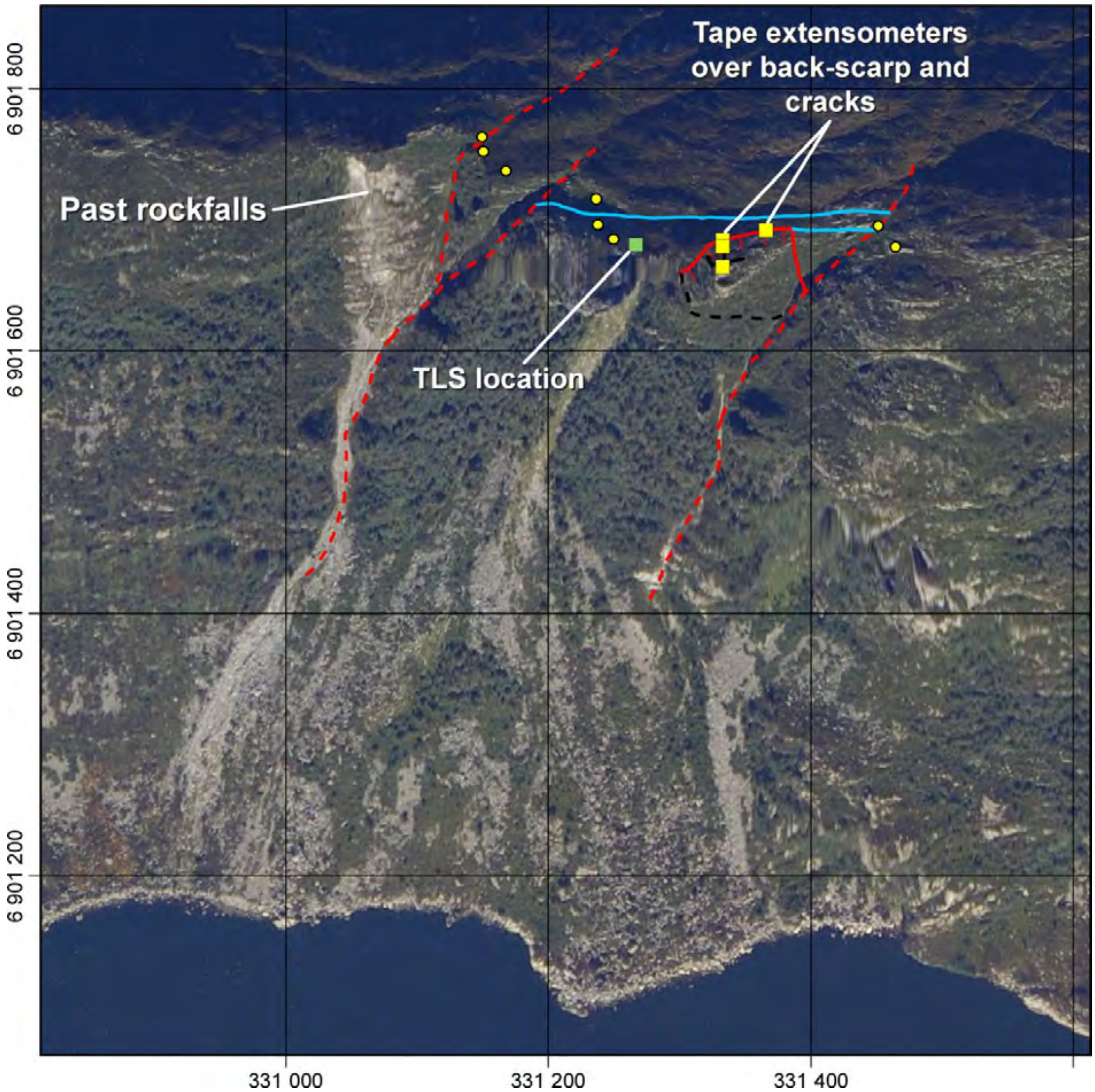

Figure 113: Map of the Laupsnipa instability showing locations of field measurements (yellow dots) and measurement instrumentation (tape extensometer & TLS).

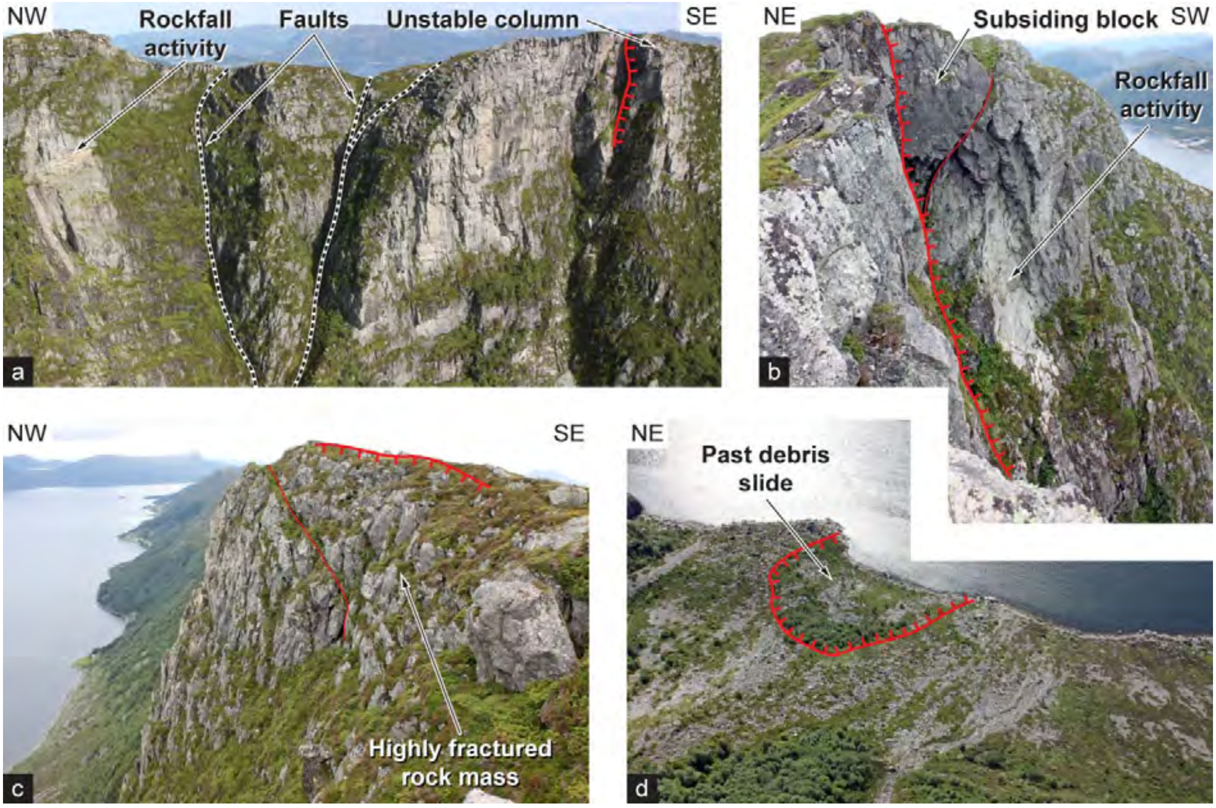

Figure 114: Photographs of the Laupsnipa instability: a) steeply S-dipping joints act as back-crack and as potential sliding surfaces. Large rockfall scars and potential rockfall blocks are observed at the front cliff; b) large talus slope at the foot of Laupsnipa with a past debris slide along the shoreline.

7.3 Ulstein municipality

There is one known site located in Ulstein municipality, which is described in this report (Figure 110).

7.3.1 Haddalura

Haddalura (Figure 110) is a steep talus slope with large blocks on the west-facing slope of Ringstadhornet 370 m above Haddalsvika. The slope was investigated by Anda et al. (2000), field mapped in 2009 and visited again in 2011 by helicopter. There is no visible rockslide scar that could explain this large block field (Figure 115), but there are indications of in-situ disintegration of the large, relatively intact rock blocks (inset in Figure 115a). Furthermore, the foliation is moderately SE-dipping and thus not favourably oriented to form basal sliding surfaces along it. The extent of the block field at Haddalura appears to be lithologically controlled, since it is limited to a metagabbro outcrop (Lutro et al. 1998).

Haddalura was measured periodically with dGNSS in 2005 and 2009, but all 6 points on the slope show no significant displacements over the 4 years measurement period (Figure 116). The slope below 200 m a.s.l. is 35–40° steep (Figure 115a), which is close to the stability limit of talus slopes. Smaller debris slides from this steep talus might impact the road and Haddalsvika, but will likely have too small volume and energy to create a significant displacement wave.

Recommendation: There are no signs that the Haddalura block field might fail in a massive rock slope failure. Periodic displacement measurements with dGNSS did not reveal significant displacements. No further investigations or displacement measurements are necessary and the hazard and risk classification will not be made. However, rockfalls are possible and their run-out area is given by the rockfall susceptibility map or more detailed hazard maps, where available.

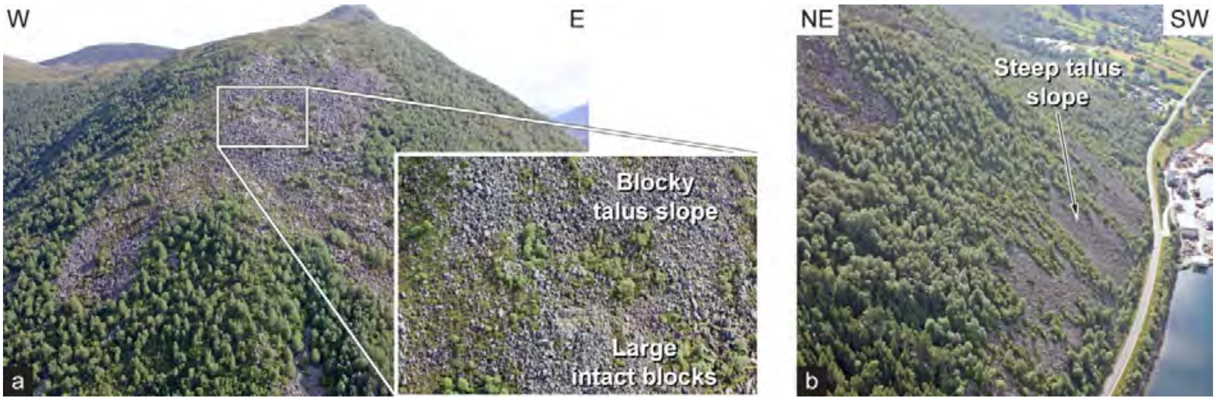

Figure 115: **Photographs of the Haddalura block field: a) gentle, blocky talus slope with large, relatively intact blocks and sings of in-situ disintegration; b) steep talus slope in the lower part.**

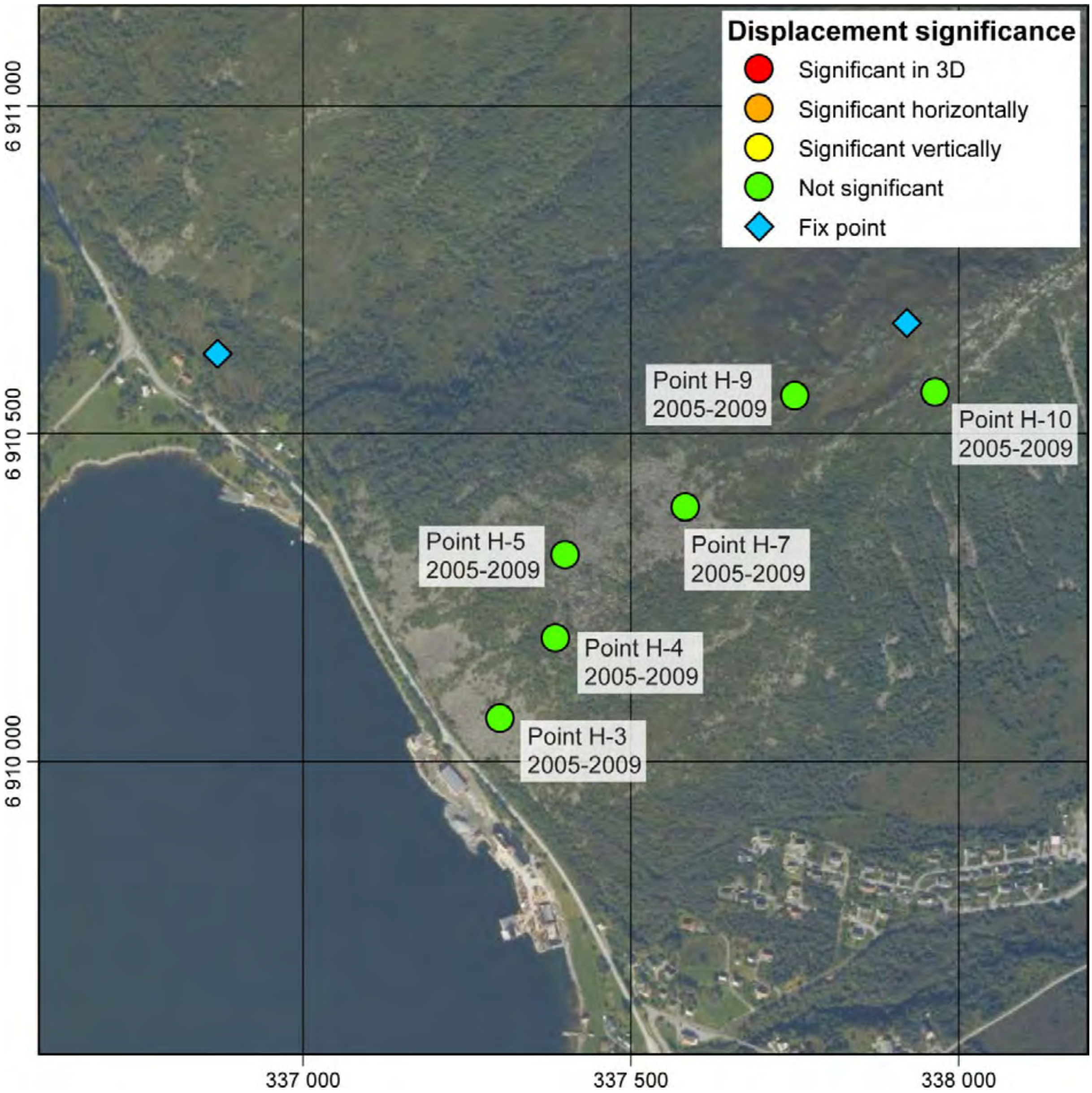

Figure 116: **Map of the Haddalura block field with the location of dGNSS points for periodic displacement measurements. No significant displacements were detected over the 2005–2009 measurement period.**

7.4 Vanylven municipality

There are three known sites located in Vanylven municipality, which are all described in this report (Figure 117).

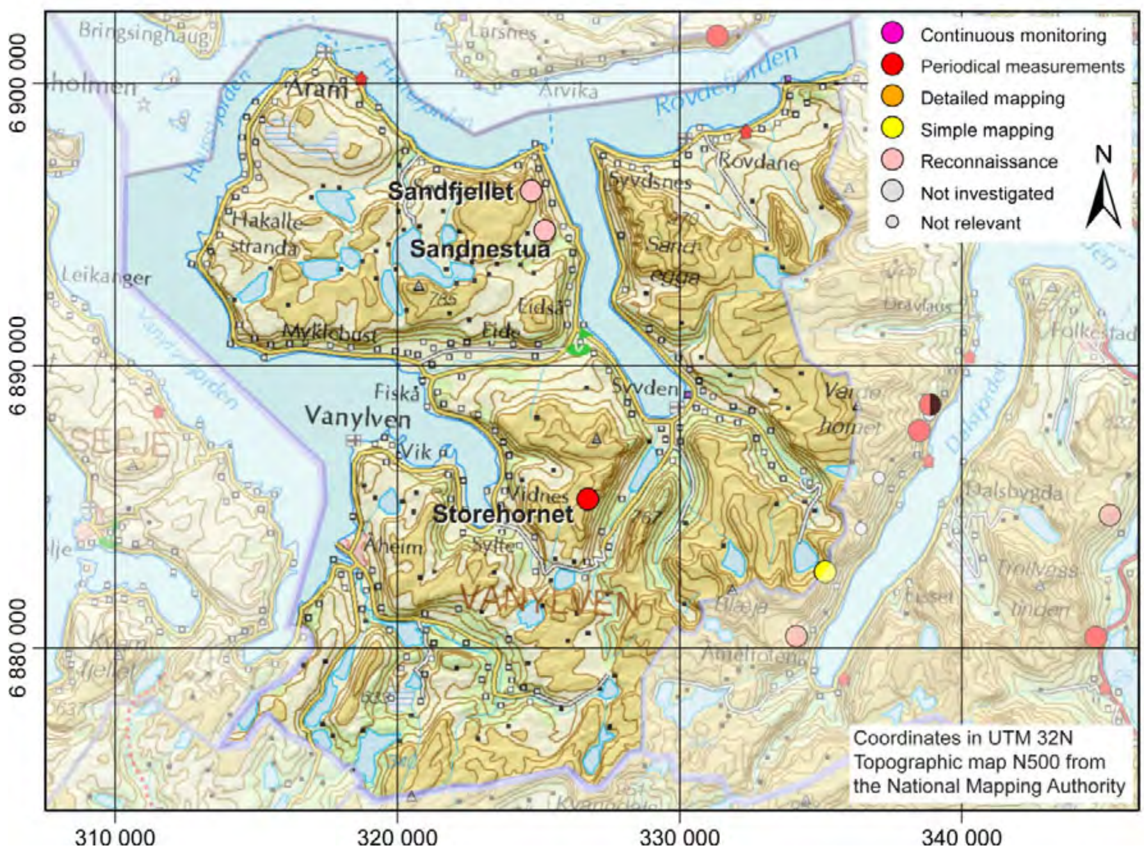

Figure 117: Map of the three known sites in the Vanylven municipality with their investigation status. The name of the sites described in this report is shown.

7.4.1 <u>Sandfjellet</u>

Sandfjellet (Figure 117) is a steep west-facing slope 545 m above Syvdsfjord. Road observations in 2011 identified a potential instability NNW of large scars of past rockslides and of well visible fjord-dipping basal sliding surfaces. However, aerial photographs do not reveal open cracks that may indicate present-day gravitational deformation in the area NNW of the rockslide scars (Figure 118).

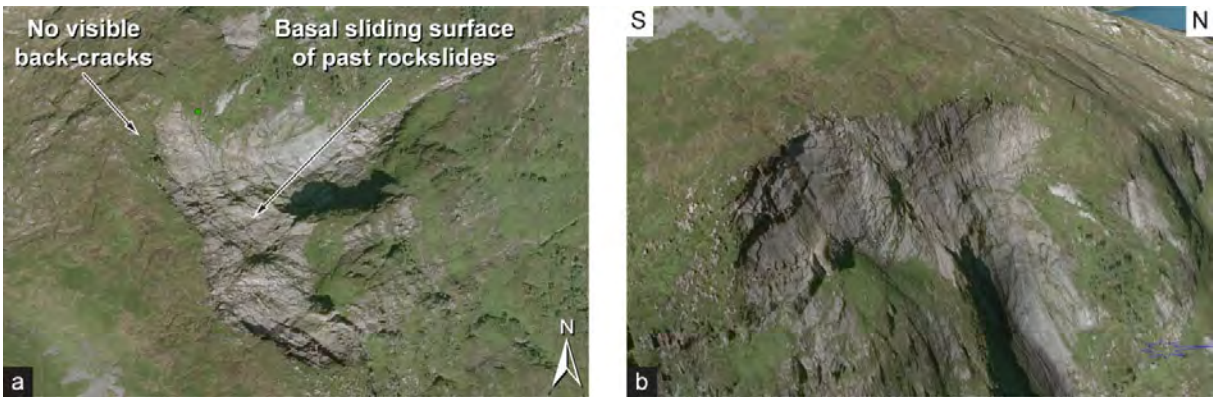

Figure 118: Photographs of the Sandfjellet rockslide scars: a) orthophoto of the scars with a remaining potential instability in the NNW of the scar; b) 3D view from Norge i 3D.

Recommendation: A helicopter reconnaissance flight is planned to have a closer look at the past rockslide scars and the remaining potential instability at Sandfjellet.

7.4.2 Sandnestua

Sandnestua is a southeast-facing blocky rock slope 420 m above Sandnesdalen Valley and Sandnes (Figure 117). A helicopter reconnaissance flight was made in 2011. The unstable rock slope shows two distinct deformation styles with (1) rockfalls from small cliffs in the SW-part and (2) in the NE-part a heavily disintegrated rockslide that has moved several meters (Figure 119a). Some larger, more intact blocks are observed in both the rockfall area and the rockslide area (inset in Figure 119b). At the north-eastern limit of the rockslide area, basal sliding surfaces crop out (Figure 119b). These might be parallel to the basal sliding surface under the present rockslide area, leading to a relatively shallow rockslide, a few meters to tens of meters thick. The shallow sliding surface combined with the high disintegration of the rockslide area likely prevent from the development of large collapses.

Recommendation: A possible rock avalanche from Sandnestua will have no consequences. No further investigations or displacement measurements are necessary. The hazard and risk classification will be made after a simple run-out assessment. Further follow-up activities will be based on this classification.

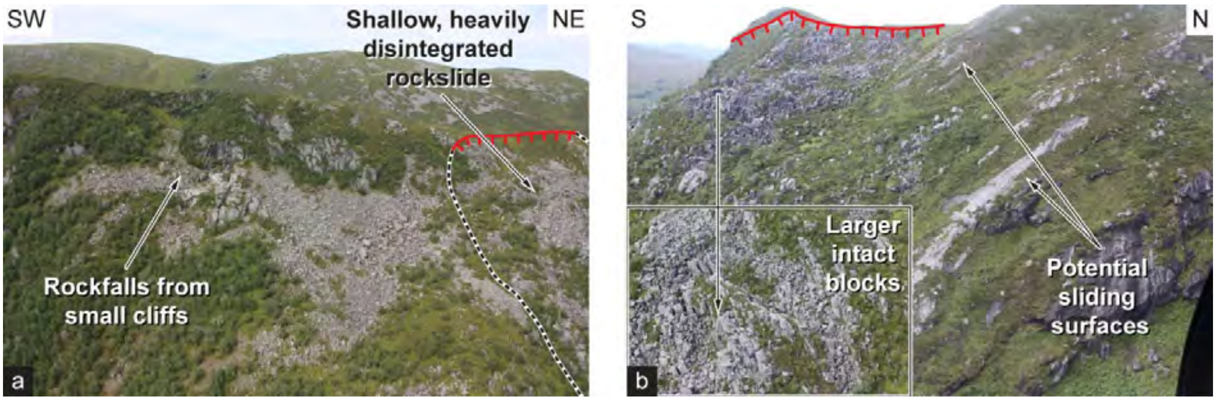

Figure 119: Photographs of the Sandnestua unstable rock slope: a) different deformation styles with rockfalls in the SW and a shallow rockslide in the NE; b) the rockslide is heavily disintegrated with the exception of some blocks (inset). Basal sliding surfaces are exposed at the NE limit of the rockslide area.

7.4.3 Storehornet

Storehornet (Figure 117) is located on a southeast-facing slope 710 m above Saurdalen Valley. A helicopter reconnaissance flight and field mapping were carried out in 2011, followed in 2012 by further field mapping, installation of periodic displacement measurement points (dGNSS, tape extensometer and TLS) and sampling of sliding surfaces and rock avalanche deposits for cosmogenic nuclide dating (Figure 120). Anda et al. (2000) and Blikra et al. (2002a) briefly described the Storehornet unstable rock slope and the deposits of past rock avalanches that are younger than the Younger Dryas (~11 500 years BP).

In the NE the Storehornet slope has formed a complex rockslide that already led to past failures with rock avalanches (Figure 121a, f), while in the SW part several localized instabilities (blocks A to D) are observed (Figure 121). In addition, a fully detached, large block (F) is located at the front of the complex rockslide (Figure 121a, f). Basal sliding surfaces parallel to the gneiss foliation dipping down towards the valley are observed in the back-scarp area of the complex rockslide. These structures enable a relatively simple planar sliding mechanism.

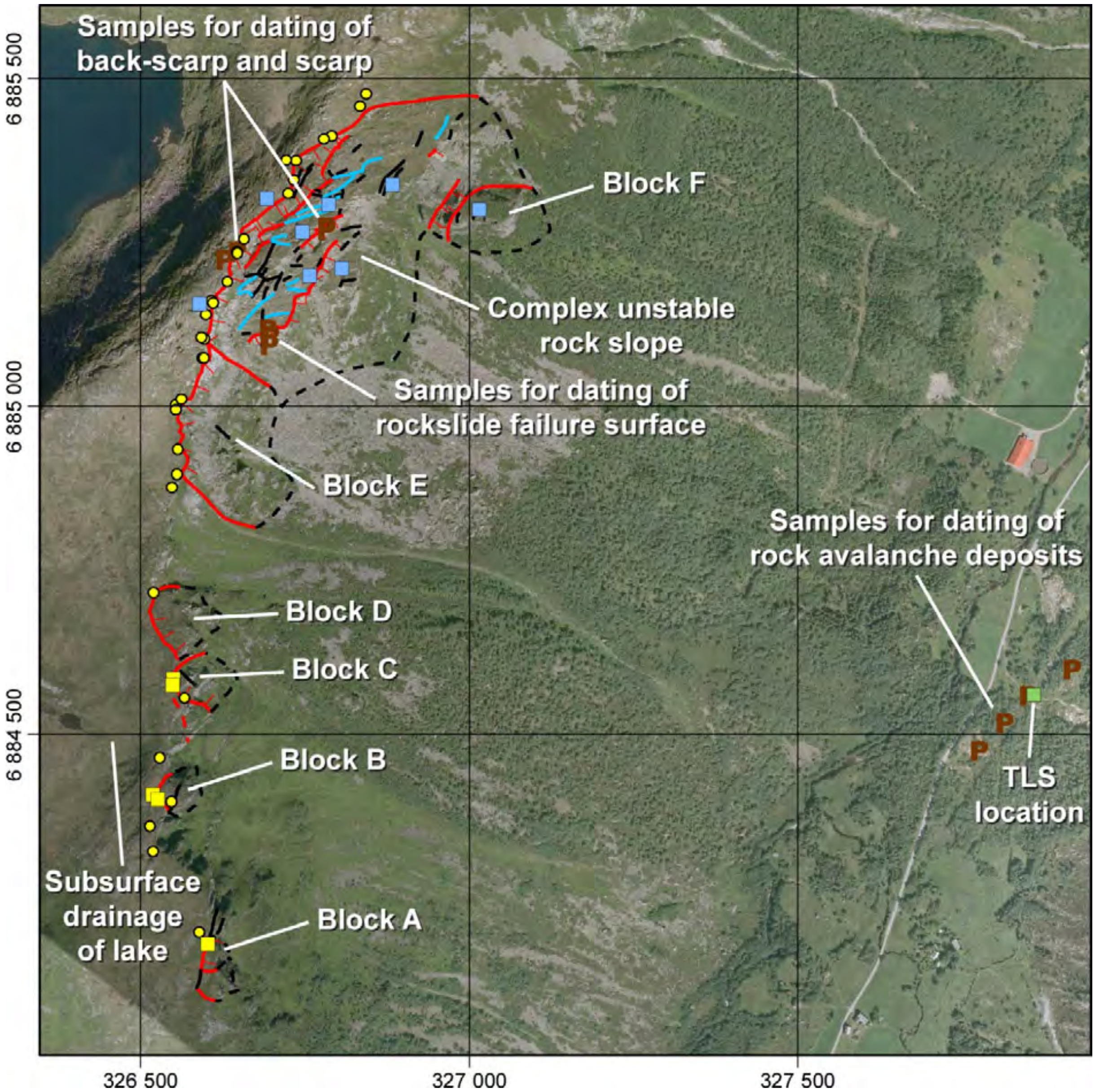

Figure 120: **Map of the Storehornet unstable rock slope showing locations of field measurements (yellow dots), measurement instrumentation (blue squares: dGNSS; yellow squares: tape extensometer; green square: TLS) and sampling locations for terrestrial cosmogenic nuclide dating (letters P).**

However, the past deformations increase from the NE to the SW of the rockslide, leading to a complex deformation pattern, notably with several scarps and even a well delimited compartment (block E) in the SW (Figure 121a, b). This change in deformation coincides with a decrease in foliation dip angle from approximately 70° in the NE to 35–45° in the SW. Furthermore, one or several past rockslides originated from this SW part of the complex rockslide area.

Further to the S in the area between Storehornet and Høgefjellet, the gneiss foliation steepens and turns again leading to another deformation style. Along the high cliff four localised instabilities (blocks A to D) are mapped. These are all delimited by steep to subvertical, open back-cracks and more or less well developed lateral release surfaces (Figure 121c, d, e). The rockfall deposits in the valley with several large, single boulders let suppose that these instabilities are prone to large rockfalls, but less to rock avalanche. This assumption is supported by an important disintegration of unstable blocks (Figure 121d, e). A subsurface drainage of a small lake south of Storehornet further indicated a significant open fracturing of the rock mass in that area.

A massive failure from Storehornet would likely form a rock avalanche that will reach the bottom of Saurdalen Valley. Several buildings might be impacted and the rock avalanche deposits might dam the Saurdalselva River with the possibility of subsequent dam breach and outburst flooding (Dahle et al. 2011a).

Recommendation: Periodic displacement measurements are started at the Storehornet unstable rock slope, but the time-series is not sufficiently long to determine displacement rates. Periodic displacement measurements using dGNSS, tape extensometer and TLS should be continued with 1–3 years interval. The hazard and risk classification needs to be made and further follow-up activities will be decided based on this classification.

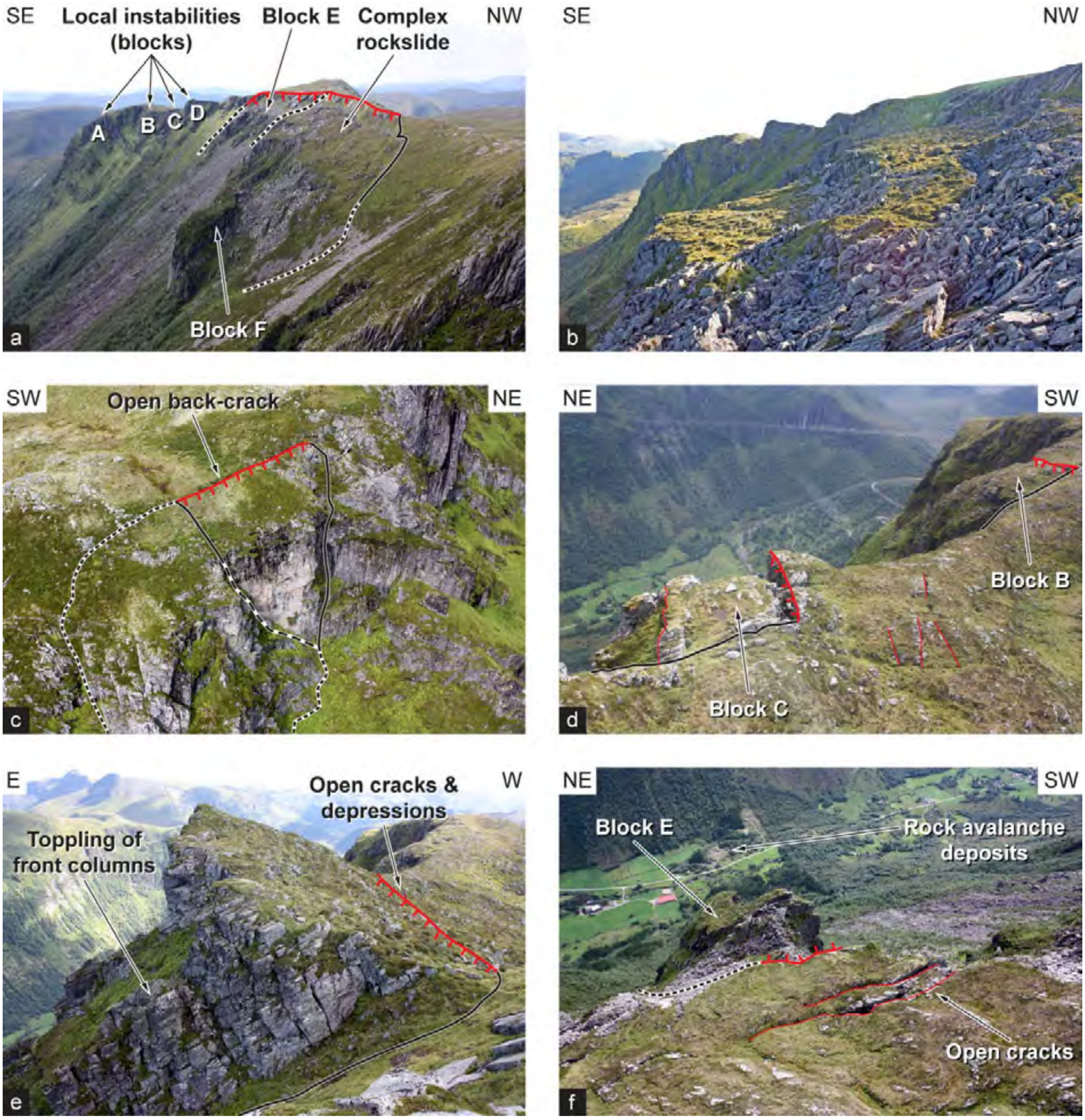

Figure 121: Photographs of the Storehornet instability: a) overview of the complex rockslide and of five localised instabilities; b) a series of scarps divided the complex rockslide into several compartments; c) block A is delimited by an open back-crack, but the lateral limits are uncertain; d) blocks B and C are delimited by open back-cracks and well-defined lateral release surfaces. Open cracks parallel to the back-crack of block C are visible; e) block D shows toppling movement of columns at its front and is delimited to the back by open cracks and surface depressions; f) block E is fully detached from the complex rockslide body. Rock avalanche deposits have crossed Saurdalen Valley and run-up on the opposite valley flank.

7.5 Volda municipality

There are 12 known sites located in Volda municipality. Ten of them are described in this report (Figure 122).

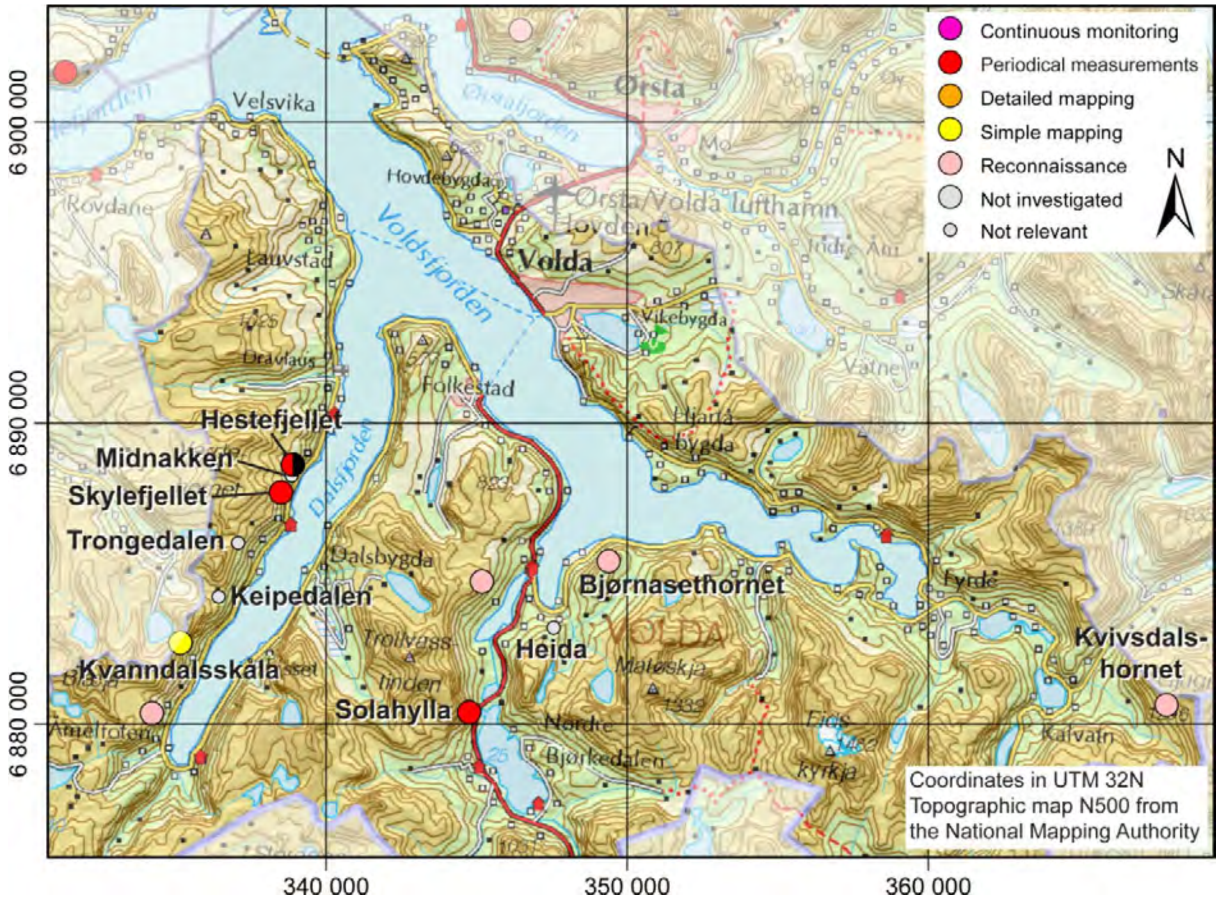

Figure 122: Map of the 12 known sites in the Volda municipality with their investigation status. Potential unstable rock slopes are also shown with a half-masked symbol (◑). The name of the sites described in this report is shown.

7.5.1 Bjørnasethornet

Bjørnasethornet (Figure 122) is situated on a southeast-facing slope 300 m above Stølselva Valley. During helicopter reconnaissance flight in 2011 a small unstable rock slope was observed (Figure 123). A closer inspection shows a high disintegration of the rocks into small blocks, which is likely due to the superficial collapse of relatively thin slices of rock. Only few, partially open cracks could be observed at the back. This deformation style will most likely not lead to a large rock slope failure. Furthermore, an eventual rock avalanche would affect the uninhabited Stølselva Valley and therefore have no major consequences.

Recommendation: A possible rock avalanche from Bjørnasethornet will have no consequences. No further investigations or displacement measurements are necessary. The hazard and risk classification will be made after a simple run-out assessment. Further follow-up activities will be based on this classification.

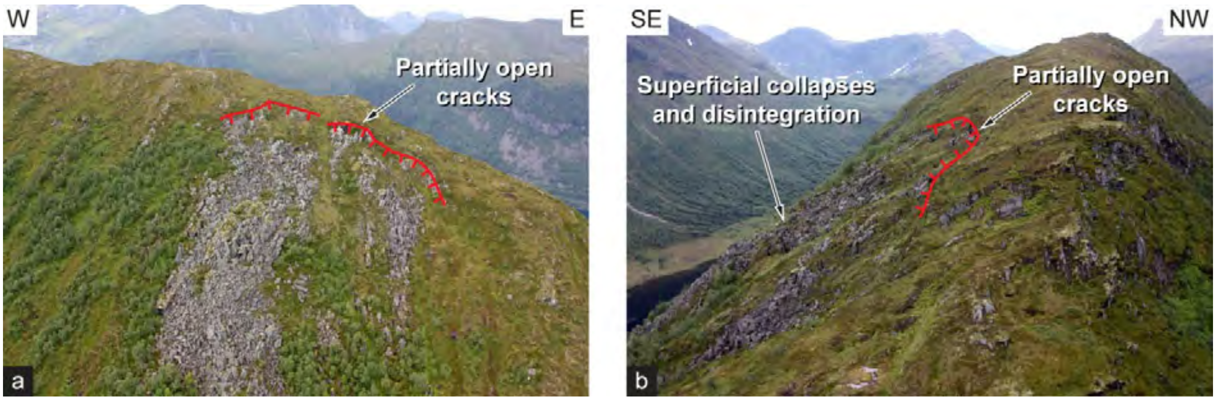

Figure 123: Photographs of the Bjørnasethornet unstable rock slope: a) the block field is on a SE-facing slope above the uninhabited Stølselva valley; b) lateral view of the block field formed by superficial collapses and disintegration of rock slices.

7.5.2 Heida

Heida (Figure 122) is located on a north-facing slope 420 m above Botnavika. The slope with a fresh rockfall scar was observed during helicopter reconnaissance in 2011 (Figure 124). The rock mass is highly fractured with a subvertical NE-dipping foliation and a perpendicular vertical discontinuity set, forming small volumes leading to rockfalls. A slightly visible surface depression is seen at the back of the rockfall scar, but there are no indications for a large unstable rock slope.

Recommendation: There are no signs that the Heida rock slope might fail in a massive rock slope failure. No further investigations or displacement measurements are necessary and the hazard and risk classification will not be made. However, rockfalls are possible and their run-out area is given by the rockfall susceptibility map or more detailed hazard maps, where available.

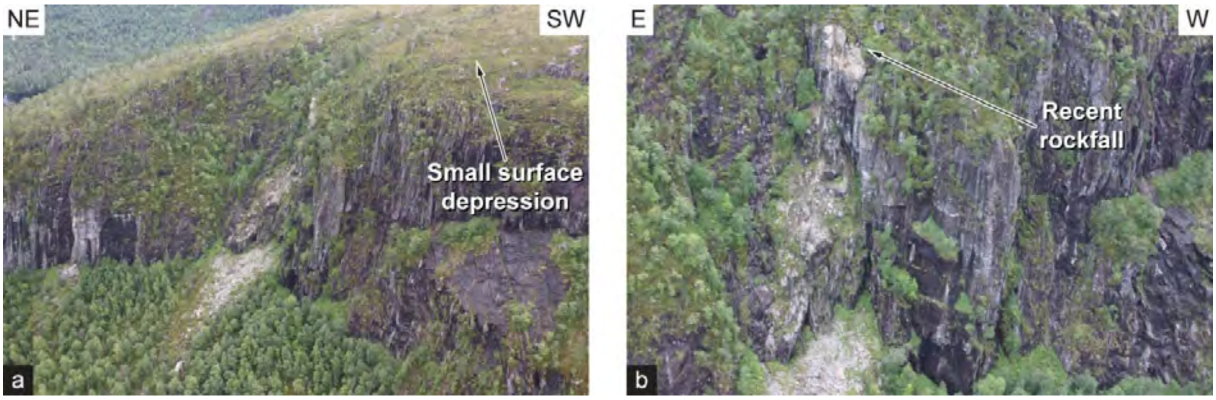

Figure 124: Photographs of the Heida rockfall area: a) the rock mass is highly fractured leading to small volumes prone to rockfall; b) detail photograph of a recent rockfall scar.

7.5.3 Hestefjellet, Midnakken & Skylefjellet

Hestefjellet, Midnakken and Skylefjellet are located on the southeast-facing slope above Dalsfjord at an altitude of 420 m, 410 m and 490 m, respectively (Figure 122, Figure 125). Site reconnaissance was done in 2011 from helicopter and along the road. Field work was made in 2012 on Hestefjellet, while Skylefjellet is inaccessible to field work. The potential instability at Hestefjellet and the instability at Skylefjellet were scanned by TLS from several locations in the valley for structural characterization and providing a reference dataset for periodic displacement measurements (Figure 125).

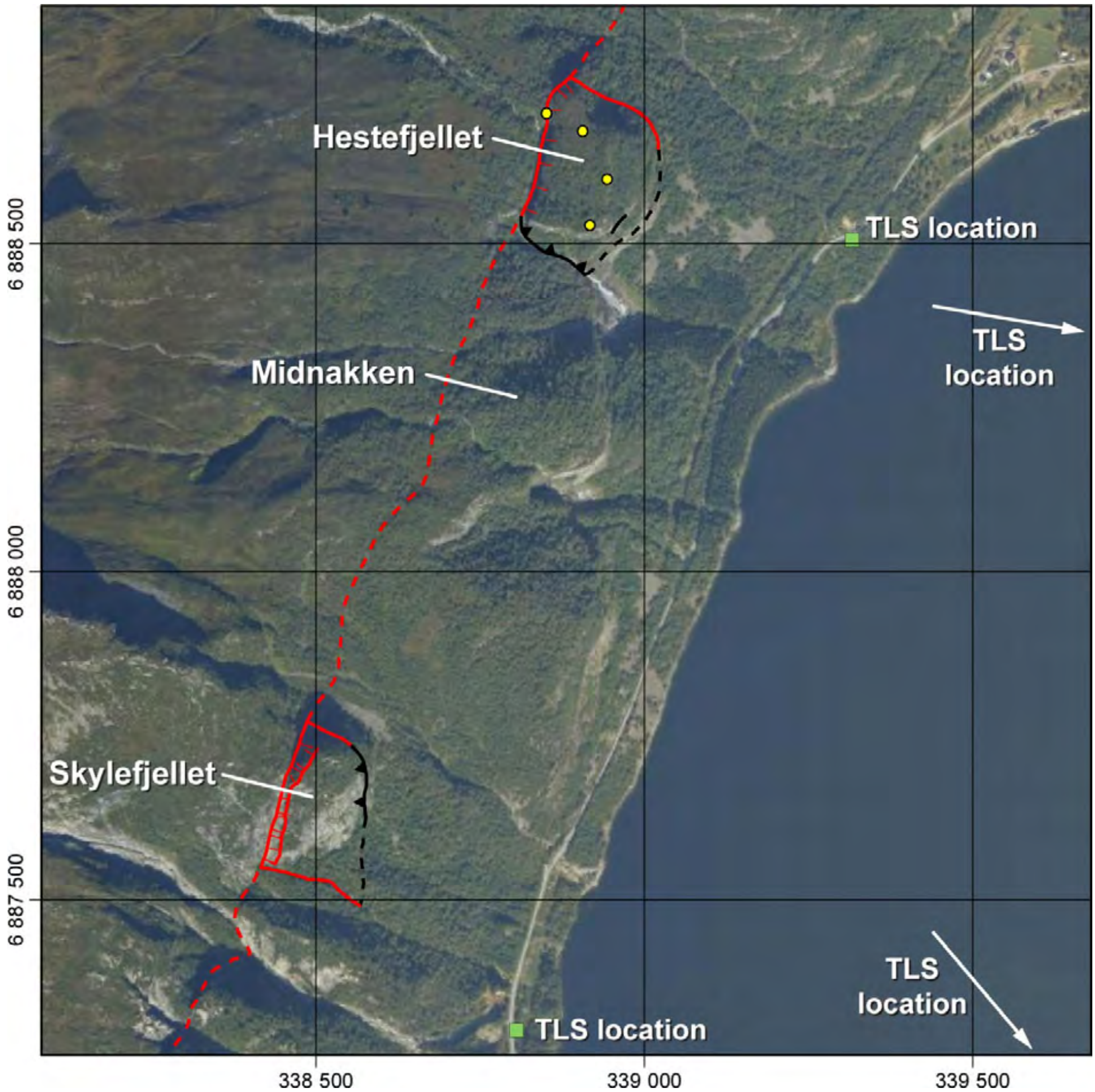

Figure 125: Location map of the Hestefjellet and Skylefjellet instabilities and the Midnakken rock slope showing locations of field measurements (yellow dots) and measurement instrumentation (TLS).

An ancient eroded fault that is followed over several km acts as the back-bounding structure for all the three sites (Figure 125, Figure 126a, b, d). At Hestefjellet the Fosselva River runs into this fault before running down on the southern side of the block (Figure 126b). There are no signs of opening along this fault at Hestefjellet. The gneiss foliation is moderately-dipping towards the fjord, but no sliding surface is visible at the base of the potential instability (Figure 126c). There are some visible rockfall scars on the frontal cliff although the scree slopes are well vegetated indicating only small rockfall activity (Figure 126b, c). The volume cannot be estimated due to the lack of basal sliding surface localization, but would certainly reach several million m³.

The Skylefjellet instability located 1 km SSW of Hestefjellet follows the same back-bounding fault (Figure 126a, d). The fault is deeply eroded and about 20 m wide. The foliation is moderately SSE-dipping and is slightly undulating (Figure 126e). A basal sliding surface parallel to the foliation is observed at the base of the Skylefjellet instability. There are no signs of recent openings along the back-crack and the rock mass at the instability is relatively intact.

However, relatively fresh rockfall scars are observed at the frontal cliff. The volume of the instability is estimated to 2–3 million m³ and thus large enough to generate a displacement wave in Dalsfjord in case of a massive failure (Dahle et al. 2011a).

The Midnakken spur located between Hestefjellet and Skylefjellet (Figure 125, Figure 126a) has a similar morphology, but the fault at its back is not eroded. There are no visible structures delimiting a large unstable rock slope. Rockfalls occur from the very steep cliff at Midnakken, but there are no signs of other deformation or activity.

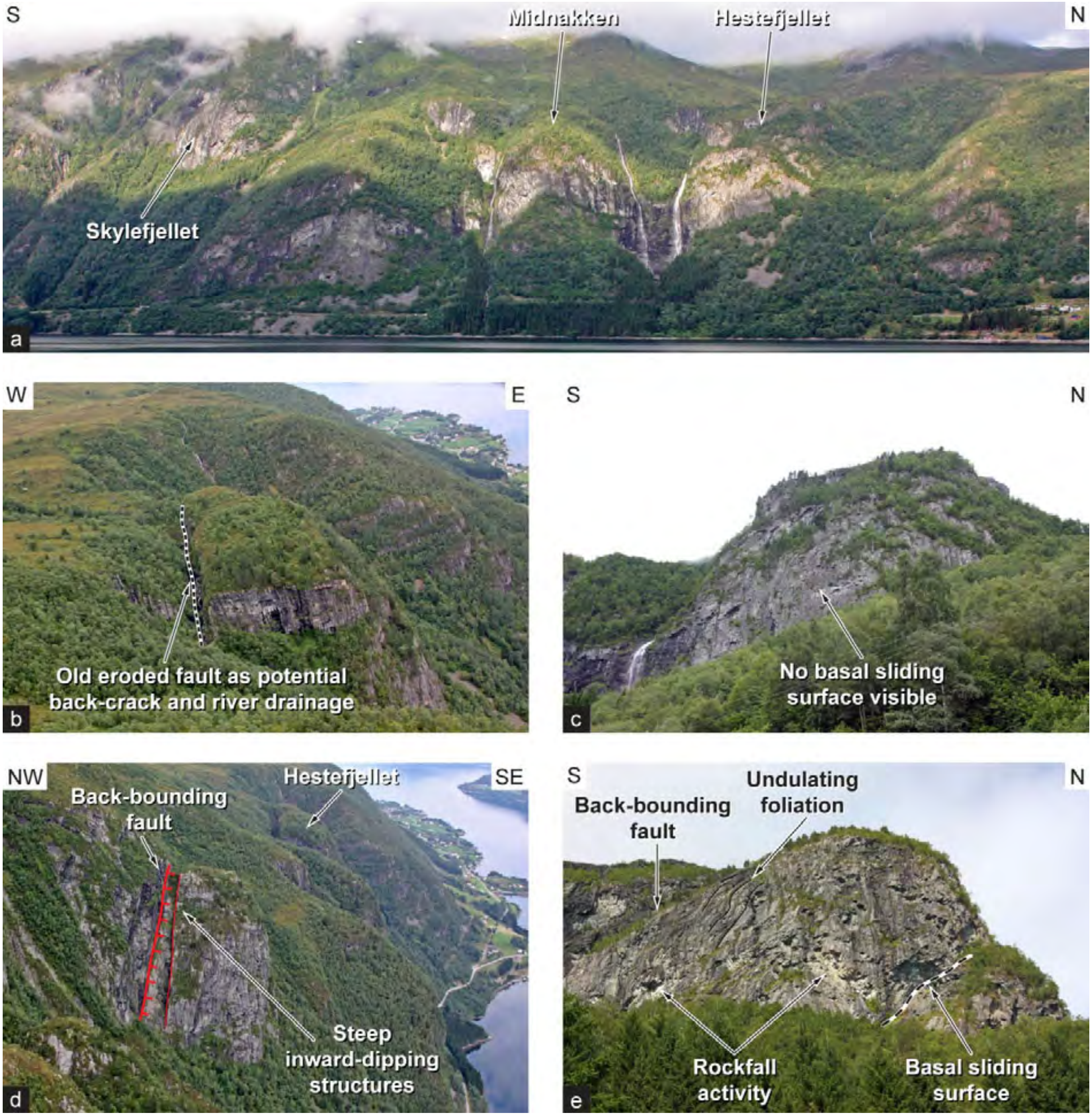

Figure 126: Photographs of the potential instability at Hestefjellet, the Skylefjellet instability and the Midnakken spur: a) overview photograph; b) Hestefjellet is back-bounded by an old eroded fault that guides the river drainage; c) no basal sliding surface is visible at the frontal cliff of Hestefjellet; d) Skylefjellet is back-bounded by the same old fault as Hestefjellet; e) a basal sliding surface parallel to the foliation is visible at Skylefjellet, along with relatively recent rockfall activity.

Recommendation: Periodic displacement measurements are started at the Skylefjellet instability, but the time-series is not sufficiently long to determine displacement rates. Periodic displacement measurements using TLS should be continued with 1–3 years interval. The hazard and risk classification needs to be made and further follow-up activities will be decided based on this classification.

Hestefjellet is classified as a potential unstable rock slope. At present the remaining rock slope does not show any signs of past or present displacements or deformation of a large volume. No further investigations or displacement measurements are necessary and the hazard and risk classification will not be made. However, this site may lead to rockfalls and develop over time into an unstable rock slope, due to structural and geological conditions. The site should be revisited after years to decades to detect any changes and be followed-up on InSAR data.

There are no signs that Midnakken spur might fail in a massive rock slope failure. No further investigations or displacement measurements are necessary and the hazard and risk classification will not be made. However, rockfalls are possible and their run-out area is given by the rockfall susceptibility map or more detailed hazard maps, where available.

7.5.4 Keipedalen

Keipedalen is located on a southeast-facing slope 580 m above Dalsfjord (Figure 122). Helicopter reconnaissance in 2011 and field mapping in 2012 showed isolated open N-S-trending cracks on the rock slope (Figure 127). The Keipedalsvatnet Lake has no superficial outflow and might drain across the rock mass through open cracks or fractures.

The gneiss foliation is dipping northwards and is thus not favourably oriented to develop basal sliding surfaces. Two other discontinuity sets were observed: one subvertical set along which the open crack forms and another steeply SSE-dipping set. The latter is too steep to daylight the slope at Keipedalen. Except the isolated open cracks, there are no signs of past deformation at Keipedalen. Necessary structures to enable sliding or toppling are missing.

Recommendation: There are no signs that the Keipedalen rock slope might fail in a massive rock slope failure. No further investigations or displacement measurements are necessary and the hazard and risk classification will not be made. However, rockfalls are possible and their run-out area is given by the rockfall susceptibility map or more detailed hazard maps, where available.

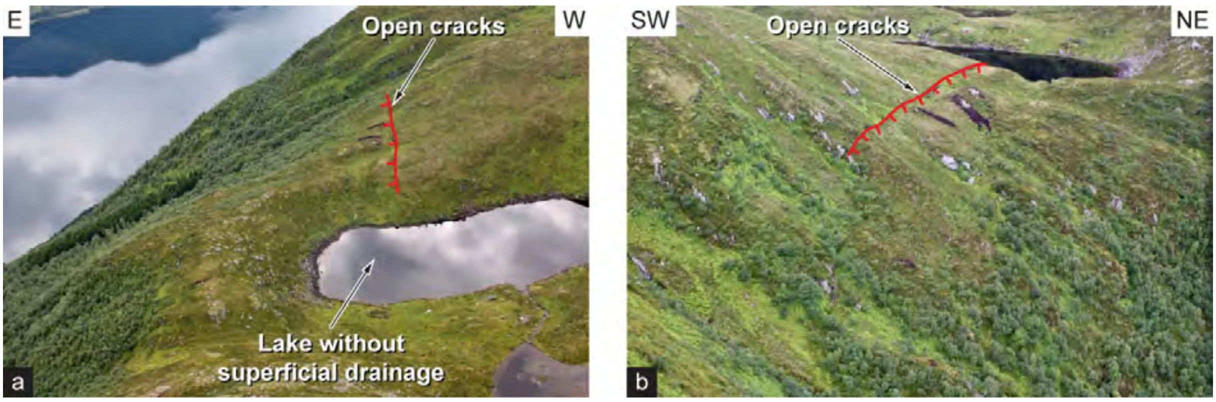

Figure 127: Photographs of Keipedalen: a) Keipedalsvatnet Lake has no superficial outflow and might drain across the rock mass through open fractures; b) open cracks south of Keipedalsvatnet.

7.5.5 Kvanndalskåla

Kvanndalsskåla is located on a southeast-facing slope 740 m above Dalsfjord (Figure 122). The site was observed from helicopter in 2011 and mapped in 2012. A shallow depression on the top of the plateau developed along an ancient fault zone that currently forms the south-western limit of the instability (Figure 128, Figure 129). The gneiss foliation is steeply-dipping towards the fjord, but does not daylight the slope. Other structures are a subvertical NW-SE-trending discontinuity set and a shallowly WSW-dipping discontinuity set. With these structures no sliding or toppling mechanism is feasible. However, a moderately valley-dipping discontinuity set was found locally on the instability and would enable a planar sliding mechanism.

The current site knowledge does not allow to ascertain whether the small depression on the top is caused by past slope deformation or preferential erosion of the fault zone. Several necessary structures to delimit an unstable rock slope are missing, such as the lateral release surface in the NE (Figure 128b) and a basal sliding surface. The toe lines shown in Figure 129 are provisional and correspond to the bottom of the steepest slope sections. There are no signs of activity on the instability itself, but the surrounding slope is affected by several landslide processes such as debris flows and rock avalanches. The latter include the 1867 event from Floget that created a displacement wave in Dalsfjord (Figure 128b), as would a rock avalanche from Kvanndalskåla likely do too.

Recommendation: A possible rock avalanche from the Kvanndalskåla instability will have consequences, which will be assessed in the hazard and risk classification. Further follow-up activities will be decided based on this classification.

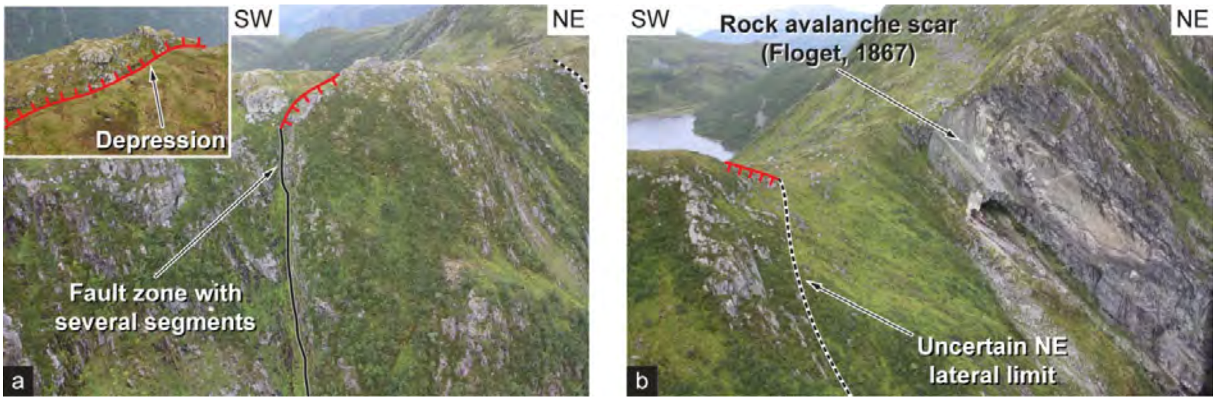

Figure 128: Photographs of the Kvanndalsskåla instability: a) a fault zone delimits the instability laterally to the SW and to the back, where it is marked by a shallow depression (see inset); b) detail of the NE-limit and the scar of the 1867 rock avalanche from Floget.

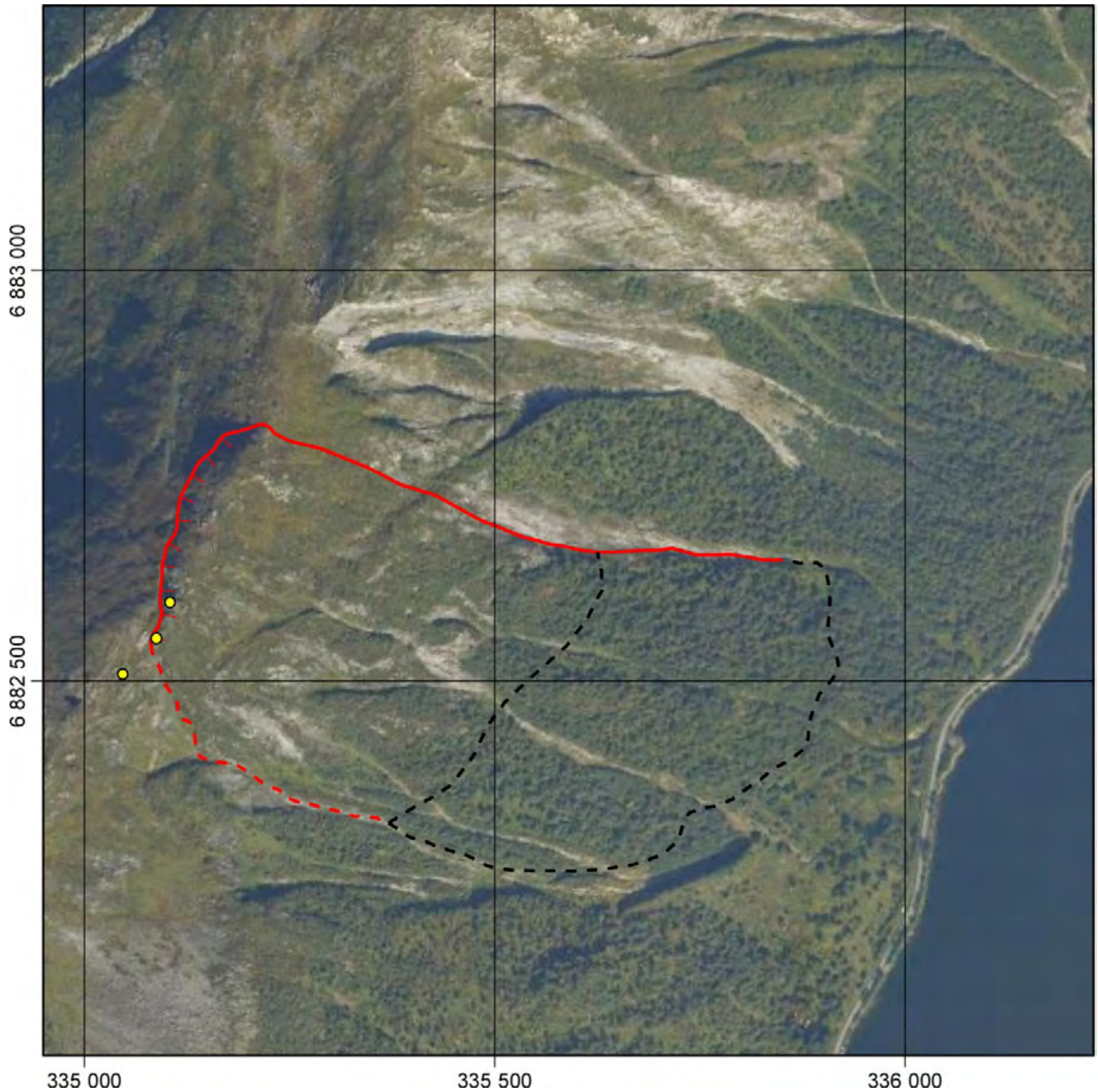

Figure 129: Map of the Kvanndalskåla instability showing locations of field measurements (yellow dots). The locations of the toe lines are provisional.

7.5.6 Kvivsdalshornet

Kvivsdalshornet is located on a southwest-facing slope 680 m above Kvivsdalen Valley (Figure 122). During helicopter reconnaissance flight in 2011 a highly disintegrated rock slope was observed (Figure 130). There are several open back-cracks that – together with other subvertical cracks – delimit blocks with small volumes (tens to hundreds of m^3). The foliation is parallel to the slope and might enable sliding of the small blocks. Several of them have already collapsed in the past, but did not have a long run-out distance and came to rest on the slope (Figure 130). The deformation style can be described as a superficial retrogressive sliding that leads to collapses of small blocks. In the unlikely event of a massive rock slope failure from Kvivsdalshornet only the uninhabited upper part of Kvivsdalen Valley would be reached and therefore not cause significant consequences.

Recommendation: A possible rock avalanche from the Kvivsdalshornet instability will have no consequences. No further investigations or displacement measurements are necessary. The hazard and risk classification will be made after a simple run-out assessment. Further follow-up activities will be based on this classification.

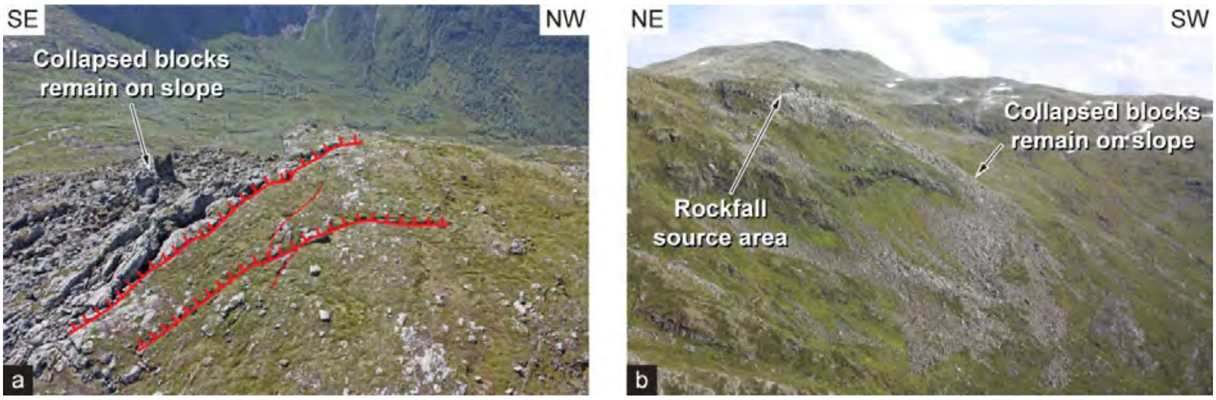

Figure 130: Photographs of the Kvivsdalshornet: back-cracks and transverse cracks delimit small blocks, which generally come to rest on the slope after failure.

7.5.7 Solahylla

Solahylla is located on an east-facing slope 550 m above Bjørkedalsvatnet Lake (Figure 122). A helicopter reconnaissance flight was made in 2011 and showed an instability that is delimited by a vertical N-S-trending back-crack (Figure 131a). On the top of the instability no opening or escarpment is visible due to vegetation cover (Figure 131b). Yet, this indicates only small to no past displacements. The foliation is undulating and in average very steeply dipping to the south. A basal sliding surface at the foot of the instability may form on a moderately east-dipping discontinuity set (Figure 131a). The structures present at Solahylla enable sliding and toppling of the instability.

The Solahylla instability is inaccessible to field work. Therefore it was scanned by TLS from two locations in the valley providing a reference dataset for periodic displacement measurements (Figure 132). The TLS dataset and the observed structures allowed measuring a width of 90 m, a height of 130 m and a volume of 184 000 m³ for Solahylla instability. A failure from Solahylla is expected to reach Bjørkedalsvatnet Lake and will provoke a displacement wave (Dahle et al. 2011a).

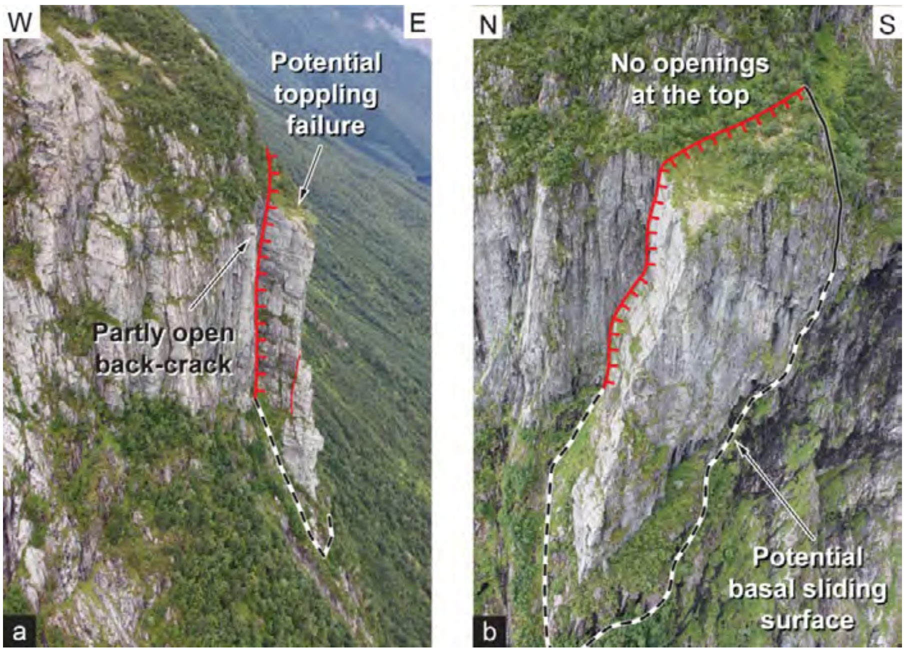

Figure 131: Photographs of the Solahylla instability: a) lateral view showing the vertical back-crack and the moderately valley-dipping basal sliding surface; b) no recent openings or escarpments are visible on the top of the instability.

Figure 132: Map of the Solahylla instability showing locations of measurement instrumentation (TLS).

Recommendation: Periodic displacement measurements are started at the Solahylla instability, but the time-series is not sufficiently long to determine displacement rates. Periodic displacement measurements using TLS should be continued with 1–3 years interval. The hazard and risk classification needs to be made and further follow-up activities will be decided based on this classification.

7.5.8 Trongedalen

Trongedalen is located on a southeast-facing slope 660 m above Dalsfjord (Figure 122). Since the small Trangedalsvatna Lake has no superficial outflow, the hill located in front of the lake was supposed highly fractured and thus a possible unstable rock slope (Figure 133a). However, no open cracks, no structures delimiting an unstable rock slope and no other signs of activity were observed by a helicopter survey in 2011. The outflow of the lake occurs likely through a more fractured zone in the north, where an ancient fault is visible. Some rockfalls or small rockslides (with volumes of less than 10 000 m³) have however failed in the past from the observed slope (Figure 133b), but such small failures will not cause a significant displacement wave in Dalsfjord.

Recommendation: There are no signs that the Trongedalen rock slope might fail in a massive rock slope failure. No further investigations or displacement measurements are necessary and the hazard and risk classification will not be made. However, rockfalls are possible and their run-out area is given by the rockfall susceptibility map or more detailed hazard maps, where available.

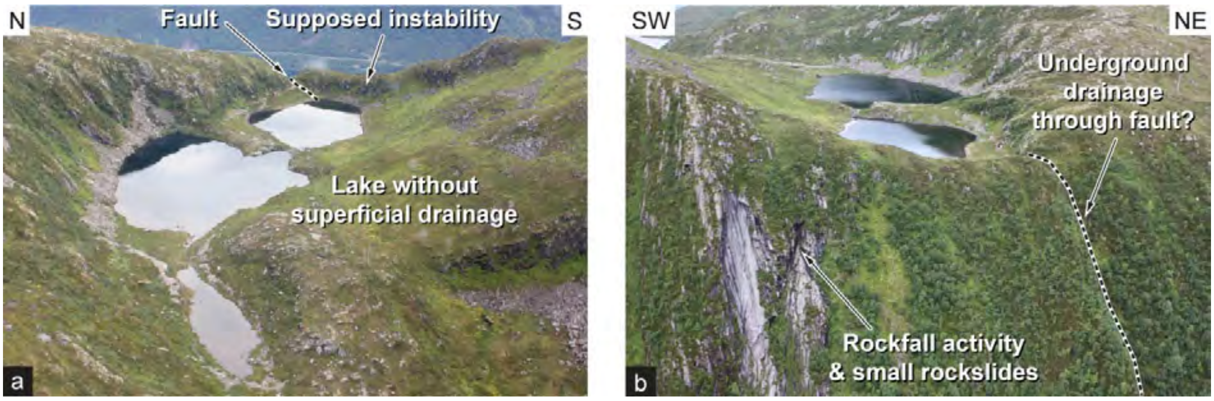

Figure 133: Photographs of the Trongedalen rock slope: a) the supposed instability is located in front of a lake without superficial outflow; b) rockfalls and small rockslides occurred, but no large unstable rock slope is visible.

7.6 Ørsta municipality

There are seven known sites located in Ørsta municipality, which are all described in this report (Figure 134).

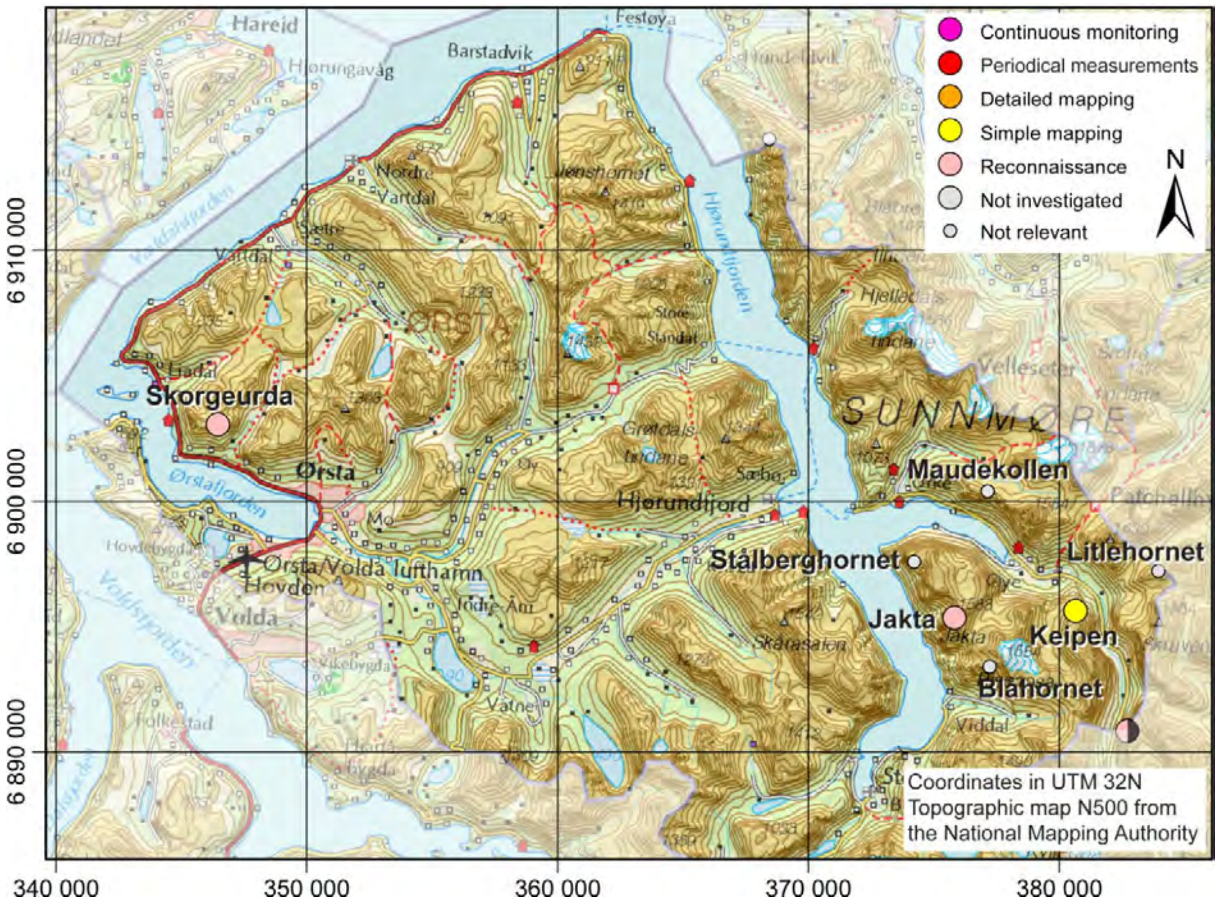

Figure 134: Map of the seven known sites in the Ørsta municipality with their investigation status. The name of the sites described in this report is shown.

7.6.1 Blåhornet

Blåhornet (Figure 134) is situated on a south-facing slope 1060 m above Viddalen Valley. A helicopter reconnaissance flight in 2011 showed evident rockfall activity from the steep cliffs at Blåhornet, but no large unstable rock slope is visible (Figure 135). This can be explained by the structural setting of the slope: the foliation is flat-laying and cross-cut by two perpendicular sets of vertical joints, which delimits relatively small rock volumes that fail as rockfalls or small toppling failures. The absence of less steeply-dipping discontinuities impedes the development of a large instability. A failure from Blåhornet will probably not reach inhabited areas of Viddalen Valley.

Recommendation: There are no signs that the Blåhornet rock slope might fail in a massive rock slope failure. No further investigations or displacement measurements are necessary and the hazard and risk classification will not be made. However, rockfalls are possible and their run-out area is given by the rockfall susceptibility map or more detailed hazard maps, where available.

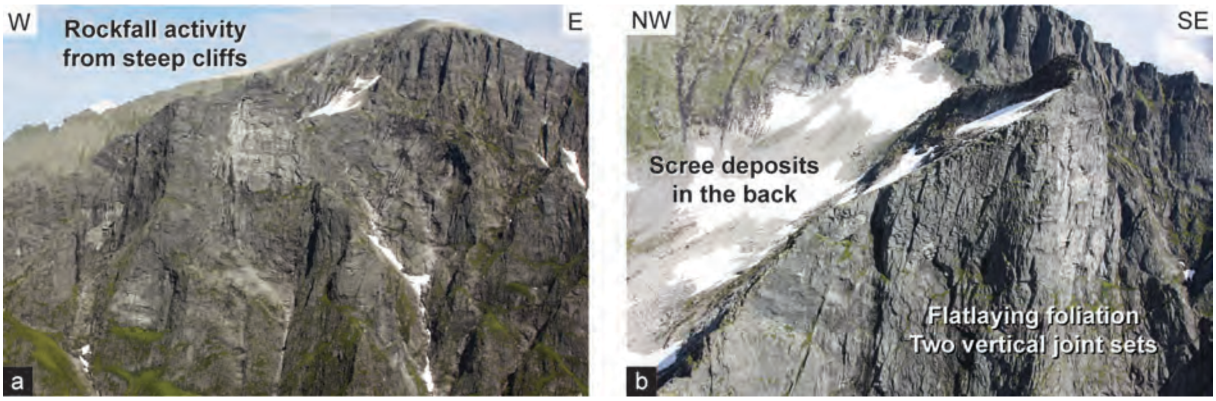

Figure 135: Photographs of the Blåhornet rock slope: a) rockfalls originate from the steep cliffs; b) no large unstable rock slope is visible.

7.6.2 Jakta

Jakta is located on a west-facing slope 1580 m above the southern end of Hjørundfjord (Figure 134). A helicopter reconnaissance flight in 2011 revealed past rock slope failures and a remaining instability (Figure 136a). The foliation is moderately SW-dipping and has served as a basal sliding surface for a past rockslide. The lateral release surface of this rockslide can be followed inwards joining an open crack observed on the mountain top (Figure 136). A massive rock slope failure would likely cause a displacement wave in Hjørundfjord.

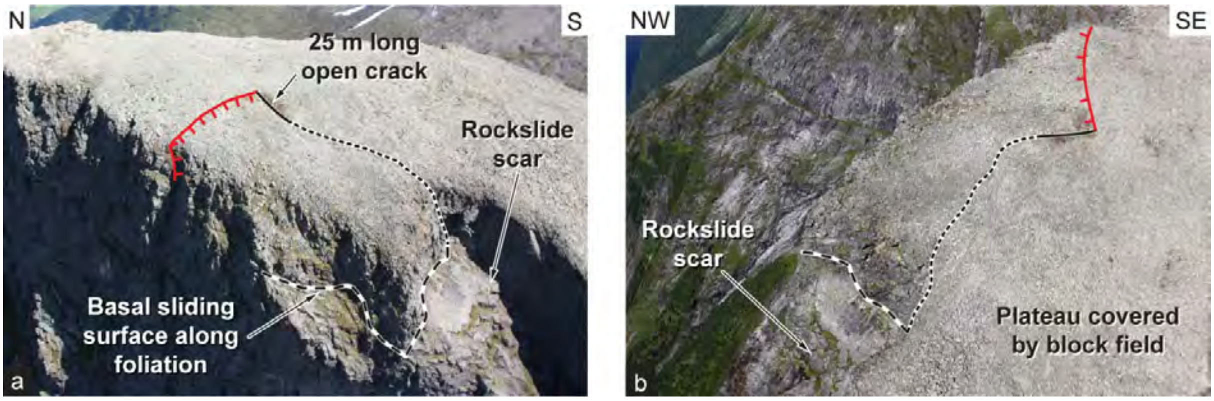

Figure 136: Photographs of the Jakta instability: a) the foliation acts as basal sliding surface in a previous rockslide and for the remaining instability; b) the lateral release surface of the past rockslide follows inwards to join an open crack.

Recommendation: A possible rock avalanche from the Jakta instability will have consequences. Geological field mapping is necessary to evaluate the structural and geological conditions, to quantify past displacements and assess the structures involved in the previous rockslide. The hazard and risk classification will be made after this field mapping. Further follow-up activities will be decided based on this classification.

7.6.3 Keipen

Keipen (Figure 134) is located on a northeast-facing slope 790 m above Lyngnstøylvatnet Lake in Norangsdalen Valley. In May 1908 occurred a rock avalanche that created 40 m high deposits and dammed the river. Several buildings were destroyed and flooded by Lyngnstøylvatnet Lake. The rock slopes at Keipen were investigated by helicopter in 2011. They are inaccessible to field work and were therefore scanned by TLS from the road in 2012 in order to characterise the structures and estimate volumes.

The upper, rear part is characterised by very steep cliffs and a highly fractured rock mass, which leads to rockfalls but not to a large rock slope failure (Figure 137b). Along a N-S-trending, old, brecciated fault crossing the slope, open cracks develop and can act as a back-crack (Figure 137a). Moderately SE-dipping foliation could be activated as basal sliding surface of a large potential rock slope instability with an estimated volume ranging from 0.5 to 1.8 million m³. This instability uses therefore similar structures as the 1908 rockslide, even though the exact location of this past event is not evident (Figure 137a). Anyhow, this indicates that failure is kinematically possible with the given structural setting. However, there are no signs of present active displacement at the instability.

A failure of the Keipen instability would impact the dam generated by the 1908 rock avalanche and the Lyngnstøylvatnet Lake, which might lead to a dam breach followed by downstream flooding of Norangsdalen Valley.

Recommendation: A possible rock avalanche from the Keipen instability will have consequences, which will be assessed in the hazard and risk classification. Further follow-up activities will be decided based on this classification.

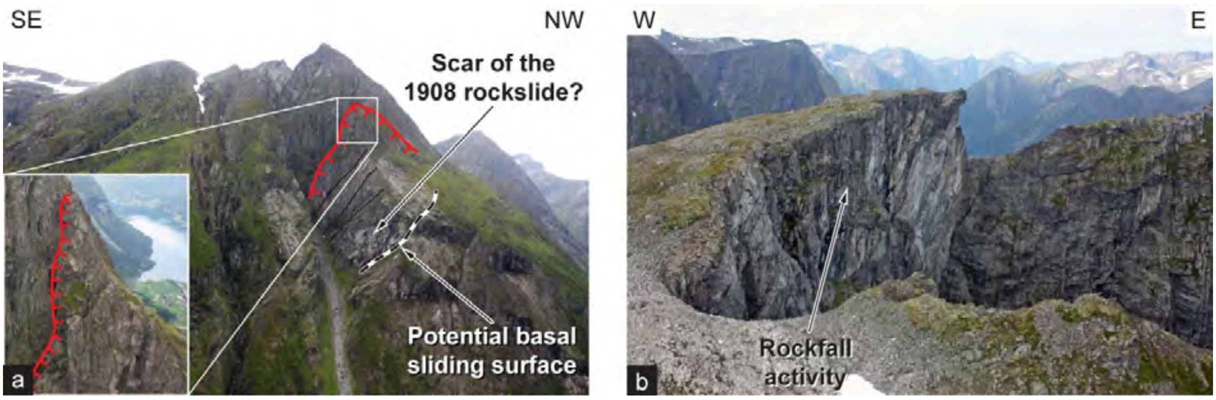

Figure 137: Photographs of the Keipen instability: a) an old fault guides the development of a possible back-crack for the instability (inset). The scar of the 1908 rock avalanche is likely located in front of the remaining instability, which uses the foliation as possible sliding surfaces; b) the upper part of Keipen is characterised by rockfall activity, but no large instability is currently delimited.

7.6.4 Litlehornet

Litlehornet (Figure 134) is located on a south-facing slope 350 m above Svartedalen Valley, a small tributary valley of Norangsdalen Valley. With a helicopter reconnaissance flight in 2011 a glacially fractured rock surface forming a block field was observed (Figure 138). Open cracks are visible on the mountain crest indicating creep of the block field to the SE into the uninhabited Svartedalen Valley (Figure 138a). The rock mass is highly fractured into small blocks (Figure 138b). There are no indications for a large unstable rock slope at Litlehornet.

Recommendation: There are no signs that the Litlehornet rock slope might fail in a massive rock slope failure. No further investigations or displacement measurements are necessary and the hazard and risk classification will not be made. However, rockfalls are possible and their run-out area is given by the rockfall susceptibility map or more detailed hazard maps, where available.

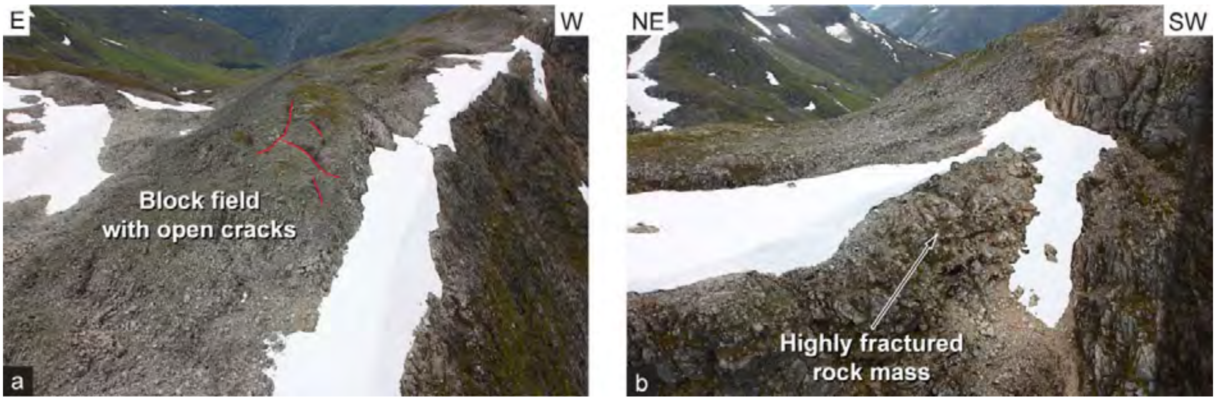

Figure 138: Photographs of the Litlehornet rock slope: the highly fractured rock mass forms a block field; open cracks indicate creep movements of the block field to the SE.

7.6.5 Maudekollen

Maudekollen (Figure 134) is located at 1020 m a.s.l. above Norangsfjord. A helicopter reconnaissance flight in 2011 has allowed the identification of a highly fractured rock mass on the northern side of the crest leading to small toppling failures (Figure 139a). These tend to fall toward the uninhabited Langesæterdalen Valley. The moderately S-dipping foliation forms possible sliding surfaces on the fjord-facing slope, but there are no visible back-cracks or lateral release surfaces that would delimit a large unstable rock slope (Figure 139b).

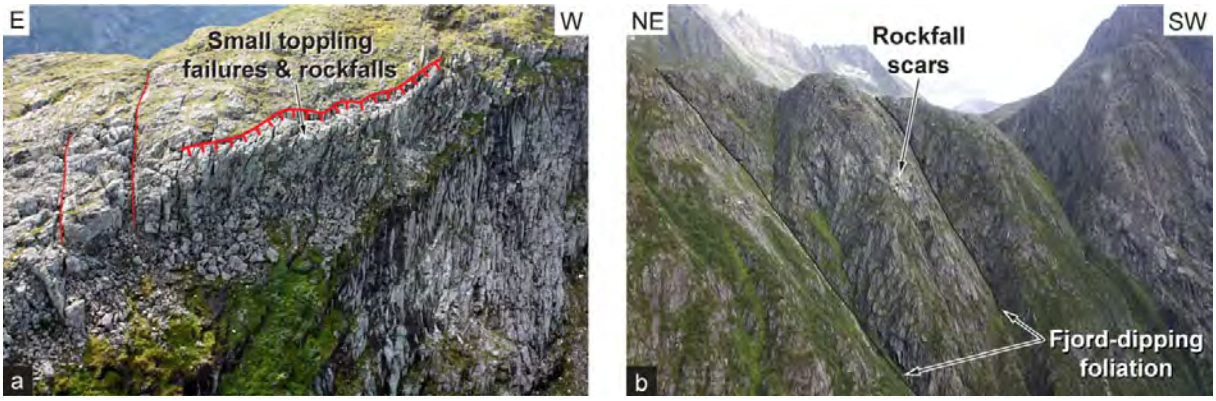

Figure 139: Photographs of the Maudekollen: a) highly fractured rock mass leads to rockfalls and small toppling failures towards the north; b) fjord-dipping foliation surfaces might form basal sliding surfaces, but other structures to delimit a large unstable rock slope are not observed.

Recommendation: There are no signs that Maudekollen rock slope might fail in a massive rock slope failure. No further investigations or displacement measurements are necessary and the hazard and risk classification will not be made. However, rockfalls are possible and their run-out area is given by the rockfall susceptibility map or more detailed hazard maps, where available.

7.6.6 Skorgeurda

Skorgeurda is located on a south-facing slope 830 m above Ørstafjord (Figure 134). The scars and deposits of a large prehistoric rock avalanche were observed during a helicopter survey in 2011 (Figure 140). This rock avalanche occurred 11 000 to 11 800 years ago. It incorporated moraine material, impacted the fjord on a width of over 1 km and crossed Ørstafjord (Blikra 1994). The morphology of the rock avalanche is complex with large boulders remaining on the slope, where the slope flattens in the region of Nakkane spur at 477 m a.s.l. (Figure 140b).

The planar basal sliding surfaces formed on steeply valley-dipping gneiss foliation are conspicuous in the upper section of the slope. Remaining blocks and rock slabs with a thickness of tens of meters might slide on these surfaces (Figure 140c). Another failure, even of small volume, could remobilize deposits and large boulders of the prehistoric rock avalanche and would impact settled areas along the shoreline and possibly cause a displacement wave in Ørstafjord (Dahle et al. 2011a).

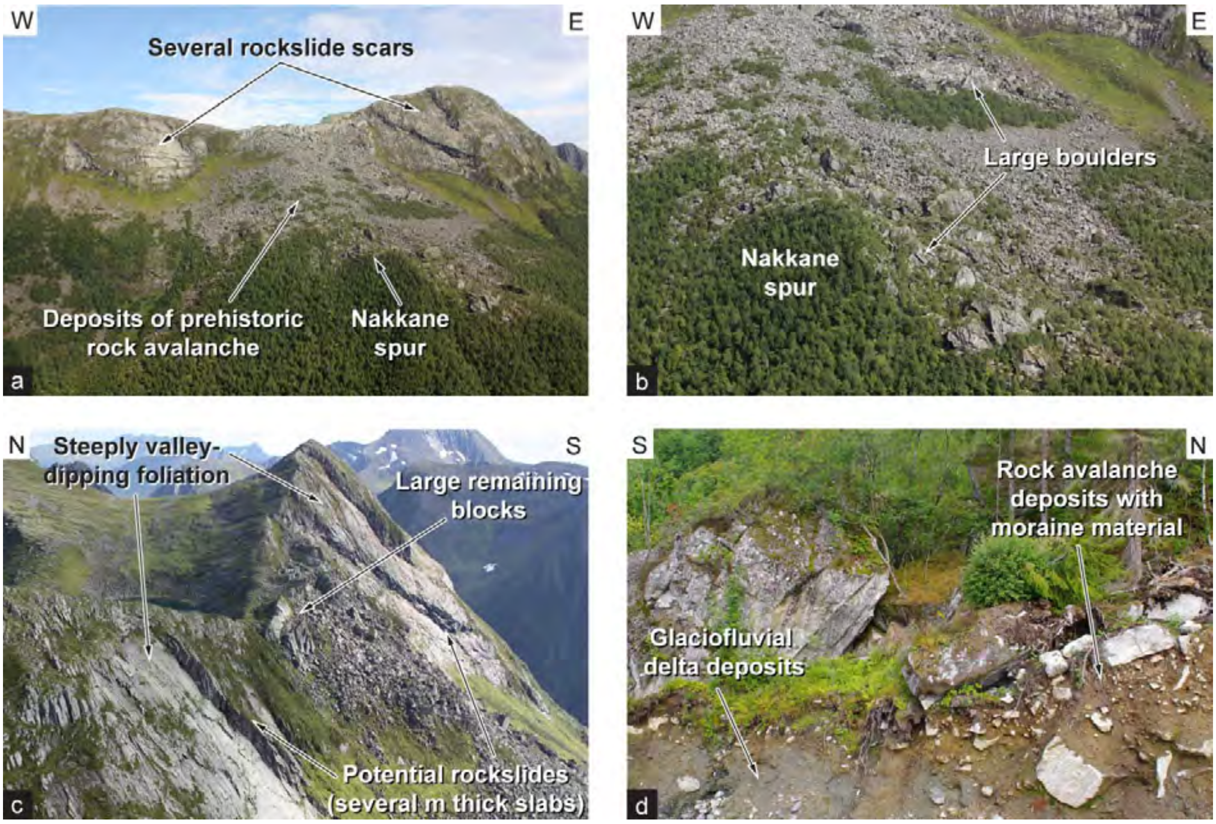

Figure 140: Photographs of the Skorgeurda unstable rock slope: a) frontal view of the rock avalanche deposits and scars; b) large boulders deposited on the slope at Nakkane spur; c) remaining blocks and slabs may slide on the steeply valley-dipping foliation that formed already the basal sliding surfaces of the prehistoric rock avalanche; d) rock avalanche deposits with incorporated moraine material and large boulders overlaying glaciofluvial deposits.

A brief investigation of the rock avalanche deposits was done in 2012 and samples for cosmogenic nuclide dating were collected from three locations in Skorgedalen Valley (Figure 140d). Stratigraphic sections show sand and gravel that were likely deposited in a delta setting, while the shoreline was up to 48 m higher than today (Svendsen and Mangerud 1987). When the mountain side collapsed moraine material deposited in the valley was included in the massive flow of coarse rock material. This explains the matrix of angular blocks incorporated by finer sand and soil overlaying the delta deposits. On top of this matrix, and further upslope, the bouldery deposit is typically openwork. Details about the stratigraphy of the deposits can be found in Blikra (1994), Blikra and Nemec (1998) and Wolden (2005).

Recommendation: A possible rock avalanche from the Skorgeurda will have consequences. Geological field mapping is necessary to evaluate the structural and geological conditions, assess the structures involved in the previous rockslide and better understand the morphology of the rock avalanche deposits. The hazard and risk classification will be made after this field mapping. Further follow-up activities will be decided based on this classification.

7.6.7 Stålberghornet

Stålberghornet is located on a south-facing slope 1060 m above the southern end of Hjørundfjord (Figure 134). A lineament observed on aerial photographs has been interpreted as a back-crack delimiting a possible instability. A helicopter reconnaissance flight showed, however, that this lineament is caused by superficial sliding of glacial deposits or a vegetated block field (Figure 141a). The highly fractured rock mass at the SW-facing slope close to the investigated lineament is a possible source area for rockfalls (Figure 141b), although only a little amount of deposits is visible down-slope. No structures delimiting a large unstable rock slope are visible.

Recommendation: There are no signs that the Stålberghornet rock slope might fail in a massive rock slope failure. No further investigations or displacement measurements are necessary and the hazard and risk classification will not be made. However, rockfalls are possible and their run-out area is given by the rockfall susceptibility map or more detailed hazard maps, where available.

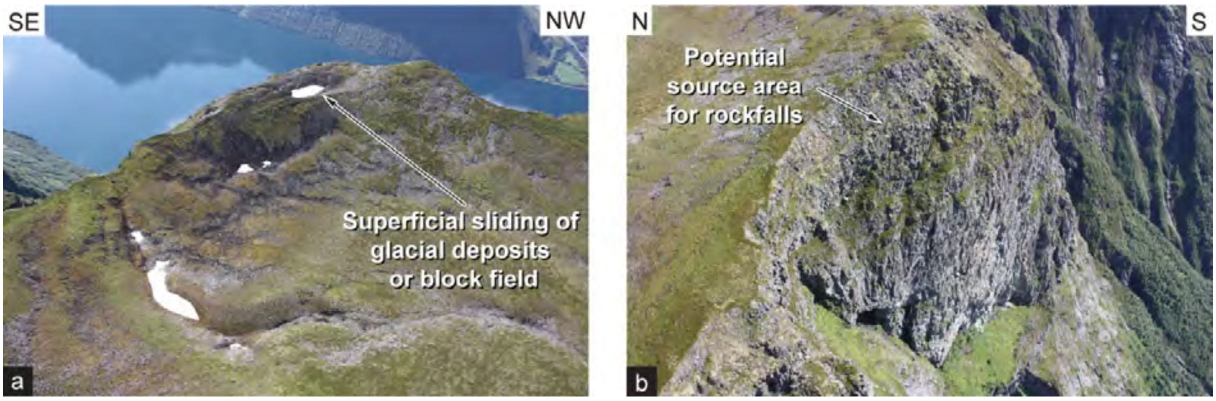

Figure 141: Photographs of the Stålberghornet rock slope: a) superficial sliding or creep of glacial deposits forming depressions on the mountain top; b) highly fractured rock mass that is prone to rockfalls.

8. ÅLESUND REGION

8.1 Haram municipality

There are ten known sites located in Haram municipality, which are all described in this report (Figure 142).

Figure 142: Map of the ten known sites in the Haram municipality with their investigation status. The name of the sites described in this report is shown.

8.1.1 Branddalsryggen

Branddalsryggen is located on a southeast-facing slope 280 m above Nymark village on Skuløya Island (Figure 142). A deep-seated gravitational slope deformation with a clear escarpment as back-scarp (Figure 143) was mapped and reported in Ganerød and Lutro (2011) and newly observed during a helicopter reconnaissance flight in 2012.

The unstable rock slope developed clearly on a band made of different rocks that also shape the slope (Ganerød and Lutro 2011). Several counter-scarps, sinkholes and ridges testify of past deformations, especially in the southwestern part and in the upper parts of the rock slope (Figure 143a). There are some scree deposits at the front of the unstable rock slope, but no clear signs of recent activity. The volume is not accurately calculated, but likely in the order of several tens of million m^3. A massive collapse of the Branddalsryggen rock slope will affect several settlements on the southern end of Skuløya Island (Dahle et al. 2011a).

Recommendation: A possible rock avalanche from the Branddalsryggen will have consequences. Geological field mapping is necessary to evaluate the structural and geological conditions, estimate the volume and quantify past displacements. The hazard and risk classification will be made after this field mapping. Further follow-up activities will be decided based on this classification.

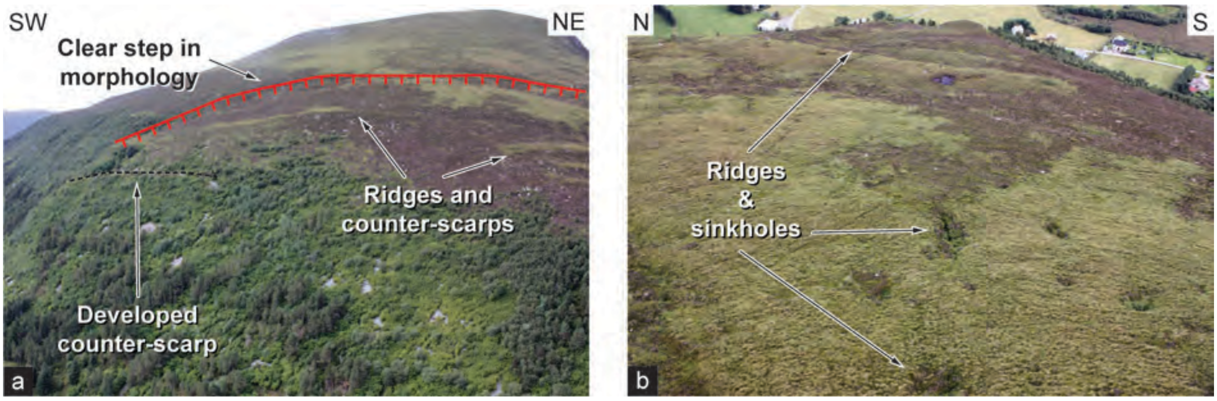

Figure 143: Photographs of the Branddalsryggen rock slope: a) morphology of the deep-seated gravitational slope deformation with an escarpment in the back and several ridges and counter-scarps on the rock slope; b) some sinkholes and open cracks are visible in the upper part of the rock slope.

8.1.2 Byrkjevollhornet

Byrkjevollhornet (Figure 142) is located on a north-facing slope 295 m above Eikedalen Valley. A helicopter reconnaissance flight in 2012 revealed a well-developed translational slide with more than 10 m apparent offset at the back-scarp (Figure 144a, b). The basal sliding surface is parallel to the moderately NW-dipping foliation and the western lateral release fracture is distinctly developed. The detached slab is only a few meters thick, 130 m wide and daylights probably 120 m further down slope, where there is a change in vegetation. The volume of this instability is between 100 000 and 200 000 m³. A massive rock slope failure from Byrkjevollhornet would therefore likely not form a rock avalanche with a run-out distance exceeding the run-out of rockfalls. The cabins on the northeastern flank of Eikedalen Valley will thus not be reached by a failure from Byrkjevollhornet.

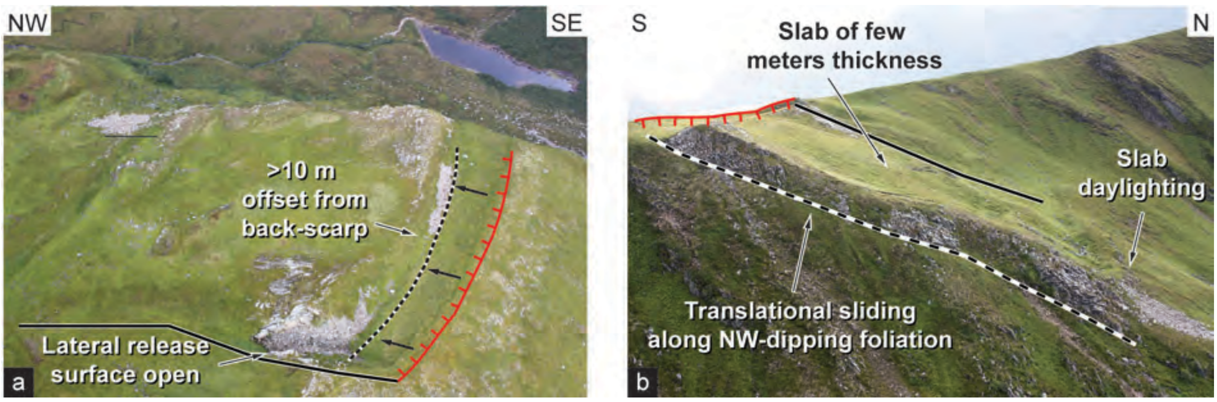

Figure 144: Photographs of the Byrkjevollhornet rockslide: a) past displacements along the back-scarp might have exceeded 10 m; b) a several meters thick slab is sliding on the NW-dipping foliation and daylights the slope.

Recommendation: A possible rock avalanche from the Byrkjevollhornet instability will have no consequences. No further investigations or displacement measurements are necessary. The hazard and risk classification will be made after a simple run-out assessment. Further follow-up activities will be based on this classification.

8.1.3 Hellenakken

Hellenakken (Figure 142) is a N-S-trending mountain ridge 420 m a.s.l. between Vestrefjord and Vatnefjord. A helicopter reconnaissance flight was made in 2012. In the northern part of the mountain ridge a depression indicates past deformations along a back-crack (Figure 145). Small ponds of water in this depression indicate poor drainage and therefore no recent openings of this possible back-crack. Further north this depression evolves to narrow, partly open cracks. These depression and cracks possibly delimit an unstable block towards the east (Figure 145). Recent rockfall activity is noticed at the frontal cliff of this instability. However, Blikra et al. (2002b) identified an unstable rock slope that extends further north and supposed moving to the west. The gneiss foliation is subhorizontal. Together with two subvertical discontinuity sets the foliation delimits small blocks that may fail as rockfalls. In any case, the current structures are not favourably oriented for sliding, both towards the east and the west.

Recommendation: A possible rock avalanche from the Hellenakken instability will have consequences. Geological field mapping is necessary to evaluate the structural and geological conditions, to quantify past displacements and assess the possible sliding direction. The hazard and risk classification will be made after this field mapping. Further follow-up activities will be decided based on this classification.

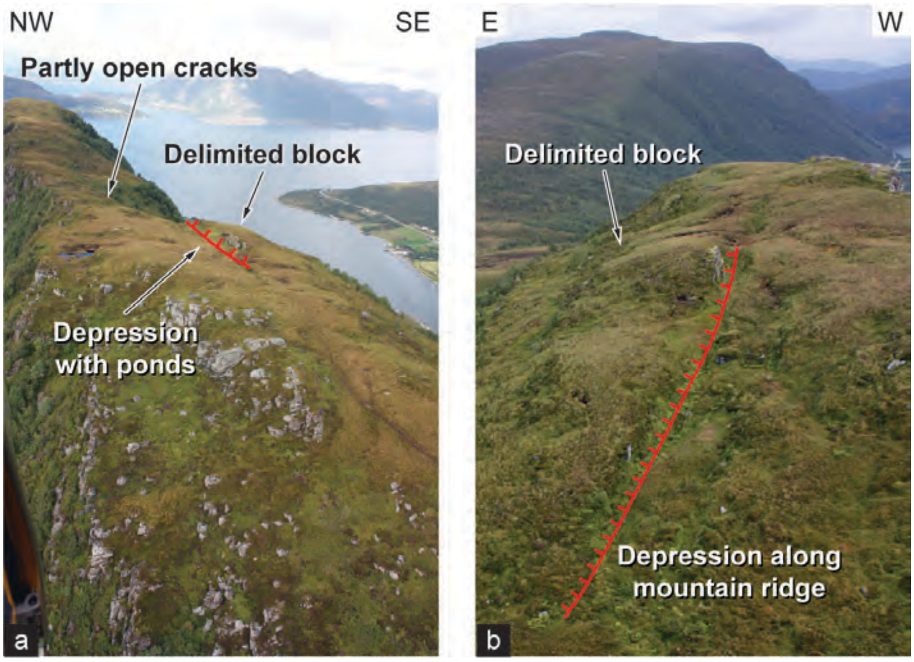

Figure 145: Photographs of the Hellenakken rock slope: an instability is delimited by a back-bounding depression and cracks along the mountain ridge.

8.1.4 Otrefjellet

Otrefjellet (Figure 142) is located at 629 m a.s.l. between Dysadalen and Gåsdalen Valleys. An extensive deformation with a multitude of open cracks and past rock slope failures (Figure 146) of this 2 km long mountain ridge was observed during a helicopter reconnaissance flight in 2012. The site is already reported in Anda et al. (2000) and Blikra et al. (2002a).

The failures occurred on both the eastern and western sides of the ridge forming talus slopes with some large boulders. On the western side a rock avalanche deposit displays a very steep front (Figure 146a) suggesting that the deposit was remobilised after the rock avalanche as a rock glacier. Rock glaciers occur in permafrost environments, which, given the altitude of the site, dates the rock avalanche from shortly after the deglaciation. A partly developed graben can be followed along the top of the ridge (Figure 146b). The structure pattern indicates toppling failures as possible mechanism on both mountain sides (Figure 146a, d) producing relatively small unstable volumes. The only larger instability is located on the eastern slope and displays a partly open back-crack and a free lateral release surface to the north (Figure 146c). The volume of this instability ranges from 100 000 to 200 000 m³. A massive failure of this instability would therefore likely not form a rock avalanche with a run-out distance exceeding the run-out of rockfalls. No settlements would be affected by such a failure.

Recommendation: A possible rock avalanche from the unstable rock slope at Otrefjellet will have no consequences. No further investigations or displacement measurements are necessary. The hazard and risk classification will be made after a simple run-out assessment. Further follow-up activities will be based on this classification.

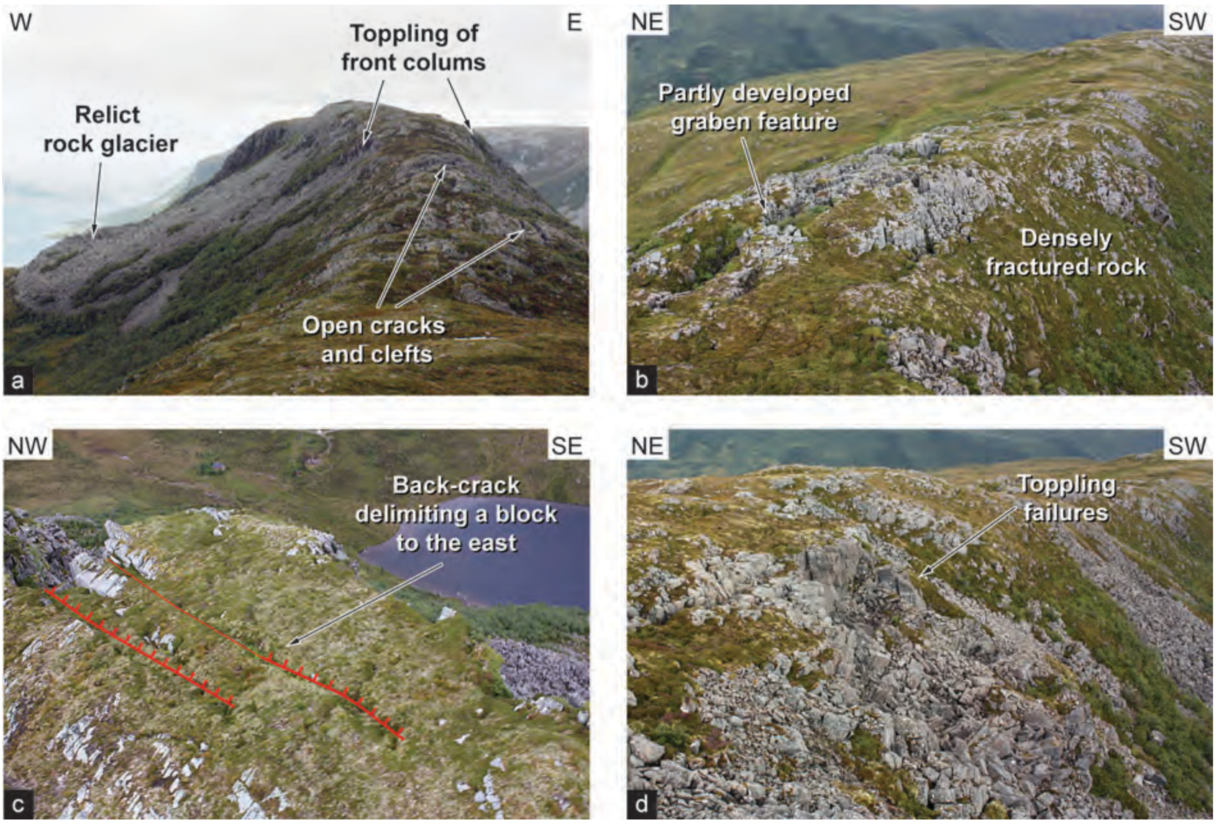

Figure 146: Photographs of the Otrefjellet rock slope: a) the mountain ridge is highly fractured and disintegrates towards the east and west by toppling; b) open cracks and grabens affect the densely fractured rock mass; c) back-cracks of a localised instability on the eastern flank; d) toppled blocks on the western flank.

8.1.5 Skjerveheian

Skjerveheian (Figure 142) is located on a northeast-facing slope 650 m above Skoradalen Valley. A helicopter reconnaissance flight in 2012 revealed a circular escarpment on the flat plateau (Figure 147a). There are no visible cracks or other structures delimiting an unstable rock slope, but the terrain above the escarpment presents signs of creep movements (Figure 147b). This suggests that the circular escarpment is the scar of an old soil/debris slide that removed the few meters thick upper layer. The loose debris moved close to the steep frontal cliff (Figure 147a). The relatively steep slope created by the slide scar favours the creep movements of the debris above. Possible rockfalls or debris falls from Skjerveheian will only affect the uninhabited Skoradalen Valley.

Recommendation: There are no signs that the Skjerveheian rock slope might fail in a massive rock slope failure. No further investigations or displacement measurements are necessary and the hazard and risk classification will not be made. Rockfalls or debris falls are however possible and their run-out area is given by the rockfall susceptibility map or more detailed hazard maps, where available.

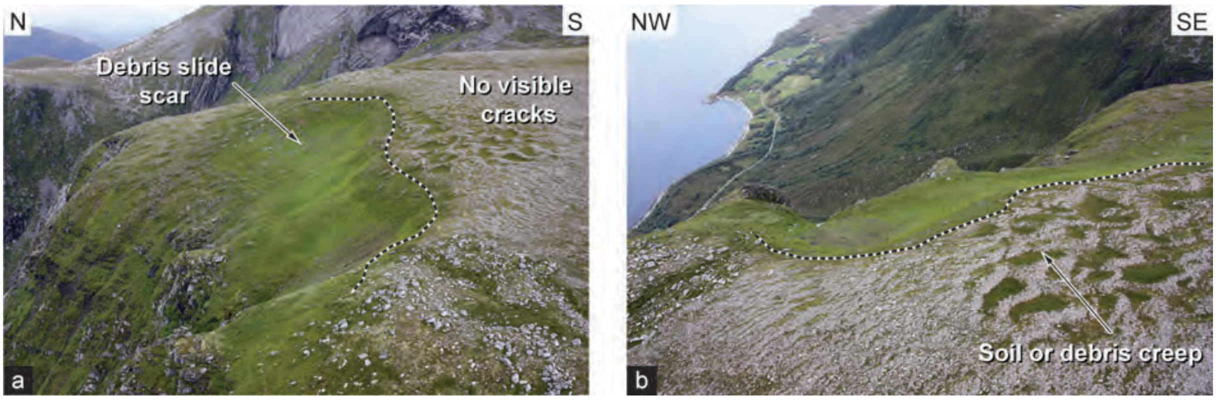

Figure 147: Photographs of the Skjerveheian rock slope: a) scar of a past debris slide forming an escarpment; b) creep movements of soil/debris above the debris slide scar.

8.1.6 Skulen

Skulen is located on a northeast-facing slope 330 m above Nogvafjord (Figure 142). A helicopter reconnaissance flight in 2012 showed a circular shaped back-scarp of an unstable rock slope (Figure 148a). The back-scarp is partly open, but extensively filled and vegetated. A depression marks the NW lateral release surface, which is totally filled (Figure 148b). There is no visible daylighting sliding surface and the instability appears unaffected by recent deformation. Two subvertical discontinuity sets are visible, and one corresponds to the foliation steeply dipping to NNW. The escarpment along the back-crack shows a few meters of past deformation and there are signs of rockfall activity along the SE lateral release surface which follows the foliation. The volume of Skulen instability is estimated to 2 million m³. A massive failure from Skulen would reach Nogvafjord and create a displacement wave (Dahle et al. 2011a).

Recommendation: A possible rock avalanche from the Skulen instability will have consequences. Geological field mapping is necessary to evaluate the structural and geological conditions and to quantify past displacements. The hazard and risk classification will be made after this field mapping. Further follow-up activities will be decided based on this classification.

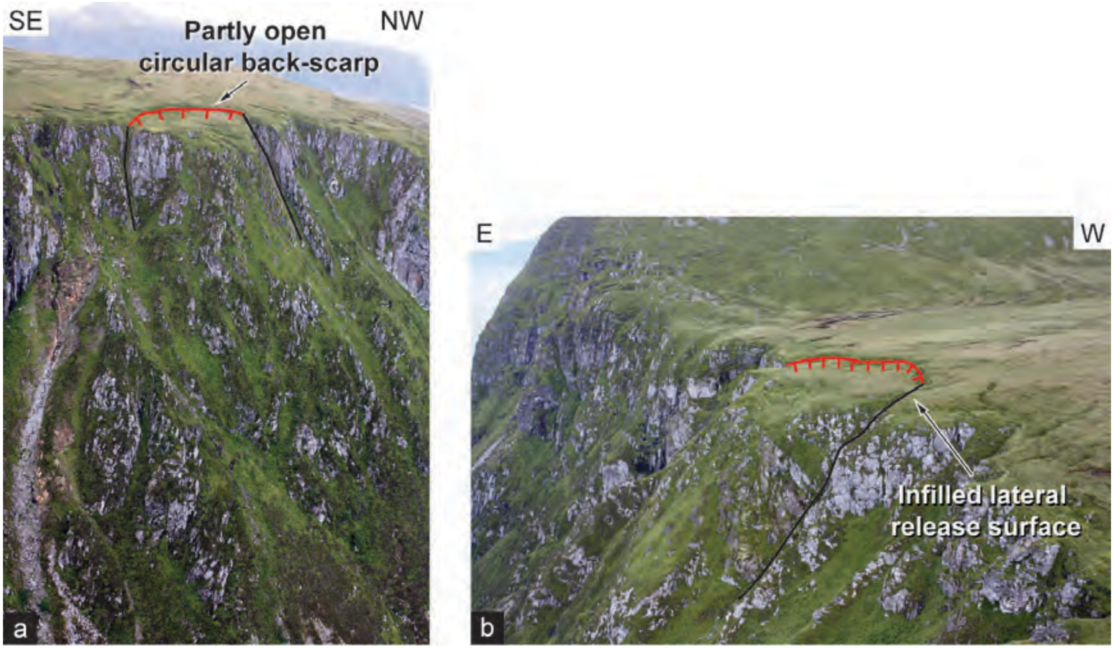

Figure 148: Photographs of the Skulen instability: the circular back-scarp and the lateral release surfaces are partly open, but generally filled with soil and vegetation.

8.1.7 Skoraegga

Skoraegga is located on the north-facing slope 525 m above Skor settlement and Midfjord (Figure 142). The rock slope was investigated by Blikra et al. (2002b) and during a helicopter reconnaissance flight in 2012. The gneiss foliation is steeply N-dipping and does not daylight the topography further downslope (Figure 149a). Even though there are foliation-parallel depressions on the mountain top, there are no structures delimiting a large unstable rock slope and no signs of activity. A vertical joint set perpendicular to foliation delimits small blocks that might fail as rockfalls (Figure 149b).

Recommendation: There are no signs that the Skoraegga rock slope might fail in a massive rock slope failure. No further investigations or displacement measurements are necessary and the hazard and risk classification will not be made. However, rockfalls are possible and their run-out area is given by the rockfall susceptibility map or more detailed hazard maps, where available.

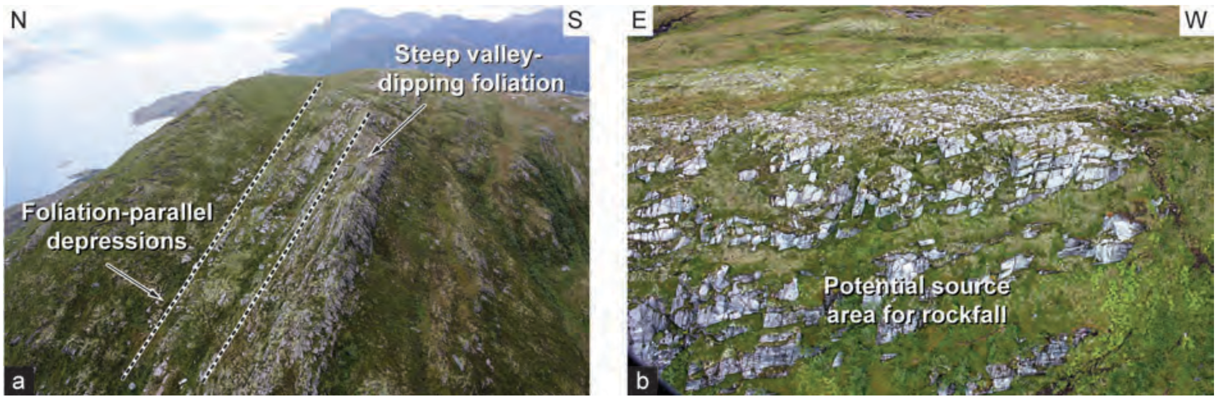

Figure 149: Photographs of the Skoraegga rock slope: a) depressions parallel to the steeply N-dipping foliation are visible on the mountain top; b) small blocks delimited the foliation and vertical discontinuities may fail as rockfalls.

8.1.8 Tindfjellet

Tindfjellet (Figure 142) is located on a west-facing slope 665 m above the Vestrevatna Lake. A helicopter reconnaissance flight was made in 2012 showing a large block field formed by rockfalls from the Tindfjellet mountain top or from in-situ disintegration of highly fractured rock masses (Figure 150a). Some open cracks developed in this block field, but no large unstable rock slope is actually shaped. A small instability with a maximum volume of 50 000 m³ is located along the south-western crest of Tindfjellet and displays a fully open back-crack and a lateral release surface formed by the steeply N-dipping foliation (Figure 150b). A failure of this instability would not travel further than rockfalls (Dahle et al. 2011a).

Recommendation: There are no signs that the Tindfjellet rock slope might fail in a massive rock slope failure. No further investigations or displacement measurements are necessary and the hazard and risk classification will not be made. However, rockfalls are possible and their run-out area is given by the rockfall susceptibility map or more detailed hazard maps, where available.

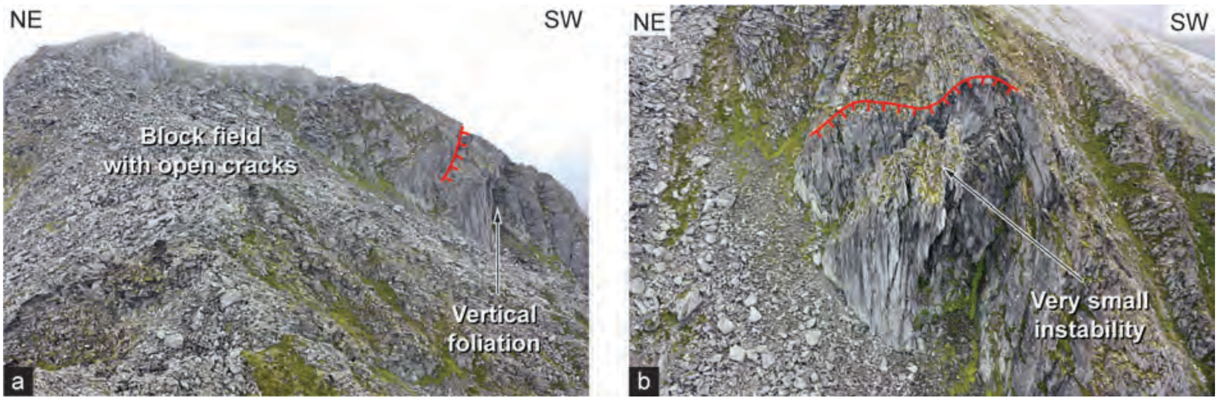

Figure 150: Photographs of the Tindfjellet rock slope: a) a highly disintegrated block field forms the western mountain slope; b) a small instability is located on the SW-ridge of Tindfjellet.

8.1.9 Vassbotnen 1 & 2

Vassbotnen 1 & 2 (Figure 142) are located on a north-facing to northeast-facing slope 270–280 m above the Eikedalen Valley, close to the Byrkjevollhornet rockslide. Shallow surface depressions were observed on aerial photographs and interpreted as possible back-cracks and lateral release surfaces (Figure 151). A helicopter reconnaissance flight made in 2012 showed that these depressions are only superficial and not related to open cracks at depth. There are no structures present at Vassbotnen 1 & 2 to delimit an unstable rock slope and no signs of past displacements. Rockfalls occur however from both sites forming a talus slope at the foot of the cliff (Dahle et al. 2011a).

Recommendations: There are no signs that the Vassbotnen 1 & 2 rock slopes might fail in massive rock slope failures. No further investigations or displacement measurements are necessary and the hazard and risk classification will not be made. Rockfalls or debris falls are however possible and their run-out area is given by the rockfall susceptibility map or more detailed hazard maps, where available.

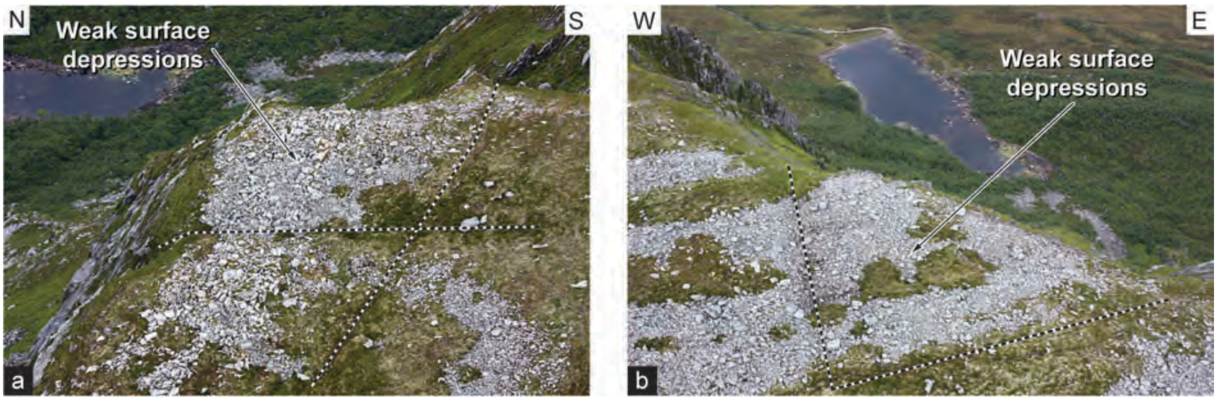

Figure 151: Photographs of the Vassbotnen rock slopes: a) Vassbotnen 1; b) Vassbotnen 2. Both rock slopes display weak surface depressions that are not related to open cracks at depth.

8.2 Sula municipality

There are three known sites located in Sula municipality that all developed on Tverrfjellet mountain and are all described in this report (Figure 152).

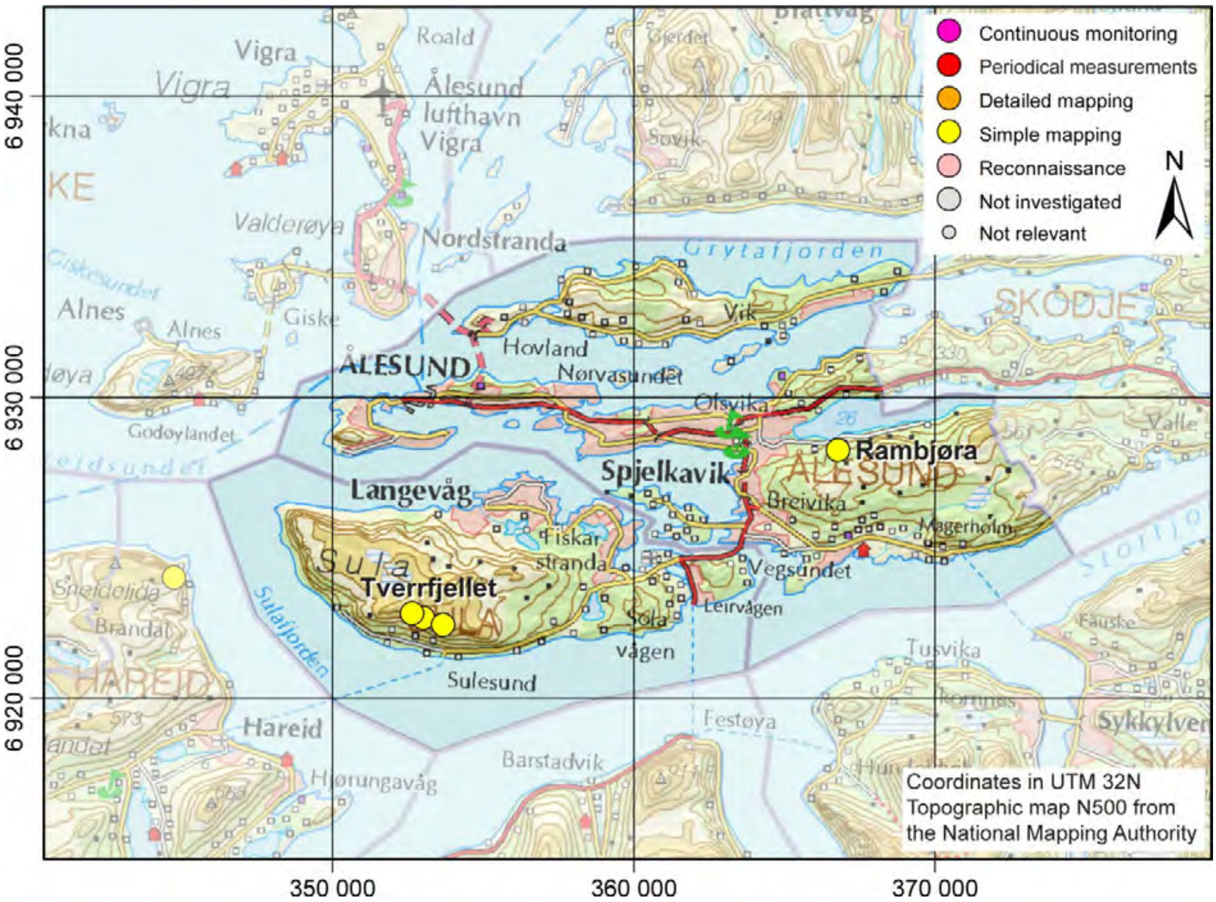

Figure 152: Map of the known sites in the Sula municipality (3 sites) and Ålesund municipality (1 site) with their investigation status. The name of the sites described in this report is shown.

8.2.1 Tverrfjellet 1, 2 & 3

Tverrfjellet 1, 2 & 3 are located on a southwest-facing slope 650–670 m above Sulesund (Figure 152). A helicopter reconnaissance flight made in 2011 showed a deep-seated gravitational slope deformation of the mountain side over a width of more than 2 km (Figure 153). Field mapping in 2012 allowed to map relevant structures and to delimit the deformed area into three distinct unstable rock slopes, named Tverrfjellet 1, 2 & 3, respectively (Figure 153a, Figure 154).

Tverrfjellet 1 is delimited to the NW by a moderately SE-dipping lateral release surface forming a 3–4 m high escarpment (Figure 153b, d). The back-scarp is formed by a complex pattern of valley-parallel cracks and transverse cracks and has a downthrow of 0.5–2.0 m. The southeastern limit on the Tverrfjellet 1 unstable rock slope is a W-dipping lateral release surface with a throw of up to 75 cm that joins a gully (Figure 154). The basal failure surface is not visible and the toe line shown in Figure 154 is thus speculative. Past deformations are relatively small given the size of the unstable rock slope and there are only few open cracks observed within the instability (Figure 153b, d). Highly fractured spurs are located on the moderately SW-dipping slope in the front of Tverrfjellet 1 (Figure 154).

Tverrfjellet 2 is a site of complex deep-seated gravitational slope deformation with distinct lateral and rear limits and internal scarps and ridges (Figure 153a, e, f, Figure 154). The downthrow of the back-scarp increases from 1–2 m in the NW to 20–30 m in the SE, but is overgrown by vegetation and small blocks (Figure 153e). A 10–15 m high, E-W-trending ridge is located at the front of the eastern part of the unstable rock slope (Figure 153a, f, Figure 154). This ridge might be formed by differential movement between two compartments of the gravitationally deformed slope. Similarly to Tverrfjellet 1, the basal failure surface is inconspicuous so the toe line drawn in Figure 154 is uncertain and several highly fractured spurs are located on the moderately fjord-dipping slope in the front of Tverrfjellet 2 (Figure 154).

The gneiss foliation at Tverrfjellet 2 is folded and its orientations range from gently S-dipping to gently E-dipping and moderately NE-dipping. Four other discontinuity sets have quite variable orientation, but are generally subvertical. Planar sliding is a possible failure mechanism, where the foliation is S-dipping. Toppling failures are also possible along a vertical WNW-ESE-trending discontinuity set.

Glacial deposits with tills and centimetric to decimetric clasts are observed along the back-scarp of Tverrfjellet 2. The tills create a relatively impermeable layer that explains the swamp and small lakes on the flat top of the unstable rock slope (Figure 153a) and a bog formed above the back-scarp. This indicates a relatively intact rock mass with only few open cracks.

Tverrfjellet 3 is located between the Tverrfjellet 1 & 2 unstable rock slopes and is relatively small compared to both other sites (Figure 154). The instability is delimited by an open back-scarp with a downthrow of 1–2 m (Figure 153c). The lateral limits are defined by gullies on both sides of the instability. The basal failure surface is not visible and the toe line in Figure 154 is thus questionable. On Tverrfjellet 3 instability, a subblock is delimited by a 5 m wide graben (Figure 153c) without displaying traces of recent openings or signs of activity.

The gneiss foliation is folded and the formed surfaces are very rough. The foliation orientation changes from gently SW-dipping to subhorizontal and gently NE-dipping. Three other discontinuity sets are steeply dipping towards the NNE, E and SE, respectively. Planar sliding is feasible when the foliation is dipping to the SW, while toppling may occur along the NNE-dipping discontinuity set.

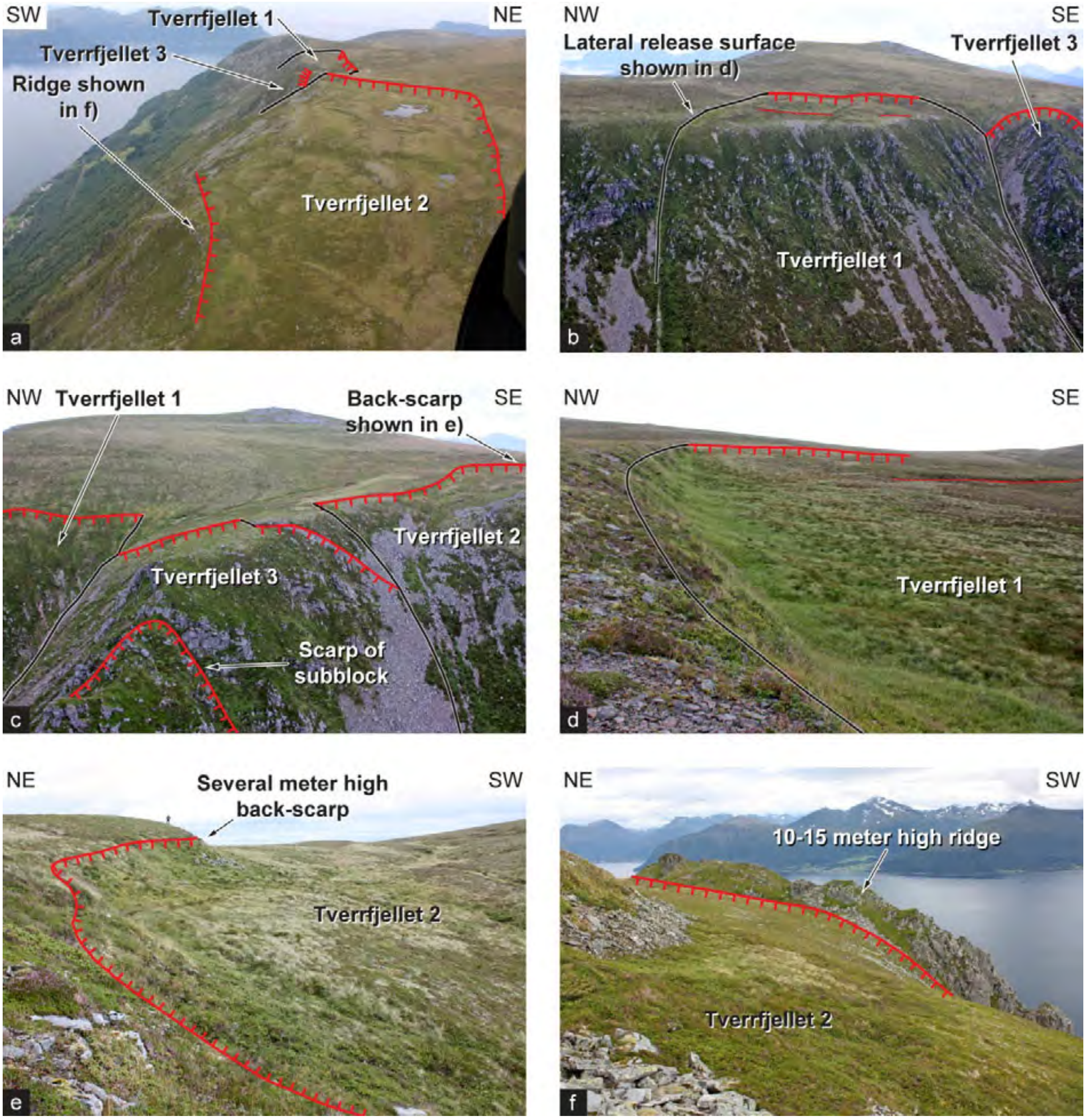

Figure 153: Photographs of the three Tverrfjellet unstable rock slopes: a) overview photograph displaying the ridge and lakes on Tverrfjellet 2; b) frontal view of Tverrfjellet 1 with few open cracks on the plateau; c) Tverrfjellet 3 is delimited by a 1–2 m open back-crack, a subblock is separated from the main instability by a 5 m wide graben; d) lateral release surface of Tverrfjellet 1 with a decreasing throw towards the back-scarp; e) back-scarp of Tverrfjellet 2; f) 10–15 m high ridge located in the eastern part of Tverrfjellet 2 indicates differential movement of two compartments of the unstable rock slope.

All the three sites of deep-seated gravitational slope deformation at Tverrfjellet do not display signs of recent displacements, since the delimiting structures are completely overgrown by vegetation. The Tverrfjellet 1 & 3 instabilities are still in an early-stage of deformation, while past deformations were larger at Tverrfjellet 2 with internal scarps and ridges. Massive failures of these large unstable rock slopes have thus only a small probability, but they would cause a displacement wave in the fjord with catastrophic consequences (Dahle et al. 2011a). The localised blocks and spurs at the front of the Tverrfjellet unstable rock slopes (Figure 154) have relatively small volumes (<100 000 m^3). Their failure would likely not form rock avalanches with run-out distances exceeding the run-out of rockfalls, but might still impact buildings in Sulesund.

Recommendations: Possible rock avalanches from the Tverrfjellet 1, 2 & 3 unstable rock slopes will have consequences, which will be assessed in the hazard and risk classification. Further follow-up activities will be decided based on this classification.

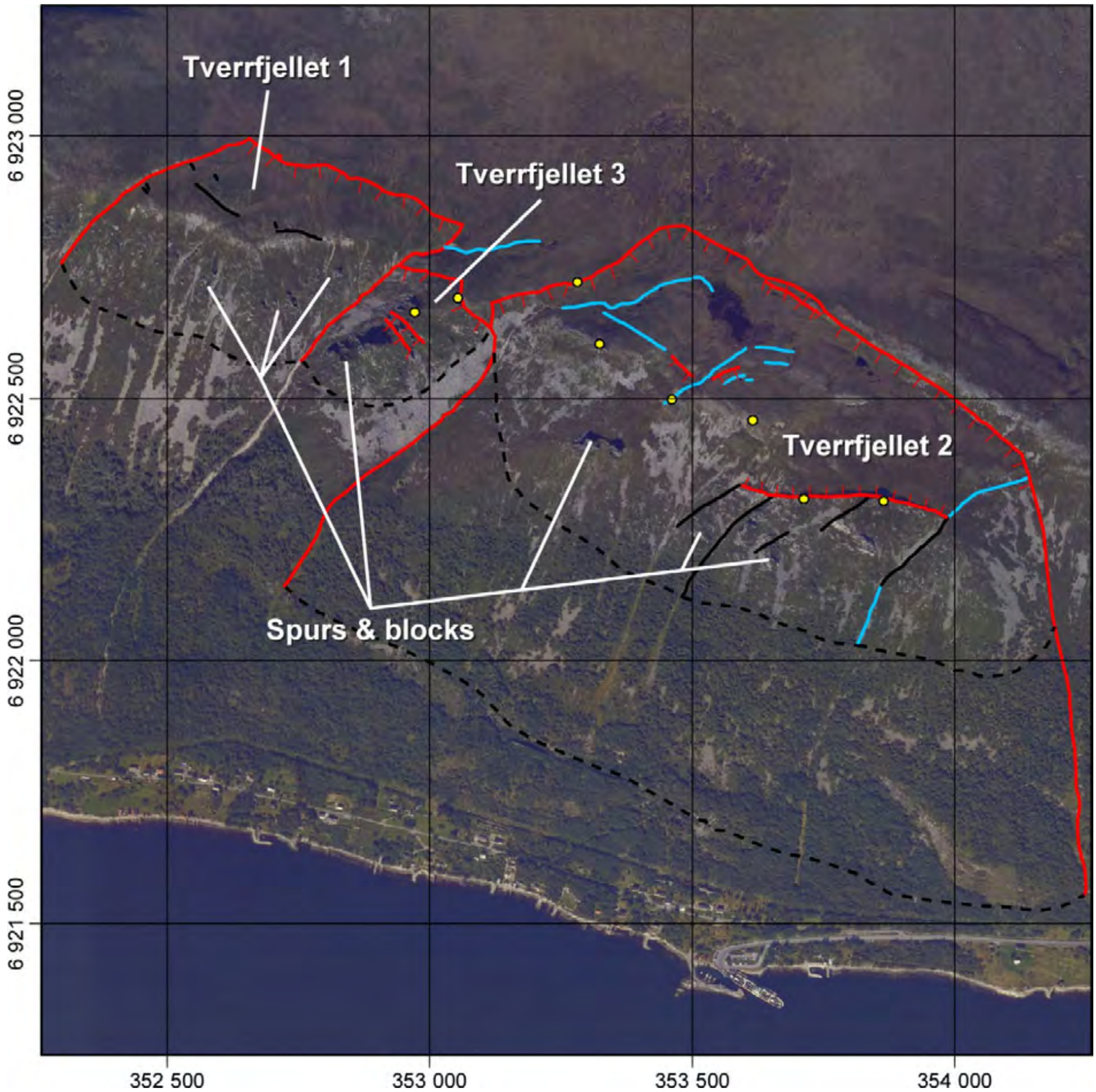

Figure 154: Map of the three Tverrfjellet unstable rock slopes showing locations of field measurements (yellow dots). The locations of the toe lines are uncertain.

8.3 Ålesund municipality

There is one known site located in Ålesund municipality, which is described in this report (Figure 152).

8.3.1 Rambjøra

Rambjøra (Figure 152) is located on a northwest-facing slope 300 m above Litlestølen settlement and Brusdalsvatnet Lake. A helicopter reconnaissance flight in 2011 revealed an unstable rock slope that is bounded to the east and to the SW by two distinct faults (Figure 155, Figure 156). The SW-bounding fault is eroded and shows typical mineralisation with laumonite and chlorite (Figure 155c), while the eastern fault forms a marked surface depression that can be followed inward of the plateau (Figure 156). A several meter high back-scarp is observed at the southwestern corner of the instability in direct continuation of the cliff west of Rambjøra instability. The back-scarp might thus persist into the instability and a shallow depression is indeed visible inline with the back-scarp toward the east (Figure 156). Past deformations have probably been very small, because (1) the rock mass in the instability is relatively intact and only affected by few internal cracks and (2) the back-scarp is poorly developed. At the front cliff of the instability, there is a completely detached block to the NW (Figure 155a, b) and a partly open crack delimiting a column to the east (Figure 155d).

The gneiss foliation has variable orientations and is subparallel to the faults at the SW and E limits (steeply NNE-dipping and steeply W-dipping, respectively). On the top of the instability the foliation is gently E-dipping. Four other discontinuity sets are measured and are all subvertical. Two of them form the open cracks that delimit the detached blocks and columns along the front cliff of the Rambjøra instability. These might fail by a combination of sliding and toppling, while the entire instability might fail along the intersection line formed by the faults.

A massive failure of Rambjøra instability would create a rock avalanche that would impact Litlestølen settlement and create a displacement wave in Brusdalsvatnet Lake that counts several other settlements along its shoreline (Dahle et al. 2011a).

Recommendation: A possible rock avalanche from the Rambjøra and the created displacement wave instability will have consequences, which will be assessed in the hazard and risk classification. Further follow-up activities will be decided based on this classification.

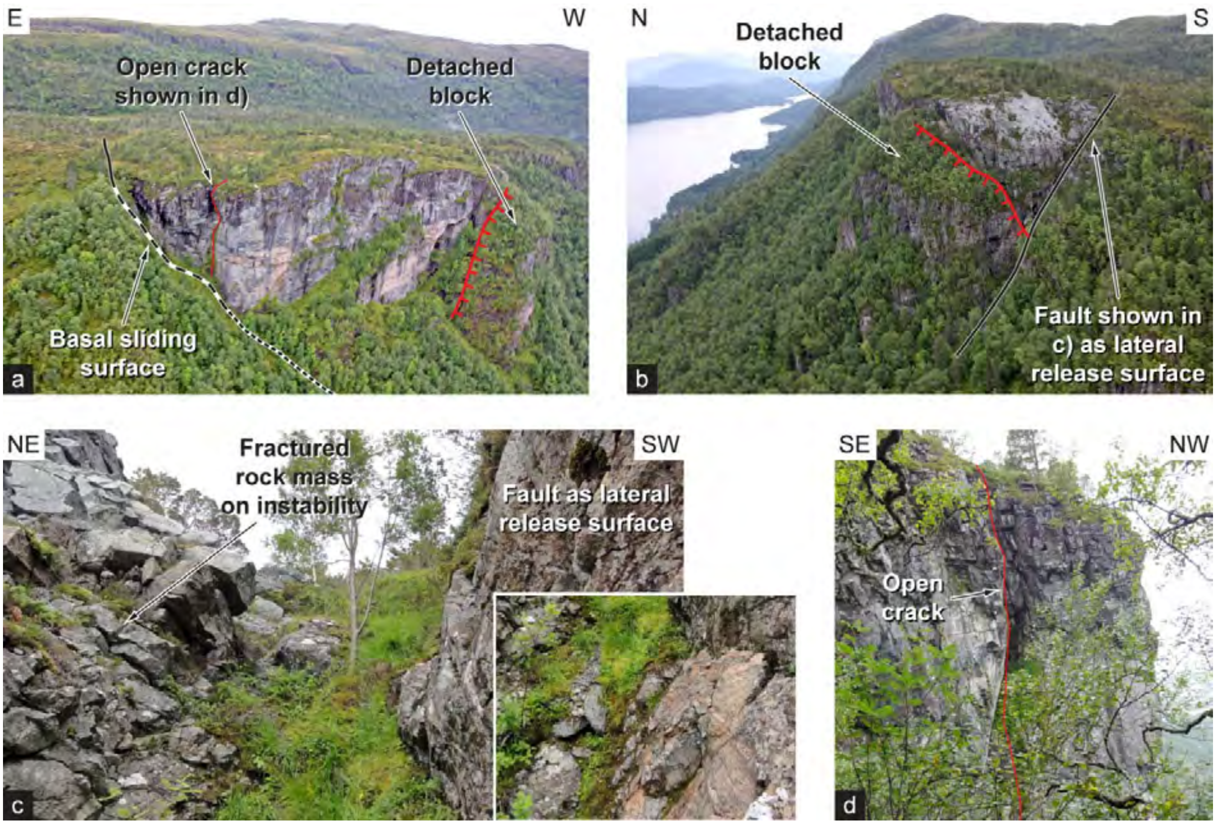

Figure 155: Photographs of the Rambjøra instability. a) frontal view of the instability with the basal sliding surface as eastern limit and detached blocks at the front; b) a fault forms the lateral release surface in the SE; c) detail of the SE-bounding fault (inset: mineralisation of the fault zone); d) open subvertical crack delimiting a column along the front cliff.

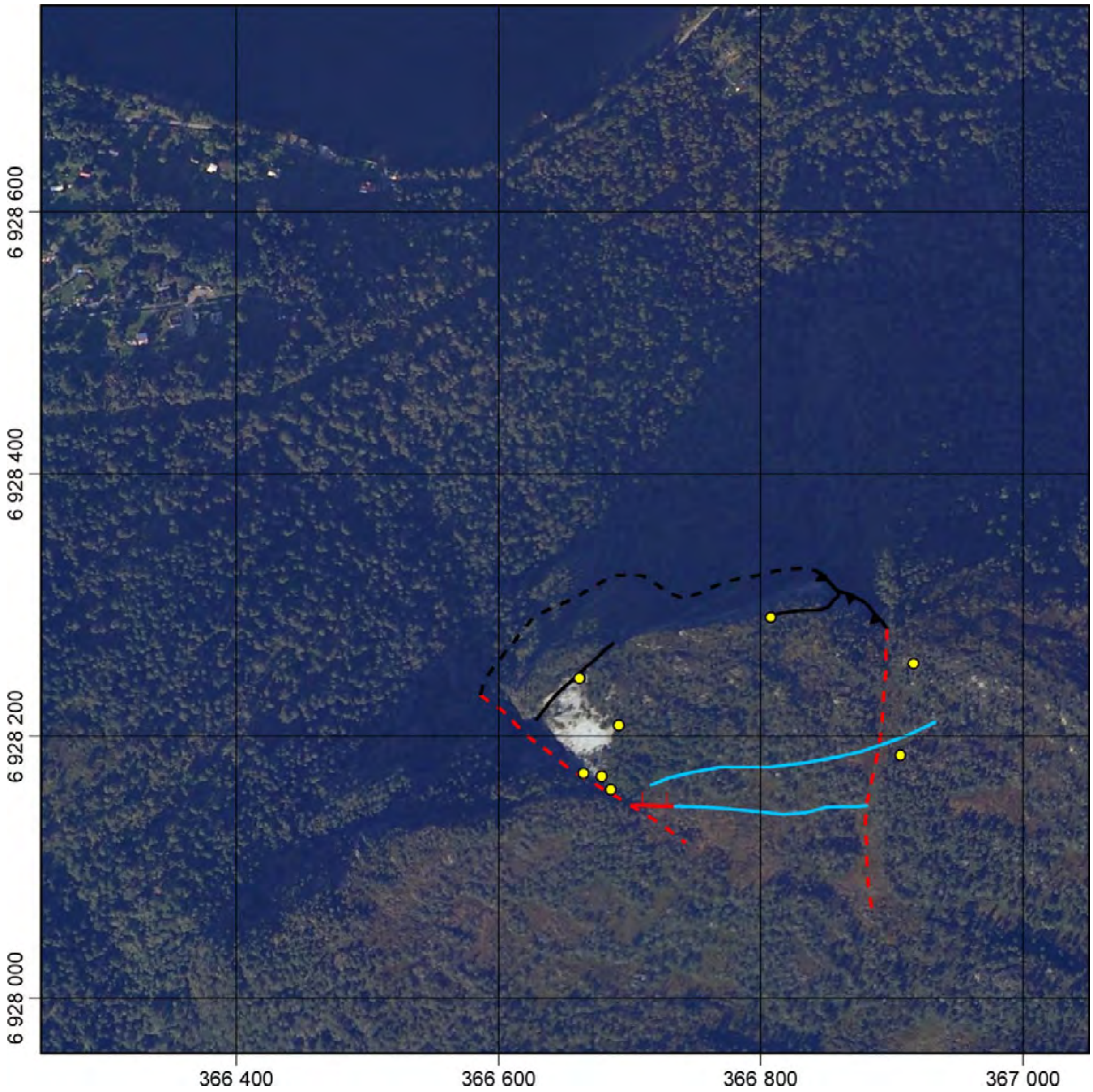

Figure 156: Map of the Rambjøra instability showing locations of field measurements (yellow dots).

9. INVESTIGATIONS ON PAST ROCK AVALANCHES

The knowledge of past partial or total rock slope failures is a fundamental to understand present unstable rock slopes and assess their hazard. It issues from basic mapping of rock avalanche deposits, from modelling of already failed rock slopes as well as from dating of deposits and of cracks or/and other structures associated to past rock slope deformation.

9.1 Rock avalanche inventory in Romsdalen Valley

An inventory of rock avalanches in Romsdalen Valley was made by T.Ø. Farsund during a project thesis at NTNU in collaboration with NGU (Farsund 2010). The study was mainly based on the interpretation of a high-resolution digital elevation model and aerial photographs, but involved also brief field validation. Forty-one rock avalanche deposits were mapped in Romsdalen Valley including their corresponding source areas (rockslide scars) (Figure 157).

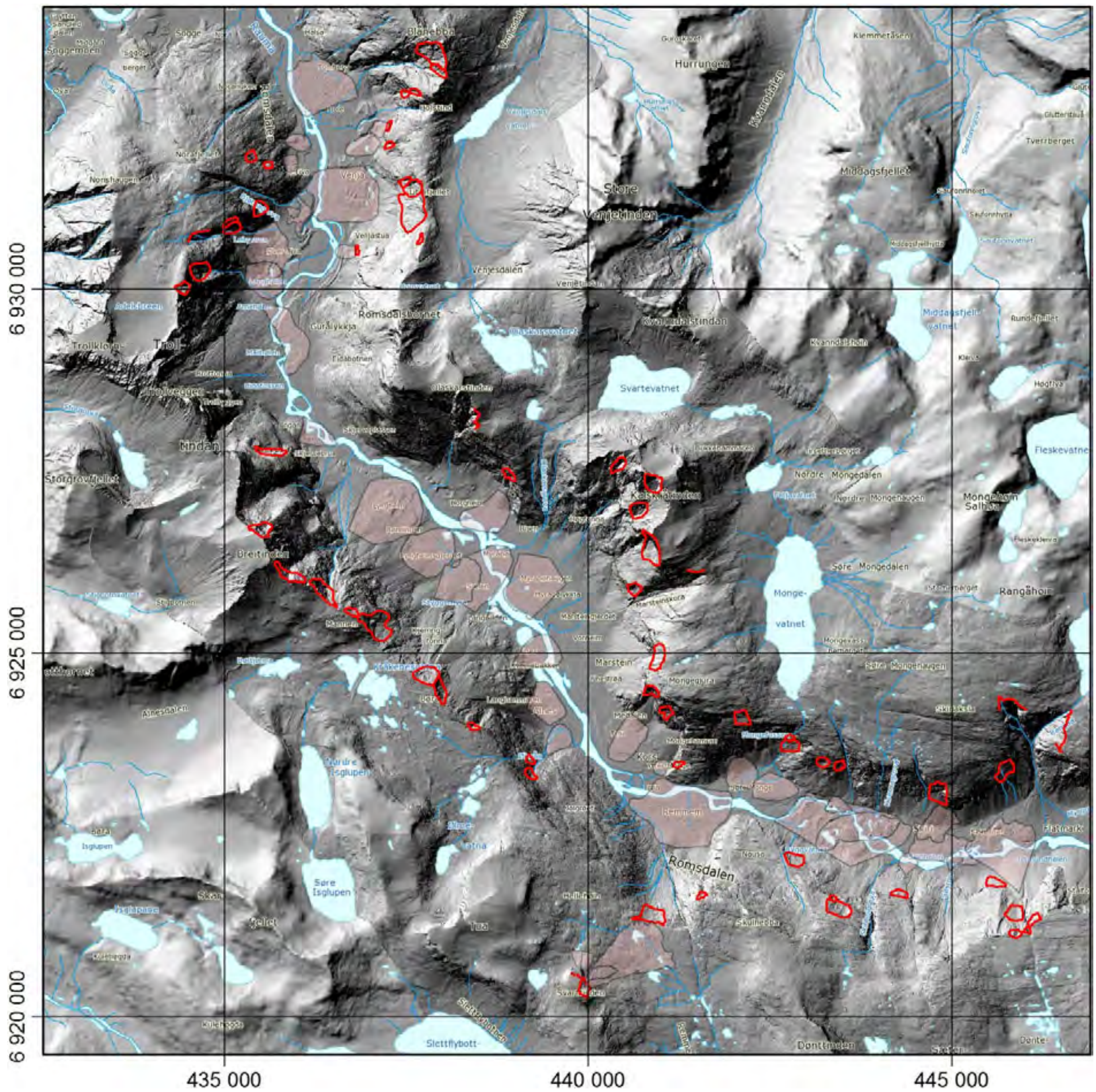

Figure 157: Rock avalanche inventory map in Romsdalen Valley (red polygons: rock avalanche deposits; red lines: rockslide scars) (modified from Farsund 2010).

It can be noted that some of the mapped deposits did not display an excessive run-out distance and cannot be rock avalanches *sensu strictu* as defined in section 1.1. Some deposits superpose or overlap with other deposits and their stratigraphic relationship is difficult to elucidate based on the high-resolution digital elevation model and aerial photographs. It cannot be ruled out that some of the deposits were formed by the same rock avalanche event, but appear to be distinct based on different morphologies. These drawbacks reduce the likely number of post-glacial rock avalanches in Romsdal Valley to approximately ten, which is comparable to a total of 15 rock avalanche deposits identified in Romsdalen Valley by previous studies (Anda and Blikra 1998, Elvebakk and Blikra 1999, Blikra et al. 2002a).

9.2 Rock avalanche inventory in Innerdalen Valley

An inventory of rock avalanches in Innerdalen Valley was made by M. Schleier during an internship at NGU in 2009 and now as part of his PhD thesis at University of Erlangen, Germany, in collaboration with NGU and under R. Hermanns' co-supervision. Preliminary results are summarized in Schleier et al. (2013):

Multiple rock avalanche deposits composed of rock boulders several meter in diameter occur in Innerdalen Valley. The blocky deposits are divided into six units (A to F in Figure 158). The main rock avalanche deposits (A) have an estimated volume of 39 million m^3 and typical lateral levees and frontal rims. The rock avalanche crossed the valley, ran-up on the opposite valley side by up to 65 m and dammed the river to form Innerdalvatnet Lake. Boulders are several meter to tens of meter in diameter and cover the entire surface of the deposits.

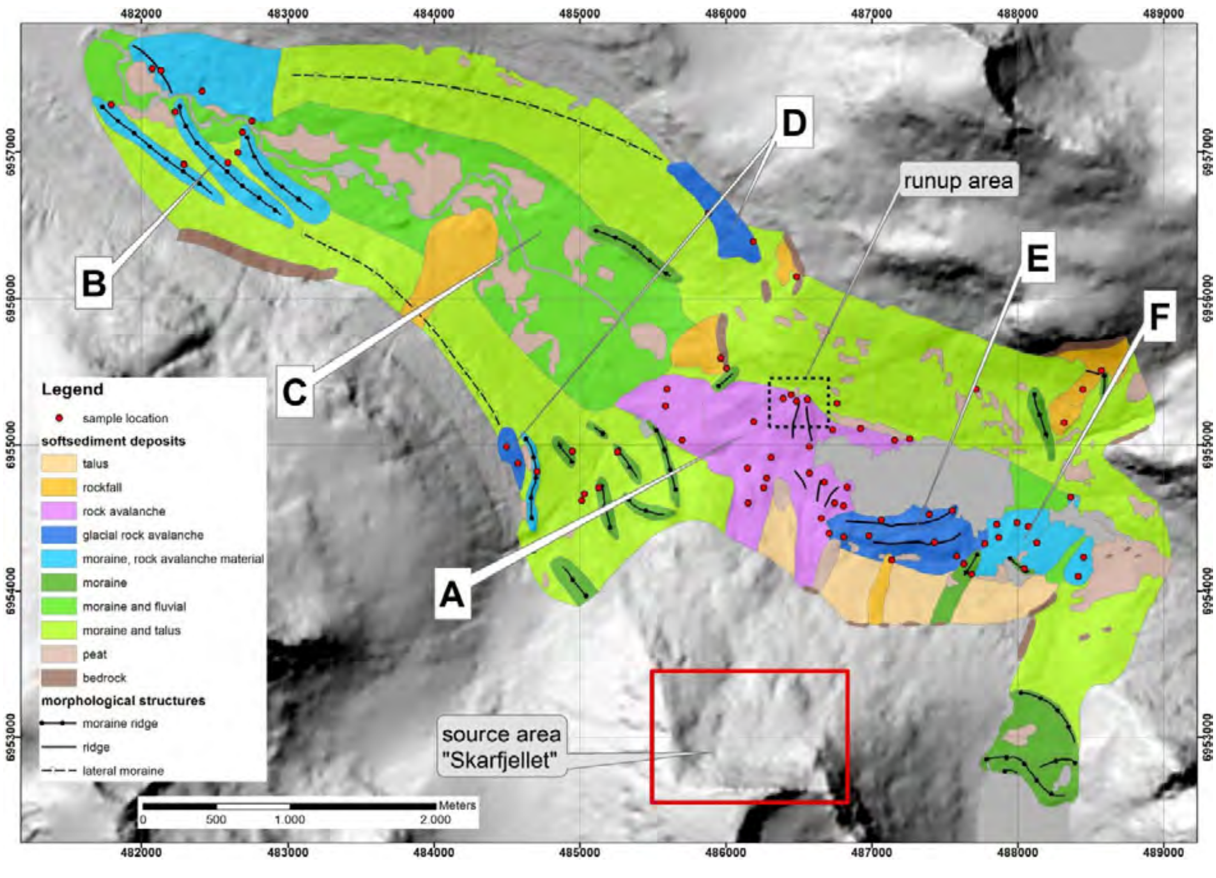

Figure 158: Rock avalanche inventory map in Innerdalen Valley (Schleier et al. 2013).

Other boulder deposits are interpreted to be related to another rock avalanche that would have occurred in Innerdalen Valley when it was filled by a glacier at the end of the Younger Dryas. This rock avalanche would have travelled over the glacier and deposited patches of boulders (D) on the slope at 270–370 m above the valley floor. However, most of the material would have been deposited onto the glacier and then redeposited with the normal supra- and subglacial load into three closely spaced 12–15 m high frontal moraine ridges covered with metric boulders (B) and isolated hills composed of rock boulders surrounded by fluvial sediments (C). Two distinctive valley-parallel ridges (E) 30–50 m above Innerdalvatnet Lake are likely related to rock avalanche debris deposited onto the glacier. This protects the ice from melting and leads to an accumulation of boulders by washing out of fine-grained material by supraglacial processes. A flat boulder patch within moraine deposits southeast of Innerdalvatnet Lake (F) should be related to transported rockfall and rock avalanche material from upstream the Innerdalen Valley.

9.3 Rock avalanche inventory in Innfjorddalen Valley

An inventory of rock avalanches in Innfjorddalen Valley was made by S. Seljesæter as part of a MSc thesis and by M. Schleier as part of his PhD thesis at University of Erlangen, Germany, in collaboration with NGU and under R. Hermanns' co-supervision . Preliminary results are summarized in Schleier et al. (2013):

In the lower Innfjordalen Valley a succession of three rock avalanche deposits is mapped. The deposits have lobate forms, overlay each other and boulders of several meters in diameter (Figure 159). Several distinguishable morphological features can be mapped: a terrace of a marine delta at an altitude of 120 m a.s.l. (A), which is overlain by a first rock avalanche deposit (B). It has a volume of approximately 21 million m^3 and the rock avalanche ran-up the opposite valley side by 110 m. These deposits can be divided into a continuous deposit located between 130 and 35 m a.s.l. (B) and a distal part at 15 m a.s.l. showing only isolated hills of boulder deposits (E). In between there is an area of deformed valley fill deposits with isolated boulders (C) and undisturbed valley fill deposits without boulders (D) (Figure 159). The distal part of the oldest rock avalanche in Innfjorddalen Valley (E) is interpreted to have deposited into the fjord approximately 3000 years ago when the shoreline was still approximately 20 m higher than today. The main part of that rock avalanche (B) is however deposited onshore. The limit between disturbed and undisturbed valley fill sediments (C and D) is supposed to mark the shoreline at that time and the disturbed sediments were liquefied and deformed by the rock avalanche.

The proximal part of first rock avalanche deposit is overlain by a second rock avalanche deposit with an estimated volume of 5.4 million m^3 (F), which dammed the river and formed a lake. Cosmogenic nuclide dating of one rock avalanche deposit sample gives an age of 1200 ± 400 years BP. These deposits are overlain by a third rockfall deposit (G), which has a relatively small volume (190 000 m^3) and occurred in 1611 or 1612 (Furseth 2006).

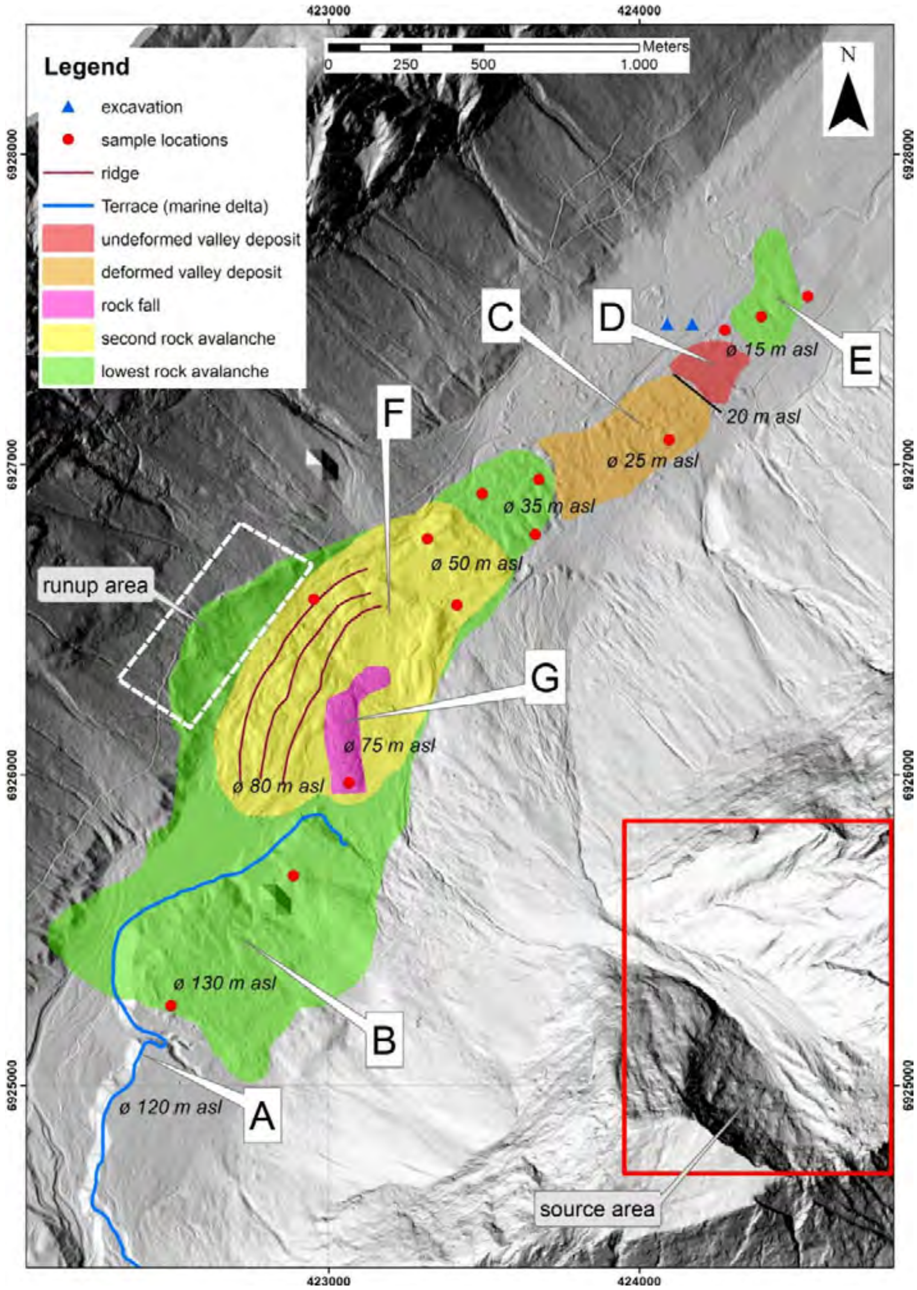

Figure 159: Rock avalanche inventory map in Innfjorddalen Valley (Schleier et al. 2013).

9.4 Back-analysis of rockslides in Tafjord

The back-analysis of past rockslides in Tafjord was part of T. Oppikofer's PhD thesis (Oppikofer 2009) and made within the Åknes/Tafjord project. Detailed results will be published in a scientific journal (Oppikofer et al. in prep.):

The analysis of rockslide scars in Tafjord is based on a combined approach using detailed geomorphic, structural and geological field mapping along with interpretation of high-resolution digital elevation models and orthophotos. Seventeen rockslide scars are mapped (Figure 160) and back-analyzed, including the identification of major discontinuity sets and of relevant rockslide structures (basal sliding surface, back-scarp, lateral release surface…), the rockslide mechanisms and the volume calculation. The computed volumes range from 29'000 m^3 to 63.6 million m^3. These back-analyses highlight the strong control of pre-existing planar structures on the development of large rockslides in the study area. The gneiss foliation is implied in mostly all the ancient rockslides and serves mainly as basal sliding surfaces.

However, the basal sliding surfaces are often buttressed by the topography and an additional sliding surface had to develop to enable displacement in a wedge failure mechanism. Shallow-plunging sliding directions (as low as 25°) are kinematically feasible because of the presence of low friction angle and low cohesion fault breccia, fault gouges or mica-rich layers along the basal sliding surface. This study of rockslide scars in Tafjord provides useful findings for the understanding of present rock slope instabilities, which also appear to be controlled by pre-existing structures.

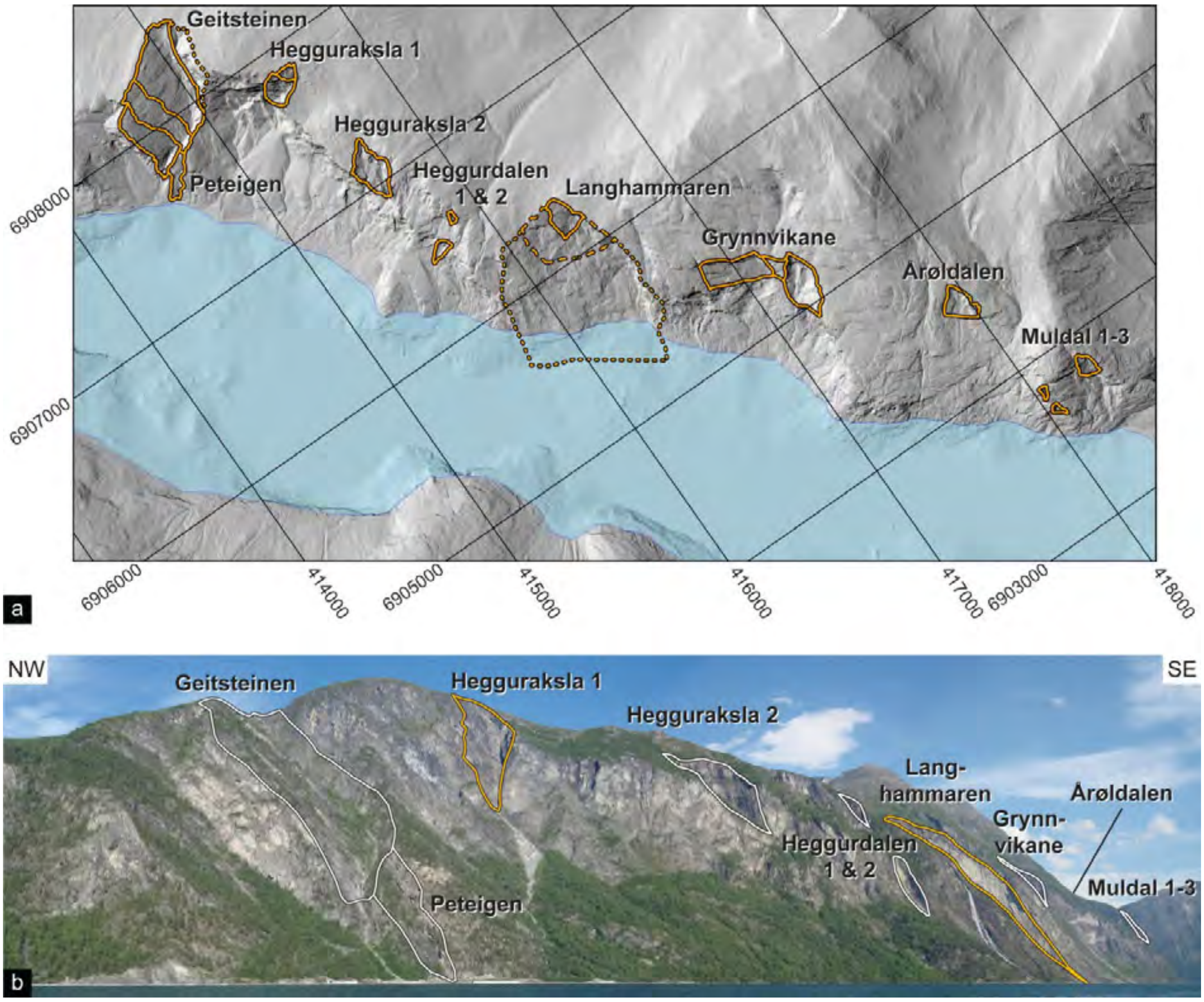

Figure 160: a) Map of the 14 rockslide scars in the Tafjord study area; b) Panorama picture of the study area showing the main rockslide scars (Oppikofer et al. in prep.).

9.5 Back-analysis of the 1756 Tjellefonna rockslide, Langfjord

The back-analysis of the 1756 Tjellefonna rockslide was made by G. Sandøy in a MSc thesis at NTNU in collaboration with NGU and under T. Oppikofer's co-supervision (Sandøy 2012):

On 22 February 1756 the largest historically recorded rockslide in Norway took place at Tjelle in Langfjord. Three displacement waves of up to 50 m were created in Langfjord by the impact of the failed rock mass constituting the Tjellefonna rockslide. A total of 32 people were killed, and 168 houses and 196 boats around the fjord were destroyed.

This MSc thesis focuses on a back-analysis of the Tjellefonna rockslide. The ante-rockslide topography (ART) is reconstructed and a detailed volume calculation of the rockslide is carried out using two modern techniques: the Slope Local Base Level (SLBL) and a manual ART reconstruction in the PolyWorks® software (InnovMetric 2013). The reconstructed topography is then used in the Phase^2 numerical modelling software (Rocscience 2013) for a detailed study of the parameters and trigger factors that affected the slope stability.

The volume of the deposits (on- and offshore) is calculated to be around 11.5 million m^3, giving an initial volume of the rockslide between 9 and 10 million m^3. Only one third of the total rockslide volume impacted the fjord. This new volume estimation of the Tjellefonna rockslide is less than the earlier calculations of 12 to 15 million m^3 (Furseth 2006), and could have consequences for previous rockslide-generated tsunami modelling, which used these larger volumes as input parameter.

The Phase^2 analyses include shear strength reduction investigations and parameter sensitivity tests. It is demonstrated that the failure of the Tjellefonna slope might have required strain softening in combination with triggering factors, where high groundwater is an essential feature. Earthquake, on the other hand, is ruled out as a triggering factor. Additionally, the analyses show that a shallow-dipping structure is critical in order to induce slope instability. This could be represented either by a joint set or an observed sub-horizontal fault. Fieldwork and modelling indicates that the fault is the most important to reduce slope stability.

The sliding surface has been evaluated using the Phase^2 and SLBL results. It is concluded that the Tjellefonna rockslide was not lying on a uniform plane, but on a complex surface made of joints, faults, foliation and intact rock bridges (Figure 161). Moreover, it is obvious that the Tjellefonna failure was closely related to the tectonic deformation of the rocks in this area. The failure was likely also a consequence of progressive accumulation of rock weakening (strain softening), acting to degrade the equilibrium state of the slope. This could have generated a hillside creep explaining the growing tension cracks observed at the present crown prior to the rockslide.

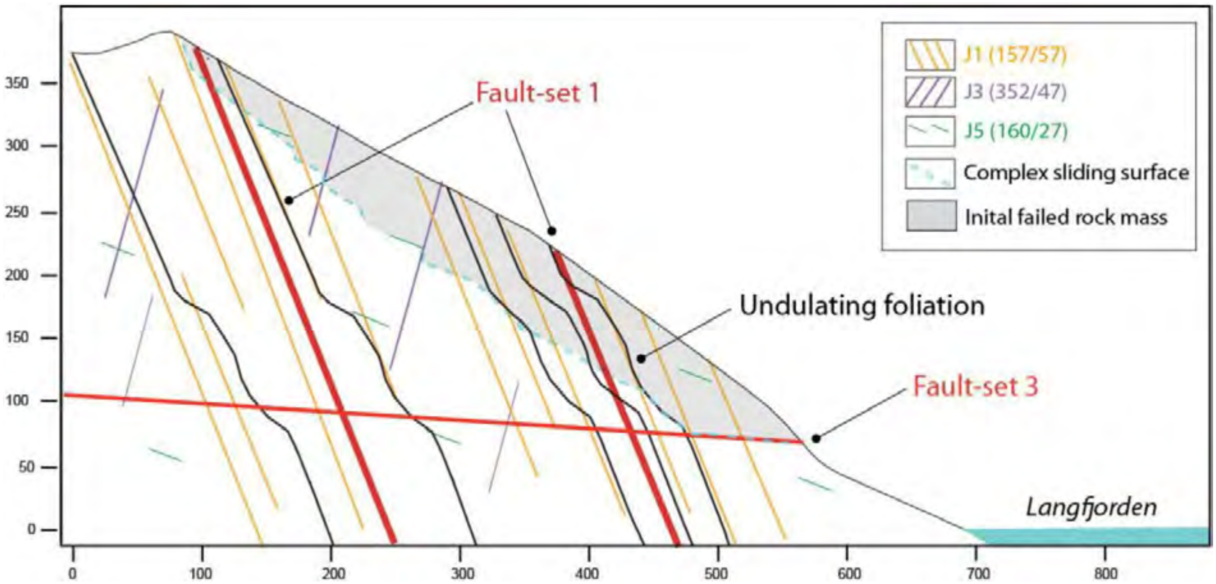

Figure 161: Conceptual model of the Tjellefonna rockslide based on fieldwork and numerical modelling results (Sandøy 2012).

9.6 Cosmogenic nuclide dating of sliding surfaces, rockslide scars and rock avalanche deposits

Results from terrestrial cosmogenic nuclide dating of sliding surfaces, scars and rock avalanche deposits, which are related to unstable rock slopes described in the present report, can be found in the corresponding sections:

- Alstadfjellet: rock avalanche deposits (p. 83)
- Flatmark: rock avalanche deposits (p. 68)
- Fremste Blåhornet: rock avalanche scar (p. 99)
- Ivasnasen: sliding surface, rock avalanche scar and deposits (p. 37)
- Kallen: rock avalanche deposits (p. 87)
- Kjøtåfjellet: rock avalanche deposits (p. 61)
- Mannen: sliding surface (p. 72)
- Nokkenibba 2: rock avalanche scar (p. 103)
- Oppstadhornet: sliding surface (p. 54)
- Skorgeurda: rock avalanche deposits (p. 133)
- Storehornet: sliding surface, rock avalanche scar and deposits (p. 117)
- Svarttinden: rock avalanche deposits (p. 77)
- Veten: rock avalanche deposits (p. 79)

Two other datings of past rock slope failures are available. They are not linked to any registered unstable or potential unstable rock slopes in Møre og Romsdal County:

- The Nakkeneset rock avalanche scar on the southern side of Geirangerfjord was sampled at two locations for cosmogenic nuclide dating giving an average age of 6700 ± 900 years. This age is in agreement with the age of the related rock avalanche deposits in the fjord, which are dated to 5000–8000 years BP (Longva et al. 2009).
- Two samples of the rock avalanche deposits at Sætra in Eikesdalen Valley were dated to 11'400 ± 1400 years BP using cosmogenic nuclide dating. The source area of this rock avalanche is not exactly known, but is likely located on the northeast-facing slopes of Seteraksla.

10. RECOMMENDATIONS FOR FUTURE WORK

The current status of investigations of unstable rock slopes in Møre og Romsdal County is presented in chapters 4 to 8. Based on the recommendations in the site descriptions in this report a list with recommended site investigations is proposed (Figure 162, Table 2). Note that not relevant sites (standard recommendation #1) and potential unstable rock slopes (standard recommendation #2) will not be classified in terms of hazard and risk and do therefore not require further investigations. These sites are thus not included in Figure 162 and Table 2.

Recommended measurement intervals for unstable rock slopes that are currently measured periodically by dGNSS, TLS or tape extensometer are given in Figure 163 and Table 3.

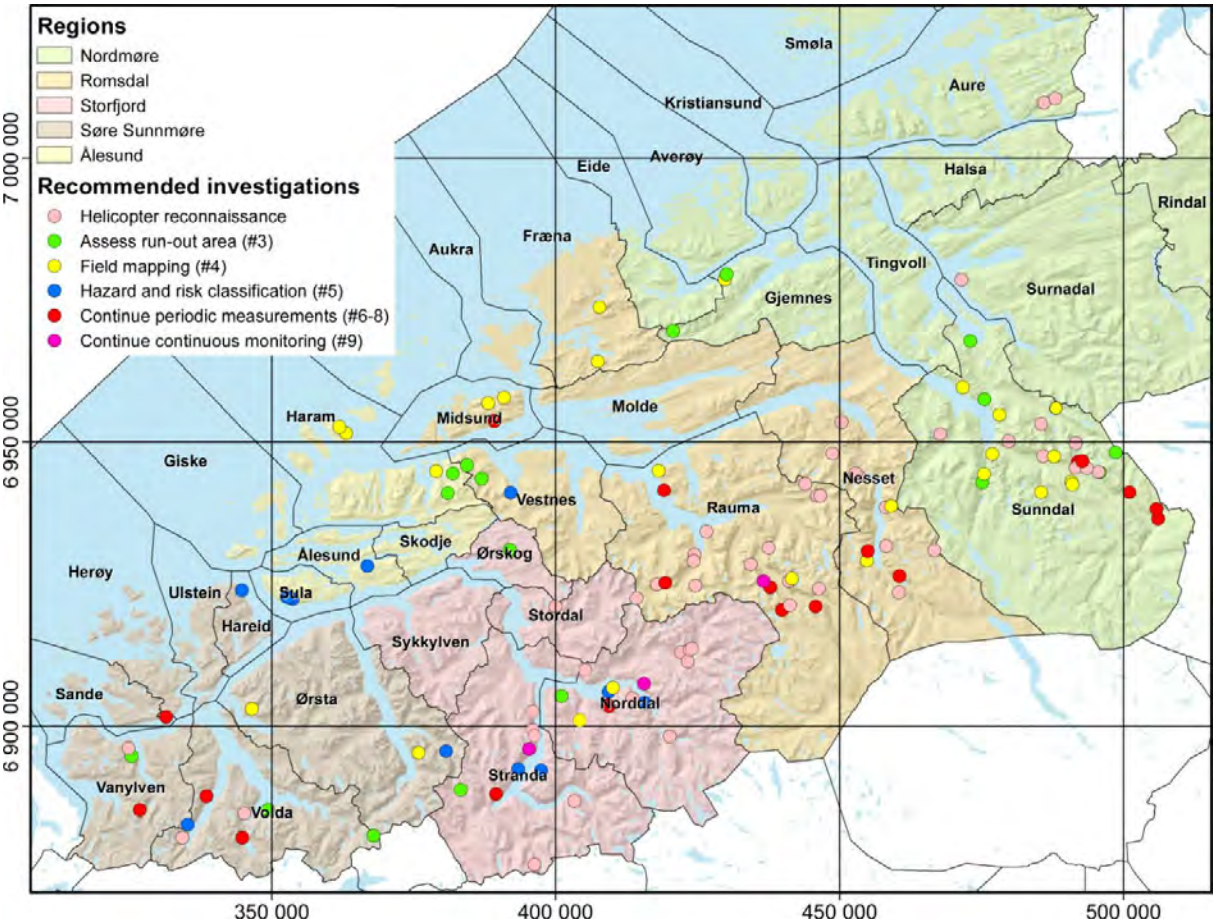

Figure 162: Map of unstable rock slopes in Møre og Romsdal County with recommended investigations and analyses. Note: not relevant sites (standard recommendation #1) and potential unstable rock slopes (standard recommendation #2) are not shown in this map; sites not described in this report are shown according to recommended investigations in Appendix 3.

Recommendations for future investigations can be grouped into following classes according to the standard recommendations in chapter 2.1.2 and Figure 1:

- Continuously monitored unstable rock slopes (3 sites in Møre og Romsdal): continue continuous monitoring (standard recommendation #9);
- Periodically measured unstable rock slopes with significant displacements (4 sites): continue periodic displacement measurements with 1–3 years interval and make the final hazard and risk classification (standard recommendation #8);
- Periodically measured unstable rock slopes without significant displacements (9 sites): continue periodic displacement measurements with 3–5 years interval and make the final hazard and risk classification (standard recommendation #7)

- Periodically measured unstable rock slopes with unknown displacements (7 sites): perform repetitive measurement within 1–3 years and make the final hazard and risk classification (standard recommendation #6);
- Mapped unstable rock slopes (12 sites): make the preliminary hazard and risk classification (standard recommendation #5);
- Reconnoitred unstable rock slopes with consequences (26 sites): make field mapping and thereafter the preliminary hazard and risk classification (standard recommendation #4);
- Reconnoitred unstable rock slopes without consequences (16 sites): assess the potential run-out area and make thereafter the preliminary hazard and risk classification (standard recommendation #3);
- Potential unstable rock slopes (28 sites): no further investigations or displacement measurements are necessary and the hazard and risk classification will not be made, but the sites should be revisited after some years or decades (standard recommendation #2). Amongst these potential unstable rock slopes are also 6 sites that were previously measured periodically with dGNSS;
- Not relevant sites (92): no further investigations or periodic displacement measurements are necessary and the hazard and risk classification will not be made (standard recommendation #1). Amongst these not relevant sites are also 2 sites that were previously measured periodically with dGNSS or TLS;
- Not investigated sites (48): helicopter reconnaissance is recommended to assess the relevance of the site and necessity for field mapping. Amongst these not investigated sites are also 5 sites that were previously reconnoitred, but where a new helicopter reconnaissance is recommended.

Recommendations for further investigations and periodic displacement measurements given in this report are preliminary. Final recommendations will be made in the next years based on the systematic hazard and risk classification system for large unstable rock slopes in Norway (Hermanns et al. 2012) and a forthcoming NVE document describing the implications of the risk classification related to the low-, medium- and high-risk classes.

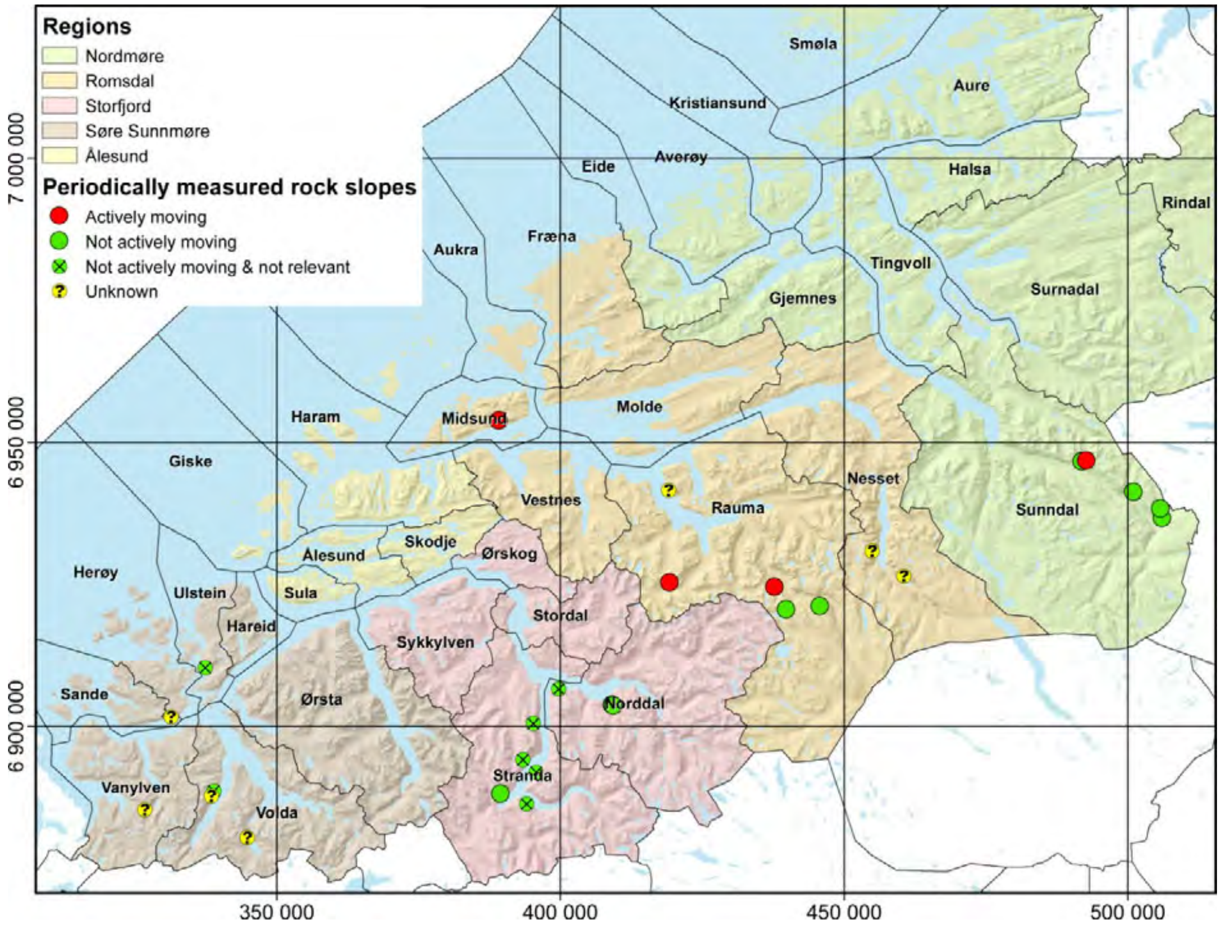

Figure 163: **Map of the 28 periodically measured unstable rock slopes in Møre og Romsdal with state of activity: actively moving = measured displacement rates are significant (4 sites); not actively moving = measured displacement rates are not significant (9 sites); unknown = no repetitive measurements made up to now (7 sites); not actively moving & not relevant = periodic displacement measurements should not be continued because the sites are no longer classified as unstable rock slopes (8 sites).**

Table 2: **Recommended investigations and analyses on unstable rock slopes. See Appendix 3 for recommendations on sites not described in this report.**

Site name	Investigation status	Recommended investigations (standard recommendation)
Nordmøre region		
Gjemnes municipality		
Geitaskaret	Reconnaissance	Assess run-out area (#3)
Trolldalsfjellet	Reconnaissance	Assess run-out area (#3)
Ørnstolen	Reconnaissance	Field mapping (#4)
Sunndal municipality		
Fulånebba	Reconnaissance	Field mapping (#4)
Gammelseterhaugen	Reconnaissance	Assess run-out area (#3)
Gikling 1	Periodic measurements	Continue periodic displacement measurements (#8)
Gikling 2	Periodic measurements	Continue periodic displacement measurements (#7)
Gjersvollsetra	Reconnaissance	Assess run-out area (#3)
Gråhøa 1	Simple mapping	Field mapping (#4)
Gråhøa 2	Reconnaissance	Field mapping (#4)
Ivasnasen	Periodic measurements	Continue periodic displacement measurements (#7)
Merrakammen	Reconnaissance	Field mapping (#4)
Ottdalskammen	Reconnaissance	Assess run-out area (#3)
Ottem 3	Periodic measurements	Continue periodic displacement measurements (#7)
Serkjenebba	Reconnaissance	Field mapping (#4)
Storbotnen	Simple mapping	Field mapping (#4)
Storurhamran	Simple mapping	Assess run-out area (#3)
Vollan	Periodic measurements	Continue periodic displacement measurements (#7)
Romsdal region		
Fræna municipality		
Røssholfjellet	Reconnaissance	Field mapping (#4)
Talstadhesten	Reconnaissance	Field mapping (#4)
Midsund municipality		
Bendsethornet	Reconnaissance	Field mapping (#4)
Oppstadhornet	Periodic measurements	Continue periodic displacement measurements (#8)
Ræstadhornet	Reconnaissance	Field mapping (#4)
Nesset municipality		
Evelsfonnhøa	Periodic measurements	Continue periodic displacement measurements (#6)
Kjøtåfjellet	Periodic measurements	Continue periodic displacement measurements (#6)
Litleaksla	Reconnaissance	New helicopter reconnaissance
Martinskora	Reconnaissance	Field mapping (#4)
Vikesoksa	Reconnaissance	Field mapping (#4)
Rauma municipality		
Børa	Periodic measurements	Continue periodic displacement measurements (#8)
Flatmark	Periodic measurements	Continue periodic displacement measurements (#7)
Kvarvesnippen	Reconnaissance	Field mapping (#4)
Kvitfjellgjølet	Periodic measurements	Continue periodic displacement measurements (#6)
Mannen	Continuous monitoring	Continue continuous monitoring (#9)
Marsteinskora 1	Reconnaissance	Field mapping (#4)
Middagstinden	Periodic measurements	Continue periodic displacement measurements (#8)
Svarttinden	Periodic measurements	Continue periodic displacement measurements (#7)
Trolltindan	Reconnaissance	New helicopter reconnaissance
Vestnes municipality		
Seteraksla	Reconnaissance	Assess run-out area (#3)
Snaufjellet	Reconnaissance	Assess run-out area (#3)
Strandastolen	Reconnaissance	Make hazard & risk classification (#5)
Storfjord region		
Norddal municipality		
Alstadfjellet	Simple mapping	New helicopter reconnaissance
Hegguraksla	Continuous monitoring	Continue continuous monitoring (#9)
Kilstiheia	Reconnaissance	Field mapping (#4)
Kleivahammaren	Reconnaissance	Field mapping (#4)
Kvitfjellet 1	Periodic measurements	Continue periodic displacement measurements (#7)
Kvitfjellet 2	Periodic measurements	Continue periodic displacement measurements (#7)

Table 2: Recommended investigations and analyses on unstable rock slopes. See Appendix 3 for recommendations on sites not described in this report.

Site name	Investigation status	Recommended investigations (standard recommendation)
Stranda municipality		
Aksla	Simple mapping	Make hazard & risk classification (#5)
Fivelstadnibba	Reconnaissance	Assess run-out area (#3)
Rindalseggene	Periodic measurements	Continue periodic displacement measurements (#7)
Åknes	Continuous monitoring	Continue continuous monitoring (#9)
Ørskog municipality		
Giskemonibba	Reconnaissance	Assess run-out area (#3)
Søre Sunnmøre region		
Hareid municipality		
Grøthornet	Simple mapping	Make hazard & risk classification (#5)
Sande municipality		
Laupsnipa	Periodic measurements	Continue periodic displacement measurements (#6)
Vanylven municipality		
Sandfjellet	Reconnaissance	Helicopter reconnaissance
Sandnestua	Reconnaissance	Assess run-out area (#3)
Storehornet	Periodic measurements	Continue periodic displacement measurements (#6)
Volda municipality		
Bjørnasethornet	Reconnaissance	Assess run-out area (#3)
Kvanndalsskåla	Simple mapping	Make hazard & risk classification (#5)
Kvivsdalshornet	Reconnaissance	Assess run-out area (#3)
Skylefjellet	Periodic measurements	Continue periodic displacement measurements (#6)
Solahylla	Periodic measurements	Continue periodic displacement measurements (#6)
Ørsta municipality		
Jakta	Reconnaissance	Field mapping (#4)
Keipen	Simple mapping	Make hazard & risk classification (#5)
Skorgeurda	Reconnaissance	Field mapping (#4)
Ålesund region		
Haram municipality		
Branddalsryggen	Reconnaissance	Field mapping (#4)
Byrkjevollhornet	Reconnaissance	Assess run-out area (#3)
Hellenakken	Reconnaissance	Field mapping (#4)
Otrefjellet	Reconnaissance	Assess run-out area (#3)
Skulen	Reconnaissance	Field mapping (#4)
Sula municipality		
Tverrfjellet 1	Simple mapping	Make hazard & risk classification (#5)
Tverrfjellet 2	Simple mapping	Make hazard & risk classification (#5)
Tverrfjellet 3	Simple mapping	Make hazard & risk classification (#5)
Ålesund municipality		
Rambjøra	Simple mapping	Make hazard & risk classification (#5)

Table 3: Periodically measured unstable rock slopes with recommended measurement intervals.

Site name	Measurement technique	Measurements First	Measurements Last	Recommended measurement interval
Nordmøre region				
Sunndal municipality				
Gikling 1 & 2	dGNSS	2007	2011	1–3 years, extend measurement network
Ivasnasen	TLS	2010	2012	3–5 years
	Tape extensometer	2010	2011	
Ottem 2	TLS	2010	-	Periodic measurements not to be continued
Ottem 3	dGNSS	2008	2009	3–5 years
	TLS	2011	-	
Vollan	dGNSS	2008	2011	3–5 years
Romsdal region				
Midsund municipality				
Oppstadhornet	dGNSS	2003	2011	1–3 years
Nesset municipality				
Evelsfonnhøa	TLS	2012	-	First repetitive measurement within 1–3 years
Kjøtåfjellet	TLS	2012	-	First repetitive measurement within 1–3 years
	Tape extensometer	2011	-	
Rauma municipality				
Børa	dGNSS	2003	2012	1–3 years
	TLS	2008	2012	
Flatmark	dGNSS	2006	2011	3–5 years
	TLS	2007	2012	
Kvitfjellgjølet	TLS	2012	-	First repetitive measurement within 1–3 years
Middagstinden	dGNSS	2008	2011	1–3 years, extend measurement network
	TLS	2010	2012	
Svarttinden	dGNSS	2005	2010	3–5 years
	TLS	2006	-	
Storfjord region				
Norddal municipality				
Kvitfjellet 1 & 2	dGNSS	2005	2011	3–5 years
	TLS	2006	2012	
Skrednakken 1	dGNSS	2006	2012	Periodic measurements not to be continued
Stranda municipality				
Fremste Blåhornet	dGNSS	2005	2009	Periodic measurements not to be continued
Furneset	dGNSS	2006	2007	Periodic measurements not to be continued
Herdalsnibba	dGNSS	2006	2012	Periodic measurements not to be continued
Nokkenibba 2	dGNSS	2006	2010	Periodic measurements not to be continued
Rindalseggene	dGNSS	2005	2012	3–5 years
	TLS	2006	2011	
Søre Sunnmøre region				
Sande municipality				
Laupsnipa	TLS	2012	-	First repetitive measurement within 1–3 years
	Tape extensometer	2012	-	
Ulstein municipality				
Haddalura	dGNSS	2005	2009	Periodic measurements not to be continued
Vanylven municipality				
Storehornet	dGNSS	2012	-	First repetitive measurement within 1–3 years
	TLS	2012	-	
	Tape extensometer	2012	-	
Volda municipality				
Hestefjellet	TLS	2012	-	Periodic measurements not to be continued
Skylefjellet	TLS	2012	-	First repetitive measurement within 1–3 years
Solahylla	TLS	2012	-	First repetitive measurement within 1–3 years

11. CONCLUSIONS & PERSPECTIVES

In the past years (2006-2012) NGU has worked on 131 unstable or potential unstable rock slopes in Møre og Romsdal County. Helicopter reconnaissance flights were made in Eikesdalen and Romsdalen Valleys, Romsdalsfjord, Søre Sunnmøre region and the coastal region between Ålesund and Molde to get an overview over unstable rock slopes in these previously uninvestigated areas. Field mapping was done on several unstable rock slopes in these areas, along with other sites in Storfjord region and Sunndal municipality. Many of the investigated unstable rock slopes are complex in terms of deformation style and deformation mechanism. Often an unstable rock slope can be divided into several compartments, which need to be assessed individually as a possible failure scenario within the hazard and risk classification system.

At 28 unstable rock slopes periodical displacement measurements are made by NGU using differential Global Navigation Satellite Systems, terrestrial laser scanning and tape extensometers. Three unstable rock slopes (Åknes, Hegguraksla and Mannen) are continuously monitored by the Åknes/Tafjord Early-Warning Centre. In addition to Åknes and Mannen do NGU's periodic measurements shows significant displacements on four unstable rock slopes (Børa, Gikling, Middagstinden, Oppstadhornet) with displacement rates ranging from 0.1 to 2.4 cm/year. Other periodically measured sites have either no significant displacements measured over several years (16 sites) or displacements are unknown as periodic measurements were only initiated in 2012 and no repetitive measurements are made up to now (8 sites). According to the recommendations given in this report, periodic measurements should not be continued at 8 sites because they are no longer classified as unstable rock slopes.

The age of eight rock avalanche deposits, three rockslide scars and one sliding surface was determined using terrestrial cosmogenic nuclide dating, providing important information about the timing of rock slope failures and long-term displacement rates of actively moving unstable rock slopes: seven out of twelve dated rockslides and rock avalanches initiated respectively occurred shortly after the last glaciation period with ages older or around 10'000 years BP.

The work plan for investigations and analyses in the next years will mainly be based on the recommendations given in this report and on the hazard and risk classification system for large unstable rock slopes in Norway. The main purpose of field investigations in the next years is the collection of data necessary for this hazard and risk classification according to NGUs mapping approach (see chapter 2.1). Highest priority will thereby be given to areas with high potential consequences and therefore on unstable rock slopes located above water bodies or densely populated areas. Additionally, the work plan will also depend on the schedule of periodic displacement measurements.

New InSAR data acquired since 2009 with the Radarsat-2 satellite over the entire Møre or Romsdal County and with the TerraSAR-X satellite over parts of Møre og Romsdal have a better resolution and better capability of obtaining coherent data even on vegetated slopes than the historical dataset of the ERS satellites. By the end of 2012 a sufficient amount of satellite scenes have been acquired and data processing and quality control is going on in spring 2013. It is possible that these new InSAR data will indicate displacements on some of the known unstable rock slopes, but also highlight currently unknown unstable rock slopes. New investigations will probably become necessary in light of these new data.

ACKNOWLEDGEMENTS

The authors would like to thank M. Böhme, H. Bunkholt, L. Fischer, I. Henderson, T. Redfield and F.X. Yugsi Molina from the Geological Survey of Norway for assistance with field work and fruitful discussions. G.M. Dreiås, T.Ø. Farsund and G. Sandøy from NTNU and I. Krieger and M. Schleier from the University of Erlangen are acknowledged for their valuable inputs and detailed studies on unstable rock slopes and rock avalanches as part of their MSc and PhD theses. The authors are grateful to C. Longchamp, F. Delasoie, D. Carrea, M.-H. Derron and M. Jaboyedoff from the University of Lausanne, Switzerland, for the processing and analysis of terrestrial laser scanning data.

REFERENCES

Anda, E. and Blikra, L.H. (1998) Rock-avalanche hazard in Møre og Romsdal, western Norway. *NGI Publication*, **203**, 53-59.

Anda, E., Blikra, L.H. and Braathen, A. (2002) The Berill Fault-first evidence of neotectonic faulting in southern Norway. *Norsk Geologisk Tidsskrift*, **82**, 3, 175-182.

Anda, E., Blikra, L.H. and Longva, O. (2000) Large-scale slope failures in Møre og Romsdal - Paleoseismic evidence? In: Dehls, J. and Olesen, O. (eds.) *NGU report 2000.01,* Geological Survey of Norway, Trondheim, Norway, pp. 20-20-25.

Balco, G., Stone, J.O., Lifton, N.A. and Dunai, T.J. (2008) A complete and easily accessible means of calculating surface exposure ages or erosion rates from 10Be and 26Al measurements. *Quaternary Geochronology,* **3**, 174-195.

Bhasin, R. and Kaynia, A.M. (2004) Static and dynamic simulation of a 700-m high rock slope in western Norway. *Engineering Geology*, **71**, 213-226.

Bigot-Cormier, F., Braucher, R., Bourlès, D., Guglielmi, Y., Dubar, M. and Stéphan, J.F. (2005) Chronological constraints on processes leading to large active landslides. *Earth and Planetary Science Letters*, **235**, 1-2, 141-150.

Blikra, L.H. (2008) The Åknes rockslide; monitoring, threshold values and early-warning. In: Chen, Z., Zhang, J., Li, Z., Wu, F. and Ho, K. (eds.) *Landslides and Engineered Slopes. From the Past to the Future - Proceedings of the 10th International Symposium on Landslides and Engineered Slopes, 30 June - 4 July 2008, Xi'an, China*, Taylor & Francis Group, London, pp. 1089-1094.

Blikra, L.H. (1994) Postglacial colluvium in western Norway. Sedimentology, geomorphology and palaeoclimatic record. PhD thesis, Geological Institute, University of Bergen, Bergen, Norway.

Blikra, L.H., Anda, E., Høst, J. and Longva, O. (2006) Åknes/Tafjord-prosjektet: Sannsynlighet og risiko knyttet til fjellskred og flodbølger fra Åknes og Hegguraksla. NGU report 2006.039, Geological Survey of Norway, Trondheim, Norway.

Blikra, L.H., Braathen, A., Anda, E., Stalsberg, K. and Longva, O. (2002a) Rock avalanches, gravitational bedrock fractures and neotectonic faults onshore northern West Norway: Examples, regional distribution and triggering mechanisms. NGU report 2002.016, Geological Survey of Norway, Trondheim, Norway.

Blikra, L.H., Braathen, A. and Skurtveit, E. (2002b) Hazard evaluation of rock avalanches; the Baraldsnes - Oterøya area. NGU report 2001.108, Geological Survey of Norway, Trondheim, Norway.

Blikra, L.H., Longva, O., Braathen, A., Anda, E., Dehls, J.F. and Stalsberg, K. (2006) Rock Slope Failures in Norwegian Fjord Areas: Examples, Spatial Distribution and Temporal Pattern. In: Evans, S.G., Scarascia Mugnozza, G., Strom, A. and Hermanns, R.L. (eds.) *Landslides from Massive Rock Slope Failure; NATO Science Series, IV. Earth and Environmental Sciences, Vol 49.* Springer, Dodrecht, Netherlands, pp. 475-496.

Blikra, L.H. and Nemec, W. (1998) Postglacial colluvium in western Norway: depositional processes, facies and palaeoclimatic record. *Sedimentology*, **45**, 909-959.

Böhme, M., Hermanns, R.L., Oppikofer, T., Fischer, L., Bunkholt, H.S.S., Eiken, T., Pedrazzini, A., Derron, M.-H., Jaboyedoff, M., Blikra, L.H. and Nilsen, B. (2013) Analyzing complex rock slope deformation at Stampa, western Norway, by integrating geomorphology, kinematics and numerical modeling. *Engineering Geology*, **154**, 116-130.

Braathen, A., Blikra, L.H., Berg, S.S. and Karlsen, F. (2004) Rock-slope failure in Norway; type, geometry, deformation mechanisms and stability. *Norwegian Journal of Geology*, **84**, 1, 67-88.

Bungum, H., Lindholm, C.D., Dahle, A., Woo, G., Nadim, F., Holme, J.K., Gudmestad, O.T., Hagberg, T. og Karthigeyan, K. (2000) New seismic zoning maps for Norway, the Northe Sea and the UK. *Seismological Research Letters*, **71**, 687-697.

Bunkholt, H., Osmundsen, P.T., Redfield, T.F., Oppikofer, T., Eiken, T., L'Heureux, J.-S., Hermanns, R.L. and Lauknes, T.R. (2011) ROS Fjellskred i Troms: status og analyser etter feltarbeid 2010. NGU report 2011.031, Geological Survey of Norway, Trondheim, Norway.

Bunkholt, H., Otterå, S., Yugsi Molina, F.X., Hermanns, R.L., Dehls, J.F., Osmundsen, P.T., Redfield, T.F. and Eiken, T. (2013) Undersøkelser av ustabile eller potensielt ustabile fjellpartier i Troms – status og planer etter feltarbeid 2011 og 2012. NGU report 2013.021, Geological Survey of Norway, Trondheim, Norway.

Dahle, H. (2004) Analyse av skråningsstabilitet for Oppstadhornet. MSc thesis, Norwegian University of Science and Technology, Trondheim, Norway.

Dahle, H., Anda, E., Sætre, S., Saintot, A., Hermanns, R.L. and Oppikofer, T. (2011a) Risiko- og sårbarheitsanalyse for fjellskred i Møre og Romsdal - FylkesROS-fjellskred. Fylkesmannen i Møre og Romsdal, Møre og Romsdal Fylkeskommune, Geological Survey of Norway, Molde, Norway.

Dahle, H., Anda, E., Saintot, A. and Sætre, S. (2008) Faren for fjellskred fra fjellet Mannen i Romsdalen. NGU report 2008.087, Geological Survey of Norway, Trondheim, Norway.

Dahle, H., Bjerke, P.L., Crosta, G.B., Hermanns, R.L., Anda, E. and Saintot, A. (2011b) Faresoner for utløp, oppdemming og flom som følge av fjellskredfare ved Mannen. NGU report 2011.058, Geological Survey of Norway, Trondheim, Norway.

Dahle, H., Saintot, A., Blikra, L.H. and Anda, E. (2011c) Geofagleg oppfølging av ustabilt fjellparti ved Mannen i Romsdalen. NGU report 2010.022, Geological Survey of Norway, Trondheim, Norway.

Dalsegg, E., Elvebakk, H. and Tønnesen, J.F. (2007) Geofysiske målinger Oppstadhornet, Midsund kommune, Møre og Romsdal. NGU report 2006.012, Geological Survey of Norway, Trondheim, Norway.

Dalsegg, E. and Rønning, J.S. (2012) Geofysiske målinger på Mannen i Rauma kommune, Møre og Romsdal. NGU report 2012.024, Geological Survey of Norway, Trondheim, Norway.

Dalsegg, E., Rønning, J.S., Tønnesen, J.F., Saintot, A. and Ganerød, G.V. (2010) Geologisk og geofysisk kartlegging av Gikling, et ustabilt fjellparti i Sunndalen, Møre og Romsdal. NGU report 2010.050, Geological Survey of Norway, Trondheim, Norway.

Dalsegg, E. and Tønnesen, J.F. (2004) Geofysiske målinger Breitind og Børa, Rauma kommune, Møre og Romsdal. NGU report 2004.008, Geological Survey of Norway, Trondheim, Norway.

Dehls, J., Fischer, L., Böhme, M., Saintot, A., Hermanns, R.L., Oppikofer, T., Lauknes, T.R., Larsen, Y. and Blikra, L.H. (2012) Landslide monitoring in western Norway using high resolution TerraSAR-X and Radarsat-2 InSAR. In: Eberhardt, E., Froese, C., Turner, A.K. and Leroueil, S. (eds.) *Landslides and Engineered Slopes: Protecting Society through Improved Understanding*, Taylor & Francis Group, London, pp. 1321-1325.

Derron, M.-H., Blikra, L.H. and Jaboyedoff, M. (2005a) High resolution digital elevation model analysis for landslide hazard assessment (Åkerneset, Norway). In: Senneset, K., Flaate, K. and Larsen, J.O. (eds.) *Landslides and Avalanches: ICFL 2005 Norway,* Taylor & Francis Group, London, pp. 101-106.

Derron, M.-H., Jaboyedoff, M. and Blikra, L.H. (2005b) Preliminary assessment of rockslide and rockfall hazards using a DEM (Oppstadhornet, Norway). *Natural Hazards and Earth System Sciences,* **5**, 2, 285-292.

Devoli, G., Eikenæs, O., Taurisano, A., Hermanns, R.L., Fischer, L., Oppikofer, T. and Bunkholt, H. (2011) Plan for skredfarekartlegging - Delrapport steinsprang, steinskred og fjellskred. NVE rapport 15/2011, Norges vassdrags- og energidirektorat, Oslo, Norway.

Dreiås, G.M. (2012) Engineering geological assessment and structural comparison of the Vollan and Ivasnasen rock slopes in Sunndalen, Norway. MSc thesis, Norwegian University of Science and Technology, Trondheim, Norway.

Eidsvig, U. and Harbitz, C.B. (2005) Åknes/Tafjord prosjektet. Innledende numeriske analyser av flodbølger som følge av mulige skred fra Åkneset. Norges Geotekniske Institutt.

Eidsvig, U.M., Medina-Cetina, Z., Kveldsvik, V., Glimsdal, S., Harbitz, C.B. and Sandersen, F. (2011) Risk assessment of a tsunamigenic rockslide at Åknes. *Natural Hazards,* **56**, 2, 529-545.

Eiken, T. (2012) Rapport om deformasjonsmålingar i potensielle fjellskred - Møre og Romsdal 2011. Technical report, Department of Geosciences, University of Oslo, Oslo, Norway.

Elvebakk, H. (2012) Borhullslogging med optisk televiewer KH-02-11, Mannen, Rauma kommune, Møre og Romsdal. NGU report 2012.032, Geological Survey of Norway, Trondheim, Norway.

Elvebakk, H. (2008) Borehullslogging, Åknes, Stranda kommune. NGU report 2008.030, Geological Survey of Norway, Trondheim, Norway.

Elvebakk, H. and Blikra, L.H. (1999) Georadarundersøkelser i forbindelse med undersøkelser av fjellskred i Romsdalen, Møre og Romsdal. NGU report 1999.025, Geological Survey of Norway, Trondheim, Norway.

Farsund, T.Ø. (2011) Geological and numerical stability modelling of Mannen, Romsdalen. MSc thesis, Norwegian University of Science and Technology, Trondheim, Norway.

Farsund, T.Ø. (2010) Geology, DEM analysis and geohazard assessment of the Romsdalen valley. Project thesis, Norwegian University of Science and Technology, Trondheim, Norway.

Fenton, C.R., Hermanns, R.L., Blikra, L.H., Kubik, P.W., Bryant, C., Niedermann, S., Meixner, A. and Goethals, M.M. (2011) Regional 10Be production rate calibration for the past 12 ka deduced from the radiocarbon-dated Grøtlandsura and Russenes rock avalanches at 69° N, Norway. *Quaternary Geochronology,* **6**, 5, 437-452.

Frei, C. (2008) Groundwater flow at the Åknes rockslide site (Norway): results of a multitracer test. MSc thesis, ETH Zürich, Zürich, Switzerland.

Furseth, A. (2009) *Dommedagsfjellet - Tafjordulykka 75 år etter,* Det Norske Samlaget, Oslo, Norway, 175 pp.

Furseth, A. (2006) *Skredulykker i Norge,* Tun Forlag, Oslo, Norway, 207 pp.

Ganerød, G.V. (2010) Structural mapping of the Åknes Rockslide, Stranda Municipality, Møre and Romsdal County, Western Norway. NGU report 2008.042, Geological Survey of Norway, Trondheim, Norway.

Ganerød, G.V. and Lutro, O. (2011) Berggrunnsgeologisk og strukturgeologisk kartlegging i forbindelse med prosjektet Fv. 659 Nordøyvegen, Møre og Romsdal. NGU report 2011.049, Geological Survey of Norway, Trondheim, Norway.

Ganerød, G.V., Grøneng, G., Aardal, I.B. and Kveldsvik, V. (2007) Logging of drill cores from seven boreholes at Åknes, Stranda municipality, Møre and Romsdal County. NGU report 2007.020, Geological Survey of Norway, Trondheim, Norway.

Ganerød, G.V., Grøneng, G., Rønning, J.S., Dalsegg, E., Elvebakk, H., Tønnesen, J.F., Kveldsvik, V., Eiken, T., Blikra, L.H. and Braathen, A. (2008) Geological model of the Åknes rockslide, western Norway. *Engineering Geology,* **102**, 1-2, 1-18.

Gosse, J.C. and Philips, F.M. (2001) Terrestrial in situ cosmogenic nuclides: theory and application. *Quaternary Science Reviews,* **20**, 1475-1560.

Grøneng, G., Lu, M., Nilsen, B. and Jenssen, A.K. (2010) Modelling of time-dependent behavior of the basal sliding surface of the Åknes rockslide area in western Norway. *Engineering Geology*, **114**, 3-4, 414-422.

Grøneng, G., Nilsen, B. and Sandven, R. (2009) Shear strength estimation for Åknes sliding area in western Norway. *International Journal of Rock Mechanics & Mining Sciences,* **46**, 479-488.

Heincke, B., Günther, T., Dalsegg, E., Rønning, J.S., Ganerød, G.V. and Elvebakk, H. (2010) Combined three-dimensional electric and seismic tomography study on the Åknes rockslide in western Norway. *Journal of Applied Geophysics*, **70**, 4, 292-306.

Henderson, I. and Saintot, A. (2007) Fjellskredundersøkelser i Møre og Romsdal. NGU report 2007.043, Geological Survey of Norway, Trondheim, Norway.

Henderson, I.H.C., Saintot, A. and Derron, M.-H. (2006) Structural mapping of potential rockslide sites in the Storfjorden area, western Norway: the influence of bedrock geology on hazard analysis. NGU report 2006.052, Geological Survey of Norway, Trondheim, Norway.

Hermanns, R.L., Fischer, L., Oppikofer, T., Böhme, M., Dehls, J.F., Henriksen, H., Booth, A.M., Eilertsen, R., Longva, O. and Eiken, T. (2011) Mapping of unstable and potentially unstable rock slopes in Sogn og Fjordane (work report 2008-2011). NGU report 2011.055, Geological Survey of Norway, Trondheim, Norway.

Hermanns, R.L., Niedermann, S., Ivy-Ochs, S. and Kubik, P.W. (2004) Rock avalanching into a landslide-dammed lake causing multiple dam failure in Las Conchas valley (NW Argentina) - evidence from surface exposure dating and stratigraphic analyses. *Landslides,* **1**, 2, 113-122.

Hermanns, R.L., Oppikofer, T., Anda, E., Berg, H., Blikra, L.H., Böhme, M., Bunkholt, H., Crosta, G.B., Dahle, H., Devoli, G., Eikenæs, O., Fischer, L., Jaboyedoff, M., Loew, S., Sætre, S. and Yugsi Molina, F.X. (2012) Classification system to propose mapping and monitoring effort on large unstable rock slopes in Norway. NGU report 2012.029, Geological Survey of Norway, Trondheim, Norway.

Hermanns, R.L., Oppikofer, T., Dahle, H., Blikra, L.H., Ivy-Ochs, S. and Eiken, T. (2013) Understanding long-term slope deformation for stability assessment of rock slopes: the case of the Oppstadhornet rockslide, Norway. In: Genevois, R. and Prestizini, A. (eds.) *International Conference Vajont, 1963-2013 - thoughts and analyses after 50 years since the catastrophic landslide*, Italian Journal of Engineering Geology and Environment, Book Series, **6**, 255-264.

Hermanns, R.L., Redfield, T.F., Bunkholt, H., Oppikofer, T., Fischer, L., Gosse, J. and Eiken, T. (2012) Cosmogenic nuclide dating of slow moving rockslides in Norway in order to assess long-term slide velocities. In: Eberhardt, E., Froese, C., Turner, A.K. and Leroueil, S. (eds.) *Landslides and Engineered Slopes: Protecting Society through Improved Understanding,* Taylor & Francis Group, London, pp. 849-854.

Hermanns, R.L., Niedermann, S., Garcia, A.V., Gomez, J.S. and Strecker, M.R. (2001) Neotectonics and catastrophic failure of mountain fronts in the southern intra-Andean Puna Plateau, Argentina. *Geology,* **29**, 7, 619-622.

Hoek, E. and Bray, J. (1981) *Rock Slope Engineering,* 3rd, E & FN Spon, London.

InnovMetric (2013) PolyWorks: 3D scanner and 3D digitizer software from InnovMetric Software Inc., http://www.innovmetric.com/polyworks/3D-scanners/home.aspx?lang=en, accessed 11.04.2013.

itmsoil (2012) Digital Tape Extensometer, itmsoil.com/pages/digital+tape+extensometer, accessed 1.11.2012.

Jaboyedoff, M., Oppikofer, T., Derron, M.-H., Blikra, L.H., Böhme, M. and Saintot, A. (2011) Complex landslide behaviour and structural control: a three-dimensional concep-

tual model of Åknes rockslide, Norway. *Geological Society, London, Special Publications,* **351**, 147-161.
Krieger, I., Hermanns, R.L., Schleier, M., Yugsi Molina, F.X., Oppikofer, T., Rønning, J.S., Eiken, T. and Rohn, J. (2013) The Berill fault and its relation to a deep-seated gravitational slope deformation (DSGSD). In: Genevois, R. and Prestizini, A. (eds.) *International Conference Vajont, 1963-2013 - thoughts and analyses after 50 years since the catastrophic landslide*, Italian Journal of Engineering Geology and Environment, Book Series, **6**, 265-273.
Kristensen, L. (2012) Feasibility study of GB radar measurements Kvitfjellet, Romsdalsfjorden, Møre og Romsdal. Åknes report 09.2012, Åknes/Tafjord Beredskap IKS, Stranda, Norway.
Kristensen, L. and Blikra, L.H. (2011) Monitoring displacement on the Mannen rockslide in Western Norway. In: Catani, F., Marggottini, C., Trigila, A. and Iadanza, C. (eds.) *Proceedings of the Second World Landslide Forum,* ISPRA - Italian National Institute for Environmental Protection and Research, Rome, Italy, pp. WLF2-2011-0381-WLF2-2011-0381.
Kristensen, L. and Blikra, L.H. (2010) Hegguraksla in Tafjorden: Monitoring and data analyses. Åknes report 04.2010, Åknes/Tafjord Early Warning Centre, Stranda, Norway.
Kristensen, L., Blikra, L.H. and Hole, J. (2010) Åknes: State of instrumentation and data analysis. Åknes report 02.2010, Åknes/Tafjord Early Warning Centre, Stranda, Norway.
Kveldsvik, V., Eiken, T., Ganerød, G.V., Grøneng, G. and Ragvin, N. (2006) Evaluation of movement data and ground conditions for the Åknes rock slide. *International Symposium on Stability of Rock Slopes in Open Pit Mining and Civil Engineering Situations, The South African Institute of Mining and Metallurgy,* , pp. 279-279-299.
Kveldsvik, V., Kaynia, A.M., Nadim, F., Bhasin, R., Nilsen, B. and Einstein, H.H. (2009a) Dynamic distinct-element analysis of the 800m high Åknes rock slope. *International Journal of Rock Mechanics and Mining Sciences,* **46**, 4, 686-698.
Kveldsvik, V., Einstein, H.H., Nilsen, B. and Blikra, L.H. (2009b) Numerical Analysis of the 650,000 m^2 Åknes Rock Slope based on Measured Displacements and Geotechnical Data. *Rock Mechanics and Rock Engineering,* **42**, 5, 689-728.
Kveldsvik, V., Nilsen, B., Einstein, H. and Nadim, F. (2008) Alternative approaches for analyses of a 100,000 m^3 rock slide based on Barton-Bandis shear strength criterion. *Landslides,* **5**, 2, 161-176.
Lacasse, S. (2008) Event tree analysis of Åknes rock slide hazard. *4th Canadian Conference on Geohazards : From Causes to Management,* Quebec, Canada, pp. 551-551-558.
Longva, O., Blikra, L.H. and Dehls, J. (2009) Rock avalanches - distribution and frequencies in the inner part of Storfjorden, Møre og Romsdal County, Norway. NGU report 2009.002, Geological Survey of Norway, Trondheim, Norway.
Lutro, O., Thorsnes, T. and Tveten, E. (1998) Bedrock map Ulsteinvik, 1:250 000, Geological Survey of Norway, Trondheim, Norway.
Nordvik, T. and Nyrnes, E. (2009) Statistical analysis of surface displacements -- an example from the Åknes rockslide, western Norway. *Natural Hazards and Earth System Sciences,* **9**, 3, 713-724.
Nordvik, T., Grøneng, G., Ganerød, G.V., Nilsen, B., Harding, C. and Blikra, L.H. (2009) Geovisualization, geometric modelling and volume estimation of the Åknes rockslide, Western Norway. *Bulletin of Engineering Geology and the Environment,* **68**, 2, 245-256.
Oppikofer, T. (2009) Detection, analysis and monitoring of slope movements by high-resolution digital elevation models. PhD thesis, Institute of Geomatics and Analysis of Risk, University of Lausanne, Lausanne, Switzerland.
Oppikofer, T., Bunkholt, H., Fischer, L., Saintot, A., Hermanns, R.L., Carrea, D., Longchamp, C., Derron, M.-H., Michoud, C. and Jaboyedoff, M. (2012a) Investigation and

monitoring of rock slope instabilities in Norway by terrestrial laser scanning. In: Eberhardt, E., Froese, C., Turner, A.K. and Leroueil, S. (eds.) *Landslides and Engineered Slopes: Protecting Society through Improved Understanding,* Taylor & Francis Group, London, pp. 1235-1241.

Oppikofer, T., Bunkholt, H., Ganerød, G.V. and Engvik, A.K. (2012b) Mannen unstable rock slope (Møre og Romsdal): Geological and engineering geological logging of drill core KH-02-11 & grain size distribution and XRD analysis of fine-grained breccia. NGU report 2012.036, Geological Survey of Norway, Trondheim, Norway.

Oppikofer, T. and Jaboyedoff, M. (2008) Åknes/Tafjord project: Analysis of ancient rockslide scars and potential instabilities in the Tafjord area & Laser scanner monitoring of instabilities at Hegguraksla. Technical report, Institute of Geomatics and Analysis of Risk, University of Lausanne, Lausanne, Switzerland.

Oppikofer, T., Jaboyedoff, M., Blikra, L.H. and Derron, M.-H. (2009) Characterization and monitoring of the Åknes rockslide using terrestrial laser scanning. *Natural Hazards and Earth System Sciences*, **9**, 3, 1003-1019.

Oppikofer, T., Jaboyedoff, M., Pedrazzini, A., Derron, M.-H. and Blikra, L.H. (2011) Detailed DEM analysis of a rockslide scar to improve the basal failure surface model of active rockslides. *Journal of Geophysical Research,* **116**, F02016.

Oppikofer, T., Jaboyedoff, M., Pedrazzini, A., Derron, M.-H. and Blikra, L.H. (in prep.) Assessing rockslide hazard in Tafjord (Norway): Part I – Past rockslides and rock avalanches. *Engineering Geology*.

Oppikofer, T., Saintot, A., Otterå, S., Sandøy, G., Hermanns, R.L., Anda, E., Dahle, H. and Eiken, T. (2013) Undersøkelser av ustabile fjellpartier i Møre og Romsdal – status og planer etter feltarbeid i 2012. NGU report 2013.053, Geological Survey of Norway, Trondheim, Norway.

Øydvin, E.K., Devoli, G., Bargel, T., Wiig, T., Taurisano, A., Berg, H., Eikenæs, O., Lyche, E., Fergus, T., Kvakland, M.R., Wasrud, J., Helle, T.E., Orvedal, K., Peereboom, I.O., Andersen, Ø.B., Hermanns, R.L., Høst, J., Hansen, L., Bunkholt, H., Eilertsen, R., Fischer, L., L'Heureux, J.-S., Oppikofer, T., Rubensdotter, L., Sletten, K., Solberg, I.-L. and Stalsberg, K. (2011) Plan for skredfarekartlegging - Status og prioriteringer innen oversiktskartlegging og detaljert skredfarekartlegging i NVEs regi. NVE rapport 14/2011, Norges vassdrags- og energidirektorat, Oslo, Norway.

Robinson, P., Tveten, E. and Blikra, L.H. (1997) A post-glacial bedrock failure at Oppstadhornet, Oteroya, More og Romsdal: a potential major rock avalanche. *NGU Bulletin,* **433**, 46-47.

Rocscience (2013) Phase2 8.0: Finite Element Analysis for Excavations and Slopes, http://www.rocscience.com/products/3/Phase2, accessed 11.04.2013.

Rønning, J.S., Dalsegg, E., Heincke, B.H. and Tønnesen, J.F. (2008) Geofysiske målinger på bakken ved Åknes og ved Hegguraksla, Stranda og Nordal kommuner, Møre og Romsdal. NGU report 2007.026, Geological Survey of Norway, Trondheim, Norway.

Rønning, J.S., Dalsegg, E., Elvebakk, H., Ganerød, G.V. and Tønnesen, J.F. (2006) Geofysiske målinger Åknes og Tafjord, Stranda og Nordal kommune, Møre og Romsdal. NGU report 2006.002, Geological Survey of Norway, Trondheim, Norway.

SafeLand (2010) Review of techniques for landslide detection, fast characterization, rapid mapping and long-term monitoring. SafeLand deliverable 4.1, Edited for the SafeLand European project by Michoud C., Abellán, A., Derron, M.-H. and Jaboyedoff, M., available at http://www.safeland-fp7.eu.

Saintot, A., Böhme, M., Redfield, T.F. and Dahle, H. (2008) Field studies of unstable slopes in Sunndalen Valley. NGU report 2008.049, Geological Survey of Norway, Trondheim, Norway.

Saintot, A., Elvebakk, H., Oppikofer, T., Ganerød, G.V. and Farsund, T.Ø. (2011a) Mannen unstable rock slope (Møre & Romsdal): Logging of borehole and drill core KH-01-10, geomorphologic digital elevation model interpretation & displacement analysis by terrestrial laser scanning. NGU report 2011.026, Geological Survey of Norway, Trondheim, Norway.

Saintot, A., Henderson, I.H.C. and Derron, M.-H. (2011b) Inheritance of ductile and brittle structures in the development of large rock slope instabilities: examples from western Norway. In: Jaboyedoff, M. (ed.) *Slope Tectonics*, , pp. 27-27-78.

Saintot, A., Oppikofer, T., Derron, M.-H. and Henderson, I. (2012) Large gravitational rock slope deformation in Romsdalen valley (Western Norway). *Revista de la Asociación Geológica Argentina*, **69**, 3, 354-371.

Sandøy, G. (2012) Back-analysis of the 1756 Tjellefonna rockslide, Langfjorden. MSc thesis, Norwegian University of Science and Technology, Trondheim, Norway.

Schleier, M., Hermanns, R.L. and Rohn, J. (2013) Spatial distribution or rockslide deposits and their morphological features suggest timing and paleo-environmental conditions for rock slope failurs in Innerdalen and Innfjorddalen, Møre og Romsdal County, Western Norway. In: Genevois, R. and Prestizini, A. (eds.) *International Conference Vajont, 1963-2013 - thoughts and analyses after 50 years since the catastrophic landslide*, Italian Journal of Engineering Geology and Environment, Book Series, **6**, 493-505.

Storrø, G. and Gaut, S. (2009) Sporstofforsøk på Akneset, Stranda kommune - Møre og Romsdal fylke. NGU report 2008.091, Geological Survey of Norway, Trondheim, Norway.

Svendsen, J.I. and Mangerud, J. (1987) Late Weichselian and holocene sea-level history for a cross-section of western Norway. *Journal of Quaternary Science*, **2**, 2, 113-132.

Terranum (2013) Coltop3D - LIDAR data processing and analyzing software for geologists, http://www.terranum.ch/coltop3d-features, accessed: 11.04.2013.

Tønnesen, J.F. (2009) Georadarmålinger ved Rønningen og Horgheim i Romsdalen for undersøkelse av løsmassetyper i dalbunnen under det ustabile fjellpartiet Mannen. NGU report 2009.062, Geological Survey of Norway, Trondheim, Norway.

Tveten, E., Lutro, O. and Thorsnes, T. (1998) Bedrock map Ålesund, 1:250 000, Geological Survey of Norway, Trondheim, Norway.

Wolden, K. (2005) Sakkyndig rapport. Skorgeura naturreservat, Ørsta kommune. NGU report 2005.056, Geological Survey of Norway, Trondheim, Norway.

Wyllie, D.C. and Mah, C.W. (2004) *Rock Slope Engineering: Civil and Mining*, Spon Press/Taylor & Francis Group, London and New York, 431 pp.

APPENDIXES

Appendix 1: Report on dGNSS displacement measurements in Møre og Romsdal

This appendix gives detailed results from periodic monitoring using dGNSS in Møre og Romsdal. It groups the yearly reports from Trond Eiken, University of Oslo, with the latest results for each of the unstable rock slopes monitored by dGNSS (in Norwegian).

Rapport

om

Deformasjonsmålingar i potensielle fjellskred

Møre og Romsdal
2007-2012

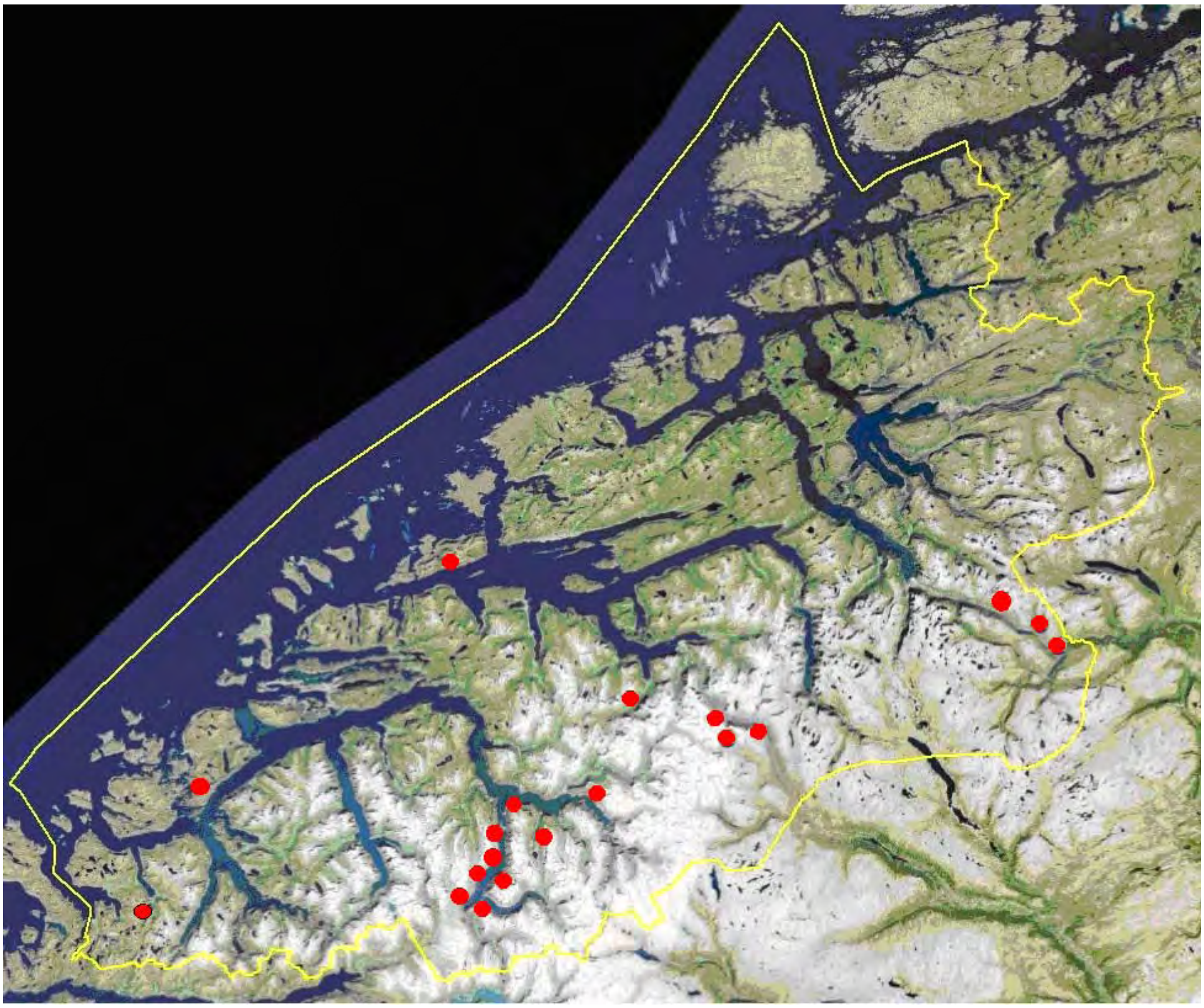

Trond Eiken
Institutt for geofag
Universitetet i Oslo

Innhald

Samandrag

Frå starten i 2003 og fram til i dag er det sett i gong måling av rørsle på lokalitetar for potensielle fjellskred i alt 20 stadar i Møre og Romsdal. Alle, med unntak av Storehornet der nye punkt vart sett ut i 2012, er målt to eller fleire gonger. Lokalitetane varierer mykje, frå to punkt til større nett med mange punkt. Presisjonen til resultata varierer difor ein del. På mange av lokalitetane er det små endringar i punkt som gir signifikante utslag i statistisk test, men overestimert presisjon i målemetoden tilseier at ein bør vere konservativ i tolking av resultat. Det er difor usikre konklusjonar når berre to, tre målingar ligg til grunn for endringar på nokre få millimeter, eller at ein ikkje har klare trendar i resultatet når fleire år vart lagt til grunn.

Resultata av målingane kan kort summerast opp til:

- På Børa er det relativt stor rørsle i to blokker, men og klare teikn til rørsle i fleire punkt når målingar over fleire år vert lagt til grunn.
- På Flatmark det ikkje klare teikn til endringar i punkta.
- På Fremste Blåhornet er det ikkje påvist signifikant endring i punkta.
- På Furneset er det ingen teikn til at punkta er i rørsle.
- På Gikling er det klare indikasjonar på endringar i to av punkta.
- I Haddalurda har mest truleg ingen punkt rørsle.
- I Hegguraksla er det teikn på rørsle i eitt punkt.
- På Herdalsnibba er det ikkje klare teikn til endringar i punkta.
- I Kvitfjellet er det ikkje klare teikn til endringar i punkta.
- På Mannen er det relativt stor rørsle i eitt punkt, både i plan og høgd.
- På Middagstinden er det klare teikn til rørsle i storleik cm/år både i plan og høgd.
- På Nokkenibba er resultata framleis noko usikre, men det er ikkje klare teikn til endringar i punktet.
- På Oppstadhornet er det klare teikna til rørsle i ein del av punkta.
- Ottem har svake indikasjonar på rørsle.
- På Rindalseggene er lite truleg at det er rørsle i punkta.
- På Skrednakken det ikkje klare teikn til endringar i punkta.
- På Svarttinden er det ikkje teikn til rørsle.
- På Vollan er det usikre indikasjonar på mindre rørsle i minst eitt av punkta.
- Åknes har rørsle i mange av punkta, resultata her samsvarar stort sett med resultat frå tidlegare år.

Innleiing

I Møre og Romsdal vart dei fyrste målingane for å avklare stabilitet i fjellsider med GPS-målingar utført i 2003 på Otrøya og Børa. Målingane vart utført tilsvarande i 2004 og i 2005 på Otrøya med utviding til fleire punkt. I 2004 vart det gjort målingar på Åknes og i 2005 vart alle punkta her målt to gonger og området utvida med fleire punkt ved ei tredje måling. I 2005 og 2006 vart det etablert nye punkt og sett i gong tilsvarande målingar på fleire nye stader i fylket. I 2005 på Heggurda, Norddal, Blåhornet, Hellesylt og Svarttind. I 2006 eitt ekstra punkt i Norddal, nye punkt på Skrenakken, Furneset, Nokkenibba, Herdalsnibba og Flatmark, og i tillegg tre nye punkt på Mannen. I 2007 vart nye punkt sett ut og målt på Gikling, og i 2008 ved Ottem og Vollan i Sunndal, og på Berill i Innfjorden. I 2012 er det sett ut punkt på Storehornet i Vanylven.

Til saman er det målt på i alt 20 ulike lokalitetar i Møre og Romsdal fylke, og alle desse med unntak av Storehornet er målt minst to eller fleire gonger.

Metode

Alle målepunkta for GPS er markert med gjenga skruvar (5/8 UNC gjengar) som er limt fast i fjell. Gjengetypen gjer at GPS-antenner ved måling kan skruvast direkte på punktet med minimale feil i sentrering. Normalt vert antenna sett på ein ”trefot” (figur 1) som kan stillast horisontal, slik at antenna vert stilt sentrisk loddrett over sentrum av skruven. Høgd på antenna vert målt ved å måle avstandar på trefoten. I nokre punkt er bolten sett så skeiv at det er uråd å stille trefoten horisontal. Desse punkta er kommentert spesielt sidan dette utgjer ei feilkjelde.

Figur 1: Trefot med antenne

Måleutstyret som er nytta er Javad/Topcon tofrekvente GPS- mottakarar, dels og med måling av GLONASS satellittar (GLONASS er eit russisk GNSS system som er svært likt GPS).

Målemetoden er statisk relativ fasemåling, med måling av eit nettverk av vektorar mellom punkt. Måleintervall (epokeintervall) er fem sekund, og måletid minst 30 minutt pr. vektor. Nettet er bygt opp slik at alle punkt skal ha samband til minst tre andre punkt. Måletida i dei fyrste åra var nokre gonger kortare enn 30 minutt. Erfaring har synt at auka måletid gir vinst i presisjon utan serleg auke i totaltida ein nyttar for målingane.

GPS-vektorar er rekna i programmet ”TPS-Pinnacle”. I nokre tilfelle der vektorar vert funne å ha dårleg eller variable presisjon, eller at det vert funne mykje støy i målingane er vektorar og prosessert i programmet GrafNet som er eit program tilsvarande Pinnacle, men frå ein annan leverandør. Programma skal teoretisk gi same resultat, men litt ulike metodar for korreksjon for meteorologi (troposfæremodell) og ulike grenser for forkasting av målingar kan gi litt ulike resultat. I 2007 er ingen data prosessert i GrafNet.

I båe programma vert GPS vektorar rekna som statiske vektorar med heiltals-løysing. I tillegg til 3D-vektorar estimerer og programma standardavvik (σ) for vektorkomponentane.

Estimert presisjon (standardavvik) på vektor komponentar er oftast betre enn 1 mm i N og E (plan), og 2 mm i høgd, men i ein del tilfelle er dei langt dårlegare enn dette. Erfaring tilseier at estimerte standardavvik på rekna vektorar er for optimistiske, slik at reell presisjon er faktor 2-3 høgare enn estimert av programma. Vektorane har best presisjon i grunnriss (X,Y), komponenten i høgd (Z) har normalt ca. 2–3 gongar høgre standardavvik. Dette skuldast geometriske eigenskapar ved GPS systemet kombinert med at måleområdet er langt mot nord. Gjennom prosesseringa av vektorane i området er det og funne at serleg høgdekomponenten i vektorane er var for satellittgeometri, utan at dette kjem fullt ut til uttrykk i standardavvika til resultatet.

Netta av GPS-vektorar er jamna ut ved nettutjamning etter minste kvadraters metode for å finne dei mest sannsynlege verda for koordinatane til punkta. Tilhøyrande standardavvik for koordinatar vert og estimert gjennom utjamninga. Koordinatar for punkt vert rekna relativt til dei eller det lokale fastpunkta(et) som er halde fast, dvs. har same koordinat frå år til år. Nokre av netta som er omtala har berre eitt fastpunkt, eller fleire fastpunkt i ein del av området. Dette gjer at ein ikkje har fullgod kontroll mot feil målingar serleg i punkt lengst borte frå fastpunkta. Eit optimalt nett har to eller fleire fastpunkt fordelt kring utkanten av nettet.

Observasjonane vert gitt vekt etter estimert standardavvik for vektorane. Dersom dette estimatet er korrekt skal utjamninga av samla nett gi det same estimat for standardavvik som vektorane. For dei aktuelle netta ligg estimert presisjon faktorar på ca. 2 høgre. Dette indikerer at estimert presisjon for vektorane er optimistisk med ein slik faktor.

Estimerte standardavvik på resultatkoordinatar er med nokre unntak på 1–2 mm i grunnriss, og 2–6 mm i høgd. Dette samsvarar godt med erfaringstal frå liknande målingar, men serleg for høgder vil det vere variasjonar med geometri som ikkje vert fanga opp, slik at standardavvika ikkje gir mål for uvisse i høve til "sanne" storleikar, men i høve til resultata ein har fått (intern presisjon). Sidan dei fleste målingane vert gjort innanfor eit relativt kort tidsrom vil fleire vektorar ha om lag den same geometriske konfigurasjon for satellittar, og dermed ha ei systematisk påverking frå denne. Endringar i meteorologiske tilhøve vil og kunne gi systematiske endringar på høgderesultat. Ommåling nokre timar seinare kan gi litt andre resultat, og den systematiske skilnaden som kan oppstå frå både geometri og meteorologi vert lite reflektert av standardavvika til resultata som kjem fram. Variasjon i presisjon på dei ulike lokalitetane gjer at endringar på t.d. 1 cm kan vere klart signifikant endring i eitt område, medan det ikkje er signifikant på ein annan lokalitet.

Konklusjonen ein må trekke av dette er at serleg for høgdekomponentane bør ein vere konservativ i tolking av endringar, serleg om alle målingar er gjort innanfor eit rimeleg kort tidsrom.

Koordinatsystem

Alle koordinatar er referert til eit system gitt ved presis absolutt fastlegging av posisjonen til eitt eller fleire punkt i kvart område ut frå GPS-målingane og presise banedata. Dei fastlagde posisjonane er i ITRF2000 referanseramme som ligg nær opptil EUREF89, men koordinatane kan avvike i høve EUREF89 med opptil ca. 1 m.
Alle høgder er gitt som ellipsoidehøgder. Alle gitte høgder er dermed ca. 45 meter høgare enn "normale" høgder over havet (h.o.h.).

Endringar

Endringane i koordinatar over tid er dels framstilt i tabellar som syner endring i koordinatar mellom målingar, med retning og avstand på endringa, eller som grafiske figurar. Figurane for endringar syner grunnriss (N,E) for seg og høgd for seg, eller alle tre dimensjonar i ein figur. I tillegg til endring syner figurane og konfidensnivå, dvs. kor stor ei endring må vere for at den skal vere statistisk signifikant. Som signifikansnivå er valt 99%. Dette tilsvarar om lag 3x standardavviket for den funne endringa.

I grunnriss er endringa synt med ein svart pil og signifikansnivået synt med ein raud ellipse, eller rettare ei fotpunktkurve (grøn) til ein ellipse som syner standardavviket til endringa i ulike retningar (figur 2). Dersom ei endringspil går utanfor fotpunktkurva er endringa signifikant, om spissen ligg innanfor er endringa ikkje signifikant. For høgde er endringane framstilt med sirklar, blå sirklar med taggar innover representerer senking (rørsle ned), raude sirklar med taggar utover representerer heving (rørsle opp). Grensa for signifikant endring er gitt med ein fiolett vertikal pil. Dersom pilspissen er innanfor sirkelen er endringa signifikant, om pilspissen er utanfor sirkelen er den ikkje det. Dette er den viktigaste testen som vert utført for å kontrollere om punkt verkeleg har flytt på seg, eller om variasjonen i koordinatar truleg berre skuldast tilfeldige feil (målestøy). Alle målingar har visse innslag av feil, og her vil feil på dei einskilde vektorane som vert målt forplante seg til feil i koordinatane som er resultatet. Verknaden av desse feila vert synt som standardavvik for koordinatane. Sjølv om det ikkje er noko som har flytta på seg kan ein ikkje forvente å få identiske resultat. Ein må difor teste om den funne endringa i koordinatar er så stor at den ikkje sannsynleg kan forklarast med feil i målingane. Teorien for dette kan kort forklarast til:

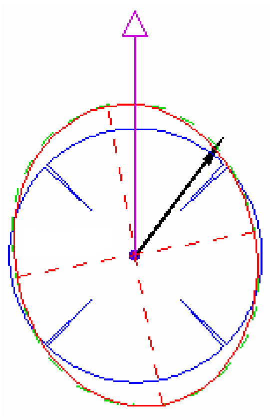
Figur 2: Konfidensfigur

Ved fyrste gongs måling vert posisjonen til punktet fastlagt som UTM-koordinatar $(N,E,h)_1$ og estimert grannsemd (standardavvik) $(\sigma N, \sigma E, \sigma h)_1$ (og korrelasjonar mellom N og E koordinat). Ved ommåling vert det estimert tilsvarande posisjon $(N,E,h)_2$ og grannsemd. Ut frå dei to fastleggingane kan ein så teste om koordinatane til dei to tidspunkta er ulike. Svaret på denne testen er i utgongspunktet ja / nei og ikkje informativ ut over det.
Ved i staden å rekne kor mykje koordinatane har endra seg mellom dei to fastleggingane kan ein fastlegge ein ”endringsvektor” i grunnriss og høgd. Vektorane er gitt ved:

Vektor lengd: $dS = \sqrt{(N_2-N_1)^2 + (E_2-E_1)^2}$

Vektor retning: $r = \operatorname{atan}((E_2-E_1)/ (N_2-N_1))$

Denne vektoren vil ha grannsemd som er ein funksjon av grannsemda til koordinatane $(N,E)_1$ og $(N,E)_2$ - $(\sigma N,\sigma E)_1$ og $(\sigma N,\sigma E)_2$ Grannsemda til vektoren i ulike retningar kan framstillast som ein ellipse (eller strengt fotpunktkurva til ein ellipse). Standardavvik har eit konfidensnivå på 67%, dvs det er 67% sannsyn for at ein tilfeldig observasjon ligg innanfor eitt standardavvik. For å auke sannsynet for at ein ikkje gjer feil slutning er det vanleg å nytte 95 eller 99% nivå for ein test, eller 5 eller 1% sannsyn for feil slutning. Varierande testnivå vil endre storleiken men ikkje forma til feilellipsen. Ein kan difor grafisk framstille endringsvektoren i høve til feilellipsen slik at om vektoren går utanfor feilellipsen så er det signifikant endring på det nivå feilellipsen er skalert til, og tilsvarande ikkje signifikant om vektoren endar inne i ellipsen.

For vertikale endringar er det skilnaden mellom målingane og tilhøyrande standardavvik på differansen som vert estimert og testa tilsvarande. I den grafiske testen vert høgdeendring framstilt som ein sirkel, der radius i sirkelen svarar til endringa. For å skilje heving frå setning vert punkt med heving teikna med raude sirklar med taggar ”utover”, og punkt med setning med blå sirklar med ”taggar” innover. Teststorleiken for signifikant endring vert framstilt som ein vertikal stolpe frå sirkelsentrum. Når radien i sirkelen er større enn lengda på stolpen, dvs. går forbi enden på denne er endringa signifikant.

Dei grafiske figurane for endring kan såleis både syne kva for endring ein har i dei ulike punkta, og i tillegg syne om denne er signifikant eller ei. Ein kan og sjå korleis endringane er i høve til grensene for signifikans. Storleiken på signifikansellipsane vil variere ut frå presisjonen til målingane som ligg til grunn og den geometriske utforminga av nettet. Til vanleg vil ein ha aukande storleik på feilellipsane di lengre ein kjem bort frå fastpunkt, og fleire godt fordelte fastpunkt er difor ein stor føremun.

Resultat

Resultata er i det vidare presentert for kvart område i form av tabellar med koordinatar og endringar og grafiske figurar. I alle tabellar er meter nytta som eining for avstandar og høgder, gon (^{g}) – 400 delt sirkel som eining for retningar. Kommentarar til endringane er gitt for kvart område.

Børa

Figur 3: Kart over Børa (Sk-N50).

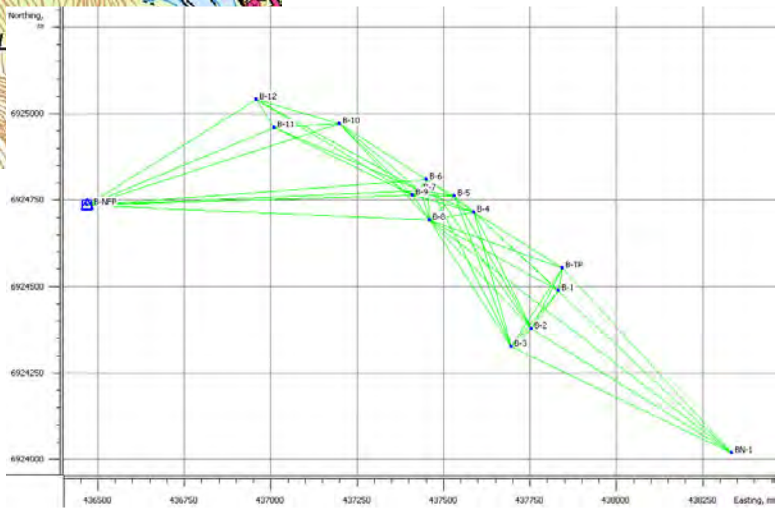

Figur 4: Nettet på Børa (komplett nett – ikkje alle punkta er målt 2012).

Punktgrunnlag

På Børa vart det fyrste gong gjort målingar i regi av Statens Vegvesen M&R i 1999 med ommålingar i 2000 og 2001, desse eldre målingane er ikkje tekne med her. I 2003 og 2004 vart målingane utført av to hovudfagstudentar ved Institutt for geofag ved Universitetet i Oslo som del av hovudfagsoppgåver til Cand. scient. graden. Nettet vart i 2003 utvida med eit nytt fastpunkt og tre nye punkt mot nord. I 2004 vart det etablert eitt punkt lengre mot søraust og to nye punkt på Mannen som vart knytt til det same nettet. I 2009 vart det etablert eitt ekstra punkt B-14 på kanten mot søraust på Børa (figurar 3 og 4).

Deler av nettet på Børa er målt om fleire gonger i åra etter 2004, med serleg vekt på punkta ut mot kanten som har synt rørsle. I 2012 er eit slikt utval med ti punkt langs kanten og mot søraust målt om.

Resultat - endringar

Resultata er gitt i tabellar 1 og 2 og i figur 5. Resultata syner at punkta B-4 og B-6, som er frittståande blokker med mindre volum, har rørsle i storleik ca 10 og 5 mm/år i plan og litt vertikal setning. Resultata for dei to punkta samsvarar godt med tidlegare målingar. Punktet B-13 som vart etablert lengst mot søraust i 2004 syner og konsistent endring over tid i storleik 2–3 mm/år i plan og litt setning (1 mm/år). Punktet B-14, etablert 2009, ca. 300 meter nærare Børa syner ikkje rørsle.

Punkta B-TP, B-1 og B-5 syner signifikant rørsle når ein legg data over fleire år til grunn, men det er tale om små endringar i storleik 1 mm/år. Dei andre punkta som er målt om syner ikkje signifikante endringar.

Konklusjon:
Det er påvist signifikant rørsle i fleire av punkta på Børa, storleik på endringar varierer frå ca. 1 til 10 mm/år. Punktet B-14, etablert 2009 syner ikkje signifikant rørsle målt over tre år.

PUNKT	År	N (UTM)	E (UTM)	H (ell.)	σN [m]	σE [m]	σH [m]	dN [m]	dE [m]	Avst. [m]	Retning [^{g} gon]	dH [m]
B-NFP	Fastp.	6924735.066	436467.732	1089.842								
B-TP	2003	6924552.3650	437843.6410	1105.3780	0.0010	0.0010	0.0030					
B-TP	2004	6924552.3660	437843.6440	1105.3820	0.0010	0.0010	0.0020	0.001	0.003	**0.003**	79.52	**0.004**
B-TP	2006	6924552.3703	437843.6433	1105.3797	0.0007	0.0005	0.0015	0.005	0.002	**0.006**	26.07	**0.002**
B-TP	2008	6924552.3730	437843.6474	1105.3814	0.0012	0.0007	0.0022	0.008	0.006	**0.010**	42.96	**0.003**
B-TP	2009	6924552.3729	437843.6457	1105.3793	0.0003	0.0002	0.0007	0.008	0.005	**0.009**	34.17	**0.001**
B-TP	2010	6924552.3727	437843.6466	1105.3805	0.0004	0.0005	0.0008	0.008	0.006	**0.010**	40.03	**0.003**
B-TP	2012	6924552.3739	437843.6461	1105.3832	0.0005	0.0004	0.0011	0.009	0.005	**0.010**	33.13	**0.005**
B-1	2003	6924487.4970	437833.0780	1094.8590	0.0010	0.0010	0.0030					
B-1	2004	6924487.4940	437833.0810	1094.6820	0.0010	0.0010	0.0020	-0.003	0.003	**0.004**	150.00	**-0.177**
B-1	2006	6924487.5020	437833.0802	1094.8645	0.0008	0.0005	0.0015	0.005	0.002	**0.005**	26.39	**0.005**
B-1	2010	6924487.5006	437833.0843	1094.8643	0.0004	0.0005	0.0008	0.004	0.006	**0.007**	66.95	**0.005**
B-1	2012	6924487.5025	437833.0833	1094.8666	0.0005	0.0004	0.0011	0.005	0.005	**0.008**	48.82	**0.008**
B-2	2003	6924376.7420	437754.9090	1078.0010	0.0010	0.0010	0.0030					
B-2	2004	6924376.7420	437754.9130	1078.0020	0.0010	0.0010	0.0020	0.000	0.004	**0.004**	100.00	**0.001**
B-2	2006	6924376.7453	437754.9090	1078.0087	0.0007	0.0005	0.0014	0.003	0.000	**0.003**	0.00	**0.008**
B-2	2009	6924376.7464	437754.9154	1078.0064	0.0004	0.0003	0.0008	0.004	0.006	**0.008**	61.66	**0.005**
B-2	2010	6924376.7448	437754.9136	1078.0052	0.0005	0.0006	0.0010	0.003	0.005	**0.005**	65.19	**0.004**
B-3	2003	6924326.4400	437695.0210	1074.6930	0.0010	0.0010	0.0030					
B-3	2004	6924326.4430	437695.0240	1074.7010	0.0010	0.0010	0.0020	0.003	0.003	**0.004**	50.00	**0.008**
B-3	2006	6924326.4434	437695.0207	1074.7003	0.0007	0.0005	0.0014	0.003	0.000	**0.003**	394.40	**0.007**
B-3	2009	6924326.4425	437695.0230	1074.6990	0.0004	0.0003	0.0008	0.002	0.002	**0.003**	42.96	**0.006**
B-3	2010	6924326.4402	437695.0219	1074.6984	0.0004	0.0006	0.0010	0.000	0.001	**0.001**	86.08	**0.005**
B-4	2003	6924714.3650	437586.6960	1096.9550	0.0010	0.0010	0.0020					
B-4	2004	6924714.3700	437586.7020	1096.9560	0.0010	0.0010	0.0020	0.005	0.006	**0.008**	55.77	**0.001**
B-4	2006	6924714.3914	437586.7144	1096.9518	0.0006	0.0004	0.0013	0.026	0.018	**0.032**	38.75	**-0.003**
B-4	2008	6924714.4190	437586.7418	1096.9454	0.0012	0.0007	0.0022	0.054	0.046	**0.071**	44.78	**-0.010**
B-4	2009	6924714.4289	437586.7515	1096.9397	0.0003	0.0002	0.0007	0.064	0.056	**0.085**	45.53	**-0.015**
B-4	2010	6924714.4351	437586.7577	1096.9386	0.0004	0.0005	0.0008	0.070	0.062	**0.093**	45.95	**-0.016**
B-4	2012	6924714.4501	437586.7728	1096.9371	0.0004	0.0004	0.0009	0.085	0.077	**0.115**	46.74	**-0.018**
B-5	2003	6924761.2500	437530.2530	1098.1660	0.0010	0.0010	0.0020					
B-5	2004	6924761.2490	437530.2560	1098.1700	0.0010	0.0010	0.0020	-0.001	0.003	**0.003**	120.48	**0.004**
B-5	2006	6924761.2538	437530.2531	1098.1683	0.0006	0.0004	0.0014	0.004	0.000	**0.004**	1.67	**0.002**
B-5	2008	6924761.2530	437530.2561	1098.1738	0.0012	0.0007	0.0021	0.003	0.003	**0.004**	51.04	**0.008**
B-5	2009	6924761.2549	437530.2552	1098.1704	0.0004	0.0003	0.0008	0.005	0.002	**0.005**	26.87	**0.004**
B-5	2010	6924761.2530	437530.2542	1098.1721	0.0003	0.0004	0.0007	0.003	0.001	**0.003**	24.22	**0.006**
B-5	2012	6924761.2551	437530.2539	1098.1757	0.0004	0.0004	0.0010	0.005	0.001	**0.005**	11.12	**0.010**
B-6	2003	6924809.3670	437450.5790	1089.7860	0.0010	0.0010	0.0020					
B-6	2004	6924809.3710	437450.5790	1089.7820	0.0010	0.0000	0.0020	0.004	0.000	**0.004**	0.00	**-0.004**
B-6	2006	6924809.3852	437450.5768	1089.7756	0.0006	0.0004	0.0013	0.018	-0.002	**0.018**	392.34	**-0.010**
B-6	2008	6924809.3980	437450.5802	1089.7695	0.0012	0.0007	0.0021	0.031	0.001	**0.031**	2.46	**-0.016**
B-6	2009	6924809.4029	437450.5798	1089.7672	0.0004	0.0003	0.0008	0.036	0.001	**0.036**	1.42	**-0.019**
B-6	2010	6924809.4052	437450.5813	1089.7636	0.0003	0.0004	0.0007	0.038	0.002	**0.038**	3.83	**-0.022**
B-6	2012	6924809.4145	437450.5810	1089.7624	0.0004	0.0004	0.0010	0.048	0.002	**0.048**	2.68	**-0.024**
B-7	2003	6924777.5950	437431.8270	1089.1590	0.0010	0.0010	0.0020					
B-7	2004	6924777.5930	437431.8290	1089.1630	0.0010	0.0000	0.0020	-0.002	0.002	**0.003**	150.00	**0.004**
B-7	2006	6924777.5956	437431.8284	1089.1645	0.0006	0.0004	0.0012	0.001	0.001	**0.002**	74.22	**0.005**
B-7	2010	6924777.5936	437431.8303	1089.1650	0.0003	0.0004	0.0007	-0.001	0.003	**0.004**	125.54	**0.006**

PUNKT	År	N (UTM)	E (UTM)	H (ell.)	σN [m]	σE [m]	σH [m]	dN [m]	dE [m]	Avst. [m]	Retning [^{g} gon]	dH [m]
B-8	2003	6924690.7890	437459.3550	1082.4170	0.0010	0.0010	0.0020					
B-8	2004	6924690.7870	437459.3550	1082.4220	0.0010	0.0010	0.0020	-0.002	0.000	**0.002**	200.00	**0.005**
B-8	2006	6924690.7906	437459.3529	1082.4220	0.0006	0.0004	0.0012	0.002	-0.002	**0.003**	341.45	**0.005**
B-8	2010	6924690.7893	437459.3564	1082.4269	0.0003	0.0004	0.0007	0.000	0.001	**0.001**	86.56	**0.010**
B-8	2012	6924690.7883	437459.3550	1082.4299	0.0004	0.0004	0.0010	-0.001	0.000	**0.001**	200.00	**0.013**
B-9	2003	6924764.5020	437410.3120	1086.7780	0.0010	0.0010	0.0020					
B-9	2004	6924764.4990	437410.3140	1086.7760	0.0010	0.0000	0.0010	-0.003	0.002	**0.004**	162.57	**-0.002**
B-9	2006	6924764.5012	437410.3117	1086.7784	0.0006	0.0004	0.0012	-0.001	0.000	**0.001**	222.84	**0.000**
B-9	2009	6924764.4996	437410.3132	1086.7825	0.0004	0.0003	0.0008	-0.002	0.001	**0.003**	170.48	**0.005**
B-9	2010	6924764.4990	437410.3134	1086.7837	0.0003	0.0004	0.0007	-0.003	0.001	**0.003**	172.20	**0.006**
B-10	2003	6924970.0380	437199.5980	1078.6970	0.0010	0.0010	0.0020					
B-10	2004	6924970.0360	437199.5990	1078.7010	0.0010	0.0000	0.0010	-0.002	0.001	**0.002**	170.48	**0.004**
B-10	2006	6924970.0374	437199.5984	1078.7055	0.0004	0.0003	0.0009	-0.001	0.000	**0.001**	162.57	**0.009**
B-10	2008	6924970.0370	437199.5992	1078.7057	0.0009	0.0005	0.0017	-0.001	0.001	**0.002**	144.23	**0.009**
B-10	2009	6924970.0349	437199.5997	1078.7041	0.0004	0.0003	0.0008	-0.003	0.002	**0.004**	168.07	**0.007**
B-10	2010	6924970.0368	437199.5985	1078.7038	0.0004	0.0005	0.0008	-0.001	0.001	**0.001**	174.87	**0.007**
B-10	2012	6924970.0345	437199.5975	1078.7039	0.0005	0.0005	0.0013	-0.003	-0.001	**0.004**	209.03	**0.007**
B-11	2003	6924959.5520	437010.5690	1069.2780	0.0010	0.0010	0.0020					
B-11	2004	6924959.5480	437010.5700	1069.2840	0.0010	0.0000	0.0010	-0.004	0.001	**0.004**	184.40	**0.006**
B-11	2006	6924959.5529	437010.5692	1069.2838	0.0008	0.0005	0.0018	0.001	0.000	**0.001**	13.92	**0.006**
B-11	2010	6924959.5515	437010.5694	1069.2879	0.0004	0.0005	0.0008	-0.001	0.000	**0.001**	157.04	**0.010**
B-11	2012	6924959.5510	437010.5694	1069.2878	0.0005	0.0005	0.0011	-0.001	0.000	**0.001**	175.78	**0.010**
B-12	2003	6925039.2040	436958.5780	1062.6410	0.0010	0.0010	0.0020					
B-12	2004	6925039.2010	436958.5780	1062.6440	0.0010	0.0000	0.0010	-0.003	0.000	**0.003**	200.00	**0.003**
B-12	2006	6925039.2045	436958.5779	1062.6459	0.0009	0.0005	0.0019	0.001	0.000	**0.001**	387.43	**0.005**
B-12	2010	6925039.2015	436958.5765	1062.6437	0.0004	0.0005	0.0008	-0.002	-0.001	**0.003**	234.40	**0.003**
B-13	2004	6924018.4570	438333.4780	1022.9320	0.0010	0.0010	0.0020					
B-13	2006	6924018.4680	438333.4805	1022.9411	0.0009	0.0006	0.0020	0.011	0.003	**0.011**	14.23	**0.009**
B-13	2008	6924018.4720	438333.4914	1022.9325	0.0013	0.0008	0.0027	0.015	0.013	**0.020**	46.42	**0.000**
B-13	2009	6924018.4737	438333.4925	1022.9291	0.0004	0.0003	0.0009	0.017	0.014	**0.022**	45.52	**-0.003**
B-13	2010	6924018.4775	438333.4908	1022.9243	0.0004	0.0005	0.0008	0.020	0.013	**0.024**	35.53	**-0.008**
B-13	2012	6924018.4796	438333.4945	1022.9198	0.0005	0.0005	0.0013	0.023	0.016	**0.028**	40.15	**-0.012**
B-14	2009	6924216.7391	438097.7364	1068.6499	0.0004	0.0003	0.0008	Nytt	2009			
B-14	2010	6924216.7385	438097.7364	1068.6496	0.0005	0.0006	0.0010	-0.001	0.000	**0.001**	200.00	**0.000**
B-14	2012	6924216.7393	438097.7358	1068.6517	0.0006	0.0005	0.0013	0.000	-0.001	**0.001**	320.48	**0.002**

Tabell 1: Koordinatar og endringar i høve til fyrste måling for punkt på Børa 2003–12. B-NFP er fastpunkt og B-TP er Statens kartverk triangelpunkt D27T0064. Punkta B-10 – B-13 og B-NFP er etablert i 2004, punktet B-14 i 2009. Punktet B-1 (merka med raudt) har ein feil i antennehøgd i 2004).

		Endring mellom målingar				
PUNKT	**ÅR**	**dN [m]**	**dE [m]**	**Avstand [m]**	**Retning [g gon]**	**dH [m]**
B-TP	2003-04	0.001	0.003	**0.003**	79.52	**0.004**
B-TP	2004-06	0.004	-0.001	**0.004**	389.73	**-0.002**
B-TP	2006-08	0.003	0.004	**0.005**	62.93	**0.002**
B-TP	2008-09	0.000	-0.002	**0.002**	296.26	**-0.002**
B-TP	2009-10	0.000	0.001	**0.001**	113.92	**0.001**
B-TP	2010-12	0.001	0.000	**0.001**	374.87	**0.003**
B-1	2003-04	-0.003	0.003	**0.004**	150.00	**-0.177**
B-1	2004-06	0.008	-0.001	**0.008**	393.65	**0.182**
B-1	2006-10	-0.001	0.004	**0.004**	120.95	**0.000**
B-1	2010-12	0.002	-0.001	**0.002**	369.16	**0.002**
B-2	2003-04	0.000	0.004	**0.004**	100.00	**0.001**
B-2	2004-06	0.003	-0.004	**0.005**	343.91	**0.007**
B-2	2006-09	0.001	0.006	**0.006**	89.16	**-0.002**
B-2	2099-10	-0.002	-0.002	**0.002**	253.74	**-0.001**
B-3	2003-04	0.003	0.003	**0.004**	50.00	**0.008**
B-3	2004-06	0.000	-0.003	**0.003**	307.68	**-0.001**
B-3	2006-09	-0.001	0.002	**0.002**	123.75	**-0.001**
B-3	2009-10	-0.002	-0.001	**0.003**	228.40	**-0.001**
B-4	2003-04	0.005	0.006	**0.008**	55.77	**0.001**
B-4	2004-06	0.021	0.012	**0.025**	33.43	**-0.004**
B-4	2006-08	0.028	0.027	**0.039**	49.77	**-0.006**
B-4	2008-09	0.010	0.010	**0.014**	49.35	**-0.006**
B-4	2009-10	0.006	0.006	**0.009**	50.00	**-0.001**
B-4	2010-12	0.015	0.015	**0.021**	50.21	**-0.001**
B-5	2003-04	-0.001	0.003	**0.003**	120.48	**0.004**
B-5	2004-06	0.005	-0.003	**0.006**	365.40	**-0.002**
B-5	2006-08	-0.001	0.003	**0.003**	116.59	**0.005**
B-5	2008-09	0.002	-0.001	**0.002**	371.84	**-0.003**
B-5	2009-10	-0.002	-0.001	**0.002**	230.84	**0.002**
B-5	2010-12	0.002	0.000	**0.002**	390.97	**0.004**
B-6	2003-04	0.004	0.000	**0.004**	400.00	**-0.004**
B-6	2004-06	0.014	-0.002	**0.014**	390.21	**-0.006**
B-6	2006-08	0.013	0.003	**0.013**	16.53	**-0.006**
B-6	2008-09	0.005	0.000	**0.005**	394.81	**-0.002**
B-6	2009-10	0.002	0.002	**0.003**	36.79	**-0.004**
B-6	2010-12	0.009	0.000	**0.009**	397.95	**-0.001**
B-7	2003-04	-0.002	0.002	**0.003**	150.00	**0.004**
B-7	2004-06	0.003	-0.001	**0.003**	385.56	**0.002**
B-7	2006-10	-0.002	0.002	**0.003**	151.63	**0.000**
B-8	2003-04	-0.002	0.000	**0.002**	200.00	**0.005**
B-8	2004-06	0.004	-0.002	**0.004**	366.38	**0.000**
B-8	2006-10	-0.001	0.003	**0.004**	122.64	**0.005**
B-8	2010-12	-0.001	-0.001	**0.002**	260.51	**0.003**
B-9	2003-04	-0.003	0.002	**0.004**	162.57	**-0.002**
B-9	2004-06	0.002	-0.002	**0.003**	348.59	**0.002**
B-9	2006-09	-0.002	0.001	**0.002**	152.05	**0.004**
B-9	2009-10	-0.001	0.000	**0.001**	179.52	**0.001**
B-10	2003-04	-0.002	0.001	**0.002**	170.48	**0.004**
B-10	2004-06	0.001	-0.001	**0.002**	374.22	**0.005**
B-10	2006-08	0.000	0.001	**0.001**	129.52	**0.000**
B-10	2008-09	-0.002	0.001	**0.002**	185.12	**-0.002**
B-10	2009-10	0.002	-0.001	**0.002**	364.14	**0.000**
B-10	2010-12	-0.002	-0.001	**0.003**	226.11	**0.000**

		Endring mellom målingar				
PUNKT	**ÅR**	**dN [m]**	**dE [m]**	**Avstand [m]**	**Retning [^{g} gon]**	**dH [m]**
B-11	2003-04	-0.004	0.001	**0.004**	184.40	**0.006**
B-11	2004-06	0.005	-0.001	**0.005**	389.70	**0.000**
B-11	2006-10	-0.001	0.000	**0.001**	190.97	**0.004**
B-11	2010-12	-0.001	0.000	**0.001**	200.00	**0.000**
B-12	2003-04	-0.003	0.000	**0.003**	200.00	**0.003**
B-12	2004-06	0.003	0.000	**0.004**	398.18	**0.002**
B-12	2006-10	-0.003	-0.001	**0.003**	227.80	**-0.002**
B-13	2004-06	0.011	0.003	**0.011**	14.23	**0.009**
B-13	2006-08	0.004	0.011	**0.012**	77.61	**-0.009**
B-13	2008-09	0.002	0.001	**0.002**	36.56	**-0.003**
B-13	2009-10	0.004	-0.002	**0.004**	373.22	**-0.005**
B-13	2010-12	0.002	0.004	**0.004**	67.14	**-0.005**
B-14	2009-10	-0.001	0.000	**0.001**	200.00	**0.000**
B-14	2010-12	0.001	-0.001	**0.001**	359.03	**0.002**

Tabell 2: Endringar mellom målingar for punkt på Børa 2003–12. Det er primært punkta B-4 og B-6 som har konsistente endringar frå år til år.

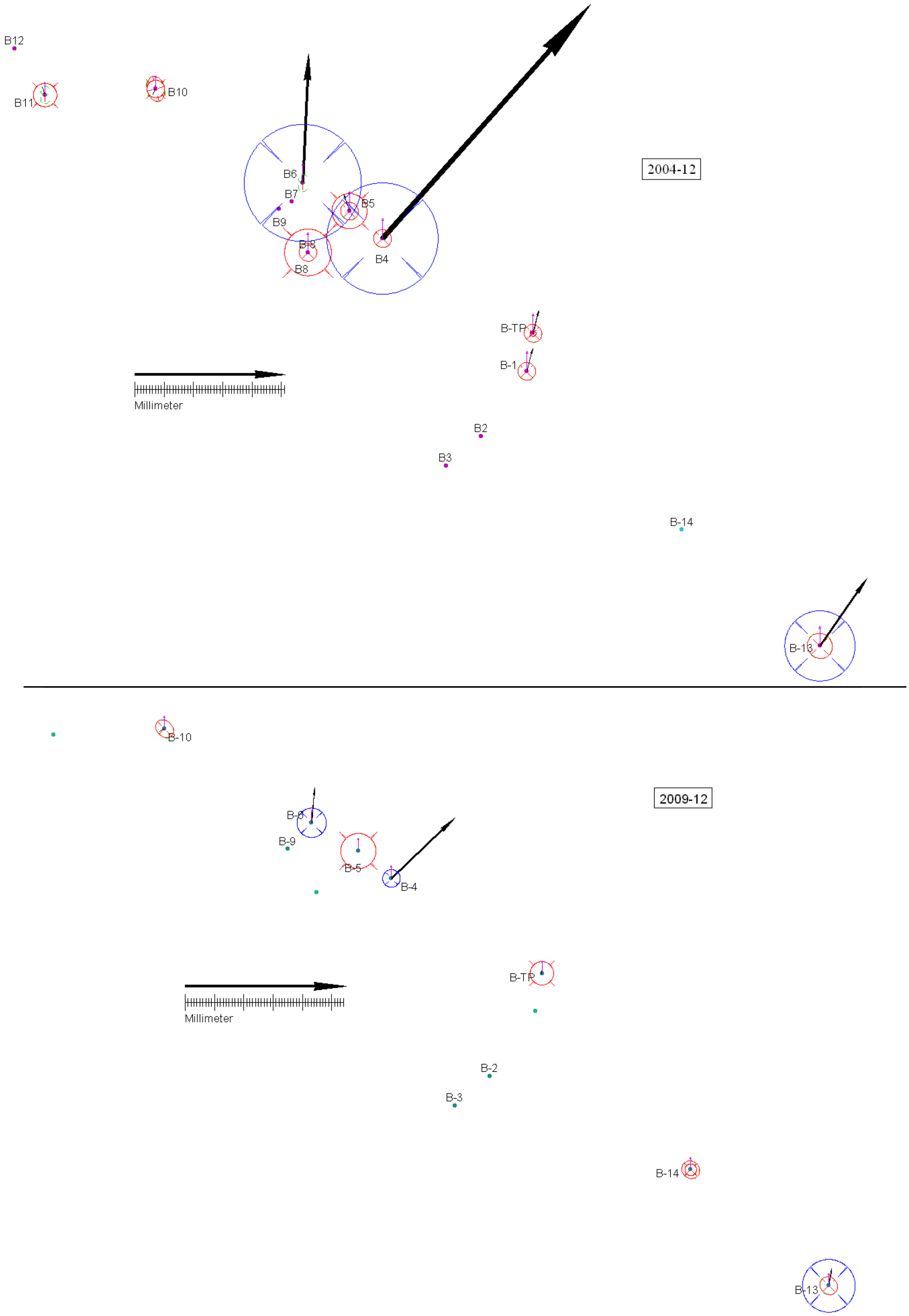

Figur 5: Grafisk endring grunnriss og høgde 2004–12 (øvst), 2009–12 (nedst), det siste inkluderer punktet B-14 etablert 2009.

Flatmark

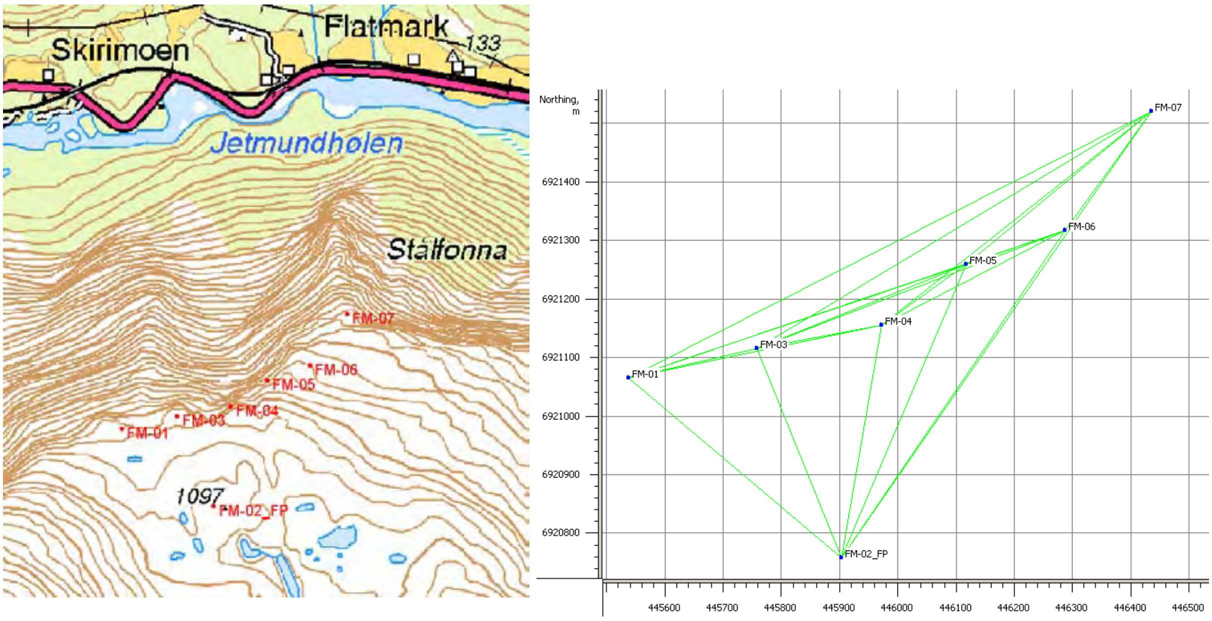

Figur 6: Vektorriss og kart (Sk-N50).

Punktgrunnlag
I 2006 vart det etablert seks nye punkt på potensielt ustabile blokker på kanten ned mot dalen sør for Flatmark, pluss eitt fastpunkt i fjell på platået innanfor (figur 6). Punkta er målt om i 2007, 2008 og 2011.

Resultat – endringar
Resultata er synt i tabellar 3 og 4 og endringar grafisk i figur 7. Målingane både i alle tre åra syner god presisjon, men standardavvik for posisjon er klart underestimert som eit resultat av at sju mottakarar måler samstundes og det vert ei stor grad av korrelasjon i observasjonsmaterialet.

Resultata for 2011 kan indikere at det har vore ein sentreringsfeil i fastpunktet (FM-02_FP). Alle indikerte endringar for 2011 resultata peiker i same retning, ca. 170^g med storleik ca. 6 mm, men samstundes stemmer målingar for antennehøgd godt med tidlegare år og indikerer korrekt horisontering. Det er difor vanskeleg å peike på konkrete feil men resultata vert ekstra usikre.

Med unntak av den systematiske endringa for alle punkt er det ingen signifikante endringar over tid, og serleg i høgd er det i sum stabile resultat over dei åra det er målt.

Konklusjon
Det er ikkje klare teikn til endringar i punkta så langt, men noko variable resultat gjer konklusjonen litt usikker og det tilseier at ein bør gjere nye målingar seinare.

PUNKT	År	N	E	H	sN	sE	sH	dN	dE	Avst	Retning	dH
FM-02_FP	F.P.	6920757.380	445904.058	1141.960								
FM-01	2006	6921065.003	445537.768	1084.280	0.000	0.000	0.000					
FM-01	2007	6921065.004	445537.767	1084.280	0.001	0.000	0.001	0.001	-0.001	**0.001**	372.47	**0.000**
FM-01	2008	6921065.007	445537.7686	1084.2811	0.0004	0.0002	0.0008	0.004	0.001	**0.004**	8.83	**0.001**
FM-01	2011	6921065.0005	445537.7711	1084.2812	0.0002	0.0002	0.0005	-0.002	0.003	**0.004**	139.29	**0.001**
FM-03	2006	6921114.727	445758.542	1080.160	0.000	0.000	0.000					
FM-03	2007	6921114.729	445758.540	1080.159	0.001	0.000	0.001	0.003	-0.002	**0.003**	361.98	**-0.001**
FM-03	2008	6921114.73	445758.5404	1080.165	0.0004	0.0002	0.0008	0.004	-0.001	**0.004**	378.97	**0.005**
FM-03	2011	6921114.7258	445758.5431	1080.1610	0.0002	0.0002	0.0005	-0.001	0.002	**0.002**	127.80	**0.001**
FM-04	2006	6921154.777	445972.221	1080.242	0.000	0.000	0.000					
FM-04	2007	6921154.780	445972.219	1080.239	0.001	0.000	0.001	0.003	-0.001	**0.003**	373.75	**-0.003**
FM-04	2008	6921154.778	445972.2178	1080.2479	0.0004	0.0003	0.0009	0.001	-0.003	**0.003**	326.62	**0.006**
FM-04	2011	6921154.7742	445972.2203	1080.2445	0.0002	0.0002	0.0005	-0.003	0.000	**0.003**	204.89	**0.002**
FM-05	2006	6921259.147	446116.901	1020.707	0.000	0.000	0.000					
FM-05	2007	6921259.146	446116.901	1020.702	0.001	0.000	0.001	-0.001	0.000	**0.001**	209.03	**-0.005**
FM-05	2008	6921259.153	446116.9003	1020.7168	0.0004	0.0002	0.0008	0.006	-0.001	**0.006**	390.97	**0.010**
FM-05	2011	6921259.1471	446116.9021	1020.7134	0.0002	0.0002	0.0005	0.000	0.001	**0.001**	73.38	**0.006**
FM-06	2006	6921317.510	446286.753	987.029	0.000	0.000	0.000					
FM-06	2007	6921317.509	446286.752	987.022	0.001	0.000	0.001	-0.001	0.000	**0.001**	220.48	**-0.007**
FM-06	2008	6921317.514	446286.7503	987.0319	0.0004	0.0002	0.0008	0.004	-0.002	**0.005**	369.34	**0.003**
FM-06	2011	6921317.5089	446286.7529	987.0339	0.0002	0.0002	0.0005	-0.001	0.000	**0.001**	174.22	**0.005**
FM-07	2006	6921520.331	446435.220	893.493	0.000	0.000	0.001					
FM-07	2007	6921520.321	446435.220	893.487	0.001	0.000	0.001	-0.010	0.001	**0.010**	194.76	**-0.006**
FM-07	2008	6921520.335	446435.220	893.4934	0.0004	0.0002	0.0008	0.004	0.000	**0.004**	5.91	**0.001**
FM-07	2011	6921520.3302	446435.2229	893.4992	0.0002	0.0002	0.0005	-0.001	0.003	**0.003**	109.57	**0.007**

Tabell 3: Koordinatar og endring frå fyrste måling for punkta på Flatmark.

		Endring mellom målingar				
PUNKT	**ÅR**	**dN [m]**	**dE [m]**	**Avstand [m]**	**Retning [^{g} gon]**	**dH [m]**
FM-01	2006-07	0.001	-0.001	**0.001**	372.47	0.000
FM-01	2007-08	0.003	0.001	**0.003**	24.22	0.001
FM-01	2008-11	-0.007	0.003	**0.007**	176.62	0.000
FM-03	2006-07	0.003	-0.002	**0.003**	361.98	-0.001
FM-03	2007-08	0.001	0.001	**0.001**	29.52	0.006
FM-03	2008-11	-0.004	0.003	**0.005**	163.63	-0.004
FM-04	2006-07	0.003	-0.001	**0.003**	373.75	-0.003
FM-04	2007-08	-0.002	-0.001	**0.002**	236.69	0.009
FM-04	2008-11	-0.004	0.003	**0.005**	162.95	-0.003
FM-05	2006-07	-0.001	0.000	**0.001**	209.03	-0.005
FM-05	2007-08	0.007	-0.001	**0.007**	392.76	0.014
FM-05	2008-11	-0.006	0.002	**0.006**	181.15	-0.003
FM-06	2006-07	-0.001	0.000	**0.001**	220.48	-0.007
FM-06	2007-08	0.005	-0.002	**0.005**	374.69	0.010
FM-06	2008-11	-0.005	0.003	**0.006**	169.99	0.002
FM-07	2006-07	-0.010	0.001	**0.010**	194.76	-0.006
FM-07	2007-08	0.014	0.000	**0.014**	398.18	0.006
FM-07	2008-11	-0.005	0.003	**0.006**	165.40	0.006

Tabell 4: Endring mellom målingar for punkt på Flatmark 2006–11.

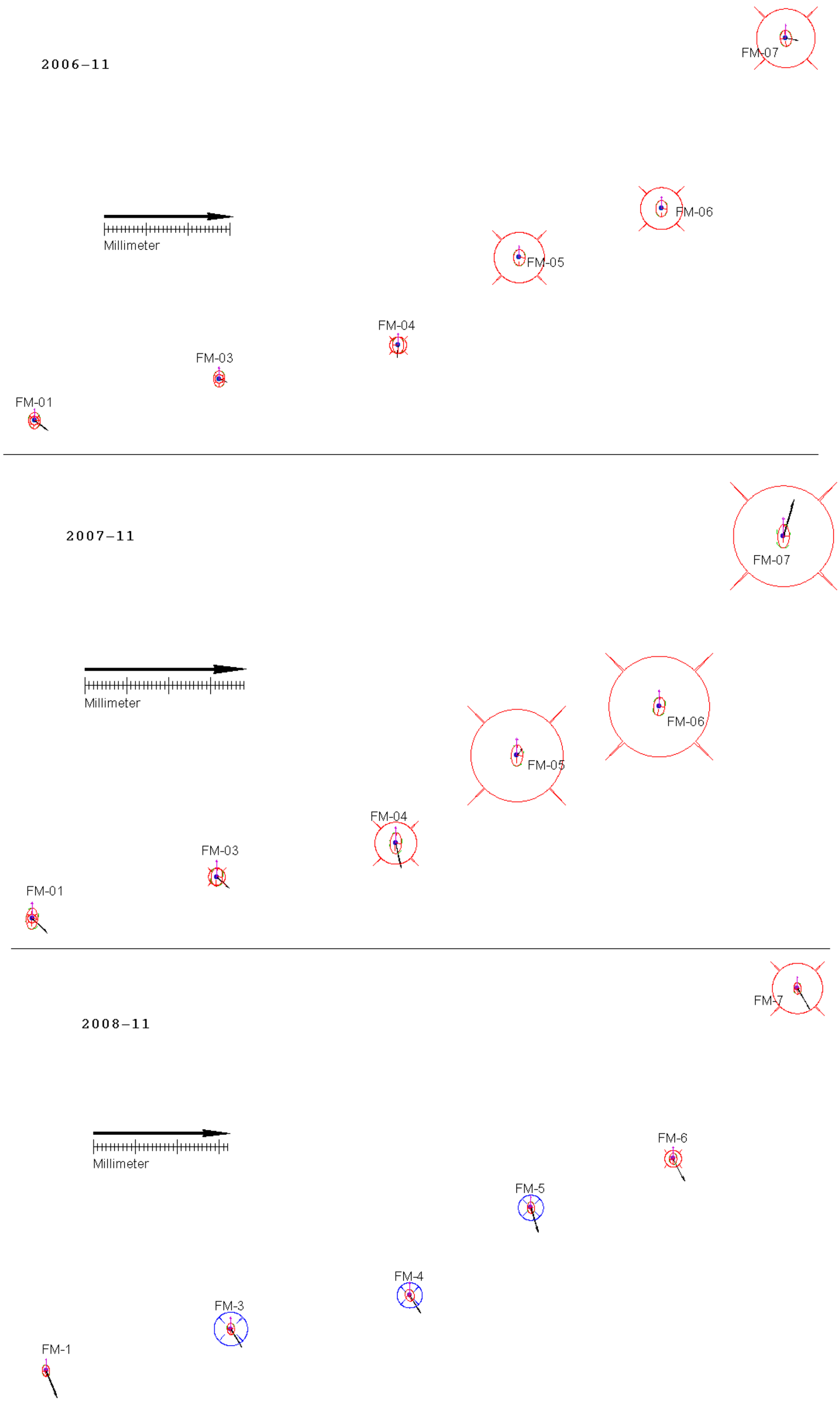

Figur 7: Grafisk framstilling av endring i punkta på Flatmark 2006–11 (øvst), 2007–11 (midt) og 2008–11 (nedst), med konfidensnivå for 99%. Grunnriss (pil), høgde (sirkel). Blå sirklar indikerer setning, raude heving.

Fremste Blåhornet

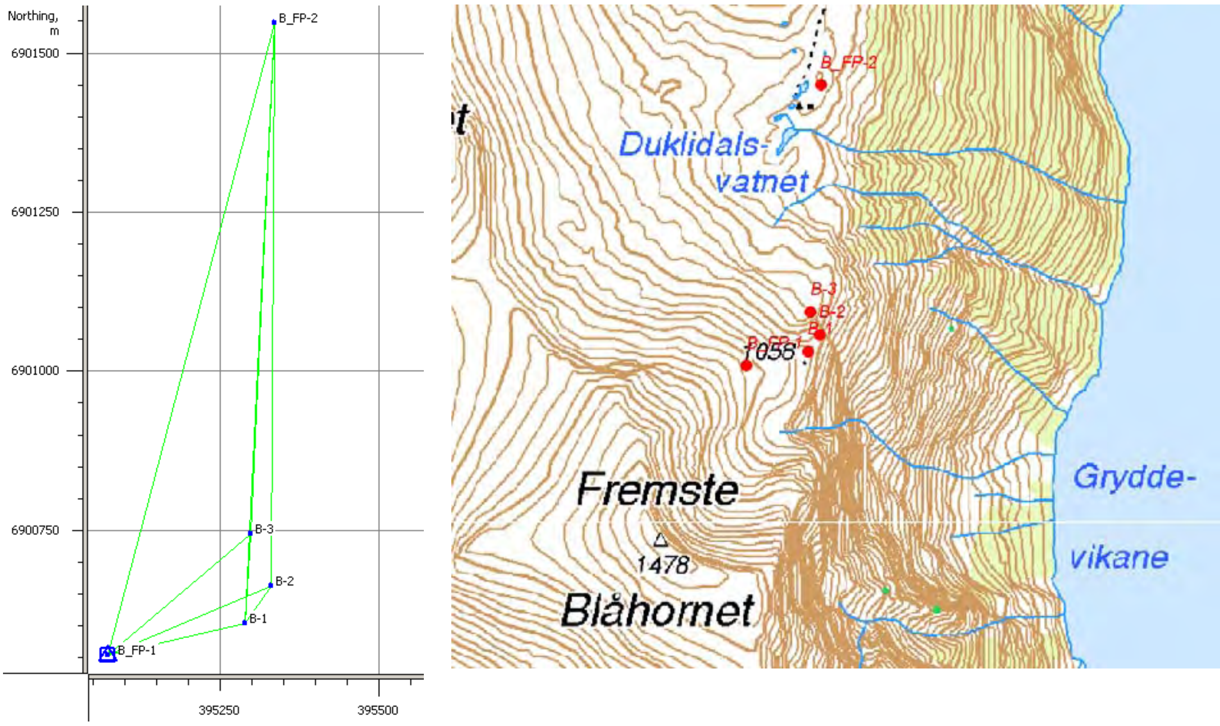

Figur 8: Nett på Blåhornet og plassering på kart (Sk N50).

Punktgrunnlag
I august 2005 vart tre punkt etablert nær stupkanten nord for Fremste Blåhornet i eit område med mogeleg rørsle. I tillegg vart det sett ut to fastpunkt (figur 8). Punkta er målt om att i 2006, 2007 og 2009.

Resultat – endringar, 2009
Det er ingen klare signifikante endringar, korkje i grunnriss eller høgd i noko av punkta (tabellar 5 og 6, figur 9). BL-1 har på grensa til signifikant endring i grunnriss frå 2006–07, men ikkje i høve til målingane i 2005. Punktet BL-3 syner og litt endring når 2005 resultata vert lagt til grunn, men ein av vektorane i denne målinga var dårleg, og kan vere forklaring til dette. Mellom 2006 og 2007 syner ikkje punktet endring ut over tilfeldig målestøy.

Konklusjon
Endringane i punkta gir så langt lite grunnlag for å påvise rørsle, men det kan ikkje utelukkast at det er små rørsler i punkta.

PUNKT	År	N (UTM)	E (UTM)	H (ell.)	σN [m]	σE [m]	σH [m]	dN [m]	dE [m]	Avst. [m]	Retning [g gon]	dH [m]
BL_FP-1	F.P.	6900554.355	395073.013	1160.178								
BL_FP-2	F.P.	6901546.682	395336.175	887.310								
BL-1	2005	6900604.4152	395290.5032	1096.8086	0.0017	0.0010	0.0032					
BL-1	2006	6900604.4154	395290.5002	1096.8063	0.0009	0.0007	0.0023	0.000	-0.003	0.003	304.238	-0.002
BL-1	2007	6900604.4190	395290.5031	1096.8054	0.0010	0.0007	0.0024	0.004	0.000	0.004	398.325	-0.003
BL-1	2009	6900604.4166	395290.5030	1096.8114	0.0009	0.0007	0.0019	0.001	0.000	0.001	390.967	0.003
BL-2	2005	6900662.5349	395331.4742	1073.9890	0.0010	0.0007	0.0024					
BL-2	2006	6900662.5335	395331.4749	1073.9924	0.0009	0.0007	0.0027	-0.001	0.001	0.002	170.483	0.003
BL-2	2007	6900662.5342	395331.4768	1073.9851	0.0011	0.0007	0.0027	-0.001	0.003	0.003	116.743	-0.004
BL-2	2009	6900662.5341	395331.4776	1073.9953	0.0009	0.0007	0.0020	-0.001	0.003	0.003	114.712	0.006
BL-3	2005	6900743.8041	395299.4135	1003.1301	0.0015	0.0008	0.0035					
BL-3	2006	6900743.8069	395299.4148	1003.1393	0.0026	0.0014	0.0053	0.003	0.001	0.003	27.672	0.009
BL-3	2007	6900743.8094	395299.4135	1003.1264	0.0018	0.0010	0.0034	0.005	0.000	0.005	0.000	-0.004
BL-3	2009	6900743.8025	395299.4159	1003.1304	0.0013	0.0007	0.0023	-0.002	0.002	0.003	137.433	0.000

Tabell 5: Koordinatar og endringar Fremste Blåhornet, 2005–2009.

PUNKT	ÅR	dN [m]	dE [m]	Avstand [m]	Retning [g gon]	dH [m]
BL-1	2005-06	0.0002	-0.0030	0.003	304.238	-0.0023
BL-1	2006-07	0.0036	0.0029	0.005	43.170	-0.0009
BL-1	2007-09	-0.0024	-0.0001	0.002	202.651	0.0060
BL-2	2005-06	-0.0014	0.0007	0.002	170.483	0.0034
BL-2	2006-07	0.0007	0.0019	0.002	77.528	-0.0073
BL-2	2007-09	-0.0001	0.0008	0.001	107.917	0.0102
BL-3	2005-06	0.0028	0.0013	0.003	27.672	0.0092
BL-3	2006-07	0.0025	-0.0013	0.003	369.473	-0.0129
BL-3	2007-09	-0.0069	0.0024	0.007	178.690	0.0040

Tabell 6: Fremste Blåhornet, endring mellom år 2005–2009.

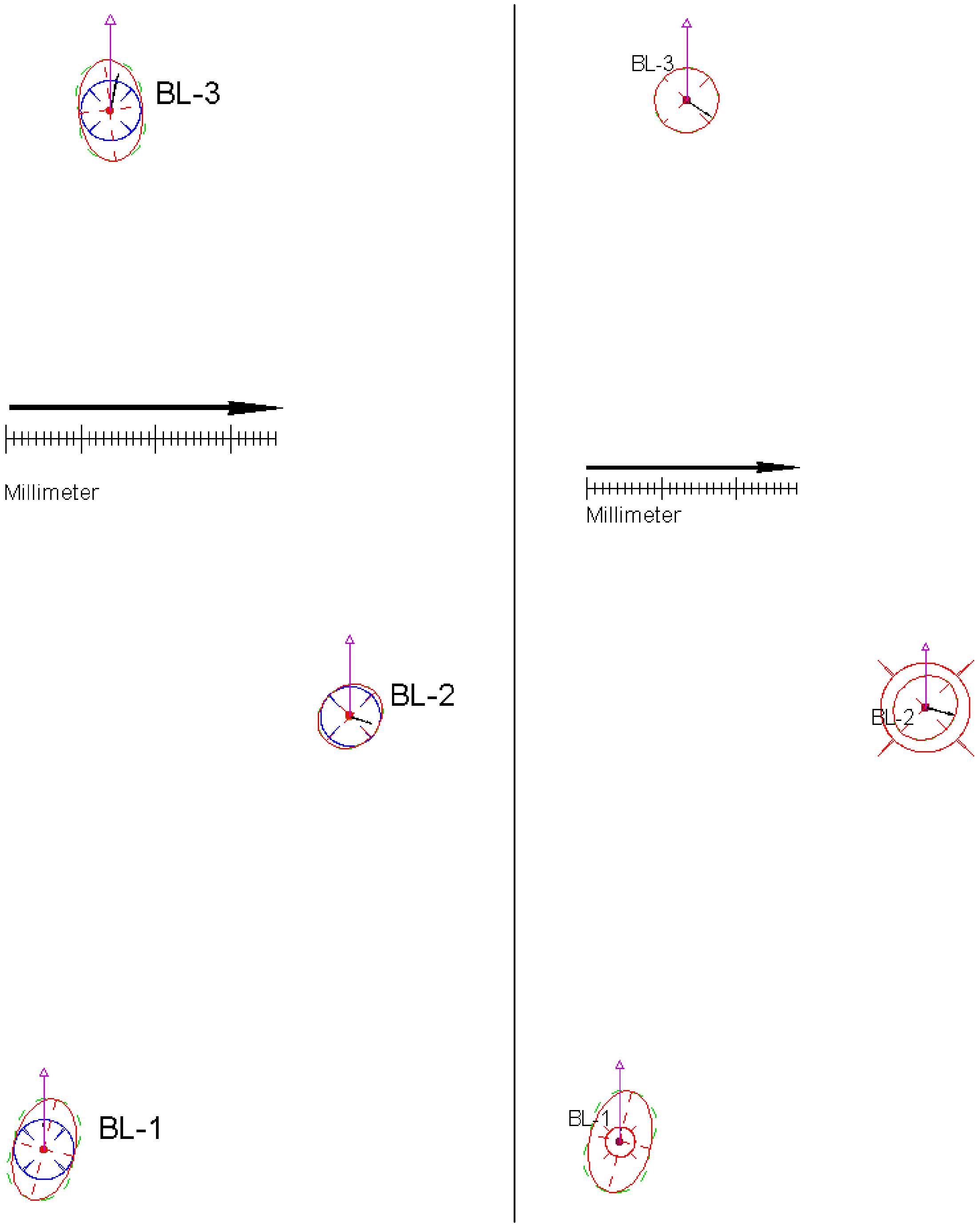

Figur 9: Endringar i grunnriss og høgder for 2005–07 til venstre, 2005–09 til høgre, med konfidensellipser (horisontal) og stolpe (vertikal). Blå sirklar indikerer senking, raude heving.

Furneset

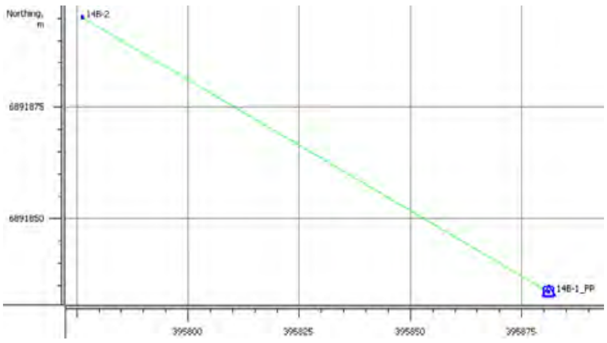

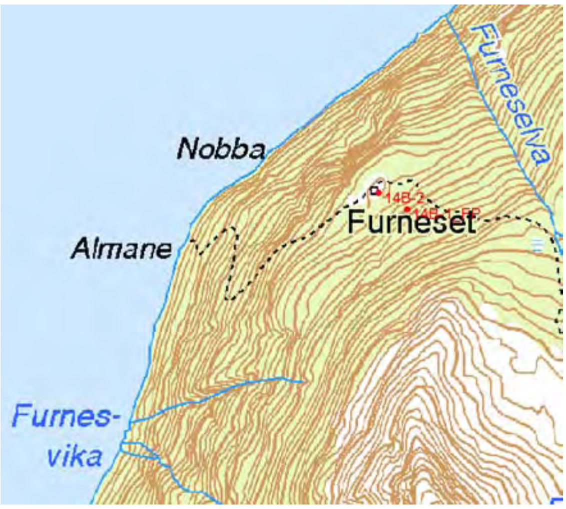

Figur 10: Vektor og plassering på kart (Sk–N50).

Punktgrunnlag
To punkt vart etablert i 2006. Eitt punkt i fast fjell i bratt skråning ovanfor gardstunet på Furneset, og eitt punkt i fjellknaus like ved husa på garden (figur 10). I 2007 er punkta målt om att.

Resultat – endringar, 2007
Resultatkoordinatane for punkt 14-B2 samsvarar i 2007 godt med det som vart funne i 2006 (tabell 7, figur 11). Det er berre ein enkeltvektor som ligg til grunn for resultatet, men det er så godt samsvar at fei på det næraste kan utelatast. Skilnadane mellom dei to åra kan forklarast med tilfeldig målestøy.

Konklusjon
Det kan ikkje påvisast rørsle i punktet.

PUNKT	ÅR	N	E	H	sN	sE	sH	dN	dE	Avstand	Retning	dH
14B-1_FP	2007	6891833.390	395881.126	553.044								
14-B2	2006	6891896.040	395775.216	492.601	0.001	0.000	0.001					
14-B2	2007	6891896.039	395775.216	492.602	0.001	0.000	0.001	-0.001	-0.001	0.001	223.375	0.001

Tabell 7: Koordinatar og endringar for punkt på Furneset 2006–07.

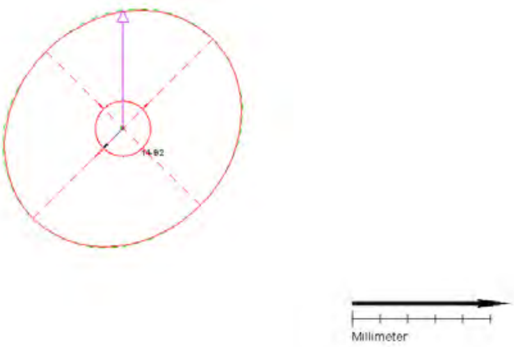

Figur 11: Endringar i punktet 14-B2, 2006–07.

Gikling

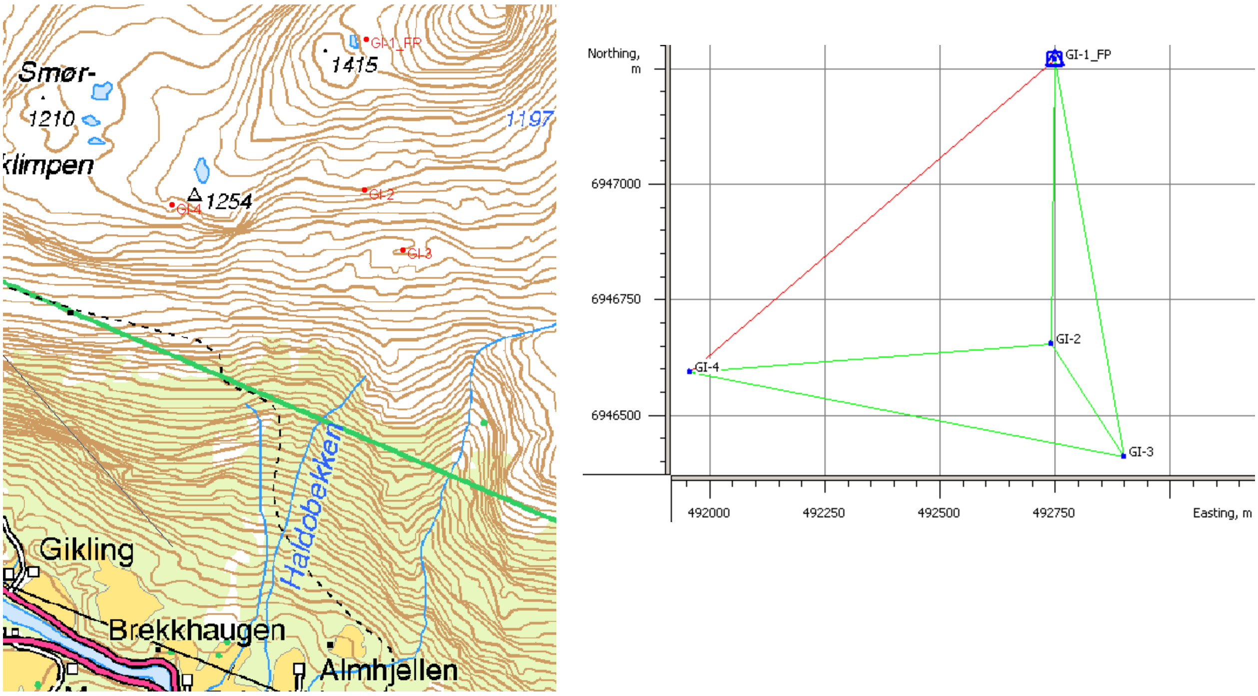

Figur 12: Vektorriss og kart (Sk-N50).

Punktgrunnlag
I 2007 er det etablert tre nye punkt på potensielt ustabile blokker på kanten ned mot dalen ovanfor Gikling, og eitt fastpunkt på platået bak (figur 12). Fastpunktet er fastlagt ved absolutt presis metode, dei andre punkta er rekna relativt til fastpunktet ved vektormålingar. Punkta er målt om i 2008, 2009 og 2011.

Resultat - endring
Resultata er synt i tabellar 8 og 9 og endringar grafisk i figur 13. Målingane i alle åra er gode, det er til dels lange observasjonstider, meir enn to timar og det gir ved støyfrie observasjonar overestimert presisjon, dvs urealistisk låge standardavvik.

I 2011 var dei meteorologiske tilhøva ei utfordring. Målingane vart utført på ein dag med mild svært fuktig luft (det var skodde i lågare deler over heile fylket), og resultat ut frå standard prosessering med normalatmosfære (50% RH) ga til resultat heving på fleire cm i punkta på Gikling. Resultata som er gitt i rapporten er basert på relativ luftråme på 70%. Dette verdet gir ”fornuftige” resultat på høgder for alle punkta, og er i tillegg eit rimeleg verde ut frå meteorologiske observasjonar på Sunndalsøra (90% kl 08 og 66% kl 14) og Mannen i Romsdal (81 % heile dagen). Målingane vart utfør i tida 08–10, og det var klart fuktigare lengre vest i dalen, med meir skodde. Høgare relativ luftfukt gir setningar i alle punkt og tilsvarande gir lågare fukt heving i alle punkt. Horisontale koordinatar vert lite påverka av endringar i meteorologiske parametrar, men nordkoordinat kan endre seg i storleik ±1 mm. Endring av meteorologiske standardverde påverkar resultata systematisk, og introduserer ei ekstra uvisse i resultata, men i dette tilfellet er det klare indikasjonar på at det ikkje var standard meteorologiske tiløve under målinga, og bruka verde er sannsynlege.

Resultata mellom 2007 og 2008 indikerte signifikante endringar i planet i alle tre punkta, om enn små endringar i planet (ca. 5 mm). I høgd var det signifikant setning i punkta GI-2 og GI-3 på meir enn 1 cm.

Fram til 2011 er det framleis teikn til endringar i dei to punkta, men mindre enn den fyrste målinga indikerte. Dei to punkta syner ein trend i horisontal endring over fleire år som indikerer rørsle. Statistisk er det klart signifikant endring, men ein må her ta omsyn til at det er lange observasjonstider og svært små estimerte standardavvik i resultata og dermed tilsvarande låge grenser for signifikant endring.

Konklusjon
Det er teikn til rørsle i punkta GI-2 og GI-3, med årleg endring i storleik 2–3 mm i GI-2 og noko mindre i GI-3. For GI-4 er det ikkje klare teikn til rørsle.

PUNKT	År	N (UTM)	E (UTM)	H (ell.)	σN [m]	σE [m]	σH [m]	dN [m]	dE [m]	Avst. [m]	Retning [^{g} gon]	dH [m]
GI-FP	FP	6947270.135	492750.056	1456.196								
GI-2	2007	6946653.8345	492742.2087	1240.8316	0.0007	0.0006	0.0016					
GI-2	2008	6946653.8288	492742.2090	1240.8199	0.0002	0.0001	0.0004	-0.006	0.000	**0.006**	196.65	**-0.012**
GI-2	2009	6946653.8282	492742.2059	1240.8194	0.0005	0.0004	0.0010	-0.006	-0.003	**0.007**	226.62	**-0.012**
GI-2	2011	6946653.8222	492742.2083	1240.8179	0.0003	0.0002	0.0005	-0.012	0.000	**0.012**	202.07	**-0.014**
GI-3	2007	6946409.7674	492898.8172	1106.6376	0.0008	0.0007	0.0017					
GI-3	2008	6946409.7628	492898.8161	1106.6246	0.0002	0.0001	0.0004	-0.005	-0.001	**0.005**	214.94	**-0.013**
GI-3	2009	6946409.7630	492898.8137	1106.6249	0.0005	0.0004	0.0010	-0.004	-0.003	**0.006**	242.78	**-0.013**
GI-3	2011	6946409.7603	492898.8143	1106.6271	0.0003	0.0002	0.0005	-0.007	-0.003	**0.008**	224.69	**-0.011**
GI-4	2007	6946592.4316	491956.9424	1282.3409	0.0012	0.0010	0.0025					
GI-4	2008	6946592.4280	491956.9457	1282.3378	0.0002	0.0001	0.0004	-0.004	0.003	**0.005**	152.77	**-0.003**
GI-4	2009	6946592.4270	491956.9448	1282.3428	0.0005	0.0004	0.0011	-0.005	0.002	**0.005**	169.39	**0.002**
GI-4	2011	6946592.4306	491956.9459	1282.3385	0.0003	0.0002	0.0006	-0.001	0.003	**0.004**	117.72	**-0.002**

Tabell 8: Koordinatar og endring frå fyrste måling for punkta på Gikling.

PUNKT	ÅR	dN [m]	dE [m]	Avstand [m]	Retning [^{g} gon]	dH [m]
GI-2	2007-08	-0.006	0.000	**0.006**	196.65	**-0.012**
GI-2	2008-09	-0.001	-0.003	**0.003**	287.83	**0.000**
GI-2	2009-11	-0.006	0.002	**0.006**	175.78	**-0.002**
GI-3	2007-08	-0.005	-0.001	**0.005**	214.94	**-0.013**
GI-3	2008-09	0.000	-0.002	**0.002**	305.29	**0.000**
GI-3	2009-11	-0.003	0.001	**0.003**	186.08	**0.002**
GI-4	2007-08	-0.004	0.003	**0.005**	152.77	**-0.003**
GI-4	2008-09	-0.001	-0.001	**0.001**	246.65	**0.005**
GI-4	2009-11	0.004	0.001	**0.004**	18.88	**-0.004**

Tabell 9: Endring mellom målingar for punkta på Gikling.

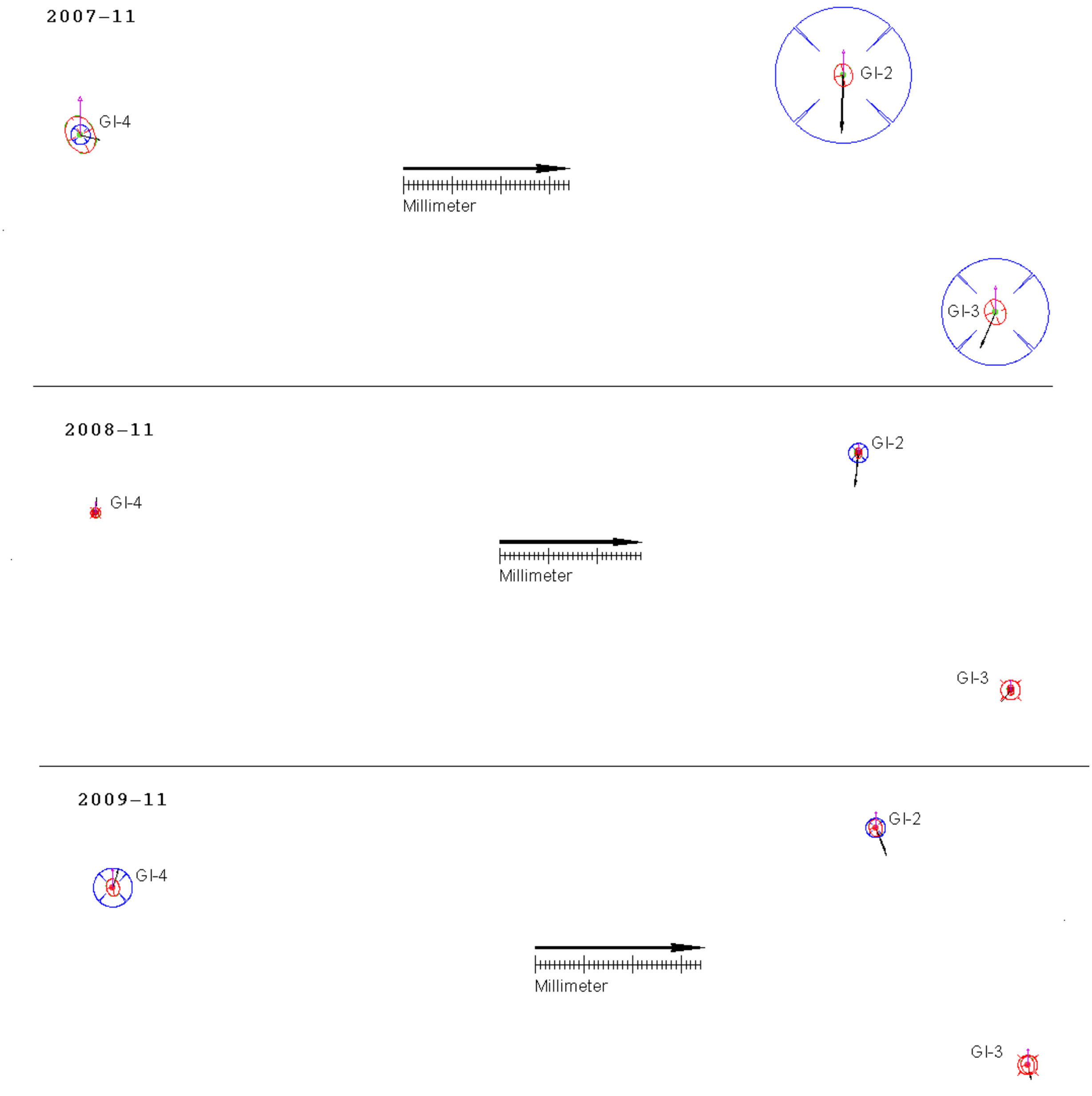

Figur 13: Grafisk framstilling av endring i punkta på Gikling 2007–11 (øvst), 2008–11 (midten) og 2009–11 (nedst), med konfidensnivå for 99%. Grunnriss (pil), høgde (sirkel). Blå sirklar indikerer setning.

Haddalura

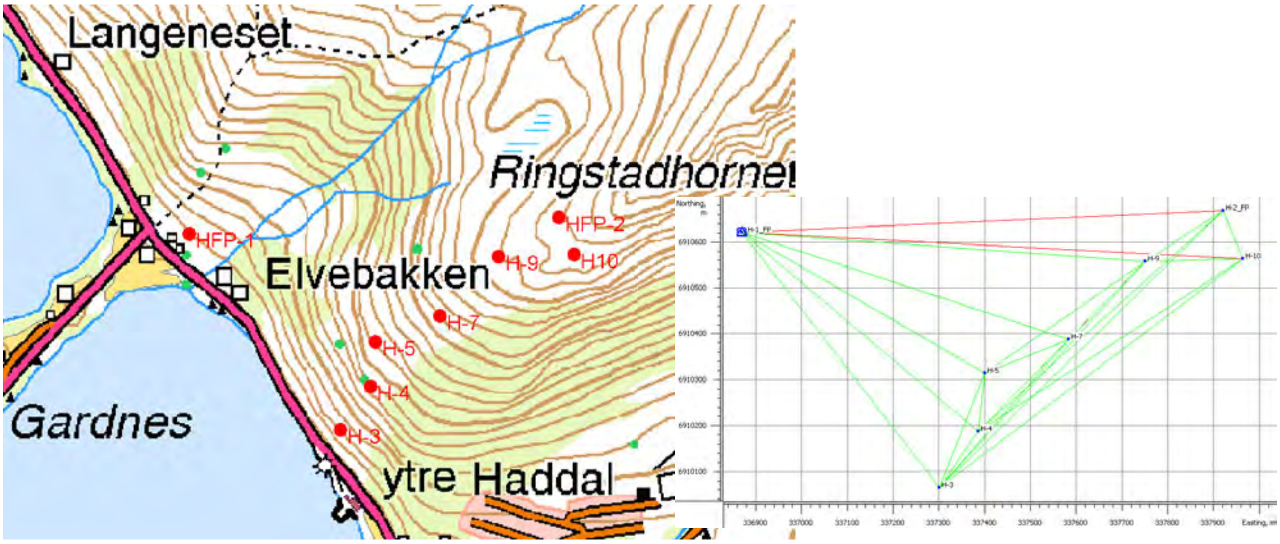

Figur 14: Vektorriss og kart (Sk-N50).

Punktgrunnlag
I 2005 vart det etablert seks punkt på potensielt ustabile blokker i Haddalura i tillegg til to fastpunkt (figur 14). Fastpunkta er fastlagt ved absolutt presis metode, og relative vektor mellom punkta i 2009. Dei andre punkta er rekna relativt til fastpunkta ved vektormålingar. Resultata syner god presisjon.

Resultat - endring
Resultata er synt i tabell 10 og endringar grafisk i figur 15. Resultata indikerer knapt signifikante endringar. Eitt punkt har heving så vidt over grense for signifikans, men det er lite som talar for at dette er reell endring. I plan er det ingen signifikante endringar.

Konklusjon
Det er lite teikn til rørsle i punkta i Haddalura.

PUNKT	År	N (UTM)	E (UTM)	H (ell.)	σN [m]	σE [m]	σH [m]	dN [m]	dE [m]	Avst. [m]	Retning [^{g} gon]	dH [m]
H-1_FP	FP	6910621.7610	336869.8210	94.7960								
H-2_FP	FP	6910668.8045	337920.9825	501.1846								
H-3	2005	6910065.0164	337300.6932	115.5070	0.0012	0.0010	0.0027					
H-3	2009	6910065.0186	337300.6923	115.5156	0.0007	0.0006	0.0014	0.002	-0.001	**0.002**	375.28	**0.009**
H-4	2005	6910187.7642	337385.6315	222.5031	0.0012	0.0010	0.0026					
H-4	2009	6910187.7661	337385.6330	222.5134	0.0007	0.0005	0.0013	0.002	0.001	**0.002**	42.54	**0.010**
H-5	2005	6910314.8696	337400.3318	276.6267	0.0011	0.0010	0.0024					
H-5	2009	6910314.8707	337400.3322	276.6338	0.0008	0.0008	0.0017	0.001	0.000	**0.001**	22.20	**0.007**
H-7	2005	6910387.7566	337583.6651	366.3850	0.0012	0.0009	0.0022					
H-7	2009	6910387.7583	337583.6665	366.3885	0.0009	0.0007	0.0017	0.002	0.001	**0.002**	43.86	**0.004**
H-9	2005	6910557.3137	337750.8352	462.9283	0.0010	0.0007	0.0020					
H-9	2009	6910557.3144	337750.8366	462.9287	0.0006	0.0005	0.0012	0.001	0.001	**0.002**	70.48	**0.000**
H10	2005	6910562.9172	337964.7820	493.0369	0.0012	0.0008	0.0019					
H-10	2009	6910562.9177	337964.7822	493.0340	0.0007	0.0005	0.0013	0.001	0.000	**0.001**	24.22	**-0.003**

Tabell 10: Koordinatar og endring frå fyrste måling for punkta i Haddalura.

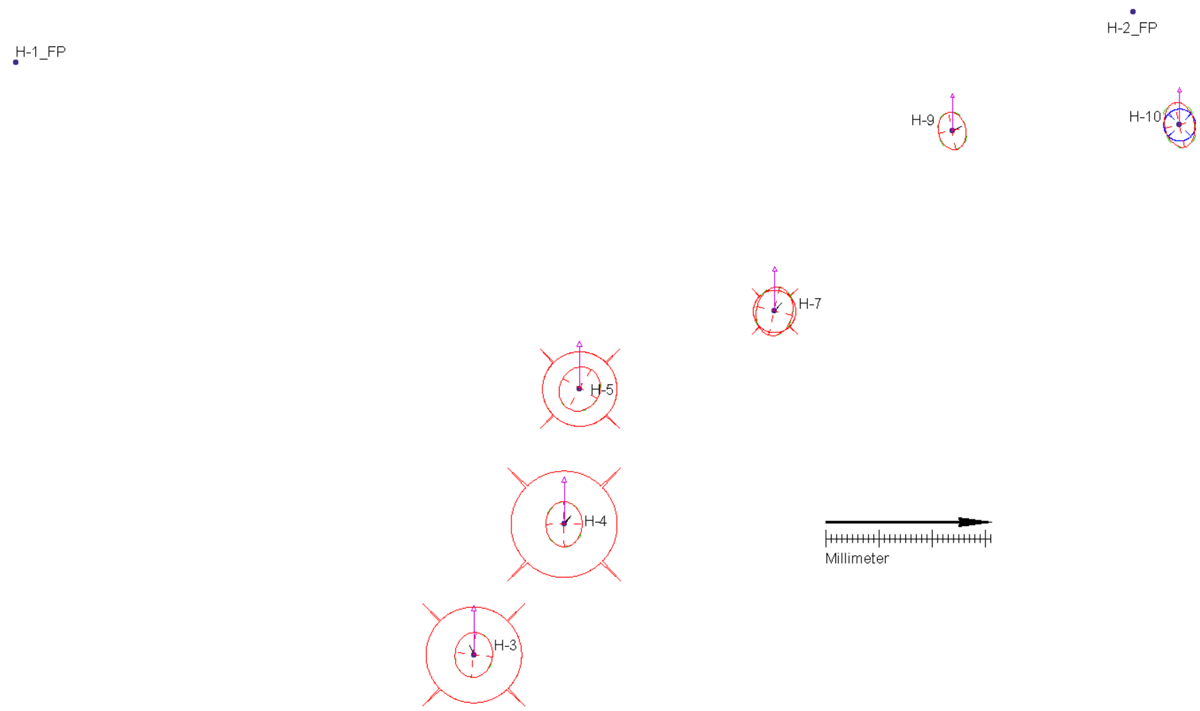

Figur 15: Grafisk framstilling av endring i punkta i Haddalura 2005–09, med konfidensnivå for 99%. Grunnriss (pil), høgde (sirkel). Raude sirklar indikerer heving.

Hegguraksla

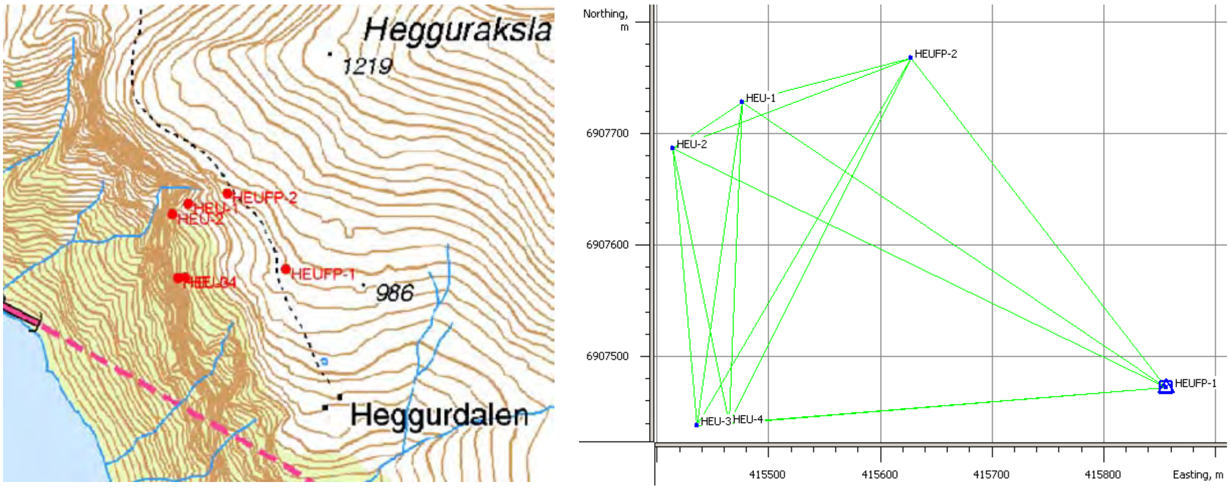

Figur 16: Plassering av punkt (Sk-N50) og riss over vektormålingar i Hegguraksla.

Punktgrunnlag
I Hegguraksla vart det i august 2005 sett ut to fastpunkt i ca. 980 meters høgd, og fire punkt i Hegguraksla, to på utsida av markerte sprekker, og to innanfor sprekkene (figur 16). Plasseringa av punkta er til dels lite optimal for GPS-måling, og serleg punktet HEU-4 har svært dårleg horisont for GPS-måling. Dette gjer at forventa presisjon for dette punktet og i noko grad HEU-2 er lågare enn for dei andre. Punkta vart målt om att i oktober 2005 og sidan i august 2006, 2007 og 2008.

Resultat – endringar, 2008
Tidlegare resultat har synt enkelte signifikante endringar i punkta, men det har vore til dels sprikande resultat (tabell 11, figur 17). HEU-3 er punktet som har peika seg ut til å ha mogeleg rørsle, men målingane i 2008 stadfestar ikkje dette. Resultata i 2008 er meir usikre enn fleire av dei tidlegare på grunn av uheldig satellittgeometri. Koordinatresultata for alle punkta er relativt stabile, og tilseier ikkje at det er klar rørsle i punkta.

Konklusjon
Tidlegare påvist rørsle i punktet HEU-3 er ikkje stadfesta, og det er ikkje klare teikn til rørsle i nokon av punkta i Hegguraksla.

PUNKT	Tidspkt	N	E	H	sN	sE	sH	dN	dE	Dist	Retn	dH
HEUFP-1	2007	6907472.491	415855.534	1023.320								
HEUFP-2	2007	6907767.222	415627.218	1029.626								
HEU-1	aug.05	6907727.350	415475.906	918.277	0.001	0.001	0.004					
HEU-1	okt.05	6907727.356	415475.908	918.264	0.001	0.001	0.003	0.006	0.002	0.006	20.48	-0.013
HEU-1	2006	6907727.354	415475.908	918.273	0.001	0.001	0.002	0.004	0.002	0.005	28.29	-0.004
HEU-1	2007	6907727.357	415475.906	918.271	0.001	0.001	0.002	0.007	0.000	0.007	0.00	-0.006
HEU-1	2008	6907727.355	415475.907	918.270	0.001	0.001	0.002	0.005	0.001	0.005	14.18	-0.007
HEU-2	aug.05	6907685.878	415414.331	862.179	0.003	0.003	0.004					
HEU-2	okt.05	6907685.882	415414.334	862.166	0.001	0.001	0.002	0.004	0.003	0.005	40.97	-0.013
HEU-2	2006	6907685.880	415414.334	862.175	0.001	0.001	0.003	0.002	0.003	0.004	55.99	-0.004
HEU-2	2007	6907685.883	415414.331	862.176	0.001	0.001	0.002	0.005	0.000	0.005	395.85	-0.003
HEU-2	2008	6907685.878	415414.331	862.186	0.002	0.001	0.003	0.000	0.000	0.000	329.52	0.007
HEU-3	aug.05	6907437.951	415435.271	775.541	0.001	0.001	0.002					
HEU-3	okt.05	6907437.953	415435.272	775.520	0.001	0.001	0.002	0.002	0.001	0.002	29.52	-0.021
HEU-3	2006	6907437.947	415435.270	775.540	0.001	0.001	0.002	-0.004	-0.001	0.004	215.60	-0.001
HEU-3	2007	6907437.949	415435.264	775.541	0.001	0.001	0.002	-0.003	-0.007	0.007	277.57	0.000
HEU-3	2008	6907437.947	415435.270	775.529	0.002	0.001	0.003	-0.004	-0.001	0.004	213.13	-0.012
HEU-4	aug.05	6907439.612	415464.117	794.003	0.001	0.002	0.002					
HEU-4	okt.05	6907439.618	415464.125	793.970	0.001	0.001	0.002	0.006	0.008	0.010	59.03	-0.033
HEU-4	2006	6907439.617	415464.127	793.986	0.001	0.002	0.002	0.005	0.010	0.011	71.78	-0.017
HEU-4	2007	6907439.617	415464.113	793.999	0.002	0.002	0.003	0.005	-0.004	0.007	360.96	-0.004
HEU-4	2008	6907439.617	415464.112	794.000	0.002	0.003	0.005	0.005	-0.005	0.007	350.00	-0.004

Tabell 11: Hegguraksla – målingar 2005–08, resultatkoordinatar og endringar august 2005 til august 2008. Resultata for HEU-4 er usikre.

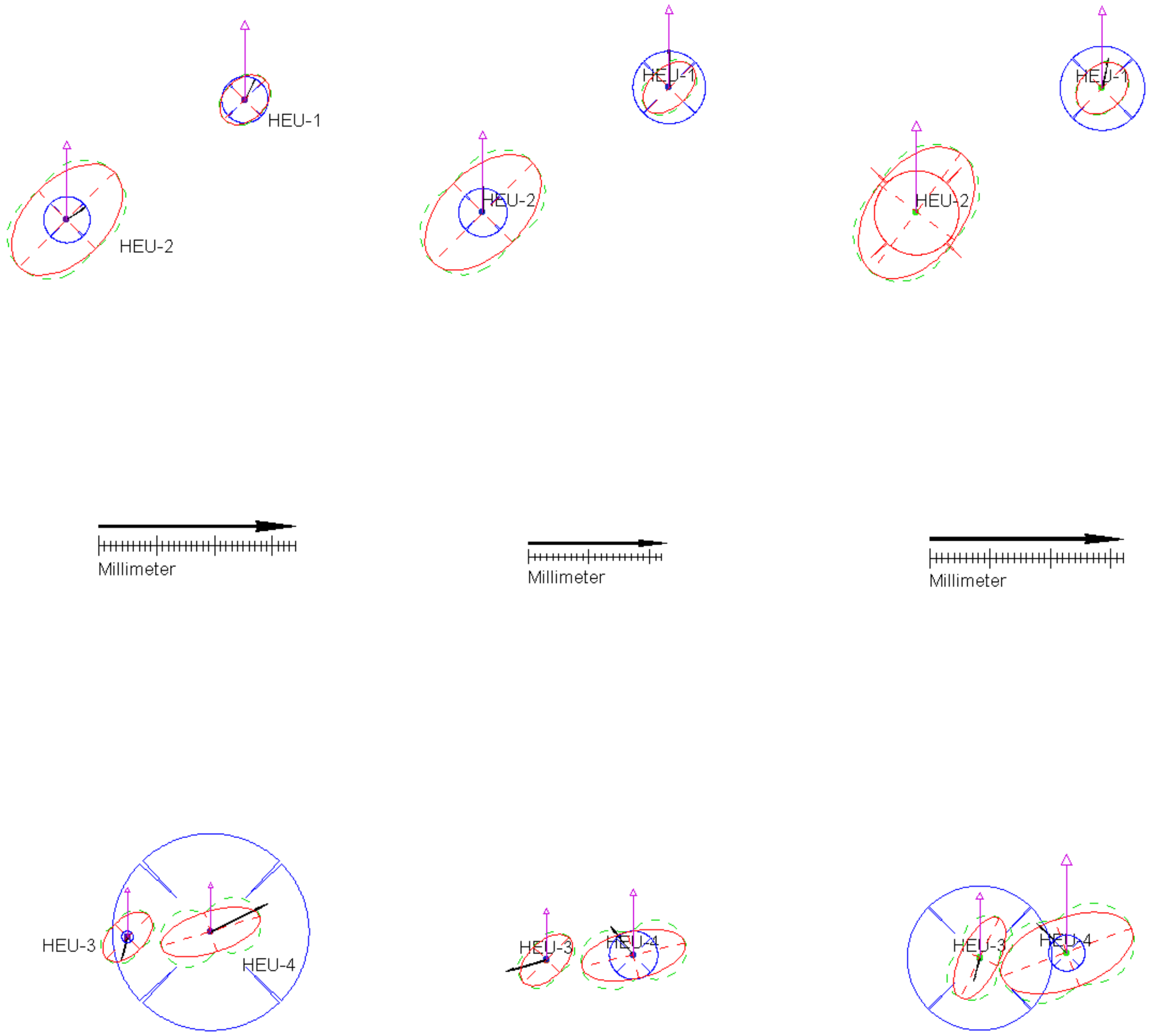

Figur 17: Endringar august 2005–august 2006 (venstre), endring august 2005–07 (midten) og endring 2005–08 (høgre).

Herdalsnibba

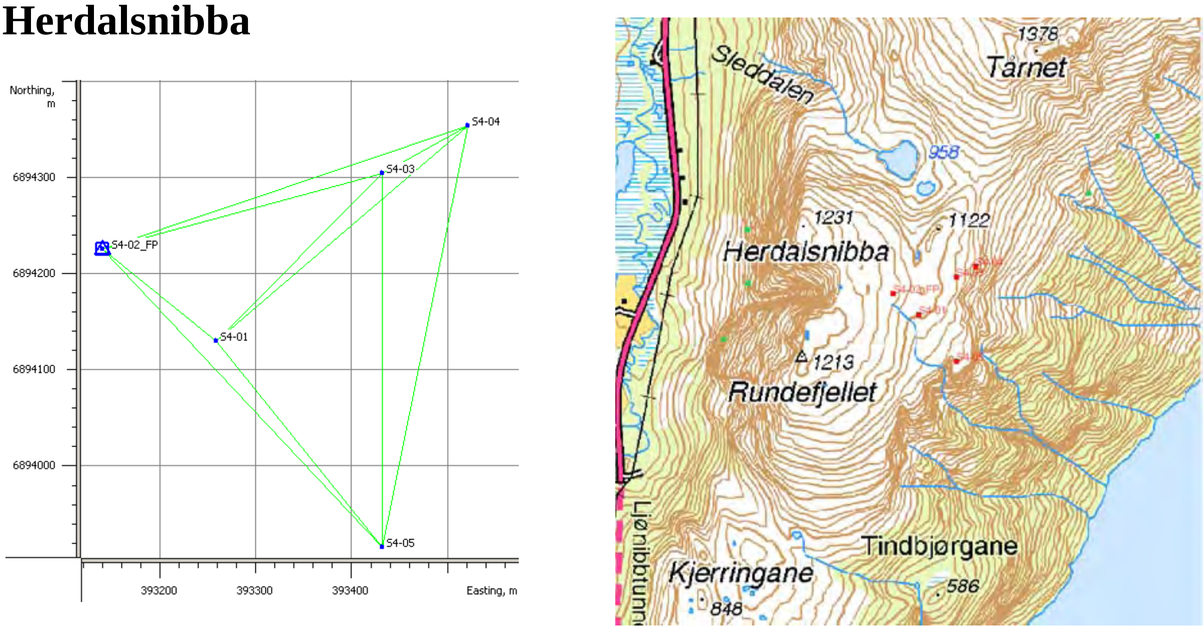

Figur 18: Riss og kart (Sk-N50).

Punktgrunnlag
Fire punkt vart etablert på Herdalsnibba i 2006 (figur 18). Eitt punkt er fastpunkt på lokal topp bak markert søkk (S4-02_FP), og eitt punkt (S4-01) like utanfor søkket. Punkta S4-03 og S4-04 er plassert nedover mot stupkanten, S4-04 på mogeleg blokk som har sige litt ned i høve til fjellet bak. Vegetasjonsdekket på blokka gjer det noko usikkert om punktet er i fjell eller i ei større steinblokk. Det vart i 2010 sett ut og målt inn eit nytt punkt (S4-05) mot SV i området.

Resultat – endringar, 2012
Analysane i 2007 synte at det var klart signifikant horisontal endring i punkt S4-04, og så vidt signifikant endring i S4-01 (tabellar 12 og 13, figur 19). Resultata for seinare år stadfestar ikkje desse endringane. Det kan sjå ut til at resultata for 2006 og 2007 ligg i ytterpunkt i motsette retningar, slik at jamført med andre år peikar endringar i motsette retningar. For perioden 2008–12 er det ingen signifikante endringar.

Konklusjon
Dei nyaste målingane gir ikkje klare teikn til at det er rørsle i nokon av punkta på Herdalsnibba, men for å få eit sikrare grunnlag bør det eventuelt målast fleire gonger.

PUNKT	År	N (UTM)	E (UTM)	H (ell.)	σN [m]	σE [m]	σH [m]	dN [m]	dE [m]	Avst. [m]	Retning [^{g} gon]	dH [m]
S4-02_FP	FP	6894225.883	393140.174	1195.559								
S4-01	2006	6894129.9800	393258.5747	1151.2174	0.0006	0.0005	0.0013					
S4-01	2007	6894129.9822	393258.5800	1151.2169	0.0005	0.0005	0.0011	0.002	0.005	0.006	74.95	-0.001
S4-01	2008	6894129.9805	393258.5793	1151.2163	0.0006	0.0004	0.0010	0.000	0.005	0.005	93.11	-0.001
S4-01	2009	6894129.9810	393258.5788	1151.2155	0.0008	0.0007	0.0019	0.001	0.004	0.004	84.77	-0.002
S4-01	2010	6894129.9838	393258.5766	1151.2122	0.0003	0.0005	0.0008	0.004	0.002	0.004	29.52	-0.005
S4-01	2012	6894129.9824	393258.5785	1151.2115	0.0005	0.0005	0.0011	0.002	0.004	0.004	64.14	-0.006
S4-03	2006	6894303.9330	393432.2193	1121.3613	0.0008	0.0007	0.0020					
S4-03	2007	6894303.9333	393432.2226	1121.3555	0.0007	0.0006	0.0016	0.000	0.003	0.003	94.23	-0.006
S4-03	2008	6894303.9329	393432.2223	1121.3574	0.0008	0.0005	0.0013	0.000	0.003	0.003	102.12	-0.004
S4-03	2009	6894303.9333	393432.2215	1121.3532	0.0008	0.0007	0.0019	0.000	0.002	0.002	91.37	-0.008
S4-03	2010	6894303.9344	393432.2200	1121.3547	0.0004	0.0005	0.0008	0.001	0.001	0.002	29.52	-0.007
S4-03	2012	6894303.9341	393432.2204	1121.3571	0.0005	0.0005	0.0012	0.001	0.001	0.002	50.00	-0.004
S4-04	2006	6894353.9962	393520.7547	1079.9456	0.0012	0.0006	0.0019					
S4-04	2007	6894353.9979	393520.7659	1079.9496	0.0005	0.0005	0.0012	0.002	0.011	0.011	90.41	0.004
S4-04	2008	6894354.0018	393520.7600	1079.9473	0.0008	0.0005	0.0012	0.006	0.005	0.008	48.25	0.002
S4-04	2009	6894353.9969	393520.7607	1079.9409	0.0009	0.0008	0.0021	0.001	0.006	0.006	92.61	-0.005
S4-04	2010	6894353.9988	393520.7596	1079.9457	0.0004	0.0005	0.0008	0.003	0.005	0.006	68.94	0.000
S4-04	2012	6894353.9962	393520.7604	1079.9488	0.0005	0.0005	0.0011	0.000	0.006	0.006	100.00	0.003
S4-05	2010	6893915.0623	393432.3114	1067.2570	0.0004	0.0005	0.0008		Nytt punkt 2010			
S4-05	2012	6893915.0631	393432.3131	1067.2540	0.0005	0.0005	0.0011	0.001	0.002	0.002	72.00	-0.003

Tabell 12: Herdalsnibba, koordinatar og endring 2006–12 i høve til fyrste måling.

PUNKT	ÅR	dN [m]	dE [m]	Avstand [m]	Retning [^{g} gon]	dH [m]
S4-01	2006-07	0.002	0.005	**0.006**	**74.95**	-0.001
S4-01	2007-08	-0.002	-0.001	**0.002**	**224.87**	-0.001
S4-01	2008-09	0.001	0.000	**0.001**	**350.00**	-0.001
S4-01	2009-10	0.003	-0.002	**0.004**	**357.60**	-0.003
S4-01	2010-12	-0.001	0.002	**0.002**	**140.43**	-0.001
S4-03	2006-07	0.000	0.003	**0.003**	**94.23**	-0.006
S4-03	2007-08	0.000	0.000	**0.000**	**240.97**	0.002
S4-03	2008-09	0.000	-0.001	**0.001**	**329.52**	-0.004
S4-03	2009-10	0.001	-0.002	**0.002**	**340.28**	0.002
S4-01	2010-12	0.000	0.000	**0.000**	**140.97**	0.002
S4-04	2006-07	0.002	0.011	**0.011**	**90.41**	0.004
S4-04	2007-08	0.004	-0.006	**0.007**	**337.18**	-0.002
S4-04	2008-09	-0.005	0.001	**0.005**	**190.97**	-0.006
S4-04	2009-10	0.002	-0.001	**0.002**	**366.59**	0.005
S4-01	2010-12	-0.003	0.001	**0.003**	**181.00**	0.003
S4-03	2010-12	0.001	0.002	**0.002**	**72.00**	-0.003

Tabell 13: Herdalsnibba, endring mellom målingar 2006–12.

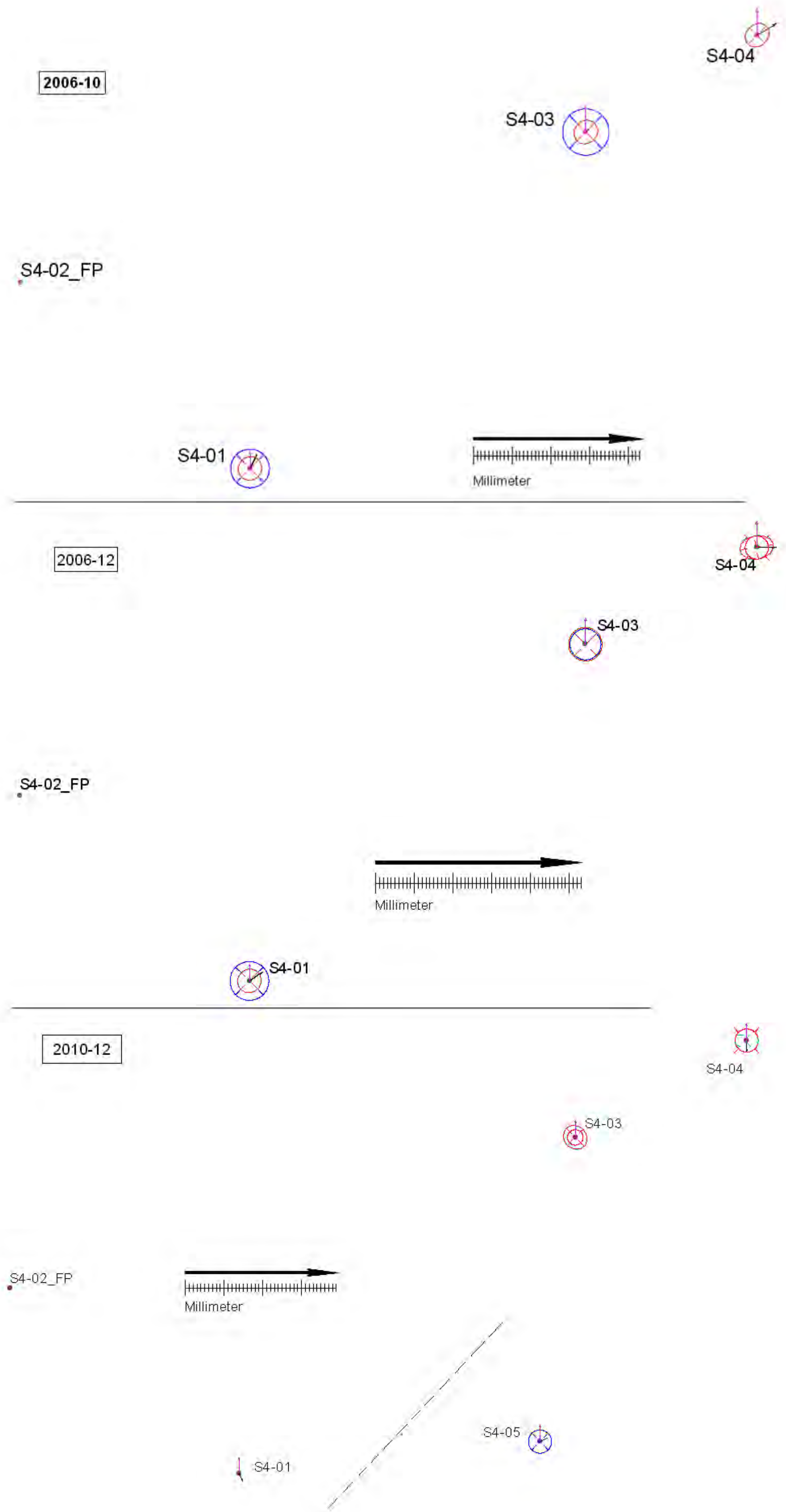

Figur 19: Endringar i grunnriss og høgder for ulike år, med konfidensellipser (horisontal) og stolpe (vertikal). Blå sirklar indikerer senking, raude heving. 2010–12 nedst inkluderer det nye punktet S4-05 lengs sør – plassering er ikkje korrekt på figuren.

Kvitfjellet

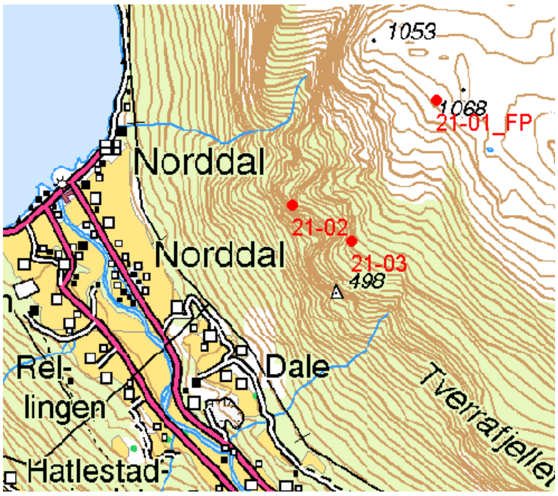

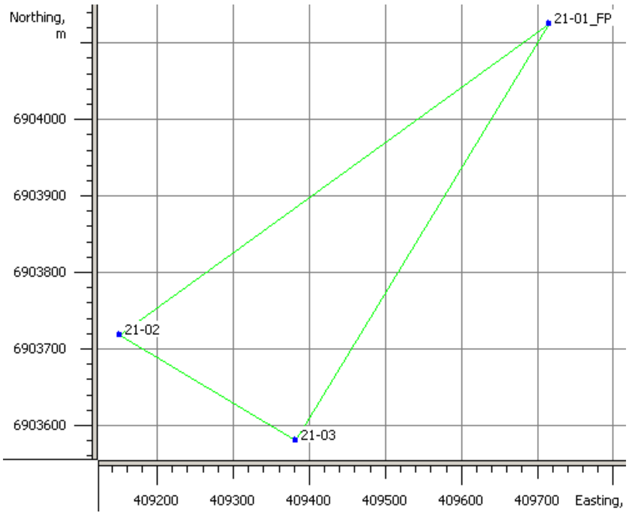

Figur 20: Vektornett og plassering av punkt ved Kvitfjellet (Kart Sk-N50).

Punktgrunnlag
I 2005 vart to punkt etablert ved Kvitfjellet. Eitt fastpunkt i fjellrygg på topplatået NV for Kyrkjefjellet (21-01), og eitt punkt på mogeleg blokk i fjellsida ned mot bygda (21-02) (figur 20). Dei to punkta vart målt om i 2006, og eitt nytt punkt sett ut på mogeleg blokk lengre mot sør (21-03). I 2007 vart ikkje punktet 21-02 målt sidan helikopteret ikkje kunne lande der. I 2011 er alle punkta målt om.

Fastpunktet i Kvitfjellet (21-01_FP) er litt problematisk sidan bolten er så skeiv at trefot ikkje alltid kan stillast i lodd på punktet. Det har difor i 2006 og 2007 vore nytta antenne direkte på bolt i punktet, medan det ved eit mistak vart nytta vanleg oppstilling med trefot i 2011 (som i 2005). Sentreringsfeil i fastpunktet som skuldast skeiv bolt kan utgjere 2–8 mm i planfeil (utan/med trefot), og gjer tolking av resultata ekstra usikre.

Resultat – endringar, 2011
Resultatet er synt i tabellar 14 og 15 og grafisk i figurere 21 og 22. Resultata er ekstra usikre sidan fastpunktet på toppen har så skeiv bolt at det ikkje er råd å stille sentrisk over bolten. I 2005 og 2011 vart det stilt opp antenne på trefot slik at den kan vere eksentrisk i høve til bolten. I 2006 og 2007 vart antenna skruva direkte på bolten slik at eventuell sentreringsfeil er så liten som råd. Dei ulike oppstillingane i fastpunktet kan ha påverka resultata men storleik og retning på dette er ukjent. I 2005 og 2007 er det berre einskildvektorar til grunn for resultata og det gir mangelfull kontroll.

Feil som skuldast ulik sentrering ved målingane kan vere forklaringa til dei variable endringane som kjem fram mellom dei ulike åra. Resultata må karakteriserast som noko usikre, og einaste klare trend ved alle målingar er ei lita heving i dei to punkta..

Konklusjon
Det er lite grunnlag til å slå fast om noko av punkta 21-02 og 21-03 verkeleg har rørsle, men resultata indikerer at det er endringar i koordinatane sjølv om det er usikre resultat.

Storleiken til endringane er ikkje større enn det som kan ha si årsak i feil i oppstillinga i fastpunktet, og konklusjon om mogeleg endring er difor ekstra usikker. At årlege endringar peikar i ulike og til dels motsette retningar kan og indikere påverking frå feil i fastpunktet (eksentrisk antenne).

PUNKT	År	N	E	H	sN	sE	sH	dN	dE	Avstand	Retning	dH
21-01_FP	F.P.	6904124.813	409718.403	1068.065								0
21-02	2005	6903718.061	409153.343	633.539	0.002	0.002	0.003					
21-02	2006	6903718.068	409153.345	633.543	0.001	0.001	0.002	0.007	0.002	0.007	20.48	0.0034
21-02	2007	ikkje målt										
21-02	2011	6903718.061	409153.3492	633.5608	0.001	0.0008	0.0019	0.000	0.006	0.006	103.03	0.022
21-03	2006	6903579.001	409386.112	743.302	0.001	0.001	0.002					
21-03	2007	6903579.005	409386.118	743.315	0.001	0.001	0.002	0.004	0.006	0.007	62.04	0.0125
21-03	2011	6903578.996	409386.1166	743.3158	0.001	0.0008	0.0018	-0.005	0.004	0.007	157.76	0.014

Tabell 14: Endring i koordinatar Kvitfjellet 2005–11.

PUNKT	ÅR	dN	dE	Avstand	Retning	dH
21-02	2005-06	0.007	0.002	**0.007**	20.48	**0.003**
21-02	2006-11	-0.007	0.004	**0.008**	167.72	**0.018**
21-03	2006-07	0.004	0.006	**0.007**	62.04	**0.013**
21-03	2007-11	-0.009	-0.001	**0.009**	208.84	**0.001**

Tabell 15: Kvitfjellet, endring mellom målingar frå 2005 til 2011.

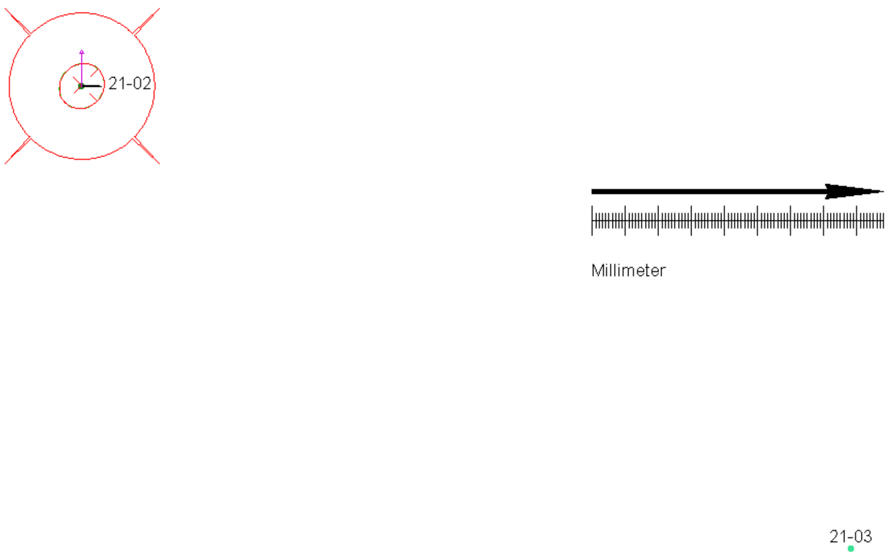

Figur 21: Endring i punkt 21-02, 2005–11 med konfidensnivå for 99%. Grunnriss (pil), høgde (sirkel). Raud sirkel indikerer heving. (Punkt 21-03 vart etablert i 2006).

Figur 22: Endring i punkta, 2006–11 med konfidensnivå for 99%. Grunnriss (pil), høgde (sirkel). Raud sirkel indikerer heving.

Mannen

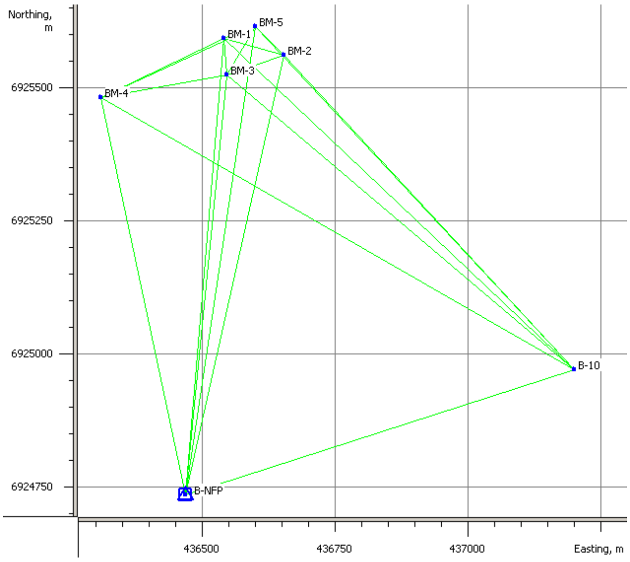

Figur 23: Nett på Mannen. Punkta B-NFP og B-10 frå Børa er med i nettet (frå målingane 2006).

Figur 24: Kart over Børa – Mannen (Sk-N50).

Punktgrunnlag

I 2004 vart det etablert to punkt på Mannen som vart knytt til det same nettet som Børa. I 2007 er det etablert tre nye punkt på Mannen, av desse eitt fastpunkt (figurar 23 og 24).

Resultat - endringar

Resultata er gitt i tabellar 16 og 17 og i figur 25. Etter at fastpunktet BM-4_FP vart etablert er det primært resultat for det lokale nettet på Mannen som er lagt til grunn. Dette reduserer eventuell påverking av vektorar frå Børa med stor høgdeskilnad. I 2008 var det problem med logginga i mottakaren i punktet BM-1, slik at det her berre er logga litt data. Dette gjer resultata i dette punktet vesentleg meir usikre.

Resultata for Mannen syner at punktet BM-5 som vart etablert i 2006 framleis har stor rørsle (jfr. figur 25). Dette punktet ligg på ”sigeblokka” utanfor pinnakelen Mannen. Punktet har utan tvil rørsle, sjølv om endringane i koordinatar varierer litt mellom åra er det utan tvil horisontale endringar på 2–3cm/år og vertikale på 3–4 cm/år i punktet.

For dei andre punkta er det ikkje klare trendar i resultata, og sjølv om enkelte endringar er signifikante er det usikkert om det er utslag ut over støy i målingane.

Konklusjon:
Målingane på Mannen 2006–10 syner at punktet BM-5 har stor rørsle, på 2–3cm i plan og 3–4 cm/år i høgd (senking). For dei andre punkta kan det ikkje påvisast sikker rørsle.

PUNKT	År	N (UTM)	E (UTM)	H (ell.)	σN [m]	σE [m]	σH [m]	dN [m]	dE [m]	Avst. [m]	Retning [^{g} gon]	dH [m]
BM-4_FP	2008	6925480.779	436308.721	1331.414								
BM-1	2004	6925591.5400	436540.1010	1332.6470	0.0010	0.0000	0.0020					
BM-1	2006	6925591.5411	436540.0995	1332.6425	0.0004	0.0003	0.0009	0.001	-0.002	**0.002**	340.28	**-0.005**
BM-1	2007	6925591.5398	436540.0997	1332.6367	0.0005	0.0004	0.0012	0.000	-0.001	**0.001**	290.28	**-0.010**
BM-1	2008	6925591.5468	436540.0976	1332.6609	0.0048	0.0031	0.0147	0.007	-0.003	**0.008**	370.48	**0.014**
BM-1	2009	6925591.5412	436540.0987	1332.6364	0.0006	0.0005	0.0011	0.001	-0.002	**0.003**	330.61	**-0.011**
BM-1	2010	6925591.5413	436540.0980	1332.6386	0.0004	0.0006	0.0009	0.001	-0.003	**0.003**	326.03	**-0.008**
BM-2	2004	6925559.9220	436653.8620	1337.1790	0.0010	0.0000	0.0020					
BM-2	2006	6925559.9245	436653.8628	1337.1777	0.0005	0.0004	0.0010	0.002	0.001	**0.003**	19.72	**-0.001**
BM-2	2007	6925559.9212	436653.8614	1337.1680	0.0005	0.0004	0.0012	-0.001	-0.001	**0.001**	240.97	**-0.011**
BM-2	2008	6925559.9263	436653.8627	1337.1756	0.0011	0.0006	0.0020	0.004	0.001	**0.004**	10.27	**-0.003**
BM-2	2009	6925559.9254	436653.8615	1337.1684	0.0006	0.0005	0.0011	0.003	-0.001	**0.003**	390.70	**-0.011**
BM-2	2010	6925559.9252	436653.8624	1337.1751	0.0004	0.0006	0.0009	0.003	0.000	**0.003**	7.92	**-0.004**
BM-3	2006	6925523.8553	436546.6976	1329.7139	0.0005	0.0003	0.0009					
BM-3	2007	6925523.8551	436546.6976	1329.7066	0.0005	0.0004	0.0012	0.000	0.000	**0.000**	200.00	**-0.007**
BM-3	2008	6925523.8598	436546.6991	1329.7109	0.0011	0.0006	0.0020	0.004	0.002	**0.005**	20.48	**-0.003**
BM-3	2009	6925523.8564	436546.6974	1329.7077	0.0005	0.0004	0.0011	0.001	0.000	**0.001**	388.55	**-0.006**
BM-3	2010	6925523.8575	436546.6969	1329.7111	0.0004	0.0006	0.0010	0.002	-0.001	**0.002**	380.39	**-0.003**
BM-5	2006	6925614.9248	436600.8499	1320.1309	0.0005	0.0004	0.0010					
BM-5	2007	6925614.9397	436600.8764	1320.0862	0.0007	0.0005	0.0014	0.015	0.027	**0.030**	67.39	**-0.045**
BM-5	2008	6925614.9545	436600.9119	1320.0553	0.0011	0.0006	0.0021	0.030	0.062	**0.069**	71.56	**-0.076**
BM-5	2009	6925614.9628	436600.9348	1320.0207	0.0006	0.0004	0.0012	0.038	0.085	**0.093**	73.21	**-0.110**
BM-5	2010	6925614.9688	436600.9534	1319.9894	0.0004	0.0006	0.0010	0.044	0.104	**0.112**	74.41	**-0.142**

Tabell 16: Koordinatar og endringar for punkt på Mannen 2006–08. Resultat for BM-1 og 2 som vart etablert i 2004 er ikkje teke med sidan dei ikkje er relatert til same fastpunkt. BM-4_FP er lokalt fastpunkt. BM-1 i 2008 er usikkert pga. kort observasjonstid.

		Endring mellom målingar				
PUNKT	**ÅR**	**dN [m]**	**dE [m]**	**Avstand [m]**	**Retning [^{g} gon]**	**dH [m]**
BM-1	2004-06	0.001	-0.002	**0.002**	340.28	**-0.005**
BM-1	2006-07	-0.001	0.000	**0.001**	190.28	**-0.006**
BM-1	2007-08	0.007	-0.002	**0.007**	381.45	**0.024**
BM-1	2008-09	-0.006	0.001	**0.006**	187.65	**-0.024**
BM-1	2009-10	0.000	-0.001	**0.001**	309.03	**0.002**
BM-2	2004-06	0.002	0.001	**0.003**	19.72	**-0.001**
BM-2	2006-07	-0.003	-0.001	**0.004**	225.54	**-0.010**
BM-2	2007-08	0.005	0.001	**0.005**	15.89	**0.008**
BM-2	2008-09	-0.001	-0.001	**0.002**	259.03	**-0.007**
BM-2	2009-10	0.000	0.001	**0.001**	113.92	**0.007**
BM-3	2006-07	0.000	0.000	**0.000**	200.00	**-0.007**
BM-3	2007-08	0.005	0.002	**0.005**	19.67	**0.004**
BM-3	2008-09	-0.003	-0.002	**0.004**	229.52	**-0.003**
BM-3	2009-10	0.001	-0.001	**0.001**	372.84	**0.003**
BM-5	2006-07	0.015	0.027	**0.030**	67.39	**-0.045**
BM-5	2007-08	0.015	0.035	**0.038**	74.85	**-0.031**
BM-5	2008-09	0.008	0.023	**0.024**	77.86	**-0.035**
BM-5	2009-10	0.006	0.019	**0.020**	80.13	**-0.031**

Tabell 17: Endringar mellom målingar for punkt på Mannen 2004–10. Den store variasjonen i høgd i BM-1 er ikkje reell. Det skuldast svake målingar i 2008. Det er berre punktet BM-5 som syner konsistente endringar over tid.

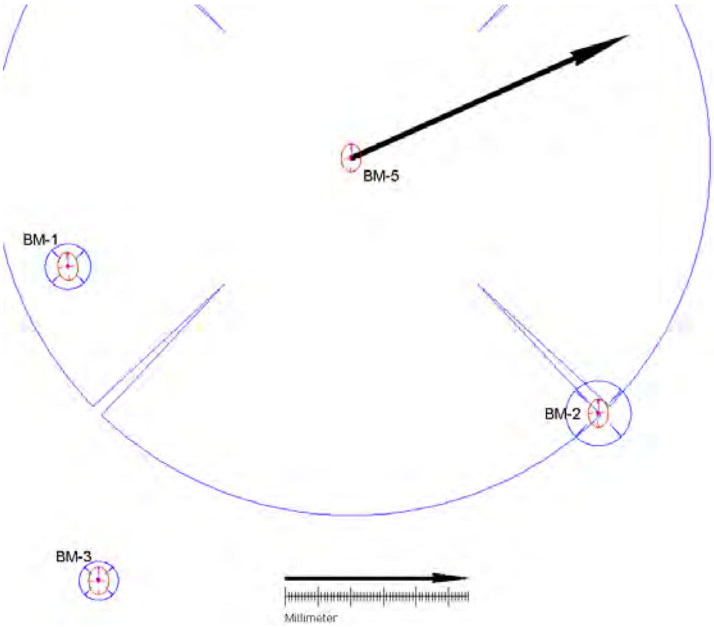

2006-2009

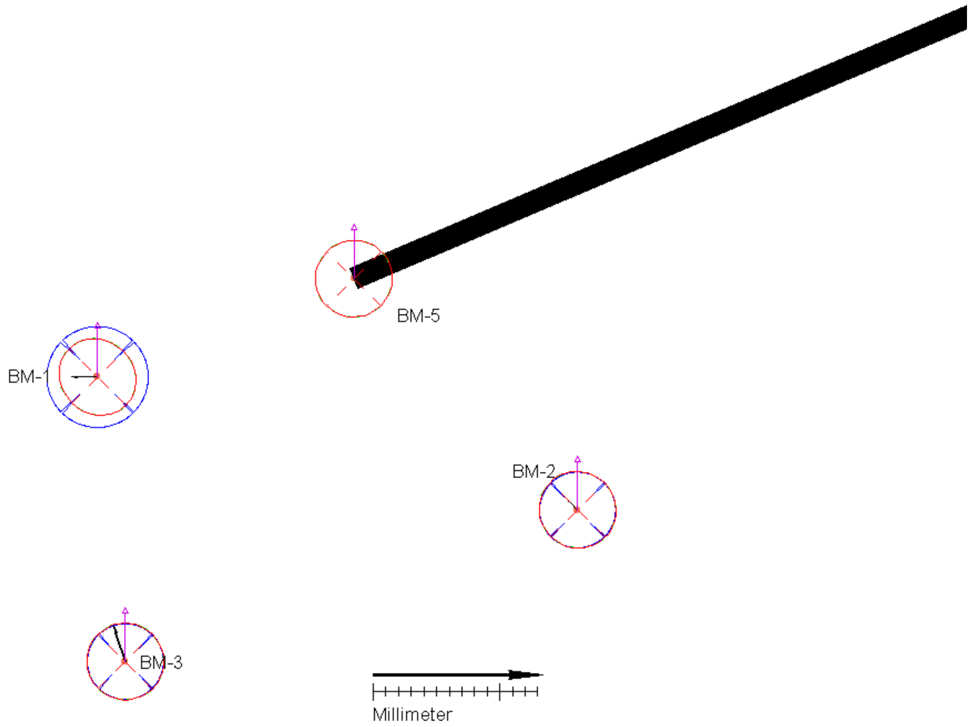

2006-2010

Figur 25: Grafisk endring grunnriss og høgde for punkta på Mannen, 2006–2009 (øvst) og 2006–2010 (nedst). Figuren for 2006–10 er i meir detaljert skala slik at horisontal og vertikal endring i punktet BM-5 går utanfor figuren. Fastpunktet på Mannen (BM-4), etablert 2006 er ikkje med på figuren.

Middagstinden

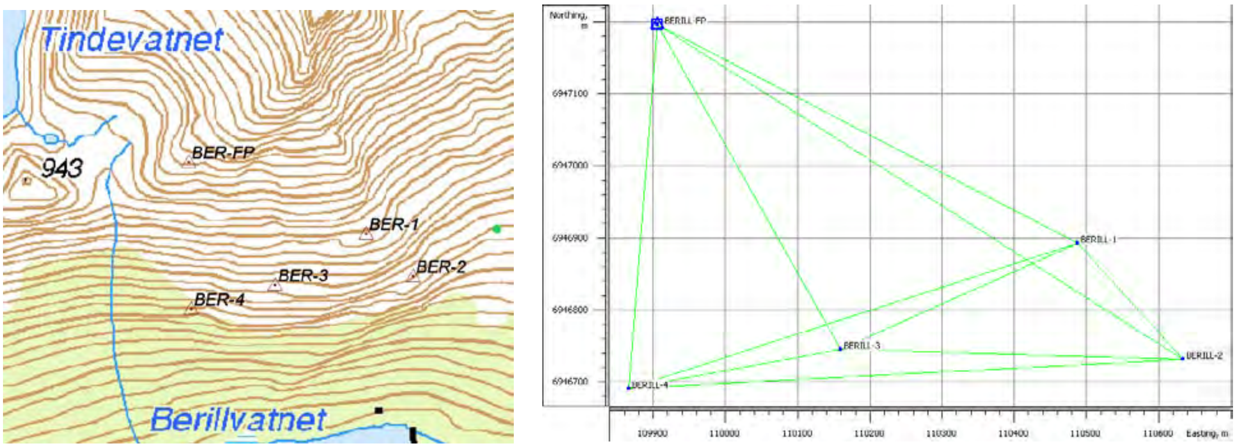

Figur 26: Vektorriss og kart (Sk-N50).

Punktgrunnlag

I 2008 er det etablert tre nye punkt på potensielt ustabile blokker i dalsida ned mot Berillvatnet, og eitt fastpunkt på sør-ryggen til Middagstinden (figur 26). Fastpunktet er fastlagt ved absolutt presis metode, dei andre punkta er rekna relativt til fastpunktet ved vektormålingar. Eitt nytt punkt er etablert ved nyare sprekk mot sør i 2009. Punkta er målt om i 2010 og 2011.

Resultat - endring

Resultata er synt i tabellar 18 og 19 og endringar grafisk i figur 27. Målingane både i alle åra er gode, men det er noko usikkert med omsyn til i antennehøgd i fastpunktet for 2008. Etter montering av bolten var det anten ein eller to mutterar på bolten i punktet BER-FP, mest sannsynleg to, men det kan ha vore ein. Frå og med 2009 er det ikkje råd å montere antenna med ein mutter, men dette var mogeleg i 2008 før mutteren vart endeleg fastskrudd. Skilnaden mellom desse to alternativa er ca. 14 mm. Resultata er laga for det mest sannsynlege, to mutterar i fastpunktet.

Det er signifikante endringar i planet i alle fire punkta på Middagstinden, med størst endring i punktet BER-4 med meir enn 1 cm pr år i plan og ca. 2 cm i høgd. I dei tre andre punkta er endringane i storleik 5 mm pr. år både i plan og høgd.

Konklusjon

Punkta på Middagstinden har klare teikn til rørsle.

PUNKT	År	N (UTM)	E (UTM)	H (ell.)	σN [m]	σE [m]	σH [m]	dN [m]	dE [m]	Avst. [m]	Retning [g gon]	dH [m]
BER-FP	2009	6925281.6220	418878.8850	1016.7880								
BER-1	2008	6925033.2275	419485.9159	844.7852	0.0009	0.0006	0.0018					
BER-1	2009	6925033.2219	419485.9144	844.7812	0.0005	0.0003	0.0009	-0.006	-0.002	**0.006**	216.66	**-0.004**
BER-1	2010	6925033.214	419485.9173	844.7758	0.0004	0.0004	0.0007	-0.014	0.001	**0.014**	193.61	**-0.009**
BER-1	2011	6925033.2087	419485.9161	844.7710	0.0009	0.0005	0.0013	-0.019	0.000	**0.019**	199.32	**-0.014**
BER-2	2008	6924887.0769	419646.5779	712.1617	0.0009	0.0005	0.0020					
BER-2	2009	6924887.0697	419646.5770	712.1663	0.0005	0.0003	0.0009	-0.007	-0.001	**0.007**	207.92	**0.005**
BER-2	2010	6924887.069	419646.5789	712.1582	0.0004	0.0004	0.0007	-0.008	0.001	**0.008**	192.37	**-0.004**
BER-2	2011	6924887.0630	419646.5743	712.1489	0.0009	0.0005	0.0013	-0.014	-0.004	**0.014**	216.13	**-0.013**
BER-3	2008	6924857.1432	419173.2247	740.1638	0.0010	0.0006	0.0019					
BER-3	2009	6924857.1342	419173.2242	740.1638	0.0005	0.0003	0.0009	-0.009	-0.001	**0.009**	203.53	**0.000**
BER-3	2010	6924857.128	419173.2245	740.1557	0.0004	0.0004	0.0008	-0.015	0.000	**0.015**	200.85	**-0.008**
BER-3	2011	6924857.1245	419173.2193	740.1454	0.0008	0.0004	0.0013	-0.019	-0.005	**0.019**	217.90	**-0.018**
BER-4	2009	6924775.1287	418886.5785	671.7474	0.0005	0.0004	0.0010		Nytt	2009		
BER-4	2010	6924775.114	418886.5772	671.7275	0.0004	0.0004	0.0008	-0.014	-0.001	**0.014**	205.73	**-0.020**
BER-4	2011	6924775.1013	418886.5770	671.7069	0.0008	0.0004	0.0014	-0.027	-0.002	**0.027**	203.48	**-0.040**

Tabell 18: Koordinatar og endring mellom målingar 2008–11 for punkta ved Middagstinden. Korrigert for to mutterar på FP i 2008.

		Endring mellom målingar				
PUNKT	**ÅR**	**dN [m]**	**dE [m]**	**Avstand [m]**	**Retning [g gon]**	**dH [m]**
BER-1	2008-09	-0.006	-0.002	**0.006**	216.66	**-0.004**
BER-1	2009-10	-0.008	0.003	**0.009**	178.60	**-0.005**
BER-1	2010-11	-0.005	-0.001	**0.005**	215.29	**-0.005**
BER-2	2008-09	-0.007	-0.001	**0.007**	207.92	**0.005**
BER-2	2009-10	-0.001	0.002	**0.002**	133.41	**-0.008**
BER-2	2010-11	-0.006	-0.005	**0.007**	243.78	**-0.009**
BER-3	2008-09	-0.009	-0.001	**0.009**	203.53	**0.000**
BER-3	2009-10	-0.006	0.000	**0.006**	196.77	**-0.008**
BER-3	2010-11	-0.004	-0.005	**0.006**	259.82	**-0.010**
BER-4	2009-10	-0.014	-0.001	**0.014**	205.73	**-0.020**
BER-4	2010-11	-0.013	0.000	**0.013**	200.98	**-0.021**

Tabell 19: Endringar mellom målingar for punkt på Middagstinden 2008–11.

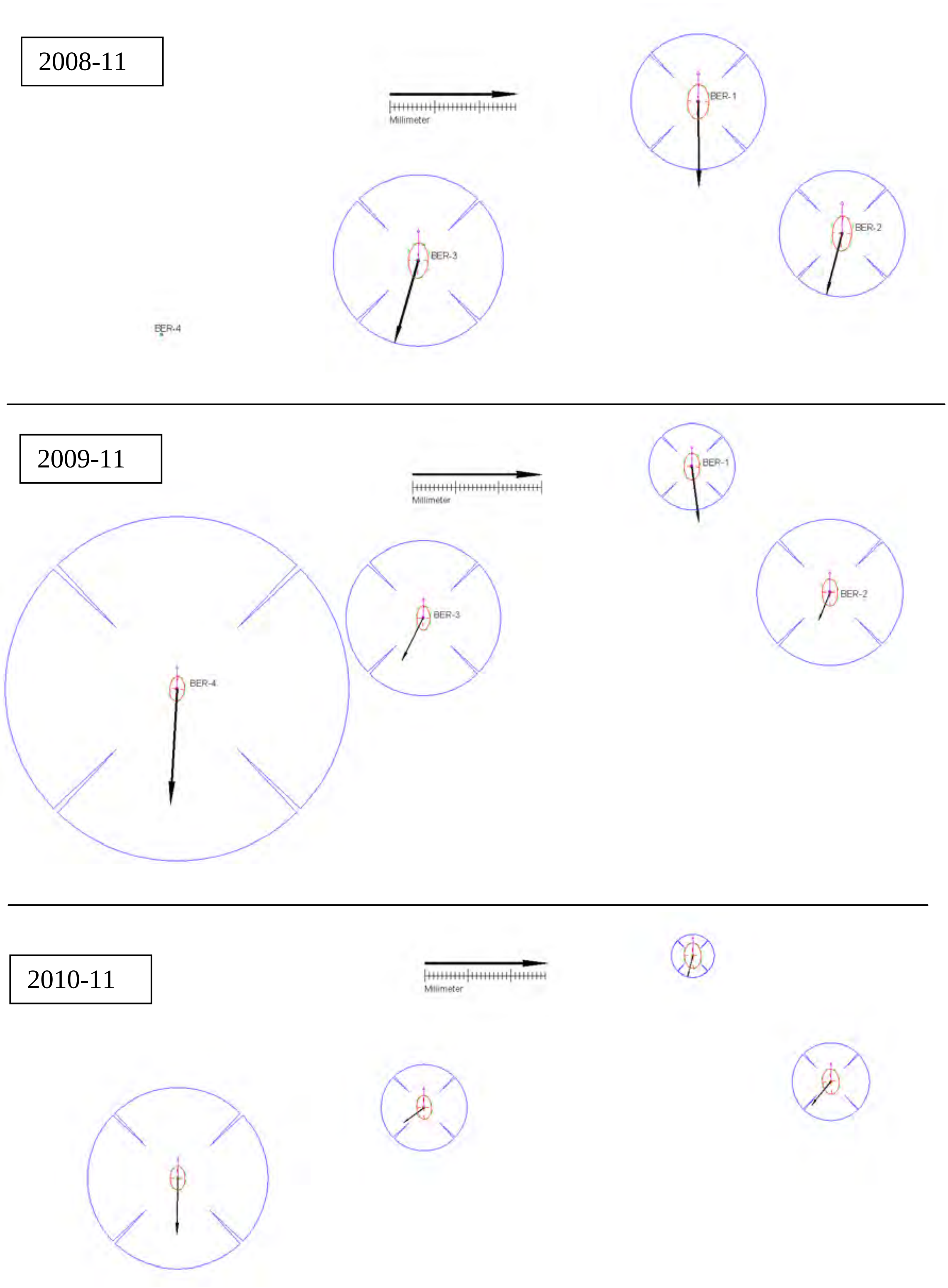

Figur 27: Grafisk framstilling av endring i punkta ved Middagstinden 2008–11 (øvst), 2009–11 (midten) og 2010–11 (nedst) med konfidensnivå for 99%. Grunnriss (pil), høgde (sirkel). Blå sirklar indikerer setning. (Punktet BER-4 vart etablert 2009).

Nokkenibba

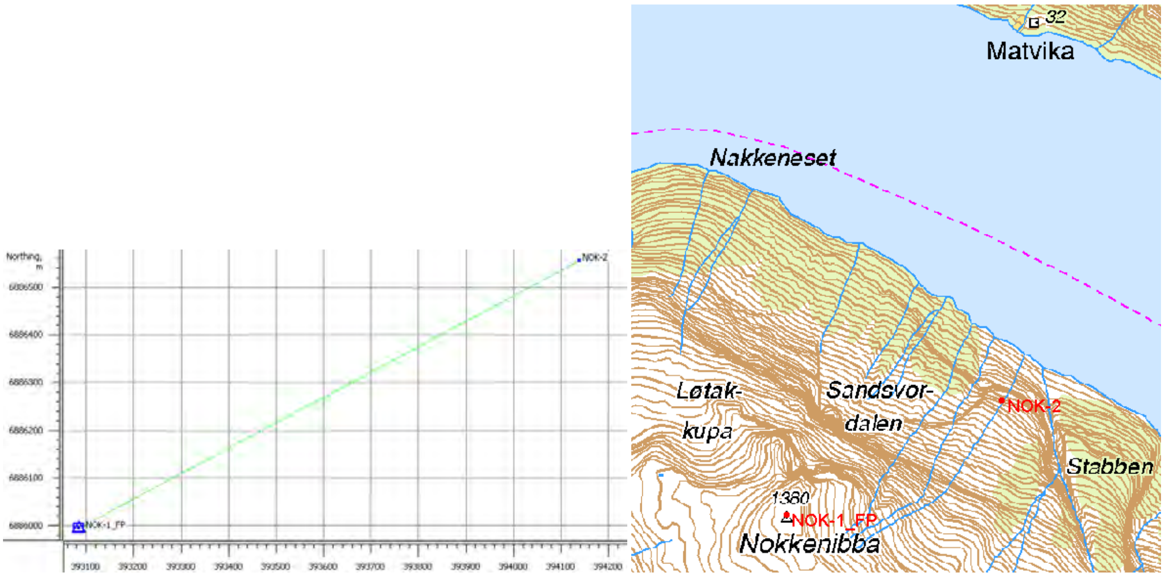

Figur 28: Vektorriss og kart (Sk-N50).

Punktgrunnlag
I 2006 er det sett ut eitt punkt like ved triangelpunktet på toppen av Nokkenibba, og eitt punkt ved eit elvegjel ned mot fjorden (figur 28). Punkta er målt om i 2007 og 2010.

Resultat – endringar, 2010
Den målte vektoren i 2006 var ikkje god. Punktet NOK-2 er svært vanskeleg å måle i sidan satellittane vert sterkt skjerma av den bratte fjellveggen mot sør. I måleperioden i 2006 var det problem med tilstrekkeleg satellittdekning, slik at vektoren til punktet fekk redusert kvalitet. Målingane i 2007 og 2010 er vesentleg betre. Punkta vart då målt samstundes med Hellesylt/Herdalsnibba, slik at fleire vektorar ligg til grunn for resultatet. Vektoren for 2006 er nyprosessert med eit betre resultat enn tidlegare og er presentert i resultata, men har vesentleg lågare presisjon enn dei nyare målingane.

Resultata er noko sprikande, serleg for høgder (tabellar 20 og 21, figur 29). Indikert horisontal endring for 2006–10 og 2007–10 går i same retning og kan vere eit teikn på mogeleg rørsle, men sidan ingen av endringane er statistisk signifikante er dette berre ein svak indikasjon.

Konklusjon.
Etter tre målingar er det ingen signifikante endringar i punktet på Nokkenibba

PUNKT	År	N (UTM)	E (UTM)	H (ell.)	σN [m]	σE [m]	σH [m]	dN [m]	dE [m]	Avst. [m]	Retning [g gon]	dH [m]
NOK-1_FP	2010	6885994.5487	393084.7871	1425.7699								
NOK-2	2006	6886556.0691	394139.7875	419.3133	0.0041	0.0008	0.0109					
NOK-2	2007	6886556.0666	394139.7919	419.2941	0.0025	0.0018	0.0070	-0.003	0.004	0.005	132.89	-0.019
NOK-2	2010	6886556.0805	394139.7903	419.3154	0.0008	0.0010	0.0017	0.011	0.003	0.012	15.33	0.002

Tabell 20: Koordinatar og endring i høve til fyrste måling 2006–10 for punkt på Nokkenibba.

		Endring mellom målingar				
PUNKT	**ÅR**	**dN [m]**	**dE [m]**	**Avstand [m]**	**Retning [^{g} gon]**	**dH [m]**
NOK-2	2006-07	-0.003	0.004	0.005	132.89	-0.019
NOK-2	2007-10	0.014	-0.002	0.014	392.70	0.021

Tabell 21: Endring mellom målingar 2006–10 for punkt på Nokkenibba.

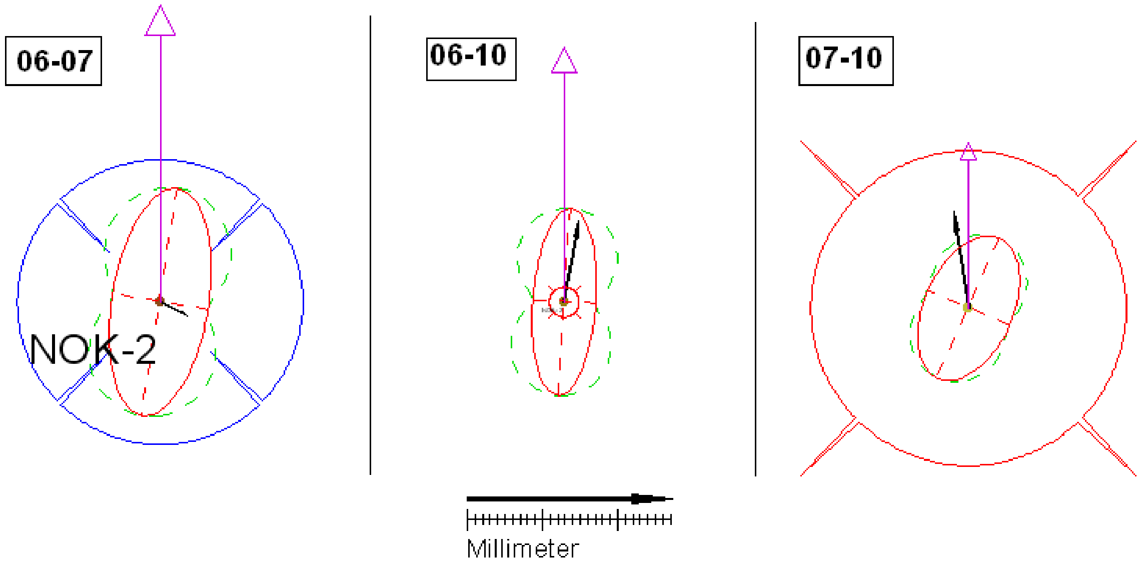

Figur 29: Horisontal- og vertikal-endringar på Nokkenibba. 2006–07 (til venstre) og 2006–10 (midten) og 2007–10 (til høgre), med 99% signifikansgrenser.

Oppstadhornet

Figur 30: Kart Oppstadhornet merka med raud sirkel (Kart: Statens kartverk)

Generelle kommentarar

Nettet på Oppstadhornet (figurar 30 og 31) vart etablert i 2003, og målt om årleg til 2008 og deretter i 2011. I 2004 vart det etablert eit nytt punkt i det ustabile området (OT-11), og eit nytt fastpunkt i sjøkanten nedanfor området (OFP-3). I 2005 vart det etablert åtte nye punkt lengre mot nordaust på toppryggen, av desse eitt fastpunkt under toppen mot nordaust for å sikre god kontroll (OFP-23). I 2006 vart det utført ekstra måling mellom fastpunkta slik at desse er gitt nye verde som er haldne fast i nettutjamningane (figur 31).

Punktet OT-3 er ikkje målt i 2008 og seinare. Her er bolten skeiv og eksakt sentrering er difor vanskeleg, og punktet er difor utelate. I 2008 vart det ikkje målt i OT-10 (Linhamaren) og OFP-3, og serleg resultata i høgd kan avvike frå resten av serien ettersom tilkytinga til OFP-3 manglar.

Endringar

Endringane er framstilt i tabellar 22 og 23 og i figurar 33 og 34 for horisontal og vertikal endring, og i tillegg er endringar i høgd for alle punkta over tid synt i figur 32. Endringane varierer noko om ein tek utgongspunkt i resultata frå 2003, 2004 eller 2005, men i store trekk er biletet relativt konsistent. Resultat i høve til 2003 inkluderer dei fyrste etablerte punkta, 2004 har med eitt ekstra punkt (OT-11) og endringar i høve til 2005 tek med dei nye punkta mot aust på toppen.

Endringane er generelt små, men relativt konsistente for dei fleste punkta i alle tre analysane. I dei eldste punkta, som dekker fjellskråninga i den vestre delen, er det små men signifikant rørsler i dei fleste punkta, med unntak av punkta heilt på toppen. Endringane er klarast frå 2003–11, men det same mønsteret for rørsle er å finne for dei to andre analyseperiodane. Dei lågare punkta har litt større endringane i plan, men meir variabel vertikale endring, og berre punktet OT-9 har konsistent vertikal endring over tid (dette er eit punkt på ei ca. 2 m^3 blokk i urda). Dei lågaste punkta har synt variable resultat i høgder over tid (jfr. figur 32), noko som skuldast variasjon i meteorologiske tilhøve i ulike år. Men trend over alle målingar er med nokre unntak relativt konsistent.

I dei nyaste punkta mot aust, etablert 2005, er det etter seks år så vidt signifikant endring i planet i nokre punkt. Vertikal endring er så vidt signifikant i dei fleste punkta, men med bakgrunn i noko underestimert storleik på standardavvik (og dermed signifikansnivå) kan det ikkje klart konkluderast med at det er rørsle i dette området, men det kan heller ikkje konkluderast med at området er stabilt.

Konklusjon
Det er påvist små men signifikante rørsler i punkta i den vestre delen. Ganske lik trend over fleire år styrkjer konklusjonen om at det er rørsle i punkta på om lag 1 mm/år.

I nokre av dei nye punkta (2005) på toppryggen er det og indikasjonar på rørsle, men dette er meir usikkert. I dei nedre punkta er endringane litt større, ca. 2 mm/år, og serleg horisontal trend er konsistent for dei ulike analysane.

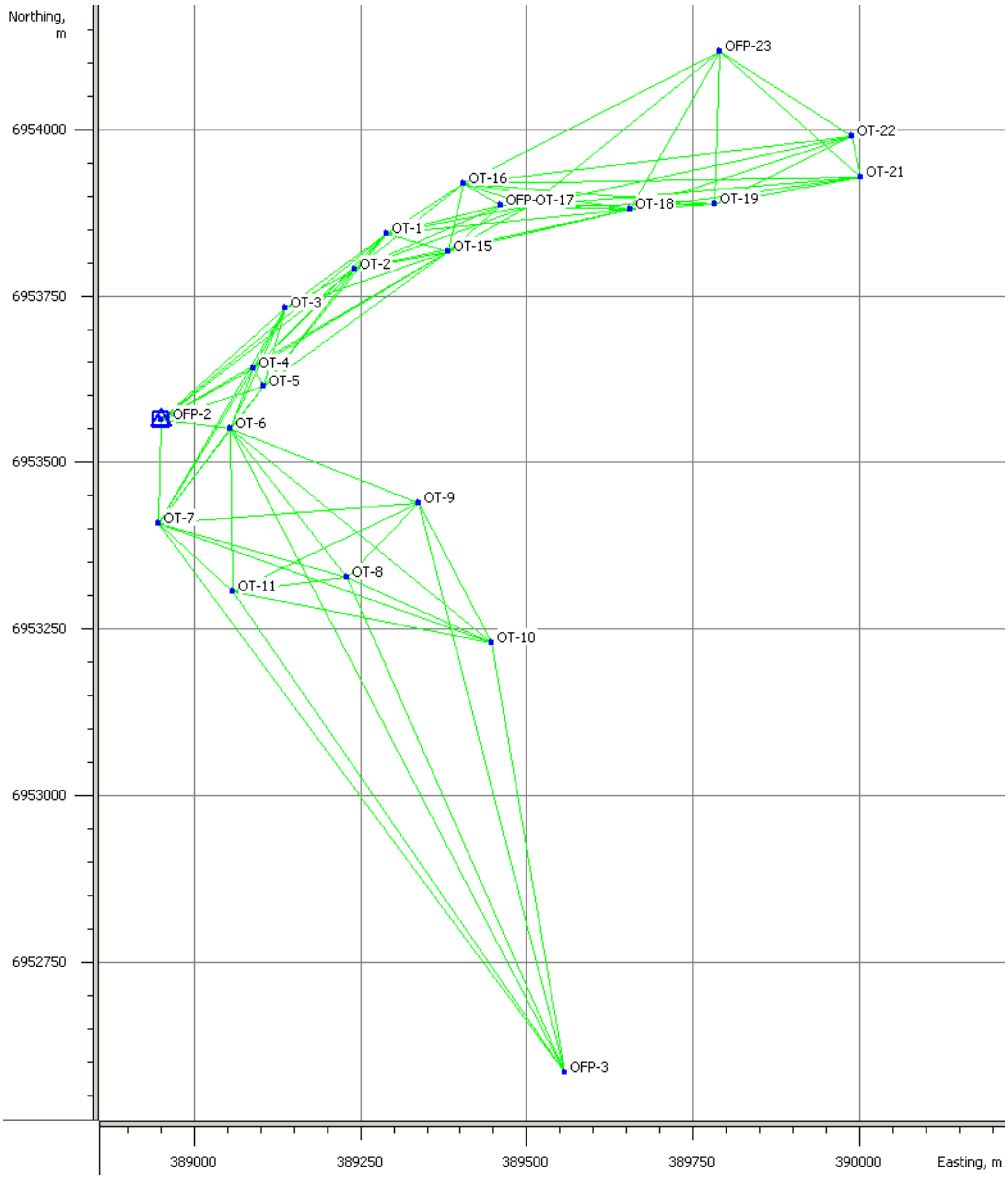

Figur 31: Vektornett på Oppstadhornet 2007.

PUNKT	År	N	E	H	sN	sE	sH	dN	dE	Avstand	Retning	dH
OFP-2	FP	6953563.683	388951.073	583.305								
OFP-3	FP	6952583.887	389557.245	47.669								
OFP-23	FP	6954117.309	389790.182	656.534								
OFP-1	2003	6953885.893	389460.060	777.032	0.001	0.001	0.003					
OFP-1	2004	6953885.891	389460.060	777.027	0.001	0.001	0.002	-0.002	-0.001	0.002	228.00	-0.005
OFP-1	2005	6953885.890	389460.059	777.030	0.001	0.001	0.001	-0.003	-0.002	0.003	236.87	-0.002
OFP-1	2006	6953885.893	389460.061	777.028	0.001	0.000	0.001	0.000	0.001	0.001	87.43	-0.004
OFP-1	2007	6953885.892	389460.063	777.030	0.001	0.001	0.002	-0.001	0.002	0.002	127.16	-0.002
OFP-1	2008	6953885.891	389460.060	777.038	0.001	0.000	0.001	-0.002	0.000	0.002	196.65	0.006
OFP-1	2011	6953885.890	389460.059	777.017	0.001	0.000	0.001	-0.003	-0.002	0.003	238.55	-0.015
OT-1	2003	6953843.412	389289.928	755.474	0.002	0.001	0.004					
OT-1	2004	6953843.406	389289.926	755.463	0.002	0.001	0.003	-0.006	-0.002	0.007	222.95	-0.011
OT-1	2005	6953843.412	389289.929	755.466	0.001	0.001	0.002	-0.001	0.001	0.001	154.89	-0.008
OT-1	2006	6953843.411	389289.931	755.468	0.001	0.000	0.001	-0.001	0.002	0.003	137.43	-0.006
OT-1	2007	6953843.410	389289.930	755.463	0.001	0.001	0.002	-0.002	0.002	0.003	160.77	-0.011
OT-1	2008	6953843.408	389289.929	755.472	0.001	0.000	0.001	-0.004	0.001	0.004	190.52	-0.003
OT-1	2011	6953843.411	389289.927	755.460	0.001	0.000	0.001	-0.002	-0.001	0.002	244.23	-0.014
OT-2	2003	6953789.325	389241.248	730.794	0.002	0.001	0.004					
OT-2	2004	6953789.320	389241.248	730.785	0.001	0.001	0.002	-0.005	0.000	0.005	205.29	-0.010
OT-2	2005	6953789.320	389241.246	730.785	0.001	0.001	0.001	-0.005	-0.002	0.005	222.00	-0.009
OT-2	2006	6953789.321	389241.250	730.787	0.001	0.000	0.001	-0.004	0.002	0.004	168.55	-0.007
OT-2	2007	6953789.320	389241.249	730.781	0.001	0.001	0.002	-0.005	0.001	0.005	192.24	-0.013
OT-2	2008	6953789.319	389241.247	730.786	0.001	0.000	0.001	-0.006	-0.001	0.006	209.03	-0.008
OT-2	2011	6953789.316	389241.245	730.770	0.001	0.001	0.001	-0.009	-0.003	0.009	218.75	-0.025
OT-3	2003	6953731.229	389137.074	675.219	0.002	0.002	0.004					
OT-3	2004	6953731.225	389137.074	675.206	0.002	0.002	0.003	-0.003	0.001	0.003	190.70	-0.013
OT-3	2005	6953731.234	389137.073	675.207	0.001	0.001	0.002	0.006	-0.001	0.006	387.65	-0.012
OT-3	2006	6953731.226	389137.076	675.208	0.001	0.001	0.002	-0.003	0.002	0.004	165.31	-0.010
OT-3	2007	6953731.212	389137.064	675.209	0.001	0.001	0.002	-0.017	-0.010	0.020	234.01	-0.010
OT-4	2003	6953640.857	389089.457	645.521	0.001	0.001	0.002					
OT-4	2004	6953640.854	389089.460	645.514	0.001	0.001	0.002	-0.003	0.002	0.004	159.97	-0.008
OT-4	2005	6953640.854	389089.457	645.514	0.001	0.000	0.001	-0.003	-0.001	0.003	213.71	-0.008
OT-4	2006	6953640.853	389089.457	645.515	0.001	0.000	0.001	-0.004	-0.001	0.004	212.27	-0.006
OT-4	2007	6953640.852	389089.456	645.516	0.001	0.001	0.002	-0.005	-0.002	0.005	222.70	-0.005
OT-4	2008	6953640.853	389089.458	645.510	0.001	0.000	0.001	-0.005	0.000	0.005	197.35	-0.011
OT-4	2011	6953640.848	389089.456	645.503	0.001	0.001	0.001	-0.010	-0.002	0.010	209.87	-0.019
OT-5	2003	6953614.196	389104.899	636.605	0.002	0.001	0.003					
OT-5	2004	6953614.190	389104.901	636.594	0.001	0.001	0.002	-0.006	0.002	0.007	182.28	-0.010
OT-5	2005	6953614.190	389104.898	636.602	0.001	0.001	0.002	-0.006	0.000	0.006	204.38	-0.003
OT-5	2006	6953614.189	389104.900	636.597	0.001	0.000	0.001	-0.007	0.001	0.008	188.10	-0.008
OT-5	2007	6953614.189	389104.898	636.598	0.001	0.001	0.002	-0.007	-0.001	0.007	206.26	-0.006
OT-5	2008	6953614.187	389104.899	636.597	0.001	0.000	0.001	-0.009	0.000	0.009	197.81	-0.008
OT-5	2011	6953614.183	389104.898	636.587	0.001	0.001	0.001	-0.013	-0.001	0.013	204.40	-0.018

PUNKT	År	N	E	H	sN	sE	sH	dN	dE	Avstand	Retning	dH
OT-6	2003	6953551.498	389054.335	602.946	0.001	0.001	0.002					
OT-6	2004	6953551.497	389054.334	602.944	0.001	0.001	0.002	-0.002	-0.001	0.002	234.40	-0.002
OT-6	2005	6953551.495	389054.334	602.953	0.001	0.001	0.003	-0.004	-0.001	0.004	216.80	0.007
OT-6	2006	6953551.494	389054.336	602.941	0.001	0.000	0.001	-0.005	0.000	0.005	194.71	-0.005
OT-6	2007	6953551.495	389054.330	602.953	0.001	0.001	0.002	-0.003	-0.005	0.006	266.69	0.007
OT-6	2008	6953551.494	389054.334	602.938	0.001	0.000	0.001	-0.004	-0.001	0.004	216.69	-0.008
OT-6	2011	6953551.488	389054.335	602.928	0.001	0.001	0.001	-0.010	-0.001	0.010	204.41	-0.018
OT-7	2003	6953407.521	388946.469	533.909	0.001	0.001	0.002					
OT-7	2004	6953407.523	388946.469	533.907	0.001	0.001	0.002	0.003	0.000	0.003	4.89	-0.002
OT-7	2005	6953407.522	388946.469	533.909	0.001	0.000	0.002	0.001	0.000	0.001	390.97	0.000
OT-7	2006	6953407.520	388946.470	533.909	0.001	0.000	0.001	-0.001	0.001	0.001	168.21	0.000
OT-7	2007	6953407.518	388946.465	533.916	0.001	0.001	0.002	-0.002	-0.004	0.005	267.45	0.007
OT-7	2008	6953407.517	388946.470	533.899	0.001	0.000	0.001	-0.003	0.001	0.003	188.88	-0.010
OT-7	2011	6953407.510	388946.470	533.893	0.001	0.000	0.001	-0.011	0.001	0.011	192.82	-0.016
OT-8	2003	6953327.905	389229.402	409.697	0.002	0.001	0.003					
OT-8	2004	6953327.903	389229.402	409.698	0.003	0.001	0.004	-0.001	0.000	0.001	189.49	0.001
OT-8	2005	6953327.905	389229.407	409.698	0.002	0.001	0.003	0.000	0.005	0.005	100.00	0.001
OT-8	2006	6953327.910	389229.408	409.693	0.001	0.001	0.002	0.005	0.006	0.008	58.40	-0.004
OT-8	2007	6953327.901	389229.412	409.712	0.002	0.001	0.003	-0.003	0.010	0.011	121.04	0.016
OT-8	2008	6953327.895	389229.407	409.681	0.003	0.002	0.005	-0.010	0.005	0.011	172.55	-0.016
OT-8	2011	6953327.896	389229.411	409.697	0.001	0.001	0.002	-0.009	0.009	0.012	149.28	0.000
								OT-8 er dårleg i 2008				
OT-9	2003	6953439.175	389338.215	468.343	0.002	0.001	0.002					
OT-9	2004	6953439.177	389338.219	468.336	0.001	0.001	0.003	0.002	0.003	0.004	68.34	-0.007
OT-9	2005	6953439.172	389338.218	468.343	0.001	0.001	0.002	-0.003	0.003	0.004	154.71	0.000
OT-9	2006	6953439.169	389338.219	468.341	0.001	0.000	0.001	-0.007	0.004	0.008	165.60	-0.002
OT-9	2007	6953439.167	389338.219	468.355	0.001	0.001	0.002	-0.008	0.003	0.008	174.52	0.012
OT-9	2008	6953439.168	389338.222	468.319	0.001	0.001	0.002	-0.007	0.007	0.010	150.45	-0.023
OT-9	2011	6953439.149	389338.229	468.323	0.001	0.001	0.002	-0.026	0.013	0.029	169.80	-0.020
OT-10	2003	6953228.498	389447.378	305.347	0.005	0.003	0.009					
OT-10	2004	6953228.502	389447.381	305.365	0.004	0.002	0.007	0.003	0.003	0.004	42.73	0.017
OT-10	2005	6953228.499	389447.375	305.360	0.002	0.001	0.004	0.001	-0.003	0.003	318.73	0.013
OT-10	2006	6953228.488	389447.386	305.378	0.002	0.001	0.003	-0.010	0.008	0.013	156.52	0.030
OT-10	2007	6953228.496	389447.377	305.391	0.002	0.001	0.003	-0.003	-0.002	0.003	236.24	0.043
OT-10	2011	6953228.483	389447.382	305.372	0.001	0.001	0.002	-0.015	0.004	0.015	185.22	0.024
OT-11	2004	6953305.675	389057.875	437.772	0.002	0.001	0.002					
OT-11	2005	6953305.670	389057.875	437.781	0.001	0.001	0.002	-0.005	0.000	0.005	201.18	0.009
OT-11	2006	6953305.671	389057.876	437.781	0.001	0.000	0.001	-0.004	0.001	0.004	189.96	0.009
OT-11	2007	6953305.668	389057.875	437.796	0.001	0.001	0.002	-0.007	0.000	0.007	200.87	0.024
OT-11	2008	6953305.667	389057.877	437.763	0.001	0.001	0.002	-0.008	0.002	0.009	183.51	-0.009
OT-11	2011	6953305.660	389057.880	437.772	0.001	0.001	0.002	-0.015	0.004	0.016	181.45	0.000
OT-15	2005	6953815.791	389381.972	735.100	0.001	0.001	0.002					
OT-15	2006	6953815.793	389381.973	735.099	0.001	0.000	0.001	0.002	0.001	0.002	25.78	-0.002
OT-15	2007	6953815.790	389381.973	735.098	0.001	0.001	0.002	-0.001	0.001	0.001	133.62	-0.002
OT-15	2008	6953815.791	389381.971	735.100	0.001	0.001	0.001	0.000	-0.001	0.001	292.08	0.000
OT-15	2011	6953815.786	389381.975	735.084	0.001	0.000	0.001	-0.005	0.003	0.006	166.82	-0.017

PUNKT	År	N	E	H	sN	sE	sH	dN	dE	Avstand	Retning	dH
OT-16	2005	6953918.319	389404.196	762.292	0.001	0.001	0.001					
OT-16	2006	6953918.320	389404.199	762.289	0.001	0.000	0.001	0.001	0.002	0.003	72.64	-0.003
OT-16	2007	6953918.318	389404.200	762.289	0.001	0.001	0.002	-0.001	0.003	0.004	114.31	-0.003
OT-16	2008	6953918.318	389404.198	762.295	0.001	0.000	0.001	-0.001	0.001	0.002	133.05	0.003
OT-16	2011	6953918.318	389404.198	762.283	0.001	0.000	0.001	-0.001	0.002	0.002	126.62	-0.009
OT-17	2005	6953886.563	389504.610	781.515	0.001	0.001	0.001					
OT-17	2006	6953886.565	389504.609	781.513	0.001	0.000	0.001	0.001	0.000	0.001	385.56	-0.002
OT-17	2007	6953886.564	389504.610	781.512	0.001	0.001	0.002	0.000	0.001	0.001	62.57	-0.004
OT-17	2008	6953886.563	389504.609	781.520	0.001	0.000	0.001	0.000	-0.001	0.001	270.48	0.005
OT-17	2011	6953886.563	389504.607	781.506	0.001	0.000	0.001	0.000	-0.003	0.003	297.64	-0.010
OT-18	2005	6953879.869	389655.709	779.394	0.001	0.001	0.002					
OT-18	2006	6953879.867	389655.711	779.391	0.001	0.000	0.001	-0.002	0.002	0.003	158.55	-0.003
OT-18	2007	6953879.867	389655.711	779.388	0.001	0.001	0.002	-0.002	0.001	0.003	165.19	-0.006
OT-18	2008	6953879.863	389655.710	779.400	0.001	0.000	0.001	-0.006	0.001	0.006	189.82	0.006
OT-18	2011	6953879.868	389655.709	779.384	0.001	0.000	0.001	-0.002	0.000	0.002	196.26	-0.011
OT-19	2005	6953888.593	389782.466	779.762	0.001	0.001	0.001					
OT-19	2006	6953888.592	389782.466	779.760	0.001	0.000	0.001	-0.001	0.000	0.001	217.72	-0.001
OT-19	2007	6953888.590	389782.467	779.763	0.001	0.001	0.002	-0.003	0.001	0.003	187.43	0.002
OT-19	2008	6953888.589	389782.467	779.769	0.001	0.000	0.001	-0.004	0.000	0.004	195.23	0.007
OT-19	2011	6953888.590	389782.466	779.755	0.001	0.001	0.001	-0.003	0.000	0.003	208.73	-0.007
OT-21	2005	6953928.216	390002.391	729.512	0.001	0.001	0.002					
OT-21	2006	6953928.213	390002.389	729.506	0.001	0.001	0.002	-0.003	-0.002	0.003	234.40	-0.006
OT-21	2007	6953928.210	390002.390	729.506	0.001	0.001	0.002	-0.005	-0.001	0.005	213.03	-0.005
OT-21	2008	6953928.211	390002.391	729.516	0.001	0.001	0.001	-0.004	0.000	0.004	201.48	0.005
OT-21	2011	6953928.212	390002.390	729.500	0.001	0.001	0.001	-0.004	-0.001	0.004	213.92	-0.012
OT-22	2005	6953989.553	389987.658	700.342	0.001	0.001	0.002					
OT-22	2006	6953989.555	389987.658	700.334	0.001	0.000	0.002	0.002	0.000	0.002	8.44	-0.008
OT-22	2007	6953989.552	389987.659	700.335	0.001	0.001	0.003	-0.001	0.001	0.001	170.48	-0.007
OT-22	2008	6953989.551	389987.658	700.344	0.001	0.001	0.001	-0.002	-0.001	0.002	218.81	0.001
OT-22	2011	6953989.554	389987.659	700.334	0.001	0.001	0.002	0.000	0.000	0.001	40.97	-0.008

Tabell 22: Koordinatar med standardavvik og endringar for Oppstadhornet 2003–2011. Endringar gitt i meter, retning i gon (400 deling av sirkel). Alle endringar er rekna i høve til den fyrste målte koordinaten for punktet.

PUNKT	ÅR	dN [m]	dE [m]	Avstand [m]	Retning [^{g} gon]	dH [m]
OFP-1	2003-04	-0.0017	-0.0008	0.0019	228.00	-0.0055
OFP-1	2004-05	-0.0009	-0.0009	0.0013	250.00	0.0034
OFP-1	2005-06	0.0028	0.0027	0.0039	48.84	-0.0018
OFP-1	2006-07	-0.0012	0.0012	0.0017	150.00	0.0018
OFP-1	2007-08	-0.0009	-0.0021	0.0023	274.22	0.0082
OFP-1	2008-11	-0.0007	-0.0019	0.0020	277.53	-0.0215
OT-1	2003-04	-0.0061	-0.0023	0.0065	222.95	-0.0109
OT-1	2004-05	0.0054	0.0029	0.0061	31.37	0.0028
OT-1	2005-06	-0.0007	0.0015	0.0017	127.80	0.0017
OT-1	2006-07	-0.0010	-0.0004	0.0011	224.22	-0.0049
OT-1	2007-08	-0.0016	-0.0011	0.0019	238.34	0.0087
OT-1	2008-11	0.0022	-0.0021	0.0030	351.48	-0.0115
OT-2	2003-04	-0.0048	-0.0004	0.0048	205.29	-0.0095
OT-2	2004-05	-0.0002	-0.0014	0.0014	290.97	0.0006
OT-2	2005-06	0.0011	0.0039	0.0041	82.50	0.0020
OT-2	2006-07	-0.0010	-0.0015	0.0018	262.57	-0.0059
OT-2	2007-08	-0.0007	-0.0014	0.0016	270.48	0.0047
OT-2	2008-11	-0.0033	-0.0019	0.0038	233.26	-0.0165
OT-3	2003-04	-0.0034	0.0005	0.0034	190.70	-0.0127
OT-3	2004-05	0.0090	-0.0016	0.0091	388.80	0.0009
OT-3	2005-06	-0.0089	0.0031	0.0094	178.66	0.0014
OT-3	2006-07	-0.0136	-0.0120	0.0181	246.03	0.0003
OT-4	2003-04	-0.0033	0.0024	0.0041	159.97	-0.0079
OT-4	2004-05	0.0001	-0.0031	0.0031	302.05	0.0000
OT-4	2005-06	-0.0009	-0.0001	0.0009	207.04	0.0015
OT-4	2006-07	-0.0010	-0.0011	0.0015	253.03	0.0013
OT-4	2007-08	0.0003	0.0021	0.0021	90.97	-0.0059
OT-4	2008-11	-0.0048	-0.0017	0.0051	221.67	-0.0076
OT-5	2003-04	-0.0063	0.0018	0.0066	182.28	-0.0102
OT-5	2004-05	0.0005	-0.0022	0.0023	314.23	0.0077
OT-5	2005-06	-0.0016	0.0018	0.0024	146.26	-0.0053
OT-5	2006-07	0.0003	-0.0021	0.0021	309.03	0.0015
OT-5	2007-08	-0.0016	0.0010	0.0019	164.44	-0.0014
OT-5	2008-11	-0.0043	-0.0012	0.0045	217.33	-0.0104
OT-6	2003-04	-0.0015	-0.0009	0.0017	234.40	-0.0023
OT-6	2004-05	-0.0022	-0.0001	0.0022	202.89	0.0093
OT-6	2005-06	-0.0011	0.0014	0.0018	142.40	-0.0118
OT-6	2006-07	0.0018	-0.0056	0.0059	319.80	0.0122
OT-6	2007-08	-0.0011	0.0041	0.0042	116.69	-0.0151
OT-6	2008-11	-0.0060	0.0004	0.0060	195.76	-0.0101
OT-7	2003-04	0.0026	0.0002	0.0026	4.89	-0.0020
OT-7	2004-05	-0.0012	-0.0004	0.0013	220.48	0.0020
OT-7	2005-06	-0.0025	0.0008	0.0026	180.28	-0.0004
OT-7	2006-07	-0.0012	-0.0047	0.0049	284.09	0.0073
OT-7	2007-08	-0.0011	0.0047	0.0048	114.64	-0.0166
OT-7	2008-11	-0.0072	0.0006	0.0072	194.71	-0.0062

PUNKT	ÅR	dN [m]	dE [m]	Avstand [m]	Retning [^{g} gon]	dH [m]
OT-8	2003-04	-0.0012	0.0002	0.0012	189.49	0.0007
OT-8	2004-05	0.0012	0.0045	0.0047	83.41	0.0005
OT-8	2005-06	0.0049	0.0017	0.0052	21.26	-0.0049
OT-8	2006-07	-0.0084	0.0038	0.0092	172.95	0.0193
OT-8	2007-08	-0.0065	-0.0056	0.0086	245.27	-0.0313
OT-8	2008-11	0.0013	0.0043	0.0045	81.31	0.0160
OT-9	2003-04	0.0019	0.0035	0.0040	68.34	-0.0070
OT-9	2004-05	-0.0048	-0.0010	0.0049	213.08	0.0074
OT-9	2005-06	-0.0036	0.0014	0.0039	176.39	-0.0022
OT-9	2006-07	-0.0013	-0.0006	0.0014	227.53	0.0135
OT-9	2007-08	0.0006	0.0038	0.0038	90.03	-0.0351
OT-9	2008-11	-0.0187	0.0062	0.0197	179.62	0.0032
OT-10	2003-04	0.0034	0.0027	0.0043	42.73	0.0174
OT-10	2004-05	-0.0024	-0.0060	0.0065	275.78	-0.0046
OT-10	2005-06	-0.0112	0.0116	0.0161	148.88	0.0174
OT-10	2006-07	0.0077	-0.0099	0.0125	342.08	0.0133
OT-10	2007-11	-0.0123	0.0051	0.0133	174.98	-0.0193
OT-11	2004-05	-0.0054	-0.0001	0.0054	201.18	0.0087
OT-11	2005-06	0.0010	0.0008	0.0013	42.96	0.0005
OT-11	2006-07	-0.0029	-0.0008	0.0030	217.14	0.0145
OT-11	2007-08	-0.0010	0.0023	0.0025	126.11	-0.0326
OT-11	2008-11	-0.0067	0.0023	0.0071	178.95	0.0093
OT-15	2005-06	0.0021	0.0009	0.0023	25.78	-0.0015
OT-15	2006-07	-0.0028	0.0003	0.0028	193.20	-0.0004
OT-15	2007-08	0.0006	-0.0020	0.0021	318.55	0.0014
OT-15	2008-11	-0.0053	0.0039	0.0066	159.61	-0.0160
OT-16	2005-06	0.0011	0.0024	0.0026	72.64	-0.0028
OT-16	2006-07	-0.0019	0.0011	0.0022	166.59	-0.0005
OT-16	2007-08	0.0000	-0.0021	0.0021	300.00	0.0066
OT-16	2008-11	0.0000	0.0004	0.0004	100.00	-0.0124
OT-17	2005-06	0.0013	-0.0003	0.0013	385.56	-0.0023
OT-17	2006-07	-0.0009	0.0009	0.0013	150.00	-0.0015
OT-17	2007-08	-0.0007	-0.0012	0.0014	266.38	0.0085
OT-17	2008-11	0.0002	-0.0021	0.0021	306.04	-0.0144
OT-18	2005-06	-0.0021	0.0016	0.0026	158.55	-0.0034
OT-18	2006-07	-0.0002	-0.0002	0.0003	250.00	-0.0028
OT-18	2007-08	-0.0039	-0.0004	0.0039	206.51	0.0120
OT-18	2008-11	0.0045	-0.0009	0.0046	387.43	-0.0164
OT-19	2005-06	-0.0014	-0.0004	0.0015	217.72	-0.0015
OT-19	2006-07	-0.0016	0.0010	0.0019	164.44	0.0031
OT-19	2007-08	-0.0010	-0.0003	0.0010	218.55	0.0053
OT-19	2008-11	0.0011	-0.0007	0.0013	363.92	-0.0142

PUNKT	ÅR	dN [m]	dE [m]	Avstand [m]	Retning [^{g} gon]	dH [m]
OT-21	2005-06	-0.0030	-0.0018	0.0035	234.40	-0.0057
OT-21	2006-07	-0.0023	0.0007	0.0024	181.19	0.0006
OT-21	2007-08	0.0010	0.0010	0.0014	50.00	0.0098
OT-21	2008-11	0.0007	-0.0007	0.0010	350.00	-0.0163
OT-22	2005-06	0.0015	0.0002	0.0015	8.44	-0.0080
OT-22	2006-07	-0.0025	0.0003	0.0025	192.40	0.0007
OT-22	2007-08	-0.0013	-0.0012	0.0018	247.45	0.0088
OT-22	2008-11	0.0027	0.0010	0.0029	22.58	-0.0095

Tabell 23: Endringar mellom målingar for Oppstadhornet 2003–11. Endringar gitt i meter, retning i gon (400 deling av sirkel). Endringane er over eitt år fram til 2008, og deretter over tre år fram til 2011.

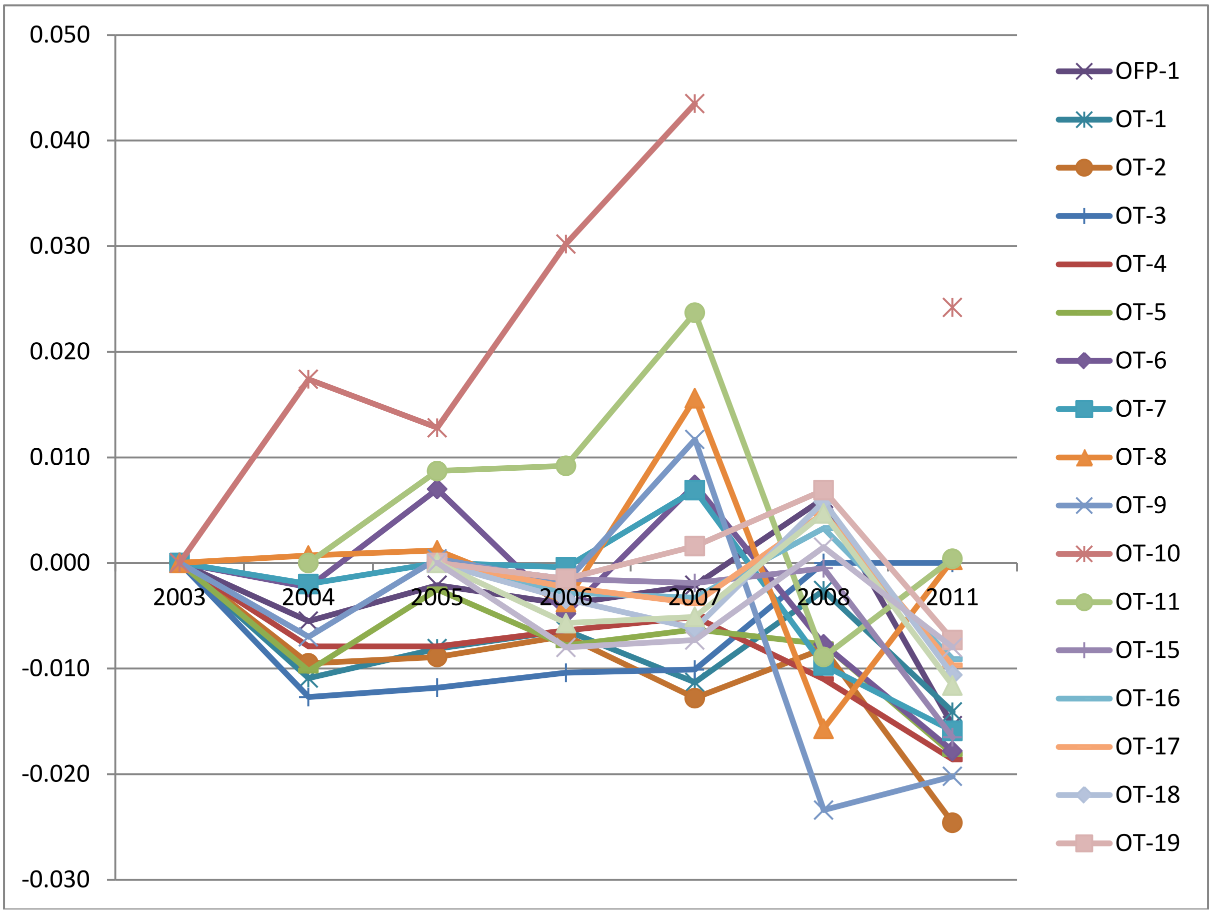

Figur 32: Relative høgdeendringar for punkta på Oppstadhornet. Punkta med store positive utslag er punkta i den nedre delen av området der variasjonar i meteorologiske tilhøve verkar sterkt inn på resultatet.

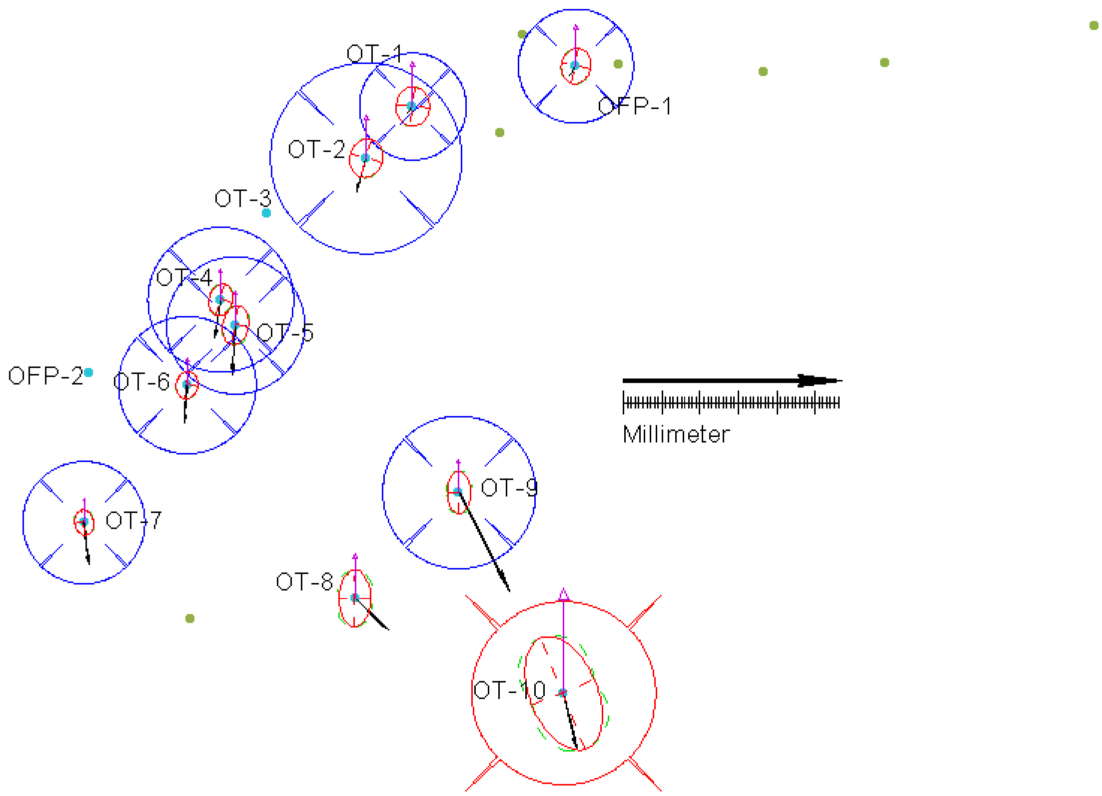

Figur 33: Endringar Oppstadhornet, 2003–2011, med konfidensnivå for 99% (raud ellipse/ fiolett pil). Grunnriss (pil), høgde (sirkel). Blå sirklar indikerer setning, raude sirklar heving.

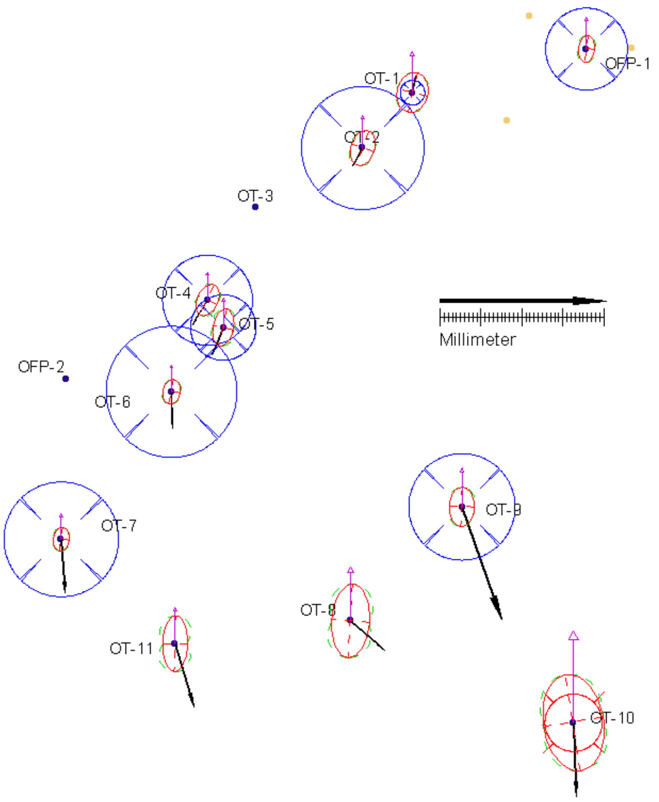

Figur 34: Endringar Oppstadhornet, 2004–2011.

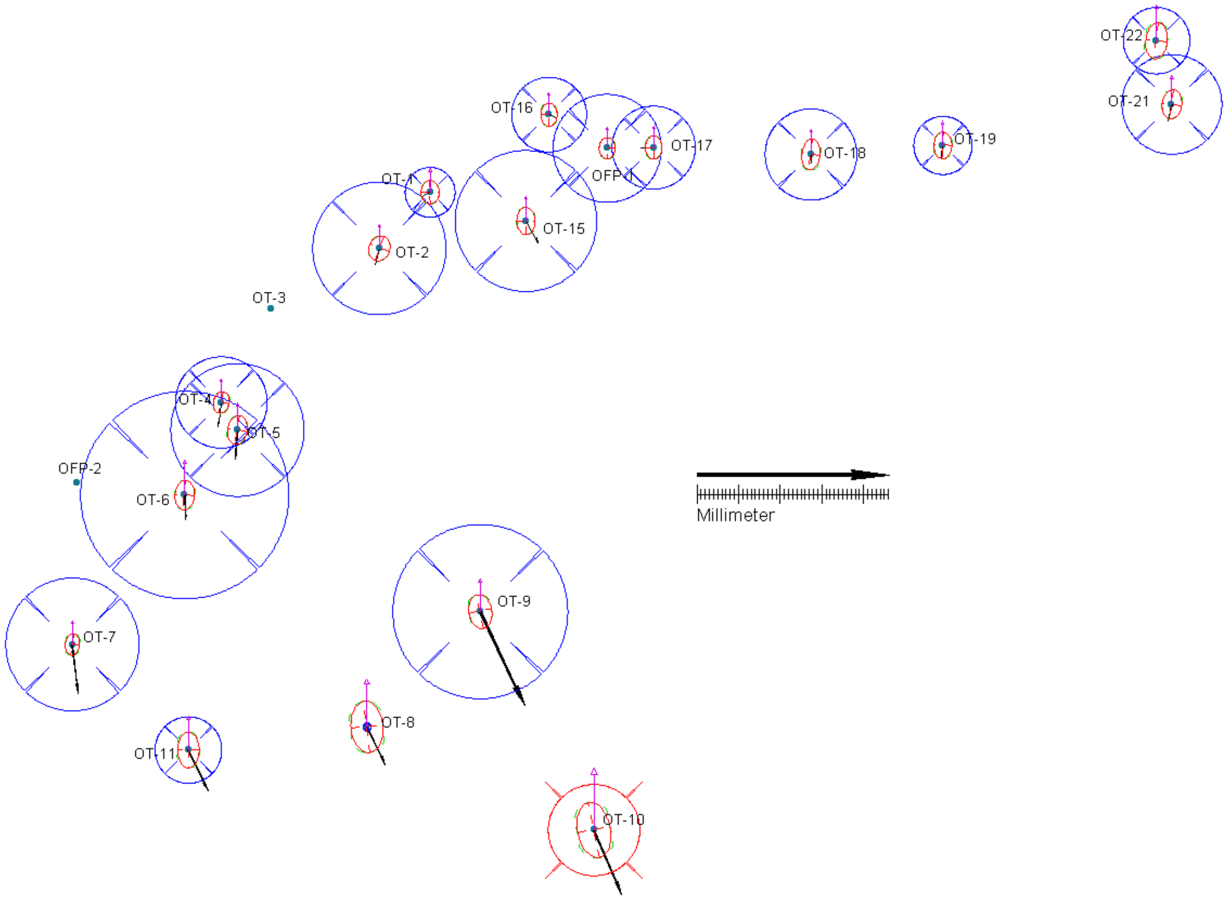

Figur 35: Endringar 2005–2011 for alle punkt, inkluderer dei nye punkta frå 2005.

Ottem

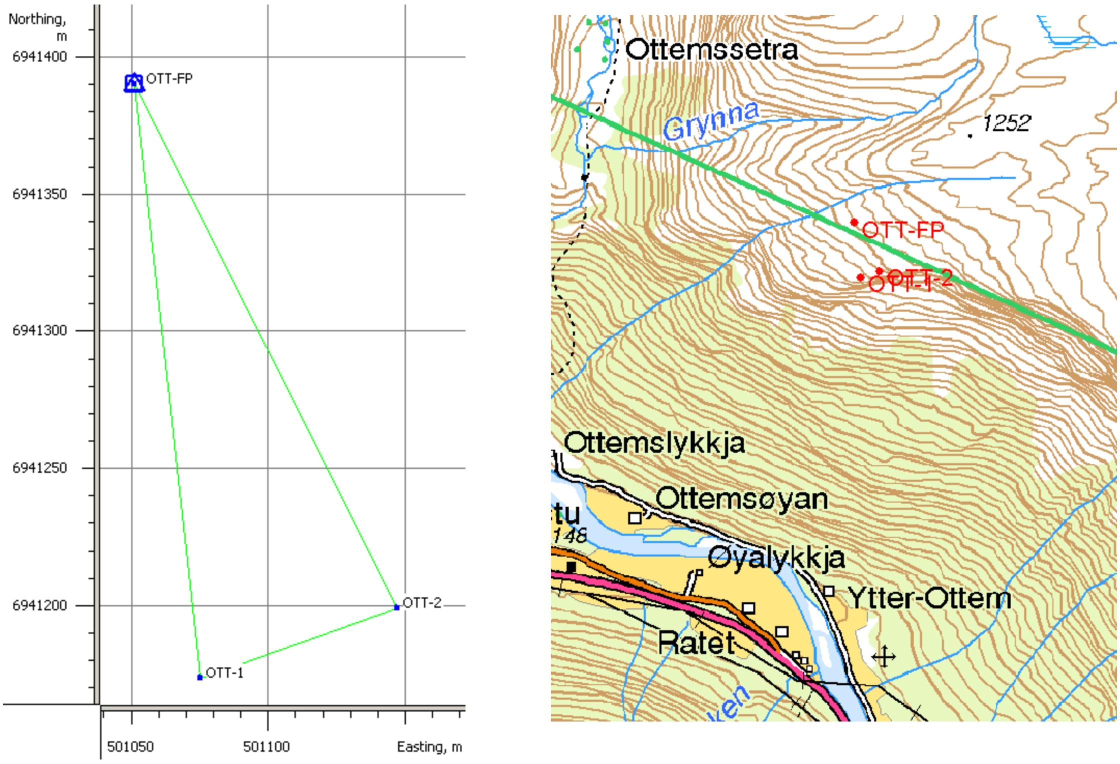

Figur 36: Vektorriss og kart (Sk-N50).

Punktgrunnlag
I 2008 er det etablert to nye punkt i potensielt ustabilt område på kanten ned mot dalen ovanfor Ottem, og eitt fastpunkt i stabilt område lengre opp (figur 36). Fastpunktet er fastlagt ved absolutt presis metode, dei andre punkta er rekna relativt til fastpunktet ved vektormålingar. Resultata syner god presisjon.

Resultat - endring
Punkta er målt om i 2009. Resultata er synt i tabell 24 og endringar grafisk i figur 37. I høgd er det på grensa til signifikant setning i punkta OTT-1 og OTT-2 på 7 og 6 mm. Sidan resultat i høgd er meir usikre, og standardavvik kan vere underestimert, er det usikkert om dette er reelle endringar.

Konklusjon
Det er visse teikn til rørsle i punkta, men fleire målingar bør gjerast for å få eit sikrare materiale.

PUNKT	År	N (UTM)	E (UTM)	H (ell.)	σN [m]	σE [m]	σH [m]	dN [m]	dE [m]	Avst. [m]	Retning [g gon]	dH [m]
OTT-FP	FP	6941389.8560	501051.2300	1167.2220								
OTT-1	2008	6941173.6664	501075.1488	1099.9874	0.0005	0.0004	0.0008					
OTT-1	2009	6941173.6681	501075.1494	1099.9806	0.0009	0.0009	0.0022	0.002	0.001	**0.002**	21.60	**-0.007**
OTT-2	2008	6941199.0090	501147.0337	1121.8104	0.0004	0.0003	0.0008					
OTT-2	2009	6941199.0094	501147.0339	1121.8042	0.0008	0.0008	0.0020	0.000	0.000	**0.000**	29.52	**-0.006**

Tabell 24: Koordinatar og endring frå fyrste måling for punkta på Ottem.

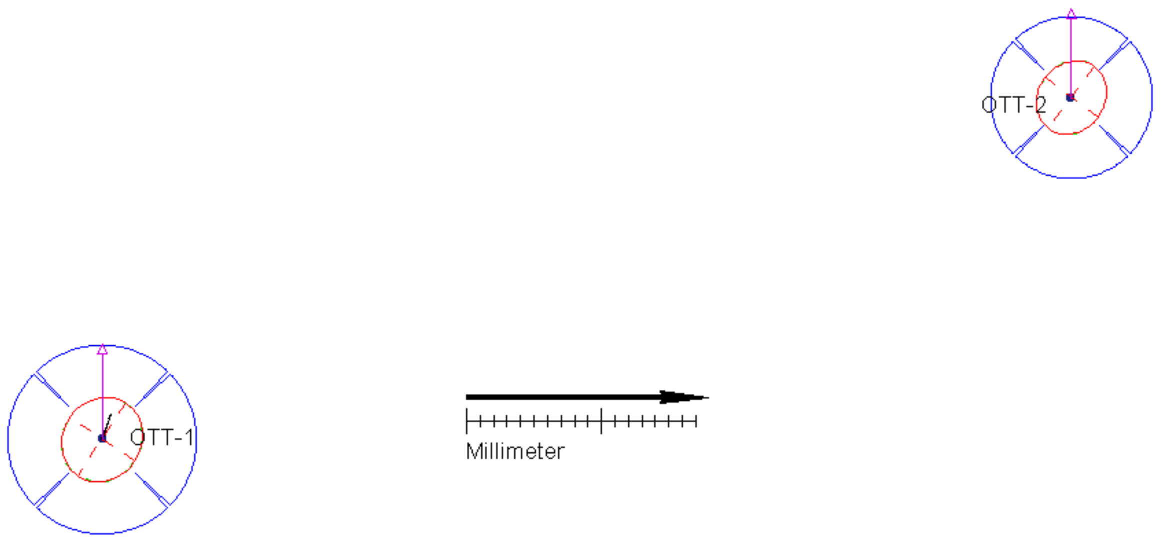

Figur 37: Grafisk framstilling av endring i punkta på Ottem 2008–09, med konfidensnivå for 99%. Grunnriss (pil), høgde (sirkel). Blå sirklar indikerer setning.

Rindalseggene

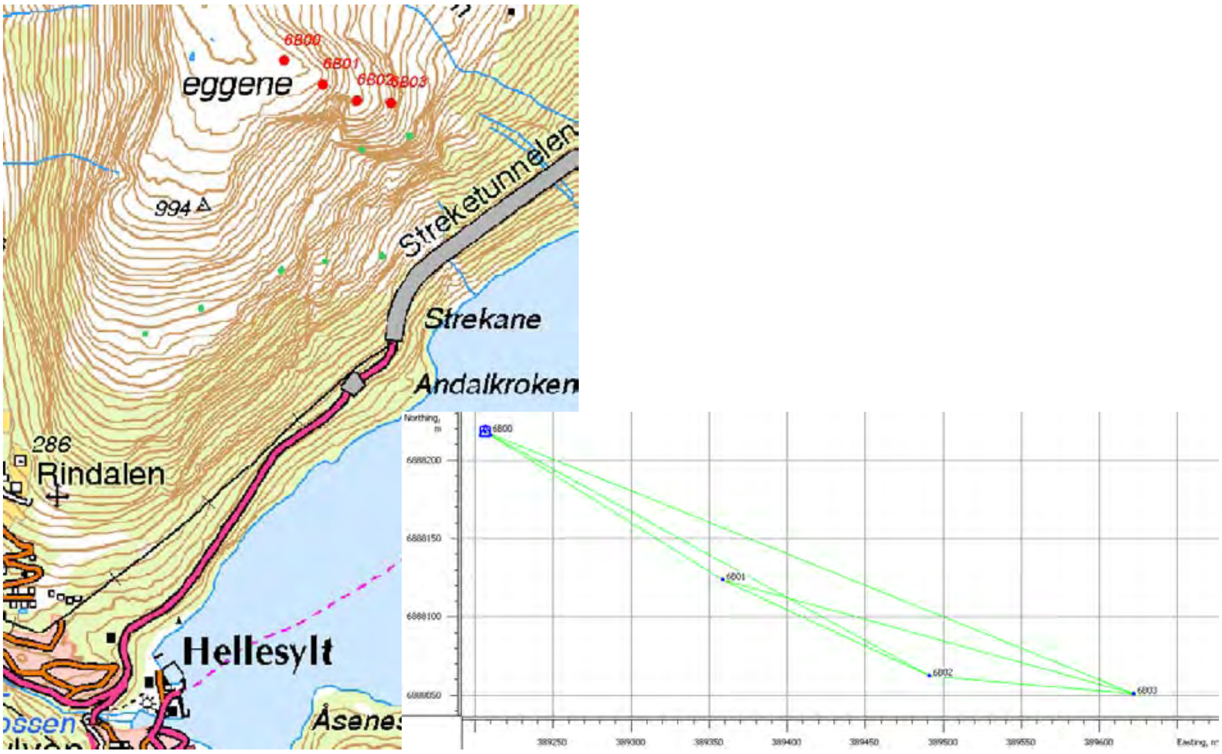

Figur 38: Plassering av punkt (Sk-N50) og riss over vektormålingar – 6B00 er fastpunkt.

Punktgrunnlag

I august 2005 vart det sett ut og målt fire punkt på søraustre del av Rindalseggene over Streketunnellen (figur 38). Eitt fastpunkt på det relativt flate topp-partiet og tre punkt nedover i lia. Det nedste utanfor markert sprekk. Punkta er sidan målt om kvart år med unntak av 2009.

Resultat – endringar, 2012

Dei fyrste resultata i området synte mogleg signifikant rørsle i nokre av punkta. Resultata frå seinare målingar syner ikkje tilsvarande klare teikn til endringar, men serleg punktet 6B-03 har vertikale variasjonar frå år til år som er større enn forventa ut frå presisjon i målingane.
I 2011 var antenna i punktet 6B-02 ikkje i lodd, men avviket vart målt med klinometer og koordinatane er korrigert. Det er likevel noko større uvisse i resultatet i dette punktet enn i dei andre punkta. Punktet får for 2011 signifikant horisontal endring, men tidlegare observasjonar syner ikkje slik endring og utslaget skuldast mest truleg manglande eller feilaktig korreksjon.

Resultata i tabell 25 med endring i høve til fyrste måling, og i tabell 26 med endringar mellom kvar måling (år) syner ingen klar trend over tid, men ein del store utslag i enkeltår. Grafisk framstilling i figur 39 syner og at nokre årskombinasjonar gir signifikante endringar i enkeltpunkt, men det er lite konsistent trend over tid. Trendliner (figur 40) for endring i høgd syner ingen trend for 6B-03 om 2005 vert er sett som start, men ein svak setningstrend om 2006 er startpunkt, men det er låge korrelasjonar.

Konklusjon

Det er ingen klare indikasjonar på rørsle i punkta sjølv om det er indikasjonar både på setning og heving i punkt med signifikante endringar både mellom enkeltmålingar og over tid.

Resultata er likevel så variable både i retning (plan) og høgd gjennom dei sju målingane, at det med høgt sannsyn kan konkluderast at det ikkje er reelle endringar i punkta.

PUNKT	ÅR	N	E	H	sN	sE	sH	dN	dE	Avstand	Retning	dH
6B00_FP	F.P.	6888217.859	389206.542	1142.490								
6B-01	2005	6888123.6132	389358.7811	1090.2478	0.0006	0.0005	0.0011					
6B-01	2006	6888123.6111	389358.7815	1090.2525	0.0002	0.0002	0.0004	-0.002	0.000	0.002	188.02	0.005
6B-01	2007	6888123.6096	389358.7806	1090.2547	0.0009	0.0006	0.0027	-0.004	-0.001	0.004	208.79	0.007
6B-01	2008	6888123.6107	389358.7822	1090.2517	0.0009	0.0007	0.0019	-0.002	0.001	0.003	173.61	0.004
6B-01	2010	6888123.6102	389358.7810	1090.2525	0.0013	0.0015	0.0023	-0.003	0.000	0.003	202.12	0.005
6B-01	2011	6888123.6123	389358.7807	1090.2545	0.0009	0.0009	0.0019	-0.001	0.000	0.001	226.63	0.007
6B-01	2012	6888123.6119	389358.7816	1090.2540	0.0007	0.0005	0.0013	-0.001	0.000	0.001	176.62	0.006
6B-02	2005	6888062.1725	389491.5485	991.1988	0.0006	0.0005	0.0011					
6B-02	2006	6888062.1715	389491.5477	991.2002	0.0002	0.0002	0.0004	-0.001	-0.001	0.001	242.96	0.001
6B-02	2007	6888062.1739	389491.5472	991.2001	0.0008	0.0005	0.0023	0.001	-0.001	0.002	352.36	0.001
6B-02	2008	6888062.1742	389491.5497	991.2030	0.0009	0.0007	0.0018	0.002	0.001	0.002	39.13	0.004
6B-02	2010	6888062.1707	389491.5495	991.2042	0.0012	0.0015	0.0022	-0.002	0.001	0.002	167.72	0.005
6B-02	2011	6888062.1718	389491.5530	991.2075	0.0008	0.0009	0.0018	-0.001	0.005	0.005	109.82	0.009
6B-02	2012	6888062.1729	389491.5497	991.1998	0.0006	0.0005	0.0012	0.000	0.001	0.001	79.52	0.001
6B-03	2005	6888050.9934	389622.3389	904.4080	0.0008	0.0006	0.0015					
6B-03	2006	6888050.9891	389622.3386	904.4414	0.0003	0.0003	0.0007	-0.004	0.000	0.004	204.43	0.033
6B-03	2007	6888050.9871	389622.3420	904.4314	0.0009	0.0009	0.0029	-0.006	0.003	0.007	170.89	0.023
6B-03	2008	6888050.9919	389622.3402	904.4242	0.0011	0.0010	0.0021	-0.002	0.001	0.002	154.54	0.016
6B-03	2010	6888050.9889	389622.3378	904.4170	0.0015	0.0018	0.0025	-0.004	-0.001	0.005	215.26	0.009
6B-03	2011	6888050.9883	389622.3394	904.4338	0.0010	0.0012	0.0023	-0.005	0.001	0.005	193.78	0.026
6B-03	2012	6888050.9936	389622.3404	904.4210	0.0008	0.0007	0.0016	0.000	0.002	0.002	91.56	0.013

Tabell 25: Rindalseggene, Koordinatar og endring 2005 til 2012 (i høve til fyrste måling). (Raude tal for 6B-02 i 2011 pga. skeiv trefot. Resultatet er søkt korrigert, men er usikkert).

PUNKT	ÅR	dN	dE	Avstand	Retning	dH
6B-01	2005-06	-0.002	0.000	0.002	188.02	0.005
6B-01	2006-07	-0.002	-0.001	0.002	234.40	0.002
6B-01	2007-08	0.001	0.002	0.002	61.66	-0.003
6B-01	2008-10	-0.001	-0.001	0.001	274.87	0.001
6B-01	2010-11	0.002	0.000	0.002	390.97	0.002
6B-01	2011-12	0.000	0.001	0.001	126.63	-0.001
6B-02	2005-06	-0.001	-0.001	0.001	242.96	0.001
6B-02	2006-07	0.002	-0.001	0.002	386.92	0.000
6B-02	2007-08	0.000	0.003	0.003	92.40	0.003
6B-02	2008-10	-0.004	0.000	0.004	203.63	0.001
6B-02	2010-11	0.001	0.003	0.004	80.61	0.003
6B-02	2011-12	0.001	-0.003	0.003	320.48	-0.008
6B-03	2005-06	-0.004	0.000	0.004	204.43	0.033
6B-03	2006-07	-0.002	0.003	0.004	133.85	-0.010
6B-03	2007-08	0.005	-0.002	0.005	377.16	-0.007
6B-03	2008-10	-0.003	-0.002	0.004	242.96	-0.007
6B-03	2010-11	-0.001	0.002	0.002	122.84	0.017
6B-03	2011-12	0.005	0.001	0.005	11.87	-0.013

Tabell 26: Rindalseggene, Endring mellom år frå 2005 til 2012. (Raude tal for 6B-02 i 2011 pga. skeiv trefot. Resultatet er søkt korrigert, men er usikkert).

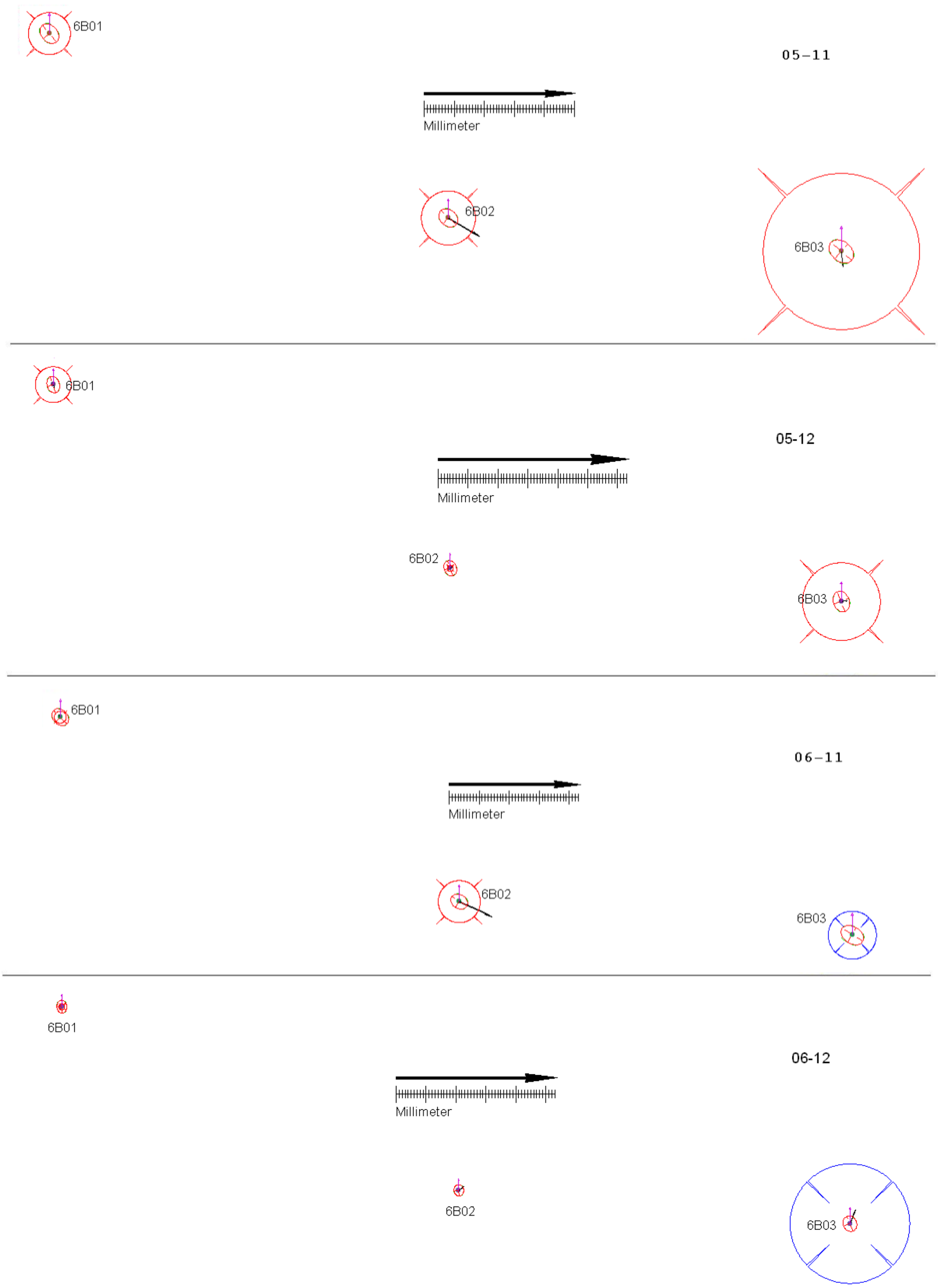

Figur 39: Endringar for ulike periodar 2005–12 med konfidensgrenser for 99% . Grunnriss (svarte piler) og høgd (sirklar). Raude sirklar indikerer heving, blå setning. 2005 resultatet var svært lav høgd i 6B03, medan 2006 var relativt høg og er årsak til det ulike biletet med 2005 og 2006 som utgongspunkt.

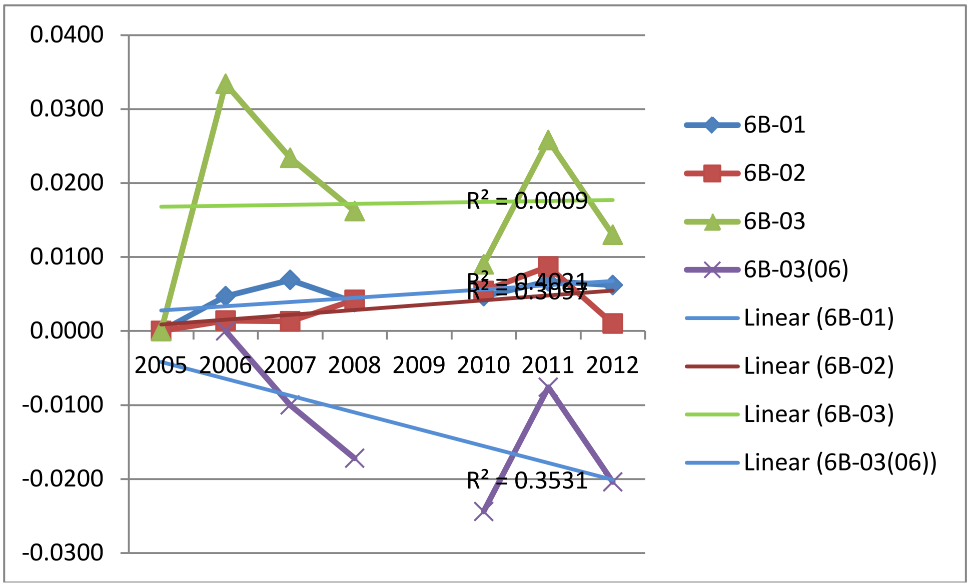

Figur 40: Endringar i høgd, med trendliner for endring.

Skrednakken

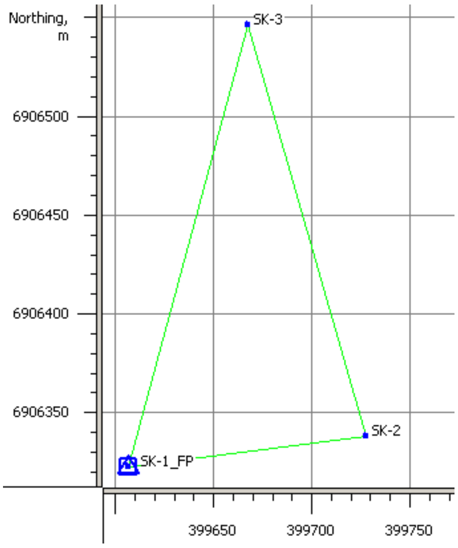

Figur 41: Vektorriss og kart (Sk-N50).

Punktgrunnlag
I august 2006 vart det etablert to fastpunkt i skogkanten litt ovanfor husa på garden Skrednakken, og eitt punkt i fjellknaus på innmarka utanfor mogeleg sprekk (figur 41). Punkta vart målt om i 2007 og 2012.

Resultat – endringar, 2012
Resultata er synt i tabellar 27 og 28 og grafisk i figur 42. Målinga i 2007 synte ingen signifikante endringar, og det gjer heller ikkje målinga i 2012.

Konklusjon
Det er ingen teikn på rørsle i punktet på Skrednakken.

PUNKT	År	N	E	H	sN	sE	sH	dN	dE	Avstand	Retning	dH
SK-1_FP	F.P.	6906322.390	399606.603	509.107								
SK-2_FP	F.P.	6906337.913	399727.783	517.916								
SK-3	2006	6906546.3870	399667.4895	476.2300	0.0011	0.006	0.0024					
SK-3-07	2007	6906546.3858	399667.4900	476.2273	0.0008	0.005	0.0015	-0.001	0.001	0.001	162.567	-0.003
SK-3	2012	6906546.3856	399667.4875	476.2301	0.0031	0.0026	0.0067	-0.001	-0.002	0.002	266.590	0.000

Tabell 27: Koordinatar og endringar i høve til fyrste måling for punkt på Skrednakken.

PUNKT	ÅR	dN	dE	Avstand	Retning	dH
6B-01	2005-06	-0.002	0.000	0.002	188.02	0.005
6B-01	2006-07	-0.002	-0.001	0.002	234.40	0.002

Tabell 28: Endringar mellom år for punkt SK-3 på Skrednakken.

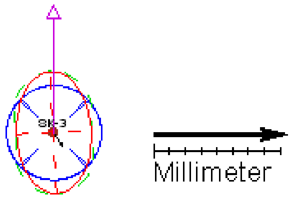

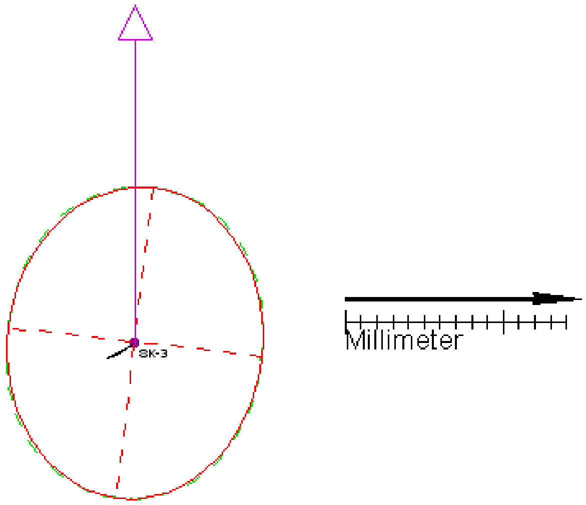

Figur 42: Grafisk illustrasjon av endringar i punkt SK-3, 2006–07 til venstre, 2006–12 til høgre – ingen signifikant endring (høge standardavvik i 2012 gir stor konfidensellipse).

Storehornet

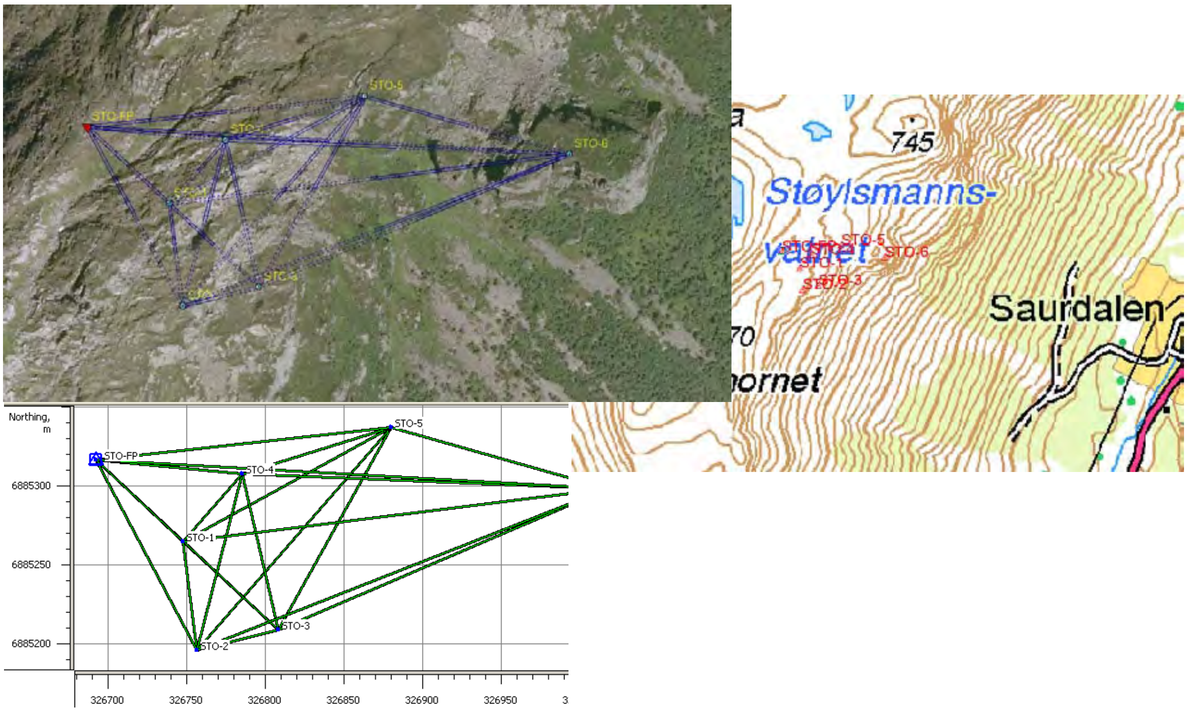

Figur 43: Vektorriss og kart (Sk-N50).

Punktgrunnlag

I september 2012 er det etablert eit fastpunkt på toppen av fjellryggen og seks punkt på blokker i det oppsprekte området aust for ryggen (figur 43).

Resultat

Resultat frå målinga i 2012 er gitt i tabell 29.

PUNKT	År	N	E	H	sN	sE	sH	dN	dE	Avstand	Retning	dH
STO-FP	2012	6885316.5470	326692.5480	764.2500								
STO-1	2012	6885264.9521	326747.8077	751.6576	0.0005	0.0004	0.0011					
STO-2	2012	6885196.2136	326756.7543	746.1957	0.0005	0.0004	0.0011					
STO-3	2012	6885208.9295	326808.2048	729.9537	0.0005	0.0004	0.0012					
STO-4	2012	6885307.8984	326785.6724	750.5380	0.0005	0.0004	0.0011					
STO-5	2012	6885336.8724	326879.9337	737.1742	0.0005	0.0004	0.0012					
STO-6	2012	6885298.1395	327017.6038	671.0902	0.0005	0.0004	0.0012					

Tabell 29: Koordinatar for punkt på Storehornet.

Svarttinden

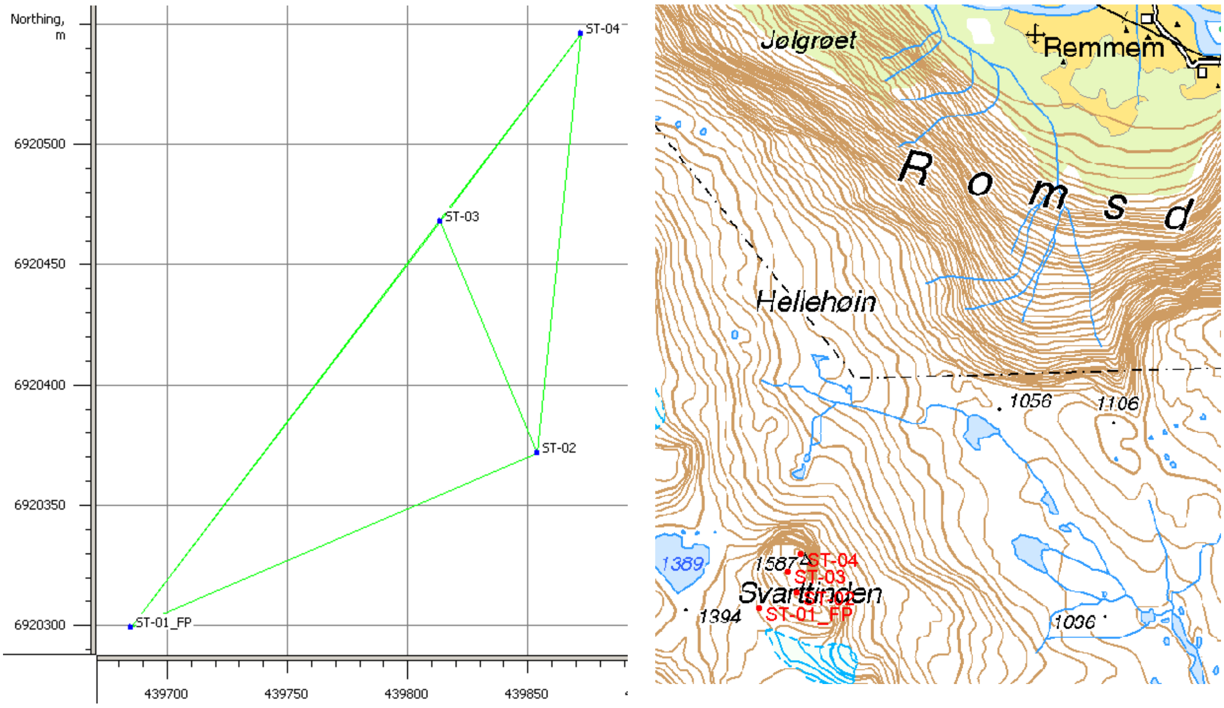

Figur 44: Riss over GPS-vektorar, ST-01_FP er fastpunkt. Kartskisse med punkt (Sk-N50).

Punktgrunnlag
Nær toppen av Svarttinden vart det etablert tre punkt i august 2005 i tillegg til eit fastpunkt ved foten av toppen på sørvestsida av fjellet (figur 44). Punkta er målt om att i 2006, 2007 og 2010.

Resultat – endringar, 2010
Resultata for perioden 2005–10 er gitt i tabellar 30 og 31 og figur 45, og syner ingen signifikante endringar, korkje i plan eller høgd. Det er stor høgdeskilnad frå referansepunktet til dei tre andre punkta, og det gir noko høge standardavvik for vektorane i prosjektet. Dette fører til at sjølv om det er vertikale endringar på meir enn 1 cm er dette, som det går fram av figur 45, ikkje signifikant endring. Variasjonane ein finn i koordinatane ligg elles innanfor testgrensene, og det er ikkje grunnlag for å seie at punkta er i rørsle.

Konklusjon:
Det er ut frå materialet ikkje grunn til å hevde at det er rørsle i punkta på Svarttinden.

PUNKT	År	N	E	H	sN	sE	sH	dN	dE	Avst	Retning	dH
ST-01_FP	F.P.	6920298.875	439684.609	1513.045								
ST-2	2005	6920371.0094	439853.4908	1602.9556	0.0020	0.0010	0.0030					
ST-2	2006	6920371.0109	439853.4889	1602.9667	0.0016	0.0013	0.0036	0.002	-0.002	**0.002**	342.54	**0.011**
ST-2	2007	6920371.0114	439853.4934	1602.9600	0.0018	0.0013	0.0030	0.002	0.003	**0.003**	58.26	**0.004**
ST-2	2010	6920371.0145	439853.4901	1602.9583	0.0009	0.0012	0.0017	0.005	-0.001	**0.005**	391.32	**0.003**
ST-3	2005	6920467.4928	439813.3207	1613.4763	0.0020	0.0010	0.0030					
ST-3	2006	6920467.4938	439813.3163	1613.4812	0.0012	0.0009	0.0027	0.001	-0.004	**0.005**	314.23	**0.005**
ST-3	2007	6920467.4957	439813.3211	1613.4845	0.0017	0.0012	0.0029	0.003	0.000	**0.003**	8.73	**0.008**
ST-3	2010	6920467.4944	439813.3174	1613.4818	0.0007	0.0010	0.0014	0.002	-0.003	**0.004**	328.74	**0.005**
ST-4	2005	6920545.2694	439871.6420	1629.0190	0.0020	0.0010	0.0030					
ST-4	2006	6920545.2676	439871.6399	1629.0174	0.0016	0.0010	0.0036	-0.002	-0.002	**0.003**	254.89	**-0.002**
ST-4	2007	6920545.2656	439871.6402	1629.0312	0.0032	0.0017	0.0050	-0.004	-0.002	**0.004**	228.16	**0.012**
ST-4	2010	6920545.2627	439871.6369	1629.0294	0.0009	0.0012	0.0018	-0.007	-0.005	**0.008**	241.42	**0.010**

Tabell 30: Koordinatar og endring i høve til fyrste måling 2005–10 for punkt på Svarttinden.

		Endring mellom målingar				
PUNKT	**ÅR**	**dN [m]**	**dE [m]**	**Avstand [m]**	**Retning [^{g} gon]**	**dH [m]**
ST-2	2005-06	0.002	-0.002	**0.002**	342.54	**0.011**
ST-2	2006-07	0.001	0.004	**0.005**	92.96	**-0.007**
ST-2	2007-10	0.003	-0.003	**0.005**	348.01	**-0.002**
ST-3	2005-06	0.001	-0.004	**0.005**	314.23	**0.005**
ST-3	2006-07	0.002	0.005	**0.005**	76.01	**0.003**
ST-3	2007-10	-0.001	-0.004	**0.004**	278.49	**-0.003**
ST-4	2005-06	-0.002	-0.002	**0.003**	254.89	**-0.002**
ST-4	2006-07	-0.002	0.000	**0.002**	190.52	**0.014**
ST-4	2007-10	-0.003	-0.003	**0.004**	254.10	**-0.002**

Tabell 31: Endring mellom målingar 2005–10 for punkt på Svarttinden.

Figur 45: Horisontal- og vertikal-endringar for punkt på Svarttinden for 2005–07 (til venstre), 2005–10 (midten) og 2007–10 (til høgre) med signifikansgrenser for 99%.

Vollan

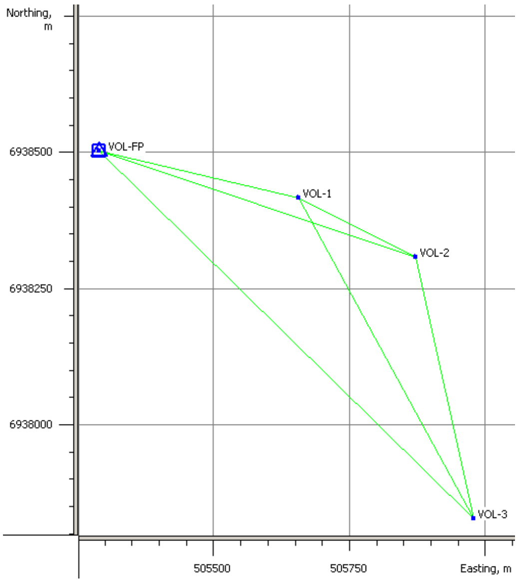

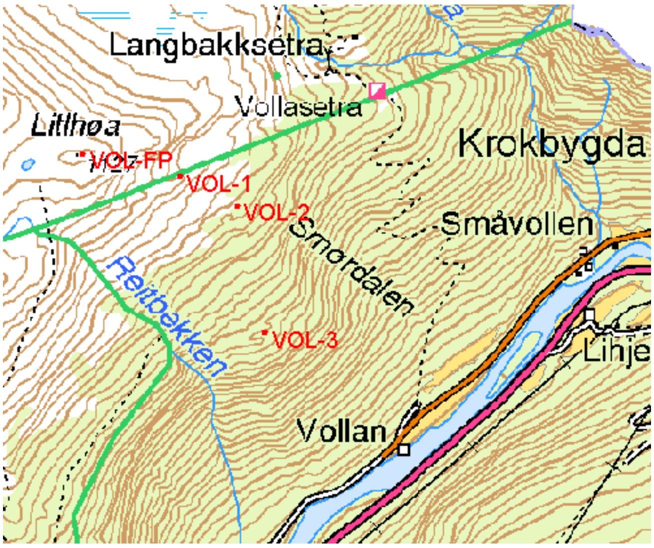

Figur 46: Vektorriss og kart (Sk-N50).

Punktgrunnlag
I 2008 er det etablert tre nye punkt på potensielt ustabile blokker i dalsida ned mot Vollan, og eitt fastpunkt på den lokale toppen Litlhøa (figur 46). Fastpunktet er fastlagt ved absolutt presis metode, dei andre punkta er rekna relativt til fastpunktet ved vektormålingar.

Resultat - endring
Punkta er målt om i 2009 og 2011. Resultata er synt i tabellar 32 og 33 og endringar grafisk i figur 47.

Målingane i alle åra er gode. Resultata for 2008–09 indikerte små signifikante endringar i planet i to av punkta (VOL-1 og VOL-3) med 5 og 8 mm. Resultata for 2011 peiker i planet til dels i motsett retning av 2009, og er såleis inga eintydig stadfesting av rørsle i området.
Målingane på Vollan i 2011 har dei same meteorologiske ”problema” som på Gikling med ekstremt fuktig luft, og resultat prosessert med normalatmosfære gir urealistiske resultat for høgder, med heving i alle punkta. Bruk av same parameter som på Gikling – 70 % RH – gir nesten uendra høgder i dei to øvre punkta, men relativt stor setning i det nedste. Dette resultatet er difor ekstra usikkert grunna uvissa som er knytt til dei meteorologiske tilhøva.

Konklusjon
Det er teikn til rørsle i punktet VOL-3, med signifikante endringar, men estimert presisjon er urealistisk høg slik at kriteria for signifikant endring er svært små. For sikrare konklusjonar bør resultata stadfestast med nye målingar.

PUNKT	År	N (UTM)	E (UTM)	H (ell.)	σN [m]	σE [m]	σH [m]	dN [m]	dE [m]	Avst. [m]	Retning [g gon]	dH [m]
VOL-FP	2009	6938503.1310	505290.3200	1167.6560								
VOL-1	2008	6938416.0699	505655.5185	1025.7763	0.0003	0.0002	0.0006					
VOL-1	2009	6938416.0732	505655.5153	1025.7702	0.0005	0.0004	0.0011	0.003	-0.003	**0.005**	350.98	**-0.006**
VOL-1	2011	6938416.0719	505655.5194	1025.7695	0.0003	0.0003	0.0007	0.002	0.001	**0.002**	26.92	**-0.007**
VOL-2	2008	6938306.9079	505871.7872	939.6603	0.0003	0.0002	0.0006					
VOL-2	2009	6938306.9080	505871.7856	939.6603	0.0006	0.0005	0.0012	0.000	-0.002	**0.002**	303.97	**0.000**
VOL-2	2011	6938306.9064	505871.7903	939.6599	0.0003	0.0003	0.0007	-0.002	0.003	**0.003**	128.69	**0.000**
VOL-3	2008	6937827.3006	505977.5721	723.3831	0.0003	0.0003	0.0007					
VOL-3	2009	6937827.3008	505977.5640	723.3808	0.0011	0.0008	0.0022	0.000	-0.008	**0.008**	301.57	**-0.002**
VOL-3	2011	6937827.2954	505977.5743	723.3685	0.0004	0.0004	0.0009	-0.005	0.002	**0.006**	174.52	**-0.015**

Tabell 32: Koordinatar og endring frå fyrste måling for punkta ved Vollan.

PUNKT	ÅR	dN [m]	dE [m]	Avstand [m]	Retning [g gon]	dH [m]
VOL-1	2008-09	0.0033	-0.0032	**0.005**	350.98	**-0.006**
VOL-1	2009-11	-0.0013	0.0041	**0.004**	119.55	**-0.001**
VOL-2	2008-09	0.0001	-0.0016	**0.002**	303.97	**0.000**
VOL-2	2009-11	-0.0016	0.0047	**0.005**	120.89	**0.000**
VOL-3	2008-09	0.0002	-0.0081	**0.008**	301.57	**-0.002**
VOL-3	2009-11	-0.0054	0.0103	**0.012**	130.74	**-0.012**

Tabell 33: Endring mellom målingar for punkta på Vollan.

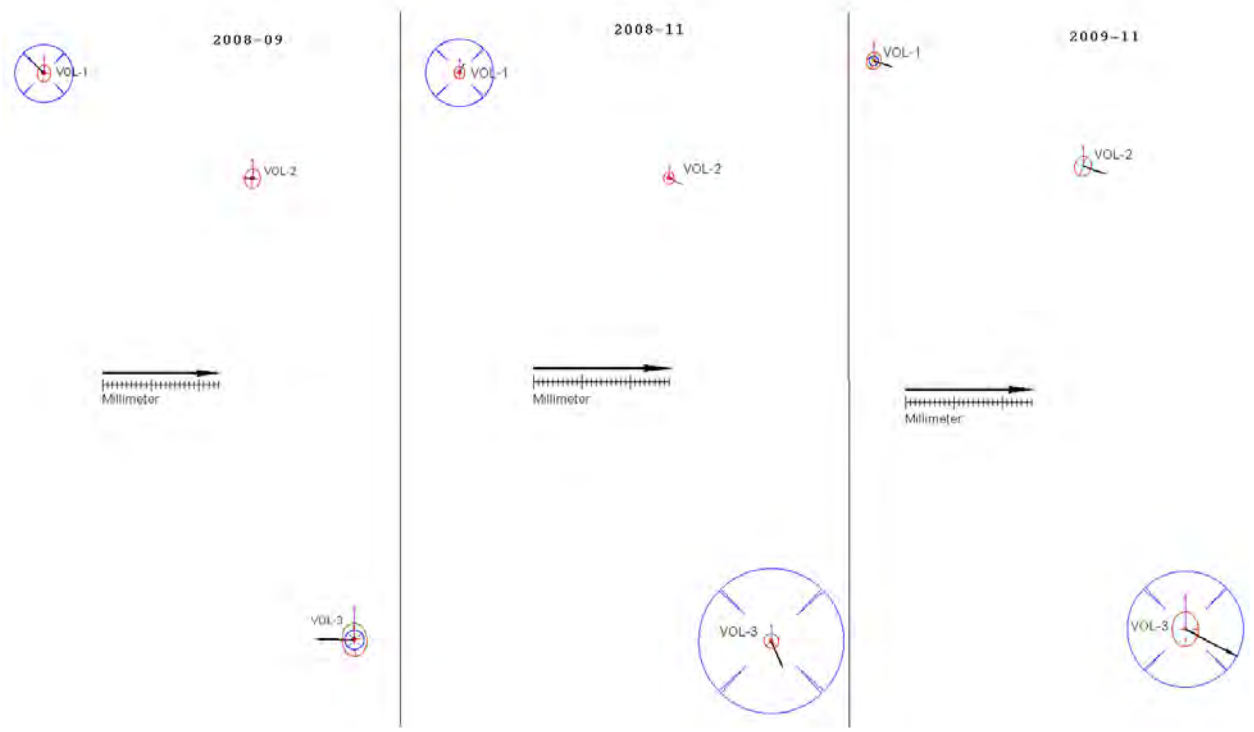

Figur 47: Grafisk framstilling av endring i punkta ved Vollan 2008–11, med konfidensnivå for 99%. Grunnriss (pil), høgde (sirkel). Blå sirklar indikerer setning.

Åknes

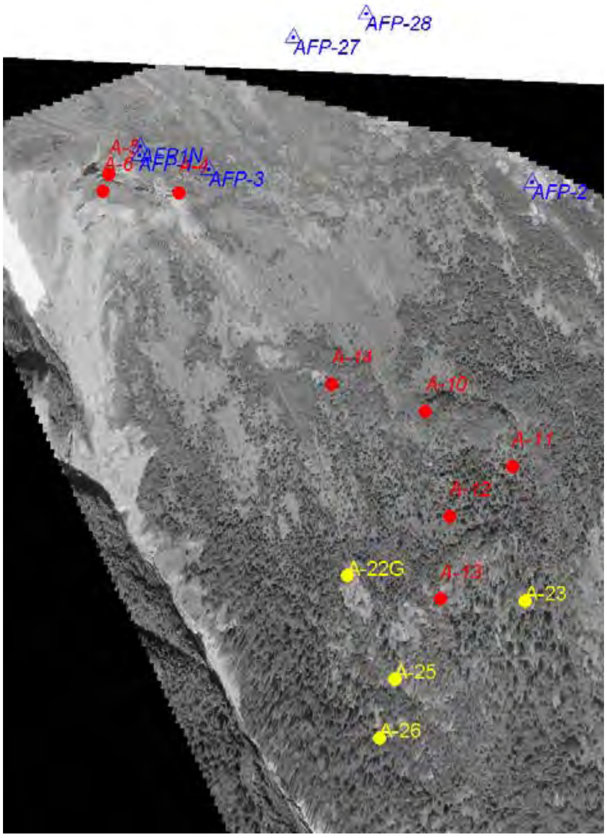

Figur 48: GPS-punkt Åknes. Blå, fastpunkt; raude, punkt etablert oktober 2004; gule, punkt etablert august 2005.

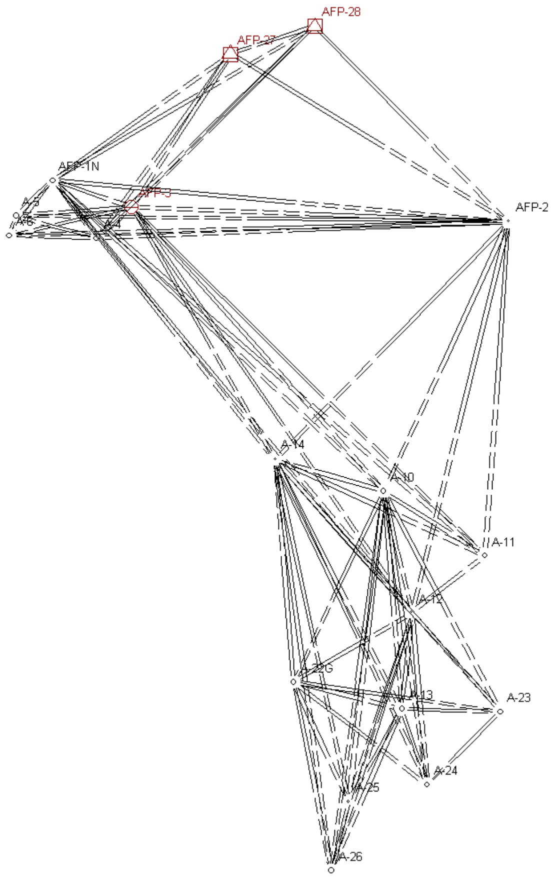

Figur 49: GPS-nett – vektorar målt august 2006.

Punktgrunnlag
GPS punkta på Åknes er etablert i to omgongar, med nokre endringar av enkeltpunkt i tillegg. Tre fastpunkt og åtte punkt i det ustabile området vart etablert i oktober 2004 (figurar 48 og 49). I august 2005 vart det etablert to nye fastpunkt og fem nye punkt i det ustabile området. I 2007 er det etablert eitt nytt fastpunkt i fast fjell ved gardstunet (AFP-29). Hausten 2005 vart eitt av fastpunkta erstatta med eit nytt etter at nye konstruksjonar vart sett opp over punktet (AFP-1). Vinteren 2006–07 vart eit anna fastpunkt delvis øydelagt av eit snøras (AFP-2), dette er ikkje målt i 2007. I 2006–07 er det sett opp mange nye fundament/master nær fleire av dei gamle GPS-punkta, og det gjer at målingane i desse ikkje får den same kvalitet som tidlegare. Konstruksjonar nær punkta reduserer horisont frå antenne, og dermed talet på satellittar ein kan måle til. Metallkonstruksjonar aukar og risiko for multipath, eller fleirvegsinterferens som kan vere ei stor feilkjelde ved GPS-målingar. Eitt av punkta (A-4) med nytt fundament rett ved punktet vart ikkje målt i 2007.

I 2008 var og fastpunktet på øvre bunkers endra av konstruksjonar og i eitt fastpunkt (AFP-27) var dataserien frå mottakaren mangelfull slik at det var vanskeleg å få samanheng til tidlegare målingar. Målingane vart difor rekna saman med data frå dei permanente stasjonane, og tilsvarande prosessering var utført for deler av 2007 målingane. Endringane i fastpunkt og endringar i enkeltpunkt på grunn av konstruksjonar ved punkta gjer at måleresultata ikkje er like konsistente som dei kunne vere utan dette. Resultata frå målingane er difor relativt usikre.

Målingar og resultat 2008

Ved målingane i 2007 var det permanente GPS systemet for overvaking på Åknes operativt, og målingane vart knytt saman med dette. Dette er vidareført ved målingane i 2008. Dei permanente GPS-stasjonane er knytt til og gitt koordinatar relativt dei gitte punkta i det gamle nettet. Dei andre målepunkta er deretter fastlagt dels ved vektorar til dei permanente punkta, og dels ved direkte vektorar slik det er gjort tidlegare.

Målepresisjonen er noko dårlegare i 2007 og 2008 enn i tidlegare år, og dette skuldast mest truleg at mange av punkta har vorte delvis ”øydelagde” ved at master for permanente stasjonar er sett opp like ved punkta, og vektorar til desse syner eit vesentleg dårlegare (mindre presist) resultat enn tidlegare. Fleire vektorar med høge standardavvik gjer at estimert standardavvik for det samla nettet og for utjamna koordinatar aukar. Dette får konsekvensar for den totale presisjonen for nettet, men påverkar i lita grad koordinatresultat for enkeltpunkta som ikkje er ”øydelagde”

Presisjonen til GPS-målingane er dårlegare på Åknes enn i dei fleste andre områda som har tilvarande målingar. Den store høgdeskilnaden og meteorologiske tilhøve som ikkje vert fanga opp gjennom vanleg måling og prosessering av GPS-vektorar kan vere noko av årsaka. Målingane vert gjennomført over relativt kort tid, slik at lokale kortperiodiske tilhøve, som m.a. inversjonar påverkar målingane utan at ein kan korrigere for det. Mange av punkta på Åknes ligg og slik at det er sikt til færre satellittar enn i fleire av dei tilsvarande måleområda. Dette fører til dårlegare geometrisk kvalitet på målingane og vidare til redusert presisjon, høgare standardavvik på resultatkoordinatane samanlikna med andre område. Ei anna feilkjelde som påverkar ein del av punkta er boltar som står så skeivt at det er uråd å sentrere, stille antenna i lodd i punkta. Denne feilen påverkar berre grunnrisskoordinaten og kan utgjere ein del millimeter og er uråd å korrigere for. Over tid vil denne feilen utgjere mindre ettersom den vert ein mindre del av den totale flyttinga til eit punkt.

Standardavvik for utjamna koordinatar er typisk 3–5 mm i grunnriss (gjennomsnitt 4 mm) og litt større i høgde (gjennomsnitt 6 mm) – men nokre punkt har standardavvik på 10 mm eller meir både i grunnriss og høgd. Serleg punkta A-11, A-12 og A-13 får i 2007 og -08 vesentleg høgare standardavvik enn tidlegare. Dette skuldast fundamenta ved punkta som reduserer kvaliteten til målingane. Basert på gjennomsnittsverda vil måleresultata indikere signifikant rørsle ved flyttingar på meir enn ca. 17 mm i grunnriss og 25 mm i høgd, men dette vil variere med presisjonen for dei ulike punkta ved dei ulike målingane.

Endringar i koordinatar er i det fylgjande synt i tabell 34 og figurar 50–53 som syner endringar mellom målingar.

Konklusjon

Resultata syner at punkta kan delast i tre grupper:

- A-5 og A-6 ved ”graben” strukturen syner stor rørsle og denne er så godt som konstant mellom alle målingar.
- A-10, A-11 og A-14 (over, på og under ”kollen”) syner relativt konstante og signifikante endringar, men mindre enn dei øvste punkta.
- Dei øvrige punkta syner ingen konsistente trendar, sjølv om enkeltresultat er signifikante.

Punkt	År	Nord	Aust	Høgd	sN	sE	sH	dN	dE	Avst.	Retn	dH
AFP-1N	aug.07	6896082.779	395315.300	955.310								
AFP-27	aug.07	6896248.858	395549.162	902.362								
AFP-28	aug.07	6896285.099	395659.440	867.172								
AFP-29	aug.07	6895166.929	396067.375	140.557	0.005	0.002	0.006					
AFP-29	aug.08	6895166.94	396067.3755	140.5105	0.0019	0.0012	0.0037	0.011	0.000	**0.011**	2.29	-0.046
A-FP3	okt.04	6896046.846	395420.033	885.806	0.002	0.002						
AFP-3	jun.05	6896046.845	395420.036	885.806	0.002	0.001		-0.001	0.003	0.003	126.25	
AFP-3	okt.05	6896046.841	395420.039	885.806	0.001	0.001		-0.005	0.006	0.008	143.60	
AFP-3	aug.06	6896046.840	395420.022	885.806	0.001	0.001		-0.006	-0.011	0.012	267.92	
AFP-3	aug.07	6896046.845	395420.046	885.806	0.002	0.001		-0.001	0.013	0.013	104.81	
AFP-3	aug.08	6896046.84	395420.0391	885.804	0.0017	0.0013	0.003	-0.006	0.007	**0.009**	146.92	-0.002
A-4	okt.04	6896007.202	395374.055	875.480	0.002	0.001	0.003					
A-4	jun.05	6896007.191	395374.062	875.446	0.002	0.001	0.003	-0.011	0.008	0.013	162.17	-0.034
A-4	okt.05	6896007.197	395374.047	875.449	0.002	0.002	0.003	-0.005	-0.008	0.010	263.31	-0.031
A-4	aug.06	6896007.186	395374.038	875.416	0.001	0.001	0.002	-0.016	-0.017	0.024	251.91	-0.064
A-4	aug.07	IKKJE MÅLT										
A-5	okt.04	6896010.366	395258.222	918.611	0.002	0.001	0.003					
A-5	jun.05	6896010.330	395258.219	918.551	0.002	0.001	0.003	-0.035	-0.002	0.035	204.13	-0.059
A-5	okt.05	6896010.318	395258.215	918.540	0.002	0.001	0.004	-0.048	-0.007	0.048	208.57	-0.071
A-5	aug.06	6896010.304	395258.208	918.485	0.002	0.001	0.003	-0.062	-0.013	0.064	213.51	-0.126
A-5	aug.07	6896010.263	395258.203	918.430	0.002	0.001	0.003	-0.103	-0.019	0.105	211.55	-0.180
A-5	aug.08	6896010.22	395258.194	918.3594	0.002	0.0016	0.0037	-0.146	-0.028	**0.149**	211.94	-0.251
A-6	okt.04	6896035.838	395267.114	918.996	0.003	0.001	0.004					
A-6	jun.05	6896035.756	395267.154	918.870	0.002	0.001	0.003	-0.081	0.040	0.091	170.86	-0.125
A-6	okt.05	6896035.729	395267.167	918.858	0.015	0.009	0.022	-0.108	0.053	0.121	170.91	-0.138
A-6	aug.06	6896035.682	395267.190	918.770	0.002	0.001	0.003	-0.156	0.076	0.174	171.11	-0.226
A-6	aug.07	6896035.599	395267.225	918.655	0.002	0.001	0.003	-0.239	0.112	0.264	172.14	-0.341
A-6	aug.08	6896035.505	395267.2679	918.5206	0.0024	0.0017	0.0042	-0.333	0.154	**0.367**	172.36	-0.475
A-10	okt.04	6895673.676	395750.805	550.918	0.003	0.002	0.004					
A-10	jun.05	6895673.663	395750.813	550.935	0.001	0.001	0.003	-0.013	0.009	0.015	162.00	0.017
A-10	okt.05	6895673.665	395750.819	550.922	0.002	0.001	0.003	-0.011	0.015	0.019	141.99	0.004
A-10	aug.06	6895673.657	395750.828	550.930	0.001	0.001	0.002	-0.019	0.023	0.030	143.55	0.011
A-10	aug.07	6895673.642	395750.837	550.904	0.002	0.002	0.005	-0.034	0.033	0.047	151.34	-0.014
A-10	aug.08	6895673.631	395750.8477	550.8852	0.0015	0.0011	0.0028	-0.045	0.043	**0.062**	151.37	-0.033
A-11	okt.04	6895589.596	395883.325	437.913	0.004	0.002	0.008					
A-11	jun.05	6895589.585	395883.335	437.920	0.002	0.001	0.003	-0.012	0.010	0.015	154.12	0.007
A-11	okt.05	6895589.589	395883.342	437.892	0.003	0.002	0.006	-0.007	0.016	0.018	125.22	-0.021
A-11	aug.06	6895589.572	395883.353	437.915	0.001	0.001	0.004	-0.024	0.028	0.037	144.61	0.001
A-11	aug.07	6895589.557	395883.363	437.878	0.003	0.002	0.010	-0.039	0.038	0.054	151.16	-0.035
A-11	aug.08	6895589.547	395883.3703	437.8621	0.003	0.002	0.0051	-0.049	0.045	**0.067**	152.69	-0.051
A-12	okt.04	6895513.898	395787.797	431.558	0.003	0.002	0.004					
A-12	jun.05	6895513.898	395787.790	431.592	0.002	0.002	0.004	0.000	-0.006	0.006	300.99	0.034
A-12	okt.05	6895513.902	395787.798	431.563	0.004	0.003	0.007	0.004	0.001	0.004	11.60	0.005
A-12	aug.06	6895513.901	395787.799	431.593	0.001	0.001	0.003	0.004	0.002	0.004	34.40	0.034
A-12	aug.07	6895513.897	395787.799	431.566	0.011	0.009	0.029	-0.001	0.002	0.002	120.48	0.008
A-12	aug.08	6895513.9	395787.8028	431.5387	0.004	0.0026	0.007	0.003	0.006	**0.007**	73.08	-0.019
Punkt	**År**	**Nord**	**Aust**	**Høgd**	**sN**	**sE**	**sH**	**dN**	**dE**	**Avst.**	**Retn**	**dH**

A-13	okt.04	6895387.389	395773.560	370.329	0.004	0.002	0.004					
A-13	jun.05	6895387.399	395773.559	370.363	0.002	0.002	0.004	0.011	-0.001	0.011	392.23	0.034
A-13	okt.05	6895387.396	395773.571	370.335	0.004	0.003	0.007	0.007	0.011	0.013	62.30	0.006
A-13	aug.06	6895387.391	395773.570	370.382	0.002	0.002	0.004	0.002	0.010	0.010	87.69	0.053
A-13	aug.07	6895387.398	395773.563	370.340	0.005	0.003	0.008	0.010	0.003	0.010	20.48	0.010
A-13	aug.08	6895387.387	395773.5714	370.3444	0.003	0.0021	0.0048	-0.002	0.012	**0.012**	110.87	0.015
A-14	okt.04	6895715.598	395607.158	602.753	0.004	0.004	0.007					
A-14	jun.05	6895715.585	395607.165	602.744	0.003	0.002	0.005	-0.012	0.007	0.014	168.86	-0.009
A-14	okt.05	6895715.588	395607.173	602.727	0.002	0.002	0.004	-0.009	0.014	0.017	137.33	-0.027
A-14	aug.06	6895715.562	395607.182	602.732	0.001	0.001	0.003	-0.036	0.024	0.043	163.02	-0.021
A-14	aug.07	6895715.545	395607.191	602.710	0.003	0.002	0.006	-0.053	0.032	0.062	164.93	-0.043
A-14	aug.08	6895715.526	395607.2017	602.6904	0.0017	0.0012	0.0032	-0.072	0.043	**0.084**	165.49	-0.063
A-22G	aug.05	6895422.691	395632.252	417.850	0.003	0.002	0.006					
A-22G	okt.05	6895422.690	395632.257	417.857	0.004	0.003	0.007	-0.001	0.005	0.005	116.59	0.007
A-22G	aug.06	6895422.688	395632.259	417.894	0.002	0.001	0.004	-0.003	0.007	0.007	125.20	0.043
A-22G	aug.07	6895422.684	395632.255	417.869	0.002	0.002	0.004	-0.007	0.003	0.008	173.04	0.019
A-22	aug.08	6895422.682	395632.2598	417.8633	0.003	0.002	0.0049	-0.009	0.008	**0.012**	155.91	0.013
A-23	aug.05	6895384.032	395903.448	318.907	0.009	0.007	0.015					
A-23	okt.05	6895384.058	395903.442	318.863	0.006	0.004	0.011	0.026	-0.006	0.027	385.38	-0.044
A-23	aug.06	6895384.024	395903.461	318.930	0.005	0.003	0.009	-0.008	0.014	0.016	133.65	0.022
A-23	aug.07	6895384.033	395903.455	318.895	0.005	0.003	0.008	0.001	0.007	0.007	90.97	-0.012
A-23	aug.08	6895384.038	395903.4591	318.8854	0.0033	0.0021	0.006	0.007	0.011	**0.013**	66.00	-0.022
A-24	aug.05	6895287.506	395807.594	282.036	0.005	0.004	0.009					
A-24	aug.06	6895287.525	395807.599	282.063	0.006	0.003	0.007	0.019	0.005	0.020	16.59	0.027
A-24	aug.07	6895287.522	395807.594	282.020	0.004	0.002	0.007	0.016	0.001	0.016	2.37	-0.016
A-24	aug.08	6895287.531	395807.603	282.0176	0.0046	0.0031	0.0094	0.025	0.009	**0.027**	22.56	-0.018
A-25	aug.05	6895264.638	395704.122	292.408	0.006	0.004	0.012					
A-25	okt.05	6895264.652	395704.117	292.379	0.006	0.004	0.010	0.014	-0.005	0.015	376.62	-0.029
A-25	aug.06	6895264.645	395704.124	292.433	0.003	0.002	0.006	0.007	0.002	0.007	19.07	0.025
A-25	aug.07	6895264.636	395704.121	292.397	0.008	0.005	0.010	-0.002	-0.001	0.002	223.17	-0.011
A-25	aug.08	6895264.617	395704.161	292.422	0.0071	0.0051	0.0149	-0.021	0.039	**0.044**	131.46	0.014
A-26	aug.05	6895174.491	395681.194	236.789	0.004	0.003	0.010					
A-26	okt.05	6895174.480	395681.201	236.782	0.010	0.006	0.015	-0.011	0.006	0.013	165.25	-0.007
A-26	aug.06	6895174.490	395681.200	236.804	0.003	0.002	0.008	-0.001	0.006	0.006	106.94	0.014
A-26	aug.07	6895174.481	395681.195	236.787	0.004	0.002	0.006	-0.010	0.001	0.010	193.39	-0.002
A-26	aug.08	6895174.482	395681.2014	236.7539	0.003	0.0016	0.0048	-0.009	0.007	**0.012**	155.84	-0.035

Tabell 34: Koordinatar og endringar for punkta på Åknes. Endringar er rekna i høve til fyrste gong punkta er målt – anten oktober 2004 eller august 2005. Koordinatar for fastpunkt har ikkje standardavvik.

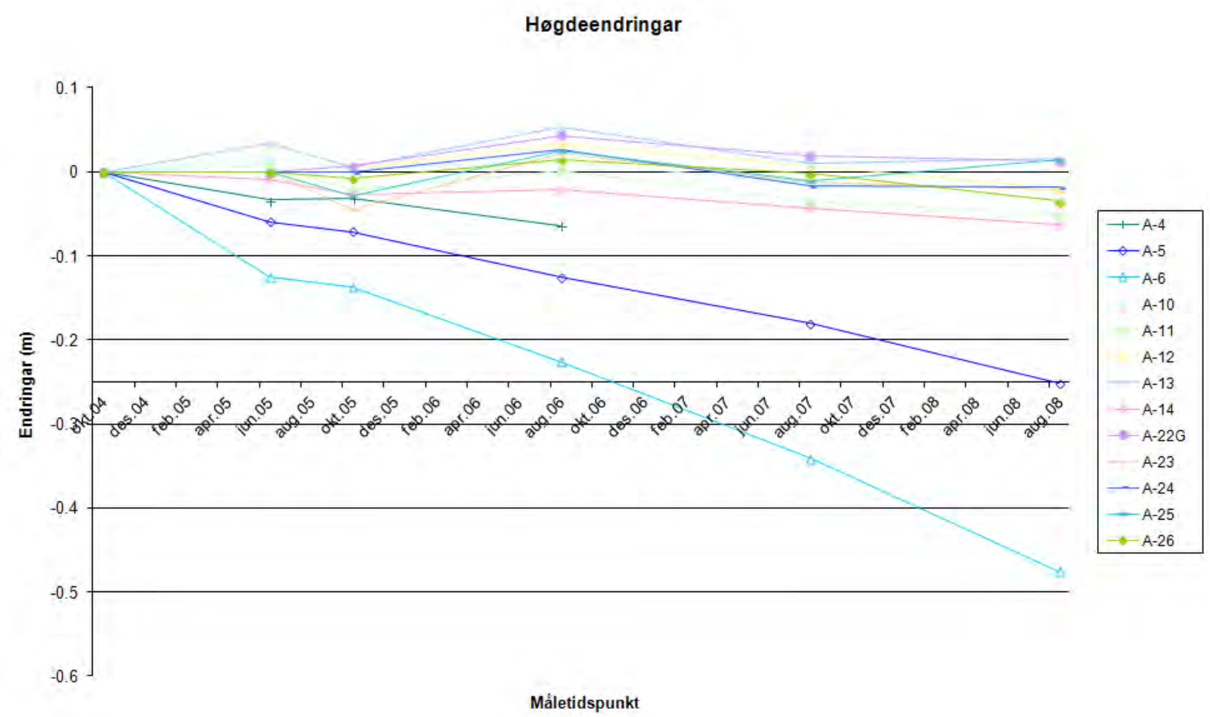

Figur 50: Alle målte endringar i høgd framstilt over tid for kvart punkt.

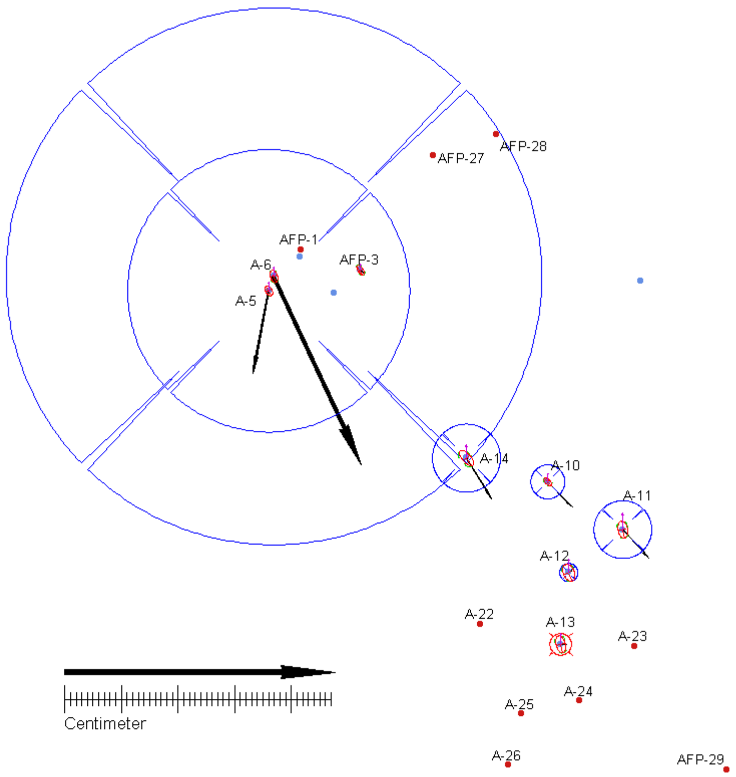

Figur 51: Endringar oktober 2004 – august 2008. Grunnriss er svarte piler, høgde er sirklar. Blå sirklar indikerer senking, raude heving.

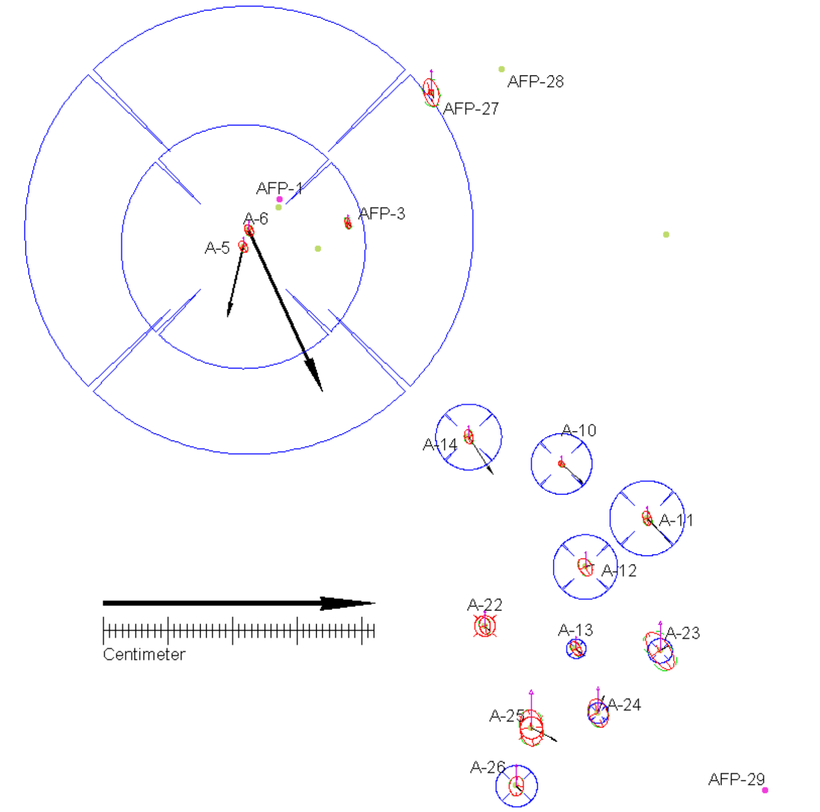

Figur 52: Endringar juni/august 2005 til 2008.

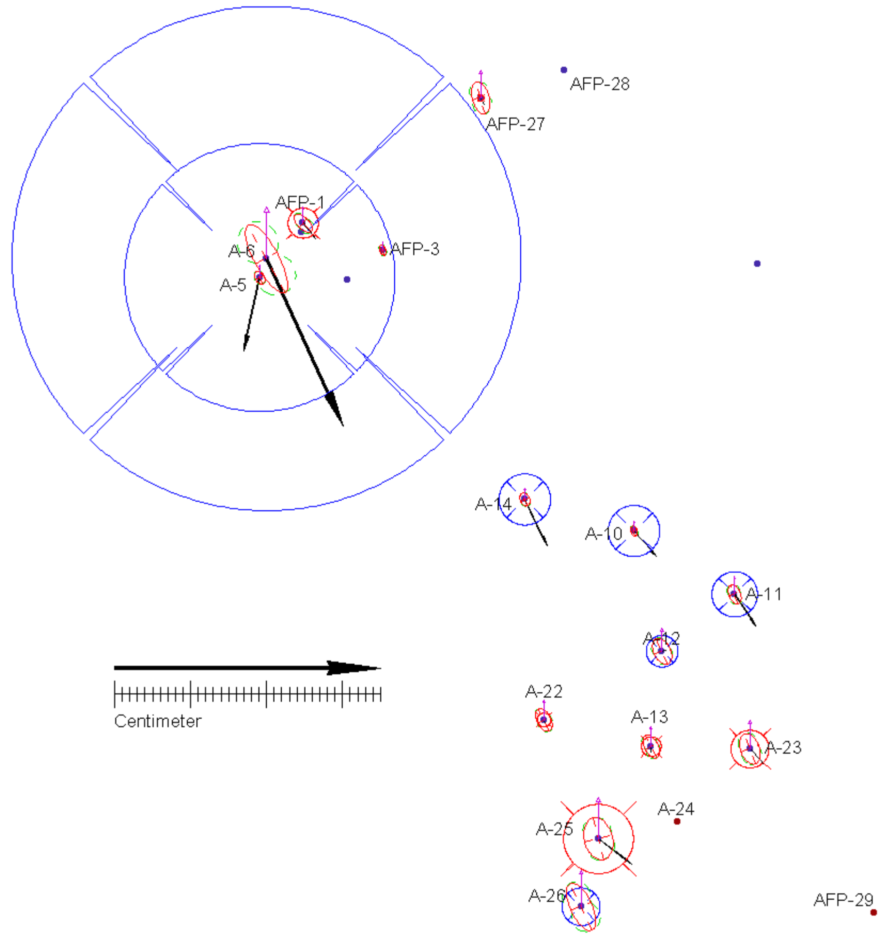

Figur 53: Endringar oktober 2005 – august 2008.

Appendix 2: Report on terrestrial laser scanning measurements in Møre og Romsdal

This appendix gives detailed results from terrestrial laser scanning measurements in Møre og Romsdal in the years 2006-2009. The data have been acquired, processed and analysed by the University of Lausanne, Switzerland, on behalf of the Geological Survey of Norway.

Note: The site Kvitfjellet in Norddal municipality is named "Nordal_21" in this report and Rindalseggene in Stranda municipality is named "Hellesylt_6b".

UNIL | Université de Lausanne
Faculty of Geosciences and Environment
Institute of Geomatics and Risk Analysis
Amphipôle
CH-1015 Lausanne

Analysis of groundbased Lidar data from Møre og Romsdal County (Norway)

C. Longchamp, F. Delasoie, D. Carrea, M.-H. Derron, T. Oppikofer, M. Jaboyedoff

IGAR - June 2010

Faculty of Geosciences and Environment
Institute of Geomatics and Risk Analysis
Phone +41 21 692 35 32 | Fax +41 21 692 35 35 | michel.jaboyedoff@unil.ch

UNIL | University of Lausanne

Executive Summary

We summarize here the main outcomes of the lidar datasets analysis for eight sites. In addition, we make some recommendations to optimize the future lidar acquisition campaigns. If a full cover of the site has been done once, it is usually not necessary to scan the entire site again, but some specific well-chosen scans are sufficient to monitor changes and displacements.

The goal of this work is to present and discuss the information extracted from the TLS scans in a way that this information can be used for future geological interpretations. As only observations from the lidar datasets are discussed here, this report does not intend to provide a complete analysis of the sites.

FLATMARK	
Year of scanning	2007
Area scanned	Upper part from two different sites of the unstable block
Discontinuity sets	Mean topography : [065/60] Site1: J1 [298/54], J2 [089/49], J3 [254/69], J4 [097/69], J5 [178/48]. Site2: J1 [263/47], J2 [235/83], J3 [088/74], J4 [193/81], J5 [039/25].
Kinematics test	Site1:toppling on J2 and J3, potential planar sliding along J4, wedge sliding on J1^J5 Site 2: mainly toppling involving J2, potentially planar sliding along J5, J3 and J2, potential wedge sliding on J1^J4. Central part: planar sliding on the foliation.
Displacements	Not done (only one year of data).
Remarks	Complex landslide with several compartments. The toppling observed on the top is certainly part of a much larger slope deformation that has to be investigated.
Main recommendations	Structural analysis of the new airborne lidar dataset and monitoring of the eastern blocks.
BØRA	
Year of scanning	2008
Area scanned	Top of the moving part, main scarp, sliding block. The area was divided into two parts: the Graben site and the Upper cliff.
Discontinuity sets	Mean topography: [044/50] Graben site: J1 [179/77], J2 [218/83], J3 [063/50], J4 [255/69]. Upper cliff: J1 [139/89], J2 [177/86], J3 [258/67], J4 [237/85], J5 [079/55], J6 [357/31].
Kinematics test	Upper cliff: toppling with J4, wedge sliding on J1^J5, planar sliding along J5 and J6.
Displacements	Not done (only one year of data)
Remarks	The top part of the instability surveyed is part of a much bigger slope deformation. Large rockfalls already happened.
Main recommendations	Detect if large volumes are moving (GPS), complete the analysis of the airborne lidar dataset.
MANNEN	
Year of scanning	2008
Area scanned	Top of the moving part, main scarp, sliding block.
Discontinuity sets	Mean topography : [045/558] J1 [254/87], J2 [112/38], J3 [067/34], J4 [124/78].
Kinematics test	Planar sliding on J3 and J2, possible wedges on J3^J2 and J3^J4, toppling on J1.
Displacements	Not done (only one year of data).
Remarks	Strongly dislocated rock mass, open fractures along J4.
Main recommendations	Scan again from the top to detect changes and displacements. Extend the area covered by TLS.

SVARTTINDEN	
Year of scanning	2006
Area scanned	The eastern old sliding surface, the western “pyramid”.
Discontinuity sets	Mean topography : [014/60] J1 [014/60], J2 [091/70], J3 [069/63], J4 [320/70], J5 [197/72], J6 [266/72].
Kinematics test	Planar sliding along J1, J3 and J4, toppling with J5, wdge sliding on J4^J2, J4^J3, J2^J3
Displacements	Not done (only one year of data).
Remarks	Prolongation of the old sliding plane under the pyramid, strong fragmentation in prisms of the rock mass.
Main recommendations	Movement detection (GPS, crack monitoring, terrestrial laser scanning)
HELLESYLT_6b	
Year of scanning	2006
Area scanned	Side of the displaced block.
Discontinuity sets	Mean topography:[150/40] J1 [280/86], J2 [343/67], J3 [033/75], J4 [175/45], J5 [214/51].
Kinematics test	Planar sliding on J4 and J5, potential wedge on J4^J3 and J4^J5..
Displacements	Not done (only one year of data).
Remarks	Open back crack.
Main recommendations	Movement detection (GPS), similar scanning if movement detected.
NORDAL_21	
Year of scanning	2006 and 2009
Area scanned	The entire cliff and the rockfall deposit fan.
Discontinuity sets	Mean topography: [22070] J1 [273/65], J2 [205/87], J3 [165/65], J4 [091/58], J5 [068/13].
Kinematics test	Toppling with J2, J5 and J4, large wedge on J1^J3, small wedges on J1^J2, planar sliding along J1 and J2.
Displacements	No movement detected for the whole block. Some smaller volume rockfalls.
Remarks	Vertical open crack in the face. Houses and fields at risk for rockfalls.
Main recommendations	Movement detection (GPS, total station, crackmeters) and periodic scan of the face from the road.

UNIL | University of Lausanne

Table of content

I Introduction

This report is made in the frame of the collaboration between the Geological Survey of Norway (NGU) and the Institute of Geomatics and Risk Analysis of the University of Lausanne (IGAR). NGU asked IGAR to monitor some of the Møre og Romsdal County instabilities by Terrestrial Laser Scanning (TLS). In complement to this report some sites (Aaknes, Tafjord, Rundefjellet and Taarnet) were analyzed by T. Oppikofer during his PhD thesis (IGAR).
All the data for 2006, 2007, 2008 and 2009 were cleaned, aligned, georeferenced and finally delivered to NGU in December 2009. That was the first part of this work. The goal of this second part is to present and discuss the information extracted from the TLS scans, so that this information can be used for future geological interpretations. Only the observations from the lidar datasets are discussed here, this report does not intend to provide a complete analysis of the sites.

II Sites Locations

All the sites discussed in this report are located in the Møre og Romsdal. The unstable areas are mountainsides above Storfjorden (Sunnylvsforden and Nordal) and Romsdalen (Figure 1).

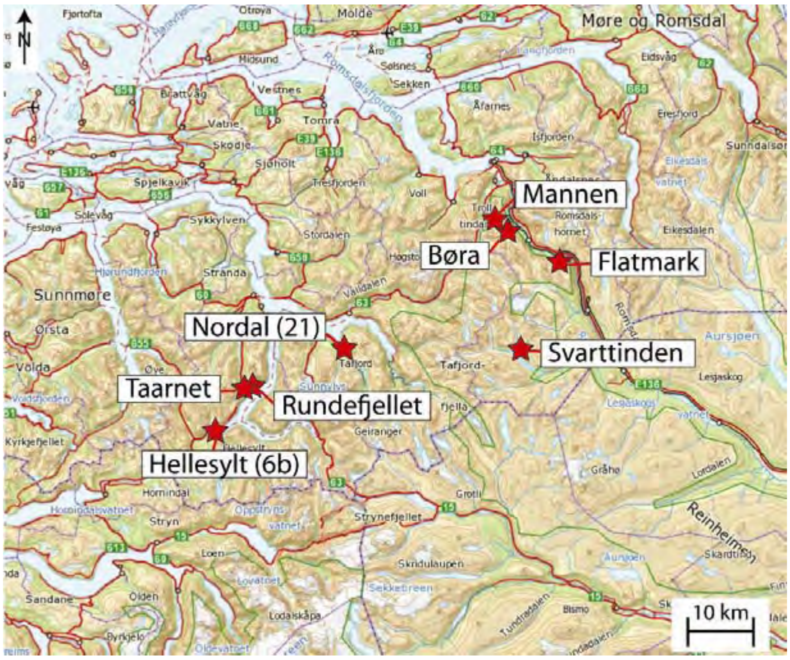

Figure 1: Location map of the sites of instabilities presented in this report.

III Data and processing

III.1 Data acquisition

At the exception of the site of Nordal, all the sites were scanned by T. Oppikofer with others between 2006 and 2008. The area of Nordal was scanned a first time in 2006 by M. Jaboyedoff and a second time in 2009 by M.-H. Derron. All the scans were done in mode « Enhanced Range », last pulse, with a device Optech-Ilris3d.

III.2 Processing method

The scans were processed at IGAR during the winter 2009-2010. The main processing steps are:

(1) Parsing with the Optech parser.
(2) Cleaning: deleting outsiders and vegetation where it masks the rock, with Pifedit (InnovMETRIC).
(3) Alignment with PolyWorks® (InnovMETRIC) v10.1 ImAlign™.
(4) Georeferencing: with PolyWorks® v10.1 ImAlign and ImInspect™ using the references mentioned hereafter. The coordinates/projection/geoid system is UTM Zone 32N – WGS84, in meter. Except for Svarttinden that were georeferenced on a 5m DEM, all the sites were georeferenced on an airborne Lidar DEM.

III.3 Geological and structural interpretation

Main steps:

- The point clouds from the terrestrial scans were interpreted using a beta-version of Coltop3D (www.coltop3d.ch): discontinuities identification, dips measurements and color coding of rock faces. The measurements of discontinuities were, if possible, made on stable parts in order to avoid variations induced by slope movement.
- When all the discontinuity sets were identified, the different families were imported in Dips 5.1 (Rocscience). The stereoplot are in lower hemisphere and equal area and the measurements are given as dip direction and dip angle. For each stereoplot, the mean topography is represented in green. Kinematic tests were performed for planar sliding, wedge sliding and toppling with a frictional angle of 35°. This value of 35° is to use with caution because the frictional angle can significantly changes, i.e., it decreases with the presence of a gouge.
- The displacements are measured using PolyWorks® v10.1 ImInspect™. The method use is the shortest distance from referential point cloud to data point cloud. A full point cloud grouping all the scans of one year includes some internal alignment errors in between the scans (usually around 3 cm) according to the method of alignment. That makes then difficult to use this overall point cloud to detect small displacements (less than 3 cm). So, according to Oppikofer and Jaboyedoff (2009), when it was possible a piece-wise comparison was used, i.e. the comparison was done between single scans of two different years instead of using the full point cloud. This requires that these single scans include a stable part that can be used as reference in addition of the part which is supposed to move. Directions of movement are obtained with the observations made on point cloud in ImInspect™. No roto-translation matrixes were applied to calculate the directions movement.

Interpretations and analysis of different locations:

This chapter contains six subchapters corresponding to the different study areas. Every subchapter contains:

(1) Discontinuity analysis: The analysis of discontinuity sets made with Coltop3D and in some cases kinematic tests.

(2) Movement analysis: A description of the displacements monitored. This second part is absent if there is only one year of lidar scanning or no superposition of scans of different years.

(3) Discussions: A synthesis of the main observations and recommendations about each site.

IV Møre Og Romsdal study areas

IV.1 Flatmark

IV.1.1 Introduction

The Flatmark site is located along the valley of Romsdalen, south-east of Mannen and Børa. Its main part is a block of 15 Mm^3 sliding toward the Nord (Figure 2a and Figure 3). A 700 m long and opened back scarp is visible on the plateau at the top. It has a 25-50 m opening and is oriented W-E (Figure 2b).

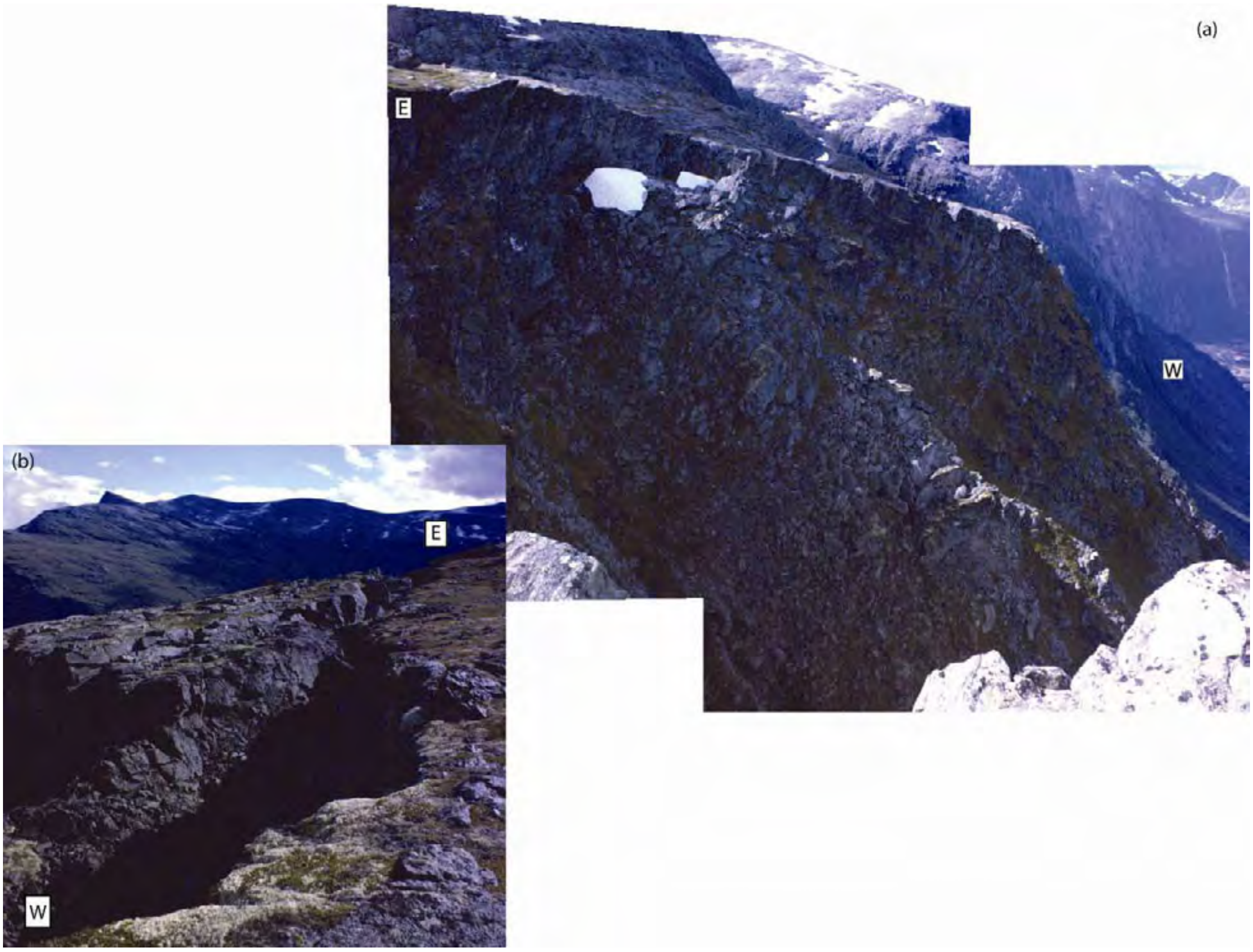

Figure 2: (a) Panorama view of the instability of Flatmark and (b) its back scarp

The Flatmark area was scanned with the terrestrial lidar in 2007. A total of 19 scans were acquired. The scanner positions and parameters are recorded in M. Böhme's fieldbook (NGU) (a copy of the fieldbook is in the dvd of data provided few months ago). Figure 3 shows the projection of the point cloud on the DEM of the studied area.

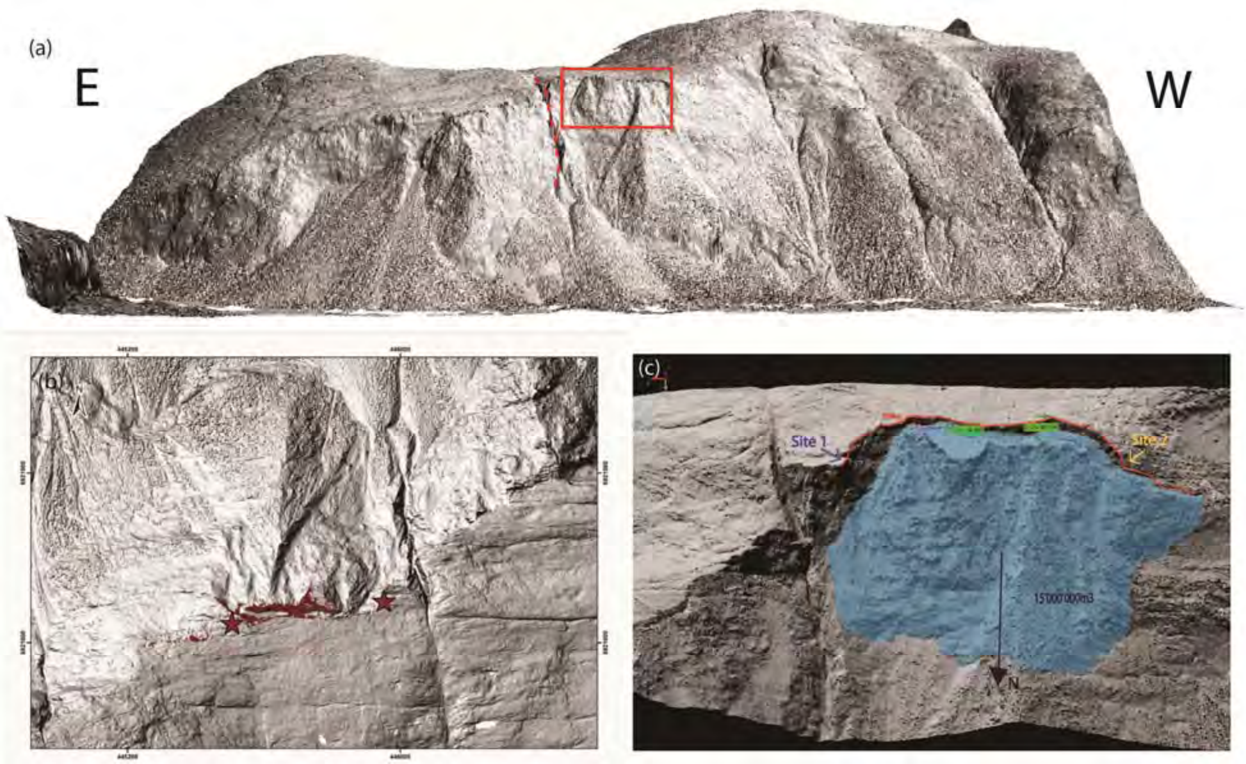

Figure 3: (a) View of the Southern side of Rosmdalen with the Flatmark site in the red box (airborne lidar data), (b) Point clouds projected on the hillshade in red and position of the Lidar during the acquisition (red stars), (c) the unstable compartment (blue), sliding down toward the North, and location of the two sites.

Three sectors, the back-scarp and the sites 1 and 2, were analyzed and discontinuity sets compared (Figure 3c)

IV.1.2 Site 1: structural analysis

The identification of the different discontinuity sets affecting the studied area was done with the software COLTOP-3D. The representation with the colors coding of COLTOP-3D (Figure 4) shows clearly the predominance of facets dipping towards NW (blue).

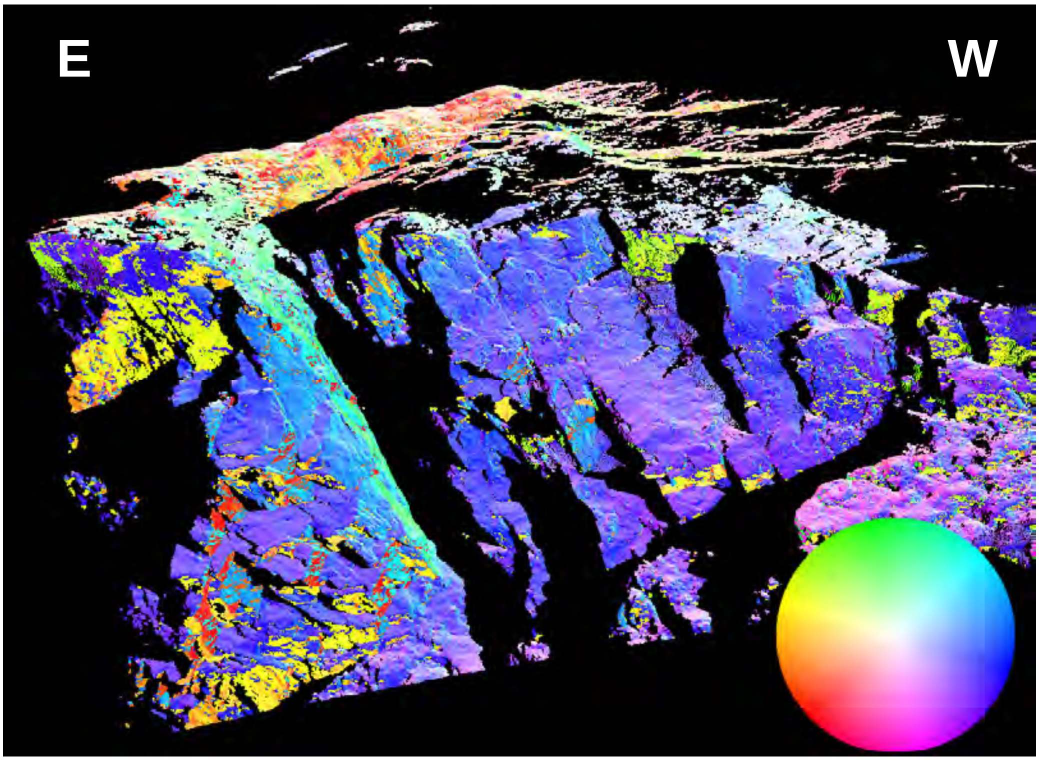

Figure 4: Coltop3D view of the cloud of points of the site1.

Five main sets of discontinuities were identified and imported into Dips. These measurements are presented below in the Table 1 and in the Figure 5:

Table 1: Characteristics of the discontinuity sets of the Site1 of the Flatmark area.

Sets	Dip Direction	Dip	Std. deviation
J1	298	54	17°
J2	089	49	9°
J3	254	69	10°
J4	097	69	8°
J5	178	48	11°

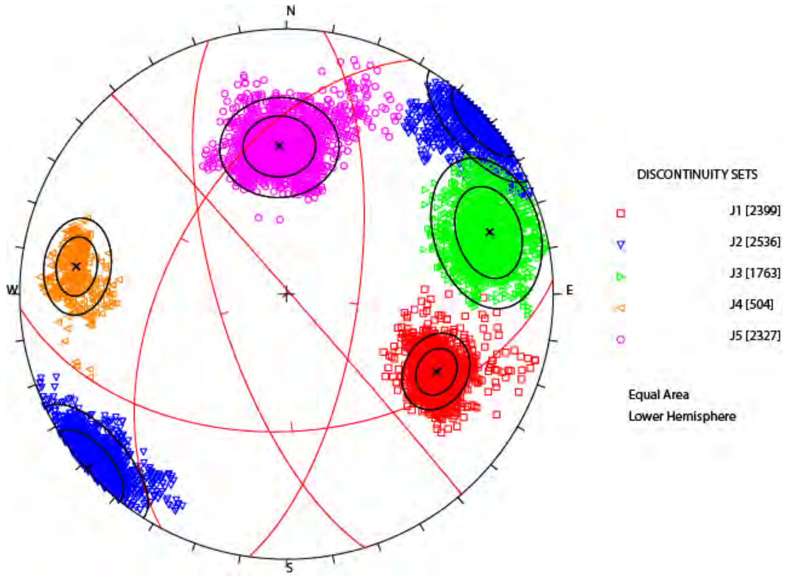

Figure 5: Stereoplot of the main surfaces of discontinuity for the first site of Flatmark. The circles represent the ± 1-sigma and 2-sigma dispersion.

When all the points of the scan are classified according to the 5 sets of discontinuities (using mean ± 2 sigma), it appears that the rock face is almost entirely composed of facets belonging to one of this discontinuity set (Figure 6).

UNIL | University of Lausanne
Faculty of Geosciences and Environment
Institute of Geomatics and Risk Analysis

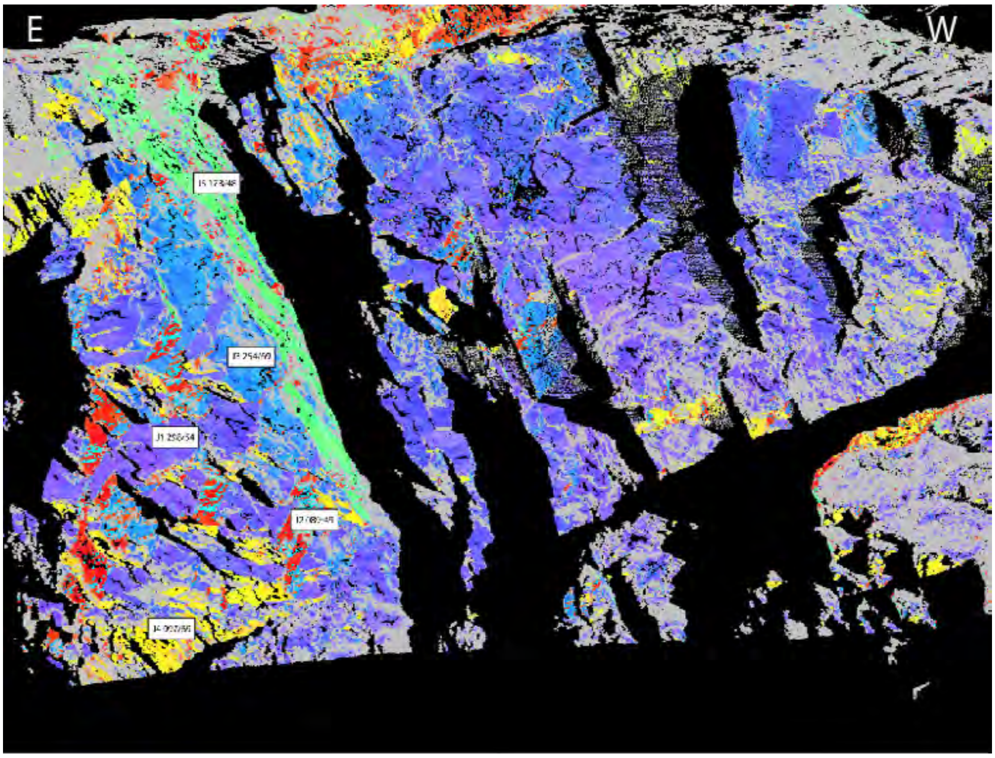

Figure 6: Lidar points cloud classified according to the main sets of discontinuities (blue=J1, red =J2, light blue=J3, yellow=J4, green=J5, gray=other)

IV.1.3 Site 1: kinematic tests

According to the kinematic tests, toppling is the most important mechanism in this zone (Figure 7b). The two discontinuity sets that could likely generate toppling are J2 and J3. Planar sliding is also possible along J4 (Figure 7a) and the discontinuity sets J1^J5 could generate wedge sliding.

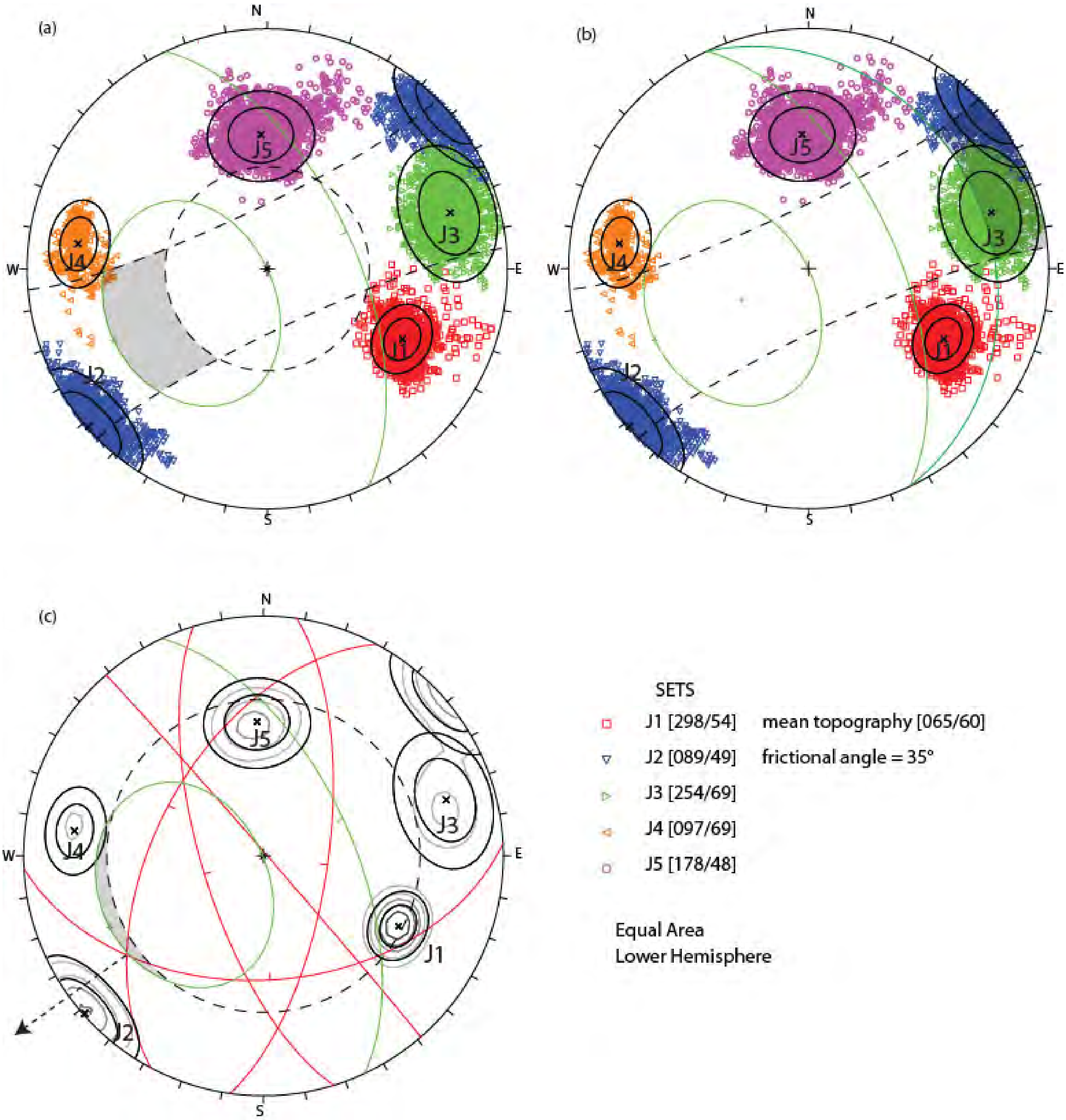

Figure 7: Kinematic test on site 1 for planar sliding (a), toppling (b and wedge sliding (c).

Some E-W cracks are visible on Figure 3c and Figure 8 in the sector of the site 1. The prolongation of these cracks makes steps in the topography of the plateau. They may be developed along a sub-vertical foliation (to be checked with field measurements). The dip angles of these cracks are steeper in the top part than in the lower part, indicating a potential down-bending with an important toppling component of the all eastern side. This toppling may be part of a much larger sagging affecting the whole mountain side below the site 1.

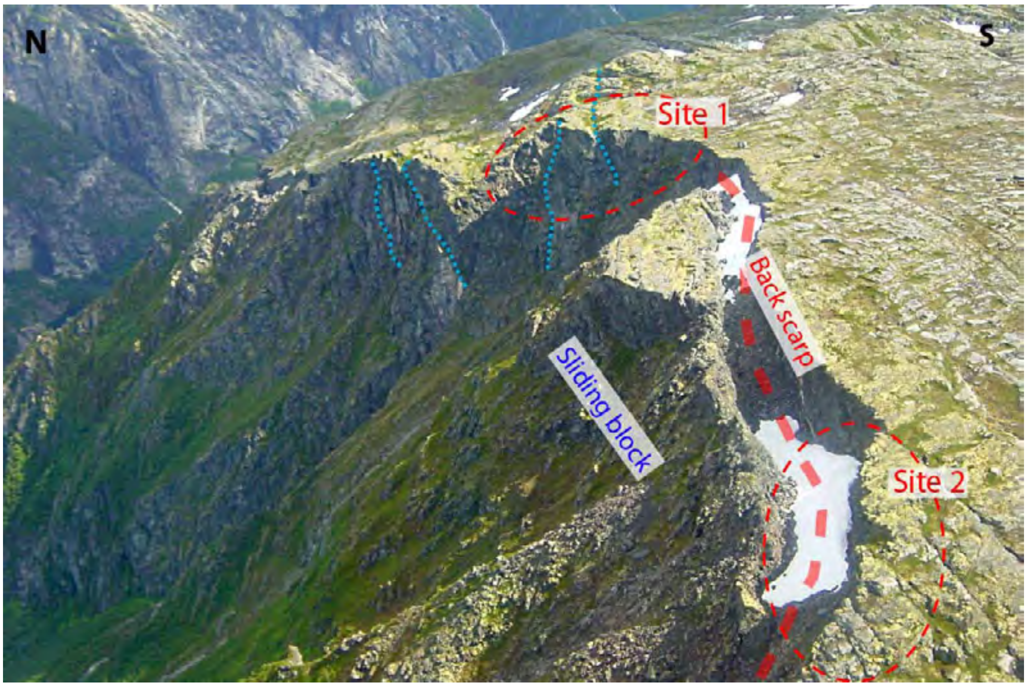

Figure 8: view of the main sliding block of Flatmark and of the two sites analyzed in details.Light blue line: steep E-W cracks.

IV.1.4 Site 2: structural analysis

The Coltop3D representation (Figure 9) shows the predominance of sub-vertical facets dipping towards NE (red) or SW (light blue) and shaping the cliff

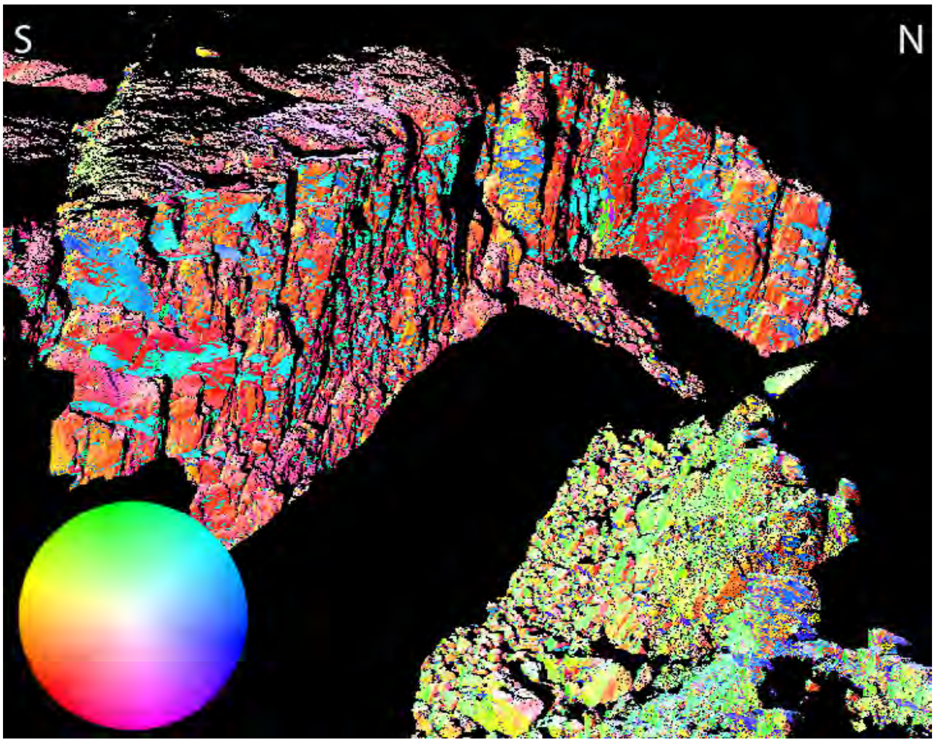

Figure 9: Coltop3D view of the cloud of points of the site 2.

Five main sets of discontinuities were identified and measured. These measurements are presented in the Table 2 and in the Figure 10:

Table 2: discontinuity sets of the Site 2 of the Flatmark area.

Sets	Dip Direction	Dip	Std. deviation
J1	263	47	7°
J2	235	83	10°
J3	088	74	9°
J4	193	81	5°
J5	039	25	14°

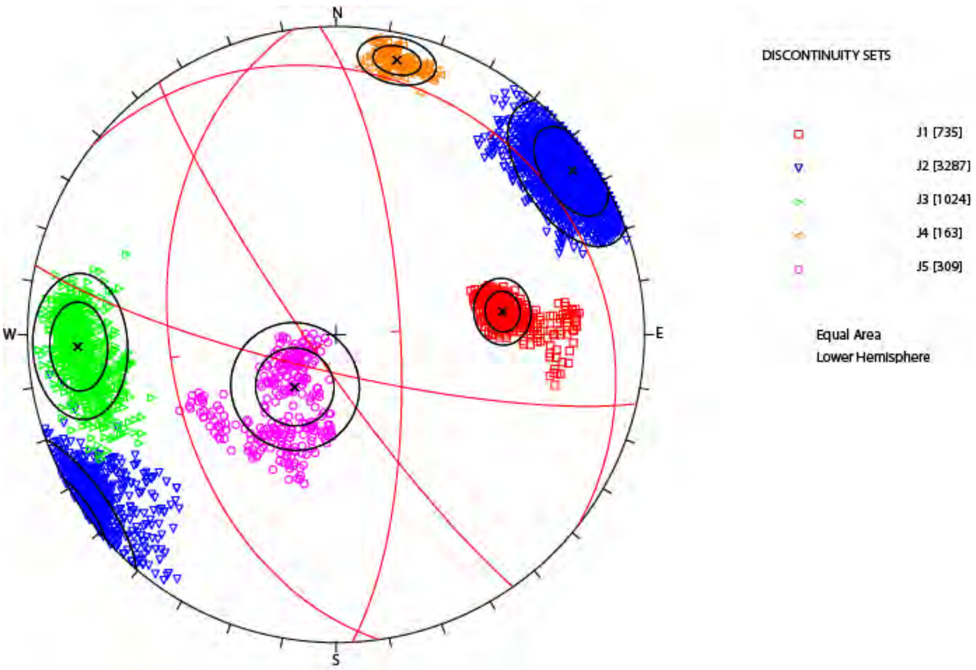

Figure 10: Stereoplot of the main surfaces of discontinuity for the second site of Flatmark. The circles represent the ± 1-sigma and 2-sigma dispersion.

The family sets J1, J2, J3 and J4 are present in both sites 1 an 2. An additional horizontal discontinuity (J5) is present on site 2. J5 is visible in the photography of Figure 11.

Figure 11: view of the upper site with the 6 discontinuity sets.

If we represent the site 2 according to these five discontinuity sets, the J2 discontinuity set makes the major part of the cliff. The combination of J2, J3 and J4 divide the rock mass in columns (Figure 12).

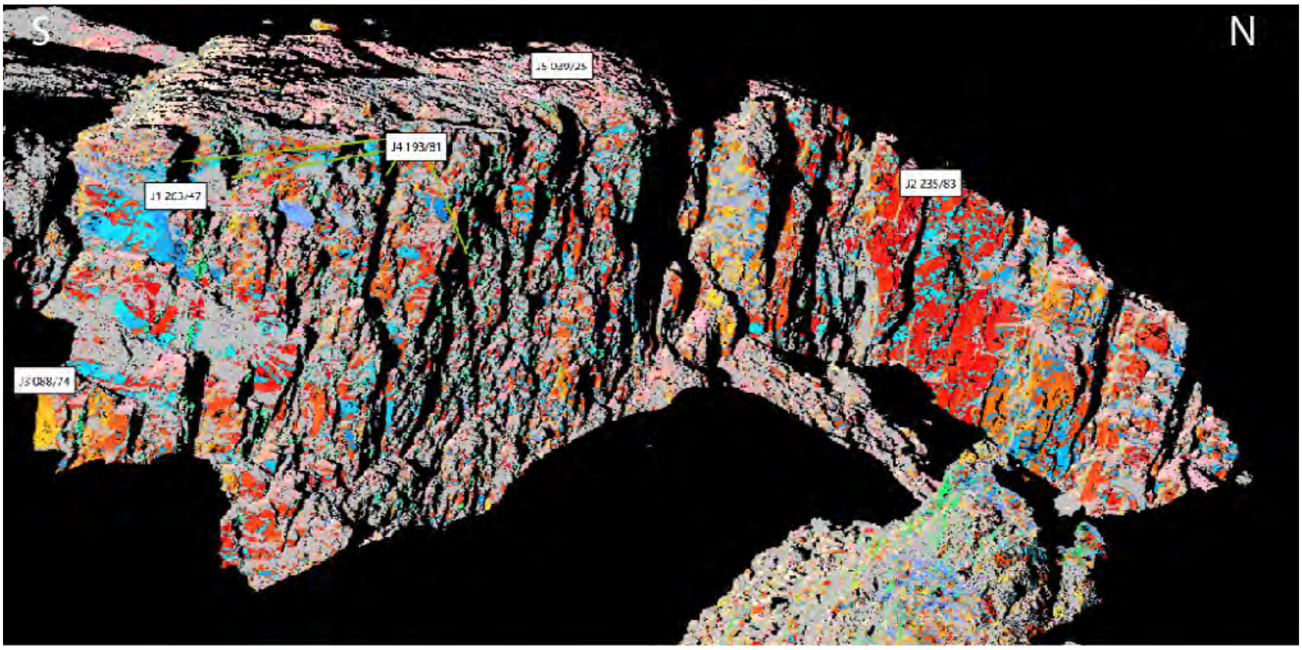

Figure 12: Lidar points cloud classified according to the main sets of discontinuities (blue=J1, red=J2, yellow =J3, green=J4, light pink=J5, gray=other)

IV.1.5 Site 2: kinematic tests

A mean topography of [061/67] was chosen based on the airborne lidar DEM. According to the kinematic tests, planar sliding is possible along J5, J3 and J2 and toppling along J1 (Figure 13) but the most important failure mechanism affecting the area is toppling due to J2. J1^J4 could eventually generate a wedge.

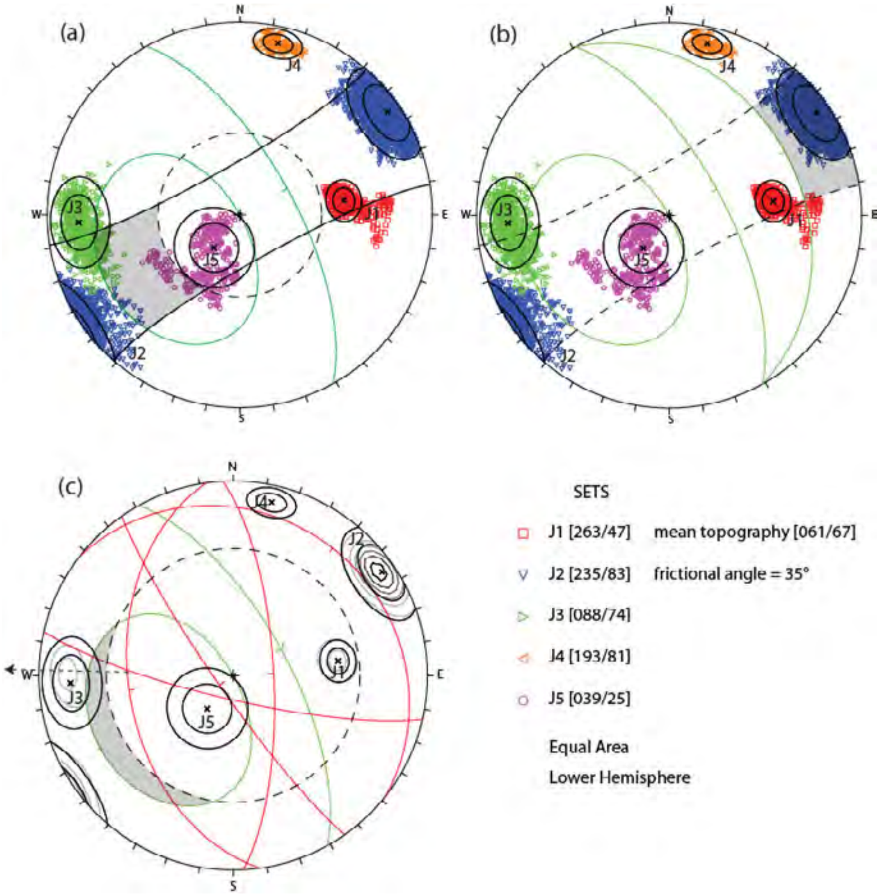

Figure 13: Kinematic test on sector 2 for planar sliding (a), toppling (b) and wedge sliding (c).

IV.1.6 Back scarp

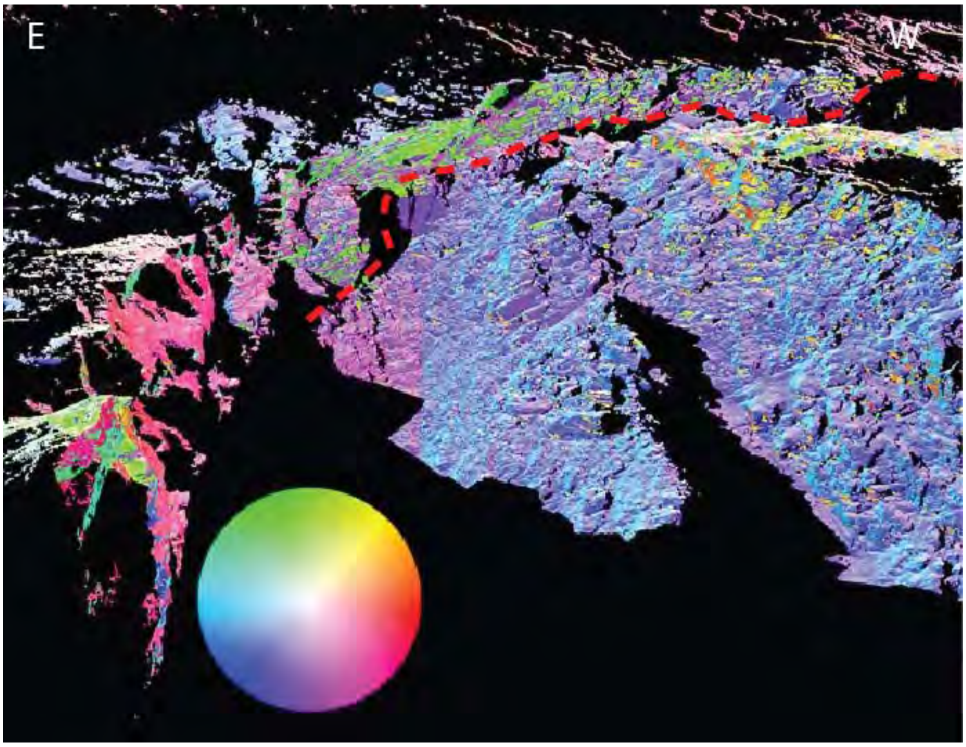

Figure 14: View of the central back scarp (red line: limit between the scarp and slided block) in Coltop 3D.

The orientation of the back scarp plane has an average orientation of [175/85], corresponding to the foliation S1 [176/78] measured in the field. Some part are south dipping (green) and some part north dipping (violet). In this area, folding influences the foliation orientation. If the lower prolongation of this sub-vertical foliation is slightly turning it can form a steep north-dipping sliding surface and it can be the cause of the displacement observed in the field. Presently we have only data for the top part of this instability.

IV.1.7 Discussion

Flatmark is a complex landslide, made of several sectors and involving several type of mechanisms. The eastern side (site 1) is affected by toppling of blocks in the upper part. But morphological features indicate that this toppling may be part of a much bigger deformation (sagging) affecting the mountain side. In the central part, with the large slided block and the main back-scarp, the sub-vertical foliation seems to play a major role. We can suspect that this foliation behaves as sliding surface lower in the face. On the western side of Flatmark, site 2, toppling is the most obvious mechanism in the top 20 m part. Again, this toppling may be the shallow expression of a large and deep slow deformation.
Then two types of hazards should be distinguished: (1) rockfalls due to block toppling, (2) a large rock slide involving large block of the mountain side. Considering the deposits in the valley, rockfalls (possibly quite large) are common in this location and will continue to occur. About large potential rockslides, a >100

m wide block has already moved of some tens of meter in the central part of Flatmark (based on field observations). Considering the morphology, slow movements affecting deeply the mountain sides on both sides of the main scarp can be expected.
For further investigations, we suggest to extend the investigation area lower in the mountain flank. First a detailed analysis of the new airborne lidar dataset acquired by NGU should be performed. The goal of this analysis will be to characterize the main structures on the whole valley side, to check if the structures described on the top are similar to those at the base, to delineate the most critical blocks (as well for rockfall than for sliding). It is important to understand how the foliation evolves lower in the face. If practicable, some fieldwork at base of the flank would be very useful. Further terrestrial lidar investigations may be of interest for monitoring once the overall instability is better characterize, but do not appear as a priority at this stage.
For rockfalls, the most critical blocks should be identified and monitored (possibly with a radar system), particularly in the eastern part of Flatmark. A GPS monitoring of the central sliding block should be performed on a yearly basis. A similar monitoring would be useful on the sides of the main scarp to detect slow displacements. In general, any rockfall activities should be announced and recorded as they can represent a direct hazard but also because they can be early indicators of a much bigger slope movement.

IV.2 Børa

IV.2.1 Introduction

The Børa site is located in Romsdalen, in between the sites of Flatmark and Mannen. It was scanned by terrestrial lidar by T. Oppikofer in 2008. The area is divided in two parts: the “graben site” and the “upper cliff”. A total of 13 scans were done (scanner positions and parameters are recorded in M. Böhme's fieldbook – NGU -a copy of the fieldbook is in the dvd of data provided few months ago-). The Figure 15 presents the projection of the scans on a hillshade view of the site. The Upper cliff and Graben site positions and the open fracture at the back (red line) are shown on the Figure 16. A panoramic view of the site is presented in the Figure 17.

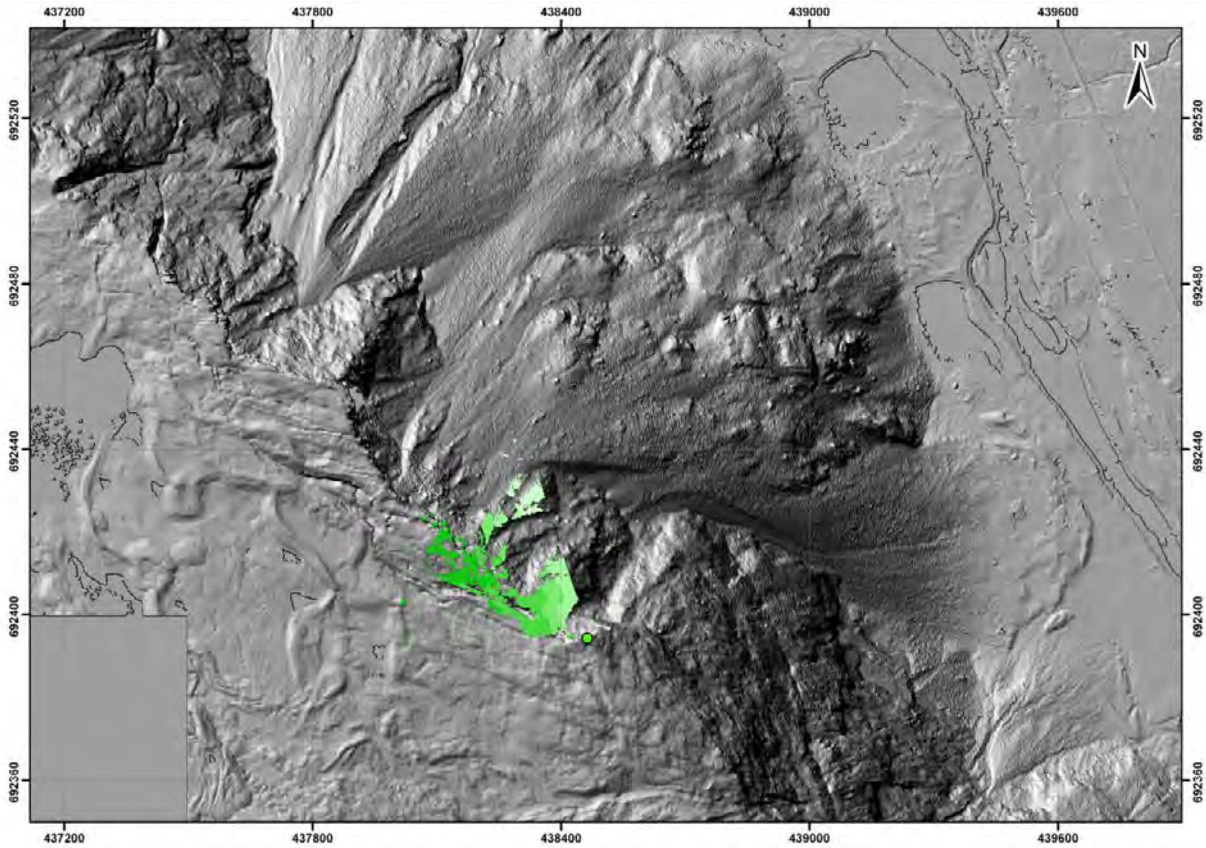

Figure 15: Upper and lower scanned sites and lidar positions (green circle) at Børa.

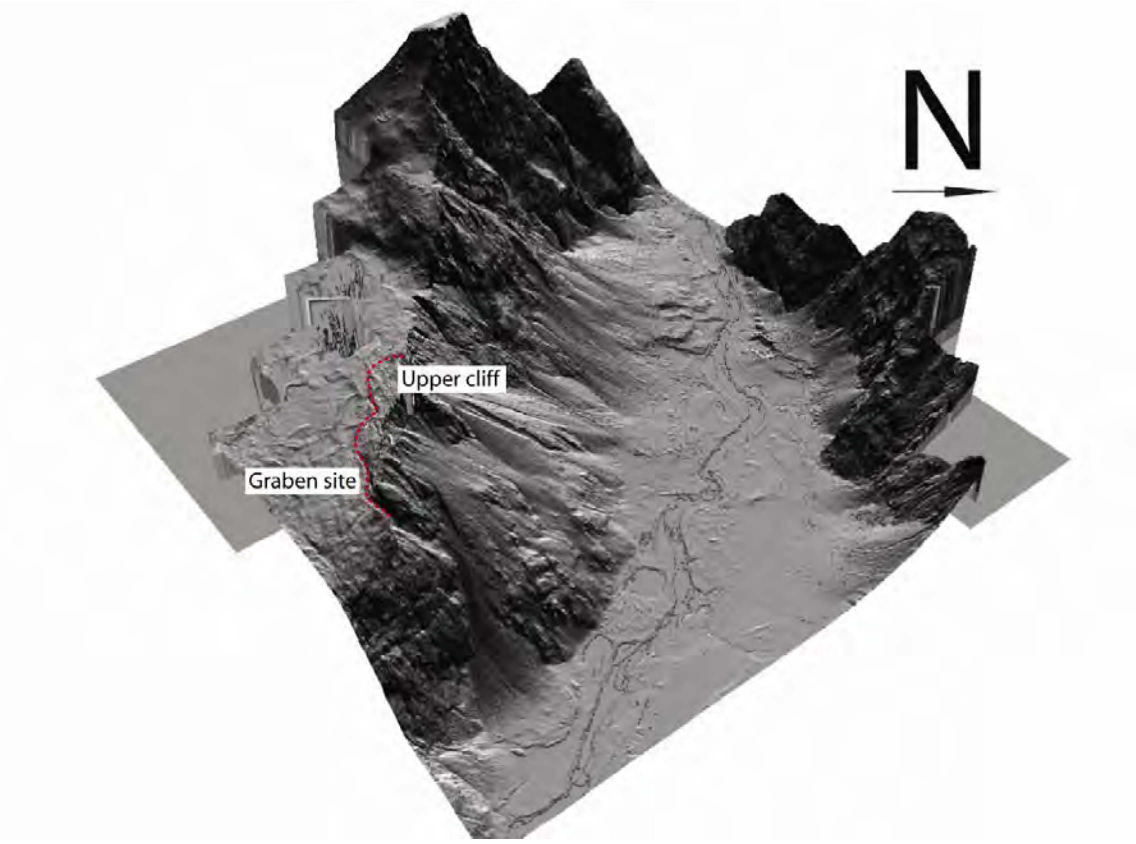

Figure 16: 3D view of Børa site, with the opened fracture in red.

Figure 17: View of Børa from the scanner position (438'395/6'923'925).

IV.2.2 Graben site: structural analysis

The graben site is an opening fracture oriented WNW-ESE and 600 m long. The North compartment slides toward NE, creating an opening on the plateau in the back part. The colors coding of Coltop3D (Figure 18) shows clearly the predominance of facets dipping towards NE to SE (from blue to green).

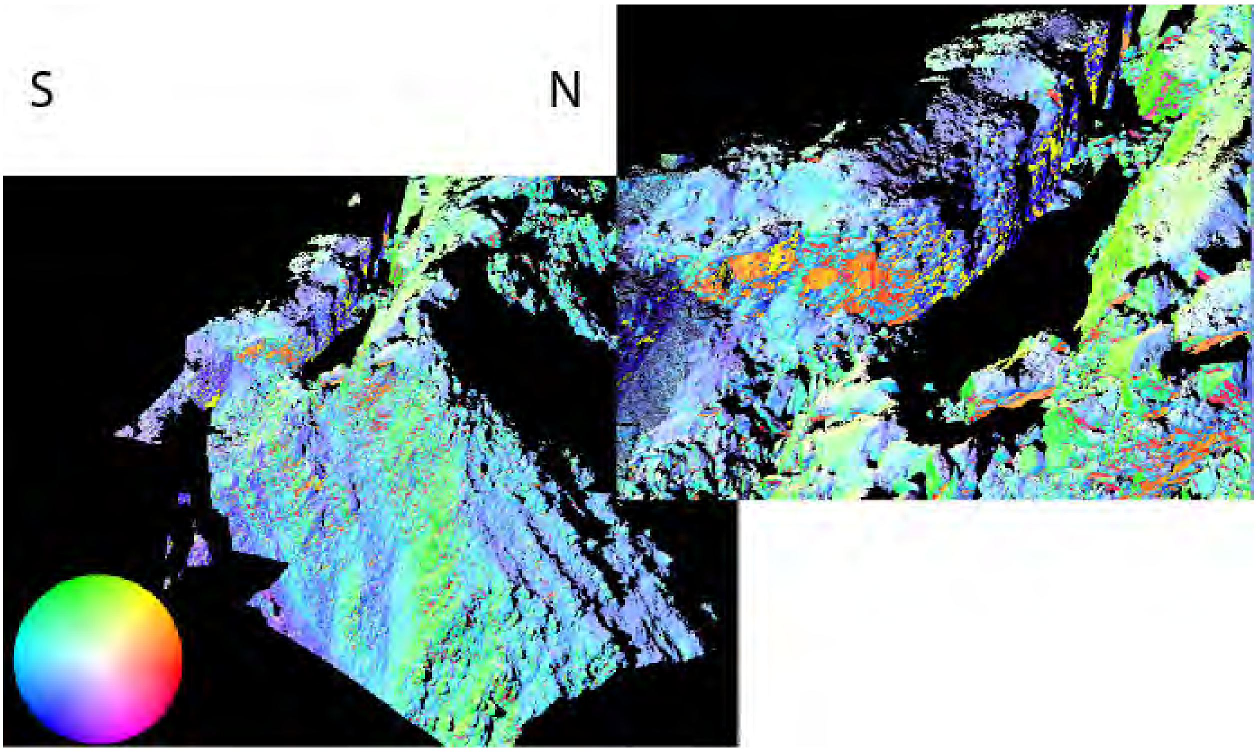

Figure 18: Coltop3D view of the cloud of points for the graben site

Four main sets of discontinuities were identified and imported into Dips (Figure 19). These measurements are presented in the Table 3.

Table 3: detail of the different discontinuity sets of the Børa area.

Sets	Dip Direction	Dip	Std. deviation
J1	179	77	15°
J2	218	83	14°
J3	063	50	25°
J4	255	69	11°

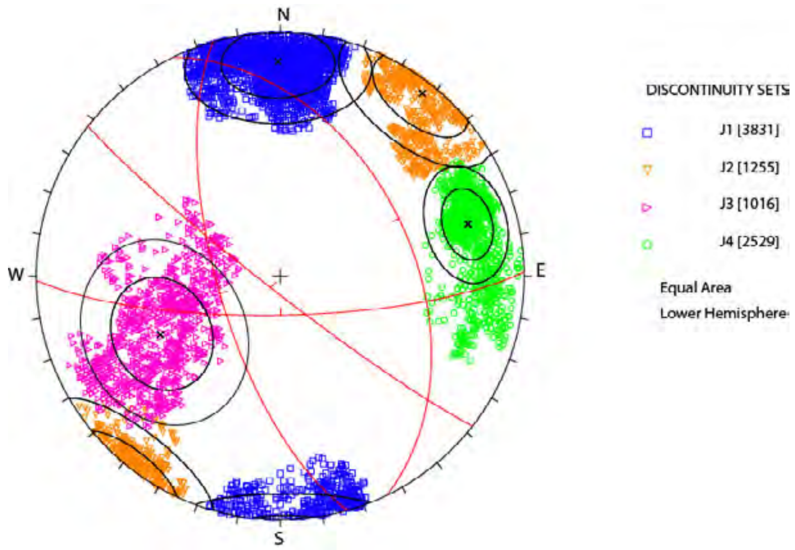

Figure 19: Stereoplot of the main surfaces of discontinuity for the graben site of Børa. The circles represent the ± 1-sigma and 2-sigma dispersion.

In Figure 20, all the points of the scan are classified according to the 4 sets of discontinuity. These discontinuities are displayed on the picture of the Figure 21. Interestingly discontinuities with orientations similar to J1, J3 and J4 were measured at the base of the cliff under Børa (Derron fieldbook 2004), with J1 corresponding to main foliation. That may indicate that these sets of discontinuities are present over a wide area.

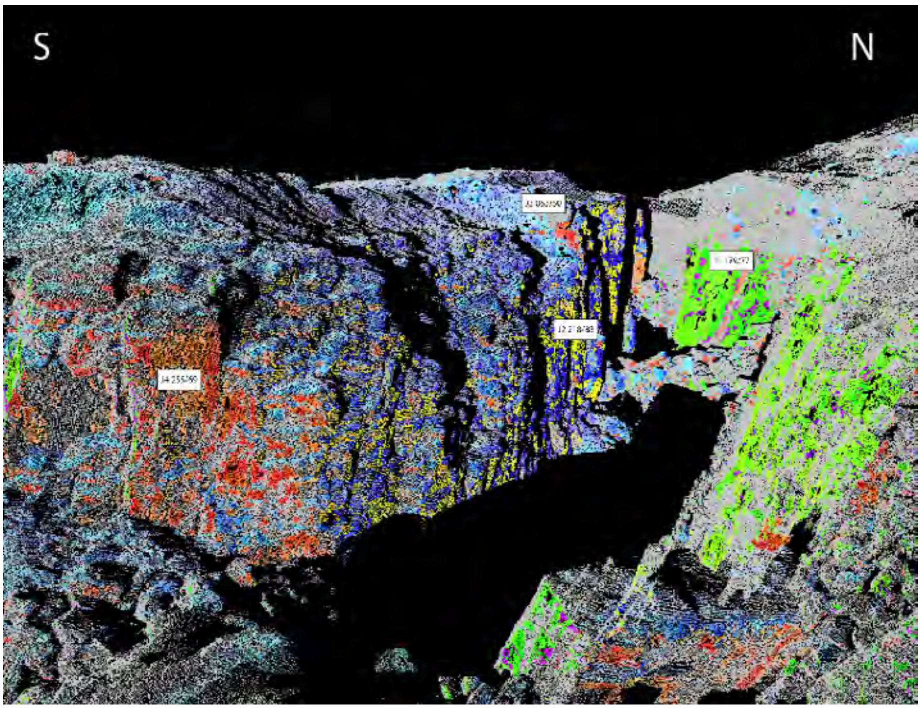

Figure 20: Coltop3D according the 4 discontinuity sets: J1=green, J2=yellow-dark blue, J3=light blue, J4=orange-red

Figure 21: Panoramic view of the back graben site. 4 dicontinuity sets are visible (green=J1, yellow=J2, blue=J3, red=J4).

IV.2.3 Upper cliff site: structural analysis

The upper cliff is 25 meters high and dipping NE. The color coding of Coltop3D (Figure 22) shows that the cliff is divided in compartments separated by sub-vertical discontinuities (J1, J2 and J4).

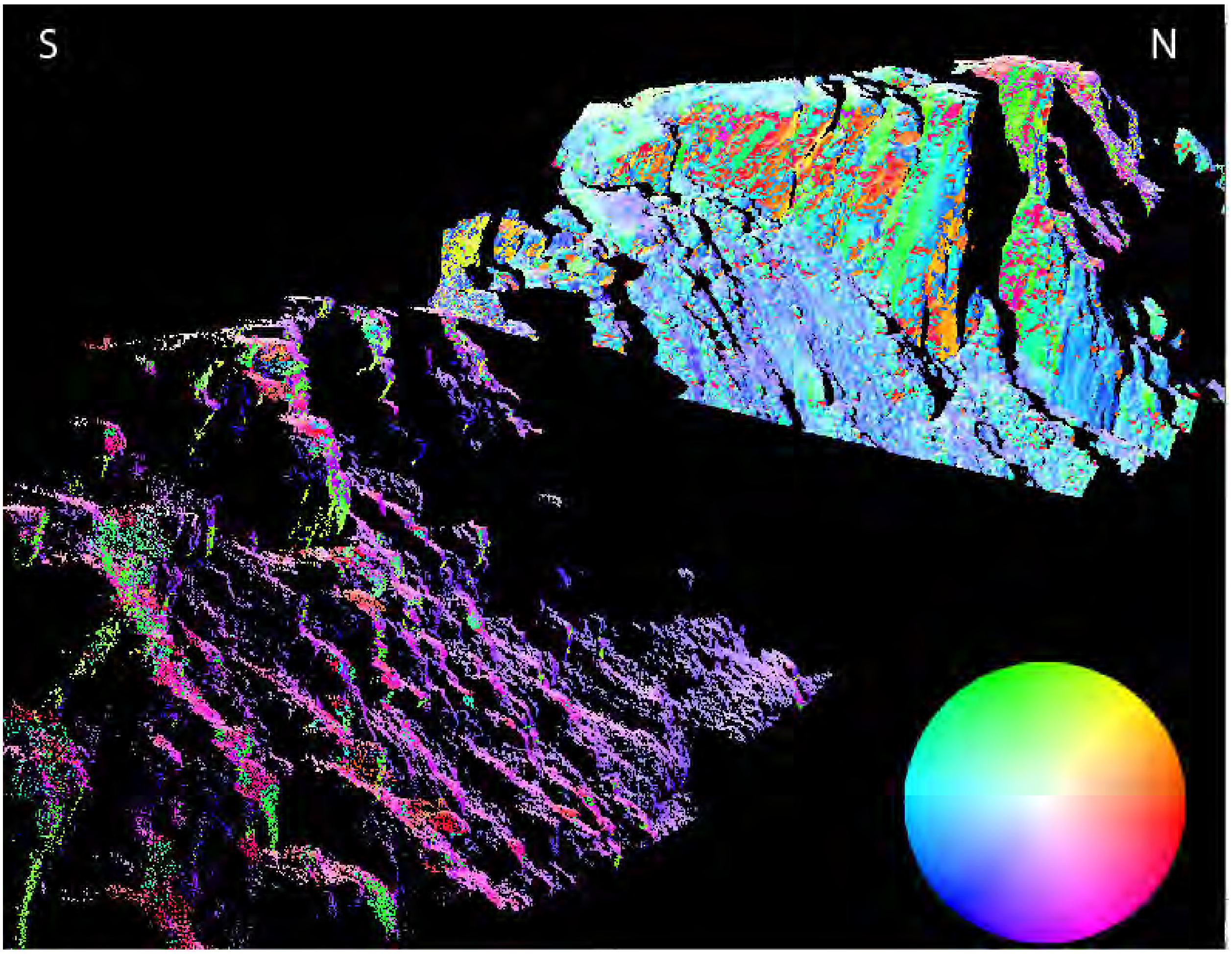

Figure 22: Example of a Coltop3D view of the cloud of points. The color of each point of the scan is given by the orientation (using the pole) of the surface at this point in the color wheel.

Six main orientations of discontinuities can be identified on this outcrop and their average orientations were estimated with Dips (Figure 23). These measurements are presented in the *Table 4*.

Table 4: orientations of the different discontinuity sets of the upper cliff of Børa.

Sets	Dip Direction	Dip	Std. deviation
J1	139	89	7°
J2	177	86	16°
J3	258	67	9°
J4	237	85	7°
J5	079	55	13°
J6	357	31	11

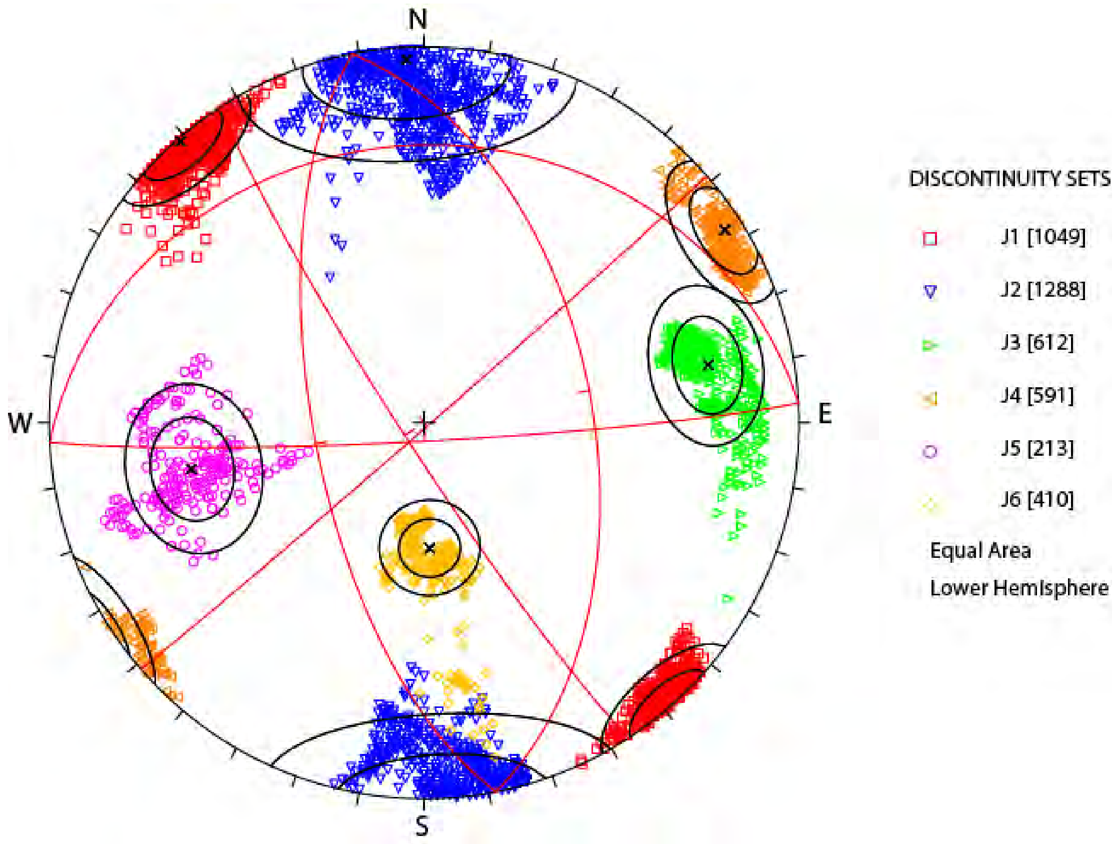

Figure 23: Stereoplot of the main surfaces of discontinuity for the upper site of Børa. The circles represent the ± 1-sigma and 2-sigma dispersion.

Some of these discontinuity surfaces are qualitatively displayed on the Figure 24. The overall surface of the cliff can be classified according to the six discontinuities (Figure 25).

Figure 24: view of the upper cliff with some examples of the 5 main discontinuity sets (green=J1-J2, red=J3, yellow=J4, blue=J5, violet=J6)

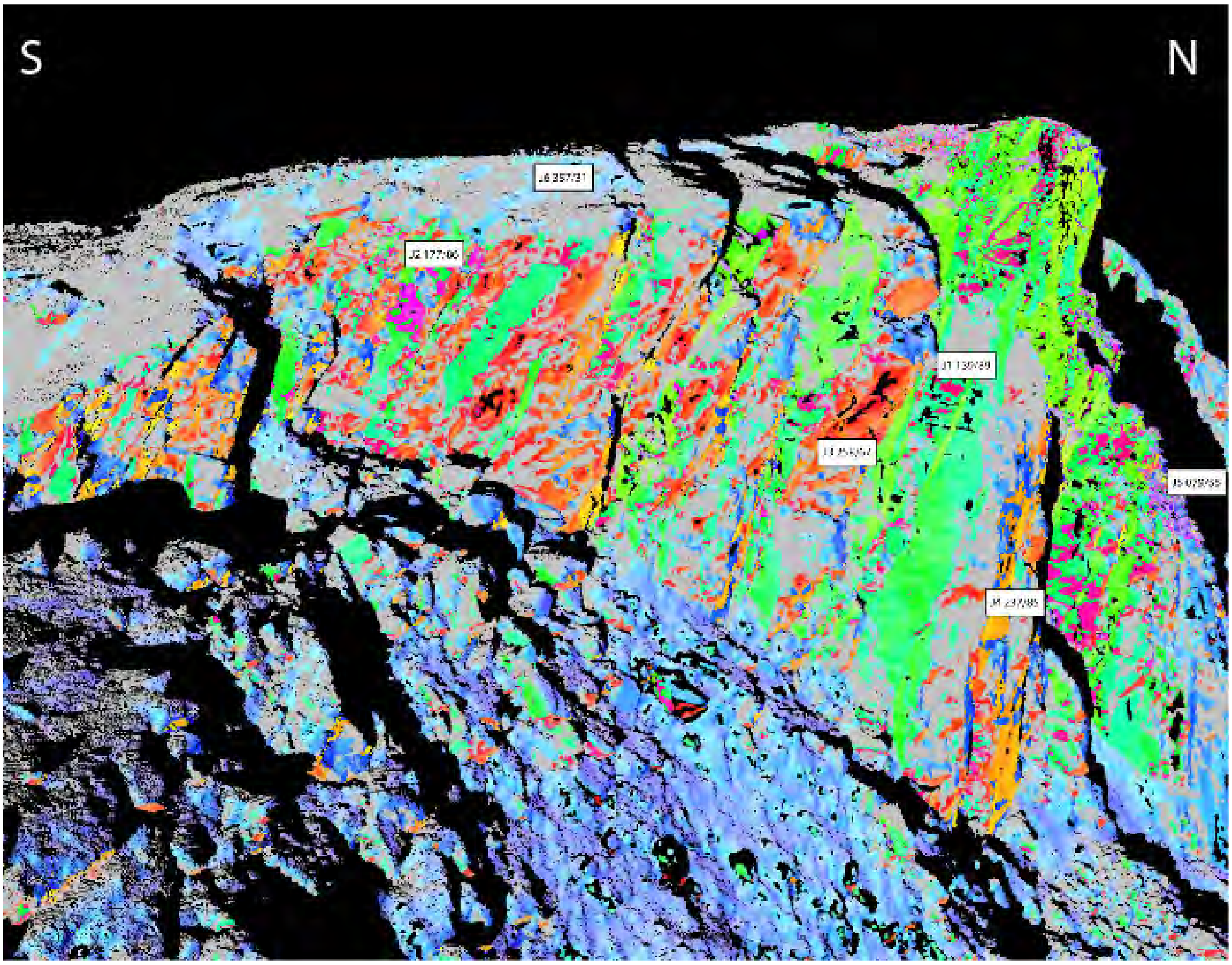

Figure 25: lidar points cloud classified according to the main sets of discontinuities, (green-pink=J1, green-violet=J2, red=J3, yellow=J4, blue=J5, violet=J6, gray=other)

IV.2.4 Upper cliff: kinematic tests

Kinematic tests (Figure 26) were done for the Upper cliff. It appears that the discontinuity J4 promotes toppling of rock columns. There is also a possibility of wedge sliding on J1^J5 with a sliding direction of [050/51]. Locally, planar mechanism is possible along J5 and J6.

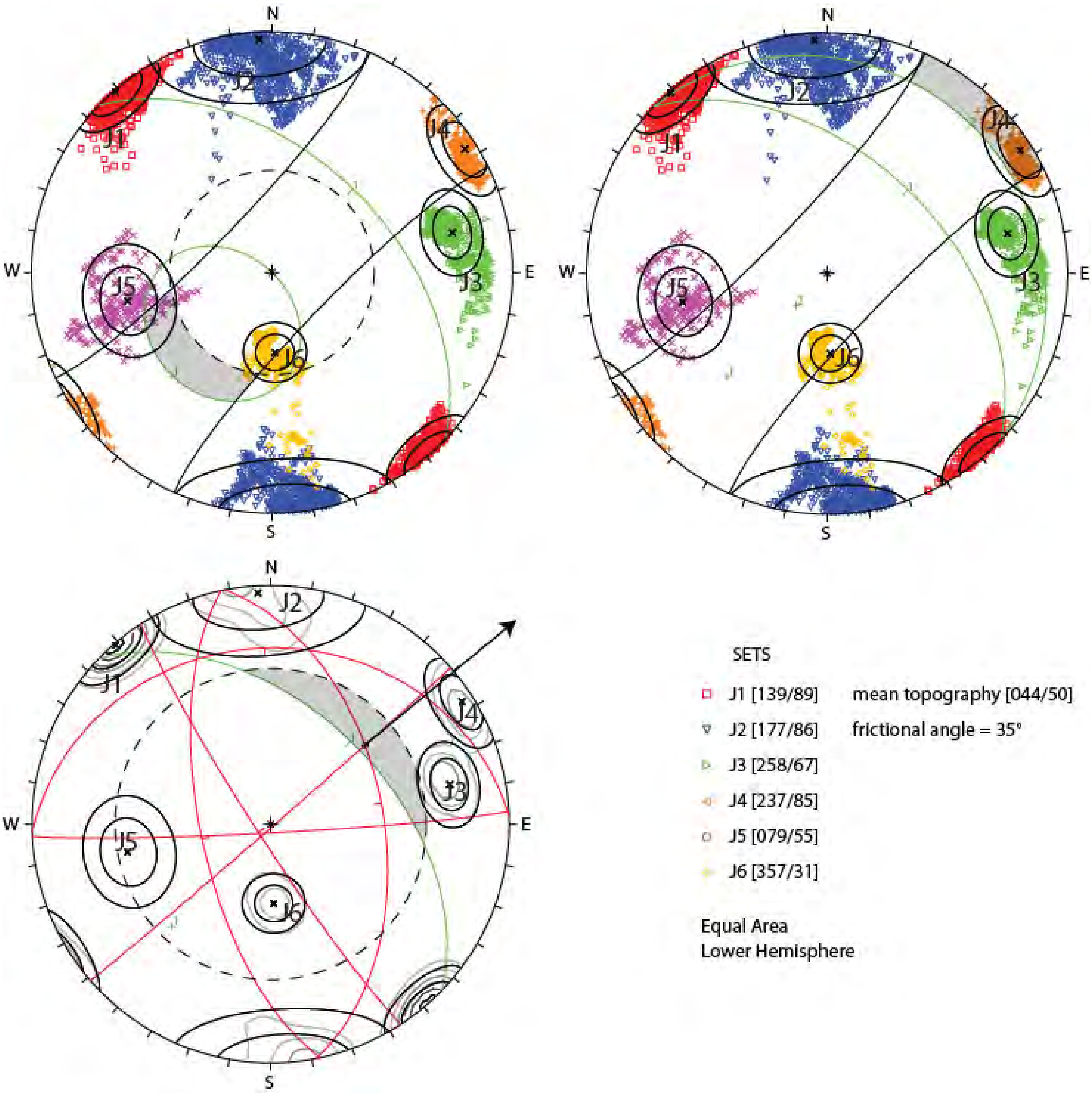

Figure 26: kinematic tests (planar sliding, toppling and wedge sliding) for the studied area.

As this cliff is very small, it is difficult to assess how these measurements are representative of larger structures affecting the entire slope. They may be only local features, perhaps produced during the block displacement. For instance we cannot define from these data if the toppling mechanism affects a bigger part of the site. That is why we have tried to match these measurements with bigger features extracted from the airborne lidar DEM.

IV.2.5 Airborne lidar DEM: structural analysis

An inspection of the airborne DEM was done with COLTOP-3D in order to find the principal sets of discontinuity at regional scale (Figure 27). Four families were identified on the DEM (Table 5).

Table 5: detail of the different discontinuity sets identified on the airborne lidar DEM of the Børa area.

Sets	Dip Direction	Dip	Std. deviation
J1	157	48	15°
J2	032	83	13°
J3	060	42	7°
J4	358	53	17°

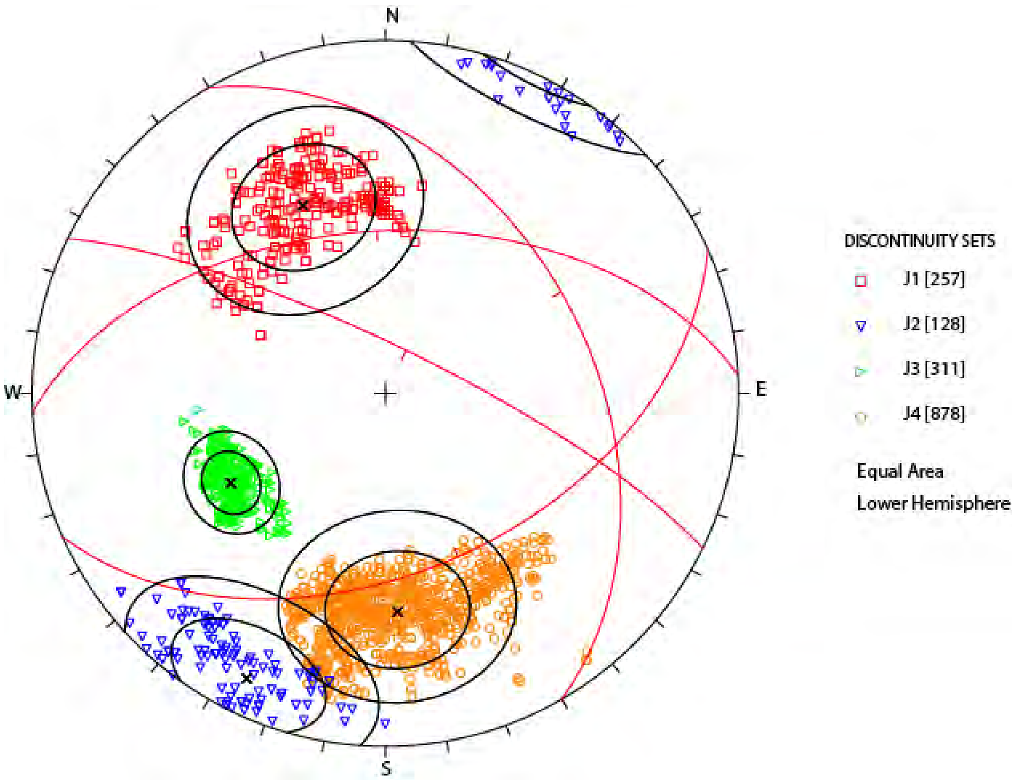

Figure 27: Stereoplot of the main surfaces of discontinuity for the upper site of Børa. The circles represent the ± 1-sigma and 2-sigma dispersion.

These four sets have approximate matches in at least one of the terrestrial scans. On both sites, the graben and the upper cliff sites, a west dipping sub-vertical discontinuity is well marked. This orientation was not detected on the airborne lidar dataset.

IV.2.6 Airborne data: kinematic tests

The kinematic tests done with the airborne data (Figure 28) show that, for a regional topography orientation [044/50], a sliding movement along J3 and J4 is possible. This discontinuity orientation is present on the whole site (= J3 "grabben site", = J5 "upper cliff") and may be related to movement of large slabs of the mountain side (and formation of the graben ?). For smaller volumes toppling due to J2 or wedge sliding J4^J3 with a sliding direction of [047/41] are possible too.

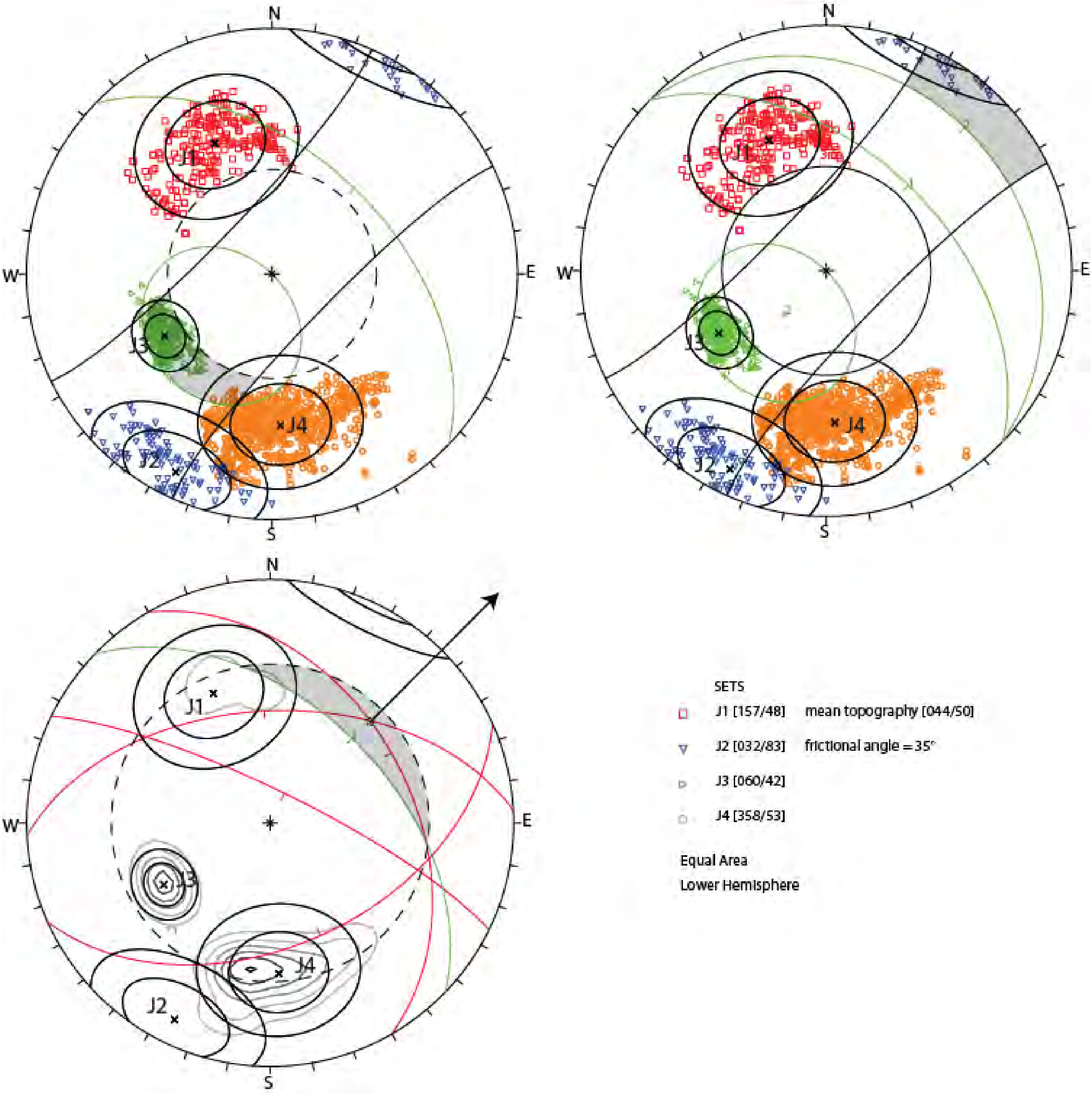

Figure 28: Kinematic tests on the MNT (planar sliding, toppling, wedge sliding).

IV.2.7 Discussion

Many other geological observations were done these last years in Børa by NGU. But only the information extracted from lidar datasets are addressed here. All these pieces of information should be put together to get a better view on this site.
On the same line than Flatmark, Børa is affected by two types of phenomena: (1) a large gravitational deformation (sagging) that formed the graben structure on the top, and (2) a dislocation of the rock in the upper part that generates rockfalls. The rockfall activity is obvious looking at the airborne lidar data. The terrestrial lidar data cover only the top part of the unstable area, and investigations at the base should complete these observations to assess the possibility of a large rockslide (by the way, if not already performed, a more detailed analysis of this dataset will be certainly fruitful).
Monitoring of points around the graben and along the edge of the cliff is important to know if slow movements of large volumes are occurring and to delimit the different blocks. Important rockfalls already happened as it can be observed in the eastern part of Figure 15, with a run-out almost down to the Rauma river.
A terrestrial lidar campaign could be used to complete the airborne dataset (graben) and to monitor the displacement of some blocks once they have been clearly indentified.

IV.3 Mannen

IV.3.1 Introduction

Mannen is the most westward of the sites studied in Romsdalen. It was scanned with the terrestrial lidar in 2008 by T. Oppikofer. Three scans were recorded during this field campaign. The Figure 29 shows the projection of the scans on the DEM. Note the open back scarp visible on the DEM. In August 2009 an attempt was made to scan again Mannen, but due to heavy snow falls that was impossible.

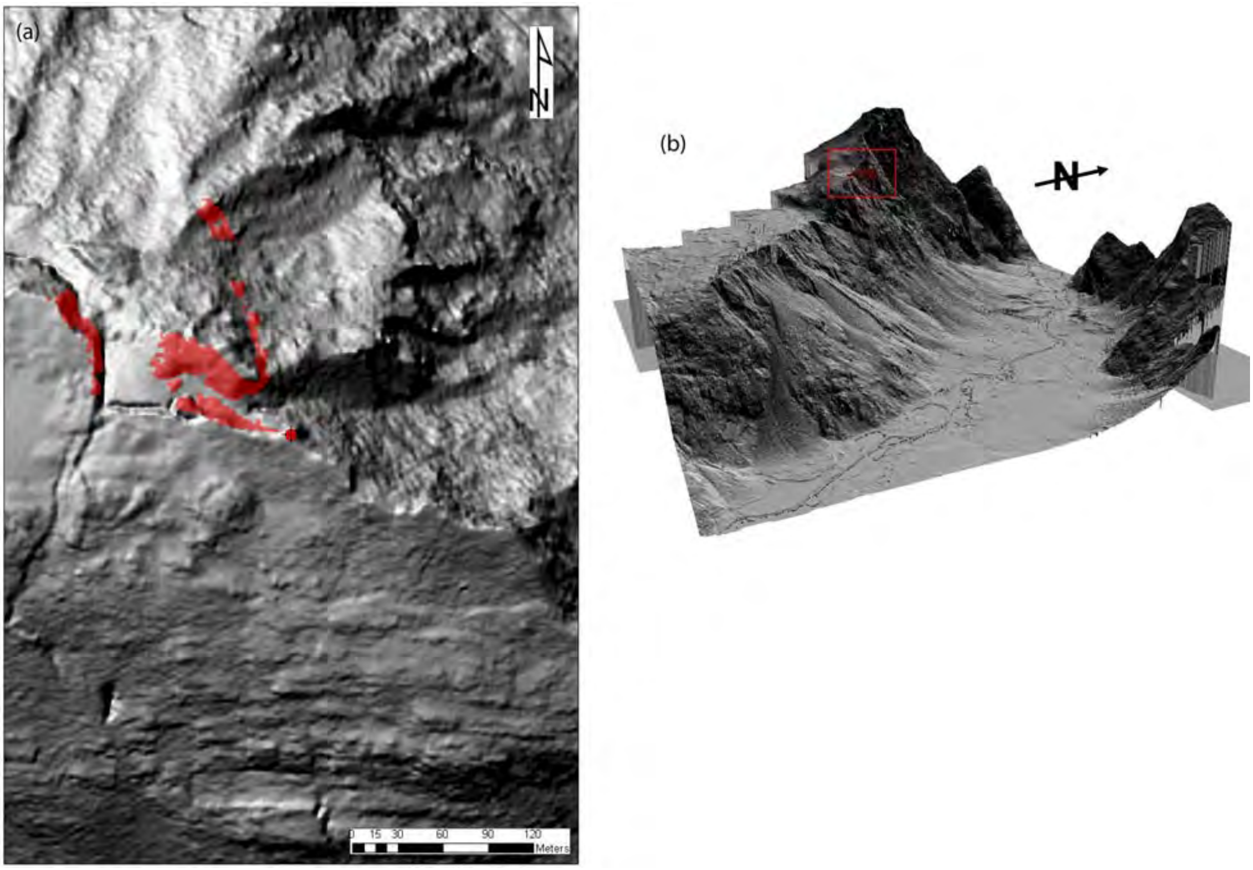

Figure 29: (a) scanned site of Mannen with the lidar position (red point), (b) 3D view of Mannen area (the scanned area is in the red square)

IV.3.2 Structural analysis

The cliff at Mannen is a sub-vertical wall with a northward orientation and the average local topography is oriented [045/55] (estimated on the DEM). The structural analysis was carried out with COLTOP-3D and four discontinuity sets were distinguished (Figure 30).

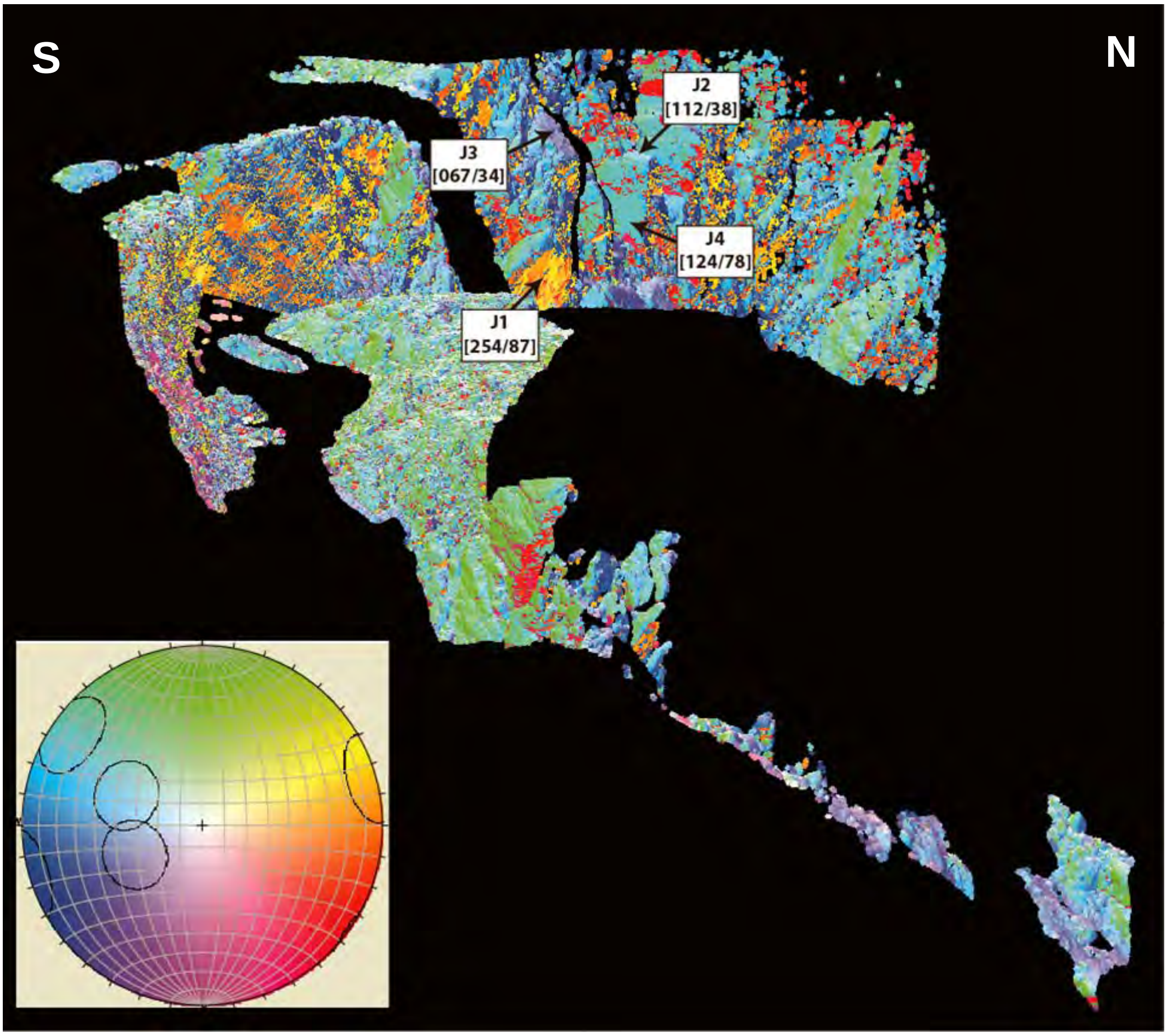

Figure 30: COLTOP-3D view of the studied area (the result is a colorful point cloud where each color is assigned to a spatial orientation)

These four main sets were imported into Dips (Figure 31) in order to estimate their orientation and standard deviation. The results are summarized in the Table 6:

Table 6: orientations of the different discontinuity sets of the Mannen area.

Sets	Dip Direction	Dip	Std. deviation
J1	254	87	11°
J2	112	38	9°
J3	067	34	10°
J4	124	78	9°

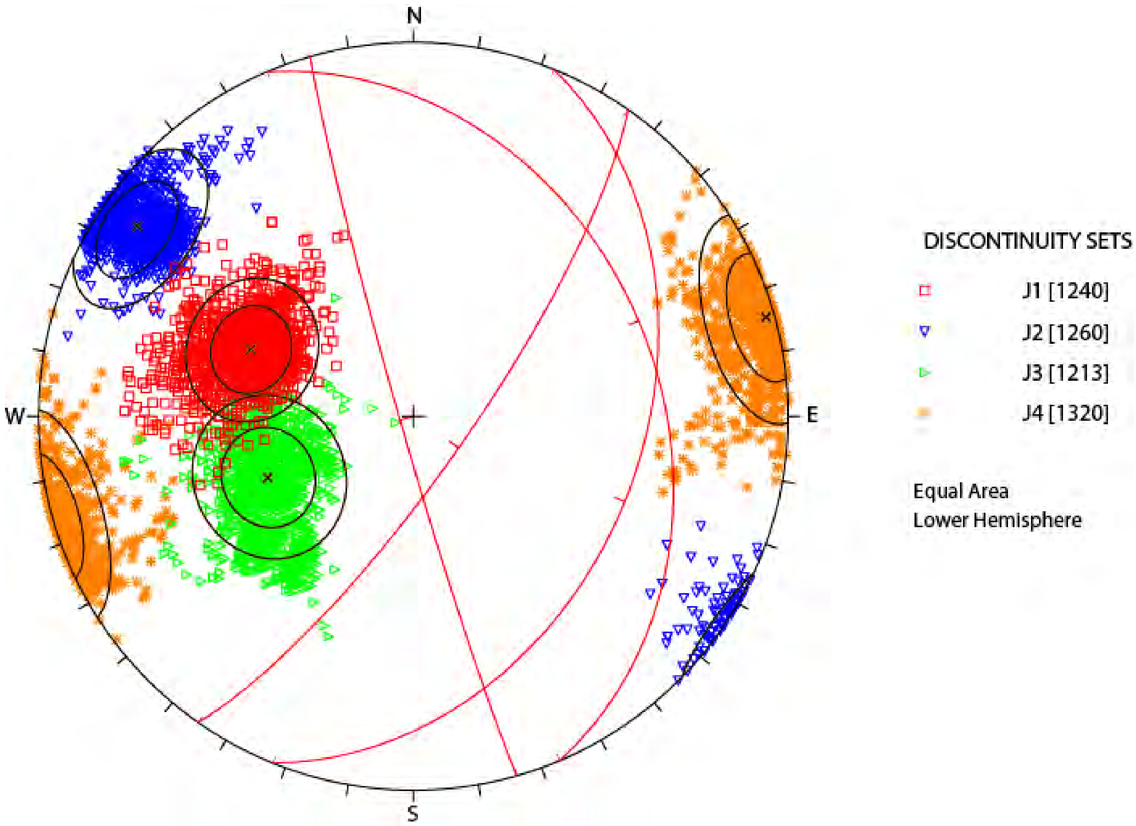

Figure 31: Stereoplot (lower hemisphere, equal area) of the discontinuity sets detected with COLTOP-3D. The circles represent the ± 1-sigma and ± 2-sigma dispersion.

The Figure 32 is a view of the cliff with the repartition of the four detected discontinuity sets. It appears that a large part of the cliff is shaped by one these discontinuities.

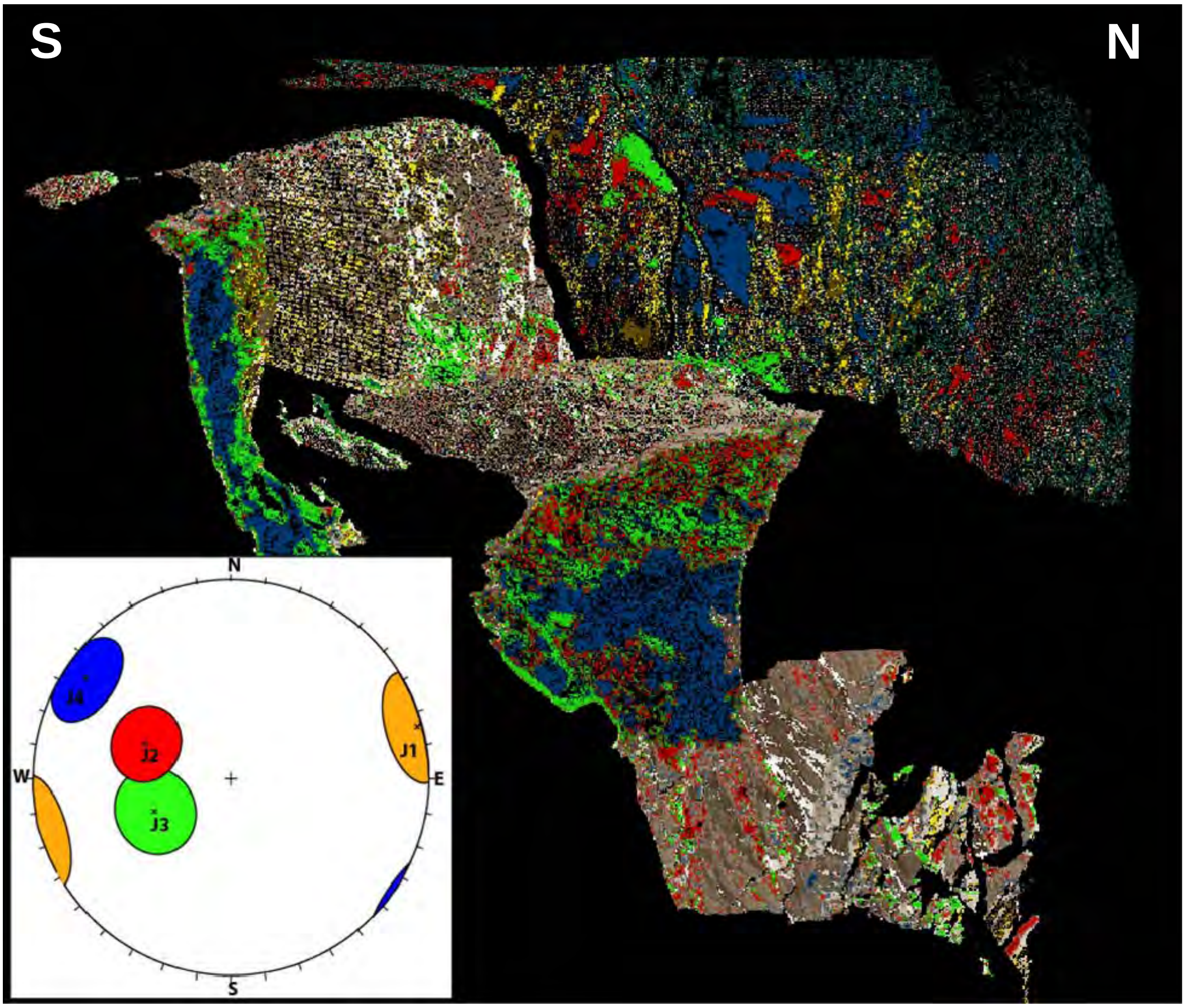

Figure 32: representation of the four families extracted with Coltop 3D.

IV.3.3 Kinematic tests

Kinematic tests were carried out with a mean topography of [045/55]. It appears that the discontinuity sets J3 and possibly J2 enables planar sliding (darker area in Figure 33a). Based on the point cloud analysis (Figure 34) the blocks seem to be laterally delimited by J4 and at the back by J1. The discontinuity J1 could involve toppling. In Figure 33c, we observe two possibilities of wedge sliding: J3^J2 with a plunging direction of [079/33] and J3^J4 with a plunging direction of [041/31].

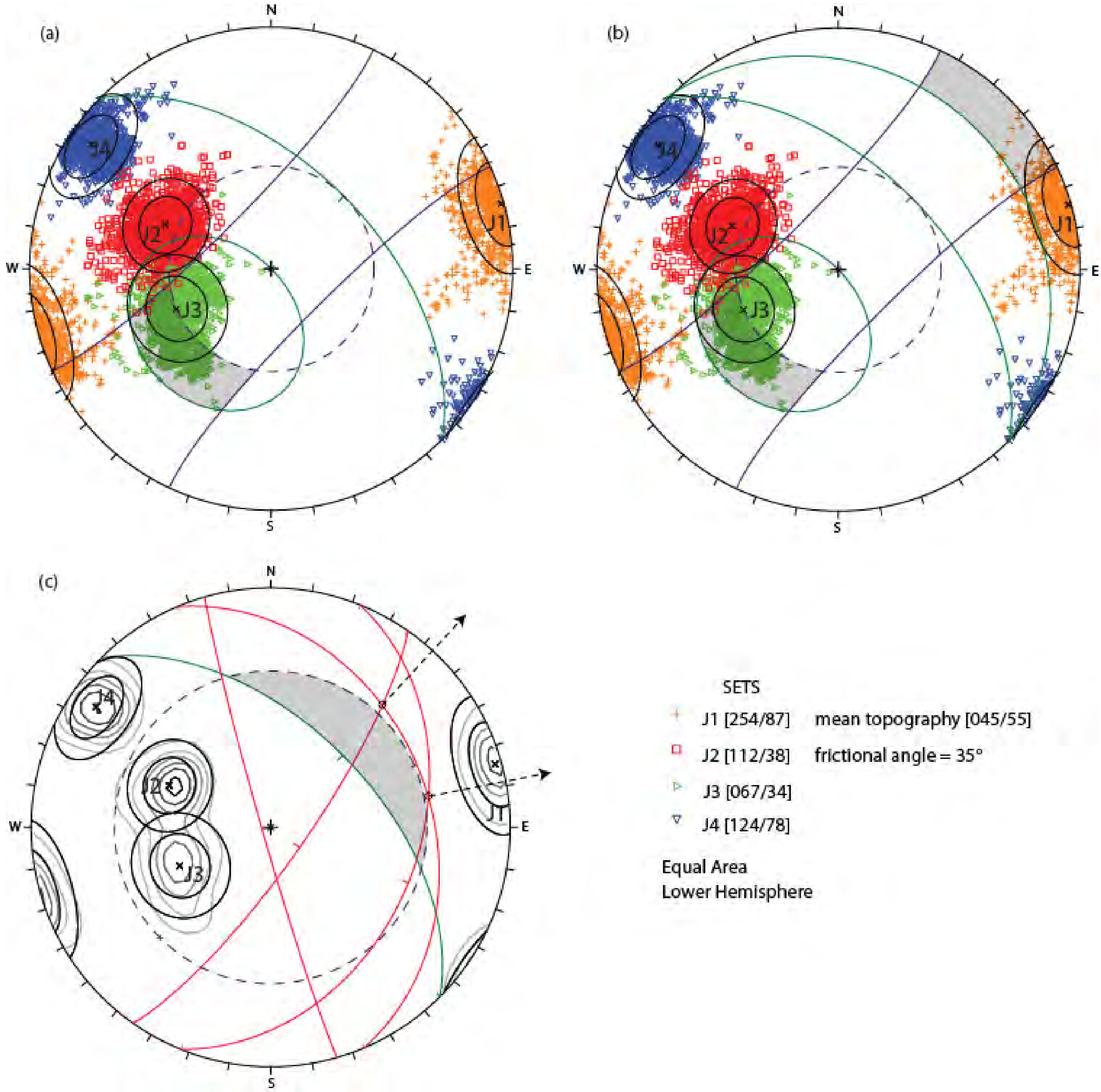

Figure 33: kinematic tests for (a) planar failure (b),toppling and (c) wedge failure (equal area, lower hemisphere stereoplot).

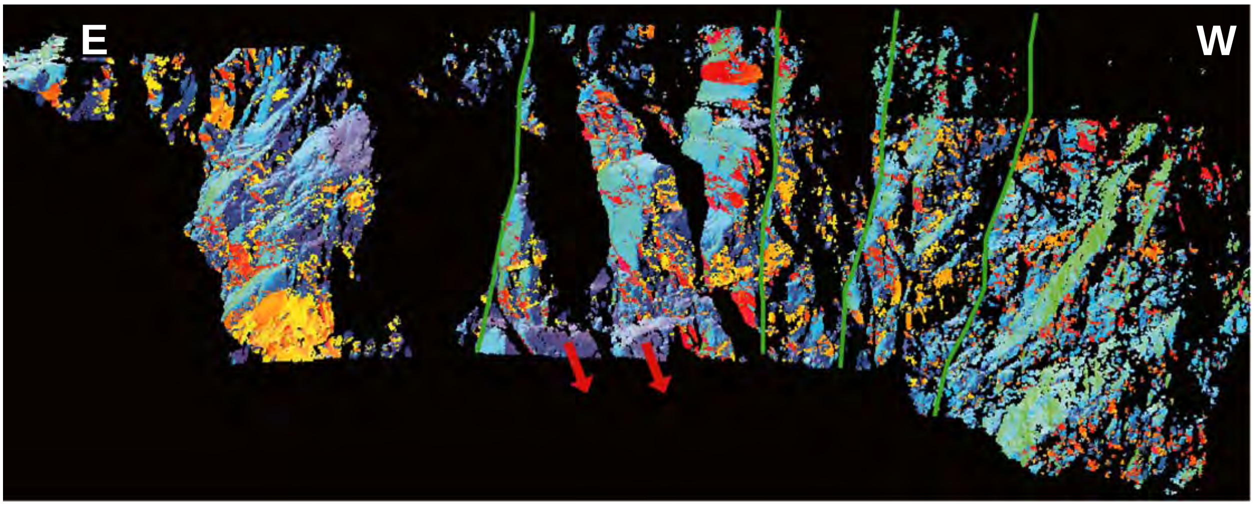

Figure 34: detail of the upper part: the blocs a laterally delimited by J4 (green lines) and at the back by J1 (dark blue – yellow in this Coltop 3D representation) and slide along J3 (red arrows).

IV.3.4 Discussion

A preliminary study was carried out by L H Blikra to estimate the volumes and the possible run-out for the unstable area of Mannen. The cliff has been divided into two possible scenarios (Figure 35a). The volume A1 has been estimated to 2-3 million m^3 and a more extreme scenario corresponding to the volume A2 around 15-25 million m^3. In the Figure 35a, at the exception of J3 that is not visible in the picture, the main discontinuity sets are highlighted (J4 = blue, J2 = red, J1 = orange). The Figure 35b is a view of the open back crack.

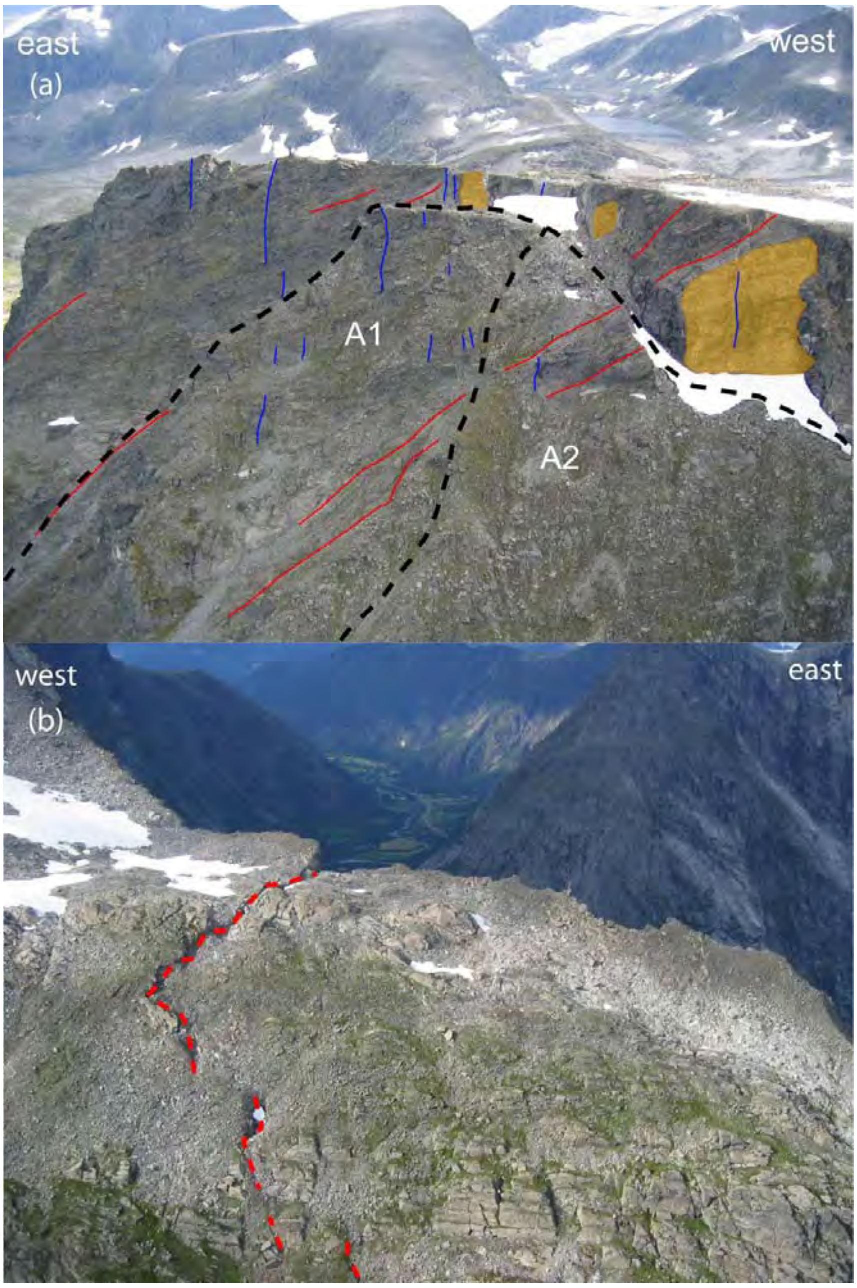

Figure 35: (a) general view of the instability with the two scenarios for the unstable volumes (A1 and A2) and (b) view of the back scarp (red dashed line) Pictures from Blikra (A/T -IKS)

Several points have to be noticed: (1) the moving mass is strongly dislocated, with numerous vertical open cracks along J4 (in blue in Figure 35a), (2) the valley side under Mannen is steeper than in the neighboring Børa, (3) the Figure 29b shows that Mannen forms a large convex volume hanging above the valley.
Mannen is known as one the most critical site in Norway and many investigations are presently running on this site. Additional terrestrial lidar scanning would be interesting to follow the evolution of this dislocation, even if the point of view is not optimal, because this is a very active instability.

IV.4 Svarttinden

IV.4.1 Introduction

The area of Svarttinden is located southward of the sites of Mannen, Børa and Flatmark. Even if it is relatively far away from any infrastructure, a collapse of this mountain could generate important rockfalls in the Romsdalen valley. This site is composed of two distinct parts (Figure 36): (1) the western part is a kind of 200 m high pyramid, (2) in the eastern part a similar volume of rocks collapsed some thousands years ago and presently the sliding surface of this event is outcropping. This sliding surface continues to the West cutting the pyramid in two parts. Nineteen scans of Svarttinden were acquired in 2006 (by T. Oppikofer and M. Jaboyedoff).

Figure 36: general view of the area of Svarttinden.

IV.4.2 Structural analysis

The sliding surface of the eastern part has a dip direction and angle of [014/60]. The structural analysis was carried out with COLTOP-3D on the western part and six different discontinuity sets were distinguished (Figure 37).

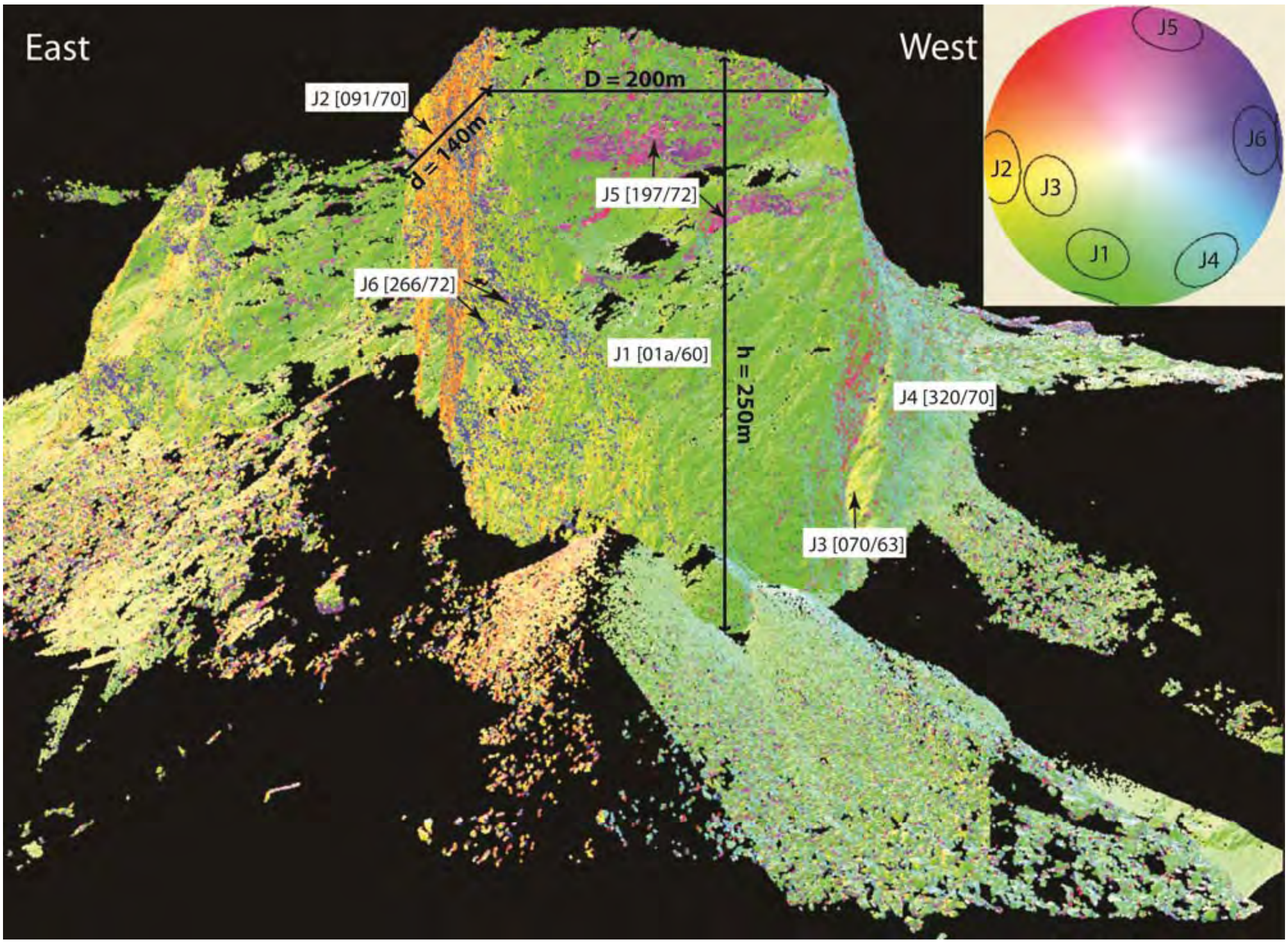

Figure 37: Coltop3D view of the studied area.

Measurements of theses six discontinuity sets were imported in Dips (Figure 38) in order to estimate their average orientation and standard deviation (*Table 7*).

Table 7: orientations of discontinuity sets identified at Svarttinden

Sets	Dip Direction	Dip	Std. deviation
J1	014	60	8°
J2	091	70	11°
J3	069	63	11°
J4	320	70	12°
J5	197	72	11°
J6	266	72	14°

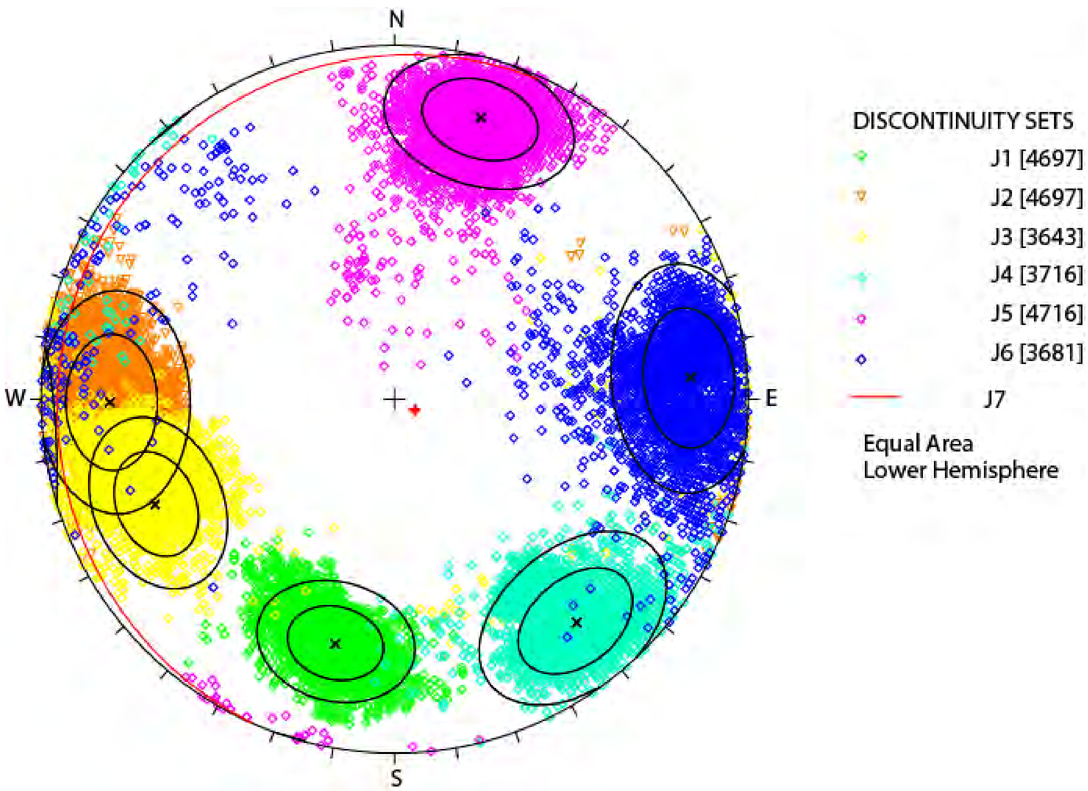

Figure 38: Stereoplot (lower hemisphere, equal area) of the main surfaces of discontinuity for the instable block of Svarttinden. The circles represent the ± 1-sigma and 2-sigma dispersion.

The study of the point cloud with COLTOP-3D brings up that the block (pyramid) is mainly formed by three major discontinuity sets: J1 [014/60] corresponds to the topography of the old sliding plane as well as a large part of the North face of the unstable block. The East face of the block is formed by the steep discontinuity J2 [091/70] and the West one by J4 [320/70].
Based on field observations and pictures analysis it appears that the entire block is affected by persistent horizontal joints J7 [294/005]. A persistent foliation is also observed.

IV.4.3 Kinematic tests

Kinematic tests were carried out in the studied area in order to see the different failure mechanisms potentially affecting the cliff. The [014/60] topography of the North face and a frictional angle of 35° are used (Figure 39). Figure 39a shows that planar sliding on J1, J3 and J4 is possible. The kinematic tests show that the discontinuity J5 enables the toppling and that there are three possibilities for wedge sliding (J4^J2, J4^J3 and J2^J3).

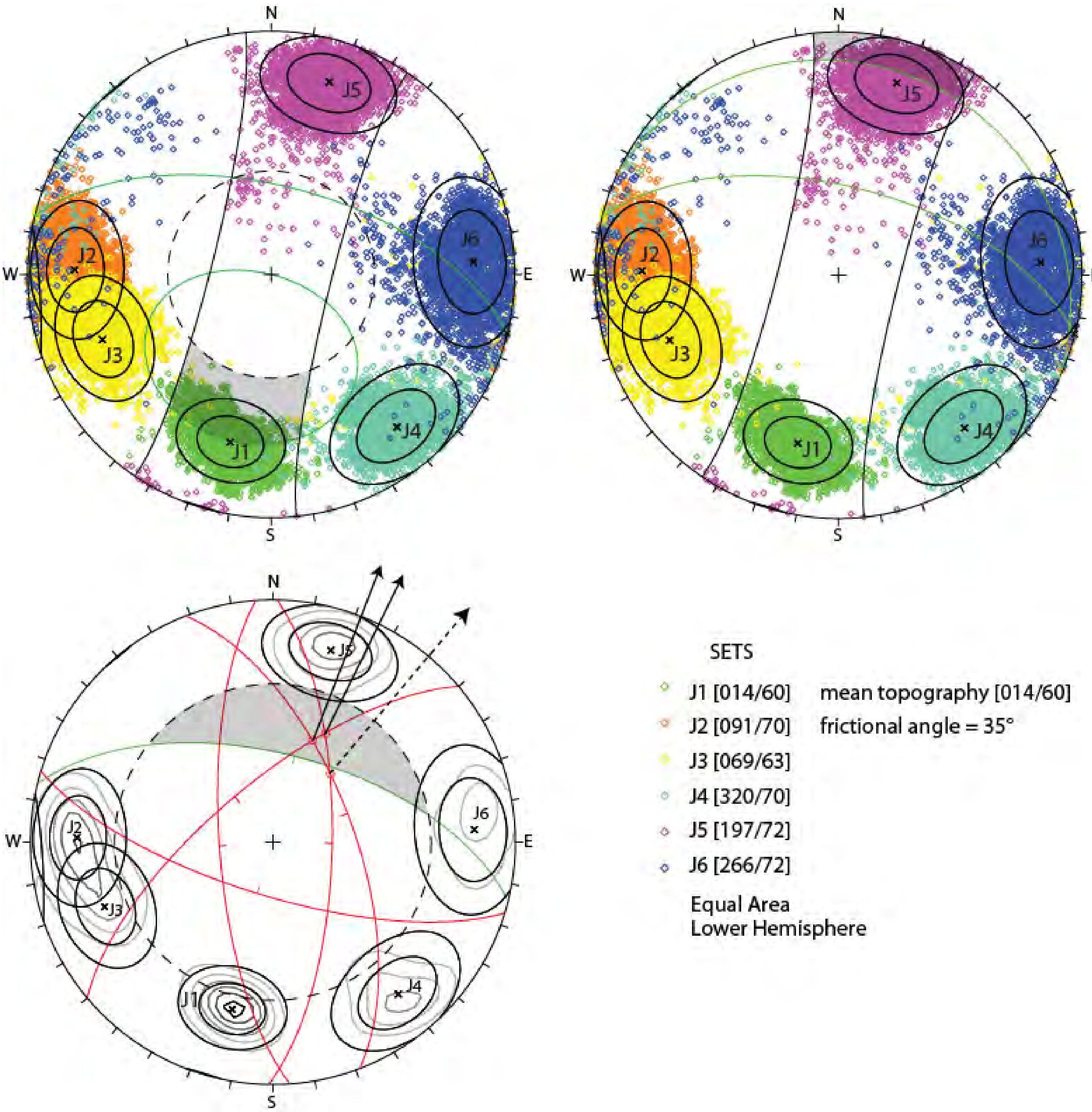

Figure 39: Kinematic tests of Svarttinden. Top left: planar sliding, top right: toppling, bottom: wedge sliding).

Based on field and pictures observations, the most probable failure mechanism for the bigger volume is planar sliding on the continuation of the sliding surface outcropping in the eastern part. This surface cut the base of the pyramid but it is not a plane as its orientation changes slightly from one side to the other: in the eastern part of the pyramid the sliding surface has a J1 orientation (Figure 42a) but on the western side the surface is less steep than J1 (Figure 42c). We can then suspect it is curved as suggested in early works (Figure 40)

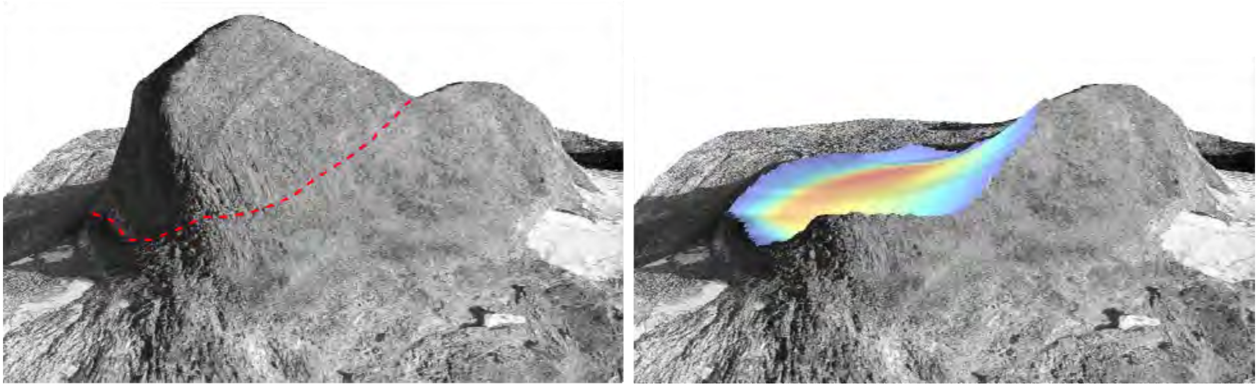

Figure 40: Left: view from SE of Svarttinden (red line: apparent trace of the sliding surface). Right: example of possible sliding surface interpolated using the SLBL method

Toppling could affect some blocks in the North face (J5 correspond to the pinkish discontinuity set in the Figure 37) and the wedge failure seems to affect only smaller volumes.
Another important feature at Svarttinden is the dense fragmentation in prisms of the rock body. As we can see in the Figure 41, the decimeter to meter prisms are cut according to J1, J7 and J2.

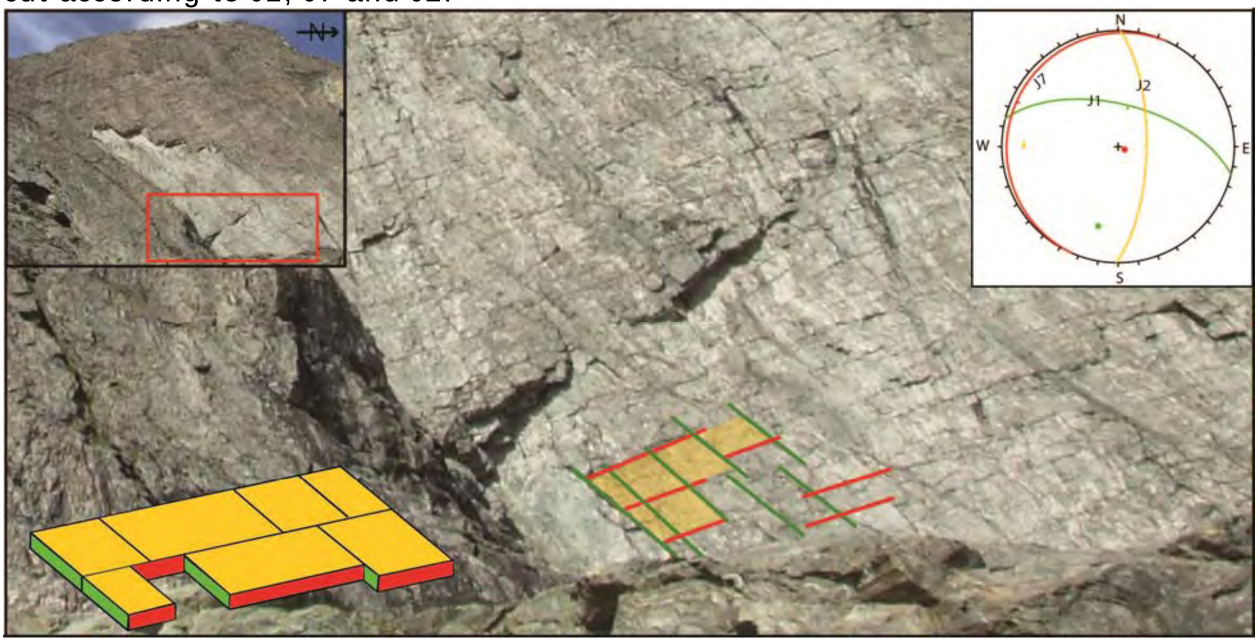

Figure 41: Cutting of the blocks in the East wall of the block.

The same mechanism affects bigger blocks (Figure 42b). In this case, the sides of the blocks are delimited by J4 and J1 instead of J7 and J1.

IV.4.4 Discussion

As discussed previously, the old sliding plane seems to extend through the present potentially unstable block. The East wall is cut by an important fracture that has the same orientation than the sliding plane [014/60] (Figure 42a) and it can be followed in the West wall but with a slightly different orientation [070/63] (Figure 42c). The volume of the block (pyramid) is estimated up to 5 Mm^3.
The presence of seepage in different places of the cliff suggests that the entire block is completely fractured and that the water can infiltrate the massif (Figure 42).

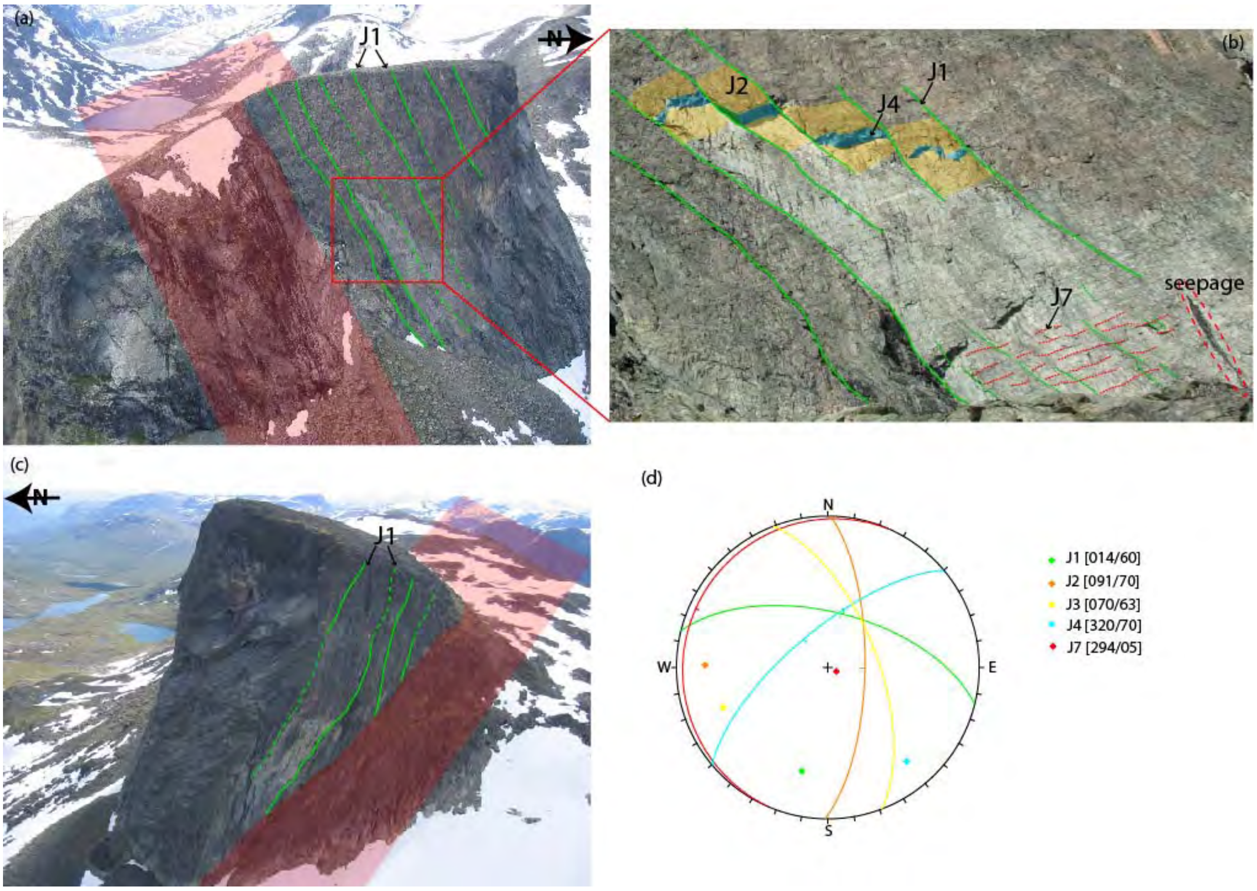

Figure 42: detailed view of the instable block of svarttinden, (a) east wall, (b) zoom of the east wall, (c) western wall, (d) stereonet of the sets highlighted in (a), (b) and (c).

The major hazard at Svarttinden is a large planar sliding that may turn into a rock avalanche that would reach the Romsdalen valley. Other smaller volumes may fall, but considering the location of this mountain they represent only minor risks (geologists at the foot of the faces for instance). A regular GPS monitoring of the top of the pyramid seems a good start to detect if there is any movement. That can be completed by some measurements along cracks. Occasionally it would be interesting to compare scans of the faces of the pyramids to estimate the rockfall activity.

IV.5 Hellesylt_6b

IV.5.1 Introduction

Hellesylt_6b is along Sunnylvsforden (Storfjorden) close to the village of Hellesylt (Stranda Kommune), in Møre og Romsdal. It consists in large block sliding on an east-dipping plane (Figure 43) towards the fjord. The interest for this site is that a catastrophic failure of this block could trigger a tsunami. Five scans were done by T. Oppikofer and M. Jaboyedoff in 2006.

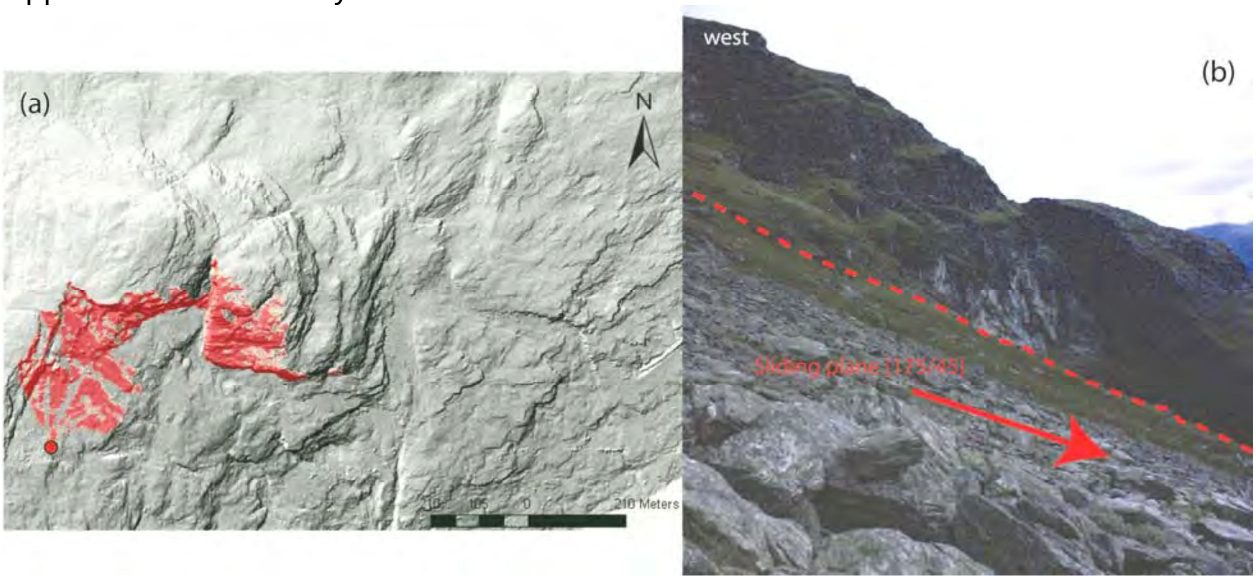

Figure 43: (a) projection of the scans on the DEM, (b) General view of the Hellesylt_6b area.

IV.5.2 Structural analysis

The structural analysis was carried out with COLTOP-3D and five discontinuity sets were distinguished (Figure 44). A average topography [150/40] was chosen for the tests.

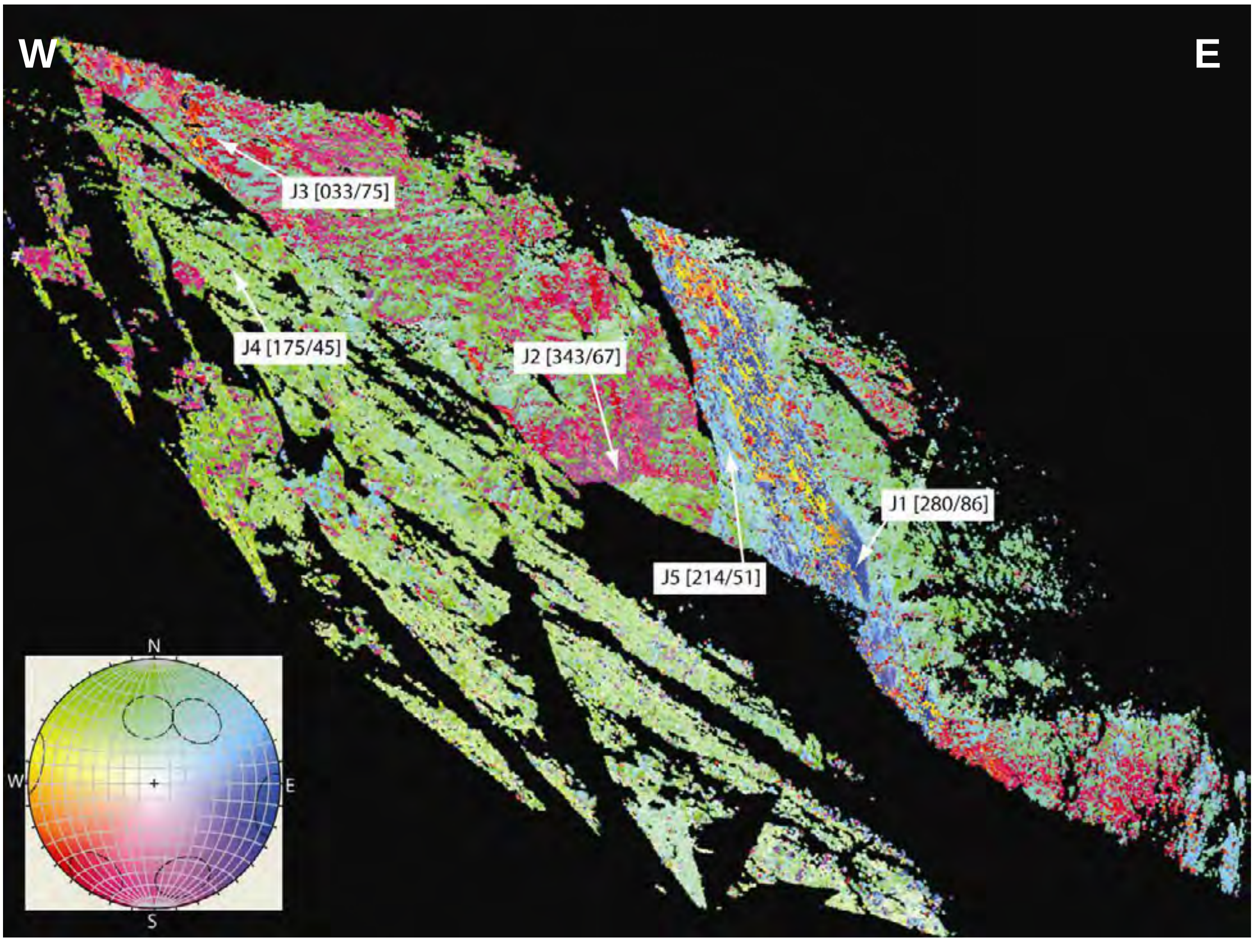

Figure 44: Coltop-3D view of the studied area (the result is a colorful point cloud where each color is assigned to a spatial orientation)

These five main sets were imported in Dips (Figure 45) and the results are summarized in the Table 8.

Table 8: orientations discontinuity sets of the Hellesylt area.

Sets	Dip Direction	Dip	Std. deviation
J1	280	86	14°
J2	343	67	14°
J3	033	75	10°
J4	175	45	13°
J5	214	51	17°

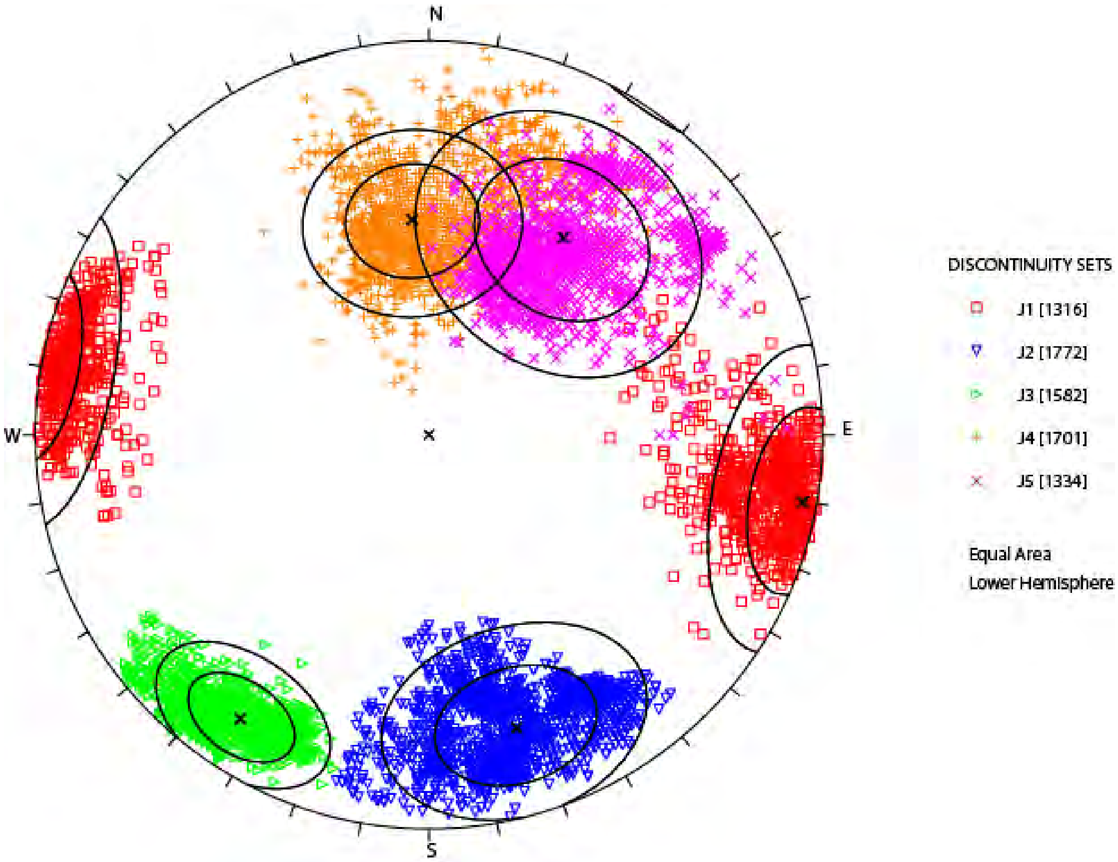

Figure 45: Setreoplot (lower hemisphere, equal area) of the discontinuity sets detected with COLTOP-3D. The circles represent the ± 1-sigma and ± 2-sigma dispersion.

IV.5.3 Kinematic tests

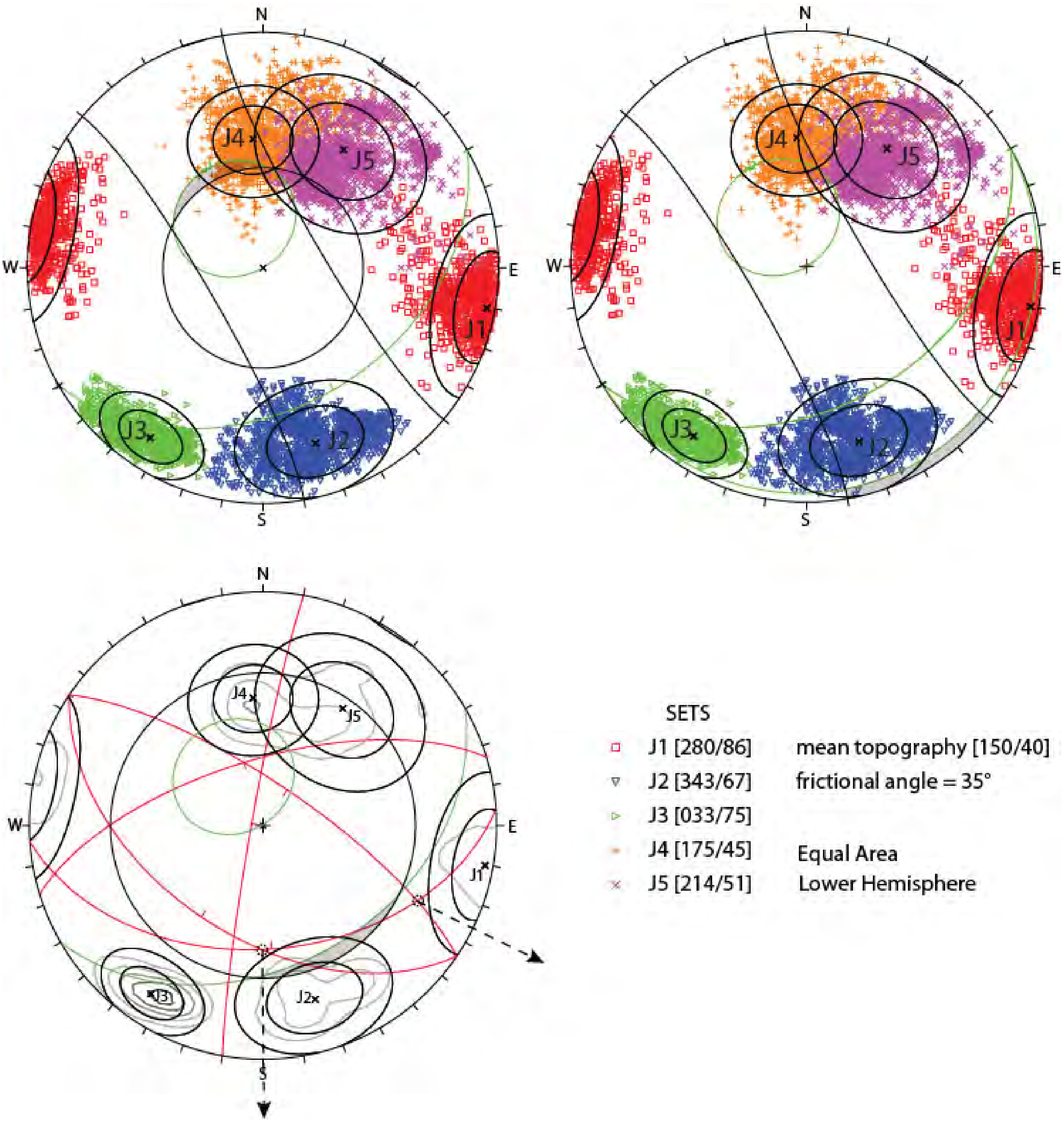

Figure 46: kinematic tests (planar sliding, toppling and wedge sliding) for the studied area.

Based on the kinematic tests (Figure 29), it appears that planar along J4 is the most probable mechanism. Based on field observations, J2 can generate toppling but it is more probable that it affects only small volumes/blocks. The tests suggest also that J4^J3 and J4^J5 could generate wedge sliding but, again, it seems to affect lesser volumes.

IV.5.4 Discussion

As suggested previously, planar sliding is the most probable failure mechanism affecting an important volume of the Hellesylt area. In fact, on the field, there is evidence of an old sliding plane (Figure 47). An important volume delimited backward by a large open fracture (X on the picture) could potentially fall down along a failure plane of orientation J4. Other vertical fractures may delimit small volume in the front of the large block.

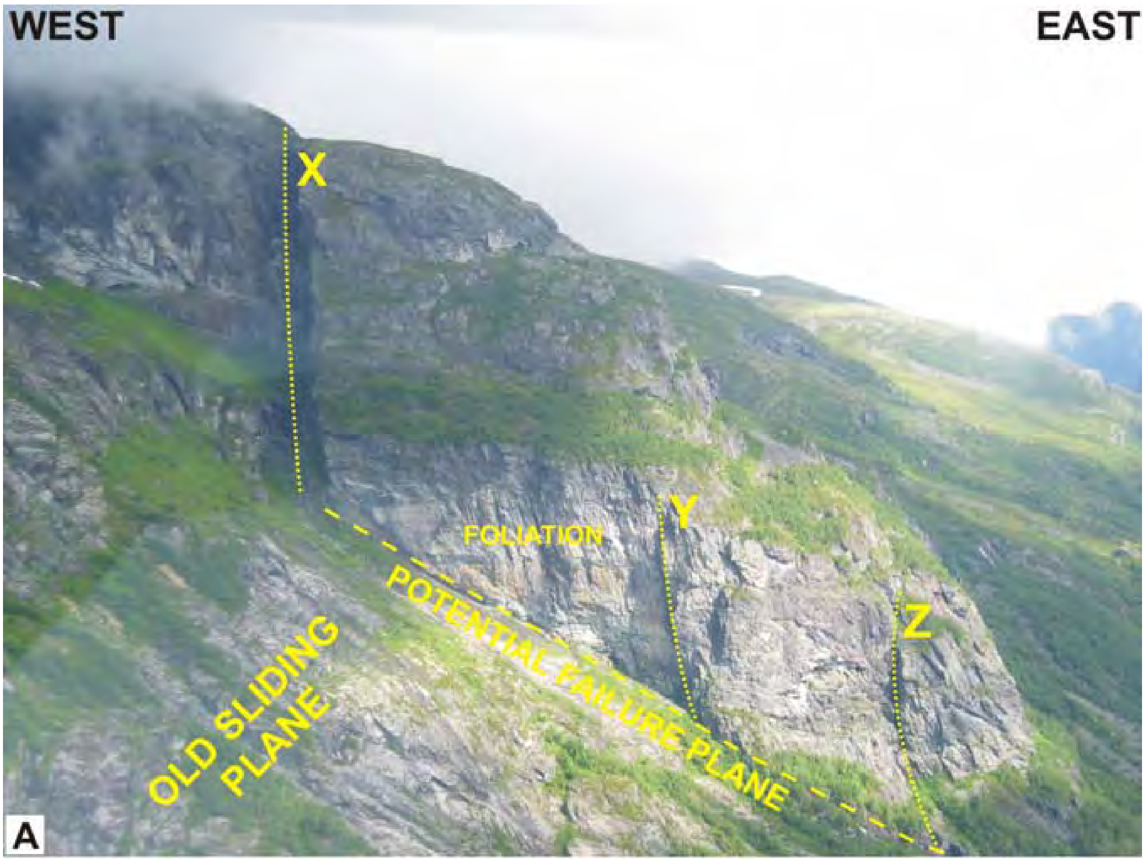

Figure 47: Photo of the structures of the Hellesylt_6b site. X is a large opened extensional fracture, suggesting several meters cumulative displacement. Y and Z are extensional fractures, trending NE-SW. The sliding plane is well defined on the picture (after the NGU-report of Henderson et al, 2006).

For the Hellesylt-6b site only collapses of large volumes are of interest because of the tsunami risk in the fjord. The block is well delimited with a widely open crack at the back and well identified sliding plane. The next step is to know if there is presently any movement of the block. This is currently done by yearly GPS monitoring. If a movement is detected, that could be interesting to return scanning in some years to check if any dislocation is taking place in the rock mass. But the site is difficult to access and a regular monitoring by terrestrial lidar does not seem a priority.

IV.6 Nordal_21

IV.6.1 Introduction

The site of Nordal_21 is located above the village of Nordal (Nordal Kommune) . The unstable part of this site is an upper steep cliff with a large rockfall deposit fans at the foot (Figure 48). According to local people, rockfalls occurred with a run-out down to the road during the XX century, but the blocks were removed from the fields.

Figure 48: panoramic view of the instability of Nordal_21

A first lidar campaign was done in 2006 by M. Jaboyedoff and T. Oppikoffer with eight scans of the site. A second campaign took place in 2009 where four scans were made by M.-H. Derron.

IV.6.2 Structural analysis

The mean topography orientation of [220/70] was estimated on the DEM. The structural analysis was carried out with COLTOP-3D and five discontinuity sets were highlighted (Figure 49).

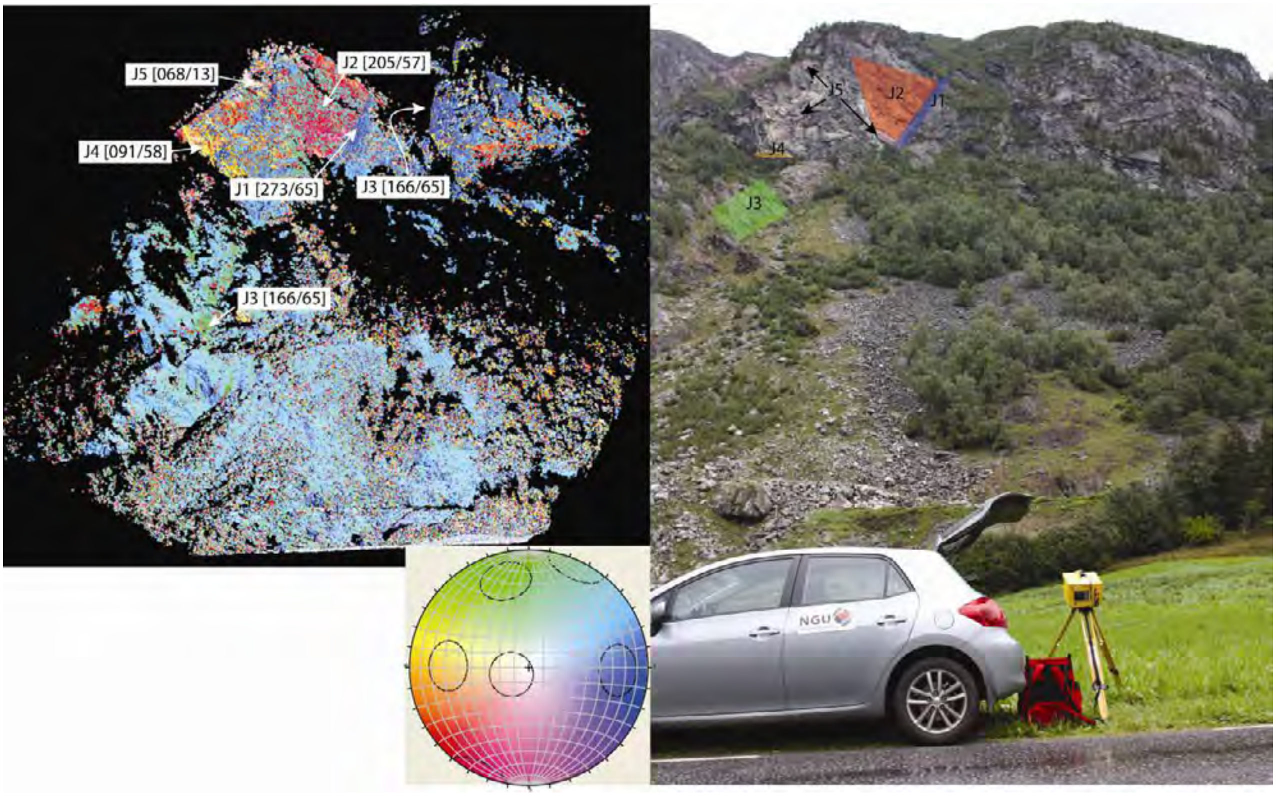

Figure 49: coltop view of the cliff (left) and a general view with the main sets (right).

These five main sets were imported in Dips (Figure 50) in order to estimate their orientation and standard deviation. The results are summarized in the Table 9.

Table 9: detail of the different discontinuity sets of the Nordal area.

Sets	Dip Direction	Dip	Std. deviation
J1	273	65	11°
J2	205	87	12°
J3	165	65	12°
J4	091	58	15°
J5	068	13	10°

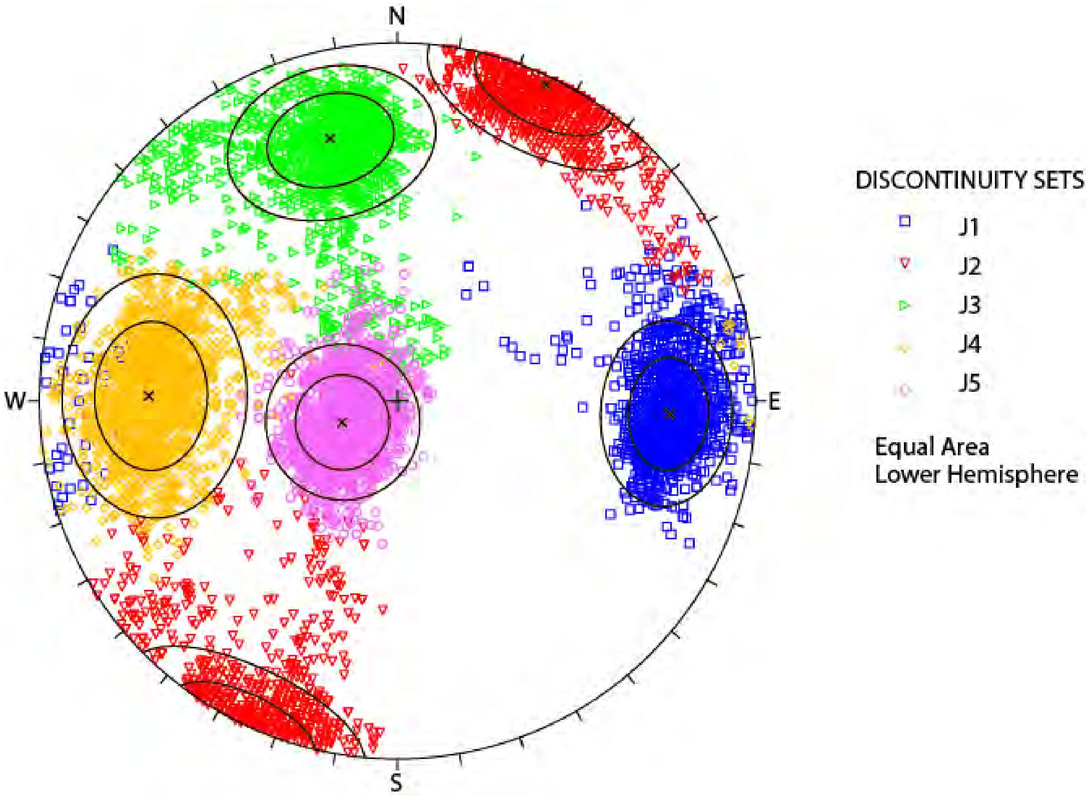

Figure 50: Stereoplot of the main surfaces of discontinuity for the site of Nordal_21. The circles represent the ± 1-sigma and 2-sigma dispersion.

A detailed analysis of the pictures allowed the identification of vertical and parallel fractures that did not appeared on the lidar data (Figure 51b). In particular, one of these fractures crosses the totality of the cliff (in red in Figure 51a) and should be a concern of future investigation.

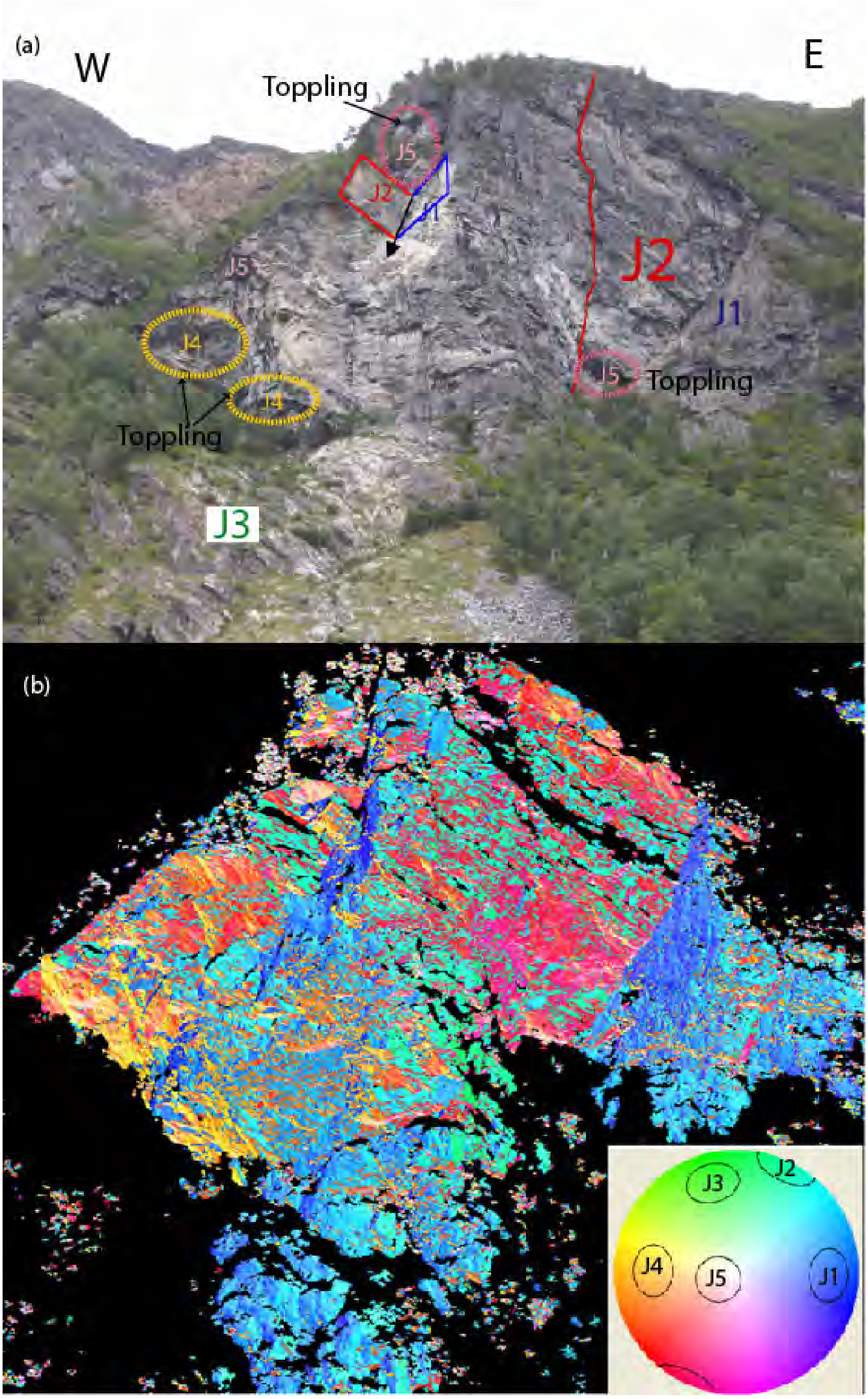

Figure 51: (a) detailed view of the potentially unstable block with the discontinuity sets and the vertical fracture F1 crossing the cliff (red line), (b) a detailed view of the cliff with COLTOP-3D.

IV.6.3 Kinematic tests

Kinematic tests were carried out in the studied area in order to see the different failure mechanisms that may affect the cliff. The [220/70] topography and a frictional angle of 35° were used. J1 and J2 could involve planar sliding (Figure 52a). It appears that the discontinuity set J2 enables toppling (Figure 52b) as well as J5 and J4, based on the Figure 51a. In Figure 52c, we observe a possibility of wedge failure on J1^J3 with a plunging direction of [219/52].

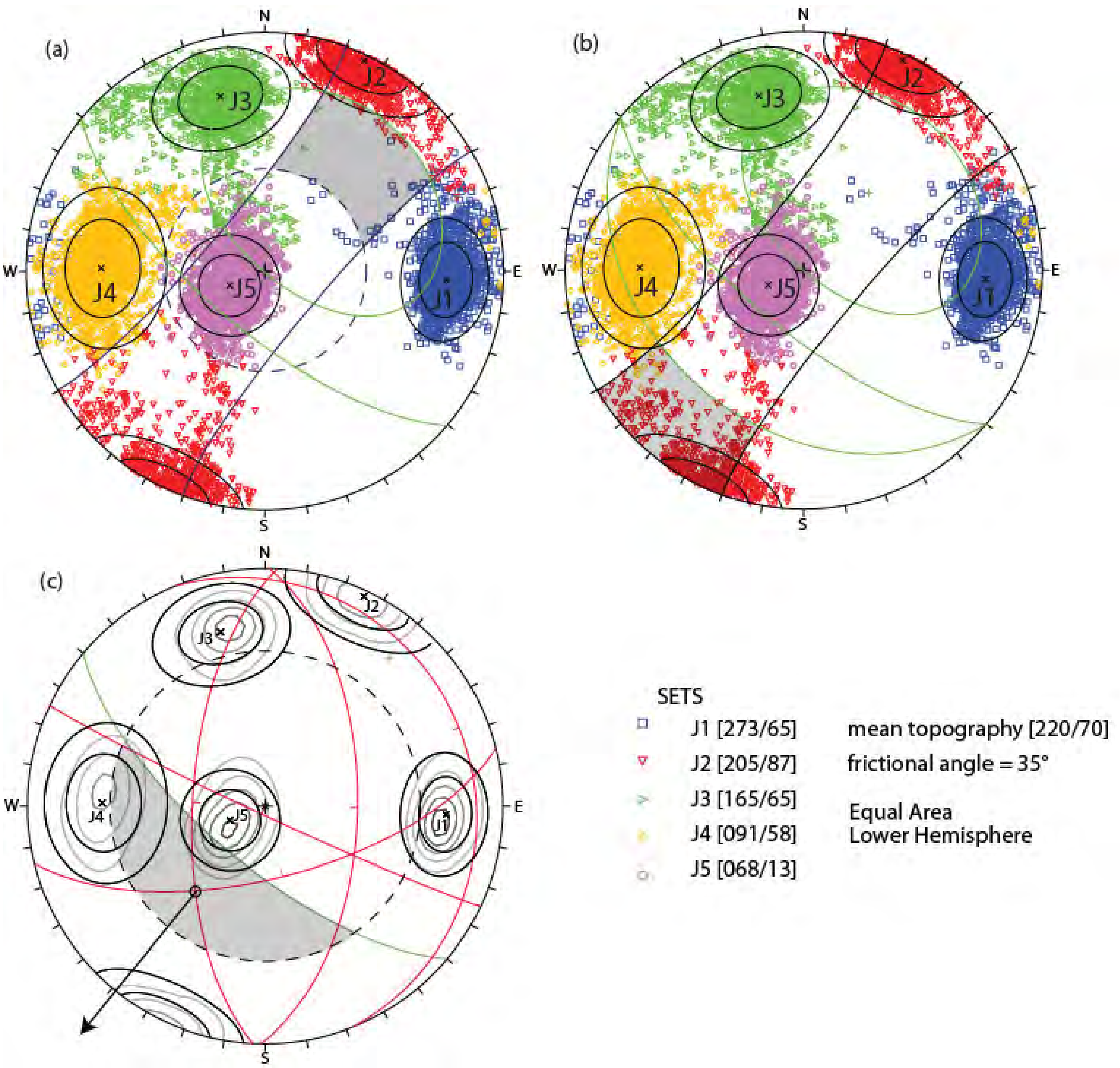

Figure 52: kinematic tests (a) planar sliding, (b) toppling and (c) wedge sliding.

Based on observations on photos, there is another possibility for wedge sliding in the rockface (with a different orientation of the topography). In fact, a fallen wedge involving J1^J2 with a plunging direction of [289/64] is present in Figure 51a. But this wegde is of much smaller volume than the one on J1^J3 which may affect the whole block.

IV.6.4 Movement analysis

A movement analysis was done by comparing the 2006 scans and with the 2009, but no evidence of movements of the overall cliff was detected. This is partly due to the low quality of the 2009 scan at long range (it was raining during the acquisition). Then this movement detection should be checked again with a new acquisition.

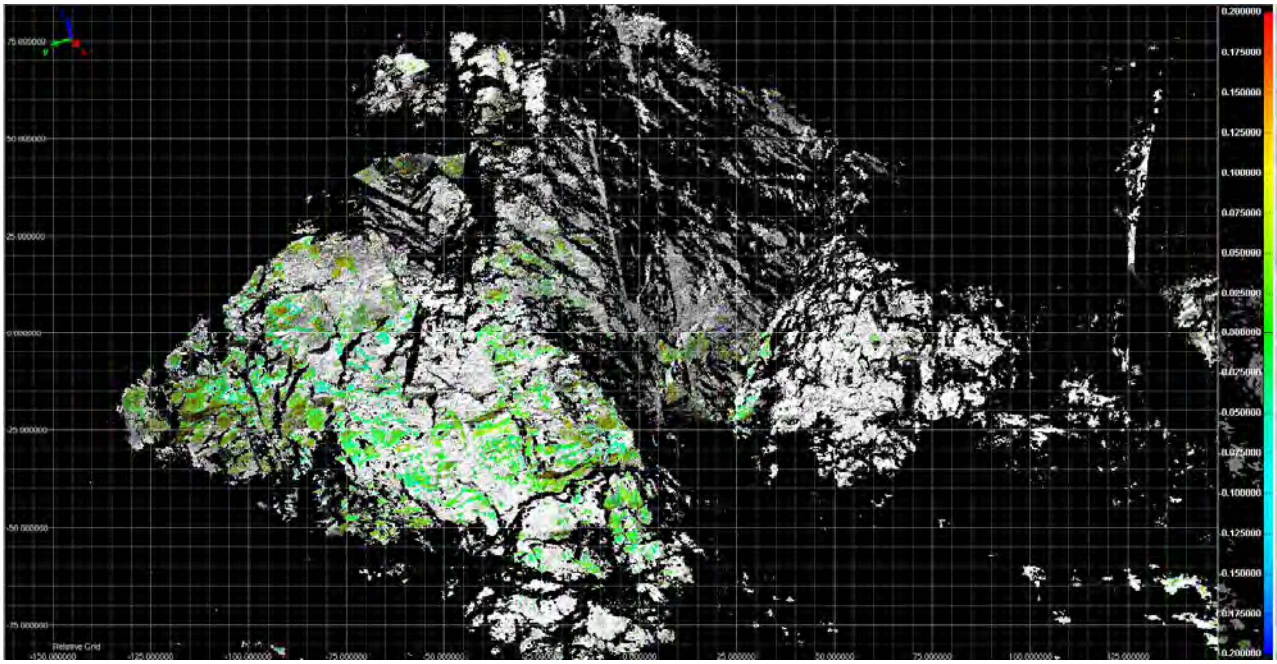

Figure 53: Scan comparison 2006-2009 (maximum distance = 0.2m). Due to difficult atmospheric conditions (rain) the quality of the 2009 scan is poor and the top of the cliff is not covered.

IV.6.5 Discussion

Wedge failures are the main concerns for the area of Nordal_21. Moreover, as discussed before, an important vertical fracture is present in the vertical face. A more detailed analysis in the field of this structure is necessary, in particular to check if this crack is visible on the top of the block.
The wedge J1^J2 is apparently the most active and responsible for the last events. But a rupture of the wedge J1^J3 at the base of the cliff would provide a much bigger volume of rockfalls. It is possible that this wedge is stopped by a buttress at the foot of the cliff (to be confirmed). Nevertheless this case has to be considered seriously as there is already an open crack (F1) in the face.
Considering that this site is above houses and fields, even small rockfalls may have consequences. At least, any rockfall activities should be recorded and announced to

the authorities (IKS-Beredskap Senter for instance). For the hazard of failure of the whole block, it has to be first determined if this block moves or not. A GPS point was implemented on the top and will provide a first answer. It would be good to complete it by measurements of the crack opening and regular geodetic monitoring (total station on target from the road). As lidar scanning is easy from the road, it should be continued to monitor the activity in the face.

V General conclusions

This report describes the analysis by terrestrial laser scanning of six instabilities in Møre og Romsdal. Three sites are located directly on the southern edge of the Romsdalen valley (Flatmark, Børa, Mannen), one on a plateau a bit more South (Svarttinden), and two in the Storfjorden area (Hellesylt, Nordal). Except for Nordal, the main concern is the potential failure of large volumes that may either trigger a tsunami (Hellesylt) or dam the Rauma river (Flatmark, Børa, Mannen, Svarttinden). For Nordal, smaller volumes are expected, but due to the presence of houses in the neighbourhood and some recent rockfall activities this site must be considered with cautions. The other most critical site is Mannen, with an extremely dislocated large volume of rocks, on a very steep valley flank (this site is already a priority of Åknes/Tafjord Beredskap IKS). For both sites, terrestrial laser scanning monitoring should be continued. For the other sites it is important first to establish if any movement is taking place in order to asses the priorities of investigation.
We can note that Flatmark, Børa and Mannen are in similar geomorphologic locations, aligned along the Rosmdalen valley, but have different particularities that may correspond to different evolution stages of this valley side. Using the terrestrial and airborne lidar datasets, combined with the field observations, and perhaps some datations, it would be interesting to decipher this evolution.

As already mentioned, this report is based on terrestrial lidar datasets only. Then these results have to be combined with the other pieces of knowledge collected by NGU or Åknes/Tafjord Beredskap IKS.

Appendix 3: Known unstable or potentially unstable rock slopes in Møre og Romsdal

The following tables show an overview of unstable rock slopes in Møre og Romsdal extracted from the database on unstable rock slopes with the current status of site investigations, recommendations for further work and references to previous reports. A list with other (former) names for the unstable rock slope is given where applicable.

List of unstable or potentially unstable rock slopes in Møre og Romsdal.

Name	Coordinates (UTM 32N)	Investigations	Recommendations	Unstable rock slope?	References	Former names
Nordmøre region						
Aure municipality						
Hardfjellet	486036 / 7009868	Aerial photographs	Helicopter reconnaissance planned	Unknown	Dahle et al. 2011a	-
Todalsdalen	487991 / 7010548	Aerial photographs	Helicopter reconnaissance planned	Unknown	Dahle et al. 2011a	-
Gjemnes municipality						
Geitaskaret	430102 / 6979632	Helicopter reconnaissance in 2012	Assess run-out area	Yes	Dahle et al. 2011a	-
Trolldalsfjellet	420668 / 6969622	Helicopter reconnaissance in 2012	Assess run-out area	Yes	Dahle et al. 2011a	-
Ørnstolen	429803 / 6978752	Helicopter reconnaissance in 2012	Field mapping planned	Yes	-	-
Sunndal municipality						
Bjørnahjellen	485858 / 6947633	Aerial photographs	Helicopter reconnaissance planned	Unknown	-	-
Blåbotnhalsen	466718 / 6931036	Aerial photographs	Helicopter reconnaissance planned	Unknown	-	-
Bytdalen	473469 / 6958093	Helicopter reconnaissance in 2007	No further investigations	No	Henderson & Saintot 2007	Sunndalen 22
Bårsveinhamran	491262 / 6945862	Helicopter reconnaissance in 2011	No further investigations	Potential	-	-
Ekkertinden 1	504722 / 6937537	Helicopter reconnaissance in 2007	No further investigations	No	Henderson & Saintot 2007	Sunndalen 7
Ekkertinden 2	504297 / 6938026	Helicopter reconnaissance in 2007	No further investigations	No	Henderson & Saintot 2007	Sunndalen 8
Fulånebba	478127 / 6954843	Helicopter reconnaissance in 2011	Field mapping planned	Yes	-	-
Gammelseterhaugen	472984 / 6967832	Helicopter reconnaissance in 2011	Assess run-out area	Yes	-	-
Gammelurkollen	474807 / 6936546	Helicopter reconnaissance in 2011	No further investigations	No	-	-
Gikling 1	492757 / 6946726	Mapped in 2006 & 2007, periodic displacement measurements with dGNSS since 2007	Continue periodic measurements with 1–3 year interval	Yes	Henderson & Saintot 2007 Saintot et al. 2008, 2011b Dalsegg et al. 2010 Dahle et al. 2011a	Sunndalen 12
Gikling 2	491958 / 6946575	Mapped in 2006 & 2007, periodic displacement measurements with dGNSS since 2007	Continue periodic measurements with 1–3 year interval	Yes	Henderson & Saintot 2007 Saintot et al. 2008 Dahle et al. 2011a	Sunndalen 12
Gjersvollsetra	475481 / 6957568	Helicopter reconnaissance in 2011	Assess run-out area	Yes	-	Karihaugen
Glennfjellet	462321 / 6946392	Aerial photographs	No further investigations	No	-	-
Grønsletta	479744 / 6950222	Aerial photographs	Helicopter reconnaissance planned	Unknown	-	-
Grøvelnebba	477595 / 6954369	Helicopter reconnaissance in 2011	No further investigations	Potential	-	-
Gråhøa 1	491028 / 6942632	Field mapping in 2010	Field mapping planned	Yes	Dahle et al. 2011a	-
Gråhøa 2	490873 / 6943040	Helicopter reconnaissance in 2007 and 2011	Field mapping planned	Yes	Henderson & Saintot 2007	Sunndalen 4
Gråhøa 3	490340 / 6943341	Helicopter reconnaissance in 2011	No further investigations	No	-	-

List of unstable or potentially unstable rock slopes in Møre og Romsdal.

Name	Coordinates (UTM 32N)	Investigations	Recommendations	Unstable rock slope?	References	Former names
Hallarvassfjellet 1	472856 / 6935205	Aerial photographs	No further investigations	No	-	-
Hallarvassfjellet 2	473443 / 6936681	Aerial photographs	No further investigations	No	-	-
Hisdalsholet	468441 / 6961495	Helicopter reconnaissance in 2007	No further investigations	No	Henderson & Saintot 2007	Almskårneset, Sunndalen 18
Hjorthaugen	466378 / 6949159	Aerial photographs	No further investigations	No	-	Botnen
Hornet	483365 / 6944169	Helicopter reconnaissance in 2007	No further investigations	No	Henderson & Saintot 2007	Sunndalen 3
Hovennebba	479893 / 6944152	Helicopter reconnaissance in 2011	No further investigations	No	-	-
Hovsnebba 1	477560 / 6950295	Reconnaissance from road in 2010 and helicopter in 2011	No further investigations	No	-	-
Hovsnebba 2	478999 / 6949621	Aerial photographs	No further investigations	No	-	-
Husmannen	493532 / 6945493	Aerial photographs	Helicopter reconnaissance planned	Unknown	Henderson & Saintot 2007	Sunndalen 27
Høghamran	477433 / 6969955	Helicopter reconnaissance in 2011	No further investigations	No	-	Vardhaugen
Ivasnasen	506143 / 6936593	Helicopter reconnaissance in 2007, field mapping in 2008 and 2011, periodic displacement measurements with tape extensometer and TLS since 2010	Continue periodic measurements with 3–5 year interval	Yes	Henderson & Saintot 2007 Saintot et al. 2008, 2011b Dahle et al. 2011a Dreiås 2012	Sunndalen 6
Jøthjellhamran	470824 / 6960277	Helicopter reconnaissance in 2007	No further investigations	No	Henderson & Saintot 2007	Sunndalen 19
Jøtulavlan 1	487798 / 6947551	Helicopter reconnaissance in 2007	Field mapping planned	Yes	Henderson & Saintot 2007	Sunndalen 15
Jøtulavlan 2	488375 / 6946767	Aerial photographs	No further investigations	No	-	-
Kamman	466835 / 6948704	Aerial photographs	No further investigations	No	-	-
Kammen	476659 / 6969969	Helicopter reconnaissance in 2011	No further investigations	No	-	-
Kjeskrødalen	471722 / 6959701	Helicopter reconnaissance in 2007	Field mapping planned	Yes	Henderson & Saintot 2007	Jøthjellen, Sunndalen 20
Kleiva	468969 / 6940498	Aerial photographs	No further investigations	No	-	-
Klingfjellet 1	498895 / 6941539	Helicopter reconnaissance in 2007	No further investigations	No	Henderson & Saintot 2007	Sunndalen 10
Klingfjellet 2	497990 / 6941478	Helicopter reconnaissance in 2011	No further investigations	No	-	-
Klingråket 1	495807 / 6944719	Helicopter reconnaissance in 2007	Assess run-out area	Yes	Henderson & Saintot 2007 Dahle et al. 2011a	Sunndalen 11, Snø-vasskjerdingane
Klingråket 2	495588 / 6944792	Aerial photographs	Helicopter reconnaissance planned	Unknown	-	-
Klomra 1	491582 / 6945572	Aerial photographs	Helicopter reconnaissance planned	Unknown	-	-
Klomra 2	491803 / 6945489	Helicopter reconnaissance in 2007	No further investigations	No	Henderson & Saintot 2007	Sunndalen 13
Litlkalkinn 1	477161 / 6947403	Helicopter reconnaissance in 2007	No further investigations	No	Henderson & Saintot 2007	Sunndalen 2

List of unstable or potentially unstable rock slopes in Møre og Romsdal.

Name	Coordinates (UTM 32N)	Investigations	Recommendations	Unstable rock slope?	References	Former names
Litlkalkinn 2	477024 / 6947442	Helicopter reconnaissance in 2007	No further investigations	No	Henderson & Saintot 2007	Litlekalken, Sunndalen 23
Litlkalkinn 3	476819 / 6947278	Helicopter reconnaissance in 2011	No further investigations	No	-	-
Merrakammen	488331 / 6955734	Helicopter reconnaissance in 2011	Field mapping planned	Yes	-	-
Mjosundet	471906 / 6959605	Helicopter reconnaissance in 2007	No further investigations	No	Henderson & Saintot 2007	Sunndalen 21
Mohaugen 1	478696 / 6957003	Helicopter reconnaissance in 2011	No further investigations	No	-	-
Mohaugen 2	477304 / 6957752	Helicopter reconnaissance in 2011	No further investigations	No	-	-
Navardalsnebba	491565 / 6949852	Aerial photographs	Helicopter reconnaissance planned	Unknown	Dahle et al. 2011a	-
Ottdalskammen	498615 / 6948252	Helicopter reconnaissance in 2011	Assess run-out area	Yes	Dahle et al. 2011a	-
Ottem 1	501600 / 6941211	Helicopter reconnaissance in 2007	No further investigations	No	Saintot et al. 2008	Sunndalen 9
Ottem 2	501124 / 6941029	Helicopter reconnaissance in 2007, periodic displacement measurements with TLS since 2010	Periodic measurements not to be continued	No	-	Sunndalen 9
Ottem 3	501067 / 6941181	Helicopter reconnaissance in 2007, field mapping in 2008, periodic displacement measurements with dGNSS since 2008 and TLS since 2011	Continue periodic measurements with 3–5 year interval	Yes	Henderson & Saintot 2007 Saintot et al. 2008, 2011b Dahle et al. 2011a	Sunndalen 9
Serkjenebba	485501 / 6941240	Helicopter reconnaissance in 2011	Field mapping planned	Yes	-	-
Seterbruna	494464 / 6931329	Aerial photographs	No further investigations	No	-	-
Skarfjellet	485485 / 6953275	Aerial photographs	Helicopter reconnaissance planned	Unknown	Dahle et al. 2011a	-
Skrommelnebba	465716 / 6950382	Aerial photographs	No further investigations	No	-	-
Steinbruhøa	473455 / 6938497	Helicopter reconnaissance in 2011	No further investigations	Potential	-	-
Steinrabbgrovin	495608 / 6940218	Aerial photographs	No further investigations	No	-	-
Storaurhøa	488002 / 6924438	Aerial photographs	No further investigations	No	-	-
Storbotnen	475433 / 6944471	Helicopter reconnaissance in 2007 and 2011, field mapping in 2008	Field mapping planned	Yes	Henderson & Saintot 2007 Saintot et al. 2008, 2011b	Sunndalen 26
Storhaugen 1	467755 / 6951472	Aerial photographs	Helicopter reconnaissance planned	Unknown	-	-
Storhaugen 2	468459 / 6951702	Aerial photographs	No further investigations	No	-	-
Storhaugen 3	468813 / 6952325	Aerial photographs	No further investigations	No	-	-
Storkalkinn	479088 / 6943935	Aerial photographs	No further investigations	No	-	-
Storskraven	471345 / 6959947	Helicopter reconnaissance in 2007	No further investigations	No	Henderson & Saintot 2007	-

List of unstable or potentially unstable rock slopes in Møre og Romsdal.

Name	Coordinates (UTM 32N)	Investigations	Recommendations	Unstable rock slope?	References	Former names
Storurhamran	475164 / 6943002	Helicopter reconnaissance in 2007, TLS in 2010 for structural analysis	Assess run-out area	Yes	Henderson & Saintot 2007	Sunndalen 24
Svarthamran	476907 / 6947951	Helicopter reconnaissance in 2007	Field mapping planned	Yes	Henderson & Saintot 2007 Dahle et al. 2011a	Sunndalen 1
Sviskura	497021 / 6939832	Helicopter reconnaissance in 2007	No further investigations	No	Henderson & Saintot 2007	Høgslåa, Sunndalen 5
Såtbakkleiva	490243 / 6946640	Helicopter reconnaissance in 2007	No further investigations	No	Henderson & Saintot 2007	Sunndalen 14
Trolla	487117 / 6950433	Aerial photographs	No further investigations	No	-	-
Vardfjelltangan	482714 / 6933827	Aerial photographs	No further investigations	No	-	-
Vollan	505839 / 6938250	Field mapping in 2008 and 2011, periodic displacement measurements with dGNSS since 2008	Continue periodic measurements with 3–5 year interval	Yes	Saintot et al. 2008 Dahle et al. 2011a Dreiås 2012	-
Surnadal municipality						
Brøskja	471478 / 6978613	Aerial photographs	Helicopter reconnaissance planned	Unknown	-	Brøske, Stangvik
Tingvoll municipality						
Bleberga	464110 / 6964303	Helicopter reconnaissance in 2007	No further investigations	No	Henderson & Saintot 2007	Aksla Svala, Sunndalen 17
Skrøhammaren	459134 / 6966917	Helicopter reconnaissance in 2007	No further investigations	No	Henderson & Saintot 2007	Sunndalen 16
Romsdal region						
Fræna municipality						
Røssholfjellet	407379 / 6964237	Helicopter reconnaissance in 2012	Field mapping planned	Yes	Dahle et al. 2011a	Alteret
Stemshesten	408928 / 6984717	Helicopter reconnaissance in 2012	No further investigations	No	Dahle et al. 2011a	-
Talstadhesten	407696 / 6973777	Helicopter reconnaissance in 2012	Field mapping planned	Yes	-	-
Midsund municipality						
Bendsethornet	390904 / 6957853	Helicopter reconnaissance in 2012	Field mapping planned	Yes	Dahle et al. 2011a	Kløvhaugen

List of unstable or potentially unstable rock slopes in Møre og Romsdal.

Name	Coordinates (UTM 32N)	Investigations	Recommendations	Unstable rock slope?	References	Former names
Oppstadhornet	389193 / 6953753	Field mapping in 2004, periodic displacement measurements with dGNSS since 2003	Continue periodic measurements with 1–3 year interval	Yes	Robinson et al. 1997 Anda et al. 2000 Blikra et al. 2002a, 2002b Bhasin & Kaynia 2004 Braathen et al. 2004 Dahle 2004 Derron et al. 2005b Dalsegg et al. 2007 Dahle et al. 2011a Saintot et al. 2011b Hermanns et al. 2013	Oterøya
Ræstadhornet	388079 / 6956921	Helicopter reconnaissance in 2012	Field mapping planned	Yes	Dahle et al. 2011a	-
Sundsbørøra	392834 / 6958671	Helicopter reconnaissance in 2012	No further investigations	No	-	-
Nesset municipality						
Bjørktinden	458221 / 6931777	Aerial photographs	Helicopter reconnaissance planned	Unknown	-	-
Børa i Eikesdalen	457582 / 6925170	Field mapping in 2010	No further investigations	No	-	-
Ellingbenken	463955 / 6924122	Helicopter reconnaissance in 2010	No further investigations	No	-	-
Evelsfonnhøa	454976 / 6930849	Helicopter reconnaissance in 2010, periodic displacement measurements with TLS since 2012	Continue periodic measurements with 1–3 year interval	Yes	Dahle et al. 2011a	-
Kaldberget	450335 / 6953557	Aerial photographs	Helicopter reconnaissance planned	Unknown	-	-
Kjøtåfjellet	460527 / 6926489	Helicopter reconnaissance in 2010, periodic displacement measurements with tape extensometer since 2011 and TLS since 2012	Continue periodic measurements with 1–3 year interval	Yes	Dahle et al. 2011a	-
Kjøvhaugen	448733 / 6948064	Aerial photographs	Helicopter reconnaissance planned	Unknown	-	-
Litleaksla	460296 / 6923756	Helicopter reconnaissance in 2010	Helicopter reconnaissance planned	Unknown	-	-
Martinskora	454798 / 6929156	Helicopter reconnaissance in 2010	Field mapping planned	Yes	-	-
Nonshaugen 1	452820 / 6944576	Aerial photographs	Helicopter reconnaissance planned	Unknown	-	-
Nonshaugen 2	453347 / 6944041	Aerial photographs	Helicopter reconnaissance planned	Unknown	-	-
Sandoddan	458099 / 6938584	Aerial photographs	Helicopter reconnaissance planned	Unknown	-	-
Vikesoksa	459061 / 6938806	Helicopter reconnaissance in 2010	Field mapping planned	Yes	-	-
Vikesætra	459195 / 6934846	Helicopter reconnaissance in 2010	No further investigations	No	-	-

List of unstable or potentially unstable rock slopes in Møre og Romsdal.

Name	Coordinates (UTM 32N)	Investigations	Recommendations	Unstable rock slope?	References	Former names
Rauma municipality						
Børa	437801 / 6924469	Field mapping in 1999, periodic displacement measurements with dGNSS since 2003 and TLS since 2008, shock loggers placed from 2009 to 2012	Continue periodic measurements with 1–3 year interval	Yes	Anda et al. 2000 Blikra et al. 2002a, 2006 Braathen et al. 2004 Dalsegg & Tønnesen 2004 Henderson & Saintot 2007 Dahle et al. 2011a Saintot et al. 2011b, 2012	-
Flatmark	445752 / 6921138	Field mapping in 2006, periodic displacement measurements with dGNSS since 2006, TLS since 2007 and tape extensometer since 2011	Continue periodic measurements with 3–5 year interval	Yes	Henderson & Saintot 2007 Dahle et al. 2011a Saintot et al. 2011b, 2012	Skiri, Stålfonna
Frisvollfjellet	421564 / 6938845	Helicopter reconnaissance in 2011	No further investigations	No	-	-
Gridsetskolten	426569 / 6934302	Aerial photographs	Helicopter reconnaissance planned	Unknown	Dahle et al. 2011a	-
Gråfonnfjellet	424603 / 6924740	Aerial photographs	Helicopter reconnaissance planned	Unknown	Dahle et al. 2011a	-
Husnebba 1	446002 / 6940635	Aerial photographs	Helicopter reconnaissance planned	Unknown	Dahle et al. 2011a	Husnebba Vest
Husnebba 2	446560 / 6940623	Aerial photographs	Helicopter reconnaissance planned	Unknown	-	Husnebba Øst
Kammen	414208 / 6922601	Aerial photographs	Helicopter reconnaissance planned	Unknown	Dahle et al. 2011a	Kamben
Kvarvesnippen	418096 / 6945028	Helicopter reconnaissance in 2011	Field mapping planned	Yes	-	-
Kvitfjellet	419303 / 6941974	Aerial photographs	Helicopter reconnaissance planned	Unknown	Dahle et al. 2011a	-
Kvitfjellgjølet	419082 / 6941599	Helicopter reconnaissance in 2011, periodic displacement measurements with TLS since 2012	Continue periodic measurements with 1–3 year interval	Yes	-	-
Kyrkjetaket	443980 / 6942715	Aerial photographs	Helicopter reconnaissance planned	Unknown	-	Grøvdal, Hen, Isfjorden
Litlefjellet	437510 / 6931460	Aerial photographs	Helicopter reconnaissance planned	Unknown	-	-

List of unstable or potentially unstable rock slopes in Møre og Romsdal.

Name	Coordinates (UTM 32N)	Investigations	Recommendations	Unstable rock slope?	References	Former names
Mannen	436599 / 6925618	Field mapping in 2006, periodic displacement measurements with dGNSS between 2004 and 2010 and TLS between 2008 and 2010, continuous monitoring since 2009 by Åknes/Tafjord Early-Warning Centre	Continue continuous monitoring	Yes	Henderson & Saintot 2007 Dahle et al. 2008, 2011a, 2011b, 2011c Tønnesen 2009 Farsund 2011 Kristensen & Blikra 2011 Saintot et al. 2011a, 2011b, 2012 Dalsegg & Rønning 2012 Dehls et al. 2012 Elvebakk 2012 Oppikofer et al. 2012b	-
Marsteinskora 1	441564 / 6926025	Helicopter reconnaissance in 2010	Field mapping planned	Yes	-	-
Marsteinskora 2	441119 / 6925589	Aerial photographs	Helicopter reconnaissance planned	Unknown	-	-
Middagstinden	419271 / 6925276	Field mapping in 2009 and 2010, periodic displacement measurements with dGNSS since 2008 and TLS since 2010	Detailed mapping in progress, continue periodic measurements with 1–3 year interval	Yes	Anda et al. 2002 Blikra et al. 2002a Dahle et al. 2011a Krieger et al. 2013	Berill
Mjølvafjellet	435815 / 6934672	Helicopter reconnaissance in 2011	No further investigations	No	-	-
Nøsa	424304 / 6929133	Aerial photographs	Helicopter reconnaissance planned	Unknown	Dahle et al. 2011a	-
Olaskarstinden	438745 / 6928008	Field mapping in 2010	No further investigations	Potential	-	-
Rangåvassherbørget	446366 / 6924295	Aerial photographs	Helicopter reconnaissance planned	Unknown	-	-
Remmem	441218 / 6921315	Aerial photographs	Helicopter reconnaissance planned	Unknown	Dahle et al. 2011a	-
Skjelbostadfjell	424436 / 6930306	Aerial photographs	Helicopter reconnaissance planned	Unknown	-	-
Svarttinden	439854 / 6920503	Field mapping in 2006, periodic displacement measurements with dGNSS since 2005 and TLS since 2006	Continue periodic measurements with 3–5 year interval	Yes	Henderson & Saintot 2007 Dahle et al. 2011a Saintot et al. 2011b, 2012	-
Tindevatnet	417843 / 6925018	Aerial photographs	Helicopter reconnaissance planned	Unknown	-	-
Trolltindan	434330 / 6928524	Helicopter reconnaissance in 2006	New helicopter reconnaissance planned	Potential	Dahle et al. 2011a	Trollveggen
Veten	424466 / 6937812	Helicopter reconnaissance in 2011	No further investigations	No	-	Raudfonna
Vestnes municipality						

List of unstable or potentially unstable rock slopes in Møre og Romsdal.

Name	Coordinates (UTM 32N)	Investigations	Recommendations	Unstable rock slope?	References	Former names
Seteraksla	384331 / 6946017	Helicopter reconnaissance in 2012	Assess run-out area	Yes	Dahle et al. 2011a	-
Snaufjellet	386934 / 6943645	Helicopter reconnaissance in 2012	Assess run-out area	Yes	Dahle et al. 2011a	-
Strandastolen	392052 / 6941173	Helicopter reconnaissance in 2012	Make hazard and risk classification	Yes	-	-
Storfjord region						
Norddal municipality						
Alstadfjellet	422109 / 6913050	Field mapping in 2007	New helicopter reconnaissance planned	Unknown	Henderson et al. 2006 Saintot et al. 2011b	Storfjord Site 39
Alvikhornet 1	415514 / 6904360	Field mapping in 2006	Make hazard and risk classification	Yes	Henderson et al. 2006 Saintot et al. 2011b	Storfjord Site 26
Alvikhornet 2	416579 / 6902927	Helicopter reconnaissance in 2005, field mapping in 2006	No further investigations	Potential	Henderson et al. 2006 Saintot et al. 2011b	Storfjord Site 27
Alvikhornet 3	416146 / 6903103	Field mapping in 2006	No further investigations	Potential	Dahle et al. 2011a	-
Blikshammaren	405148 / 6907755	Helicopter reconnaissance in 2005	No further investigations	No	Henderson et al. 2006	Longelia, Storfjord Site 33
Blåhornet	403744 / 6905447	Helicopter reconnaissance in 2005	No further investigations	No	Henderson et al. 2006	Storfjord Site 19
Brudehammaren	409305 / 6906088	Field mapping in 2005	Make hazard and risk classification	Yes	Henderson et al. 2006 Dahle et al. 2011a Saintot et al. 2011b	Storfjord Site 22
Flyene	420125 / 6898187	Aerial photographs	Helicopter reconnaissance planned	Unknown	Dahle et al. 2011a	-
Furenakken	405510 / 6904417	Field mapping in 2005	No further investigations	Potential	Henderson et al. 2006 Saintot et al. 2011b	Storåsnakken, Storfjord Site 20
Geitvikdalen	416063 / 6901673	Helicopter reconnaissance in 2007	No further investigations	No	Henderson et al. 2006	Storfjord Site 41
Gudbrandsdalen	420763 / 6913505	Helicopter reconnaissance in 2007	No further investigations	Potential	Henderson et al. 2006 Dahle et al. 2011a	Storfjord Site 38
Hegguraksla	415511 / 6907493	Field mapping from 2006 to 2008, periodic displacement measurements with dGNSS between 2005 and 2007 and TLS between 2006 and 2008, continuous monitoring since 2005 by Åknes/Tafjord Early-Warning Centre	Continue continuous monitoring	Yes	Braathen et al. 2004 Blikra et al. 2006 Oppikofer & Jaboyedoff 2008 Rønning et al. 2006, 2008 Oppikofer 2009 Kristensen & Blikra 2010 Dahle et al. 2011a Saintot et al. 2011b	-

List of unstable or potentially unstable rock slopes in Møre og Romsdal.

Name	Coordinates (UTM 32N)	Investigations	Recommendations	Unstable rock slope?	References	Former names
Hegrehamrane	405500 / 6894500	Reconnaissance from road in 2007	No further investigations	No	Henderson et al. 2006	Breiskreda, Storfjord Site 30
Hornflågrova	398848 / 6900404	Helicopter reconnaissance in 2005	No further investigations	Potential	Henderson et al. 2006 Dahle et al. 2011a Saintot et al. 2011b	Storfjord Site 16
Indreeidshornet	404000 / 6894000	Aerial photographs	No further investigations	No	Henderson et al. 2006	Storfjord Site 29
Jimdalen	419291 / 6900411	Helicopter reconnaissance in 2007	No further investigations	No	Henderson et al. 2006 Saintot et al. 2011b	Storfjord Site 42b
Kallen	416801 / 6898899	Helicopter reconnaissance in 2007	No further investigations	No	Henderson et al. 2006 Saintot et al. 2011b	Storfjord Site 41b
Kastehøgfjellet	413492 / 6905003	Aerial photographs	Helicopter reconnaissance planned	Unknown	Henderson et al. 2006	Bolthamrane, Storfjord site 25
Kilstiheia	400983 / 6905305	Helicopter reconnaissance in 2011	Field mapping planned	Yes	-	-
Kleivahammaren	403938 / 6900853	Reconnaissance from road in 2007	Field mapping planned	Yes	-	Storfjord Site 20b
Kloven	418869 / 6900866	Helicopter reconnaissance in 2007	No further investigations	Potential	Henderson et al. 2006 Saintot et al. 2011b	Storfjord Site 42
Krikeberget	423221 / 6913238	Field mapping in 2007	No further investigations	No	Saintot et al. 2011b	Storfjord Site 39b
Krikekoppen	423630 / 6913502	Aerial photographs	Helicopter reconnaissance planned	Unknown	-	Storfjord Site 39c
Kvitfjellet 1	409183 / 6903741	Field mapping in 2005, periodic displacement measurements with dGNSS since 2005 and TLS since 2006	Continue periodic measurements with 3–5 year interval	Yes	Henderson et al. 2006 Dahle et al. 2011a Saintot et al. 2011b Oppikofer et al. 2012a	Storfjord 21
Kvitfjellet 2	409376 / 6903541	Field mapping in 2006, periodic displacement measurements with dGNSS since 2006 and TLS since 2010	Continue periodic measurements with 3–5 year interval	Yes	Henderson et al. 2006 Saintot et al. 2011b	Storfjord 21b
Middagshornet	411888 / 6905973	Helicopter reconnaissance in 2005	No further investigations	No	Henderson et al. 2006	Storfjord Site 24
Nyken	404905 / 6909815	Aerial photographs	Helicopter reconnaissance planned	Unknown	-	-
Remsfjellet	419023 / 6915166	Field mapping in 2007	No further investigations	Potential	Henderson et al. 2006 Saintot et al. 2011b	-
Skorene 1	406002 / 6898608	Helicopter reconnaissance in 2007	No further investigations	No	Henderson et al. 2006 Saintot et al. 2011b	Storfjord Site 31
Skorene 2	406036 / 6896957	Helicopter reconnaissance in 2007	No further investigations	No	Henderson et al. 2006	Storfjord Site 32

List of unstable or potentially unstable rock slopes in Møre og Romsdal.

Name	Coordinates (UTM 32N)	Investigations	Recommendations	Unstable rock slope?	References	Former names
Skrednakken 1	399661 / 6906562	Field mapping in 2005, periodic displacement measurements with dGNSS since 2006	Periodic measurements not to be continued	Potential	Henderson et al. 2006 Dahle et al. 2011a Saintot et al. 2011b	Storfjord Site 18
Skrednakken 2	398634 / 6905543	Field mapping in 2005	No further investigations	No	Henderson et al. 2006 Saintot et al. 2011b	Storfjord Site 17b
Smoge	398500 / 6902000	Helicopter reconnaissance in 2005	No further investigations	No	Henderson et al. 2006	Storfjord Site 17
Svarthornet	423233 / 6911419	Aerial photographs	Helicopter reconnaissance planned	Unknown	Henderson et al. 2006	Valldal, Storfjord Site 40
Vardefjellet	406778 / 6908400	Helicopter reconnaissance in 2005	No further investigations	No	Henderson et al. 2006	Storfjord Site 34
Vindsneset	409917 / 6906864	Helicopter reconnaissance in 2005	Field mapping planned	Yes	Henderson et al. 2006 Saintot et al. 2011b	Vikasætra, Storfjord Site 23
Årøldalen	418225 / 6903911	Helicopter reconnaissance in 2007	No further investigations	Potential	Henderson et al. 2006 Oppikofer 2009 Dahle et al. 2011a	Storfjord Site 43
Stordal municipality						
Sandfjellet	399994 / 6921090	Aerial photographs	Helicopter reconnaissance planned	Unknown	-	-
Storhornet 1	399440 / 6916790	Helicopter reconnaissance in 2007	No further investigations	No	Henderson et al. 2006	Storfjord Site 36
Storhornet 2	400199 / 6916123	Helicopter reconnaissance in 2007	No further investigations	No	Henderson et al. 2006	Storfjord Site 37
Tuva	396075 / 6916854	Helicopter reconnaissance in 2007	No further investigations	No	Henderson et al. 2006	Storfjord Site 35
Stranda municipality						
Aksla	397444 / 6892294	Field mapping in 2006	Make hazard and risk classification	Yes	Henderson et al. 2006 Saintot et al. 2011b	Furneshornet, Storfjord Site 28
Brattsvødene	397000 / 6893001	Helicopter reconnaissance in 2005	No further investigations	No	Henderson et al. 2006	Aksla, Storfjord site 14
Brendefjellet	391724 / 6886409	Field mapping in 2005	No further investigations	No	Henderson et al. 2006	Storfjord Site 6
Fivelstadnibba	383276 / 6888801	Helicopter reconnaissance in 2011	Assess run-out area	Yes	Dahle et al. 2011a	-
Fremste Blåhornet	395242 / 6900486	Field mapping in 2005, periodic displacement measurements with dGNSS since 2005	Periodic measurements not to be continued	Potential	Henderson et al. 2006 Dahle et al. 2011a Saintot et al. 2011b	Blåhornet, Storfjord Site 2b
Furneset	395746 / 6891924	Field mapping in 2005, periodic displacement measurements with dGNSS since 2006	Periodic measurements not to be continued	Potential	Henderson et al. 2006 Dahle et al. 2011a Saintot et al. 2011b	Storfjord Site 14b

List of unstable or potentially unstable rock slopes in Møre og Romsdal.

Name	Coordinates (UTM 32N)	Investigations	Recommendations	Unstable rock slope?	References	Former names
Geitfonnegga	402993 / 6890148	Field mapping in 2006	No further investigations	Potential	Henderson et al. 2006 Dahle et al. 2011a Saintot et al. 2011b	Storfjord Site 12b
Herdalsnibba	393354 / 6894129	Field mapping in 2005, periodic displacement measurements with dGNSS since 2006	Periodic measurements not to be continued	Potential	Henderson et al. 2006 Dahle et al. 2011a Oppikofer et al. 2011 Saintot et al. 2011b	Rundefjellet, Storfjord Site 4
Hildeborfjellet	396011 / 6901719	Helicopter reconnaissance in 2005	New helicopter reconnaissance planned	Unknown	Henderson et al. 2006 Saintot et al. 2011b	Ildeborneset, Storfjord Site 1
Jolegrova	399808 / 6885461	Field mapping in 2005 & 2006	No further investigations	Potential	Henderson et al. 2006 Saintot et al. 2011b	Storfjord Site 9
Kvitegga	388463 / 6899705	Helicopter reconnaissance in 2011	No further investigations	No	-	-
Laushornet 1	406765 / 6888339	Field mapping in 2006	No further investigations	Potential	Henderson et al. 2006 Saintot et al. 2011b	Storfjord Site 11
Laushornet 2	406286 / 6888479	Helicopter reconnaissance in 2005	No further investigations	Potential	Henderson et al. 2006 Dahle et al. 2011a Saintot et al. 2011b	Storfjord Site 11b
Lundanesegga	395164 / 6889235	Field mapping in 2005	No further investigations	Potential	Henderson et al. 2006 Saintot et al. 2011b	Storfjord Site 13
Middagsnibba	396208 / 6875658	Aerial photographs	Helicopter reconnaissance planned	Unknown	-	-
Nokkenibba 1	393931 / 6886848	Field mapping in 2005	No further investigations	Potential	Henderson et al. 2006 Saintot et al. 2011b	Storfjord Site 7b
Nokkenibba 2	394063 / 6886301	Helicopter reconnaissance in 2005, periodic displacement measurements with dGNSS since 2006	Periodic measurements not to be continued	Potential	Henderson et al. 2006 Dahle et al. 2011a Saintot et al. 2011b	Storfjord Site 7
Oldervika	396159 / 6898228	Helicopter reconnaissance in 2005	New helicopter reconnaissance planned	Unknown	Henderson et al. 2006 Saintot et al. 2011b	Storfjord Site 3
Rindalseggene	389495 / 6888044	Field mapping in 2005, periodic displacement measurements with dGNSS since 2005 and TLS since 2006	Continue periodic measurements with 3–5 year interval	Yes	Henderson et al. 2006 Dahle et al. 2011a Saintot et al. 2011b	Storfjord Site 6b
Skafjellet	395782 / 6910984	Field mapping in 2006	No further investigations	No	Henderson et al. 2006	Storfjord Site 44
Smånipene	403292 / 6886867	Aerial photographs	Helicopter reconnaissance planned	Unknown	Dahle et al. 2011a	-

List of unstable or potentially unstable rock slopes in Møre og Romsdal.

Name	Coordinates (UTM 32N)	Investigations	Recommendations	Unstable rock slope?	References	Former names
Stokkehornet	398950 / 6894113	Helicopter reconnaissance in 2005	No further investigations	No	Henderson et al. 2006 Saintot et al. 2011b	Storfjord Site 15
Storskredholten	405397 / 6886422	Helicopter reconnaissance in 2005	No further investigations	Potential	Henderson et al. 2006 Dahle et al. 2011a Saintot et al. 2011b	Storfjord Site 10b
Svenskekjølet	396089 / 6899136	Field mapping in 2005	New helicopter reconnaissance planned	Unknown	Henderson et al. 2006 Saintot et al. 2011b	Storfjord Site 2
Syltavika	396940 / 6884865	Field mapping in 2005	No further investigations	No	Henderson et al. 2006 Saintot et al. 2011b	Storfjord Site 8
Teinnosa	401000 / 6889649	Field mapping in 2005	No further investigations	Potential	Henderson et al. 2006 Saintot et al. 2011b	Storfjord Site 12
Tenneflåna	403561 / 6888226	Field mapping in 2006	No further investigations	Potential	Henderson et al. 2006 Dahle et al. 2011a Saintot et al. 2011b	Storfjord Site 10
Tynnbjørggjølet	393362 / 6892471	Field mapping in 2005	Make hazard and risk classification	Yes	Henderson et al. 2006 Dahle et al. 2011a Saintot et al. 2011b	Storfjord Site 5
Ytstevatnet	382720 / 6890844	Helicopter reconnaissance in 2011	No further investigations	Potential	-	-

List of unstable or potentially unstable rock slopes in Møre og Romsdal.

Name	Coordinates (UTM 32N)	Investigations	Recommendations	Unstable rock slope?	References	Former names
Åknes	395295 / 6895970	Field mapping in 2004-2006, periodic displacement measurements with dGNSS from 2004 to 2007 and TLS from 2006 to 2008, continuous monitoring since 2004 by Åknes/Tafjord Early-Warning Centre	Continue continuous monitoring	Yes	Braathen et al. 2004 Derron et al. 2005a Eidsvig & Harbitz 2005 Blikra et al. 2006 Kveldsvik et al. 2006, 2008, 2009a, 2009b Rønning et al. 2006, 2008 Ganerød et al. 2007, 2008 Blikra 2008 Elvebakk 2008 Frei 2008 Lacasse 2008 Storrø & Gaut 2009 Grøneng et al. 2009, 2010 Nordvik & Nyrnes 2009 Nordvik et al. 2009 Oppikofer et al. 2009, 2011 Ganerød 2010 Heincke et al. 2010 Kristensen et al. 2010 Dahle et al. 2011a Eidsvig et al. 2011 Jaboyedoff et al. 2011 Saintot et al. 2011b Dehls et al. 2012	Åkneset, Åkerneset
Sykkylven municipality						
Hundatindan	368438 / 6914439	Helicopter reconnaissance in 2011	No further investigations	No	-	-
Ørskog municipality						
Giskemonibba	391932 / 6931106	Helicopter reconnaissance in 2011	Assess run-out area	Yes	Dahle et al. 2011a	-
Søre Sunnmøre region						
Hareid municipality						
Grøthornet	344731 / 6924004	Helicopter reconnaissance in 2011, field mapping in 2012	Make hazard and risk classification	Yes	Dahle et al. 2011a	-
Sande municipality						

List of unstable or potentially unstable rock slopes in Møre og Romsdal.

Name	Coordinates (UTM 32N)	Investigations	Recommendations	Unstable rock slope?	References	Former names
Laupsnipa	331336 / 6901669	Helicopter reconnaissance in 2011, field mapping in 2012, periodic displacement measurements with TLS and tape extensometer since 2012	Continue periodic measurements with 1–3 year interval	Yes	Dahle et al. 2011a	-
Ulstein municipality						
Haddalura	337401 / 6910313	Helicopter reconnaissance in 2011, field mapping in 2009, periodic displacement measurements with dGNSS from 2005 to 2009	Periodic measurements not to be continued	No	Anda et al. 2000 Dahle et al. 2011a	-
Vanylven municipality						
Sandfjellet	324740 / 6896180	Reconnaissance from road in 2011	Helicopter reconnaissance planned	Unknown	-	-
Sandnestua	325245 / 6894723	Helicopter reconnaissance in 2011	Assess run-out area	Yes	Dahle et al. 2011a	-
Storehornet	326750 / 6885268	Field mapping in 2011 and 2012, periodic displacement measurements with dGNSS, TLS and tape extensometer since 2012	Continue periodic measurements with 1–3 year interval	Yes	Anda et al. 2000 Blikra et al. 2002a Dahle et al. 2011a	-
Volda municipality						
Bjørnasethornet	349334 / 6885309	Helicopter reconnaissance in 2011	Assess run-out area	Yes	-	-
Heida	347553 / 6883198	Helicopter reconnaissance in 2011	No further investigations	No	-	-
Hestefjellet	338888 / 6888616	Helicopter reconnaissance in 2011, field mapping in 2012, periodic displacement measurements with TLS since 2012	Periodic measurements not to be continued	Potential	-	-
Keipedalen	336426 / 6884229	Helicopter reconnaissance in 2011, field mapping in 2012	No further investigations	No	Dahle et al. 2011a	-
Klovane	345178 / 6884732	Reconnaissance from road in 2011	Helicopter reconnaissance planned	Unknown	-	-
Kvanndalsskåla	335158 / 6882700	Helicopter reconnaissance in 2011, field mapping in 2012	Make hazard and risk classification	Yes	-	-
Kvivsdalshornet	367933 / 6880764	Helicopter reconnaissance in 2011	Assess run-out area	Yes	-	-
Midnakken	338855 / 6888260	Reconnaissance from road in 2011	No further investigations	No	-	-
Nausane	334205 / 6880365	Reconnaissance from road in 2012	Helicopter reconnaissance planned	Unknown	-	-

List of unstable or potentially unstable rock slopes in Møre og Romsdal.

Name	Coordinates (UTM 32N)	Investigations	Recommendations	Unstable rock slope?	References	Former names
Skylefjellet	338494 / 6887693	Helicopter reconnaissance in 2011, periodic displacement measurements with TLS since 2012	Continue periodic measurements with 1–3 year interval	Yes	Dahle et al. 2011a	-
Solahylla	344756 / 6880389	Helicopter reconnaissance in 2011, periodic displacement measurements with TLS since 2012	Continue periodic measurements with 1–3 year interval	Yes	Dahle et al. 2011a	-
Trongedalen	337067 / 6886024	Helicopter reconnaissance in 2011	No further investigations	No	-	Blåfjellet
Ørsta municipality						
Blåhornet	377219 / 6893416	Helicopter reconnaissance in 2011	No further investigations	No	-	-
Jakta	375820 / 6895362	Helicopter reconnaissance in 2011	Field mapping planned	Yes	Dahle et al. 2011a	-
Keipen	380647 / 6895624	Helicopter reconnaissance in 2011, TLS in 2012 for structural analysis	Make hazard and risk classification	Yes	Dahle et al. 2011a	-
Litlehornet	383941 / 6897216	Helicopter reconnaissance in 2011	No further investigations	No	Dahle et al. 2011a	-
Maudekollen	377149 / 6900404	Helicopter reconnaissance in 2011	No further investigations	No	-	-
Skorgeurda	346451 / 6903065	Helicopter reconnaissance in 2011	Field mapping planned	Yes	Dahle et al. 2011a	-
Stålberghornet	374214 / 6897591	Helicopter reconnaissance in 2011	No further investigations	No	-	-
Ålesund region						
Haram municipality						
Branddalsryggen	363044 / 6951637	Helicopter reconnaissance in 2012	Field mapping planned	Yes	Dahle et al. 2011a Ganerød & Lutro 2011	-
Byrkjevollhornet	381859 / 6944499	Helicopter reconnaissance in 2012	Assess run-out area	Yes	Dahle et al. 2011a	-
Hellenakken	378950 / 6944990	Helicopter reconnaissance in 2012	Field mapping planned	Yes	Blikra et al. 2002b Dahle et al. 2011a	-
Otrefjellet	380941 / 6941091	Helicopter reconnaissance in 2012	Assess run-out area	Yes	Anda et al. 2000 Blikra et al. 2002a Dahle et al. 2011a	Øtrefjell
Skjerveheian	372341 / 6944239	Helicopter reconnaissance in 2012	No further investigations	No	-	-
Skulen	361919 / 6952742	Helicopter reconnaissance in 2012	Field mapping planned	Yes	Dahle et al. 2011a	-
Skoraegga	374105 / 6944905	Helicopter reconnaissance in 2012	No further investigations	No	Blikra et al. 2002b	Skårahornet
Tindfjellet	382801 / 6942003	Helicopter reconnaissance in 2012	No further investigations	No	Dahle et al. 2011a	-
Vassbotnen 1	382317 / 6944116	Helicopter reconnaissance in 2012	No further investigations	No	-	-
Vassbotnen 2	382519 / 6944018	Helicopter reconnaissance in 2012	No further investigations	No	-	-
Sula municipality						

List of unstable or potentially unstable rock slopes in Møre og Romsdal.

Name	Coordinates (UTM 32N)	Investigations	Recommendations	Unstable rock slope?	References	Former names
Tverrfjellet 1	352646 / 6922821	Helicopter reconnaissance in 2011, field mapping in 2012	Make hazard and risk classification	Yes	Dahle et al. 2011a	-
Tverrfjellet 2	353022 / 6922668	Helicopter reconnaissance in 2011, field mapping in 2012	Make hazard and risk classification	Yes	Dahle et al. 2011a	-
Tverrfjellet 3	353668 / 6922446	Helicopter reconnaissance in 2011, field mapping in 2012	Make hazard and risk classification	Yes	Dahle et al. 2011a	-
Ålesund municipality						
Rambjøra	366645 / 6928245	Helicopter reconnaissance in 2011, field mapping in 2012	Make hazard and risk classification	Yes	Dahle et al. 2011a	-

NGU
Norges geologiske undersøkelse
Geological Survey of Norway

Norges geologiske undersøkelse
Postboks 6315, Sluppen
7491 Trondheim, Norge

Geological Survey of Norway
PO Box 6315, Sluppen
7491 Trondheim, Norway

Besøksadresse
Leiv Eirikssons vei 39, 7040 Trondheim

Visitor address
Leiv Eirikssons vei 39, 7040 Trondheim

Telefon 73 90 40 00
Telefax 73 92 16 20
E-post ngu@ngu.no
Nettside www.ngu.no

Tel (+ 47) 73 90 40 00
Fax (+ 47) 73 92 16 20
E-mail ngu@ngu.no
Web www.ngu.no/en-gb/